THE 12TH IAWPRC BIENNIAL INTERNATIONAL CONFERENCE

AMSTERDAM
17–20 September, 1984

HALL 1

Continued on back cover

AEROBIC FILMS

Wat. Sci. Tech. Vol.17, Amsterdam, pp.1-14.
Printed in Great Britain.

0273-1223/85 $0.00 + .50

REMOVAL OF SOLUBLE SUBSTRATES IN FIXED FILMS

Jes la Cour Jansen* and Poul Harremoës**

*I. Krüger AS, Gladsaxevej 363, DK-2860 Soeborg, Denmark
**Department of Environmental Engineering, Building 115, The Tech. Univ. of Denmark, DK-2800 Lyngby, Denmark

ABSTRACT

Experimental results with removal of soluble substrates in fixed films are presented. Experiments are performed with denitrification and with oxidation of methanol, acetic acid and glucose in a laboratory fixed film reactor.

The experiments confirm the predictions of the half order reaction model, taking diffusion of the substrates and zero order intrinsic reaction rate of the bacteria as the dominating processes in the film. The experiments enable calculation of the kinetic parameters: diffusion coefficients, intrinsic reaction rates and half order rate constants for nitrate, methanol, acetic acid, glucose and oxygen within fixed films.

KEYWORDS

Kinetics; fixed films; denitrification; oxidation of organics.

INTRODUCTION

Fixed film reactors have been reconsidered for wastewater treatment during the last twenty years. Plastic media and new process configurations such as rotating disks and fluidized filters have appeared. Furthermore the increasing need for treatment of new types of wastewater has increased the interest in fixed film reactors for treatment of both domestic and industrial wastewater. The traditional approach where the treatment plant has been considered more or less as a "black box" does not suffice. Deeper insight into all processes and phenomena related to the fixed film reactors has to be established.

Many different types of phenomena have to be considered in order to establish a sound basis for design and operation of fixed film reactors. The hydraulics, that is the macro-transportation of water and substrates within the reactors, differ very much from one reactor type to another. Transportation of gasses which take part in the biological processes also differs from system to system, just as the significance of a possible liquid film layer. However, common to all types of reactors are the processes within the fixed film. The substrates may be brought to the surface of the bacterial layer in many different ways, but inside the biofilm the substrates

have to be transported, in soluble form, to the bacteria where the reaction takes place, and the reaction products have to be transported out again. A conceptual model corresponding to this description of the fundamental processes in fixed film is illustrated in Fig. 1. The concepts are in close agreement with those stated by others, including Atkinson and Fowler, 1974; Harremoës and Riemer, 1975; Harremoës, 1978; La Motta, 1974; Williamson and McCarty 1976a, 1976b. In all cases the transportation of the substrates, and reaction products has been taken as Fick'ian diffusion, whereas several proposals for the reaction rate inside the biofilm have been given.

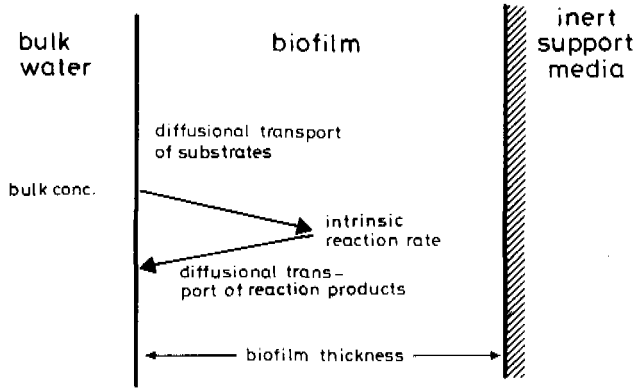

Fig. 1 Conceptual model for removal of soluble substrates focusing on phenomena inside the film.

The intrinsic process is assumed to follow Monod-type kinetics, but the Monod constant is low in many cases, which means that the intrinsic reaction rate can be taken as zero order for most practical applications, as stated by Harremoës, (1978A).

This simplicity of the mathematics leads to a very simple description of the bulk processes. As derived by Harremoës, (1976, 1978), or by Harremoës and Riemer (1975), the diffusion leads to a bulk process which is either half or zero order with respect to the bulk concentration of the substrate under consideration. The following equations summarize the results.

Zero order bulk reaction

$$r_a = k_{0a} = k_{0f} L \qquad \text{valid for} \quad \beta = \sqrt{\frac{2D\, C^*}{k_{0f} L^2}} \geq 1 \qquad (1)$$

Half order bulk reaction

$$r_a = k_{\frac{1}{2}a} C^{*\frac{1}{2}} = \sqrt{2D\, k_{0f}} C^{*\frac{1}{2}} \qquad \text{valid for } \beta < 1 \qquad (2)$$

where

r_a is the removal rate per unit area biofilm surface ($g\ m^{-2} s^{-1}$)

k_{0a} is the zero order removal rate per unit area ($g\ m^{-2} s^{-1}$)

$k_{\frac{1}{2}a}$ is the half order rate constant per unit area ($g^{\frac{1}{2}} m^{-\frac{1}{2}} s^{-1}$)

k_{0f} is the intrinsic zero order removal rate in the biofilm ($g\ m^{-3} s^{-1}$)

L	is the thickness of the biofilm (m)
D	is the coefficient of molecular diffusion in the biomass ($m^2 s^{-1}$)
C^*	is the bulk concentration at the surface of the biofilm ($g\ m^{-3}$)
β	is a dimensionless constant called the "penetration ratio"

The equations state that the bulk process becomes zero order, independent of the substrate concentration, when the substrate penetrates the biofilm fully ($\beta \geq 1$). At lower bulk concentrations, the diffusion limitation leads to partial penetration of the biofilm and a bulk reaction dependent of the bulk substrate concentration to the half power becomes the result.

Biological processes are redox processes where either electron donor or acceptor is the rate limiting substrate. In case of diffusion limitation equation (2) has to be supplemented with a calculation to show which one of the substrates is rate limiting and determines the overall reaction rate.

The component (donor or acceptor) that penetrates the least is rate limiting, leading to the following condition for change of limiting substrate:

$$\frac{C_d^*}{C_a^*} = \frac{D_a \quad k_{0fd}}{D_d \quad k_{0fa}} = \frac{D_a}{D_d} \quad M \tag{3}$$

where

C_d^* and C_a^*	are the bulk concentrations of the donor and acceptor ($g\ m^{-3}$)
D_d and D_a	are the corresponding diffusion coefficients ($m^2\ s^{-1}$)
k_{0fd} and k_{0fa}	are the corresponding zero order intrinsic reaction rates ($g\ m^{-3}\ s^{-1}$)
L	is the biofilm thickness (m)
M	is the stoichiometric consumption ratio ($g\ g^{-1}$)

Harremoës and Riemer (1975), Riemer (1977), and Riemer and Harremoës (1978) describe experiments in a denitrifying down-flow filter confirming equation (1, 2, and 3). The purpose of the experiments described in the following is to demonstrate the validity in general of these equations for removal of soluble substrates in fixed film under conditions as well defined as possible.

EXPERIMENTAL EQUIPMENT AND PROCEDURES

An experimental reactor suited for examination of the process inside fixed films was developed (details of the reactor construction and performance are given in Kristensen and Jansen (1980)). The experimental set-up for experiments with denitrification and with oxidation of organics is shown in Fig. 2.

The reactor is the result of a development based on the principles described by Kornegay and Andrews (1969) and La Motta (1974).

The reactor volume of about one litre is situated between two cylinders of which the inner is rotating. The rotation ensures a totally mixed bulk phase and creates a hydraulic shear resulting in an even distribution of the biofilm growing on the walls of the cylinder. Four dovetailed slits are placed as integrated part of the outer, stationary cylinder wall. They can be taken up and part of the film can be taken out to be used for measurements of the thickness. Details of the measuring technique can be found in Kristensen and Jansen (1980) or in Kristensen and Christensen (1982).

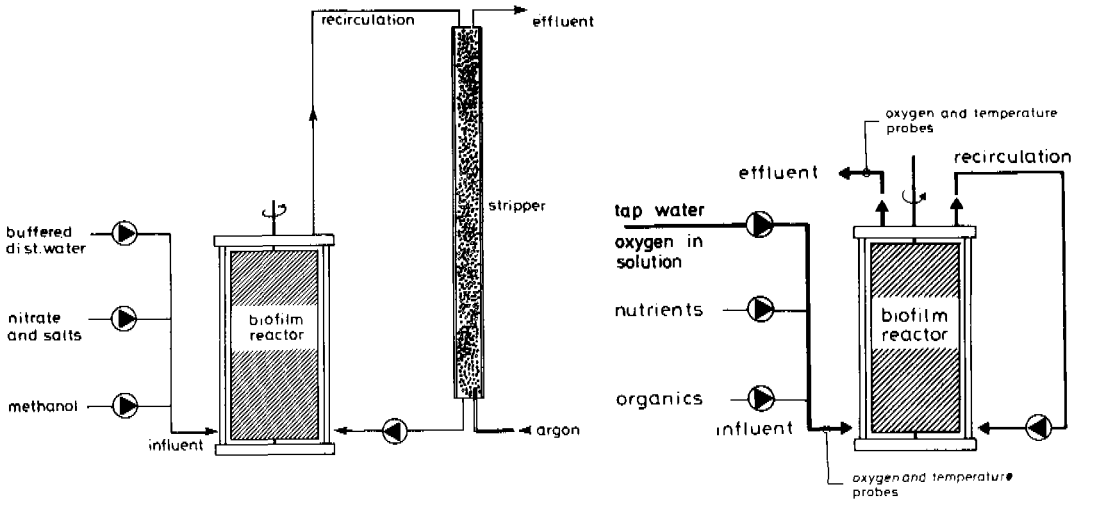

Fig. 2 Experimental set-up for examination of kinetics of soluble substrates in fixed films.

The reactor has been used for experiments with denitrification and with oxidation of organics in a slightly different set-up as seen in Fig. 2 . During denitrification, nitrogen gas is produced, leading to bubble formation at the rear of the biofilm, unless the bulk concentration of molecular nitrogen is kept low. The stripping device shown in Fig. 2 serves that purpose. The significance of nitrogen bubble formation in fixed films and the practical consequence for denitrification in fixed film reactors are described by Harremoës, Jansen and Kristensen (1980). In both cases the reactor is provided with an external recirculation serving two purposes. Total mixing of the bulk water is ensured, independently of the inflow rate. Formation of Taylor-currents (see Coles, 1965; Kristensen and Jansen, 1980; Taylor, 1923) is effectively suppressed. Such currents would disturb the homogeneous growth of the biofilm.

The experimental arrangements enable easy verification of the kinetic model and determination of the kinetic parameters: the diffusion coefficient, the intrinsic removal rate, and the half order rate constant. Considering one substrate only (all other substrates in excess), experiments at high concentrations, where equation (1) is valid, enable determination of the intrinsic removal rate, k_{0f} when the surface removal rate r_a and the biofilm thickness L are measured. At low concentrations where equation (2) is valid, the half order rate constant, $k_{1/2a}$, is found when r_a and bulk concentration C^* are known. Note that the bulk concentration equals the outlet concentration since the bulk of the water is totally mixed. Fig. 3 shows a plot of the surface removal rate of such an ideal, fictitious experiment with planned experimental results indicated, together with the prediction of the kinetic model.

Experiments with examination of change of limiting substrates (equation 3) are performed simply as an extension of the experiments with one component shown in Fig. 3. Figure 4 shows the principle. As a supplement to the one-component experiments, experiments are performed such that the level of the former substrate in excess is reduced until a level where it becomes potential limiting. The actual limitation is then

found experimentally. Accordingly, the validity of equation 3 can be tested.

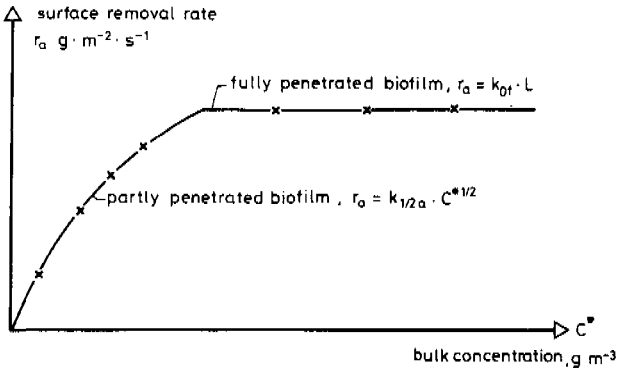

Fig. 3 Plot of an ideal, fictitious one-component experiment. Planned experimental results are indicated.

The change of limiting substrate can be illustrated directly in a dimensionless plot of all experimental data, as shown in Fig. 5, covering situations of rate limitation by either of the two substrates.

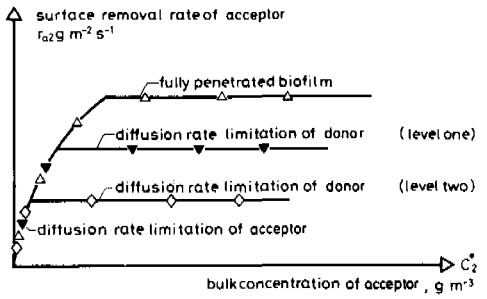

Fig. 4 Plot of an ideal fictitious two-component experiment. Planned experimental results are indicated.

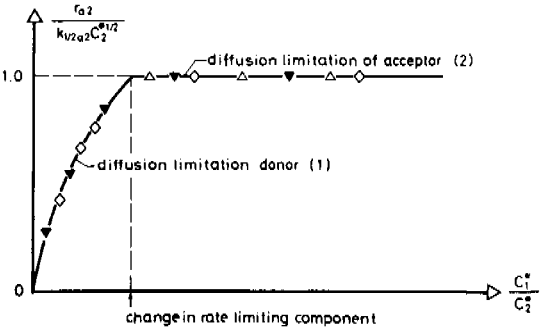

Fig. 5 Dimensionless plot of an ideal two-component experiment demonstrating change of limiting component directly.

KINETIC EXPERIMENTS

Kinetic experiments with denitrification and with oxidation of different organics have been performed. The fixed film has been grown without substrate depletion prior to the experiments. Exponential increase of the surface removal rate has been found in all cases. The film has been plane and well suited for experiments with substrate removal kinetics as described in the former section. Details of the experiments can be found in Jansen (1983).

Nitrogen Removal

Figure 6 shows results from three experiments with removal of nitrate in fixed films. The experiments are performed with a biofilm at three different thicknesses.

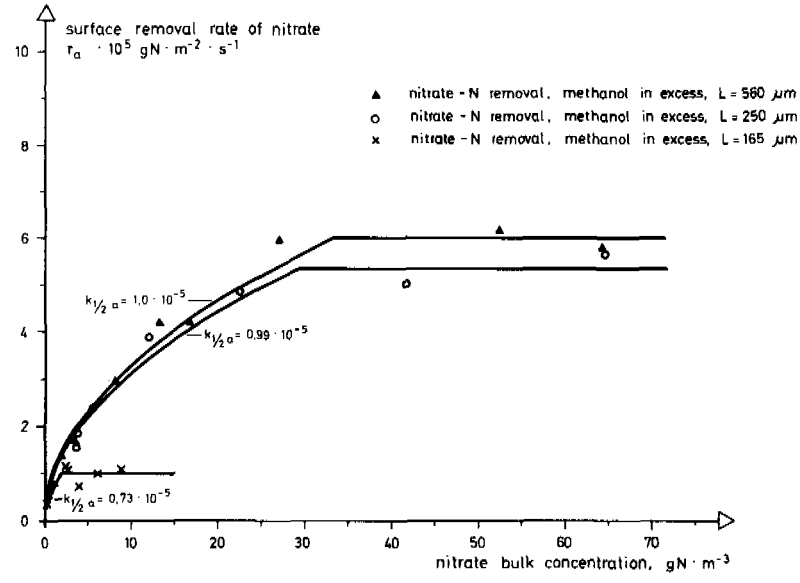

Fig. 6 Experimental results from three experiments with nitrate. The experiments are performed at biofilm thicknesses of 165, 250 and 560 µm.

The experimental points are supplemented by the best fit to the data assuming that the kinetic model is valid. It is seen that the predicted parabolic dependence of surface removal rate to bulk substrate concentration at low concentration is valid, and that the surface removal rate becomes constant at high concentrations. The half order rate constant changes a little as the biofilm thickness increases, illustrating that growth of a biofilm may change the kinetic properties of the film.

Oxygen Consumption

Figure 7 shows results from three experiments with oxygen removal in fixed films grown aerobically on methanol, acetid acid and glucose, respectively. In all cases the proposed dependence of the surface removal rate on the bulk substrate concentration is demonstrated.

Removal of Organics

Figure 8 shows results from three experiments with removal of methanol, acetic acid and glucose, respectively, in aerobic films. As for removal of nitrate and oxygen the proposed dependence exists. For glucose the bulk concentration has been too low to penetrate the biofilm fully.

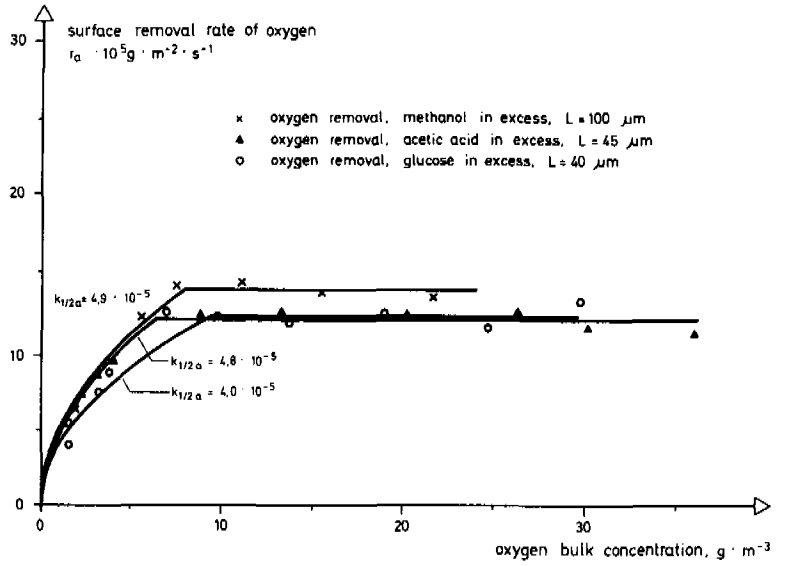

Fig. 7 Experimental results from three experiments with oxidation of organics. Methanol, acetic acid and glucose have been in excess during one experiment each.

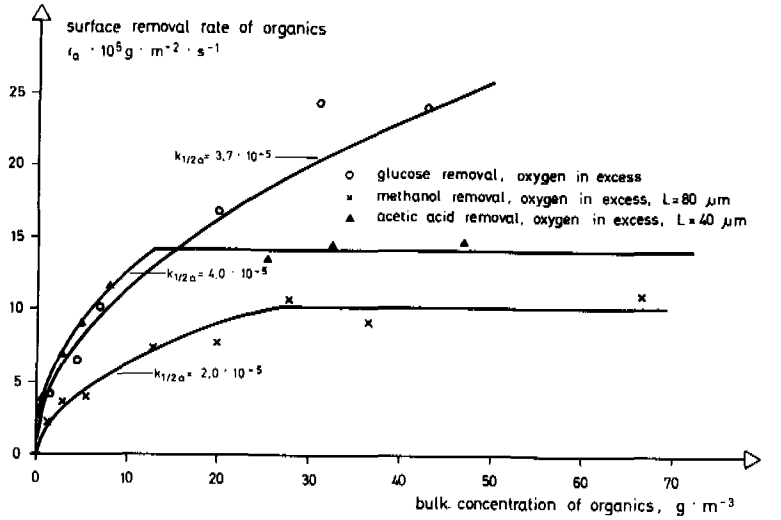

Fig. 8 Experimental results from three experiments with oxidation of methanol, acetic acid and glucose. Oxygen has been in excess in all experiments.

Methanol has been used for experiments with denitrification and oxidation of organics. Fig. 9 shows results with methanol removal in both kinds of films.

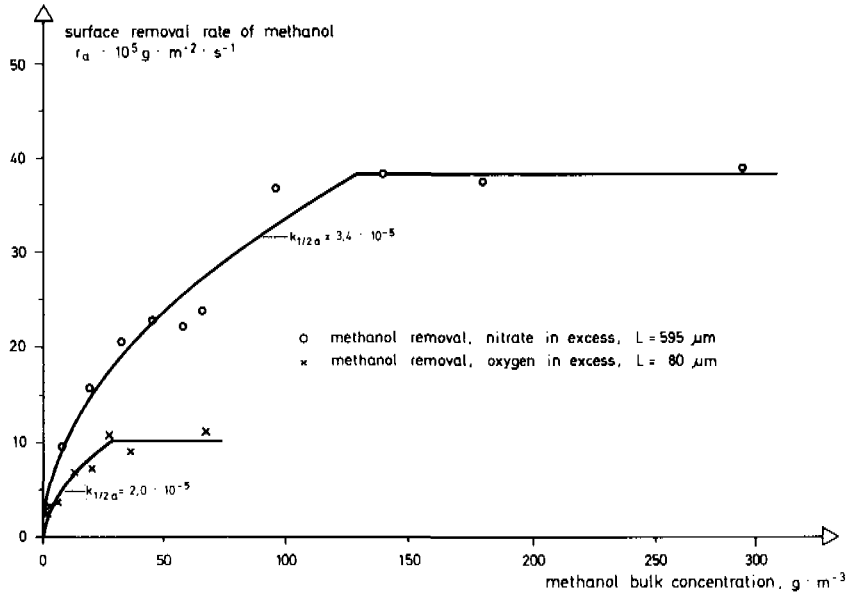

Fig. 9 Experimental results from two experiments with methanol removal. Nitrate and oxygen have been electron acceptor in one experiment each.

Change of Limiting Substrate

Figure 10 shows the results from an extended experiment with oxidation of acetic acid.

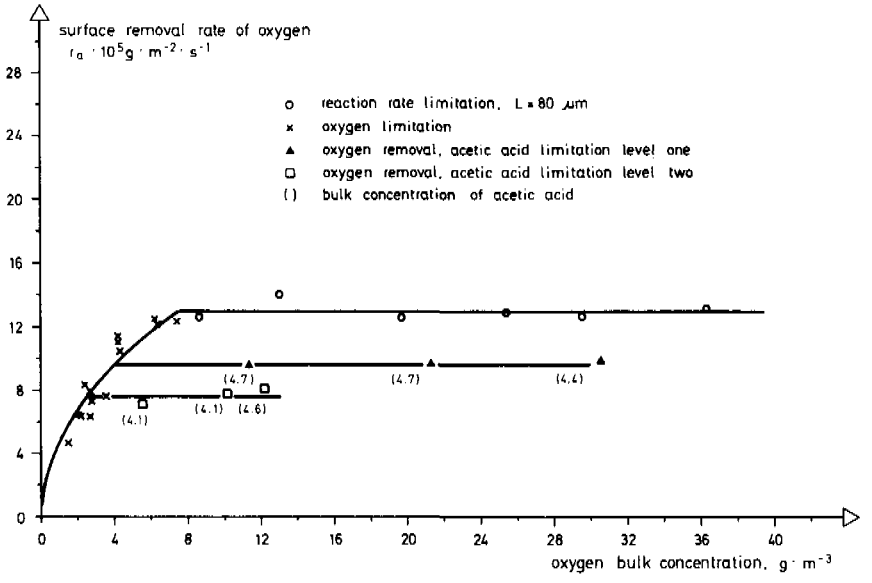

Fig. 10 Experimental results from an experiment with oxidation of acetic acid, demonstrating reaction rate limitation and diffusion limitation to oxygen and acetic acid removal.

The figure shows the oxygen removal rate, but the rates of acetic acid can be found from the stoichiometry of the process. The figure demonstrates the change of rate limitation from reaction rate limitation (no substrate limiting) to oxygen limitation. Furthermore two levels with acetic acid limitation are shown. The direct illustration of change of limiting substrate is shown in Fig. 11. Data from Fig. 10, where one of the substrates is limiting, are combined with further experimental data, where acetic acid is limiting. The change of limiting substrate is seen to take place at a proportion between bulk acetic acid and oxygen concentrations of 1.4 g acetic acid/g oxygen. Figure 12 shows the dimensionless plot of results from a kinetic experiment with denitrification similar to Fig. 11. The change of limiting substrate is seen to take place at a concentration ratio of 2 g methanol/g nitrate-N.

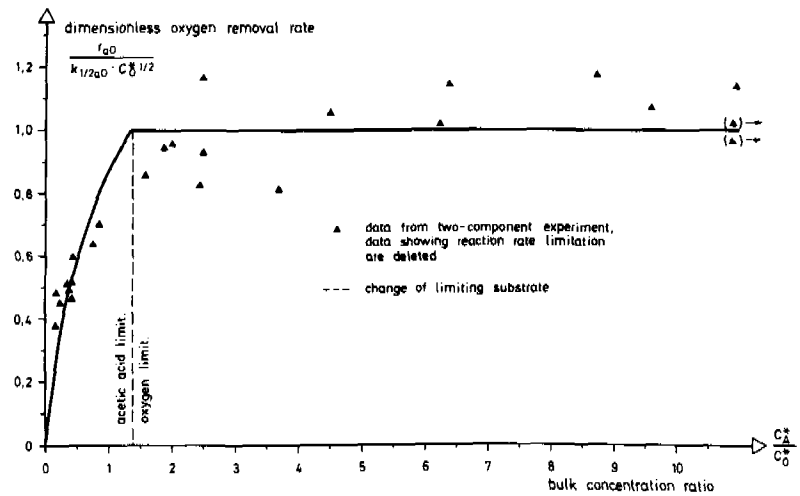

Fig. 11 Dimensionless illustration of change in rate limiting component for oxidation of acetic acid in a biofilm.

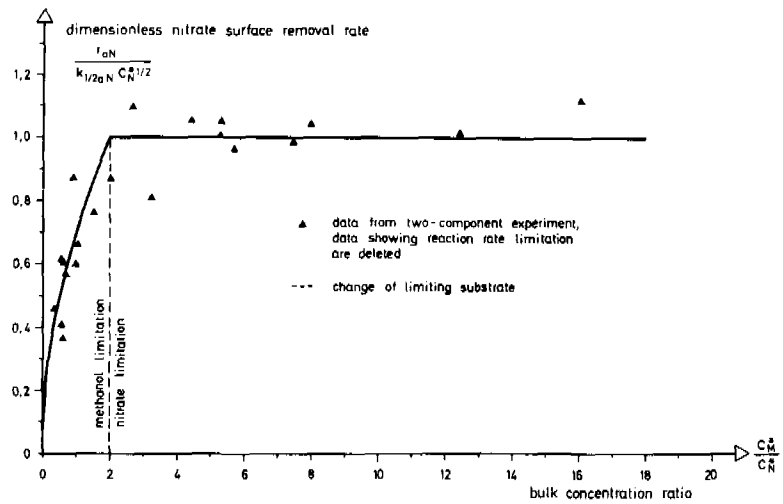

Fig. 12 Dimensionless illustration of change in rate limiting component for a denitrifying biofilm.

DISCUSSION

Figures 6 to 12 all demonstrate the significance of diffusion limitation for removal of soluble substrates in fixed films. Reduction of surface removal rate of the film at low bulk substrate concentration takes place as a half order reaction, as predicted by the model. When the bulk substrate concentration is high enough to ensure full substrate penetration of the biofilm, the removal rate becomes constant, i.e. zero order. Furthermore the distinct change of limiting substrate predicted by the model is experimentally demonstrated (see Fig. 11 and 12). It is noteworthy how well this single concept describes the experimental data, determined under laboratory conditions as well defined as possible. On this basis it can be concluded that there is little ground for introduction of more complicated models for description of the surface removal kinetics - especially when transferred to practical application.

The kinetic parameters calculated according to equation 1 and 2 are given in Table 1.

TABLE 1 Kinetic Parameters for Removal of Soluble Substrates in Fixed Films

Process	Biofilm Thickness L	Half Order Rate Const. $k_{½a}$	Intrinsic Zero Order Rate k_{0f}	Diffusion Coefficient D	Temperature T
	m	$g^{½}\ m^{-½}\ s^{-1}$	$g\ m^{-3}\ s^{-1}$	$m^2\ s^{-1}$	^oC
Denitrification			NITRATE		
	$165\ 10^{-6}$	$0.73\ 10^{-5}$	0.061	$4.3\ 10^{-10}$	22
	250 -	0.99 -	0.21	2.3 -	21
	560 -	1.0 -	0.11	5.1 -	22
	595 -	3.0 -	0.37	12.4 -	22
			METHANOL		
	595 -	3.4 -	0.64	8.9 -	22
Oxidation of organics		OXYGEN (Methanol in Excess)			
	100 -	4.9 -	1.4	8.8 -	13
		OXYGEN (Acetic Acid in Excess)			
	45 -	4.8 -	2.7	4.3 -	10
		OXYGEN (Glucose in Excess)			
	40 -	4.0 -	3.0	2.6 -	10
			METHANOL		
	80 -	2.0 -	1.3	1.5 -	9
			ACETIC ACID		
	40 -	4.0 -	3.5	2.3 -	10
			GLUCOSE		
	-	3.7 -	6.7	1.0 -	11

Note that the rates and coefficients are given for the substrate written with capital letters.

The calculated diffusivities of the soluble substrates are in all cases reduced when compared to values found in pure water given in Table 2. Diffusivities in the range of 15-80% of the values in pure water are found. The difference in reduction of diffusion coefficient for the substrates is assumed to be due to differences in the structure of the biofilm and may in case of charged substrates be caused by electrical interactions between the ions and fixed charges in the biofilm, Riemer and Harremoës (1978).

TABLE 2 Diffusion Coefficients for Some Soluble Substrates in Pure Water

	Nitrate	Oxygen	Methanol	Acetic Acid	Glucose
Diffusion Coefficient $D\ 10^{-10}\ m^2\ s^{-1}$	15	15	12	12	4.7
Temperature T ^{o}C	25	13	20	25	13
Reference	Gray (1972)	Landolt (1969)	Ans (1967)	Perry (1963)	Landolt (1969)

The intrinsic reaction rates are found to be comparable to findings in the literature. Such data based on direct measurements of the biofilm thicknesses are few and grouped in Table 3. Also literature data enabling calculation of the half order rate constant are few, but available data are collected in Table 4.

TABLE 3 Intrinsic Reaction Rates for Some Soluble Substrates

Substrate	Intrinsic Reaction k_{0f} $g\ m^{-3}\ s^{-1}$	Temp. T ^{o}C	Comments	References
$C_6H_{12}O_6$	2.8	21	Oxidation in a biofilm	Hoehn (1973)
	16.7	-	Oxidation in a biofilm	Kornegay (1969)
	1.0	-	Oxidation in a biofilm	Atkinson (1970)
	1.9-13.9	22	Oxidation in a biofilm	LaMotta (1974) (1976A) (1976B)
NO_3-N	0.23-0.42	21-29	Denitrifying biofilm	Arvin (1982)
O_2	3.0	20	Oxidation of methanol in a biofilm	Andreasen (1979)
	5.5	26	Oxidation of methanol in a biofilm	Andreasen (1979)
	0.32-0.36	25	Oxidation of nutrient broth in slime from trickling filter	Chen (1981)

TABLE 4 Half Order Rate Constants for Some Soluble Substrates

Process	Substrate	Half Order Reaction Rate Constant $k_{½a}$ $g^{½}m^{-½}s^{-1}$	Reference
Mineralisation	Glucose	$3.8\ 10^{-5}$	Harremoës (1978A)
	Glucose	4.4 -	Onuma (1982)
Denitrification	Nitrate	3.6 -	Watanabe (1978) Harremöes (1978B)

The four nitrogen experiments made with the same biofilm at different thicknesses demonstrate in all cases the significance of diffusion limitation. However, the kinetic parameters change as the film grows. The half order rate increased as the film grew older and thicker. This phenomenon is assumed to be attributed mainly to a change of the structure of the film leading to an increase of the diffusion coefficient. Furthermore the intrinsic removal rate of the film changes with the structure. The general trend is increase of the rate with age. Due to varying production of polysaccharides which make up the slimy matrix of the film, the thickness of the film may in periods increase rapidly without a corresponding increase in the number of bacteria. This leads to a decrease of the calculated removal rate based on the total biofilm volume. The present examination of the kinetics of substrate removal in fixed films is not affected by this phenomenon, since the experiments are made within very short periods, where the film properties can be taken as constants. However, the experiments demonstrate the need for combination of kinetics of substrate removal with knowledge of the development and change of the biofilm structure.

Diffusion limitation of the substrates leads to a change of limiting substrate. Fig. 11 and 12 give a direct illustration of the phenomenon for oxidation of acetic acid and for denitrification. For oxidation of acetic acid it is seen that the proportion is about 1.4 g acetic acid/g oxygen. This means that the bulk concentration of oxygen has to be close to the bulk concentration of acetic acid for oxygen not to be limiting. Due to the low solubility of oxygen in water, this requirement will seldom be fulfilled. Furthermore the low solubility means that partial penetration of the biofilm will take place in most cases. The consequence is that often oxygen will be rate limiting to aerobic degradation of organics. Consequently, in practice, the reaction rate will be dominated by half order kinetics governed by the oxygen concentration. This effect of diffusion of the substrate into fixed film is often neglected and may lead to unfavourable design and operation of fixed film reactors.

For denitrification, the change of limiting substrate takes place at a ratio of bulk concentration of methanol to nitrate of about 2 g methanol/g nitrate. This is in close agreement with the value found by Riemer (1977) for denitrification in a submerged down-flow filter. The value is remarkably lower than expected if equal reduction of the diffusivity in the biofilm of methanol and nitrate is assumed. A stronger reduction for the negatively charged nitrate than for the uncharged methanol is proposed to be caused by electrical interaction between the nitrate ions and fixed charges in the biofilm.

CONCLUSION

A basic concept involving diffusional resistance to the bulk removal rate of soluble substrates in fixed films has been verified experimentally, under well defined laboratory conditions. The results show that a simplified half order - zero order reaction concept adequately describes the phenomena and that more complicated concepts may introduce unnecessary sophistication.

Experiments with denitrification and with oxidation of organics have demonstrated the significance of diffusion limitation for the surface removal of fixed films. The model parameters diffusion coefficients, zero order intrinsic reaction rates and half order rate constants have have been found experimentally.

Diffusion coefficients for nitrate, oxygen, methanol, acetic acid and glucose inside fixed films have been found to be in the range of 15-80% of the values found in pure water.

Zero order intrinsic reaction rates and half order rate constants have been found comparable to the few values cited in the literature.

Oxygen may often be limiting for the surface removal rate of aerobic degradation of organics in fixed films due to the low solubility of oxygen in water and due to diffusional resistance to the oxygen transportation in the film.

Diffusional transportation of nitrate in denitrifying biofilms is found to be reduced as compared to transportation of methanol, supporting a theory of ion-exclusion of the negatively charged nitrate by fixed negative charges in the biofilm.

REFERENCES

Andreasen T. (1979). Kinetics of Aerobic Metabolism in Fixed Films, (in Danish). Master-Thesis, Department of Sanitary Engineering, Technical University of Denmark, Lyngby.

Ans, J. d', Lax, E. (Hrsg.) (1967). Taschenbuch für Chemiker und Physiker. Bd. 1, 3. Auflage. Springer Verlag, Berlin, Germany.

Arvin E., Kristensen, G.H. (1982). Effect of Denitrification on the pH in Biofilms. Water Science and Technology. Vol. 14, 833-848.

Atkinson, B. Daoud, T. S. (1970). Diffusion Effects within Microbial Films. Institution of Chemical Engineers. Transactions. Vol. 48, 245-254.

Atkinson, B., Fowler, H.W. (1974). The Significance of Microbial Film in Fermenters. Advances in Biochemical Engineering. Vol. 3, Chapter 6, 221-277.

Chen, Y. S., Bungay, H. R. (1981) Microelectrode Studies of Oxygen Transfer in Trickling Filter Slimes. Biotechnology and Bioengineering. Vol. 23, 781-792.

Coles D. (1965). Transitions in Circular Couette Flow. Journal in Fluid Mechanics. Vol. 21, 385-425.

Gray, D. D. (1972). American Institute of Physics Handbook. 3rd Edition. McGraw-Hill, N.Y., USA.

Harremoës, P., Riemer, M. (1975). Report on Pilot-Scale Experiments on Down-Flow Filter Denitrification. Department of Sanitary Engineering, Technical University of Denmark, Lyngby. (Rep. 75-1).

Harremoës, P. (1976). The Significance of Pore Diffusion to Filter Denitrification, Water Pollution Control Federation. Journal. Vol. 48, 377-388.

Harremoës, P. (1978A). Biofilm Kinetics. Chapter 4 in: Mitchell, R. (ed.), Water Pollution Microbiology, Vol. 2, pp. 71-109. Wiley Interscience, New York, N.Y. USA.

Harremoës, P. (1978B). Discussion to Watanabe Y. and Ishiguro M. (see below).

Harremoës, P., Jansen, J. la Cour, Kristensen, G.H. (1980). Practical Problems Related to Nitrogen Bubble Formation in Fixed Film Reactors. Progress in Water Technology. Vol. 12, (6), 253-269.

Hoehn, R. C., Ray, A. D. (1973). Effects of Thickness on Bacterial Film. Water Pollution Control Federation. Journal. Vol. 45, 2302-2320.

Jansen, J. la Cour (1983). Fixed Film Kinetics - Kinetics of Soluble Substrates. Department of Sanitary Engineering, Technical University of Denmark, Lyngby. PhD-thesis, (Rep. 81-35.).
Kornegay, B. H., Andrews, J. F. (1969). Characteristics and Kinetics of Biological Fixed Film Reactors. Department of Environmental System Engineering, Clemson University, South Carolina, USA.
Kristensen, G. H., Jansen, J. la Cour (1980). Fixed Film Kinetics - Description of Laboratory Equipment. Department of Sanitary Engineering, Technical University of Denmark, Lyngby. (Rep. 80-58).
Kristensen, G. H., Christensen, F. R. (1982). Application of Cryo-cut Method for Measurements of Bio-film Thickness. Water Research. Vol. 16, 1619-1621.
La Motta, E. J. (1974). Evaluation of Diffusional Resistances in Substrate Utilisation by Biological Films. Ph.D. Thesis, University of North Carolina, Chapel Hill, N.C., USA.
La Motta, E. J. (1976A). Internal Diffusion and Reaction in Biological Films. Environmental Science and Technology. Vol. 10, 765-769.
La Motta, E. J. (1976B). Kinetics of Growth and Substrate Uptake in a Biological Film System. Applied and Environmental Microbiology. Vol. 31, (2), 286-293.
Landolt, H., Börnstein, R. (1969). Zahlenwerte und Funktionen. Band II. Teil 5. Bandteil A, 6. Auflage. Springer Verlag, Berlin-Heidelberg, Germany.
Onuma M., Omura T. (1982). Mass-Transfer Characteristics within Microbial Systems, Water Science Technology. Vol. 14, 553-568.
Perry J. (1963). Chemical Engineer's Handbook. 4th Edition. McGraw-Hill, N.Y., USA.
Riemer, M., Harremoës, P. (1978). Multi-Component Diffusion in Dentrifying Biofilms. Progress in Water Technology. Vol. 10, (5/6), 149-165.
Taylor, G. I. (1923). Stability of a Viscous Liquid Contained between Two Rotating Cylinders. Royal Society of London. Philosophical Transactions, A. Vol. 223, 289-343.
Watanabe, Y., Ishiguro, M. (1978). Denitrification Kinetics in a Submerged Rotating Biological Disc Unit. Progress in Water Technology, Vol. 10, (5/6), 187-195.
Williamson, K., McCarty, P. L. (1976A). A Model of Substrate Utilization by Bacterial Films. Water Pollution Control Federation. Journal. Vol. 48, 9-24.
Williamson, K., McCarty, P. L. (1976B). Verification Studies of the Biofilm Model for Bacterial Substrate Utilization. Water Pollution Control Federation. Journal. Vol. 48, 281-296.

Wat. Sci. Tech. Vol.17, Amsterdam, pp.15-26.
Printed in Great Britain.

0273-1223/85 $0.00 + .50

INFLUENCE OF PARTICULATE ORGANICS ON THE REMOVAL OF DISSOLVED ORGANICS IN FIXED-FILM BIOLOGICAL REACTORS

E. Särner* and S. Marklund**

*Dept. of Environ. Eng., Lund Univ., 220 07 Lund, Sweden
**Dept. of Environ. Eng., Luleå Univ., 951 87 Luleå, Sweden

ABSTRACT

Very little is known about the interaction between dissolved and particulate organics in the fixed-film biological process used for wastewater purification, although this process has been used for many decades. The mechanisms for the removal of dissolved and particulate organics differ and it has been found that a large fraction of the organics in most wastewaters exists in particulate form.

In the experiments described here, the influence of particulate organics on the removal of glucose was studied in laboratory-scale fixed-film reactors. The particles used were starch particles and particles obtained from digested sewage sludge. The result of the experiments showed that for high glucose concentrations and high temperatures the removal of glucose was reduced when particles were adsorbed on the biofilm surface. A dramatic reduction was observed when large amounts of particles were adsorbed. This effect has also been observed in a full-scale trickling filter plant and in pilot trickling filters. At low glucose concentrations and low temperatures, however, a slight increase in glucose removal was observed when organic particles were adsorbed on the biofilm surface.

KEYWORDS

Biological treatment; biological fixed-film; organic particles; dissolved organics; removal; interaction.

INTRODUCTION

Domestic wastewater and most industrial wastewaters are very complex and the organic matter occurs in both dissolved and particulate form (see e.g. Hunter and Heukelekian, 1965). This is of importance, since the removal of dissolved substances differs from the removal

of particles in biological purification processes. In a fixed-film biological process the dissolved organics are transported into the biofilm by diffusion and the reactions take place inside the biofilm. Particulate organics are adsorbed on the biofilm surface and have to be hydrolyzed in order to make a transport into the biofilm possible.

The adsorption of particles to the microorganisms in a wastewater purification process has been used for a long time in the contact stabilization process. The production of extracellular polymers plays a central role in the coagulation of particles as shown e.g. by Pavoni and co-workers (1972) and the production depends on the growth phase of the organisms. Beccari and co-workers (1980) showed that the production of extracellular polymers was a function of the sludge age in an activated sludge process. Takahashi and co-workers (1974) showed in laboratory activated sludge experiments that the composition of the substrate had a marked influence on the reaction rate. The presence of colloids reduced the adsorption activity but a recovery was obtained when the adsorbed particles were degraded. The time for the recovery depended on the particle size and the degradation was faster for small particles than for large, which also has been shown by Balmat (1957). Takahashi and co-workers (1974) also showed that the presence of particles had a positive effect on the removal of dissolved organics. It was shown that the activity of the dehydrogenases of the activated sludge was increased by the addition of suspended matter.

The total efficiency of a biological wastewater process depends on the removal of both dissolved and particulate organics. In most wastewater treatment plants dissolved organics can only be removed in the biological process. Particles can e.g. be removed by sedimentation or by chemical coagulation followed by sedimentation. Therefore, it is important that the removal of dissolved organics is efficient in the biological process.

The effect of organic particles on the removal of dissolved organics has not been studied in detail for fixed-film biological processes. It has been shown, however, that a high recirculation of particles from the sludge treatment facilities to the influent of a wastewater treatment plant has a negative effect on the removal of dissolved organics in the trickling filter process (Särner, 1980, 1981). It was also shown that the choice of pre-treatment method (sedimentation or straining) affects the removal of dissolved organics (measured on filtered samples). These findings were made on experiments with pilot trickling filters. Recent observations show, however, a strong negative effect of sludge recirculation on full-scale trickling filters (Andersson, 1983). A negative effect of organic particles has also been observed in a submerged biological filter (Rusten, 1983).

It is obvious that the knowledge of the influence of organic particles on the removal of dissolved organics in fixed-film biological processes is minor. Therefore, experiments were carried out at laboratory scale in order to study these phenomena in conditions where most of the disturbing factors appearing in full-scale plants could be eliminated.

EXPERIMENTAL EQUIPMENT

The reactors used were made of plexiglass. Each reactor consisted of a rotating drum enclosed in an outer cylinder (Fig. 1). The rotating speed could be varied. The total liquid volume in the reactor was 1.03 l. The total area available for biological growth was 1 920 cm^2 and the surfaces were sand-blasted in order to improve the biological attachment. The distance between the rotating drum and the outer cylinder was 1.2 cm. In order to obtain a completely mixed liquid phase a pump was used to recirculate the liquid from the outlet to the inlet side of the reactor.

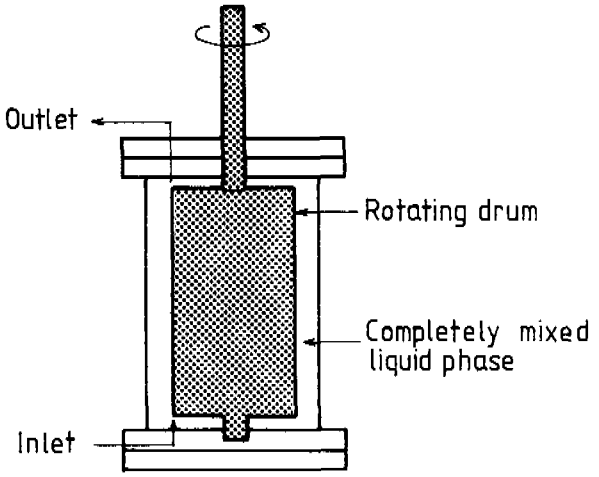

Fig. 1. Experimental reactor.

The total experimental system is schematically illustrated in Fig. 2. Tap water was passed through an activated carbon column in order to remove residual chlorine and further on to a temperature control device. A buffer solution was also added and air or oxygen was supplied in order to ensure a high concentration of dissolved oxygen in the water. The water was then pumped to the reactor. The substrate, which was stored in a refrigerator, was added to the water before it entered the reactor. Also the suspended particles were added to the flow before the reactor.

SUBSTRATE, PARTICLES AND ANALYTICAL METHODS

The same glucose-substrate and buffer solution as described by Kornegay and Andrews (1969) were used.

The major part of the experiments where particles were used was carried out with particles obtained from digested mechanical and biological sludge from a wastewater treatment plant treating domestic wastewater. The sludge was strained before use in order to avoid mechanical clogging in the reactor. The sludge was suspended in

distilled water before use. For some experiments spherical starch particles were used. The particles were allowed to swell up in water before use and after this had diameters in the range of 8-22 μm with a mean diameter of about 13 μm. The starch particles were manufactured by Pharmacia AB in Uppsala, Sweden.

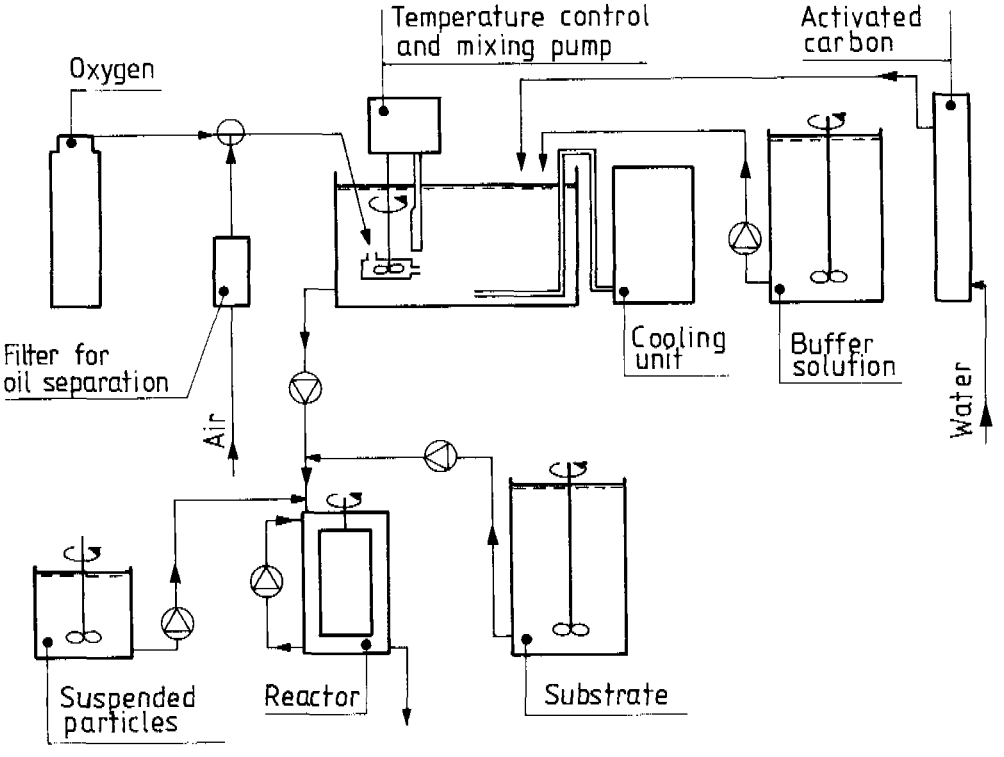

Fig. 2. Schematic presentation of the experimental equipment used.

The glucose concentration was measured by a spectrophotometer at the wavelength of 340 nm using a method described by Boehringer Mannheim Scandinavia AB (1982). The method was tested for several known concentrations and showed good accuracy. The samples were filtered before measuring the concentration of glucose. The same filter paper as used for measuring the concentration of particles was used, which was a filter paper (Sartorius-Membranfilter GmbH, Typ 11310) with a pore size of 0.05 μm.

In order to examine if a possible hydrolysis of the starch particles in the reactor resulted in a leakage of glucose into the bulk liquid ^{14}C-labelled glucose was used in four experiments. No such leak could be observed, which is in agreement with the findings of Takahashi and co-workers (1974) for an activated sludge process.

OPERATIONAL PROCEDURES

Before the reactor was fed with the glucose solution it was stored in an aeration basin at a wastewater treatment plant treating domestic wastewater for at least three days. After this the reactor was placed in the laboratory and the biofilm was allowed to acclimatize to the glucose substrate for at least five days before experiments were carried out. Normally, however, the reactor was fed with the glucose substrate for several weeks before the experiments started.

Introductory experiments showed that a reasonable fit to the complete mix situation was obtained at an inlet flow of 8.28 l/h and a recirculation flow of 54 l/h. All experiments were therefore performed at these flows. Investigation of the influence of the rotation speed showed that no increase in glucose removal was achieved at rotation speeds above 150 rpm, which is in agreement with results obtained by Kornegay and Andrews (1969) and LaMotta (1976a). Thus, in order to avoid high diffusional resistance in the liquid film outside the biofilm all experiments described here were carried out at 150 rpm.

In some initial experiments extreme glucose concentrations were used. Even at these high glucose loads an oxygen concentration of at least 1 mg/l could be maintained in the liquid phase in the reactor. In the experiments described here far lower glucose concentrations were used, which resulted in higher oxygen concentrations in the reactor. Kornegay and Andrews (1969) found that oxygen concentrations down to 2.5 mg/l had no negative effect on the glucose removal. They even conducted some tests where the oxygen concentration was below 0.5 mg/l and no adverse effect could be observed on the glucose removal.

Prior to any experiments measurements were made to ensure that steady-state conditions were achieved. No samples were taken within a period of three times the nominal retention time when changes were made that should result in a lower glucose removal (Kristensen and la Cour Jansen, 1980) except when particles were added. If changes were made that should result in an increased removal no samples were taken until 120 minutes had passed after the change. When a large increase in reduction was expected because of a change of e.g. the temperature no experiments were carried out in the next 12 hours. After the adding of particles samples were taken during a period of at least 9 times the nominal retention time. All samples were taken as grab samples.

RESULTS AND DISCUSSIONS

Removal of Dissolved Substrate

In order to get a background for the experiments with glucose and particles a number of tests were made with glucose only at different temperatures. Two rotation speeds were used - 25 and 150 rpm - but only the results from the latter will be discussed here, since all experiments with particles were carried out at 150 rpm. The theory for the removal of dissolved substrates in fixed-film biological processes will not be discussed here either. A literature review of this has been given by Harremoës (1978).

The removal of glucose could be described by the equation

$$r_a = k \cdot \theta^{T-20} \cdot C^d \qquad (1)$$

where

r_a = glucose removal rate per unit biofilm surface ($mg/(cm^2 \cdot h)$)

k = constant

θ = constant, reflecting the influence of the temperature

T = temperature (°C)

C = glucose concentration in the reactor (mg/l)

d = constant

By multiple regression analysis the following equation was obtained:

$$r_a = 0.0145 \cdot 1.037^{T-20} \cdot C^{0.650} \qquad (2)$$

The correlation coefficient was 0.89. A t-test showed that the values of θ and d were significantly different from 1 and 0 respectively at the level 0.0005. The standard deviation of the value of θ was 0.005 and of d 0.038.

From equation (2) it can be seen that the removal cannot be described as a first or zero order reaction. A partially substrate-penetrated biofilm will for a true zero order reaction give d = 0.5 (LaMotta, 1976b and Harremoës, 1978). The reaction can, however, be described as a saturation-dependent reaction using the empirical relationship according to Monod or the expression for an enzymatic phenomenon according to Michaelis-Menten. This was done e.g. by Kornegay and Andrews (1969). The saturation constant would in this case be in the order of 400 mg/l, which is far above the values reported in the literature (Harremoës, 1978). A possible explanation to the value of d is that the removal rate was influenced by the diffusional resistance in the biofilm as well as by a metabolic saturation-dependent reaction according to Michaelis-Menten. Furthermore, the removal was probably influenced by the flux of oxygen into the biofilm (see below).

Influence of Particulate Organics on the Removal of Dissolved Organics

Before particles were added to the influent to the reactor, samples were taken from the influent and effluent during a period of at least 2 hours to make sure that steady-state conditions prevailed. After the addition of particles samples were taken for at least 90 minutes. The experimental conditions during the different tests are shown in Table 1. During three tests a coagulant was added to the influent: $FeCl_3$, $MgCl_2$ and a polymer (Zetag 57 from AB CMD,Sweden) were used. This was done in an attempt to improve the adsorption

of the particles to the biofilm surface, which was low for several tests. No effect of the coagulant dose could, however, be seen.

The glucose concentrations for each test were arranged as shown in Fig. 3. The difference between the mean glucose removal before and after the addition of particles was compared by using a t-test procedure. With unknown standard deviations for the different series

TABLE 1 Experimental Conditions during the Tests with Addition of Particles

Test number	Temp.	Influent glucose conc.	Particles Type	Particles Conc.	Particles Load	Sampling period after addition of particles	Coagulant used Type	Coagulant used Conc.
	°C	mg/l		mg/l	mg/(m² min)	min		mg/l
1	15.4	536	Sludge	729	633	95		-
2	15.2	384	Sludge	693	524	150		-
3	15.2	470	Starch	759	546	150		-
4	16.2	668	Sludge	640	460	120		-
5	16.2	141	Sludge	502	361	120		-
6	20.0	151	Sludge	446	321	120		-
7	20.0	159	Starch	918	660	116		-
8	20.0	532	Sludge	668	480	120		-
9	10.5	159	Sludge	610	438	115		-
10	9.5	638	Sludge	421	303	120		-
11	5.7	127	Sludge	405	291	120		-
12	6.0	141	Sludge	483	347	90		-
13	11.4	184	Sludge	614	442	115	$FeCl_3$	30.8
14	10.6	188	Sludge	930	668	110	Z 57[3]	0.98
15	10.6	33	Sludge	530	381	120		-
16	11.5	24	Sludge	598	430	110		-
17	8.7	196	Sludge	596	428	100	$MgCl_2$	0.72

of data, the following procedure was carried out: The mean influent concentration during the experiment was $u_1 = (1/(k+n)) \cdot \sum_{1}^{k+n} x$. The mean effluent concentration before and after the addition of particles was $u_2 = (1/k) \cdot \sum_{1}^{k} y$ and $u_3 = (1/n) \cdot \sum_{k+1}^{k+n} y$ respectively. The mean difference between the influent and effluent concentrations before and after the addition of particles was $\Delta_1 = u_1 - u_2$ and $\Delta_2 = u_1 - u_3$ respectively. Calculating the difference between the influent and effluent concentrations before the adding of particles for each pair of samples, $a_1 = x_1 - y_1$, ... $a_k = x_k - y_k$, and assuming normal distribution,

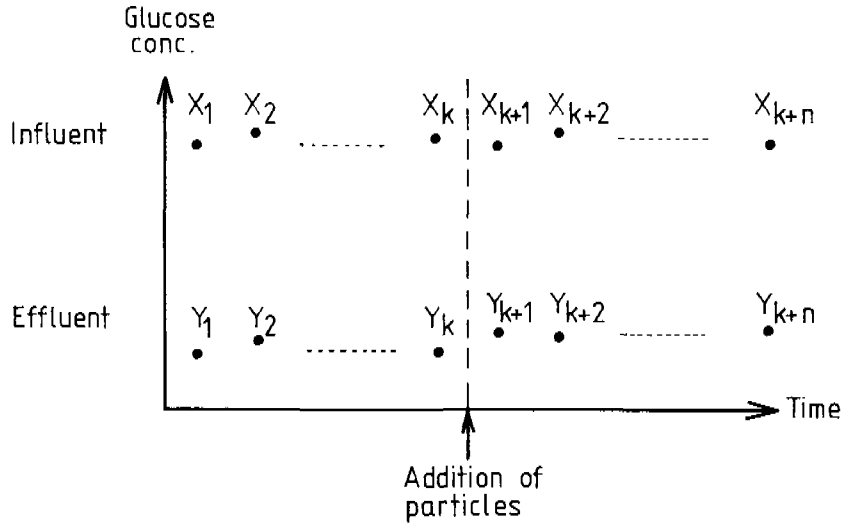

Fig. 3. Arrangement of the data from a test for statistical analysis.

i.e. $N(\Delta_1, \sigma_1)$ where σ_1 is the unknown standard deviation, the mean difference $\bar{a} = (1/k) \cdot \sum_1^k a$ will be normally distributed, $N(\Delta_1, \sigma_1/k^{1/2})$. After the addition of particles the following is obtained in a similar way:

$$b_1 = x_{k+1} - y_{k+1}, \ldots\ldots b_n = x_{k+n} - y_{k+n} \qquad N(\Delta_2, \sigma_2)$$

$$\bar{b} = (1/n) \cdot \sum_{k+1}^{n} b \qquad N(\Delta_2, \sigma_2/n^{1/2})$$

If all observations are independent the function

$$\frac{\bar{a} - \bar{b}}{\left(\frac{s_1^2}{k} + \frac{s_2^2}{n}\right)^{1/2}}$$

where s_1 and s_2 are the variances for $\bar{a}$ and $\bar{b}$ respectively will approximately be t-distributed with M degrees of freedom. M is obtained from

$$M = \left(\frac{c^2}{k-1} + \frac{1-c^2}{n-1}\right)^{-1}$$

where

$$c = \frac{s_1^2}{k \cdot s_D^2}$$

and

$$s_D^2 = \frac{s_1^2}{k} + \frac{s_2^2}{n}$$

Thus, the significance of the difference $|\bar{a}-\bar{b}|$ can be evaluated in a t-test and expressed as an α-value, and the lower the value of α the larger will be the probability that the difference between $\bar{a}$ and $\bar{b}$ exists.

The results of the statistical analyses are shown in Table 2. The maximum particle adsorption on the biofilm surface is also given in the table. The adsorption was calculated from the difference in suspended solid concentration in the influent and effluent and was consequently slightly underestimated, since also all parts of the biofilm leaving the reactor were measured. The adsorption of particles on the biofilm varied in a wide range and there seemed to be no relationship between the adsorption and the temperature. No satisfactory explanation could be found to why adsorption occurred in some cases and not in others, although the highest adsorption was obtained in tests number 1-3 and 8 when rather a high glucose concentration was used. This was not the case in tests number 4 and 10, and quite a high adsorption was obtained in test number 17 at a lower glucose concentration. It was thus not possible to confirm a theory that a low load of glucose, resulting in a low growth rate, would give a high microorganism age and thereby a high production of coagulating extracellular polymers as shown e.g. by Pavoni and co-workers (1972) for the activated sludge process (see INTRODUCTION).

One of the intentions with the experiments was to study the influence of the temperature on the interaction between particulate and dissolved organics. This influence was partly overshadowed by the varying adsorption of particles on the biofilm surface, which could not be controlled. Tables 1 and 2 show, however, that a negative effect of a load of particles on the removal of glucose only occurred at the higher temperatures. A plausible explanation for this is that a high temperature gives a high removal rate of glucose and consequently a high demand for oxygen. Thus, any reduction of the oxygen concentration close to or on the biofilm surface would result in an oxygen shortage inside the biofilm. Adsorbed organic particles which have to be degraded in order to make a further transport into the biofilm possible will bring about a local oxygen consumption on the surface, resulting in a local oxygen deficit inside the biofilm. Thus, a local reduction in the removal rate of glucose will appear. The sensitivity of the organic particles that are adsorbed should therefore increase at increased temperature and increased glucose concentration. Only the result obtained in test number 8 would contradict this explanation.

TABLE 2 Result of the Statistical Analysis of the Influence of Particles on the Removal of Glucose

Test number	The load of particles influenced the removal of glucose at the following level (α)													Maximum particle adsorption on biofilm surface
	Positive influence							No influence	Negative influence					
	0.0005	0.001	0.005	0.01	0.025	0.05	0.1		0.1	0.05	0.025	0.01	0.005	0.001	0.0005	mg/m²
1														x		14 200
2														x		12 500
3												x				10 200
4												x				2 300
5									x							2 200
6								x								4 500
7						x										5 200
8								x								7 200
9								x								1 000
10								x								2 700
11					x											20
12				x												1 500
13				x												600
14			x													4 200
15					x											3 800
16								x								0
17	x															6 600

The explanation given above to the negative effect of organic particles on the removal of glucose is supported by theoretical calculations by Williamson and McCarty (1976). They assumed that the ratio between the diffusion coefficients for glucose and oxygen in water remained the same inside a biofilm. Based on this assumption they showed that an oxygen flux limitation will occur if the bulk liquid concentration ratio of oxygen:glucose is less than 0.11. For the experiments described in this paper the oxygen concentration in the bulk water was about 3 mg/l. An oxygen flux limitation would then occur at glucose concentrations greater than approximately 25-30 mg/l. From equation (2) it can be seen that the removal is affected by the

glucose concentration. Consequently, the removal was probably flux limited by the oxygen and substrate limited by the organisms.

In consequence with the discussion above no negative effect of a load of organic particles on the removal of glucose should appear at low temperatures, low glucose concentrations and low adsorption of particles. This was also the case for tests 9-17. In 6 of the 9 experiments carried out at low temperatures, however, an increased removal of glucose was observed when organic particles were adsorbed on the biofilm surface. This is in agreement with the results obtained by Takahashi and co-workers (1974) in a laboratory-scale activated sludge process. A hypothesis that the particles obtained from digested sludge - although stored anaerobically for about four weeks - consumed glucose in the aerobic reactor could not be confirmed. This possibility can, however, not be disregarded even if a slight positive influence on the removal of glucose was observed also when starch particles were used (test number 7).

The results obtained in these experiments show that the adsorption of organic particles on a biofilm surface can have a negative effect on the removal of dissolved organics, especially if the temperature is high, the concentration of dissolved organics is high, and large amounts of particles are adsorbed. These findings are supported by results obtained in pilot-scale trickling filters (Särner, 1980, 1981) as well as by results from full-scale trickling filters (Andersson, 1983) and submerged biological filters (Rusten, 1983) treating domestic wastewater. This will have practical consequences for the design and optimization of biological processes as well as for the pre-treatment methods used. So far, however, the effect of organic particles on the removal of dissolved organics can not be quantified and the effect of other parameters is not fully understood. Further research in this field is thus needed.

ACKNOWLEDGEMENT

The authors would like to express their gratitude to the Swedish Board of Technical Development which supported the project. Mrs. Eva Cassel and Miss Kerstin Nordqvist are deeply acknowledged for their skilful operation of the system and their performance of a large number of analyses.

REFERENCES

Andersson, B. (1983). Private communication.

Balmat, J. L. (1957). Biochemical oxidation of various particulate fractions of sewage. Sewage and Ind. Wastes, 29, 757-761.

Beccari, M., P. Mappelli, and V. Tandoi (1980). Relationship between bulking and physicochemical-biological properties of activated sludge. Biotechn. and Bioeng., XXII, 969-979.

Boehringer Mannheim Scandinavia AB (1982). Test Kombination Gluco-Quant. Stockholm.

Harremoës, P. (1978). In R. Mitchell (Ed.), Water Pollution Microbiology, Vol. 2. John Wiley and Sons, New York, Chapt. 4, pp. 71-109.

Hunter, J. V., and H. Heukelekian (1965). The composition of domestic fractions. J. Wat. Pollut. Control Fed., 37, 1142-1163.

Kornegay, B. H., and J. F. Andrews (1969). Characteristics and kinetics of biological fixed film reactors. Department of Environ. Systems Eng., Clemson University, Clemson.

Kristensen, G. H., and J. la Cour Jansen (1980). Fixed film kinetics; Description of laboratory equipment. Department of San. Eng., Techn. Univ. of Denmark, Lyngby.

LaMotta, E. J. (1976a). External mass transfer in a biological film reactor. Biotechnol. Bioeng., XVIII, 1359-1370.

LaMotta, E. J. (1976b). Internal diffusion and reaction in biological films. Envir. Sci. Technol, 10, 765-769.

Pavoni, J. L., M. W. Tenney, and W. F. Echelberger (1972). Bacterial exocellular polymers and biological flocculation. J. Water Pollut. Control Fed., 44, 415-431.

Rusten, B. (1983). Rensing av kommunalt avløpsvann i aerobe dykkede filtre. SINTEF-rapport SFT21 A83076. Norges Tekniske Høgskole, Trondheim.

Särner, E. (1980). Plastic-packed trickling filters. Ann Arbor Science Publishers Inc., Ann Arbor.

Särner, E. (1981). Removal of dissolved and particulate organic matter in high-rate trickling filters. Wat. Research, 15, 671-678.

Takahashi, S., T. Fujita, M. Kato, T. Saiki, and M. Maeda (1974). In S. H. Jenkins (Ed.), Advances in Wat. Pollut. Research, Pergamon Press, Oxford, pp. 341-359.

Williamson, K., and P. L. McCarty (1976). A model of substrate utilization by bacterial films. J. Water Pollut. Control Fed., 48, 9-24.

Wat. Sci. Tech. Vol.17, Amsterdam, pp.27-44.
Printed in Great Britain.

0273-1223/85 $0.00 + .50

COMPETITION IN BIOFILMS

O. Wanner and W. Gujer

Swiss Federal Institute for Water Resources and Water Pollution Control (EAWAG), 8600 Dubendorf, Switzerland

ABSTRACT

Based on a continuum approach to the biofilm problem and on mass balance equations, the competition of several microbial species for space and substrates is described. For the case of steady state and of autotrophic and heterotrophic organisms with given biological kinetics and a common nutrient (oxygen), the effect of relative substrate concentrations on biofilm performance and composition is discussed. The approach allows for a detailed analysis and for an adequate reproduction of experimental observations.

KEYWORDS

Biofilm, Nitrification, Species competition, Model, Biological kinetics, Heterotrophic growth, Substrate limitation.

NOMENCLATURE

A	area $[L^2]$
a	specific surface of trickling filter material $[L^{-1}]$
b	biomass endogenous decay rate $[t^{-1}]$
D	substrate diffusivity within film $[L^2t^{-1}]$
dz, dh	differential length in z and h direction $[L]$
f	volume fraction of microorganisms $[-]$
h	coordinate for trickling filter height $[L]$
j, jx	substrate and biomass flux $[ML^{-2}t^{-1}]$
jL, jxL	substrate and biomass flux at z = L $[ML^{-2}t^{-1}]$
K, K_O	substrate and oxygen saturation constant in Monod kinetics $[ML^{-3}]$
k	reaction rate constant for inactivation of biomass $[t^{-1}]$
L	thickness of biofilm $[L]$
ns,nx	number of substrates and of microbial species in biofilm $[-]$
R	process rate $[ML^{-3}t^{-1}]$
r	observed conversion rate $[ML^{-3}t^{-1}]$
S	substrate concentration $[ML^{-3}]$
SL	substrate concentration in bulk liquid $[ML^{-3}]$
t	time $[t]$
u	velocity of biomass movement relative to z = 0 $[Lt^{-1}]$

V	Volume $[L^3]$
v_h	hydraulic load of trickling filter cross sectional area $[Lt^{-1}]$
Y	biomass yield coefficient $[MM^{-1}]$
z	space coordinate in biofilm $[L]$
α	conversion factor for substrate to COD $[M_O M_S^{-1}]$
$\mu, \hat{\mu}$	specific and maximum specific growth rate $[t^{-1}]$
μ_o, $\hat{\mu}_o$, $\bar{\mu}_o$	observed, maximum observed and mean observed specific growth rate $[t^{-1}]$
$\bar{\bar{\mu}}_o$	mean of $\bar{\mu}_o$ over biofilm depth $[t^{-1}]$
ν	stoichiometric coefficient $[MM^{-1}]$
ρ	biomass density $[ML^{-3}]$
σ	substrate concentration $[ML^{-3}]$

Indices

i	compound, substrate, microbial species
j	*process*
A, H, I, O	These indices are consistently applied wherever a symbol relates to autotrophs, heterotrophs, inert biological material or dissolved oxygen, respectively.

INTRODUCTION

Mueller et al. (1978) report on the performance of a full scale six stage rotating biological contactor with soluble BOD_5 degradation and nitrification. Some of their experimental results are replotted in Fig. 1. These results clearly indicate that the relative activity of heterotrophic and autotrophic microorganisms varies significantly from the entrance to the exit of the reactor. Similar phenomena have been reported for other fixed film biological reactors involving more than one microbiological species (anaerobic filter, Young and Mc Carty 1968).

The goal of this paper is to establish a link between the processes which occur within the biofilm and the phenomena which have been observed from outside. However, the goal is not to quantitatively reproduce the observed phenomena, but rather to give some insight into the mechanisms which cause them. Equally the purpose is not to make numeric predictions with regard to the selected microbial species, substrates and kinetics. Mainly they serve as an example to illustrate the principal aspects of species competition in biofilms.

THEORETICAL RATIONAL

Distribution of Microbial Species and Substrates

The discussion of the spatial distribution of several microbial species in a biofilm necessitates a simplifying description of naturally occurring systems. We assume a biofilm with gradients only perpendicular to the supporting media and composed of different microbial species that may be expressed as a continuum. The densities of the different species are assumed to be constant. At steady state biofilm thickness is kept constant due to an equilibrium of biomass net production and shear loss at the surface.

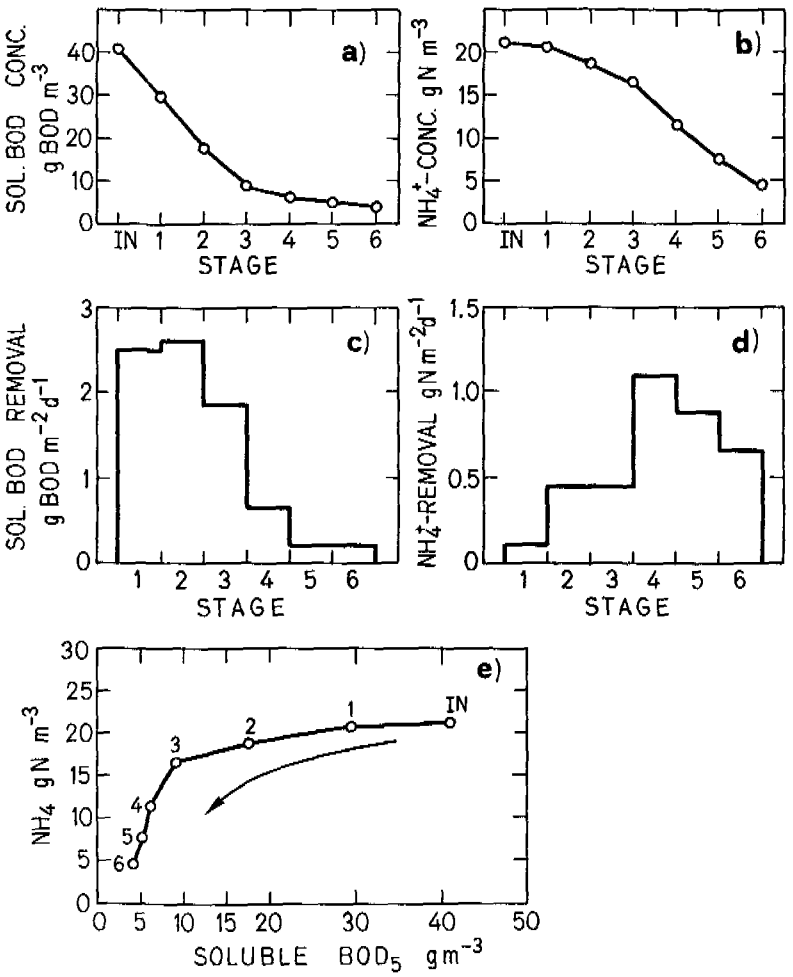

FIG. 1 Experimental results obtained from a nitrifying rotating biological contactor operated with six stages in series. IN indicates influent. Data from Mueller et al. (1978), data set 2, 15.4°C, $O_2 \leq 4.0$ mgO_2/l, hydraulic load over entire reactor = 0.036 $m^3m^{-2}d^{-1}$ of surface area.

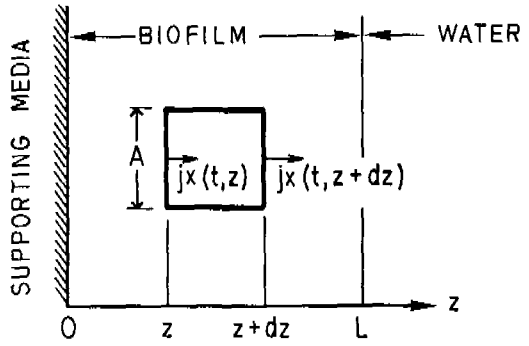

FIG. 2

Biomass flux through a differential element of the biofilm.

With these assumptions a mass balance for a single species i may be written for a differential volume element Adz of the biofilm, as shown in Fig. 2,

$$Adz\rho_i\frac{\partial f_i(t,z)}{\partial t} = Adz\mu o_i(t,z)\rho_i f_i(t,z) + Ajx_i(t,z) - Ajx_i(t,z+dz) ,$$

where ρ_i is the density, f_i the volume fraction, μo_i the observed specific growth rate and jx_i the flux of species i through area A. Division by $Adz\rho_i$ yields

$$\frac{\partial f_i(t,z)}{\partial t} = \mu o_i(t,z)f_i(t,z) - \frac{1}{\rho_i}\frac{jx_i(t,z+dz) - jx_i(t,z)}{dz} ,$$

which for $dz \to 0$ leads to

$$\frac{\partial f_i(t,z)}{\partial t} = \mu o_i(t,z)f_i(t,z) - \frac{1}{\rho_i}\frac{\partial jx_i(t,z)}{\partial z} . \qquad (1)$$

With the flux expressed by the velocity u at which the biomass moves in respect to the support media and by the concentration $\rho_i f_i$ of the microorganisms

$$jx_i = u\rho_i f_i \qquad (2)$$

and with the average net or observed specific biomass growth rate

$$\bar{\mu}o = \frac{\partial u}{\partial z} , \qquad (3)$$

which is derived in appendix A, the substitution of

$$\frac{1}{\rho_i}\frac{\partial jx_i}{\partial z} = \frac{\partial}{\partial z}\frac{jx_i}{\rho_i} = \frac{\partial}{\partial z}uf_i = f_i\frac{\partial u}{\partial z} + u\frac{\partial f_i}{\partial z} = \bar{\mu}of_i + u\frac{\partial f_i}{\partial z}$$

in eqn. (1) provides

$$\frac{\partial f_i}{\partial t} = (\mu o_i - \bar{\mu}o)f_i - u\frac{\partial f_i}{\partial z} .$$

This equation, together with the well known equation for the substrates S_i

$$\frac{\partial S_i(t,z)}{\partial t} = - \frac{\partial j_i(t,z)}{\partial z} + r_i(t,z) ,$$

where according to Fick's 1. law

$$j_i(t,z) = - D_i\frac{\partial S_i(t,z)}{\partial z}$$

and where D_i is the substrate diffusivity and r_i is the volumetric reaction rate, written for steady state, describes the spatial distribution of the nx microbial species and ns substrates in the film:

$$(\mu o_i(z) - \bar{\mu}o(z))f_i(z) - u(z)\frac{df_i(z)}{dz} = 0 \quad , \quad i = 1,..,nx \qquad (4)$$

$$\frac{d}{dz}(D_i\frac{dS_i(z)}{dz}) + r_i(z) = 0 \quad , \quad i = 1,..,ns \qquad (5)$$

The solution of eqns. (4) and (5) with the intrinsic no-flux boundary condition for the substrates $j_i(0)=0$ and for given substrate concentrations at the film-water interface

$$S_i(L) = SL_i \tag{6}$$

and $$\mu o_i(0) = \bar{\mu}o(0) \quad \text{or} \quad f_i(0) = 0 \ , \tag{7}$$

has to be done numerically and is outlined in appendix B. The condition (7) originates from

$$u(0) = 0 \ , \tag{8}$$

due to eqn. (2) and the no-flux boundary condition at the film-media interface

$$jx_i(0) = 0 \ , \tag{9}$$

which, together with eqn. (4), leads to the finding that for steady state either the specific growth rate $\mu o_i(0)$ of a species i is equal to $\bar{\mu}o(0)$ or the species cannot exist in the film ($f_i = 0$).

Kinetics of Microbial Reactions

The biological kinetics chosen for this publication are representative for two organisms that compete for a common nutrient but differ significantly in relative growth kinetics. The parameter values chosen allow for a principal discussion of the predicted phenomena with regard to the behaviour of such organisms in a biofilm, however quantitative predictions are not the goal of this paper.

The following processes are considered:
1. Growth of obligate aerobic heterotrophic organisms, with dissolved organics (acetate) as their electron donor.
2. Endogenous aerobic respiration of heterotrophic organisms.
3. Conversion of active heterotrophic biomass to inert solid material independent of oxygen.
4. Growth of obligate aerobic autotrophic organisms with ammonium as their electron donor and, for simplicity, nitrate as the product of nitrogen oxidation (nitrification).
5. Endogenous aerobic respiration of autotrophic organisms.
6. Conversion of active autotrophic biomass to inert solid material independent of oxygen.

No anaerobic processes such as denitrification are considered. There are only very few situations where these would be significant. For simplicity the nitrogen content of biomass is neglected. All compounds of interest are expressed in terms of either COD (heterotrophic, autotrophic and inert biofilm mass, dissolved organics, oxygen = negative COD) or nitrogen (NH_4^+-N).

Double Monod kinetics with substrate and oxygen limitation are used for the process of growth. This is done to a priori avoid negative concentration values and is not meant to be of microbiological significance. Endogenous respiration is described with Monod type dependence on oxygen. Inactivation stands for processes such as death, anaerobic endogenous processes, production of an inert residue etc. and is modeled by first order kinetics.

Table 1 summarizes in matrix notation the stoichiometric coefficients ν and rate laws used.

TABLE 1 Stoichiometry and rate laws for microbial processes

PROCESSES j	COMPOUNDS i: BIOMASS HET	BIOMASS AUT	BIOMASS INERT	SUBSTRATE AND PRODUCTS ORGANICS	NH_4^+-N	NO_3^--N	O_2	PROCESS RATE VECTOR R_j
HETEROTROPHIC								
1. GROWTH	+1			$\frac{-1}{Y_H}$			$-\frac{\alpha_H - Y_H}{Y_H}$	$\hat{\mu}_H f_{H\rho H} \frac{S_H}{K_H+S_H} \frac{S_O}{K_{OH}+S_O}$
2. ENDOGENOUS RESP:	-1						-1	$b_H f_{H\rho H} \frac{S_O}{K_{OH}+S_O}$
3. INACTIVATION	-1		+1					$k_H f_{H\rho H}$
AUTOTROPHIC								
4. GROWTH		+1			$\frac{-1}{Y_A}$	$\frac{+1}{Y_A}$	$-\frac{\alpha_A - Y_A}{Y_A}$	$\hat{\mu}_A f_{A\rho A} \frac{S_A}{K_A+S_A} \frac{S_O}{K_{OA}+S_O}$
5. ENDOGENOUS RESP:		-1					-1	$b_A f_{A\rho A} \frac{S_O}{K_{OA}+S_O}$
6. INACTIVATION		-1	+1					$k_A f_{A\rho A}$
OBSERVED CONVERSION RATES	$\mu_{oi} = \frac{\sum_j R_j \nu_{ij}}{f_i \rho_i}$			$r_i = \sum_j R_j \nu_{ij}$				

The maximum observed growth rate is, based on the rate expressions in table 1:

$$\hat{\mu}_o = \hat{\mu} - b - k$$

Table 2 summarizes the values of kinetic and stoichiometric coefficients used in this paper. All these values are typical in magnitude for organism growth at 20°C. Depending on the structure of the kinetic expressions, $\mu_{oi}(0)$ is not necessarily a unique function of the substrate concentrations in the bulk liquid. Therefore K_{Oi} and k_i were specifically chosen as

$$K_{OH} = K_{OA} \qquad \text{and} \qquad k_H = k_A$$

in order to exclude multiple solutions. The theoretical basis for this choice will be discussed elsewhere.

TABLE 2 Parameters for biological kinetics

		Heterotrophs		Autotrophs	
Maximum growth rate	$\hat{\mu}$	4.8	d^{-1}	0.95	d^{-1}
Substrate saturation const.	K	5	$gCODm^{-3}$	1	gNm^{-3}
Oxygen saturation const.	K_O	0.1	gO_2m^{-3}	0.1	gO_2m^{-3}
Biomass yield	Y	0.4	$gCOD_Hg^{-1}COD_S$	0.22	$gCOD_Ag^{-1}N$
Endogenous rate const.	b	0.2	d^{-1}	0.05	d^{-1}
Inactivation rate const.	k	0.1	d^{-1}	0.1	d^{-1}
Conversion factor	α	1	$gO_2g^{-1}COD$	4.57	$gO_2g^{-1}NH_4$-N

The specific densities of the different biological species were chosen equal to

$$\rho = \rho_H = \rho_A = \rho_I = 5000 \text{ gCODm}^{-3}$$

and the biofilm thickness equal to

$$L = 500 \text{ } \mu\text{m}.$$

Diffusion coefficients for dissolved organic material (acetate), ammonium and oxygen were chosen to be 80 % of the respective values in pure water at 20°C (Table 3). All electrostatic effects on ion diffusion are neglected, as are masstransfer resistances at the film water interface.

TABLE 3 Substrate diffusion coefficients within biofilm (80 % of value in water)

COD (acetate)	D_H	$83 \cdot 10^{-6} m^2 d^{-1}$
NH_4^+	D_A	$149 \cdot 10^{-6} m^2 d^{-1}$
O_2	D_O	$175 \cdot 10^{-6} m^2 d^{-1}$

Substrate Concentration in a Trickling Filter

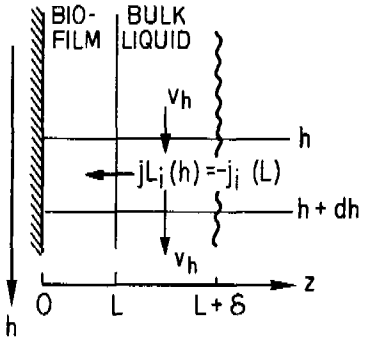

FIG. 3

Differential element of trickling filter height.

In a trickling filter pollutant concentrations SL_A and SL_H decrease with increasing depth. Neglecting external masstransfer resistance, the concentration profiles may be predicted based on a pollutant (substrate) mass balance around a differential element of trickling filter height (Fig. 3):

$$\delta a dh \frac{\partial SL_i}{\partial t} = v_h(SL_i(h) - SL_i(h+dh)) - adhjL_i(h) \ .$$

For steady state and $dh \to 0$ we obtain:

$$\frac{dSL_H}{dh} = -\frac{a}{v_h} jL_H \quad \text{and} \quad \frac{dSL_A}{dh} = -\frac{a}{v_h} jL_A \ . \tag{10}$$

Solution of eqns. (10) would yield a result as indicated in Fig. 1a,b.

Elimination of h from eqns. (10) leads to

$$\frac{dSL_A}{dSL_H} = \frac{jL_A}{jL_H} . \tag{11}$$

Solution of eqn. (11) yields a relative pollutant trajectory as indicated in Fig. 1e.
Separation of variables in eqns. (10) and integration along a trajectory yields:

$$\int_{SL_i(0)}^{SL_i(h)} \frac{d\sigma}{jL_i(\sigma)} = \frac{a}{v_h} h \tag{12}$$

Solution of eqn. (12) allows the prediction of the change of a pollutant concentration with increasing depth of the trickling filter. By this procedure equidistant points on the trajectory may be predicted as indicated by the marks for every stage in Fig. 1e.

RESULTS AND DISCUSSION

All results will be presented for biofilms at steady state only. Several reasons lead to this restriction:

a) Only at steady state there is a unique solution of the biofilm problem for a given substrate situation and for a biofilm in which both active organisms are allowed to develop.
b) Substrate concentration profiles over the depth of a biofilm respond very fast to a change of external conditions.
c) The major portion of the adaption of an established species distribution to new external conditions occurs within a few days. Changes always tend in the direction of the new steady state.
d) With time as an additional variable the biofilm history becomes important and it is not possible to establish a direct relation between external conditions and biofilm performance any more.

Using the presented mathematical description of a biofilm and the chosen biokinetics it is possible to predict for any pair of substrate concentrations in the liquid phase SL_A, SL_H and $SL_O = 8.0\ gO_2m^{-3}$ (constant for all calculations) a specific steady state biofilm. The properties of such biofilms will now be discussed. An attempt to fit experimental data is not made in this paper.

Coexistence of Microbial Species in the Biofilm

The criterion for the coexistence of different microbial species in the biofilm is given by eqn. (7) as

$$\mu o_i(0) = \bar{\mu}o(0).$$

Because inert biological material is always produced when viable microorganisms are present, all biofilms contain inert material, which is only produced, but not consumed. This means that $\mu o_I(0)$, and according to eqn. (7) also $\bar{\mu}o(0)$ and $\mu o_i(0)$ of any other microbial species present in the film, can never be negative.

Since three species compete for space within the biofilm, the mechanism which decides on the relative abundance of any single species is of interest: If $\mu o_i(0) > \mu o_{ii}(0)$ species i would expand relative to species ii and consume more substrate. Increased substrate utilization by species i would decrease $S_i(0)$ and thereby also $\mu o_i(0)$. This negative feedback mechanism would be active either until the two species are in equilibrium and $\mu o_i(0) = \mu o_{ii}(0)$ or until species ii is completely displaced by species i with $\mu o_i(0) > \mu o_{ii}(L)$. The same reasoning is applied to the opposite case or for more than two species.

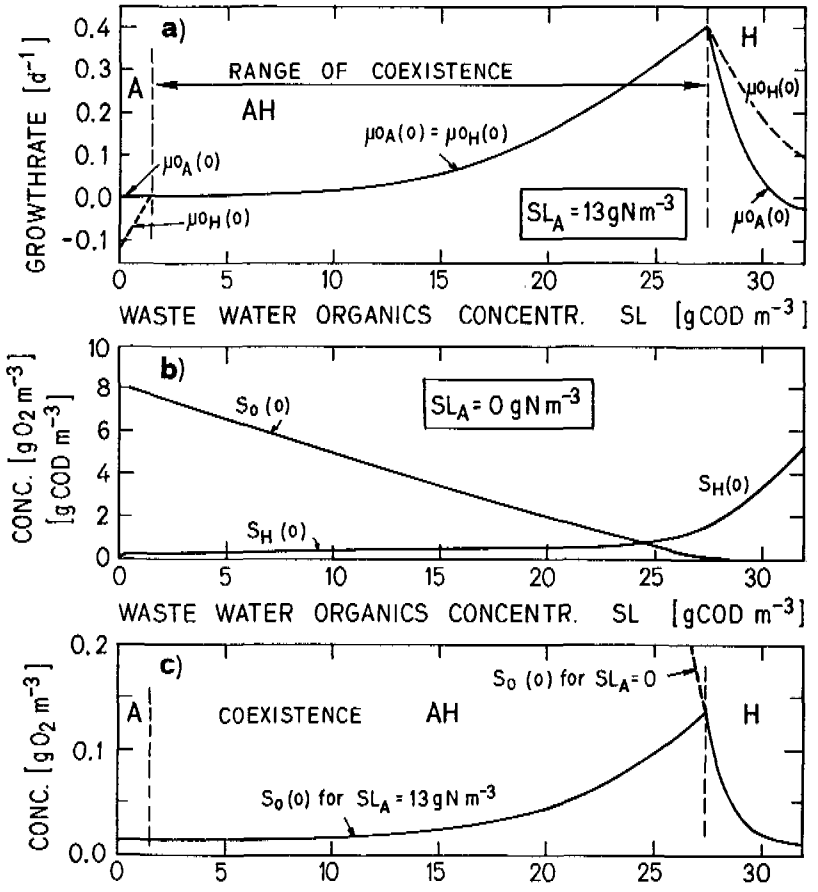

FIG. 4 Conditions at the support media in biofilms at steady state as a function of variable conditions in the bulk liquid.
a) SL_A = 13 gNm^{-3}, b) SL_A = 0 gNm^{-3}, c) SL_A = 13 gNm^{-3} and variable

Fig. 4a shows the dependence of $\mu o_H(0)$ and $\mu o_A(0)$ on SL_H for constant SL_A = 13 gNm^{-3}. For $SL_H \leq 1.35$ $gCODm^{-3}$ $\mu o_H(0)$ is negative because here the low prevailing oxygen concentration $S_O(0) = 0.014$ gO_2m^{-3} does not allow heterotrophic microorganisms to compensate for decay processes by growth. Coexistence is not possible and purely autotrophic biofilms are obtained.

For 1.35 $gCODm^{-3} \leq SL_H \leq 27.4\ gCODm^{-3}$ $\mu o_H(0) = \mu o_A(0) = \mu o_I(0) = \bar{\mu}o(0)$. This allows coexistence of heterotrophic and autotrophic organisms within the film. With increasing SL_H the model predicts a continuous increase of $\mu o_H(0)$ and a shift from mainly autotrophic to mainly heterotrophic biofilms. Above $SL_H = 27.4\ gCODm^{-3}$ even the purely heterotrophic biofilm becomes oxygen limited as indicated by a sudden increase of $S_H(0)$ (Fig. 4b). This point can be predicted by the ratio proposed by Frank and Kamenezkii (1969) if endogenous respiration is neglected:

$$\frac{SL_0\ D_0}{SL_H\ (1-Y_H)D_H} = 1.$$

Since autotrophic activity with $S_A(0)/K_A+S_A(0) = 0.93$ is very close to saturation, but heterotrophic activity with $S_H(0)/K_H+S_H(0) = 0.22$ is not, the rapid increase of $S_H(0)$ above $SL_H = 27.4\ gCODm^{-3}$ results in a rapid deviation of $\mu o_H(0)$ from $\mu o_A(0)$. Coexistence of the two species therefore is not possible in this region any more and purely heterotrophic biofilms are obtained.

Applying the same logic for different values of SL_A allows the prediction of the boundaries between three regions of possible biofilms (Fig. 5):

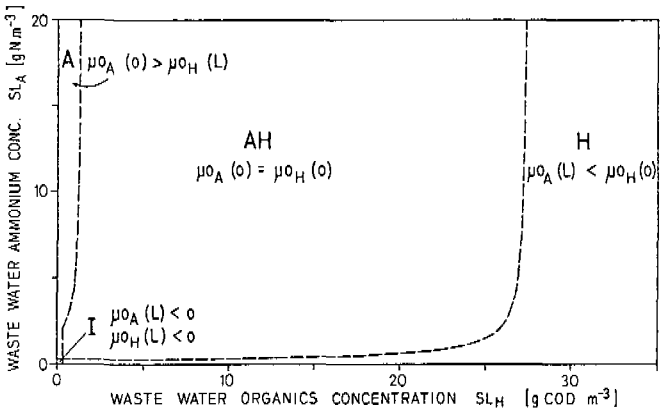

FIG. 5 Growth rate conditions for regions of purely autotrophic (A), purely heterotrophic (H) and mixed (AH) steady state biofilms and of inactive biological material (I).

Region A allows the development of autotrophic organisms only. Region AH allows coexistence of both types of viable organisms. Region H allows the development of heterotrophic organisms only. A fourth, very small region I, is defined by

$$\mu o_A(L) \leq 0 \quad \text{and} \quad \mu o_H(L) \leq 0.$$

Biofilms in region I contain inert material only and are not necessarily 500 μm thick.

Biofilm Performance

Since the ammonium and the organics concentration in the bulk liquid SL_A, SL_H are the variables which are used to discuss biofilm behaviour, it is convenient to present the predicted biofilm performance jL_A, jL_H in the SL_A-SL_H-diagram already used for Fig. 5.

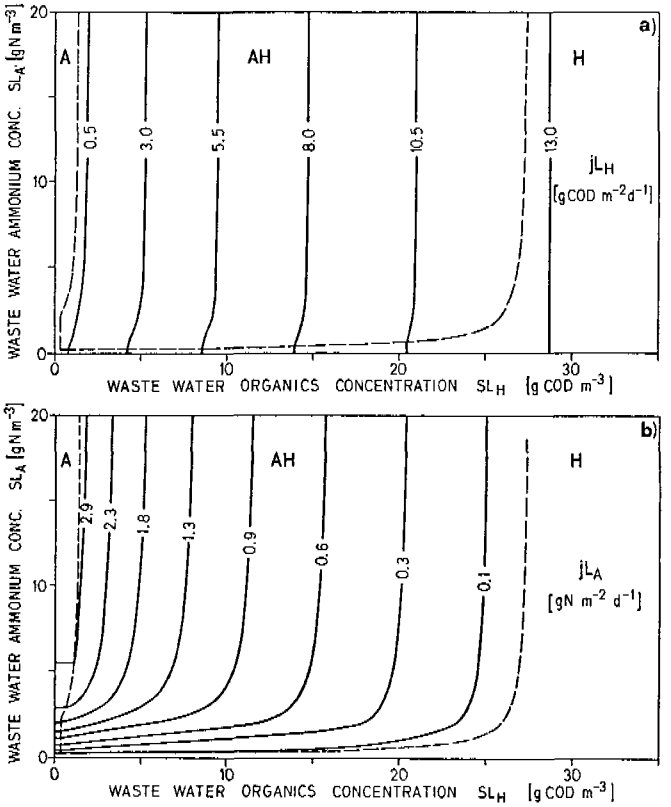

FIG. 6 Steady state substrate flux jL into the biofilm expressed as a function of waste water substrate concentrations.
a) heterotrophic activity jL_H, b) autotrophic activity jL_A.

Fig. 6a shows the heterotrophic activity jL_H as a function of substrate concentrations. The bases for Fig. 6a are the predicted values of jL_H for many pairs of substrate concentrations. Points with equal predicted performance are interconnected. Fig. 6b is identical to Fig. 6a but shows autotrophic activity jL_A.

Heterotrophic activity is barely affected by the presence of autotrophic organisms, which is illustrated by the nearly vertical lines which connect biofilms with equal heterotrophic activity jL_H. The reason for this prediction will be discussed later. Autotrophic activity depends strongly on both organic and nitrogen substrate concentration in the waste water.

In region A $jL_H = 0$ and jL_A is independent of organics concentration. The

boundary between region A and AH is identical with the line which connects biofilms where $_jL_H$ reaches zero. Symmetrical arguments can be applied for region H where $_jL_A = 0$ and to the boundary between region AH and H.

Fig. 6 once calibrated for a particular waste water, might, in combination with pollutant trajectories calculated for a particular reactor configuration, in the future be used as a basis for reactor design.

Prediction of Substrate Concentrations in Trickling Filters

On the basis of Fig. 6a,b it is possible to use eqn. (11) to predict pollutant trajectories in a trickling filter for different starting conditions as shown in Fig. 7. If eqn. (12) is solved along the trajectories it is possible to mark equidistant points over the depth of a trickling filter (constant increments of ah/v_h).

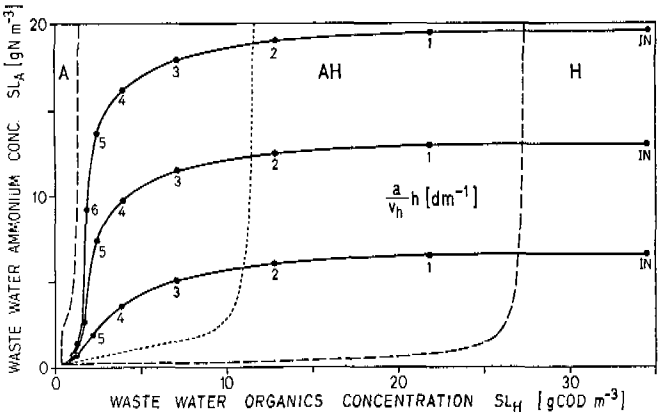

FIG. 7 Substrate trajectories for different inlet (IN) conditions into a trickling filter. Full circles indicate equidistant points along trickling filter depth. Dashed line indicates biofilms with equal oxygen consumption by heterotrophic and autotrophic activity.

Above SL_H = 10 gCODm^{-3} trajectories are close to horizontal, indicating that heterotrophic activity ($_jL_H$) dominates over autotrophic activity ($_jL_A$), whereas the inverse is valid for $SL_H \leq 3$ gCODm^{-3} independent of SL_A. All trajectories head towards a common endpoint as determined by $SL_A = S_{A,min}$ and $SL_H = S_{H,min}$, the two substrate concentrations at which biomass decay is just compensated by biomass growth ($\mu_{oi} = 0$). These two concentrations are approached asymptotically over the depth of the trickling filter. Qualitatively Fig. 7 strongly resembles the experimental observations in Fig. 1e.

Nitrification consumes significantly more oxygen than heterotrophic growth per unit mass of substrate. Neglecting endogenous decay the ratio of oxygen consumption may be predicted by

$$\frac{_jL_{O,A}}{_jL_{O,H}} = \frac{_jL_A(4.57-Y_A)}{_jL_H(1-Y_H)}$$

The dashed line in Fig. 7 separates biofilms in which heterotrophic (SL_H > 10) and autotrophic (SL_H < 10) oxygen consumption prevails.

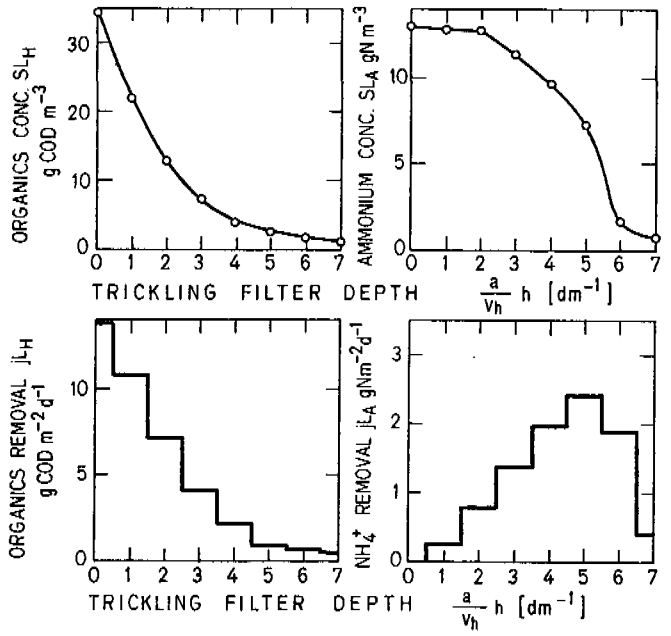

FIG. 8 Substrate concentration and biofilm activity over the depth of a trickling filter. Predictions along a pollutant trajectory (Fig. 7) starting with h = 0 at SL_H = 34.5 gCODm^{-3} and SL_A = 13 gNm^{-3}.

Fig. 8 summarizes the predicted change of substrate concentration and substrate removal over trickling filter height for one trajectory. Qualitatively this prediction is very similar to observed phenomena as shown in Fig. 1.

Species Distribution in the Biofilm

Fig. 9 presents the predicted relative fractions of the different microbial species and the dissolved oxygen concentration versus biofilm depth.

Biofilm a) belongs to region A and contains no heterotrophic organisms. Up to the penetration depth of oxygen (z = 300 μm) active autotrophic organisms dominate, whereas the anaerobic layer is dominated by inert material as expected for the chosen biokinetics (Table 1).

Biofilms b) and c) belong to region AH where coexistence of both active species is possible. Heterotrophic organisms rapidly start to dominate the top layers of the biofilm, whereas autotrophic organisms are displaced into the depth of the film.

Biofilm d) belongs to region H and contains no autotrophic organisms. Penetration depth of oxygen is at a maximum in this film, which may be explained by the fact that autotrophic organisms have a much higher oxygen consumption per unit mass than heterotrophic organisms.

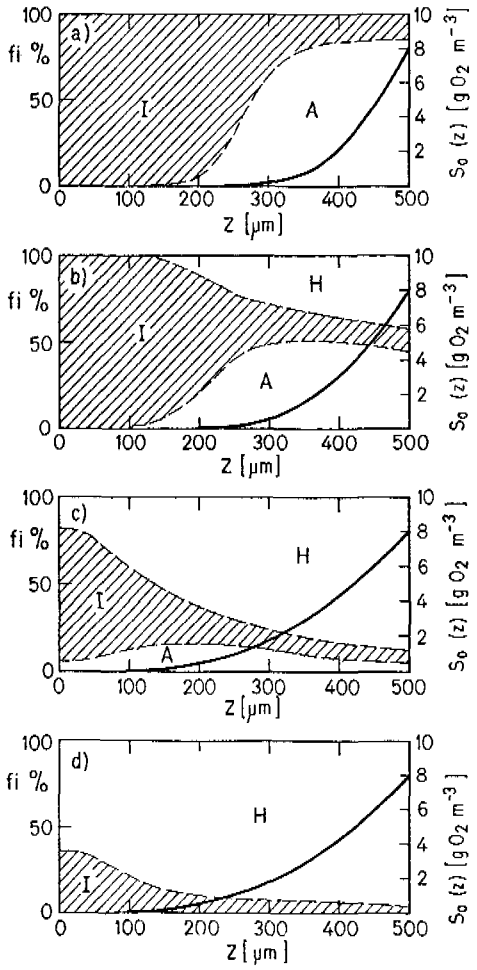

SL_A	= 13.0	gNm^{-3}	
SL_H	= 0	$gCODm^{-3}$	
jL_A	= 3.2	$gNm^{-2}d^{-1}$	
jL_H	= 0	$gCODm^{-2}d^{-1}$	
jL_O	= 13.8	$gOm^{-2}d^{-1}$	

SL_A	= 13.0	gNm^{-3}	
SL_H	= 3.0	$gCODm^{-3}$	
jL_A	= 2.3	$gNm^{-2}d^{-1}$	
jL_H	= 1.3	$gCODm^{-2}d^{-1}$	
jL_O	= 11.0	$gOm^{-2}d^{-1}$	

SL_A	= 13.0	gNm^{-3}	
SL_H	= 13.0	$gCODm^{-3}$	
jL_A	= 0.8	$gNm^{-2}d^{-1}$	
jL_H	= 7.2	$gCODm^{-2}d^{-1}$	
jL_O	= 7.9	$gOm^{-2}d^{-1}$	

SL_A	= 13.0	gNm^{-3}	
SL_H	= 30.0	$gCODm^{-3}$	
jL_A	= 0	$gNm^{-2}d^{-1}$	
jL_H	= 13.2	$gCODm^{-2}d^{-1}$	
jL_O	= 8.3	$gOm^{-2}d^{-1}$	

FIG. 9 Relative biomass distribution over the depth of a biofilm and oxygen concentration profile.

The model predicts that the first heterotrophic organism in a film on the boundary between regions A and AH is located at $z = L$, whereas the last autotrophic organism in a film on the boundary between regions AH and H is located at $z = 0$. Heterotrophs are therefore washed out from the biofilm with decreasing SL_H, whereas autotrophs are overgrown with increasing SL_H. This is the consequence of the difference of the maximum growth rates of the two organisms: $\hat{\mu}_{O_A} \ll \hat{\mu}_{O_H}$.

Relative Influence of Species Distribution on Biofilm Performance

Fig. 10 shows the change of heterotrophic and autotrophic activity jL_H, jL_A with increasing organic substrate concentration SL_H in presence and absence of ammonium SL_A.

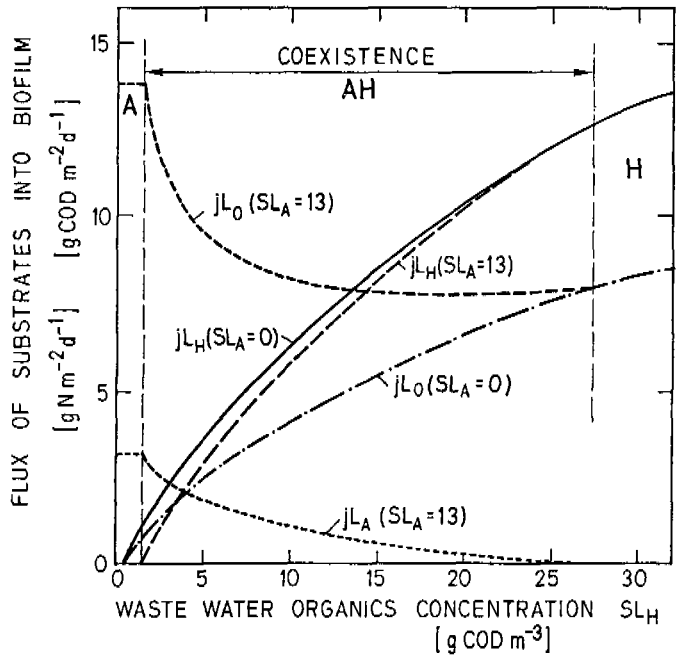

FIG. 10 Comparison of biofilm performance in presence and absence of ammonium (SL_A = 13 gNm^{-3} or SL_A = 0 gNm^{-3}).

The presence of autotrophic organisms has an effect of less than 20 % on heterotrophic activity for $SL_H \geq 5$ $gCODm^{-3}$. However the total oxygen consumption is strongly influenced by autotrophs over wide ranges of SL_H. It appears from a detailed analysis of substrate and biomass concentration profiles that autotrophic organisms are located in the depth of a biofilm and consume any oxygen which is not required by the heterotrophs.

From this prediction we may conclude that the activity of fast growing organisms may be approximately predicted with the assumption that slow growing organisms are absent. The prediction of the activity of slower growing organisms however does require complex modelling.

Biomass Production

In opposition to the steady state biofilm proposed by Rittmann and Mc Carty (1980), in which biomass growth is just compensated by biomass decay, the biological kinetics chosen in this publication, result in biofilms at steady state that always have a constant, positive biomass production which must be released into the bulk liquid to maintain a constant biofilm thickness L. This results in a biomass flux j_{XL} into the water as indicated in Fig. 11. Harremoës (1982) and Kissel et al. (1984) do not include a mechanism to release biomass into the bulk liquid in their multi species biofilm description. Their models do not describe a biofilm at steady state, but rather at ever increasing thickness.

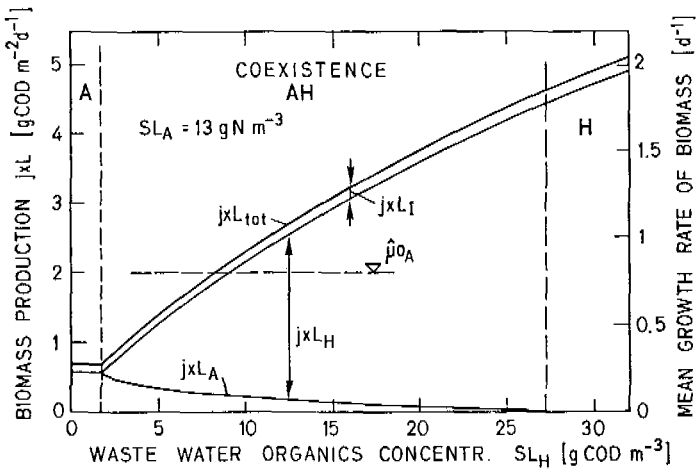

FIG. 11 Overall biomass production of biofilms as a function of organics concentration at constant SL_A = 13 gNm^{-3}.

A mean growth rate of total biomass over the entire film may be defined as:

$$\bar{\mu}o \equiv \frac{jxL_{tot}}{L\rho}$$

This mean growth rate is also shown in Fig. 11. It has to be noticed that $\bar{\mu}o$ may be significantly greater than the maximum observed growth rate of autotrophs $\hat{\mu}o_A$, in biofilms which maintain a significant nitrification activity. This prediction is an interesting contrast to suspended growth systems (washout).

Denitrification

Denitrification has been neglected in this paper for two reasons:

a) Denitrification would add another microbiological process to the model and would therefore further complicate the presentation of theoretical predictions.

b) Nitrification, a prerequisite for denitrification for most waste waters, occurs, according to model predictions, only in biofilms that are not oxygen limited if only heterotrophic activity were considered. Nowhere does the model predict anoxic conditions in the presence of significant amounts of nitrate and organic substrate. Only in nitrifying trickling filters operated with effluent recycle could, in the upper parts of a trickling filter, conditions be created which are favorable for denitrification. This situation would however just be another case of competition between two microbial processes, which may be a topic to be discussed elsewhere.

CONCLUSIONS

Differential equations are presented that describe species competition in biofilms and provide a qualitative prediction of the performance of biofilms consisting of

heterotrophic and autotrophic microorganisms. Theoretical predictions at steady state are:

1. Growth conditions at the biofilm support decide whether a microorganism may develop in the film.
2. Given the competition for a common nutrient (here oxygen), the faster growing organisms may, at low substrate concentrations, be washed out of the biofilm, whereas at high substrate concentrations they may overgrow the slower growing organisms.
3. The activity of faster growing organisms is not strongly affected by organisms with lower growth rates. Fast organisms have a tendency to be close to the biofilm surface.
4. Slower growing organisms have a tendency to reside more in the depth of a biofilm and are strongly affected by faster growing organisms.
5. Slow growing organisms may be maintained in a biofilm even if the mean growth rate of the biological material in the film exceeds the maximum growth rate of these organisms, a prediction which is in opposition to suspended growth systems.

REFERENCES

Frank-Kamenetzkii, D.A. (1969). Diffusion and Heat Transfer in Chemical Kinetics. Plenum Press, New York.

Harremoës, P. (1982). Criteria for Nitrification in Fixed Film Reactors. Wat. Sci. Tech., 14, 167-187.

Kissel, J.C., Mc Carty P.L. and Street R.L. (1984). Numerical Simulation of a Mixed-Culture Biofilm. Submitted for publication.

Mueller, J.A., Paquin P. and Famularo J. (1978). Nitrification in Rotating Biological Contactors. Presented 51st. annual Conf. WPCF, Anaheim, CA.

Powell, M.J.D. (1970). A Hybrid Method for Nonlinear Equations. Numerical Methods for Nonlinear Algebraic Equations. P. Rabinowitz, editor, Gordon and Breach.

Rittmann, B.E. and Mc Carty P.L. (1980). Model of Steady-State-Biofilm Kinetics. Biotechnology and Bioengineering, 22, 2343-2357.

Young, J.C. and Mc Carty P.L. (1968). The Anaerobic Filter for Waste Treatment. Technical Report No 87, Dept. of Civil Engin. Stanford Univ., Stanford CA (also JWPCF, 41:5, Part 2, R 160 - R 173).

APPENDICES

Appendix A: Derivation of eqn. (3)

The average net or observed specific growth rate of nx microbial species in the film is defined as

$$\bar{\mu}o \equiv \sum_{i=1}^{nx} \mu o_i f_i \quad . \tag{A1}$$

Because of

$$\sum_{i=1}^{nx} f_i = \sum_{i=1}^{nx} \frac{V_i}{V} = 1$$

summation of eqns. (1) and (2) over all microbial species yields

$$\Sigma\, \mu o_i f_i = \Sigma \frac{\partial f_i}{\partial t} + \Sigma \frac{1}{\rho_i} \frac{\partial j x_i}{\partial z} = \frac{\partial}{\partial t} \Sigma\, f_i + \frac{\partial}{\partial z} \Sigma \frac{1}{\rho_i} j x_i = \frac{\partial}{\partial z} \Sigma \frac{j x_i}{\rho_i} \tag{A2}$$

and $$\Sigma \frac{jx_i}{\rho_i} = u\Sigma f_i = u \ . \qquad \text{(A3)}$$

If eqns. (A2) and (A3) are substituted into eqn. (A1), eqn. (3) is obtained:

$$\bar{\mu}o = \Sigma \mu o_i f_i = \frac{\partial}{\partial z} \Sigma \frac{jx_i}{\rho_i} = \frac{\partial u}{\partial z}$$

Appendix B: Computation of steady state spatial profiles $f_i(z)$ and $S_i(z)$.

For steady state eqns. (1), (5), (6) and (9) provide a system of nx+2ns first order coupled ordinary differential equations

$$\frac{djx_i(z)}{dz} = \rho_i \mu o_i(z) f_i(z), \qquad jx_i(0) = 0, \qquad i=1,..,nx \qquad \text{(B1)}$$

$$\frac{dj_i(z)}{dz} = r_i(z), \qquad j_i(0) = 0, \qquad i=1,..,ns \qquad \text{(B2)}$$

$$\frac{dS_i(z)}{dz} = \frac{-1}{D_i} j_i(z), \qquad S_i(L) = SL_i, \qquad i=1,..,ns \qquad \text{(B3)}$$

With $f_i(z)$ according to eqns. (2) and (A3) given by

$$f_i(z) = \frac{\frac{jx_i}{\rho_i}}{\sum_{i=1}^{nx} \frac{jx_i}{\rho_i}} \qquad \text{if } u(z) \neq 0. \qquad \text{(B4)}$$

With the kinetics and parameter values specified in this paper eqn. (B4) may be used everywhere except for z = 0 and eqns. (B1) to (B3) may easily be solved by any standard method for numerical integration. So the steady state spatial profiles can be obtained as soon as $f_i(0)$ and $S_i(0)$ are known. However, since eqns. (B1) to (B4) represent a boundary value problem, $f_i(0)$ and $S_i(0)$ can only be found by iteration. The iteration procedure used in our work was a modification of Powell's (1970) hybrid algorithm, which searched for those values of the nx+ns unknown parameters $f_i(0)$ and $S_i(0)$, which fulfilled the nx+ns conditions

$$\left.\begin{aligned} & S_i(L) - SL_i = 0 , && i = 1,..,ns \\ & \mu o_i(0) = \bar{\mu}o(0) \quad \text{or} \quad f_i(0) = 0, && i = 1,..,nx-1 \\ \text{and} \quad & \sum_{i=1}^{nx} f_i(0) = 1. \end{aligned}\right\} \qquad \text{(B5)}$$

Wat. Sci. Tech. Vol.17, Amsterdam, pp.45-52.
Printed in Great Britain.

0273-1223/85 $0.00 + .50

THE EFFECT OF LOAD FLUCTUATIONS ON THE EFFLUENT CONCENTRATION PRODUCED BY FIXED-FILM REACTORS

Bruce E. Rittmann

Department of Civil Engineering, University of Illinois at Urbana-Champaign, Urbana, IL 61801, U.S.A.

ABSTRACT

Although time-varying loads to biological treatment processes are common, typical kinetic models are based on steady-state loads and conditions. This paper uses nonsteady-state kinetics to demonstrate the impact of load variations on the effluent concentration and load from fixed-bed biofilm reactors. The different responses for reactors having average loads that are high, intermediate, and low are compared. In most cases, time-varying input loading, in comparison with steady input loading, causes an increase in average effluent concentration; however, certain combinations of load variation and reactor type allow better performance than do steady-state loads.

KEYWORDS

Biofilms, fixed beds, fixed films, load fluctuations, modeling, nonsteady state, weighted performance.

INTRODUCTION

Input loadings to biological wastewater treatment processes usually vary over time. Flows and BOD concentrations of domestic sewage usually peak during mid-day and drop well below average at night. Some industrial operations produce load peaks on a cycle related to the work day. Other industries have irregular loads that depend on the schedule of batch operations. In almost all cases, the design flow rate, concentration, and load to a process occur rarely; instead, the design values are based on a weighted average over some appropriate time period, such as one day.

The kinetic models used for design and operation of biological processes are almost always based upon steady-state conditions within the process and steady design inputs (e.g., Lawrence and McCarty, 1970; McKinney, 1962; Eckenfelder, 1963; Velz, 1948; Rittmann and McCarty, 1980a, b; Harremöes, 1977). Purely empirical approaches to design (Galler and Gotaas, 1964; Wu and Smith, 1982; NRC, 1946; WPCF, 1977) indirectly include the effects of load variation, but still are based upon average loads. Using a steady-state assumption and average loads create two deficiencies for predictive modeling. First, the magnitude of

peaks in effluent concentration and load are ignored. In some cases, peak load discharges are of critical importance to receiving-water quality or permit compliance. Second, the average discharge concentration (or load) over the appropriate time period is a weighted composite of the concentrations that result from the various input loads experienced during that time. In other words, the average concentration should be calculated as composites of the concentrations that occur for the individual load conditions, which are ignored by conventional models.

This paper presents a kinetic analysis of the impact of load changes on fixed-bed biofilm processes. Compared to suspended-growth processes, biofilm processes are somewhat simpler to model when input loads change, since the biomass is attached and does not change significantly in concentration because of a short-term load variation. Certain trends likely are transferable to suspended-growth systems, but the specific results and conclusions are pertinent only for fixed-bed biofilm processes. Analyses of complete-mix and fluidized-bed biofilm processes are beyond the scope and limitations of this paper.

RESEARCH APPROACH AND METHODS

Overview

Development and presentation of the research results requires four steps. First, predicted biofilm masses within the reactors are based upon the weighted-average loadings, which are assumed to yield steady-state, average biofilm masses that do not change in response to short-term load variations. This assumption of quasi-steady-state biofilm mass is consistent with the relatively slow growth and loss rates for biofilm mass compared to the rate of change in input loads (Rittmann and McCarty, 1981; Rittmann and Brunner, 1983).

The second step involves modeling the response (e.g., effluent concentration) of the reactors to individual changes in input concentration, flow rate, or both. The responses are compared to the response of an ideal reactor that has first-order kinetics in substrate concentration.

Third, the predictive results for individual load conditions are appropriately added and averaged to yield weighted-average effluent concentrations for four varying-load scenarios. Finally, predicted weighted-average effluent concentrations are compared to the steady-state effluent concentration and the weighted-average effluent concentration for an ideal reactor that has first-order kinetics.

Steady-State Average Conditions

The first step is to use the average loading conditions to establish a quasi-steady-state biofilm mass within each reactor. The steady-state biofilm model of Rittmann and McCarty (1980a, 1980c) is employed for this purpose. The fundamental kinetic parameters, which are listed in Table 1, are taken from the work of Rittmann and McCarty (1980c) and are meant to be illustrative.

The fixed-bed reactor is divided into ten or twelve equal-volume segments, each having its own biofilm mass. Three average loading conditions are evaluated for each reactor type: low, intermediate, and high loading. The loading conditions are defined according to the criteria given by Rittmann (1983). Low loading means that the effluent concentration approaches S_{min} (Rittmann and McCarty, 1980a). Conversely, highly loaded reactors produce effluent concentrations significantly greater than S_{min} and have deep biofilms (Rittmann and

McCarty, 1981). Intermediate loads are those between high and low loads and have shallow biofilms. Table 2 gives the loading criteria for each condition.

TABLE 1 Fundamental Kinetic Parameters for Fixed-Bed Biofilm Reactors

Parameter	Value
k, mg/mg C-day	20
K_s, mg/l	3.9
Y, mg C/mg	0.071
b, day^{-1}	0.205
S_{min}, mg/l	0.66
X_f (active), mgC/cm^3	2.5
D, cm^2/day	1.09
D_f, cm^2/day	0.87
ε	0.34
a, cm^{-1}	13.2
D_H, cm^2/day	Eq. 16 in Rittmann and McCarty (1980b)
L, cm	Eq. 1 in Rittmann and McCarty (1980c)

TABLE 2 Three Loading Conditions

	Low Load	Intermediate Load	High Load
Actual Detention Time (θ), min	11.8	2.94	0.98
Empty-Bed Detention Time (θ_{EB}), min	34.7	8.65	2.88
Input Concentration (S°), mg/l	3.3	33	33
Volumetric Load,* $kg/1000\ m^3$-day	137	5,490	16,500
Surface Load, $kg/1000\ m^2$-day	0.104	4.16	12.5

*Based on total reactor volume.

Nonsteady-State Modeling for Individual Load Variations

The biofilm masses for each segment of reactor, as well as the same kinetic parameters (Table 1), serve as input to the nonsteady-state-biofilm model (Rittmann and McCarty, 1981). Influent concentration (S°) and/or detention time (θ) are changed from the average values, but biofilm masses are kept constant. Effluent concentrations are obtained for each new condition, which represents an individual load variation.

A concise way to compare performances for different loads is by calculating an apparent first-order reaction constant. First-order reactions are convenient and frequently used to describe biofilm reactor kinetics (Velz, 1948; Eckenfelder, 1963). For a fixed-bed, plug-flow reactor, the first-order reaction constant (k, min^{-1}) is calculated from

$$k = \frac{\ln S^\circ/S^e}{\theta} \quad (1)$$

in which, S^e = effluent concentration (mg/l)

S° = influent concentration (mg/l)

θ = detention time (min).

When the observed k for the nonsteady-state load is larger than is k for the average load, that load variation enhances performance compared to an ideal first-order reactor. When k becomes smaller, the load variation deteriorates performance, compared to an ideal first-order reactor.

Weighted-Average Concentrations

The weighted-average effluent concentrations are calculated from the effluent flows and concentrations predicted for the individual load variations. Four ideal load scenarios represent the four basic types of load variations that can occur. Table 3 presents the input concentration and detention times used to simulate each scenario.

TABLE 3 Ideal Load Scenarios Used to Estimate Weighted Average Effluent Concentration

Scenario	F_i x100%	θ/θ_{ss}	S°/S°_{ss}
1	67	2	2
	33	1/2	1/2
2	32	0.47	1
	68	2.14	1
3	32	1	2.14
	68	1	0.47
4	25	1/2	2
	8	1/2	0
	67	2	0

Note: θ_{ss} and S°_{ss} represent the detention time and input concentration for the average, steady-state loading; F_i represents the fraction of time that the individual loading condition occurs during the scenario.

1. For scenario 1, the mass load is always constant, because the concentration decreases when the flow rate increases. This scenario is representative of an industry which has almost all its mass load from one highly concentrated, constant-flow source. The flow of relatively clean water varies to change the overall flow rate and concentration.

2. In scenario 2, the input concentration stays constant, but the flow rate and mass load change. This scenario represents the periodic discharge of a uniform wastewater.

3. Scenario 3 has a constant flow rate, but S° varies. It represents the intermittent discharges of contaminant into a constant flow of relatively clean water.

4. The final scenario is similar to the input to a municipal sewage treatment plant. The highest flows and concentrations occur together over part of the cycle, while low flow and low concentrations occur during the remainder of the cycle.

The fractions of time (F_i) and ratios S°/S°_{ss} and θ/θ_{ss} were selected to give weighted average inputs of S°_{ss} and θ_{ss}.

An ideal first-order reactor would give an effluent concentration

$$S_i^e = S_i^\circ \exp(-k_{ss}\theta_i) \tag{2}$$

for a fixed-bed reactor, where k_{ss} = the apparent first-order reaction coefficient for the steady-state, average load; θ_i = the detention time for the nonsteady-state load; S_i° = the input concentration for the nonsteady-state load; and S_i^e = the resulting effluent concentration for the nonsteady-state load. If the reactor does not follow ideal first-order kinetics, the apparent first-order reaction coefficients do not equal k_{ss}. Then,

$$S_i^e = S_i^\circ \exp(-k_i\theta_i) \tag{3}$$

Over an entire loading cycle, which consists of several individual loading conditions, the weighted-average effluent concentration, $\overline{S}$, is calculated from equation 4.

$$\overline{S} = \sum_i F_i S_i^e \theta_{ss}/\theta_i \tag{4}$$

in which θ_{ss} = the average detention time and F_i = the fraction of time that loading condition i occurs. For the ideal first-order reactor, S_i^e is determined from eq. 2. For an actual reactor, S_i^e is taken from the response to individual loading conditions.

RESULTS AND DISCUSSION

Table 4 lists the steady-state-biofilm thicknesses and effluent concentrations for the three average loadings to the fixed-bed reactors. Two trends are noteworthy. First, the effluent concentration increases as the average load goes from low to intermediate to high. Second, the apparent first-order reaction goes up from low to intermediate load, but it declines somewhat from intermediate to high load. Rittmann (1983) discussed the reasons for the variations in apparent rate as loading increases.

The biofilm thicknesses listed in Table 4 are employed to give predictions of nonsteady-state performance for the individual variations in load conditions. Tables 5 through 7 present results that illustrate the ways in which fixed-bed biofilm processes respond to individual load changes. The top entry is for the average load. The next four entries are for a change to θ or S°, while the other parameter is kept at the average value. The bottom four entries are for changes to S° and θ. The apparent first-order reaction coefficients are calculated with equation 1.

The tables demonstrate that the effluent concentration responds consistently to

TABLE 4 Steady-State Results for Fixed-Bed Reactors

	Low Load	Intermediate Load	High Load
Influent Concentration, mg/l	3.3	33	33
Effluent Concentration, mg/l	0.52	3.6	16.1
Actual Detention Time, min	11.8	2.94	0.98
Apparent First-Order Reaction Coefficient, min^{-1}	0.156	0.752	0.732
Biofilm Thicknesses in μm			
Reactor Segment No.			
1	72	1,040	1,090
2	33	906	1,030
3	16	784	975
4	8.3	673	924
5	4.2	575	876
6	2.4	488	831
7	1.2	412	791
8	0.8	396	757
9	0.3	291	731
10	0.0	237	715
11	0.0	196	-
12	0.0	167	-

TABLE 5 Response of Low-Loaded Fixed-Bed Reactor to Individual Changes in Input Load

Load Changes	S^e, mg/l	k, min^{-1}
none	0.52	0.156
$\theta = \theta_{ss} \times 2.4$	0.11	0.14
$\theta = \theta_{ss} \div 2.14$	1.34	0.16
$S^\circ = S^\circ_{ss} \times 2.14$	1.41	0.14
$S^\circ = S^\circ_{ss} \div 2.14$	0.22	0.17
$S^\circ = S^\circ_{ss} \times 2$ and $\theta = \theta_{ss} \times 2$	0.31	0.13
$S^\circ = S^\circ_{ss} \div 2$ and $\theta = \theta_{ss} \times 2$	0.064	0.14
$S^\circ = S^\circ_{ss} \times 2$ and $\theta = \theta_{ss} \div 2$	3.0	0.13
$S^\circ = S^\circ_{ss} \div 2$ and $\theta = \theta_{ss} \div 2$	0.583	0.17

TABLE 6 Response of Intermediate-Loaded Fixed-Bed Reactor to Individual Changes in Input Load

Load Change	S^e, mg/l	Apparent k, min^{-1}
None	3.62	0.75
$\theta = \theta_{ss} \times 2.14$	0.80	0.59
$\theta = \theta_{ss} \div 2.14$	11.1	0.80
$S^\circ = S^\circ_{ss} \times 2.14$	10.8	0.64
$S^\circ = S^\circ_{ss} \div 2.14$	1.51	0.79
$S^\circ = S^\circ_{ss} \times 2$ and $\theta = \theta_{ss} \times 2$	2.1	0.59
$S^\circ = S^\circ_{ss} \div 2$ and $\theta = \theta_{ss} \times 2$	0.44	0.62
$S^\circ = S^\circ_{ss} \times 2$ and $\theta = \theta_{ss} \div 2$	30.8	0.52
$S^\circ = S^\circ_{ss} \div 2$ and $\theta = \theta_{ss} \div 2$	4.28	0.92

TABLE 7 Response of High-Loaded Fixed-Bed Reactor to Individual Changes in Input Load

Load Change	S^e, mg/l	Apparent k, min^{-1}
None	16.1	0.73
$\theta = \theta_{ss} \times 2.14$	9.2	0.61
$\theta = \theta_{ss} \div 2.14$	22.8	0.81
$S^\circ = S^\circ_{ss} \times 2.14$	38.4	0.63
$S^\circ = S^\circ_{ss} \div 2.14$	7.0	0.80
$S^\circ = S^\circ_{ss} \times 2$ and $\theta = \theta_{ss} \times 2$	21.6	0.57
$S^\circ = S^\circ_{ss} \div 2$ and $\theta = \theta_{ss} \times 2$	4.62	0.65
$S^\circ = S^\circ_{ss} \times 2$ and $\theta = \theta_{ss} \div 2$	47.5	0.67
$S^\circ = S^\circ_{ss} \div 2$ and $\theta = \theta_{ss} \div 2$	10.6	0.90

changes in θ or S°. An increase in S° or decrease in θ yields a higher value of S^e, whereas a decrease in S° or an increase in θ gives a lower S^e. However, the tables also show that the apparent first-order coefficient is not constant. Decreases in S° and θ alone allow removals greater than expected by a first-order reaction and have a k value greater than the k value of the average load. The opposite load changes cause an increase in k.

When both θ and S° change from their average values, the trends for k are straightforward. Increases in S° and θ, both of which alone cause k to decrease, dominate other changes of equal magnitude. For example, Tables 5, 6, and 7 show that when S° increases by a factor of 2 and θ decreases by a factor of 1/2, which give no increase in mass load, the first-order coefficient decreases. Thus, the increase in S°, which causes a decrease in k, dominates the decrease in θ, which increases k. The dominance patterns for fixed beds dictate that load changes cause poorer removal rates, compared to the steady-state rates, for more cases than they allow higher removal rates. However, relatively improved rates occur for certain load variations when S° and/or θ are smaller than their steady-state, average values.

Table 8 indicates the impact of load variations on the weighted-average effluent concentration. In general, load variations cause average concentrations to increase over steady-state values. The greatest increases in $\bar{S}$ occur for load condition 4, in which flow rate and concentration increase together for part of the loading cycle. On the other hand, loading condition 1, in which the mass load remains constant as flow rate increases are compensated by concentration decreases, gives weighted-average effluent concentrations similar to or lower than does the steady-state loading. Although Table 8 shows one exception, another general trend is that the actual effluent concentration is greater than the concentration for an ideal first-order reactor undergoing the same load changes.

TABLE 8 Weighted-Average Effluent Concentrations for Steady-State, Ideal First-Order, and Actual Fixed-Bed Biofilm Reactors (Values are concentrations in mg/1)

	Low Load	Intermediate Load	High Load
Steady State	0.52	3.62	16.1
Scenario 1			
First-Order	0.49	3.87	12.9
Actual	0.49	3.56	16.1
Scenario 2			
First-Order	0.90	7.5	18.0
Actual	0.95	7.8	18.4
Scenario 3			
First-Order	0.52	3.6	16.1
Actual	0.60	4.5	17.1
Scenario 4			
First-Order	1.3	10.9	23.0
Actual	1.5	15.4	23.8

SUMMARY

Modeling load variations to fixed-bed biofilm reactors shows that the apparent first-order rate coefficient is not the same for nonsteady-state loadings as for the average, steady-state loading. For fixed-bed reactors, the dominant effects occur for increases in S° and θ, both of which cause a decrease in k.

The impact of load variations on weighted-average effluent concentrations show three general trends. First, changes in flow rate and input concentrations that yield steady mass loads give similar or lower effluent concentrations than do steady-state loads. Second, loading variations having fluctuations in mass load give higher effluent concentrations than does a steady-state load. The greatest increase in average effluent concentration occurs when the flow rate and concentration increase together for part of the loading cycle, such as often occurs at municipal sewage treatment plants. Finally, actual biofilm reactor performance generally gives higher effluent concentrations than does an ideal first-order reactor undergoing the same loading fluctuations. In other words, using first-order kinetics to predict performance of biofilm reactors under varying loads does not adequately represent the effects of the variations.

REFERENCES

Eckenfelder, W. W., Jr. (1963). Trickling filtration design and performance. Trans. Amer. Soc. Civil Engineers, 128.

Galler, W. S. and H. B. Gotaas (1964). Analysis of biological filter variables. J. Sanitary Engineering Div., Amer. Soc. Civil Engineers, 90 (SA1), 4174.

Harremoës, P. (1977). Half-order reactions in biofilm and filter kinetics. VATTEN, 2, 122.

Lawrence, A. W. and P. L. McCarty (1970). Unified basis for biological treatment design and operation. J. Sanitary Engineering Div., Amer. Soc. Civil Engineers, 96 (SA3), 757.

McKinney, R. E. (1962). Mathematics of complete-mixing activated sludge. J. Sanitary Engineering Div., Amer. Soc. Civil Engineers, 88 (SA3), 87.

National Research Council (1946). Trickling filters in sewage treatment at military installations. Sewage Works J., 18, 787.

Rittmann, B. E. (1983). Basis of kinetics and microorganism/surface attachment in fixed-film reactors. Symposium on Application of Basic Research to the Operation and Control of Biological Waste Treatment Systems, Amer. Inst. Chem. Engineers Diamond Jubilee Meeting, Washington, D.C.

Rittmann, B. E. (1982). Comparative performance of biofilm reactor types. Biotechnology and Bioengineering, 24:1341.

Rittmann, B. E. and C. W. Brunner (1983). The nonsteady-state-biofilm process for advanced organics removal. J. Water Pollution Control Federation, in press.

Rittmann, B. E. and P. L. McCarty (1980a). Model of steady-state-biofilm kinetics. Biotechnology and Bioengineering, 22, 2343.

Rittmann, B. E. and P. L. McCarty (1980b). Design of fixed-film processes with steady-state-biofilm model. Progress in Water Technology, 12, 271.

Rittmann, B. E. and P. L. McCarty (1980c). Evaluation of steady-state-biofilm kinetics. Biotechnology and Bioengineering, 22, 2359.

Rittmann, B. E. and P. L. McCarty (1981). Substrate flux into biofilms of any thickness. J. Environmental Engineering Div., Amer. Soc. Civil Engineers, 107 (EE4), 831.

Velz, C. J. (1948). A basic law for the performance of biological beds. Sewage Works J., 20.

Water Pollution Control Federation (1977). Wastewater Treatment Plant Design Manual of Practice No. 8, Washington, D.C.

Wu, Y. C. and E. D. Smith (1982). Rotating biological contactor system design. J. Environmental Engineering Div., Amer. Soc. Civil Engineers, 108 (EE3), 578.

Wat. Sci. Tech. Vol.17, Amsterdam, pp.53-67.
Printed in Great Britain.

0273-1223/85 $0.00 + .50

EVALUATION OF TEMPERATURE EFFECTS ON TRICKLING FILTER PLANT PERFORMANCE

A. Adin*, E. R. Baumann** and F. D. Warner**

*Human Environmental Sciences, School of Applied Science and Technology, The Hebrew University, Jerusalem, Israel
**Sanitary Engineering, Department of Civil Engineering, Iowa State University, Ames, Iowa, U.S.A.

ABSTRACT

This paper presents a mathematical-statistical method to help evaluate the temperature effect on BOD and SS residual ratio during and after a trickling filter plant treatment. Mathematical relationships are developed and brought to workable linear forms which are then used for statistical examination by the F test method. The data for this purpose is provided by regular measurements of wastewater quality in a full-scale treatment plant. While settling performance did not respond consistently to temperature changes, the secondary treatment and the overall plant performance provided good correlations with the correct representative temperatures.

KEYWORDS

Trickling filter; biological filtration; temperature effects; modeling; statistical analysis.

INTRODUCTION

Wastewater temperature has an effect on both sedimentation and secondary biological treatment processes. While the trickling filter itself is mainly affected due to temperature influence on the rate at which biological oxidation occurs, the settling processes are affected mainly through the temperature influence on the physical characteristics of the wastewater. Although these basic phenomena are well known, it is felt that there is still lack of mathematical and statistical means to directly relate the efficiency of a trickling filter plant to wastewater temperature.

This work tries to establish more exactly the relationship between the temperature and trickling filter plant performance, first by developing a mathematical relationship and then using field experiments (full scale) and statistical methods. The latter enable the comparison of temperature effects during different seasons of the year.

THEORETICAL CONSIDERATIONS

Gravity settling which takes place both in the primary and in the secondary settling tanks, is generally under laminar flow conditions determined for discrete particles by the well-known Stoke's Law:

$$v_s = \frac{(\rho_s - \rho_l)\, g d_p^2}{18u} \tag{1}$$

Considering the negligible effect of temperature on the wastewater specific gravity, temperature may influence through its effect on the wastewater viscosity, approximately by (Schroepfer, 1950):

$$u = u_{50^oF} \frac{60}{T_F + 10} \tag{2}$$

Substituting eq. (2) into (1) forms a linear relationship, which may be written as:

$$v_s = a' + b'T \tag{3}$$

where a' and b' are empirical constants.
Recalling that the removal efficiency of a certain particle by settling is directly proportional to its settling velocity (divided by the overflow rates - Hazen, 1904; Camp, 1946), the fraction remaining may be expressed as:

$$f_p = 1 - (a' + b'T_p) = a + bT_p \tag{4}$$

which is a linear function too (p stands for primary).

This type of equation can be used to evaluate the effect of temperature on both suspended solids and BOD removal since the BOD removable by primary clarification is that associated with the suspended solids.

The two basic equations that link the efficiency of biochemical oxidation of organic matter with temperature are Streeter and Phelp's (1952) equation:

$$dL/dt = -kt, \text{ or, after integration} \tag{5}$$
$$L_t/L = e^{-kt} \tag{6}$$

and Van't Hoff-Arrhenius equation

$$\frac{d(\ln k)}{dT_k} = \frac{\varepsilon}{\psi T_k^2} \tag{7}$$

and, after integration between T_{k1} and T_{k2}

$$\ln (k_2/k_1) = \frac{\varepsilon(T_{k2} - T_{k1})}{\psi\, T_{k2}T_{k1}} \tag{8}$$

Since the trickling filter operations are carried out mostly within a small temperature range (Schroepfer et al, 1952), the quantity $\varepsilon/\psi(T_{k2}T_{k1})$ may be considered constant. Considering this and after some integration one gets the formula

$$k_2/k_1 = \theta^{(T_2-T_1)} \tag{9}$$

Substituting eq. (9) into eq. (6) and with further development results in an expression for the fraction of BOD remaining at two temperatures:

$$f_2 = f_1\, \theta^{(T_2-T_1)} \tag{10}$$

Rearranging this equation using logarithmic form, a new constant may be determined as follows

$$\frac{\ln f_1}{\theta^{T_1}} = \frac{\ln f_2}{\theta^{T_2}} = \alpha \qquad (11)$$

Separating and rearranging the terms brings about, for the trickling filter itself, for each temperature,

$$f_s = e^{\alpha_s \theta_s^{T_s}} \qquad (12)$$

where s stands for secondary.

For the analysis described herein, a linear regression was used and eq. (12) was modified to

$$\ln(-\ln f_s) = \ln(-\alpha_s) + T_s \ln \theta_s \qquad (13)$$

hence

$$\ln(-\ln f_s) = \alpha'_s + \theta'_s T_s \qquad (14)$$

where α'_s and θ'_s are constants. Eq. (13) enables us, therefore, to determine the value of θ for a certain filter using experimental data.

On the basis of eqs. (4) and (12), the remaining fraction of BOD or SS in a trickling filter plant, including primary settling, would be of the form

$$f_{OA} = e^{\alpha\theta^{T_s}(a + bT_p)}; \text{ OA = overall treatment} \qquad (15)$$

Eq. (15) is not theoretically correct if a single temperature is used for both T_s and T_p.

These models should theoretically predict actual removal of a dependent constituent when the correct temperature is used. The correct temperature refers to the temperature that is most representative of the process. As a reciprocal condition, it is assumed that for every temperature there is only one resulting efficiency. It is realized that in both cases a single efficiency will not actually occur because other parameters besides temperature influence process efficiency. However, all other conditions are assumed to be constant in the study and the only identifiable parameter which varied was the wastewater temperature and its effect on sloughing of filter slime.

If only one wastewater temperature is used in Eq. (15), the temperature used can be the correct temperature for at most one process. Since the wastewater temperature between stations within the plant varies, it can be assumed that the correct temperature to be used for each process also varies. Due to variations in the wastewater temperature at different points within the plant, a scattering of points will occur for at least one set of data, if plotted. When the equation for primary and secondary treatment units is evaluated for the scattered data, values of the constants will result but they will not be the same as those found for Eq. (15) when evaluated for the overall plant efficiency plotted against the data for one temperature. If another set of data is plotted for overall treatment and Eq. (15) evaluated for that data, the constants would not be the same as those found in the first instance, due to differing temperature variations within the plant.

Thus, Eq. (15) and the entire procedure of expressing the overall plant efficiency as a function of only one temperature is not theoretically correct. However, if the temperatures which are most representative of each process are not too different, an intermediate temperature may be used to approximate removal. This approach becomes increasingly desirable as the actual data becomes more scattered about a predicted value and when there is a limited amount of data. In these cases, the data can be considered not to justify the precision of a dual temperature equation. Since Eq. (15) evaluated with a single temperature is only an approximation of the true relationship, another even simpler equation may be justified due to the scatter and lack of data. Eq. (15) will form a slightly curved line when $\ln(-\ln f_{OA})$ is plotted vs temperature. If this relationship approximates a straight line within the temperature range of the observed data, a straight line relationship can be used as proposed for secondary treatment.

$$f_{OA} = e^{\alpha_{OA}\theta_{OA}^{T_{OA}}}_{\text{EXPERIMENTAL}} \qquad (16)$$

A full-scale study was conducted at the Nevada, Iowa standard-rate trickling filter plant consisting of a single primary clarifier, trickling filter and final clarifier, with a capacity of 0.5 mgd and 0.17 BOD_5/capita/day. Data was collected during nine months of operation (September to May) after plant calibration and sampling and analytical methods had been established.

In order to evaluate the performance of the plant, it was necessary to evaluate the individual performance of the primary clarifier, the trickling filter-final clarifier and also the overall plant performance. This dictated the establishment of four main sampling points:

Station A - Raw wastewater
Station B - Primary clarifier effluent
Station C - Trickling filter effluent
Station D - Plant (final clarifier) effluent

Since the experimental work was aimed to support a much broader investigation including the addition of aluminosilicate material to the raw sewage (Baumann et al, 1979)[1], the sampling at the above points served a large spectrum of wastewater quality parameters and variables. For the aim of the study presented in this paper, it is sufficient to report that the main samples (from stations A, B and D) were analyzed for BOD_5 and suspended solids using the common Standards Method procedures. Since the wastewater temperature varied throughout the plant and was expected to affect both unit performance and overall plant performance, the wastewater temperature was determined at each sampling station.

It is worthwhile noting that the plant influent wastewater flows were fairly constant throughout the study; consequently, plant loadings were also constant throughout the study. Therefore, parameters of treatment performance could be evaluated with respect to wastewater temperature and not with respect to flow-load variations.

GENERAL APPROACH TO DATA ANALYSIS

The fraction of BOD_5 or TSS remaining in a treated wastewater is used as the measure of the efficiency of the process involved. Because of major differences in plant operation during the coldest months - the second half of December and all of January, the data of these months was excluded from the

[1]It was found that the presence of the aluminosilicate material in the plant wastewater and sludge did not affect plant treatment efficiency.

analyses, as well as February data which represented a filter recovery period. The actual research period in this respect can be divided then into two phases of 3 months each - phase II (half September through half of December) and Phase III (March through May). (Phase I was a plant calibration period which should be excluded from this analysis).

Judgement as to whether or not these two phases give the same efficiency as a function of temperature is determined on a statistical basis, using the F test for a common line at the 5% level of significance (Norman and Smith, 1969). Equations of the form given above are fitted to the data of each phase using a least squares estimate and the two lines (line for each phase) are tested for similarity. If statistical analysis results in "not rejecting the hypothesis that the lines are not different", only the common line is shown in a figure, otherwise both lines are plotted. The acceptance of this hypothesis is stated then as "a common line exists."

EFFICIENCY OF PRIMARY TREATMENT

In the analysis of temperature effects on primary clarifier efficiency, two wastewater temperatures were examined, the primary effluent temperature (Station B) and an average wastewater temperature, $(T_A + T_B)/2$. The raw wastewater temperature, T_A, was not considered representative of the process. The raw wastewater is not the temperature of the clarifier influent, since secondary clarifier underflow recirculation is added and normally has a temperature different than T_A. The average primary clarifier temperature is not totally represented by $(T_A + T_B)/2$, but is satisfactory for use within the limits of this study. The actual average temperature of the primary clarifier may be closer to that of T_B depending on the wastewater temperature change between Stations A and D.

TABLE 1 Test of significance of hypothesis "that the lines are not different " $BOD_B/BOD_A = a' + b'T$, for primary removals of BOD_5

Data from Phases	Value of a'	Value of b'	Correlation coefficient, r	Number of observations
	$T=(T_A + T_B)/2$			
II	0.9323	-0.0133	-0.272	11
III	0.8419	-0.0076	-0.363	11
II & III	0.8648	-0.0092	-0.315	22
	$T = T_B$			
II	0.8890	-0.0112	-0.251	11
III	0.8322	-0.0070	-0.356	11
II & III	0.8554	-0.0089	-0.302	22
	Test for common line			
$(T_A + T_B)/2$	$F_{18}^2 = 0.181$	----------can't reject hypothesis		
T_B	$F_{18}^2 = 0.092$	----------can't reject hypothesis(Fig.1)		

Table 1 presents, for example, the results of test of significance hypothesis that the lines describing the function $f = a + bT_p$ (eq. 4) for phase II or III or their combination are not different, f being here, by definition, equal to BOD_B/BOD_A. T_p is either the average temperature or the effluent temperature of the primary settling tank. The results show poor correlation coefficients for

both temperatures, although a common line exists for the different time periods (e.g., Fig. 1). A similar picture was found to exist concerning TSS as a function of temperature in the primary clarifier, although wastewater temperature appeared to have a slightly greater effect on TSS removal than on BOD removal.

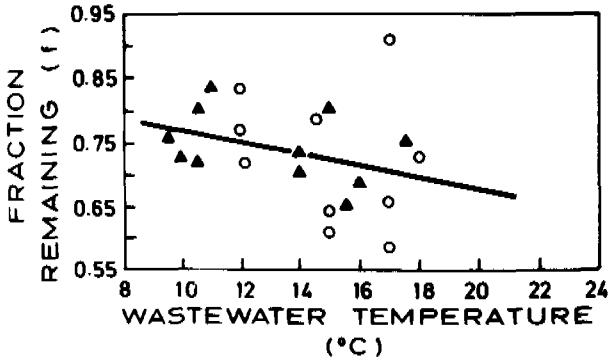

Fig. 1. Primary BOD_5 removal expressed by ratio of BOD_B/BOD_A vs primary effluent temperature, T_B. o-Phase II, Δ-Phase III.

With the low correlation and slight slopes, removal of BOD and TSS by sedimentation may be considered practically a purely random phenomenon unrelated to wastewater temperature, as reported by Lin and Heinke (1977).

EFFICIENCY OF TRICKLING FILTER-FINAL CLARIFIER SYSTEM

The theoretical basis for the model used to evaluate the removal of BOD_5 and TSS as a function of wastewater temperature has been discussed previously. In addition, the removal of TSS as a function of wastewater temperature was analyzed on a logarithmic basis. The form of the equation used in the linear regression analysis was

$$\ln f_s = \alpha''_s + \theta''_s T_s \qquad (17)$$

where α''_s and θ''_s are constants.

This model was used because of uncertainty as to how well the removal of TSS would relate to biochemical reactions in a filter which is controlled by the variations in the wastewater temperature.

The removal of BOD and TSS by the trickling filter-final clarifier is analysed against the temperature of filter influent, the temperature of filter effluent, and te average of these two temperatures. These three temperatures were utilized because of the uncertainty as to which is actually the most representative of the filter-final clarification process, although temperature B may be considered to be the best, since there is support for the idea that most of the biological action in the filter occurs in the top few feet (Hanumanula, 1970; Velz, 1948).

Plots of $\ln(-\ln [BOD_D/BOD_B])$ and $\ln(-\ln [TSS_D/TSS_B])$ vs wastewater temperature gave different results. The statistical analyses of the BOD data are summarized in Table 2. Figs 2 and 3 illustrate a "non-rejected" (one common line) and a "rejected" (two separate lines) hypothesis. BOD_5 plotted against the primary effluent temperature (Fig. 2) is the only relationship that results in not

rejecting the hypothesis that the lines derived from linear regression are not different.

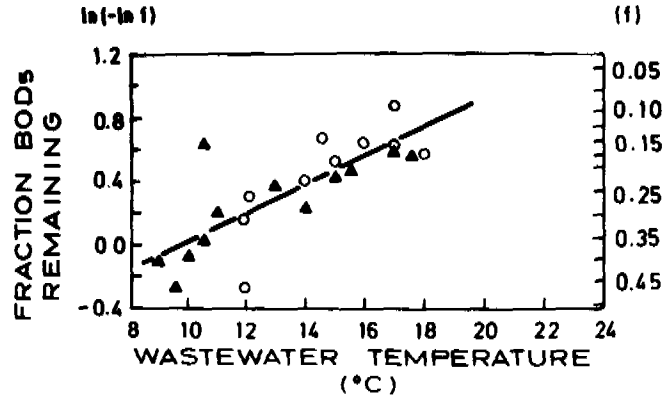

Fig. 2. Secondary BOD_5 removal expressed by ratio of BOD_D/BOD_B vs primary effluent temperature T_B. (ln [-ln f])

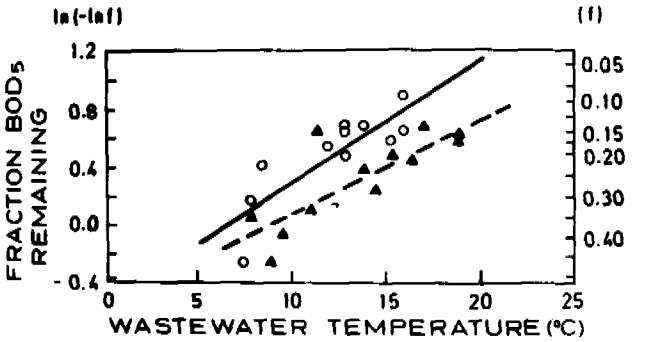

Fig. 3. Secondary BOD_5 removal expressed by ratio of BOD_D/BOD_B vs trickling filter effluent temperature, T_C. (ln [-ln f])

TABLE 2 Test of significance of hypothesis "that the lines are not different " $\ln(-\ln BOD_D/BOD_B) = \alpha' + \theta'T$, for secondary removals of BOD_5

Data from Phases	Values of α'	Values of θ'	Correlation coefficient, r	Number of observations
	$T = T_B$			
II	-1.2212	0.1128	0.799	12
III	-.7575	0.0806	0.789	14
II & III	-0.8811	0.0902	0.807	26
	$T = T_C$			
II	-0.5345	0.0821	0.843	12
III	-0.5528	0.0632	0.831	13
II & III	-0.450	0.0645	0.741	25
	$T = (T_B + T_C)/2$			
II	-0.8751	0.0988	0.841	12
III	-0.6647	0.0723	0.819	13
II & III	-0.7328	0.0828	0.804	25

Test for common line

T_B $F_{22}^2 = 0.978$----------can't reject hypothesis(Fig. 2)

T_C $F_{21}^2 = 13.789$----------reject hypothesis(Fig. 3)

$(T_B+T_C)/2$ $F_{21}^2 = 5.184$----------reject hypothesis

A plausible explanation for the observed difference between BOD_5 removal by the trickling filter-final clarifier as a function of temperature in Phases II and III is related to the time period in which the phases occurred. The Phase II portion of the study was made during the summer and fall at a time when wastewater temperatures were gradually decreasing with time. The Phase III studies were conducted during the winter and spring at a time when the wastewater temperatures were increasing with time. Logic would seem to suggest that the flora on a trickling filter would be more efficient in a period of decreasing wastewater temperature than it would during a period of increasing water temperature (Hawkes, 1960). Basically, a filter flora activated at one temperature should be able to retain the active flora more effectively during a period of decreasing wastewater temperature and reduced biological activity than it would be able to build up a more active flora as water temperature increases.

Similar results, in which lower filter-final clarifier efficiency has been observed in periods of rising wastewater temperature as compared with falling wastewater temperature, have been reported by Young, Baumann and Kleman (1969).

In the fall, the filter influent became cooler as it flowed through the filter; in the spring it became warmer with increasing air temperatures. Since the largest portion of filter media slime is in the top few feet of the filter and most removal takes place there, the wastewater temperature in that region is most important. When the wastewater temperature at Station C is used in the fall, it will predict worse removal than is actually taking place; in the late

spring better removal will be predicted. An average temperature, if skewed too far from the most representative temperature, would produce the same effect. This is apparently what is occurring in these relationships and could cause both the offset and the difference in slopes.

The statistical analyses of the TSS data for the secondary treatment are shown in Table 3 and partially illustrated in Fig. 4.

TABLE 3 Test of significance of hypothesis "that the lines are not different " $\ln [-\ln (TSS_D/TSS_B)] = \alpha' + \theta' t$, for secondary removals of TSS

Data from phases	Values of α'	Values of θ'	Correlation coefficient, r	Number of observations
	$T = T_B$			
II	-1.7956	0.1239	0.804	12
III	-0.3901	0.0345	0.561	14
II & III	-0.6766	0.0532	0.581	26
	$T = T_C$			
II	-1.0459	0.0905	0.858	12
II	-0.3112	0.0277	0.611	13
II & III	-0.5852	0.0508	0.688	25
	$T = (T_B + T_C)/2$			
II	-1.4189	0.1087	0.854	12
III	-0.3599	0.0316	0.598	13
II & III	-0.7201	0.0587	0.677	25
	Test for common line			
T_B	$F_{22}^2 = 12.42$	----------reject hypothesis		
T_C	$F_{21}^2 = 10.71$	----------reject hypothesis		
$(T_B + T_C/2)$	$F_{21}^2 = 10.83$	----------reject hypothesis(Fig. 4)		

Two basic differences exist between the removal of BOD_5 (Fig. 3) and TSS (Fig. 4) as affected by wastewater temperature. First, the lines representing TSS removal derived from linear regression of data from Phases II and III cross at a much higher temperature than do those for BOD_5. Second, the slopes of the relationship resulting from Phases II and III data differ much more for TSS results than for BOD_5 results.

The greater recirculation during Phase III could produce the flatter curves observed in both BOD_5 and TSS removal during Phase III. In early spring,

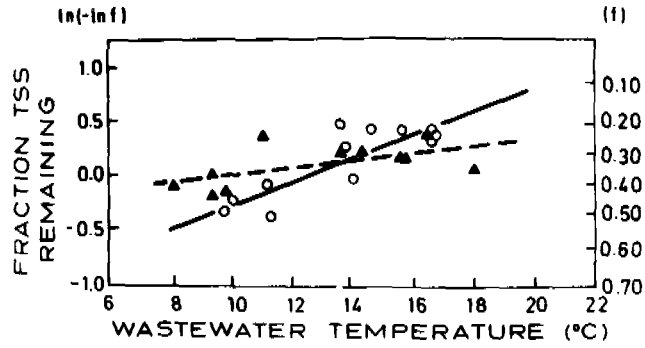

Fig. 4. Secondary TSS removal expressed by ratio of TSS_D/TSS_B vs mean wastewater temperature across trickling filter, $(T_B + T_C)/2$. (ln (-ln f)).

wastewater temperatures are cool enough to result in continued filter slime buildup, thereby lowering the final clarifier solids load and thus the effluent solids. The increased recirculation would result in an increased primary clarifier overflow rate, thus decreasing primary sedimentation efficiency. This is especially critical in the primary clarifier operation when recirculation occurs during peak flow periods. Recirculation was continued over a 24 hr period in Phase III. The poorer primary removal of SS with recirculation would produce a higher than normal secondary removal of SS. The result is an apparent improvement in solids removal for that wastewater temperature. When wastewater temperatures get warmer, spring slough-off of filter media slimes occurs and both primary and secondary clarifier loadings increase, causing higher plant effluent suspended solids and an apparent decrease in efficiency.

Analysis of the statistical data resulting from the log-normal ratio for suspended solids removal by secondary treatment results in similar figures, correlation coefficients and conclusions, as does the ln-ln analysis. The data for secondary removal of BOD_5 shows correlations that are comparable in both Phases II and III, and the correlations are high, 0.79 and 0.85 (Table 2). Total suspended solids removal results in Table 3 shows better correlation in Phase II than in Phase III, but both are high, 0.81 to 0.86 in Phase II, and 0.56 to 0.61 in Phase III. Better correlations of both TSS and BOD removal were obtained using the filter effluent temperature, T_C, or the mean trickling filter temperature, $(T_B + T_C)/2$, than it was using the filter influent temperature, T_B. The differences in the correlation coefficient for the TSS removal vs temperature between the two phases may be due to the irregularity of slough-off of slime from the filter media.

OVERALL PLANT EFFICIENCY

The analysis of the effect of wastewater temperature on overall plant treatment was made for the wastewater temperatures at Stations A, B, the average of A-D and the average of B-C.

An investigation of Eq. (15) in which $T_s = T_p$, using combinations of the maximum and minimum values for a', b', α, and θ taken from the values for both BOD_5 and TSS, showed no significant deviation from a straight line in the temperature range of 5°C to 22.5°C. Table 4 lists the values used. The actual temperature range of the data was from approximately 9°C to 22°C. As a result, Eq. (16), which uses only one temperature, was used in this

investigation to represent the effect of wastewater temperature on overall plant treatment efficiency.

TABLE 4 Maximum and minimum values of a', b', α and θ used in verifying Equation (16)

Constant	Maximum	Minimum
a'	0.95	0.55
b'	-0.0002	-0.022
α	-0.15	-0.75
θ	1.14	1.02

A straight line was also fitted to the log normal ratio of influent to effluent total suspended solids. Eq. (17) was used in this analysis.

All relationships except those relating BOD and TSS removal to the raw wastewater temperature, T_A, resulted in not rejecting the hypothesis that the lines developed from linear regression are not different (e.g., Fig. 5-9). The raw wastewater temperature was used not because it is considered representative of the temperature which best correlated with plant performance, but because it is the only wastewater temperature normally measured in plant operation control. Rejection of the hypothesis at temperature T_A and acceptance of the hypothesis at the other three temperatures is reasonable considering seasonal wastewater trends as discussed previously. Temperatures T_B, $(T_A + T_C)/2$, $(T_A + T_D)/2$ all may be considered representative of total plant temperature conditions as they affect plant performance. Correlation coefficient trends for the BOD_5 and TSS results were the same as for previous analyses, i.e., higher correlation sometimes for Phase II data than for Phase III data. Generally, high correlations resulted for all common lines for Phases II and III (0.72-0.82 for BOD and 0.46-0.75 for TSS).

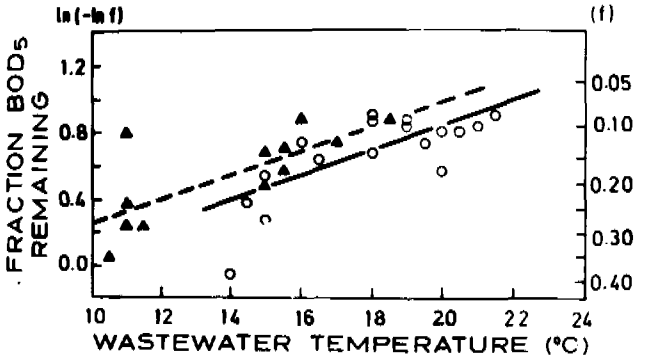

Fig. 5. Plant removals of BOD_5 expressed as ratio of BOD_D/BOD_A vs temperature of raw wastewater, T_A. (ln (-ln f)).

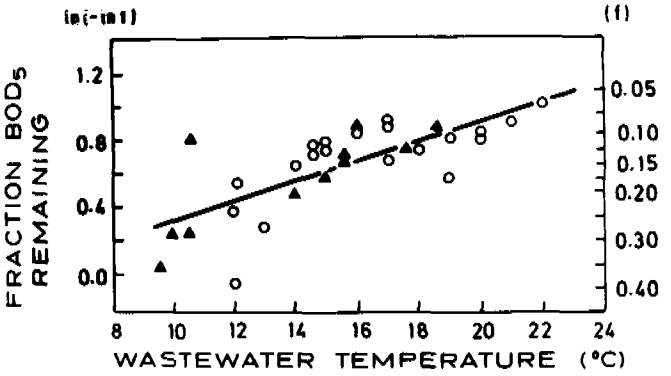

Fig. 6. Plant removals of BOD_5 expressed as ratio of BOD_D/BOD_A vs temperature of primary effluent. (ln (-ln f)).

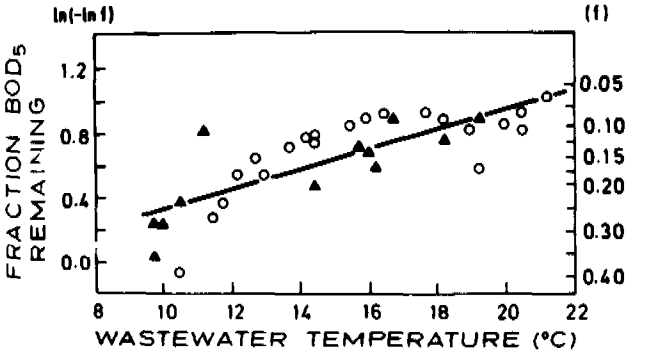

Fig. 7. Plant removals of BOD_5 expressed as ratio of BOD_D/BOD_A vs mean wastewater temperature across the plant, $(T_A + T_D)/2$. (ln (-ln f)).

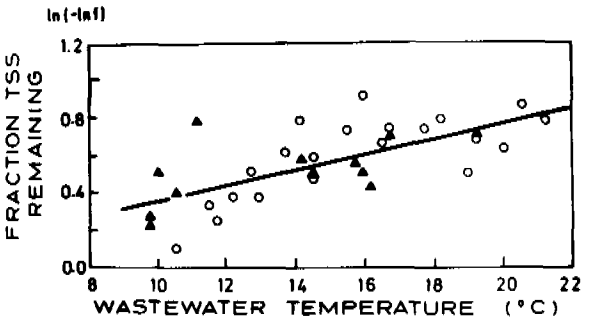

Fig. 8. Plant removals of TSS expressed as ratio of TSS_D/TSS_A vs mean wastewater temperature across the plant, $(T_A + T_D)/2$.

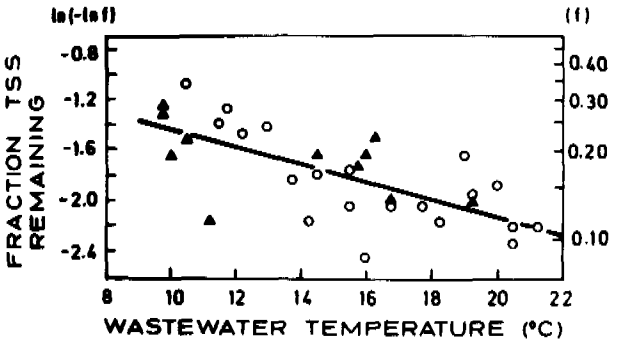

Fig. 9. Plant removal of TSS expressed as ratio of TSS_D/TSS_A vs mean wastewater temperature across the plant, $(T_A + T_B)/2$. (ln f).

An obvious question arises as to why a common line expressing removal of BOD_5 and TSS removal as a function of wastewater temperature results for overall plant treatment, when rejection of the existence of a common relationship is obtained (Tables 2 and 3) for secondary treatment alone. Three possible reasons can be advanced. First, the differences between removals in Phases II and III may be great enough to reject the hypothesis using filter influent and effluent levels of BOD and TSS, but not great enough when using the much greater overall plant levels. Second, differences between treatment units may compliment each other so that when combined, and phases are compared, a common line results. Third, variation in results, although not complimentary, serves to mask any slight differences. This explanation seems less plausible than the first if theoretical derivations are correct. This is especially true for TSS, since primary sedimentation is only included in the constant " α " and would, therefore, not affect the slope (Eq. 16).

CONCLUSIONS

The following main conclusions can be derived from the above investigation:

1. The temperature effects on trickling filter plant performance can be practically expressed in the form of linear relationships between the fractions of BOD and SS remaining and appropriate wastewater temperatures. The basis for the relationships are Stoke's Law and Streeter-Phelp's and Van't Hoff-Arrhenius equations.
2. Comparison between the performance of trickling filter plants, or possibly other treatment processes, during different seasons of the year, or during rising and falling temperature situations, can be made using linear regression analysis and a statistical test for a common line at a certain (5% in this case) level of significance.
3. Removal rates of BOD and TSS by sedimentation in the TF plant produced low correlations and may be considered practically a purely random phenomenon unrelated to wastewater temperature. On the other hand, the trickling filter itself and the overall plant results responded well to the relationships derived from the basic theoretical formulations.
4. When a correlation of plant or a process efficiency due to wastewater temperature has to be made, one should not take automatically the raw sewage temperature for this purpose. This work points out that the most representative temperatures are (a) for the trickling filter-final clarifier system - the effluent temperature on the trickling filter unit (b) for the primary sedimentation (if meaningful) - average temperature on clarifier not much

different from tank effluent temperature, and (c) for the overall plant performance - either primary effluent temperature or average plant temperature.

ACKNOWLEDGEMENT

This study was conducted at the Engineering Research Institute, Department of Sanitary Engineering, Iowa State University, as a part of Project No. 1247 which was supported by The Procter and Gamble Company.

NOMENCLATURE

a,b,a',b',a'',b'' = empirical constants
d_p = particle diameter
f = fraction remaining
f_p = fraction remaining after primary treatment
f_s = fraction remaining after secondary treatment
g = gravity constant
k = a reaction rate constant, base e, time $^{-1}$
k_D = a reaction rate constant, base e, ft^{-1}
L = removable BOD originally present, mg/l
L_t = removable BOD present at time t, mg/l
T = temperature of wastewater, ^oC
T_F = temperature, ^oF
T_k = absolute temperature, ^oK
T_p = temperature most representative of the primary clarifier
T_s = temperature most representative of the trickling filter final clarifier
t = time
v = particle settling velocity
α = a constant which along with θ relates temperature to biological wastewater treatment efficiency
ε = reaction activiation energy
θ = a temperature coefficient
θ' = ln θ_s
θ'' = a constant in Equation (17)
u = absolute viscosity
ρ_1 = wastewater density
ρ_s = discrete particle density
ψ = ideal gas constant

REFERENCES

Baumann, E.R., F.D. Warner, and A. Adin (1979). Field evaluation of effect of aluminosilicate on wastewater treatment in trickling filter plants. Final Report, Engineering Research Institute Report No. 79006, Iowa State Univ., 497 p.

Camp, T.R. (1946). Sedimentation and the design of settling tanks. Trans. ASCE, 111, Paper 2285, 895-958.

Hanamanulu, V. (1970). Performance of deep trickling filters by five methods. J. Wat. Pol. Con. Fed., 42, 1446-1457.

Hawkes, H.A. (1960). Ecology of activated sludge and bacteria beds. In P.C.G. Isaac (Ed.), Waste Treatment, Proceedings of the Symposium on the Treatment of Waste Waters, Pergamon Press, London. pp. 52-98.

Hazen, A.M. (1904). On sedimentation. Trans. ASCE, 52, 45-71.

Lin, K.C. and G.W. Heinke (1977). Variability of temperature and other process parameters, a time series analysis of activated sludge plant data. Prog. in Wat. Tech., 9, 347-363.

Schroepfer, G.J., M.B. Al-Hakim, H.F. Seidel and N.R. Ziemke (1952). Temperature effects on trickling filters. Sew. Works J., 24, 705-723.

Schroepfer, G.J., M.L. Robins and R.H. Susag (1964). The research program on the Mississippi river in the vicinity of Minneapolis and St. Paul. In Advances in Water Pollution Research, vol. 1, Peergamon Press, London.

Standard Methods for the Examination of Water and Wastewater, (1975). 14th edition. Washington, D.C., American Public Health Association.

Velz, C.J. (1968). A basic law for the performance of biological filters. Sewage Works J., 20, 607-617.

Young, J.C., E.R. Baumann and S. Kelman (1969). Design considerations for expansion of water pollution control plant, Ames, Iowa. Engineering Research Institute Special Report ERI-520.

PHOSPHORUS REMOVAL

Wat. Sci. Tech. Vol.17, Amsterdam, pp.69-80.
Printed in Great Britain.

0273-1223/85 $0.00 + .50

THE ROLE OF AN ANAEROBIC STAGE ON BIOLOGICAL PHOSPHORUS REMOVAL

T. Fukase, M. Shibata and Y. Miyaji

Kurita Central Laboratories, Kurita Water Industries Ltd., 1723 Bukko-cho, Hodogaya-ku, Yokohama, Japan

ABSTRACT

A detailed study was conducted on biological removal of phosphorus by an activated sludge process composed of an anaerobic stage followed by an aerobic stage in order to clarify the role of the anaerobic stage of the process. Two distinctive sludges, one contained approximately 10 percent phosphorus, most of which existed in the form of polyphosphates, and the other contained 1.9 percent phosphorus, were obtained by changing BOD concentration of influent and hydraulic detention time of the process. Although the polyphosphate-containing sludge released phosphorus in proportion to the absorbed BOD at anaerobic conditions, the sludge which did not contain polyphosphates also absorbed an equal amount of BOD at the identical rate without any external sources of oxygen. Both sludges accumulated identical levels of poly-β-hydroxybutyrate within the sludges as the BOD sources were absorbed. These results suggest that the polyphosphate-containing sludges have no advantage over the sludges with no polyphosphates when they uptake BOD in the anaerobic stage.

KEYWORDS

phosphorus removal, activated sludge process, anaerobic stage, polyphosphates, poly-β-hydroxybutyrate.

INTRODUCTION

Extensive studies have been conducted on biological removal of phosphorus by an activated sludge process provided with an anaerobic stage in recent years (Barnard, 1975) owing to the fact that the process is inexpensive in operational costs and can be applied easily to existing activated sludge plants. Through experiences on pilot as well as commercial plants, the process has been considered to be effective for phosphorus removal. However, the mechanism of phosphorus removal in this process is not fully understood at this moment.

Several hypotheses have been proposed to explain the mechanism (Fuhs and Chen, 1975). Among these, a hypothesis by Hong *et al.* (1982) and Marais *et al.* (1982) may give a reasonable account for phosphorus release and BOD uptake in the anaerobic stage. According to the hypothesis, polyphosphates in microorganisms

provide energy to absorb soluble BOD under anaerobic conditions by hydrolyzing to orthophosphate. The resultant orthophosphate may be then released from the microorganisms. Therefore, polyphosphate-accumulating microorganisms would have a competitive advantage over other microorganisms in BOD absorption. However, since currently available data are not sufficient enough in quality and quantity to discuss the mechanism, further study will be needed to elucidate the role of the anaerobic stage of the process. The purpose of this study is to clarify the function of the anaerobic stage of the biological phosphorus removal process.

EXPERIMENTAL PROCEDURES

Continuous Feed Experiments

A schematic diagram of the treatment unit is as shown in Figure 1.The experimental unit consisted of two anaerobic vessels, the same number of aerobic vessels, and a settling vessel. A pH controller was installed at the first anaerobic vessel to maintain pH above 6.8. The composition of the synthetic wastewater is given in Table 1. BOD sources of this synthetic wastewater were composed of acetic acid, pepton, and yeast extract.

In this study, two identical experimental units, unit A and B, were operated simultaneously. Operational conditions of unit A were fixed throughout the operational period. On the other hand, unit B was operated in three different ways by changing flow rates of the influent dilution water and/or the return sludge. Excess sludge of each unit was removed from the second aerobic vessel to keep the MLVSS concentration in the range from 3,000 to 4,000mg/l. Since MLVSS concentrations and flow rates of the synthetic wastewater were maintained constant in unit A and B throughout the operations, the BOD loading rate per MLVSS in unit B was equal to that in unit A. Details of the operational conditions for each unit are summarized in Table 2.

Batch Tests

Release of phosphorus and uptake of BOD under anaerobic conditions were examined in the batch tests using the sludges produced in unit A and phase 3 of unit B. Contents of ATP and poly-β-hydroxybutyrate(PHB) in the sludge were also determined at the start and the end of the batch tests. Nitrate and nitrite in the mixed liquor were denitrified endogeneously prior to the batch tests in order to avoid the BOD removal by denitrification. A 0.5 liter Erlenmeyer flask was used as a reactor, and gas phase in the reactor was replaced with nitrogen gas.

TABLE 1 Composition of Synthetic Wastewater

Acetic acid	20	g
Pepton	10	"
Yeast extract	10	"
KH_2PO_4	8.8	"
$(NH_4)_2SO_4$	4.0	"
NaCl	15.0	"
$MgSO_4.7H_2O$	15.0	"
$CaCl_2.2H_2O$	0.5	"
Tap water	1.0	l

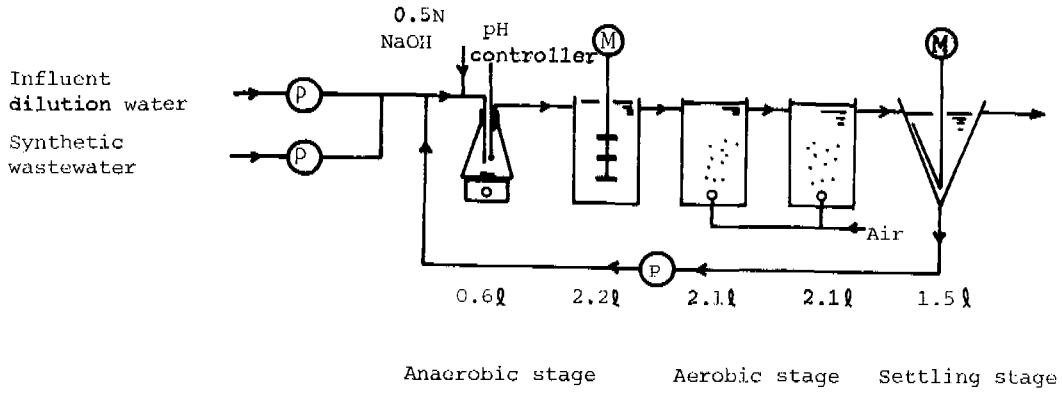

Fig. 1. Schematic diagram of biological phosphorus removal process

TABLE 2 Operational Conditions

		Unit A	Unit B		
			Phase 1	Phase 2	Phase 3
Influent BOD	(mg/l)	135	124	635	686
Influent flow rate	(l/day)	37.0	37.2	7.4	7.1
Return sludge flow rate	(l/day)	35.9	36.4	7.3	30.8
MLVSS	(mg/l)	3,470	3,650	4,120	3,790
Anaerobic stage detention time*	(hr)	1.82	1.81	9.08	9.46
Aerobic stage detention time*	(hr)	2.72	2.71	13.6	14.2
BOD loading rate**	(kg-BOD/kg-MLVSS.day)	0.20	0.18	0.16	0.18

* : Based on influent flow rate

** : Calculated by total volume of the anaerobic stage and the aerobic stage

BOD sources used in the batch tests were composed of acetic acid, pepton, and yeast extract, and the weight ratio of these constituents was 2:1:1. The pH was adjusted to 7.0 with sodium hydroxide solutions. The values of dosages of BOD sources shown in Figures 3 to 7 are the total weight of the three constituents. Temperature and pH were maintained at 25 ± 2°C and between 7.0 - 7.5, respectively. Analytical procedures were mainly based on the Japanese Industrial Standard K0102. Other analytical methods employed are listed in Table 3.

TABLE 3 Analytical Methods

Polyphosphates	1)	Hydrolysis with N hydrochloric acid at 100°C for 7 min.
	2)	Digested with alkaline hypochlorite, then extracted with distilled water(Harold,1963)
DNA		Extracted twice with 0.5N perchloric acid at 70°C for 15 min. and determined by Burton's method
RNA		Extracted with 0.5N perchloric acid at 37°C for 120 min. and determined by the orcinol reagent
ATP		Extracted with boiling tris buffer and determined by SAI ATP photometer
Protein		The Folin-Ciocalteu reagent
Carbohydrates	1)	The phenol-sulfuric acid reagent
	2)	The anthrone reagent
Poly-β-hydroxy butyrate		Digested with alkaline hypochlorite then extracted with hot chloroform and determined by the method developed by Law and Slepecky (Law and Slepecky, 1960)

TABLE 4 Averages of the Results

	Unit A		Unit B	
		Phase 1	Phase 2	Phase 3
Influent				
BOD (mg/l)	135	124	635	686
PO_4-P (mg/l)	11.7	10.7	52.9	58.2
Anaerobic stage(Filtered)				
BOD (mg/l)	5.7	6.0	41.1	8.8
PO_4-P (mg/l)	53.1	39.9	190	62.6
Filtered Effluent				
BOD (mg/l)	N.D	N.D	5.9	N.D
PO_4-P (mg/l)	2.9	1.6	46.2	56.5
NH_4-N (mg/l)	N.D	N.D	2.9	N.D
NO_x-N (mg/l)	5.2	1.3	25.8	8.2
MLSS (mg/l)	5,380	5,610	4,890	4,230
MLVSS (mg/l)	3,470	3,650	4,120	3,790
SRT* (days)	14.2	14.3	54.0	27.9
Yield (mg-cell/mg-BOD)	0.526	0.591	0.133	0.209
Phosphorus content in the sludge(%)	9.74	9.02	-	1.90**
$\Delta P/\Delta$ BOD(mg-P/mg-BOD)	0.0657	0.0734	0.0106	0.0025**

* Calculated by total volume of the anaerobic stage and the aerobic stage

** Averages for last 50 days

RESULTS

Continuous Feed Experiments

In biological wastewater treatment processes, the amount of phosphorus removed in a steady state may be expressed as following :

$$\Delta P = \Delta BOD . Y . Px$$

ΔP	:	Phosphorus removed	(mg/l)
ΔBOD	:	Removed BOD	(mg/l)
Y	:	Biomass yield	(mg-cell/mg-BOD)
Px	:	Phosphorus content in the sludge	(mg-P/mg-MLSS)

Therefore, the phosphorus removal efficiency was estimated by the phosphorus content in the sludge and the ratio of removed phosphorus to removed BOD ($\Delta P/\Delta BOD$) in this study.

Operational results are summarized in Table 4, and phosphate-phosphorus concentrations along with the phosphorus content in the sludge are as shown in Figure 2. Unit A attained 0.0657 of $\Delta P/\Delta$ BOD and 9.74 percent of phosphorus content in the sludge on the average during seven month operation. As regards unit B, the phosphorus removal efficiency was as high as that of unit A during phase 1 in which it was operated under exactly the same conditions as unit A. On the other hand, after operational conditions were changed to initiate phase 2, soluble phosphorus concentrations in the anaerobic stage increased to approximately 200mg/l, and phosphorus percent removal decreased immediately to less than 20 percent. Consequently, phosphorus content in the sludge declined gradually from 9 percent to 4.5 percent during phase 2. Though nitrate and nitrite concentrations in the effluent also increased when phase 2 started,the amount of nitrate and nitrite returned to the anaerobic stage was approximately equal to that of unit A. Therefore, adverse effects of nitrate and nitrite in the anaerobic stage were thought to be negligible. In phase 3 of unit B, the phosphorus removal efficiency remained poor, and the release of phosphorus in the anaerobic stage decreased. Averages of $\Delta P/\Delta$ BOD and phosphorus content in the sludge during last 50 days of phase 3 were calculated to be 0.0025 and 1.9 percent, respectively.

Since there was no difference in operational conditions between unit A and Phase 3 of unit B except for the flow rate of the influent dilution water, influent BOD concentration and/or hydraulic detention time had a significant influence on the phosphorus removal efficiency. It should be noted that the biomass yield decreased as much as 50 percent with decreasing the phosphorus removal efficiency.

Sludge Composition

The composition of the sludges produced in unit A and phase 3 of unit B were as compared in Table 5. Phosphorus in the sludge in unit A mainly existed in the form of polyphosphates, while the sludge in phase 3 of unit B contained virtually no polyphosphates.

Regarding inorganic constituents, magnesium and potassium contents in polyphosphate -containing sludge were higher than those in the sludge which did not contain polyphosphates, but contents of calcium, iron, and aluminium, which may react with phosphate to form insoluble compounds, showed no significant difference between the two sludges. Therefore, phosphorus removal by chemical precipitation was not taken into consideration in this study. The molar ratios of magnesium to phosphorus and potassium to phosphorus in the polyphosphate-containing sludge were 0.335 and 0.290, which indicate a good agreement with previous results(Fukase et al., 1982).

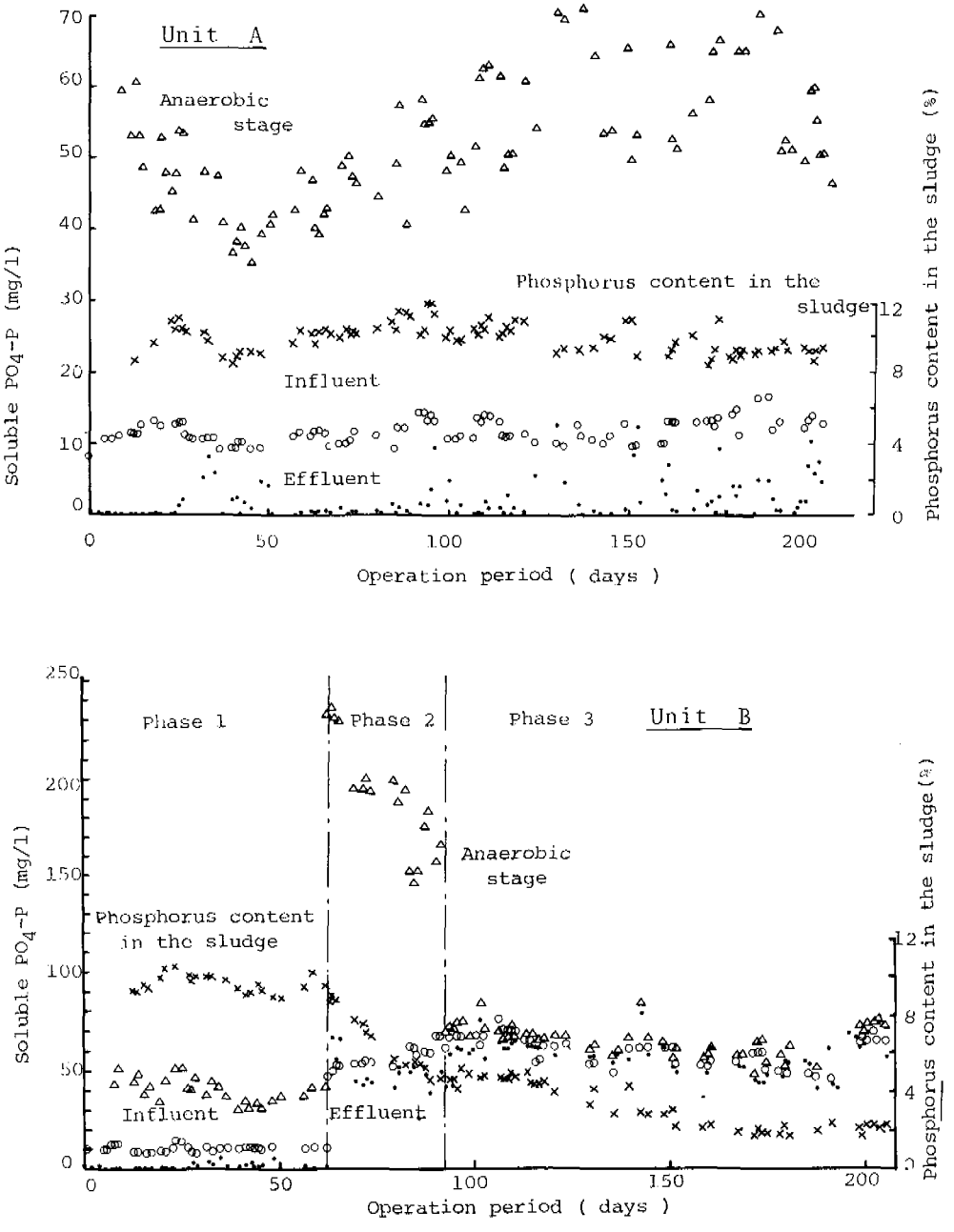

Fig. 2. Soluble phosphorus concentrations and phosphorus content in the sludge.

TABLE 5 Sludge Composition

Sludge	K	Mg	Ca	Al	Fe	P	Poly-P 1)	Poly-P 2)
Unit A	3.42	2.43	0.40	<0.1	0.08	9.38	8.04	6.47
Unit B	1.10	0.82	0.53	<0.1	0.06	2.05	1.02	0.09

Unit : % in MLSS 1) : Analyzed by N HCl hydrolysis
2) : " Harold's method

Sludge	DNA	RNA	ATP	Protein	Carbohydrates 1)	Carbohydrates 2)	PHB
Unit A	5.78	5.28	0.50	60.6	11.1	7.7	0.14
Unit B	3.50	5.30	0.33	50.2	22.4	14.4	0.22

Unit : % in MLVSS 1): Analyzed by phenol method
2): " anthrone method

With respect to the organic constituents, DNA, ATP, and protein in the polyphosphate-containing sludge were higher than those in the sludge which did not contain polyphosphates. This, together with the higher biomass yield, implies a good efficiency of cell growth. However, the RNA to DNA ratio and carbohydrate content were lower than those in the sludge with no polyphosphates.

Batch tests

It is well known that phosphorus is released from the sludge as BOD is taken up in the anaerobic stage of the biological phosphorus removal process. This phenomenon was confirmed in the batch tests using the polyphosphate-containing sludge. The effect of the concentration of the BOD sources on the release of phosphorus under anaerobic conditions is shown in Figure 3. It is clear from the figure that the phosphorus release from the sludge was greatly stimulated by the addition of the BOD sources. Since the added BOD sources were completely removed, it can be said that the amount of phosphorus released was directly proportional to the amount of removed BOD.

The influence of the MLSS concentration on the release of phosphorus and the uptake of TOC is as seen in Figure 4. The rate of the phosphorus release increased with increasing the concentration of MLSS, and this was the case with the rate of the TOC uptake. In addition, PHB in the sludge increased as the BOD sources were absorbed. The amount of increased PHB in the sludge accounted for 35.5 percent of the absorbed BOD sources by weight. From the Figures 3 and 4, the relationship between the removed TOC and the released phosphorus is shown in Figure 5, which clearly indicates a linear correlation.

The results of the test using the sludge with no polyphosphates are shown in Figure 6. Although this sludge did not release significant amounts of phosphorus, the BOD sources were taken up without any external sources of oxygen. The rate of TOC absorption and the amount of the absorbed TOC per unit weight of MLVSS were almost the same as those of polyphosphate-containing sludge. It should be noted that ATP contents at the start and the end of the test were 0.34 percent and 0.31 percent, respectively. Furthermore, PHB was also synthesized, and the amount of increased PHB in the sludge corresponded to 33.5 percent of the absorbed BOD.

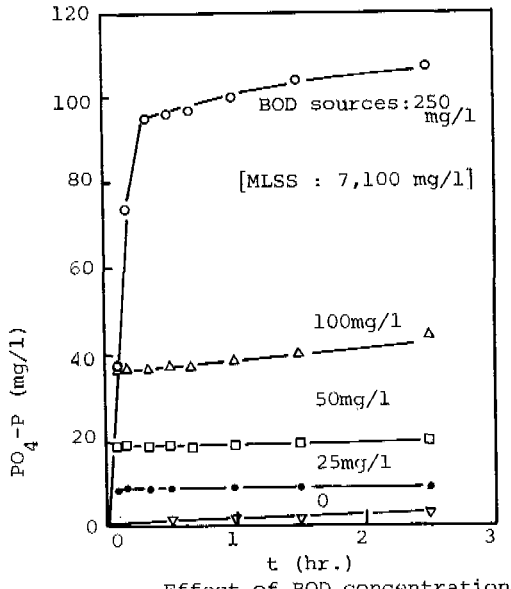

Fig.3. Effect of BOD concentration on phosphorus release

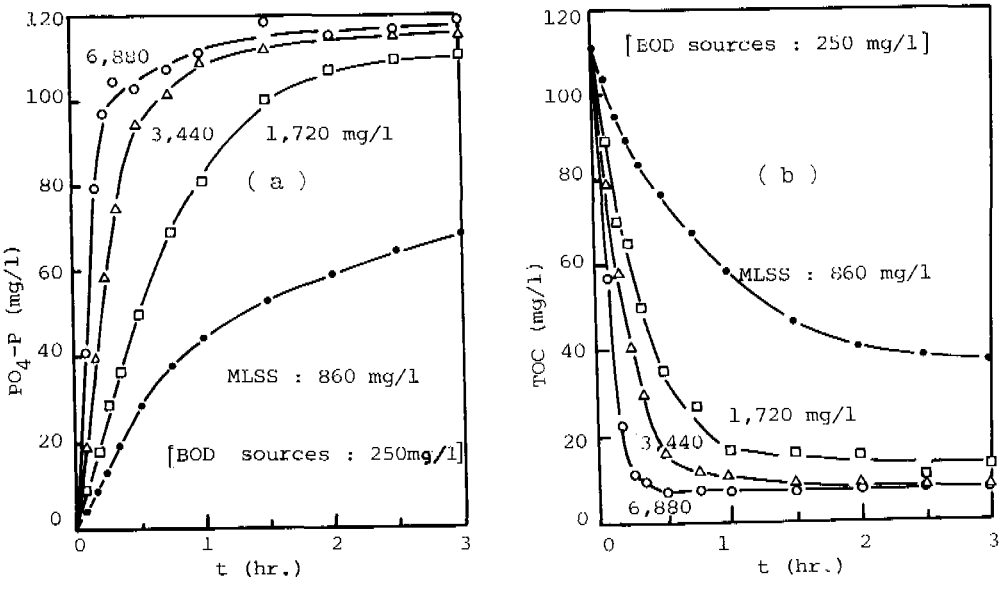

Fig. 4. Influence of MLSS concentration on phosphorus release and TOC uptake using polyphosphate-containing sludge

(a) : Profiles of phosphorus release (b) : Profiles of TOC uptake

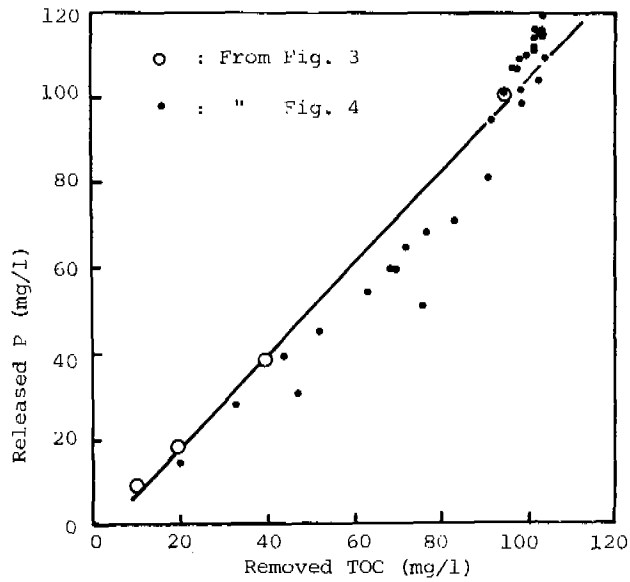

Fig. 5. Relationship between removed TOC and released phosphorus

Since it is expected from the results mentioned above that polyphosphates are not necessarily needed to absorb BOD anaerobically, BOD uptake at anaerobic conditions was examined using the sludge which had released all the polyphosphates. The excess sludge of unit A was stirred gently for three days under anaerobic conditions and washed three times with mineral solutions containing the same constituents as the influent except potassium dihydrogen phosphate. Then the sludge was aerated for one hour prior to use. Phosphorus content in the sludge was decreased from 9.18 percent to 1.28 percent by this treatment, and all of the polyphosphates were hydrolyzed. Uptake curves of the BOD sources by this sludge are as shown in Figure 7. Although the amount of TOC absorbed by this sludge was less than those by the other sludges and the rate of uptake was slower, it was evident that the BOD sources were taken up. Recovery of the added BOD sources as PHB were 28 percent by weight, and the ATP contents in the sludge at the start and the end were 0.38 percent and 0.30 percent, respectively. Therefore, it can be concluded that polyphosphates are not essential for the polyphosphate-containing sludge to absorb organic materials anaerobically.

DISCUSSION

This study presents two important findings : First, the addition of the anaerobic stage exclusive of both dissolved oxygen and oxidized nitrogen to an activated sludge process is not sufficient enough to cause excess removal of phosphorus. Second, the polyphosphates within the microorganisms are not necessarily essential to absorb BOD under anaerobic conditions.

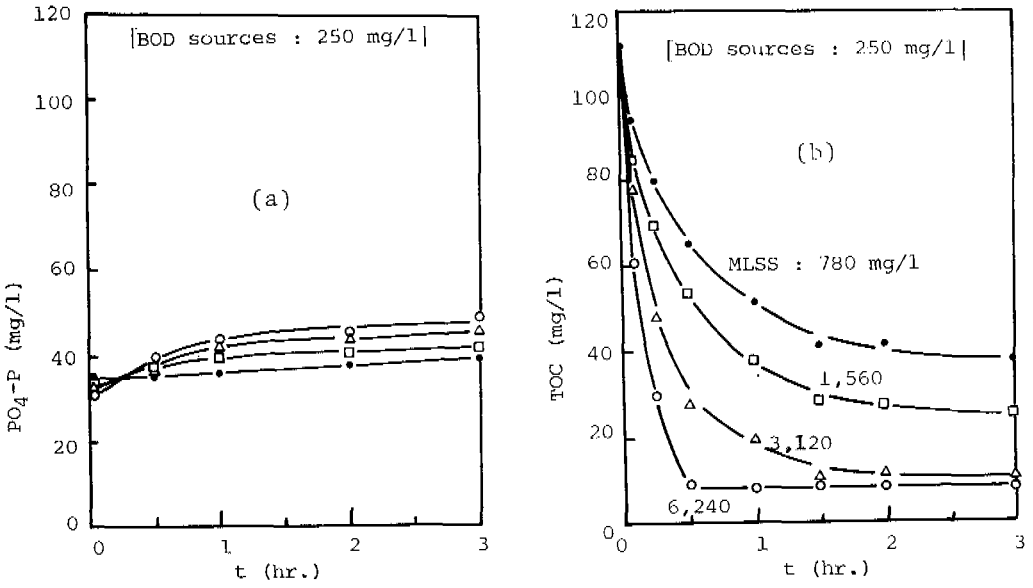

Fig. 6. Profiles of phosphorus release and TOC uptake using the sludge with no polyphosphates

(a) : Profiles of phosphorus release
(b) : Profiles of TOC uptake

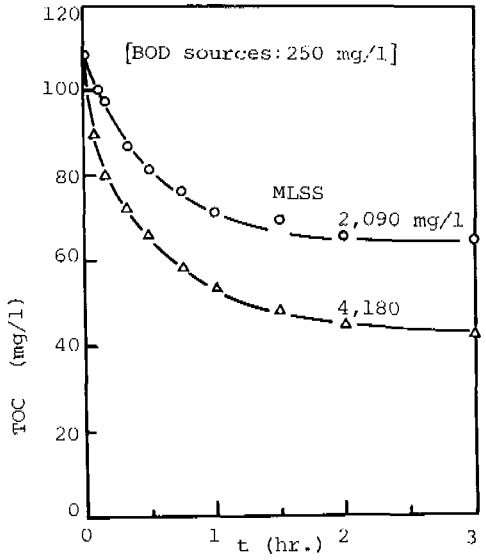

Fig.7. Profiles of TOC uptake using the sludge which had released all the polyphosphates

Unit A and B were operated using the identical apparatus provided with the anaerobic stage under identical BOD loading rate. The difference in operational conditions lies only in the concentration of influent BOD and the hydraulic detention time, but these resulted in a significant difference in the efficiency of phosphorus removal. The sludge in unit A contained almost 10 percent phosphorus, mainly in the form of polyphosphates. On the other hand, the sludge produced in phase 3 of unit B contained only 1.9 percent phosphorus, which is a representative value for regular activated sludges, and polyphosphates were not detected.

A similar experience was reported by Matsuo et al. (1982) that phosphorus was not removed excessively from night-soil by the anaerobic-aerobic activated sludge process. According to their report, COD concentration of influent was 1,500 mg/l, and nominal retention time of the process was 65 hours. Therefore, it is concluded that the addition of the anaerobic stage to the activated sludge process does not always result in removing excess amount of phosphorus, and that BOD concentration of influent and/or hydraulic retention time are important factors.

The results of the batch tests give some important information on the reason why the anaerobic-aerobic staging of the sludge does not always result in accumulating polyphosphates within the microorganisms. Though phosphorus removal efficiency decreased as soon as phase 2 was initiated, the microflora during the initial period of phase 2, not identified in this study, must be the same as those during the final period of phase 1. Therefore, even if appropriate microflora are established in the sludge, phosphorus is not always removed excessively by the anaerobic-aerobic activated sludge process. In addition, the sludge containing no polyphosphates absorbed an equal amount of BOD at the identical rate to that of the polyphosphate-containing sludge without any external sources of oxygen. These results lead to a question whether the anaerobic stage really serves as a selection zone for polyphosphate-accumulating microorganisms. Even if it is accepted that the anaerobic stage functions as a selection zone for certain microorganisms which can accumulate polyphosphates, the selected microorganisms do not always accumulate polyphosphates within the cell.

Three different sludges; polyphosphate-containing sludge, the sludge with no polyphosphates, and the sludge which had released all the polyphosphates previously contained, equally had an ability to absorb BOD and synthesize PHB under anaerobic conditions. This means that polyphosphates are not necessarily needed to absorb organic materials into microbial cell and synthesize PHB within the cell. Then, it is again emphasized that the polyphosphate-containing microorganisms appeared to have no competitive advantage over other microorganisms in BOD absorption under anaerobic conditions.

However, there still remains a possibility that polyphosphates may serve as an energy source to absorb BOD for the polyphosphate-containing sludge, for polyphosphates were hydrolyzed in proportion to the absorbed BOD. Moreover, no significant changes of ATP levels in the sludges were obtained during BOD absorption. Therefore, further study will be needed to determine if polyphosphates provide the energy for polyphosphate-containing microorganisms, and to identify the source which provides the energy for the other microorganisms to absorb organic materials under anaerobic conditions.

CONCLUSIONS

The following conclusions were obtained from the results of this study.

1. A sludge containing as high as 10 percent phosphorus in MLSS was obtained by operating an activated sludge process provided with an anaerobic stage using synthetic wastewater.
2. The same process operated at the identical BOD loading rate but with a higher influent BOD concentration and longer hydraulic retention time produced a sludge containing only 1.9 percent phosphorus.
3. Both sludges had an equivalent ability to absorb BOD and synthesize PHB without any external sources of oxygen.
4. It is suggested that polyphosphate-containing microorganisms have no advantage over other microorganisms when they uptake BOD in the anaerobic stage.

REFERENCES

Barnard, J.L. (1975). Biological phosphorus removal in the activated sludge process - Review and proposals. Paper presented at the Johannesburg branch of the Institute of Water Pollution Control.

Fuhs, G. W. and Chen, M. (1975). Microbial basis of phosphate removal in the activated sludge process for the treatment of wastewater. Microbial Ecology, 2, 119-138.

Fukase, T., Shibata, M. and Miyaji, Y. (1982). Studies on the mechanism of biological phosphorus removal. Japanese J. Water Pollut. Res. 5, 309-317.

Harold, F. M. (1963). Inorganic polyphosphate of high molecular weight from aerobacter aerogenes. J. Bact. 86, 885-887.

Hong, S. N., Krichten, D. J., Kisenbauer, K. S. and Sell, R. L. (1982). A biological wastewater treatment system for nutrient removal. Paper presented at EPA workshop on bioligical phosphorus removal.

Law, J. H. and Slepecky, R. A. (1960). Assay of poly-β-hydroxybutyric acid. J. Bact. 82, 33-36.

Marais, G. v. R. , Loewenthal, R. E. and Siebritz, I. (1982). Review : Observations suporting phosphate removal by biological excess uptake. Paper presented at IAWPR post conference seminar on phosphate removal in biological treatment processes.

Matsuo, Y.,Kitagawa, M.,Tanaka, T. and Miya, A. (1982). Sewage and Night-Soil Treatments by Anaerobic-Aerobic Activated Sludge Processes. Proc. of Environ. Sani. Eng. Research 19, 82-87.

Wat. Sci. Tech. Vol.17, Amsterdam, pp.81-92.
Printed in Great Britain.

0273-1223/85 $0.00 + .50

THE INFLUENCE OF EXTENDED ANAEROBIC RETENTION TIME ON THE PERFORMANCE OF PHOREDOX NUTRIENT REMOVAL PLANTS

A. Gerber and C. T. Winter

National Institute for Water Research, Council for Scientific and Industrial Research, P.O. Box 395, Pretoria 0001, South Africa

ABSTRACT

Laboratory-scale studies on the performance of three-stage Phoredox nutrient removal systems under nominal anaerobic retention times varying from 6 to 24 h are described. Particular attention is given to the effect of these extended periods of anaerobiosis on biological phosphate release and uptake, nitrification and denitrification. Increasing the retention time in the abovementioned range had no deleterious effect on nitrification, COD removal, sludge settleability and denitrification but resulted in significantly improved phosphate removals. Up to 15 mg/ℓ phosphate (as P) could be removed from settled wastewater at nominal anaerobic retention times of 12 h or more.

KEYWORDS

Biological phosphate removal; nitrogen removal; Phoredox process; activated sludge.

INTRODUCTION

The Phoredox wastewater treatment sequence (Fig. 1) is, by now, a well-known process for mainstream biological nutrient removal from municipal wastewater. Its performance has been studied extensively (Simpkins and McLaren, 1978; Gerber *et al.*, 1982; Ekama *et al.*, 1983; Paepcke, 1983; Pitman *et al.*, 1983).

Subjecting the sludge or mixed liquor to a period of anaerobiosis is generally accepted as a prerequisite to subsequent enhanced phosphate removal in the Phoredox process. The nature and extent of the anaerobic requirements have not been quantified, however, and designers of full-scale plants have had to rely largely on previous experience in sizing the anaerobic stage. In a survey of 11 plants designed for biological nitrogen and phosphate removal and having a physically distinct anaerobic basin, Paepcke (1983) recorded a mean nominal anaerobic retention time of 1.3 h, with individual values ranging from 0.6 to 1.9 h . Barnard (1983) states that the choice of these retention times, for what may be termed 'first generation' nutrient removal plants, was largely influenced by then prevalent predictions that overdesigning the anaerobic stage would be detrimental to the treatment processes occurring in such plants. However, subsequent studies indicated that nominal retention times in the anaero-

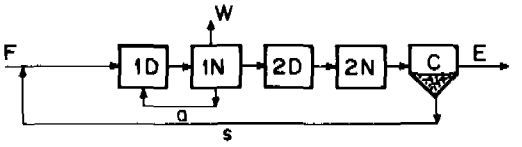

BARDENPHO®

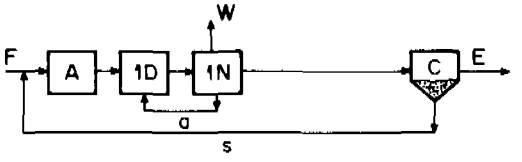

THREE-STAGE PHOREDOX

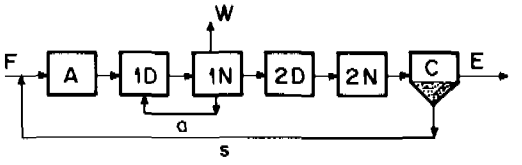

FIVE-STAGE PHOREDOX

LEGEND	
F : Feed	C : Clarifier
A : Anaerobic	E : Effluent
1D : Primary anoxic	W : Waste sludge withdrawal
1N : Primary aeration	a : a-recycle
2D : Secondary anoxic	s : s-recycle
2N : Secondary aeration	

Fig. 1. Schematic layout of the Bardenpho® and Phoredox nutrient removal systems

bic stage of 3 h and more resulted in improved and more reliable phosphate removal, with no apparent harmful effects on the other processes of interest (Gerber *et al.*, 1982). In view of the potentially important practical implications of this finding an investigation aimed at evaluating the long-term nutrient removal capacity of Phoredox plants under extended anaerobic conditions was initiated. The need for such a study was underscored by the relatively poor phosphate removal observed in many full-scale plants (Paepcke, 1983) and the realization that the deleterious effects accompanying the introduction of excessive amounts of nitrate and dissolved oxygen in the anaerobic stage may be counteracted by using longer anaerobic retention times.

This paper presents the results of studies on the influence of nominal anaerobic retention times in the range 6 to 24 h on the performance of laboratory-scale Phoredox systems. The choice of nominal retention time as a parameter was made for reasons of convenience, not necessarily because it is considered of fundamental importance *per se*. The entire range of retention times reported below are not necessarily considered practical from the design point of view. For purposes of this paper they should be viewed only as forcing functions employed to evaluate nutrient removal and other performance criteria when the mixed liquor is subjected to extreme conditions of anaerobiosis. In practical applications equivalent conditions may well be obtained by other means, such as subjecting only part or all of a sludge sidestream to extended periods of anaerobiosis.

MATERIALS AND METHODS

Four multiple reactor systems (Fig. 2), consisting of complete-mix basins in series and designated L1 to L4, were operated in parallel at a sludge age of 20 days. The study was performed at a constant temperature of 20 °C and under a nominal influent flow rate to each system of 24 ℓ/d . Sludge and mixed liquor recycle ratios with respect to influent flow rate were adjusted to target values as close as possible to s = 0.5 and a = 2.0 respectively. The actual influent and recycle flow rates were measured daily and recorded together with the rest of the data. The mixed liquor recycle was withdrawn from the penultimate aerobic basin, at which point nitrification was virtually complete, thereby achieving increased actual aerobic retention time. The dissolved oxygen level in the mixed liquor was maintained in the range 2.0 to 3.0 mg/ℓ and sludge was wasted from the final aerated basin once a day.

The influent to the experimental units consisted of settled wastewater collected around noon from the local municipal wastewater treatment plant on Mondays and Thursdays and stored in a cold room at 3 °C . Each batch was used for 3.5 days. Its COD was adjusted, by dilution with tap water, to values between 400 and 440 mg/ℓ . When the collected wastewater had a COD value of less than 440 mg/ℓ the feed was used as received. The phosphate concentration was also adjusted during part of the study, as described in the final paragraph of this section.

Daily monitoring consisted of analysing unfiltered samples of the feed and composite final effluent over 24 h, and filtered samples of the effluent, the contents of each basin and each recycle stream. AutoAnalyzers were employed for the daily analysis of nitrate, orthophosphate and ammonia while manual techniques (*Standard Methods*, 1981) were used for COD, TKN and total phosphate. Mixed liquor suspended solids (MLSS), volatile suspended solids (MLVSS) and effluent suspended solids concentrations were determined twice weekly using Whatman GF/A filters. Sodium, potassium, calcium, magnesium, sulphate, chloride, alkalinity, copper and iron were also determined twice weekly but only during the latter part of the study.

Nominal anaerobic retention times of 6, 12, 18 and 24 h were imposed on the experimental units. The corresponding unaerated volume fractions (clarifier excluded) were 60.0, 66.7, 73.3 and 77.8%. Each basin had a volume of 2 ℓ, with the exception of the third anaerobic basins of the 18 and 24 h systems, which had capacities of 10 and 16 ℓ respectively. The latter volumes were imposed by space limitations on the test bench and were not designed as such.

Batch experiments were performed occasionally to determine the phosphate uptake, nitrification and denitrification capacity of sludge deriving from the various basins in each continuous flow system. For the last anaerobic basin, which is

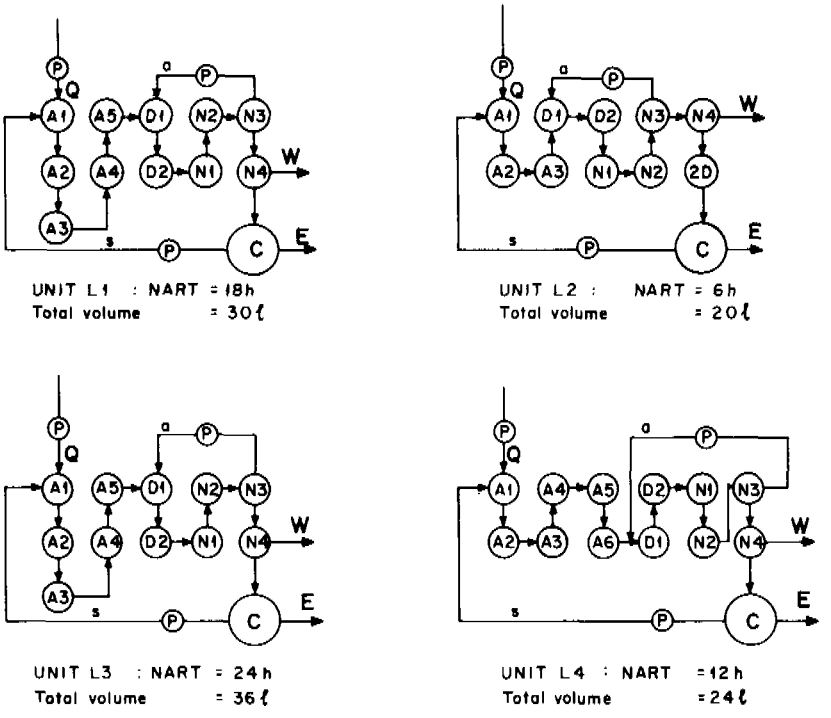

L E G E N D	
Q = Influent flowrate	A = Anaerobic
a = Mixed liquor recycle ratio	D = Anoxic
s = Sludge recycle ratio	N = Aerobic
P = Peristaltic pump	2D = Secondary anoxic
W = Waste sludge removal	E = Effluent
C = Clarifier	NART = Nominal anaerobic retention time

Fig. 2. Schematic layout of laboratory units used to study the effect of anaerobic retention time on biological nutrient removal

the only case considered below, 0.5 to 1.0 ℓ batches of mixed liquor from that basin were aerated for up to 7 h while monitoring phosphate, nitrate and ammonia concentrations. For determination of denitrification rates, similar batches of mixed liquor were introduced, without air entrainment, into a vessel pre-flushed with nitrogen. Sodium nitrate, to a concentration of 15 mg/ℓ (as N), was introduced subsequently at time zero and its disappearance monitored at discrete time steps, starting at 0.5 min . A continuous flow of nitrogen gas across the liquid surface in the container was employed to prevent the ingress of oxygen while these experiments were in progress.

This paper deals with two distinct phases of the study. From January to November 1982 the concentration of no influent compositional parameter other than COD was

adjusted, following the rule given above. During the period January to September 1983 COD adjustment was continued while the influent phosphate concentration was supplemented by the addition of approximately 20 mg/ℓ (as P) in the form of orthophosphoric acid. This was done so that the full phosphate removal capacity of the systems could be realized. In each phase the units were inoculated at start-up with fresh mixed liquor from a nitrifying-denitrifying activated sludge plant with no history of enhanced phosphate removal.

RESULTS AND DISCUSSION

Feed Characteristics

The mean feed composition during the two periods involved is summarized in Table 1. The influent was practically free of nitrate while the COD and TKN values, as well as the COD/TKN ratio, were virtually the same as those corresponding to flow-proportioned averages for the local municipal wastewater treatment plant. The increased phosphate concentration for the second phase of the study resulted from additional phosphate deliberately introduced into the feed so as to load the experimental systems beyond their normal phosphate removal capacity.

Phosphate Removal

The results in Table 2 indicate that an average influent total phosphate concentration of 10.6 mg/ℓ (as P) was reduced to values less than 1.0 mg/ℓ (orthophosphate as P). While the results for a nominal anaerobic retention time of 6 h were considered exceptionally good when seen in relation to the magnitude of the influent COD values and COD/TKN ratio, even better performance was obtained at retention times in the range 12 to 24 h, especially when appraised relative to the total mass of sludge in the corresponding anoxic and aerobic stages (Table 2). The average effluent concentrations of 0.2 mg/ℓ represent practically the detection limit of the analytical procedure used in this study and reflect the consistency with which low phosphate levels could be achieved.

Phosphate was released in the anaerobic stage to average concentrations ranging from 41 to 53 mg/ℓ (as P) in the last anaerobic basin. The minimum values in these basins practically never dropped below 35 mg/ℓ . For these relatively high values regression and correlation analysis failed to produce evidence of a relationship between the magnitude of the release and phosphate removal capacity. This is illustrated by the results for 6 h and 24 h retention times in Table 2 and leads to the conclusion that the observed values were above any minimum which may be required to induce subsequent enhanced uptake.

The *maximum* phosphate removal capacity of the four systems under the conditions of this study is illustrated by the results obtained while feeding phosphate-adjusted wastewater (Table 3). The average reductions in phosphate concentrations at nominal anaerobic retention times of 6, 12, 18 and 24 h were 9.2, 15.3, 13.9 and 15.7 mg/ℓ (as P) respectively. By increasing the retention time from 6 h to values in the range 12 to 24 h, significantly improved removals were achieved, the additional amounts varying between 50 and 70% of the levels at 6 h . Based on the relative amounts of MLSS contained in the anoxic and aerobic stages the increased reduction is even more noteworthy, being from 66 to 96% above the level of removal per unit MLSS observed at 6 h and increasing with anaerobic retention time.

TABLE 1 Average Composition of Influent to Laboratory Units (values in mg/ℓ)

Parameter	January to November 1982*	January to September 1983†
Chemical oxygen demand (COD)	369	385
Total Kjeldahl nitrogen (TKN-N)	41	39
Ammonia (NH_3-N)	27	30
Nitrate (NO_3-N)	0.3	0.2
Orthophosphate (PO_4-P)	8.5	30.7
Total phosphate (Total P)	10.6	34.5
COD/TKN-N	9.3	10.0
Sodium	-	79
Potassium	-	16.9
Calcium	-	29.3
Magnesium	-	16.7
Sulphate	-	65
Chloride	-	58
Total alkalinity (as $CaCO_3$)	-	266
Copper	-	0.09
Iron	-	0.5

*Each result based on 170 observations
†Each result based on 90 observations

TABLE 2 Average Values (in mg/ℓ where applicable) of Various Performance Parameters Measured in the Last Basin of the Indicated Process Stage (unadjusted influent phosphate concentrations, January to November 1982)

Parameter	Stage	Nominal anaerobic retention time (h)			
		6	12	18	24
PO_4-P*	Anaerobic	43	46	53	41
	Aerobic	0.9	0.3	0.2	0.2
	Effluent	0.7	0.2	0.2	0.2
NO_3-N*	Anoxic	1.2	0,6	0.4	0.3
	Effluent	5.9	6.4	6.1	6.3
NH_3-N*	Aerobic	0.2	0.2	0.2	0.2
MLSS†	Aerobic	3 355	2 522	2 432	2 072
MLVSS†	Aerobic	2 160	1 719	1 585	1 472

*Each result based on 170 observations
†Each result based on 60 observations, each in quintuplicate

Phosphate release rates declined through the anaerobic stage, being between 2.8 and 3.5 mg P/(g MLSS.h) initially (Table 4). Uptake commenced upon entry of the mixed liquor into the anoxic stage but only as long as positive nitrate concentrations were measured. These uptake rates, however, were generally less than half the 2.4 to 4.0 mg P/(g MLSS.h) recorded for the initial aerated basins. These latter values generally corresponded closely with those measured in batch uptake experiments, using mixed liquor from the last anaerobic basin (Table 5).

TABLE 3 Average Values (in mg/ℓ where applicable) of Various Performance Parameters Measured in the Last Basin of the Indicated Process Stage (supplemented influent phosphate concentrations, January to September 1983)

Parameter	Stage	Nominal anaerobic retention time (h)			
		6	12	18	24
PO_4-P*	Anaerobic	51	67	59	67
	Aerobic	25.3	19.2	20.9	18.8
	Effluent	24.2	19.3	20.8	18.0
NO_3-N*	Anoxic	2.1	0.5	0.8	0.8
	Effluent	7.4	7.6	7.1	7.6
NH_3-N*	Aerobic	0.2	0.2	0.2	0.3
	Effluent	0.2	0.2	0.2	0.2
MLSS†	Aerobic	2 924	2 932	2 495	2 593
MLVSS†	Aerobic	2 060	1 888	1 667	1 629

*Each result based on 90 observations
†Each result based on 30 observations, each in quintuplicate

That cation uptake and release should accompany phosphate uptake and release, respectively, would be expected from electroneutrality constraints on the liquid medium. The variation of cation and anion concentrations through the four experimental systems during the second phase of this study has been summarized in Tables 1 and 6. The significance of the observed changes is still being investigated but several noteworthy conclusions may be drawn from the results obtained.

Probably most important is that no significant relationship was found between phosphate release or uptake and calcium concentration in the experimental units. Along with sodium, chloride, copper and iron, calcium concentration displayed practically no variation upon passing from the influent through the anaerobic, anoxic and aerobic process stages. This indicates that calcium was not involved in precipitation or dissolution reactions involving phosphate. In contrast, the alternating release and uptake of phosphate was accompanied by an equivalent sequence for potassium and magnesium, which were released in the anaerobic stage and removed in the aerated zone. The average overall reduction in potassium concentration through the four systems ranged between 7 and 8 mg/ℓ, which is close on 50% of the mean influent concentration. Mole ratios of potassium released and taken up varied around 0.25 mol K/mol P in the anaerobic and aerated stages respectively. The corresponding net reduction in magnesium concentration ranged from 4 to 5 mg/ℓ, which is between 25 and 30% of the influent mean. The mole ratios of magnesium released and taken up were close to those observed for potassium, being about 0.25 mol Mg/mol P. The concentration pattern of potassium and magnesium was observed to hold for sulphate as well. The concentration of this anion *increased* significantly through the anaerobic stage, especially at nominal anaerobic retention times of 12 h and more. This increase was followed by a decrease in concentration, mainly through the anoxic zone, to levels near influent values (Table 6).

Nitrogen Removal

Practically complete nitrification was achieved consistently at all four nominal

TABLE 4 Average Net Removal Rates (in mg/(g MLSS.h)) of Phosphate (as P), Nitrate (as N) and Ammonia (as N) at Various Anaerobic Retention Times (negative values indicate either formation or release)

Parameter*	Basin†	Nominal anaerobic retention time (h)			
		6	12	18	24
PO_4-P	A1	-2.8	-3.4	-3.5	-3.4
	A2	-1.5	-2.3	-2.2	-2.3
	A3	-0.8	-1.5	-0.3	-0.6
	A4	NP	-1.3	-0.7	-0.4
	A5	NP	-0.8	-0.6	-0.6
	A6	NP	-0.5	NP	NP
	D1	1.3	1.6	1.6	1.7
	D2	0.0	0.3	0.1	0.7
	N1	2.4	4.0	3.8	4.0
	N2	1.3	2.9	2.6	3.4
	N3	0.9	1.5	1.8	2.1
	N4	0.6	1.2	1.3	1.3
NO_3-N	D1	0.9	1.4	1.4	1.4
	D2	0.6	0.5	0.5	0.6
	N1	-1.6	-1.6	-1.6	-1.7
	N2	-1.4	-1.6	-1.5	-1.6
	N3	-0.2	-0.5	-0.6	-0.6
	N4	0.0	-0.2	-0.2	-0.3
NH_3-N	N1	1.7	1.6	1.6	1.7
	N2	2.0	1.9	2.0	1.6
	N3	0.5	0.8	1.1	1.2
	N4	0.1	0.4	0.6	0.6

*Each result based on 60 observations in the period January to September 1983
†Refer Fig. 2 for basin configuration
NP=Not present for this retention time

TABLE 5 Average Net Removal Rates (in mg/(g MLSS.h)) of Phosphate (as P), Nitrate (as N) and Ammonia (as N) in Batch Samples from the Last Anaerobic Basin after Varying Anaerobic Retention Times (negative value indicates either formation or release)

Parameter	Condition	Nominal anaerobic retention time (h)			
		6	12	18	24
PO_4-P	Aerated	2.3	4.0	3.8	3.8
NO_3-N	Aerated	-1.8	-1.7	-1.8	-1.7
NH_3-N	Aerated	1.9	1.8	1.7	1.7
NO_3-N	Anoxic (initial NO_3-concentration 15 mg/ℓ as N)	1.0	1.4	1.4	1.5

TABLE 6 Average Concentrations (in mg/ℓ) of Selected Inorganic Constituents Measured in the Indicated Basin (supplemented influent phosphate concentrations, January to September 1983)*

Parameter†	Basin no.	Nominal anaerobic retention time (h)			
		6	12	18	24
K	First anaerobic	21.3	22.0	20.4	21.1
	Last anaerobic	24.7	29.5	27.0	28.6
	First aerobic	16.5	17.4	17.7	18.1
	Last aerobic	13.5	13.1	13.4	13.3
Ca	First anaerobic	29.3	28.4	28.5	28.5
	Last anaerobic	28.9	27.9	28.9	28.0
	First aerobic	28.6	29.1	29.2	29.0
	Last aerobic	28.8	28.9	28.9	29.9
Mg	First anaerobic	19.7	19.5	19.4	19.1
	Last anaerobic	21.5	24.4	23.0	25.1
	First aerobic	17.1	17.7	17.5	17.7
	Last aerobic	15.4	14.4	14.7	15.0
SO_4	First anaerobic	64	67	65	63
	Last anaerobic	68	78	74	76
	First aerobic	62	72	68	67
	Last aerobic	61	72	66	66
Total alkalinity (as $CaCO_3$)	First anaerobic	249	250	246	251
	Last anaerobic	248	257	248	261
	First aerobic	175	193	188	201
	Last aerobic	141	134	131	146

*Each result presented is based on 90 observations
†The concentrations of Na, Cl, Cu and Fe remained virtually unchanged from the influent values at all times

anaerobic retention times selected and effluent ammonia concentrations ranged close to the lower detection limit of the analytical procedure at all times.

Fears that extended periods of anaerobiosis may have detrimental effects on nitrification in the aerobic stage proved unfounded and average effluent ammonia concentrations of 0.2 mg/ℓ (as N) were achieved consistently during both experimental periods (Tables 2 and 3). The average net rates of nitrate formation and ammonia utilization in the initial basins of the aerobic stage (Table 4) correspond closely with previous results obtained during pilot-scale studies at the local municipal wastewater treatment plant while using nominal anaerobic retention times of less than 3 h . The results suggest that the nitrifying organisms were able to maintain the level of activity normally associated with the particular wastewater being treated, irrespective of nominal anaerobic retention time. In fact, the anaerobic stage *per se* had no detectable influence on the nitrification capacity of the four systems studied. Upon aerating batches of mixed liquor withdrawn from the last anaerobic basins nitrification rates in the range 1.7 to 1.8 mg NO_3-N/(g MLSS.h) were obtained (Table 5). These values are close to the rates obtained for the initial aerated basins (Table 4). Thus, the nitrifiers not only managed to survive nominal anaerobic retention times of up to 24 h but emerged with apparently undiminished nitrification capacity, which was resumed upon aeration without any noticeable lag.

Batch studies were also carried out to determine the denitrification capacity of mixed liquor withdrawn from the last anaerobic basin of each system. These experiments resulted in a single linear relationship between residual nitrate concentration above 0.5 mg/ℓ (as N) and elapsed time beyond 0.5 min, for all four units. Mean denitrification rates ranged from 1.0 mg N/(g MLSS.h) at 6 h nominal anaerobic retention time to about 1.4 at 12 h and beyond (Table 5). These values are practically the same as the corresponding averages observed for the first anoxic basins in each system under continuous flow conditions (Table 4). Regression analysis and analysis of variance techniques applied to the entire range of observations confirmed that the value corresponding to 6 h nominal anaerobic retention time was significantly lower than those for 12 h and more. Subjecting the mixed liquor to prolonged periods of anaerobiosis thus had a beneficial influence on initial denitrification rates.

Practically all the nitrate introduced into the anoxic stage via the mixed liquor recycle was reduced within the available retention time, leading to average effluent nitrate concentrations in the range 5.9 to 7.6 mg/ℓ (as N). It is evident from Tables 2 and 3 that these values did not prevent excellent phosphate removals from being obtained in the Phoredox systems employed in this study, in spite of average influent COD/TKN levels being between 9 and 10.

COD and Suspended Solids Removal

Effluent COD values were generally less than 25 mg/ℓ irrespective of anaerobic retention time between 6 and 24 h . Clear effluents with less than 1 mg/ℓ total suspended solids were produced consistently, based on sample volumes of 200 mℓ . As a result, there was practically no difference in the COD (as well as total phosphate and TKN values) of filtered and unfiltered effluent samples. The observed value is as good as or better than the results reported by Gerber *et al.* (1982) for pilot plant tests using settled wastewater from the same source but at nominal anaerobic retention times in the range 2 to 3 h . Under the experimental conditions of this study the removal of carbonaceous material was not in any way adversely affected by extended periods of anaerobiosis.

Sludge Separation

As in the case of COD removal, long periods of anaerobiosis had no adverse effect on the settleability of sludge in the final clarifier. Slight foaming occurred in the aeration basins at start-up but disappeared within about two days. Filamentous bulking was never observed to occur and SVI values ranged from 50 to 60 mℓ/g . These results reflect the excellent sludge settleability observed consistently during the investigation.

CONCLUSIONS

Unaerated volume fractions up to 78% of the active plant volume have no adverse effect on phosphate uptake in essentially three-stage Phoredox systems under conditions such as described.

Phosphate removal capacity per unit MLSS increased with increasing anaerobic retention time. At 6 h nominal anaerobic retention time between 9 and 10 mg/ℓ P was removed from settled wastewater, compared with about 15 mg/ℓ at 12 h or longer.

Phosphate release and uptake rates were maximal in the initial anaerobic and

aerobic basins respectively, with values in the corresponding ranges 2.8 to 3.5 and 2.4 to 4.0 mg P/(g MLSS.h) being typical.

Uptake and release of magnesium and potassium accompanied phosphate uptake and release in the experimental units. Mole ratios of approximately 0.25 of each cation/mol P were observed during release and uptake. Sulphate concentrations increased through the anaerobic stage but dropped to near influent levels in the anoxic stage.

The cations sodium, calcium, copper and iron remained constant through the process. Phosphate release and uptake could not be accounted for by dissolution or precipitation of calcium phosphate compounds.

Nitrification was unaffected by the imposition of nominal anaerobic retention times from 6 to 24 h at the experimental temperature of 20 °C . Mixed liquor from the end of the anaerobic stage exhibited a nitrification rate in the range 1.7 to 1.8 mg NO_3-N/(g MLSS.h), close to the rates for mixed liquor from the aerated zone under continuous flow conditions.

Average effluent nitrate concentrations during the study varied from 5.9 to 7.6 mg/ℓ (as N). Increased anaerobic retention time had a beneficial effect on denitrification rate, which varied from about 1.0 at 6 h to 1.4 mg NO_3-N/(g MLSS.h) at 12 h and beyond.

Removal of COD and total suspended solids was unaffected by extended periods of anaerobiosis. Average values respectively less than 25 and 1 mg/ℓ were obtained consistently.

Extended periods of anaerobiosis had no adverse effect on sludge separation characteristics. Filamentous bulking and foaming were not observed, typical SVI values being in the range 50 to 60 mℓ/g .

Overall, the benefits of extended anaerobic retention time on enhanced biological uptake have been established over a sufficiently long period that the practical application of nominal anaerobic retention times much longer than the customary 0.5 to 3 h can be recommended with confidence.

ACKNOWLEDGEMENT

This paper is published by permission of the Chief Director, National Institute for Water Research.

REFERENCES

Barnard, J.L. (1983). Background to biological phosphorus removal. *Wat. Sci. & Tech.*, 15 (3/4), 1-13.

Ekama, G.A., Siebritz, I.P. and Marais, G.v.R. (1983). Considerations in the process design of nutrient removal activated sludge processes. *Wat. Sci. & Tech.*, 15 (3/4), 283-318.

Gerber, A., Simpkins, M.J., Winter, C.T. and Scheepers, J.A. (1982). Biological Nutrient Removal from Wastewater Effluents: Performance Evaluation of the Phoredox and UCT Processes. CSIR Contract Report C WAT 52, prepared for the Water Research Commission, P.O. Box 824, Pretoria, South Africa.

Paepcke, B.H. (1983). Performance and operational aspects of biological phosphate removal plants in South Africa. *Wat. Sci. & Tech.*, 15 (3/4), 219-232.

Pitman, A.R., Venter, S.L.V. and Nicholls, H.A. (1983). Practical experience with biological phosphorus removal plants in Johannesburg. *Wat. Sci. & Tech.*, 15 (3/4), 233-259.

Simpkins, M.J. and McLaren, A.R. (1978). Consistent biological phosphate and nitrogen removal in an activated sludge plant. *Prog. Water Technol.*, 10 (5), 433-442.

Standard Methods for the Examination of Water and Wastewater (1981). Fifteenth edition, American Public Health Association, Washington, D.C.

Wat. Sci. Tech. Vol.17, Amsterdam, pp.93-106.
Printed in Great Britain.

0273-1223/85 $0.00 + .50

LOCATION OF PHOSPHORUS IN ACTIVATED SLUDGE AND FUNCTION OF INTRACELLULAR POLYPHOSPHATES IN BIOLOGICAL PHOSPHORUS REMOVAL PROCESS

Takashi Mino, Tomonori Kawakami and Tomonori Matsuo

Department of Urban and Sanitary Engineering, The University of Tokyo, 7-3-1, Hongo, Bunkyo-ku, Tokyo, 113, Japan

ABSTRACT

The STS method, a method for the fractionation of intracellular phosphorus, was introduced into the examination of the phosphorus location of activated sludges, and some basic aspects involved in the biological phosphorus removal process were investigated from biological points of view. Although both lowmolecular and highmolecular polyphosphates appeared in the sludges produced in the biological phosphorus removal process, the high phosphorus content of the sludges was caused mainly by the accumulation of lowmolecular polyphosphates and lowmolecular polyphosphates were principally responsible for the release and uptake of phosphorus. The turnover of phosphorus in lowmolecular and highmolecular polyphosphates was investigated by using ^{32}P-labelled orthophosphate as a tracer. The phosphorus turnover in lowmolecular polyphosphates was not observed under both anaerobic and aerobic conditions, while the phosphorus turnover in highmolecular polyphosphates occurred under the aerobic conditions. It was indicated that lowmolecular polyphosphates function as the energy pool under the anaerobic conditions and that highmolecular polyphosphates function as the phosphorus source for the microbial growth.

KEYWORDS

Activated sludge, biological phosphorus removal, anaerobic-oxic method, fractionation of intracellular phosphorus, polyphosphates, turnover of phosphorus.

INTRODUCTION

Phosphorus is one of the ingredients in the natural water that are responsible for the eutrophication in the closed water bodies. In order to delay the progress of the eutrophication, it is necessary to remove phosphorus from the wastewater. Recently, the anaerobic-oxic biological phosphorus removal process (Gardieri, 1979) or the phoredox process (Barnard, 1975) was developed through the investigation into the activated sludge processes where the high phosphorus removal efficiency was achieved. The flow diagram of this process is illustrated in Fig. 1. The anaerobic-oxic process is expected to be one of the most energy-saving and excellent methods for the removal of phosphorus. The unique feature of this process is the introduction of the anaerobic stage at the influent end of the

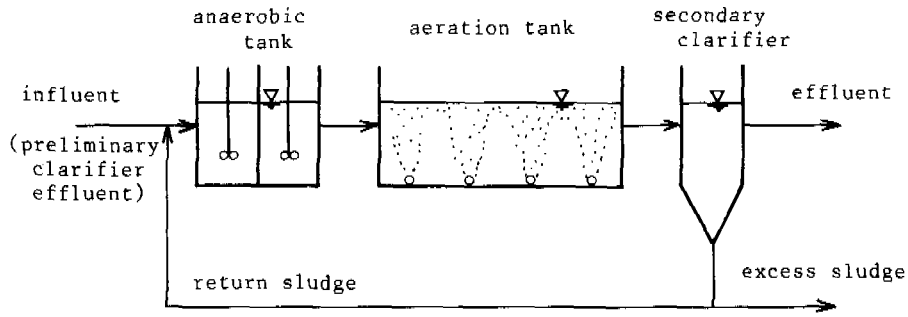

Fig. 1. Flow Diagram of Anaerobic-Oxic Process

aeration tank. Several investigators indicate (Nicholls & Osborn, 1979; Barnard, 1976) that the phosphorus content of the sludge begins to increase when the sludge passes through the anaerobic stage with the organic substrates during the routine cycle of the process. The high phosphorus removal efficiency can be achieved by this sludge with high phosphorus content.

In the anaerobic-oxic process, the following phenomena have been observed and reported (Buchan, 1982; Barnard, 1982):

(1)The anaerobic conditions with the organic substrates stimulate the accumulation of polyphosphate in the activated sludge microorganisms.

(2)In the anaerobic stage, the organic substrates are taken into the activated sludge microorganisms and at the same time orthophosphate is released from them.

(3)In the aerobic stage, more orthophosphate is taken into the sludge microorganisms than the sludge releases in the anaerobic stage.

Generally speaking, the following concepts are admitted for the explanation of these facts:

(1)In the anaerobic-oxic process, the microorganisms that have the ability to utilize the organic substrates under the anaerobic conditions become predominant.

(2)The polyphosphates accumulated in the sludge function as the energy source for the uptake of organic substrates under the anaerobic conditions, which is possible because the polyphosphates are thermodynamically "high energy" compounds.

(3)The release of phosphorus under the anaerobic conditions is the result of the polyphosphate utilization, and the followed uptake of phosphorus under the aerobic conditions is the result of polyphosphate biosynthesis by the microorganisms in the sludge.

These concepts have not been proved experimentally and the functions of polyphosphates have not been clarified satisfactorily.

In order to establish the anaerobic-oxic process as a stable technique for the phosphorus removal, it is necessary to obtain experimentally an adequate explanation of the phenomenon. The purpose of our investigation is to clarify some basic aspects involved here from biological points of view. For this purpose, the STS method, Schmidt-Thannhauser-Schneider method, (Schmidt & Thannhauser, 1945; Schneider, 1946) is employed in this study to measure the polyphosphates and other phosphorus compounds in the activated sludge. This method is a technique to fractionate the intracellular phosphorus compounds. By means of the STS method, the following three aspects are examined: (1)The differences of phosphorus location among the sludges of various phosphorus content; (2)The behaviour of polyphosphates and other phosphorus compounds during the release and uptake of phosphorus in the anaerobic-oxic process; (3)The occurence of phosphorus turnover in polyphosphates. The characteristics of phosphorus distribution and the

functions of polyphosphates in the sludges produced in the anaerobic-oxic process are discussed.

ANALYTICAL METHODS

The authors modified the original STS method to fractionate and analyze some phosphorus compounds in the activated sludge. The fractionation procedure and the analytical methods employed in this study are shown in Fig. 2. Following this procedure, some phosphorus compounds in the sludge such as intracellular polyphosphates, nucleic acids, and the phosphorus in the form of insoluble metal salts are determined.

In the present STS method, the intracellular polyphosphates are extracted into two

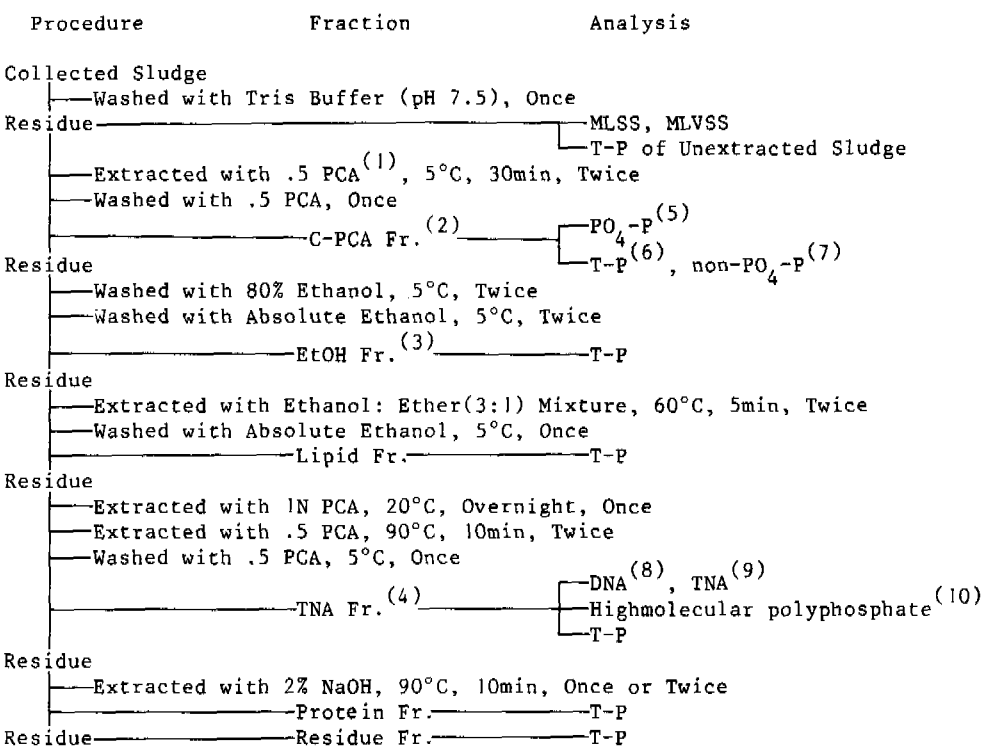

Fig. 2 Procedure of Phosphorus Fractionation by STS Method

Note: (1)Perchloric Acid (2)Cold PCA Extractable Fraction (3)Ethanol Extractable Fraction (4)Total Nucleic Acids Fraction (5)Determined by the ascorbic acid method (6)Determined by the potassium persulfate degradation method (7)Defined as T-P minus PO_4-P in C-PCA Fr. (8)Determined by the diphenylamine method (9)Determined by the UV absorption method (10)Nucleic acids are removed from TNA Fr. by charcoal adsorption and labile-P (determined by the degradation with 1N sulfuric acid at 100°C for 7 minutes) in the residue supernatant of the charcoal adsorption treatment is defined as the amount of highmolecular polyphosphates.

different fractions. The lowmolecular polyphosphates are extracted into C-PCA Fr. and determined as non-PO_4-P. The highmolecular polyphosphates are extracted into TNA Fr. and determined as labile-P after the removal of nucleic acids by the charcoal adsorption treatment. Strictly speaking, non-PO_4-P in C-PCA Fr. involves the phosphorus compounds in addition to the polyphosphates. However, it is indicated by Mino et al (1983) that the amount of phosphorus except the polyphosphates is below 0.91 mgP/gVSS in non-PO_4-P in C-PCA Fr. and that the phosphorus portion beyond this level corresponded to the lowmolecular polyphosphates. As shown later in Fig. 4. A, the sludge obtained from the anaerobic-oxic processes contain much higher level of non-PO_4-P in C-PCA Fr., therefore it is proper to consider that non-PO_4-P in C-PCA Fr. represents the amount of lowmolecular polyphosphates in most cases. The measured values of highmolecular polyphosphates must be reliable, because highmolecular polyphosphates are determined after the refining by the removal of the nucleic acids in TNA Fr.. It is very advantageous to the investigation concerning the functions of intracellular polyphosphates that the lowmolecular polyphosphates and the highmolecular polyphosphates can be determined separately.

It is indicated (Mino et al, 1983) that the chemically precipitated metal phosphates are extracted into C-PCA Fr. and determined as PO_4-P by the STS method. The orthophosphate originated from the living cells is also determined as PO_4-P. The amount of biologically originated orthophosphate is below 0.75 mgP/gVSS and the phosphorus portion beyond this level is considered to correspond to that of insoluble metal phosphates (Mino et al, 1983). The sludges produced in the practical sewage treatment plants usually contain much higher levels of metal phosphates than 0.75 mgP/gVSS. In those cases, therefore, it can be accepted that PO_4-P in C-PCA Fr. represents the amount of metal phosphates.

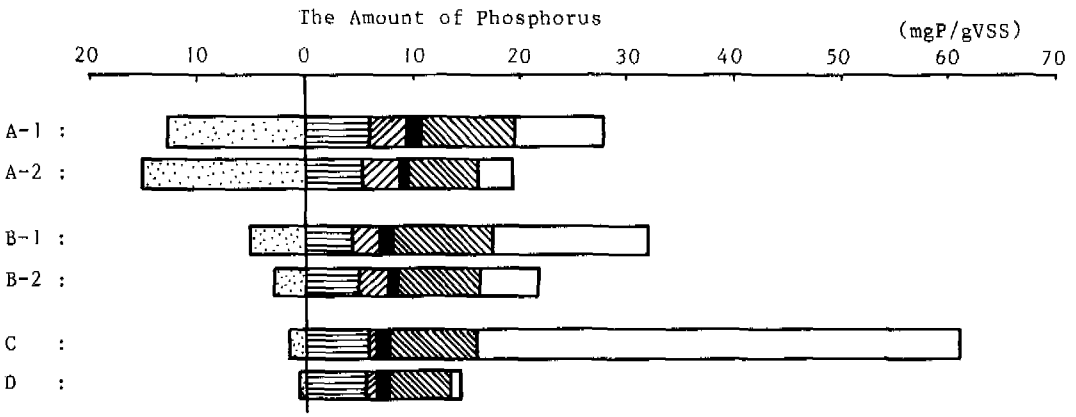

Fig. 3. Phosphorus Distribution in Various Activated Sludges

: PO_4-P in C-PCA Fr. (Metal Phosphates)
: Nucleic Acids
: Residue Fr. + Protein Fr.
: Lipid Fr. + EtOH Fr.
: Highmolecular polyphosphates
: Non-PO_4-P in C-PCA Fr. (Lowmolecular Polyphosphates)

EXPERIMENTAL AND RESULTS

The Differences of the Phosphorus Location Among Sludges

Methods. For the purpose of investigating the characteristics of phosphorus location in the sludge, various types of sludges were analyzed by the STS method. The sludge samples were obtained from the practical activated sludge plants and the pilot plants of the anaerobic-oxic process in Tokyo and its vicinity, and from the laboratory-scale systems of the anaerobic-oxic process and the conventional type activated sludge process. All the sludges were sampled at the effluent end of the aeration tank and analyzed as soon as possible.

Results. More than one hundred activated sludge samples are analyzed by the STS method in this study. The phosphorus content of the sludge ranges from 6 to 70 mgP/gMLSS. The phosphorus distribution in the sludge varied very much among sludges depending upon their phosphorus content. Some typical results of the analysis are shown in Fig. 3. In these bar graphs, the lefthand portion of the vertical line represents PO_4-P in C-PCA Fr., which approximately corresponds to the metal phosphates precipitated in the sludge. The righthand portion represents the phosphorus amount originated from microbial cells. The salient feature of these results is that the lowmolecular polyphosphates and the insoluble metal phosphates are mostly responsible for the differences of the phosphorus distribution among the sludges. In Fig. 3, the sludges sampled from the conventional type plants (A-2 and B-2) are compared with those sampled from the neighbouring anaerobic-oxic plants (A-1 and B-1, respectively). It is indicated that the amount of lowmolecular polyphosphates increase in the anaerobic-oxic process or in the system where the sludge comes into contact with the organic substrate under the anaerobic conditions. This is indicated more clearly by the results of the sludge sampled from the laboratory-scale anaerobic-oxic process (C). The sludge sampled from the laboratory-scale conventional-type process where the aerobic conditions are continuously maintained accumulates hardly any lowmolecular polyphosphates, although the accumulation of highmolecular polyphosphates is observed (D).

All the analytical data are plotted in Fig. 4, A, B, C, and D, in which the relationships between the total phosphorus amount originated from the microbial cells and the amount of some fractionated phosphorus portions are shown. In these figures, Total-P in the sludge minus PO_4-P in C-PCA Fr. is regarded as the phosphorus portion originated from the microbial cells, because PO_4-P in C-PCA Fr. approximately corresponds to the amount of precipitated metal phosphates. The lowmolecular polyphosphates appear only in the sludges which contained more than 20 mgP/gVSS of biologically originated phosphorus. The accumulation of lowmolecular polyphosphates is principally responsible for the biological increase of the phosphorus content of the sludge. It is suggested that lowmolecular polyphosphates are accumulated to a high extent in the anaerobic-oxic process. Highmolecular polyphosphates appear in almost all sludges analyzed here, but the sludges cultivated under phosphorus deficient conditions and containing not more than 10 mgP/gVSS of phosphorus accumulate hardly any highmolecular polyphosphates. The increase of intracellular phosphorus content can be reasoned out by the increase of the sum of lowmolecular and highmolecular polyphosphates, or the total polyphosphates as shown in Fig. 4, C. The amounts of biologically originated phosphorus except the polyphosphates have no significant differences among the sludges as shown in Fig. 4, D.

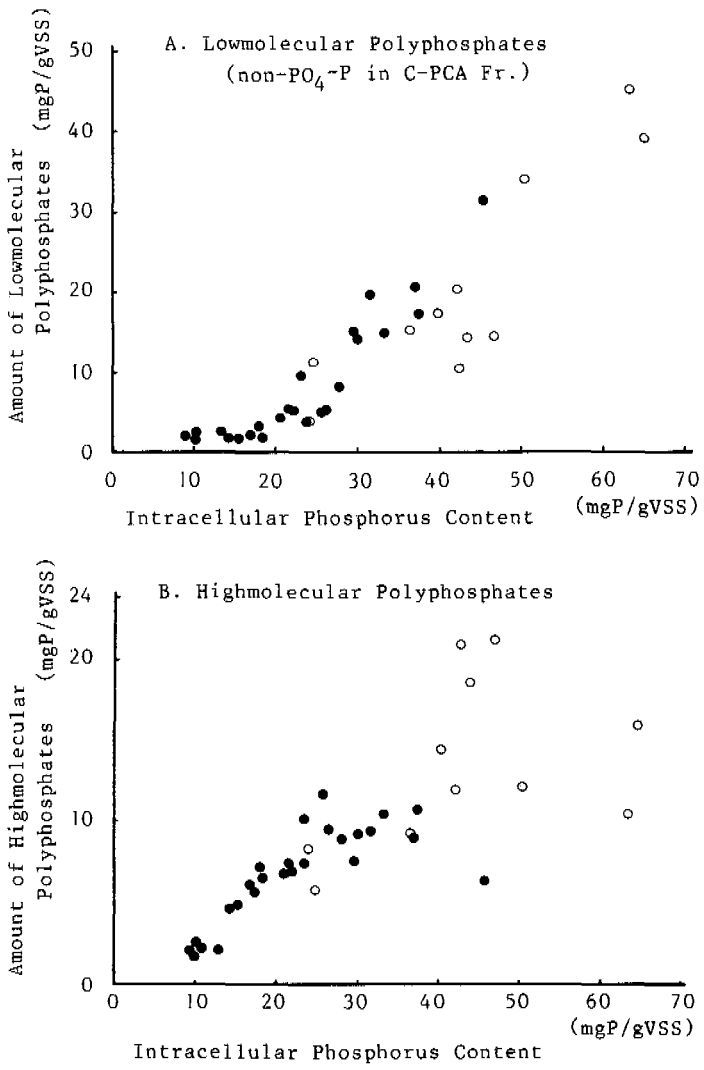

Fig. 4. The Relationships between the Total Phosphorus Amount Originated from the Microbial Cells and the Amount of the Fractionated Phosphorus Portions. (continued)

○ : Laboratory Anaerobic-Oxic Process
● : Practical Sewage Treatment Plant

Behaviour of Intracellular Phosphorus Compounds in the Course of Anaerobic-oxic process

Experimental. In order to investigate the behaviour of intracellular phosphorus compounds in the course of the anaerobic-oxic process, a series of batch experiments simulating the anaerobic-oxic process were performed. The sludges used were sampled at the effluent end of the aeration tank in the pilot plants and the

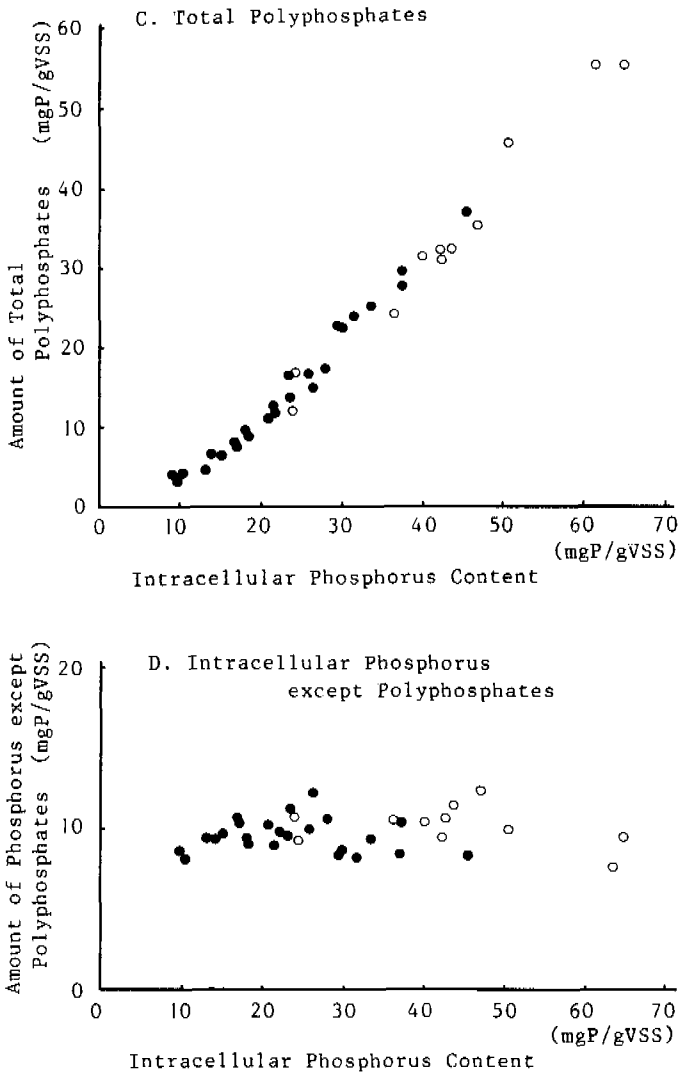

Fig. 4. The Relationships between the Total Phosphorus Amount Originated from the Microbial Cells and the Amount of the Fractionated Phosphorus Portions.

o : Laboratory Anaerobic-Oxic Process
● : Practical Sewage Treatment Plant

laboratory plants of the anaerobic-oxic process. After the addition of the organic substrate to the batch reactor, the sludge was kept under the anaerobic conditions for an hour or two and then aerated. The sludge mixed liquor was sampled at appropriate time intervals and the phosphorus distribution and some other parameters were analyzed.

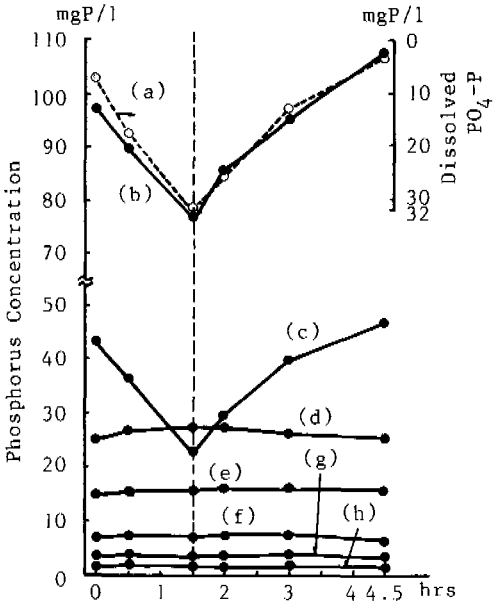

(a)Filtered PO_4-P
(b)T-P of Unextracted Sludge
(c)Non-PO_4-P in C-PCA Fr.
(Lowmolecular Polyphosphates)
(d)Highmolecular Polyphosphates
(e)Nucleic Acids
(f)PO_4-P in C-PCA Fr.
(Metal Phosphates)
(g)Lipid Fr. plus EtOH Fr.
(h)Protein Fr. plus Residue Fr.

Fig. 5. Typical Behaviour of Phosphorus Compounds in the Sludge and Filtered PO_4-P during the Anaerobic-Oxic Batch Experiment.

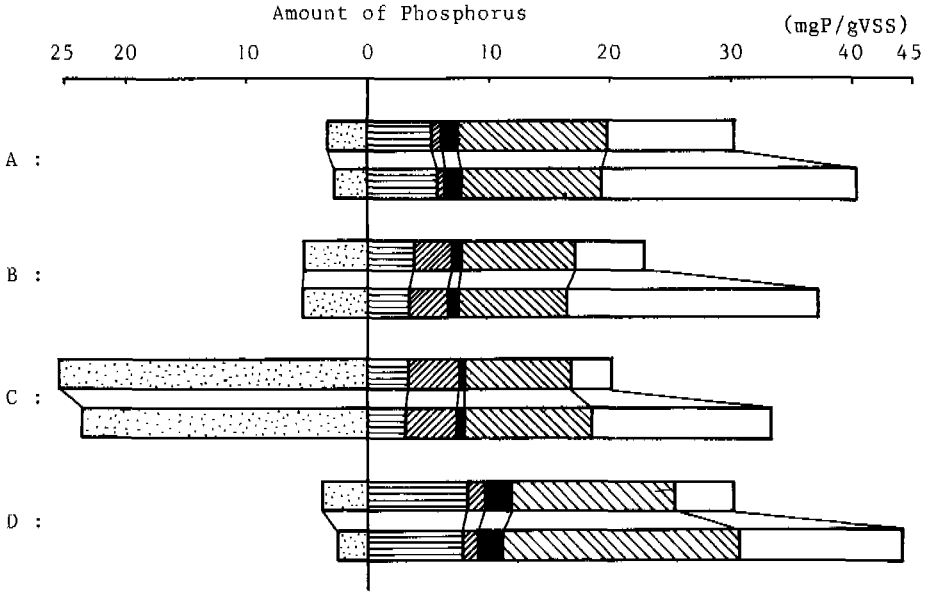

Fig.6. Intracellular Phosphorus Distributions at the End of the Anaerobic Period and after Hours of Aeration in the Anaerobic-Oxic Batch Experiment.

Legend : Refer to Fig. 3.

Results. The typical behaviour of the phosphorus compounds in the sludge and dissolved PO_4-P during the batch experiment is illustrated in Fig. 5. In the present case, 10 mgP/gMLSS of phosphorus is released to the bulk solution under the anaerobic conditions. The intracellular source of the released phosphorus is lowmolecular polyphosphates. Under the aerobic conditions, the sludge absorbs phosphorus and recovers the initial level of lowmolecular polyphosphates. Although this sludge contains higher level of highmolecular polyphosphates than the normal sludges produced in the activated sludge process of conventional type, highmolecular polyphosphates make little or no contribution to the release and uptake of phosphorus.

The phosphorus distributions at the end of the anaerobic period and after hours of aeration are picked up from the results of similar experiments, and four examples of them are illustrated in Fig. 6. In all the cases the intracellular phosphorus compound which is principally responsible for the release and uptake of phosphorus is lowmolecular polyphosphates. In the case of example D which reveals exceptionally high content of highmolecular polyphosphates, the significant amount of phosphorus release caused by highmolecular polyphosphates is observed. However, the contribution of highmolecular polyphosphates to the phosphorus release is smaller than that of lowmolecular polyphosphates. It is suggested that the physiological function proper to the anaerobic-oxic process , or the function to serve as the energy source under the anaerobic conditions, is performed by intracellular lowmolecular polyphosphates, although both lowmolecular and highmolecular polyphosphates are accumulated in the sludge in the anaerobic-oxic process.

Occurence of Phosphorus Turnover in Lowmolecular and Highmolecular Polyphosphates

Experimental. It is indicated in the above examinations that lowmolecular polyphosphates and highmolecular polyphosphates have the different functions in the metabolism under the anaerobic and oxic conditions. Two possible functions are postulated for polyphosphates (Harold, 1966). One is the function to serve as the energy pool and the other to supply the phosphorus source. If polyphosphates function as the energy source, they must be degraded under phosphorus deficient conditions and synthesized along with the active energy production. In this case, the degradation reactions and the synthesis reactions of polyphosphates must not occur at the same time, or the phosphorus turnover in the polyphosphates must not be observed. On the contrary, if polyphosphates function as the phosphorus source for the microbial growth, the polyphosphate degradation to supply required phosphorus and the polyphosphate synthesis to maintain the sufficient level of polyphosphates must occur at the same time and the phosphorus turnover in polyphosphates must be observed under the aerobic conditions. In the examination of this section, the occurrence of the phosphorus turnover in some intracellular phosphorus compounds is investigated in the course of the anaerobic-oxic process in order to clarify the functions of polyphosphates in the microbial cells.

The batch experiments including the anaerobic period and the aerobic period are set up, in which ^{32}P-labelled orthophosphate is used as a tracer to investigate the occurrence of the turnover of the polyphosphates and other phosphorus compounds. The sludges cultivated in the laboratory plants of the anaerobic-oxic process are used for these experiments. After adding the ^{32}P-labelled orthophosphate together with the organic substrates to the batch reactor, the phosphorus in the sludge is fractionated by the STS method at appropriate time intervals and the distribution of the phosphorus and the radioactivity in the sludge is examined. The radioactivity measurement is performed by the liquid scintillation spectrometer and all the experiments using the radioisotope are performed in the Radioisotope Centre of the University of Tokyo.

Results. The typical changes of the phosphorus and radioactivity distribution are illustrated in Fig. 7. During the phosphorus release under the anaerobic conditions, the transfer of the ^{32}P-orthophosphate from the bulk solution to the inside of the sludge is not observed. Under the aerobic conditions, ^{32}P-orthophosphate is taken into the sludge and the radioactivities in C-PCA Fr. containing lowmolecular polyphosphates and in highmolecular polyphosphates are increased. The radioactivities in other fractions are increased under the aerobic conditions, but their quantitative changes are very small.

In order to calculate the actual quantitative changes of the existent phosphorus from the analytical data of the radioactivities, the following assumptions can be postulated:

(1)The phosphorus transfer into the nucleic acids (DNA, RNA), Lipid Fr., and Residue Fr. are almost negligible in amount.

(2)The phosphorus transfer between lowmolecular polyphosphates and highmolecular polyphosphates does not occur. This concept is supported by Harold's indication that polyphosphates are synthesized only by the polyphosphate kinase reaction,

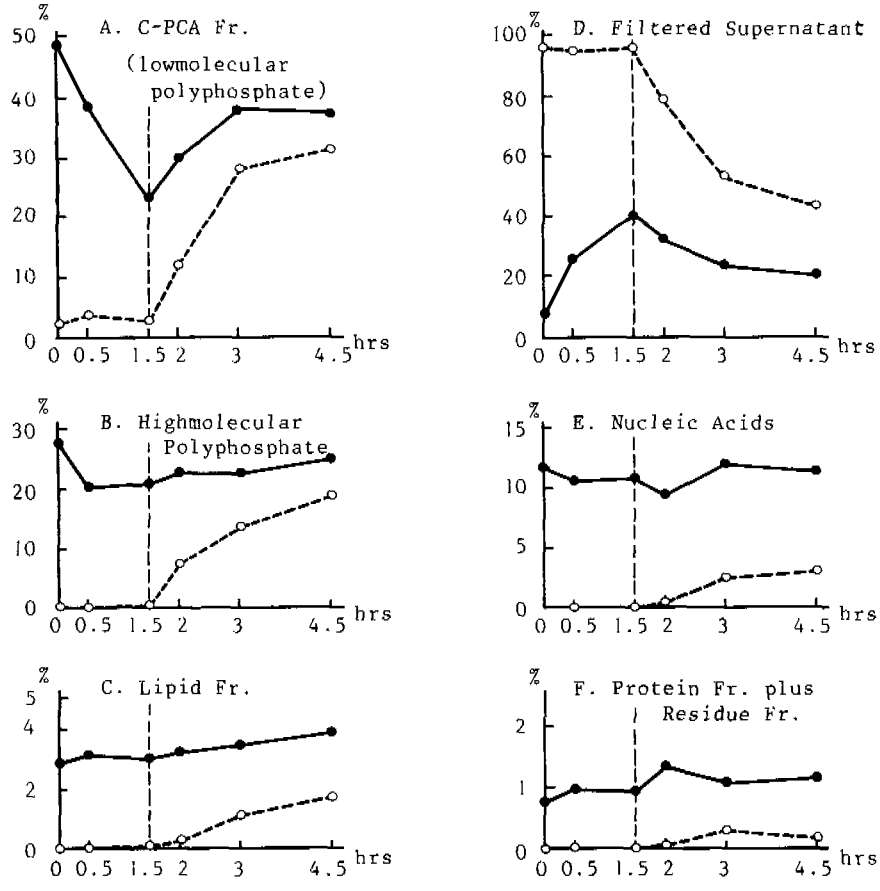

Fig. 7. Typical Changes of the Phosphorus and Radioactivity Distribution in the Anaerobic-Oxic Batch Experiment.

● : Chemically Analyzed Phosphorus
○ : Radioactivity

$(Pi)_n$ + ATP ⇌ $(Pi)_{n+1}$ + ADP, and that the depolymerization of longchain polyphosphate is inconceivable. Therefore the phosphorus utilized for the synthesis of lowmolecular or highmolecular polyphosphates is transported from the bulk solution and the phosphorus liberated along with the degradation of lowmolecular or highmolecular polyphosphates is released to the bulk solution directly.

Under these assumptions, the actual quantitative transfer of phosphorus from polyphosphates to the bulk solution can be calculated by the following equation:

(actual quantitative transfer of phosphorus) =
(change of radioactivity in polyphosphates during the calculation period) × (average specific radioactivity in the bulk solution in that period)$^{-1}$

where the specific radioactivity means the radioactivity per the unit amount of phosphorus chemically analyzed. The mean of the initial and the final radioactivity of the calculation period is regarded as the average radioactivity in that period. The quantitative change of phosphorus calculated from the radioactivity corresponds to the amount of phosphorus which actually transfers from polyphosphates to the bulk solution along with the degradation or the synthesis of polyphosphates.

In Fig. 8, the typical results of the chemically analyzed phosphorus and the calculated changes of phosphorus amounts in lowmolecular and highmolecular polyphosphates are illustrated. In the anaerobic period, the calculated changes of phosphorus amounts are negligibly small both in lowmolecular and highmolecular polyphosphates. It is indicated that the phosphorus turnover in polyphosphates does not occur along with the degradation reaction of polyphosphates during the anaerobic period. In the aerobic period, the quantitative increase of chemically analyzed phosphorus in lowmolecular polyphosphates is almost equal to the calculated change of phosphorus amount which corresponds to the amount of phosphorus actually utilized for the synthesis of lowmolecular polyphosphates. Therefore it seems the turnover of phosphorus in lowmolecular polyphosphates does not occur in the aerobic period. On the contrary, the calculated change of phosphorus amount in highmolecular polyphosphates is greater than the quantitative

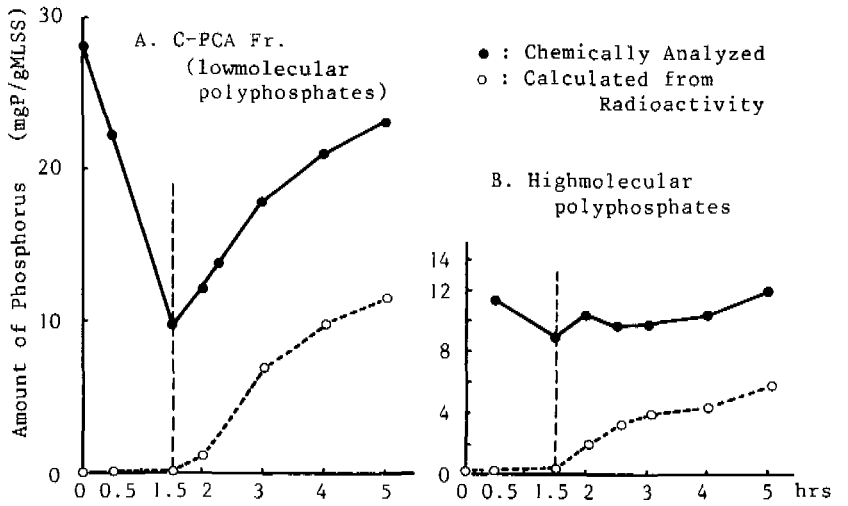

Fig. 8. Chemically Analyzed and Calculated Changes of Phosphorus Amount in Lowmolecular and Highmolecular Polyphosphates in the Anaerobic-Oxic Batch Experiment.

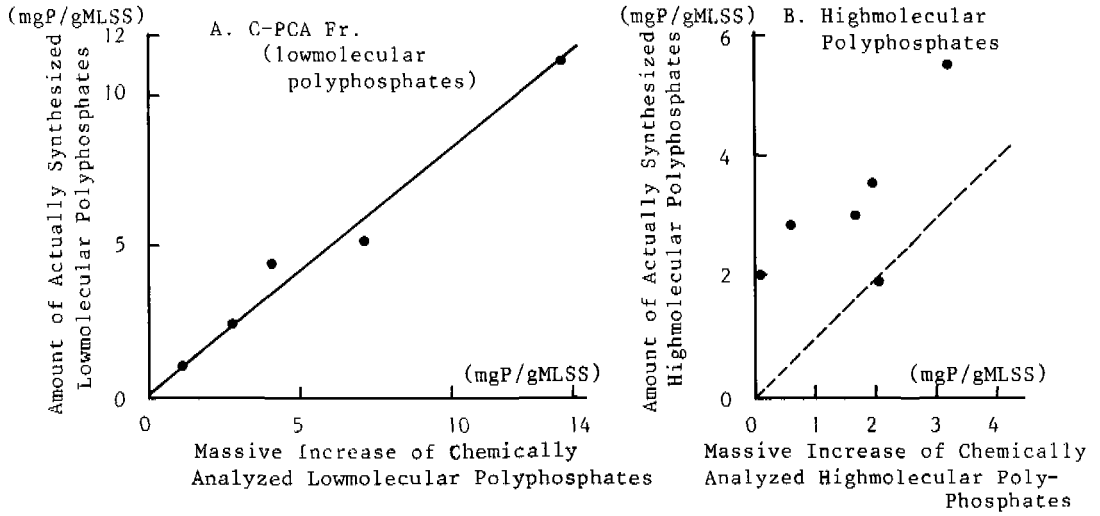

Fig. 9. Relationships between the Total Quantitative Change of Chemically Analyzed Phosphorus and the Total Change of the Phosphorus Amount Calculated from Radioactivity.

change of the chemically analyzed highmolecular polyphosphates, and the phosphorus turnover in highmolecular polyphosphates is suggested to occur in the aerobic period.

In Fig. 9, the relationships between the total quantitative change of chemically analyzed phosphorus and the total change of the phosphorus amount calculated from the radioactivity in the course of the aerobic period are depicted. There is a linear relationship between them concerning C-PCA Fr. which contains lowmolecular polyphosphates as shown in Fig. 9. A, and the slope of the regression line is calculated to be 0.84. If there occurs no turnover, the slope must be unity, and it is theoretically impossible that the slope is below unity. Therefore, the calculated value can be considered to be nearly unity. It is indicated that the phosphorus turnover does not occur in lowmolecular polyphosphates during the anaerobic period. As to highmolecular polyphosphates, there can not be found the significant relationships in Fig. 9. B. However the amounts of actually synthesized highmolecular polyphosphates exceed the increases of chemically analyzed highmolecular polyphosphates, and the occurence of the phosphorus turnover in highmolecular polyphosphates during the aerobic period is clearly indicated.

DISCUSSION

The obtained results are summarized as follows:

(1)The difference of intracellular phosphorus content among the sludges are caused by the quantitative difference of lowmolecular and highmolecular polyphosphates. Especially the accumulation of lowmolecular polyphosphates are mostly responsible for the high phosphorus content of the sludges produced in the anaerobic-oxic process.

(2)Although both lowmolecular and highmolecular polyphosphates are accumulated in the sludge produced in the anaerobic-oxic process, lowmolecular polyphosphates are principally responsible for the release and uptake of phosphorus occurring in this process.

(3)Lowmolecular polyphosphates are degraded under anaerobic conditions and synthesized under aerobic conditions without the turnover of phosphorus. The phosphorus turnover in highmolecular polyphosphates is observed under the aerobic conditions.

The phosphorus accumulation in the form of RNA is observed by Udaka et al (1980) in a pure culture of Arthrobactor. This bacterium accumulates about 30 mgP/gMLSS of RNA in its cells. In our examination, however, such high level of RNA accumulation is not observed concerning the activated sludge, a mixed culture system containing a lot of microbial species. It is clarified that the accumulation form of phosphorus in activated sludges is lowmolecular and highmolecular polyphosphates.

It is suggested from these results that the prominent characteristic of the sludges produced in the anaerobic-oxic process is their superior ability to accumulate lowmolecular polyphosphates. Judging from the fact that lowmolecular polyphosphates do not appear in the sludges whose phosphorus content is below 20 mgP/gVSS, they are expected to perform the function proper to the sludges with the high phosphorus content or the sludges produced in the anaerobic-oxic process. The fact that the turnover of phosphorus in lowmolecular polyphosphates is not observed in the course of the anaerobic-oxic process, combined with the assumption that polyphosphates are able to become the energy source for some biological reactions, gives strong support to the concept that lowmolecular polyphosphates function as the energy pool in the microbial cells.

Highmolecular polyphosphates are considered to function as the phosphorus pool for the microbial growth, because the turnover of phosphorus is observed under aerobic conditions. However, in some cases, for example in the case of D in Fig. 6, the degradation of highmolecular polyphosphates without the phosphorus turnover occurs under anaerobic conditions. Whether highmolecular polyphosphates are able to function as the energy pool or they only serve as the source of phosphorus still remains to be clarified.

In conclusion, it is suggested that lowmolecular polyphosphates function as the energy pool for the uptake of organic substrates under the anaerobic conditions and that highmolecular polyphosphates function as the phosphorus source for the microbial growth under the aerobic conditions in the anaerobic-oxic process. Lowmolecular polyphosphates reveal the prominent behaviours proper to the sludges produced in the anaerobic-oxic process as described above. Therefore, whether lowmolecular polyphosphates have the ability to serve as the energy source for the microbial reactions must be checked up positively and experimentally for the purpose of clarifing the biological mechanisms of the anaerobic-oxic process.

REFERENCES

Barnard, J. L. (1975). Biological nutrient removal without the addition of chemicals. Water Research, Vol.9, 485-490.

Barnard, J. L. (1976). A review of biological phosphorus removal in the activated sludge process. Water S. A., Vol.2, No.3, 136-144.

Barnard, J. L. (1982). Background to biological phosphorus removal. IAWPR post conference seminar on phosphate removal in biological treatment processes, Pretoria.

Buchan, L. (1982). Possible biological mechanism of phosphorus removal. IAWPR post conference seminar on phosphate removal in biological treatment processes, Pretoria.

Galdieri, J. V. (1979). Remove phosphate biologically. Water and Waste Engineering, 12.

Harold, F. M. (1966). Inorganic polyphosphates in biology: structure, metabolism,

and function. Bacteriol. Rev., Vol.30, No.4, 772-794.
Nicholls, H. A., and Osborn, D. W. (1979). Bacterial stress: prerequisite for biological removal of phosphorus. J. Water Pollut. Cont. Fed., Vol.51, No.3, 557-569.
Mino, T., Kawakami, T., and Matsuo, T. (1983). Studies on phosphorus composition and phosphorus metabolism in activated sludge, 1 and 2. J. Jap. Sewage works Assoc. Vol.20, No.228 and 229, (in Japanese)
Schmidt, G., and Thannhauser, S. J. (1945). A method for the determination of desoxyribonucleic acid, ribonucleic acid and phosphoprotein in animal tissues. J. Biol. Chem. Vol.161, p83.
Schneider, W. C. (1946). Phosphorus compounds in animal tissues. I. Extraction and estimation of desoxypentose nucleic acid and of pentose nucleic acid. J. Biol. Chem. Vol.161, p293.
Udaka, S., and Shoda, M. (1980). Screening for high phosphate accumulating bacteria. Agric. Biol. Chem. 44 (2), 319-324.

Wat. Sci. Tech. Vol.17, Amsterdam, pp.107-119.
Printed in Great Britain.

0273-1223/85 $0.00 + .50

MODELING PHOSPHATE SLUDGE PRODUCTION

R. G. Veldkamp

Laboratory of Sanitary Engineering, Dept. of Civil Engineering, Technical University Delft, The Netherlands

ABSTRACT

Sludge mass production and volumetric sludge production were measured in a series of bench scale tests. This experiment was performed as a 3-factorial design. Variables were chemical dosing level (expressed as mole ratio cation/P), P-concentration and pH. Experimental data are statistically evaluated with analysis of variance and multiple regression. Some models for the prediction of sludge production are developed.

KEYWORDS

Wastewater, modeling sludge production, chemical sludge, phosphate removal, regression analysis.

INTRODUCTION

In wastewater treatment increasing sludge quantities will be produced as a result of upgrading existing solids removal processes by chemical addition or of adding chemicals to increase the removal of phosphates.
In case of pre-precipitation primary sludge production is increased and waste activated sludge production is decreased. However, the total mass of solids will increase.
Adding chemicals in or just prior to the aeration basin (simultaneous precipitation) will increase the quantities of sludge discharged from the biological unit. Pre- and simultaneous precipitation both give a mixture of chemical/biological sludge.
In case of post precipitation the chemical sludge is discharged separately.
When designing wastewater treatment plants, the facilities for sludge handling and disposal have to be designed on expected sludge quantities. Frequently we have no idea how much sludge will be produced.
The same holds for existing biological treatment plants which are upgraded with phosphate removal facilities. In these plants the additional chemical sludge quantities are difficult to estimate.

This paper will focus on providing information on additional sludge quantities, when adding metal salts for phosphate removal.

CALCULATIONAL APPROACH

Sludge quantity estimation can be based on a calculational approach. With this approach the calculation of the additional sludge mass to be produced by chemical dosing is based on stoichiometric relationships. Furthermore, the calculations of organic and chemical sludge quantities are based on the assumption of some basic data, such as influent BOD and suspended solids, phosphorus concentration, SS removal and phosphate removal. Examples of this approach are given by Adrian & Smith (1972), Knight et al. (1973), Farrel (1974), Schmidtke (1980) and STORA (1981).
The units used for presenting sludge production values differ from each other. The STORA report expresses production data in grams per capita per day, other authors use kg dry solids per m^3 of wastewater, a more appropriate unit. When production data are given in gr/cap.day division by the daily sewage production will yield kg/m^3. Sewage production values are highly variable and in the USA much higher than in Europe.
For Dutch and USA conditions the calculated sludge production is shown in tables 1 and 2 respectively. In both tables calculation starts from different assumptions which are tabulated in table 3 for comparison.
Assuming an equal sludge production in simultaneous and post precipitation, the values given for simultaneous precipitation apply to post precipitation as well.
Both tables indicate that sludge production in the chemical/biological process is significantly higher than in the biological treatment system. The addition of iron causes somewhat higher values than alum addition.
Comparison of tables 1 and 2 shows that sludge production values in the USA are consistently lower. The same is noticed for the increase in total solids, compared with conventional treatment.

TABLE 1 Calculated Sludge Mass Production, kg/m^3 (Dutch conditions)

	conventional	alum	iron
pre precipitation:			
primary sludge	0.400 (0.150)	0.827 (0.310)	0.827 (0.310)
chemical sludge		0.109 (0.041)	0.144 (0.054)
subtotal	0.400 (0.150)	0.936 (0.351)	0.971 (0.364)
secondary sludge	0.172 (0.065)	0.072 (0.027)	0.072 (0.027)
total	0.572 (0.215)	1.008 (0.378)	1.043 (0.391)
increase primary		134 %	143 %
increase total		76 %	82 %
simultaneous precipitation:			
primary sludge	0.400 (0.150)	0.400 (0.150)	0.400 (0.150)
secondary sludge	0.172 (0.065)	0.237 (0.089)	0.237 (0.089)
chemical sludge		0.104 (0.039)	0.138 (0.052)
subtotal	0.172 (0.065)	0.341 (0.128)	0.375 (0.141)
total	0.572 (0.215)	0.741 (0.278)	0.775 (0.291)
increase secondary		98 %	118 %
increase total		30 %	36 %

TABLE 2 Calculated Sludge Mass Production, kg/m^3 (USA conditions)

	conventional	alum	iron
pre precipitation:			
primary sludge	0.150	0.225	0.225
chemical sludge		0.058	0.073
subtotal	0.150	0.283	0.298
secondary sludge	0.086	0.064	0.064
total	0.236	0.347	0.362
increase primary		89 %	99 %
increase total		47 %	53 %
simultaneous precipitation:			
primary sludge	0.150	0.150	0.150
secondary sludge	0.086	0.096	0.096
chemical sludge		0.051	0.065
subtotal	0.086	0.147	0.161
total	0.236	0.297	0.311
increase secondary		71 %	87 %
increase total		26 %	32 %

TABLE 3 Basic Data for Calculated Sludge Production

	Netherlands	USA
Influent:		
suspended solids, mg/l	600	300
BOD, mg/l	360	230
P-concentration, mg/l	20	10
Mole ratio cation/P	1.75	1.75
SS removal in primary:		
no chemicals, %	67	50
with chemicals, %	100	75
Sludge mass calculation:		
Al solids, kg/kg Al	3.59	3.80
Fe solids, kg/kg Fe	2.28	2.30

The values in table 1 are calculated by estimating a daily per capita dry solids production and dividing this value by an estimated sewage production of 150 l/cap.day. Sewage production values in the USA are about 300 to 400 l/cap.day.
Recalculation of table 1 with a 400 l/cap.day sewage production gives the sludge production values put in brackets. These values are in good agreement with those in table 2.
The calculated sludge production shown in tables 1 and 2 is based on average conditions. Production data, which have been presented in literature, reveal a fair variability. Of course sludge production is influenced by a number of variables, such as influent phosphate concentration, type of chemical and chemical dosing. Other variables like suspended solids concentration and pH can have their impact on sludge production.
To increase the reliability in estimating chemical sludge production in phosphate removal processes, a series of bench scale experiments has been carried out at the Laboratory of Sanitary Engineering in Delft. The results were used for developing some sludge production

models, resulting in a better understanding of the factors influencing chemical sludge production.

EXPERIMENTAL PROCEDURE

General

Chemical sludge production was determined in batch experiments by adding Al^{3+} or Fe^{3+} to tapwater with different phosphate concentrations. The applied chemicals were alum and ferric chloride. All experiments were done in 2 l beakers, each filled with 1.8 l of the prepared phosphate solutions.
Three variables were fixed to some predetermined values:

1. P-concentration : 5 - 10 - 20 mg/l
2. Mole ratio β (Al/P, Fe/P) : 0 - 0.375 - 0.75 - 1.125 - 1.5 - 1.875 - 2.25 - 3
3. pH (after dosing chemicals): 6.5 - 7.5

All combinations between these 3 variables were investigated, for each chemical 48 combinations altogether. For each combination the analyses were done threefold.

Phosphate solution

The phosphate solutions were prepared by adding KH_2PO_4 to tapwater. The choice of tapwater was made for it s slightly buffering capacities, thus preventing strong pH fluctuations.
The presence of calcium can give some disturbance as calciumphosphate will be precipitated. This can be prevented by reducing the pH to 6.9 or less.
Each phosphate solution was prepared in quantities, sufficient for 8 combinations of β and pH. After preparation, each solution was checked on its P-concentration and corrected if required. This check was repeated several times.

Operations

A 2 l beaker, provided with baffles, was filled with 1.8 l phosphate solution, using a graduated cylinder. The beaker was placed next to a pH-meter equipped with an automatic titrator. To end up with the desired pH the approximate amount of ash or acid was checked before. The coagulant was added simultaneously with the reagent for pH-correction. After reaching the final pH, the content was mixed for 30 seconds, followed by gentle stirring at 30 rpm for 20 minutes. After this flocculation period, 1 l was carefully poured into an Imhoff glass and settled for 30 minutes. From time to time the Imhoff glass was turned round its vertical axis to prevent any settling of flocs on the wall. After a 30 min. settling period the sludge volume was read. After determining sludge production on a volumetric base, the dry solids concentration had to be found. The content of the Imhoff glass is mixed and poured back into the beaker. After gentle stirring the mixture is filtered through a glass fibre filter. Most combinations of β and P-concentration resulted in very low mass production, making it necessary to put the whole 1.8 l over the filter. Only combinations with high β-values and high P-concentrations asked for smaller volumes to be filtered, thus preventing very long filterruns.

Dry solids concentration was measured according to Dutch NEN 3235. The filtrate is collected for analyses of phosphorus and cation concentrations. Phosphorus is measured on an auto-analyzer, according to Technicon instructions nr. 392-74-W/B. Al- and Fe-concentrations were measured on an AAS, using the Perkin-Elmer HGA instructions.

RESULTS

For both chemicals, alum and ferric chloride, 4 sets of experimental data were collected:
- sludge mass production
- volumetric sludge production
- final P-concentration
- final cation concentration

Detailed presentations of the experimental data will not be presented here as they have been elsewhere (Veldkamp,1983), except mass production data, which are presented in table 4.

DISCUSSION

Sludge mass production

In the experimental program sludge production is influenced by three factors: mole ratio β, P-concentration P and pH. In the statistical evaluation of experimental data these factors are considered as independent variables, which were given previously fixed values. Sludge production is the dependent variable.
One method to study the effects of the factors on sludge production is performing an analysis of variance on the experimental data. In such an analysis the total sum of squares is decomposed into independent components. For a three-factor experiment the total variation can be partitioned as follows:

$$SS_S = SS_\beta + SS_P + SS_{pH} + SS_{\beta P} + SS_{\beta pH} + SS_{PpH} + SS_{\beta PpH} + SS_{error}$$

The subscript S represents the dependent variable; β, P and pH the independent variables. SS_S is the total sum of squares in S. SS_β is that portion of the sum of squares in S due to the variation in the means of the categories of factor β. If the differences among the means of S in various categories of β increase, the magnitude of SS_β will become greater relative to the other components.
$SS_{\beta P}$ is the interaction term, representing the effect of β on S for different levels of P and vice versa. If all effects are additive than all interaction terms will be zero.
SS_{error} is that portion of the sum of squares not attributable to the main effects and their interactions, thus the sum of squares due to the variation within all categories of β, P and pH.
The analyses of variance were performed using the SPSS computer program. Results are shown in tables 5 and 6 for Al and Fe respectively. In these tables higher order interactions are omitted.
As can be read from table 4, differences in the replications of sludge production are very small. As a consequence the error variance is also very small.
In testing the significance of β on S the F-ratio is calculated as:

$$F = \frac{MS_{\beta}}{MS_{error}}$$

TABLE 4 Sludge Mass Production, mg/l

mole ratio	P-conc.	pH	alum sludge replications			iron sludge replications		
0	5	6.5	0	0	0	0	0	0
0	5	7.5	0	0	0	0	0	0
0	10	6.5	0	0	0	0	0	0
0	10	7.5	0	0	0	0	0	0
0	20	6.5	1.1	0.9	1.2	0	0	0
0	20	7.5	2.9	1.6	1.6	2.4	1.3	1.9
0.375	5	6.5	11.4	11.2	11.3	13.9	13.2	13.0
0.375	5	7.5	11.1	11.2	11.3	12.7	12.1	12.6
0.375	10	6.5	18.4	19.3	19.3	25.6	25.2	25.8
0.375	10	7.5	18.8	18.2	19.1	26.6	25.7	24.0
0.375	20	6.5	36.6	37.9	37.1	50.6	48.7	48.1
0.375	20	7.5	40.5	41.1	42.6	53.6	52.3	54.3
0.75	5	6.5	18.2	17.8	18.0	20.3	20.0	19.6
0.75	5	7.5	18.2	18.4	18.6	20.8	20.6	20.1
0.75	10	6.5	34.2	34.6	34.6	42.0	43.5	43.0
0.75	10	7.5	38.3	38.8	39.2	44.9	46.1	45.3
0.75	20	6.5	71.2	70.9	72.2	89.9	90.5	89.0
0.75	20	7.5	80.9	78.2	76.6	97.1	95.6	95.8
1.125	5	6.5	27.6	26.9	27.6	32.5	33.2	32.7
1.125	5	7.5	27.3	26.7	26.7	32.0	32.0	32.5
1.125	10	6.5	52.0	53.4	53.7	64.8	65.3	65.2
1.125	10	7.5	51.3	52.8	51.4	64.6	64.2	65.6
1.125	20	6.5	98.6	98.5	96.2	122.7	125.2	124.6
1.125	20	7.5	105.2	107.5	104.4	129.7	131.1	130.7
1.5	5	6.5	33.4	32.6	30.3	36.6	37.5	37.6
1.5	5	7.5	29.1	21.3	23.8	40.6	40.0	39.4
1.5	10	6.5	61.8	64.4	61.8	75.0	77.0	78.8
1.5	10	7.5	66.4	66.2	66.2	79.8	78.0	84.4
1.5	20	6.5	118.4	124.0	122.2	154.6	155.6	153.6
1.5	20	7.5	128.0	128.6	133.2	157.8	153.8	156.4
1.875	5	6.5	38.5	38.6	38.4	45.8	46.6	46.8
1.875	5	7.5	38.7	38.3	38.3	44.8	44.7	44.6
1.875	10	6.5	73.3	75.2	73.9	92.4	91.9	88.6
1.875	10	7.5	71.3	73.6	71.3	90.4	90.9	90.6
1.875	20	6.5	143.3	141.3	140.9	173.0	172.8	170.1
1.875	20	7.5	144.4	142.2	144.9	183.4	180.4	183.0
2.25	5	6.5	41.9	42.0	41.5	49.0	46.3	47.6
2.25	5	7.5	31.6	29.5	45.5	50.2	51.8	52.6
2.25	10	6.5	84.2	86.4	85.2	105.6	99.6	100.6
2.25	10	7.5	83.8	88.8	84.4	105.8	103.0	100.4
2.25	20	6.5	158.0	159.6	163.4	188.5	193.3	190.7
2.25	20	7.5	167.6	166.4	165.8	196.0	195.3	199.0
3.0	5	6.5	51.6	53.0	50.5	60.8	63.6	59.8
3.0	5	7.5	53.3	53.0	54.4	61.8	65.6	67.6
3.0	10	6.5	99.8	104.2	104.8	122.2	121.6	121.6
3.0	10	7.5	106.8	103.8	108.8	120.6	126.0	126.2
3.0	20	6.5	202.7	200.0	204.7	226.0	220.8	225.6
3.0	20	7.5	195.3	206.8	205.0	242.3	245.7	244.0

TABLE 5 Analysis of Variance for Alum Sludge

Source of variation	Sum of squares	df	Mean square	F
Main effects	351182	10	35118	5830
mole ratio	194046	7	27720	4602
P-concentration	157067	2	78533	13039
pH	68	1	68	11
Interactions	53139	23	2310	384
mole ratio·P-conc	52860	14	3775	627
mole ratio·pH	54	7	8	1
P-conc·pH	226	2	113	19
Explained	404322	33	12252	2034
Residual	662	110	6	
Total	404985	143	2832	

TABLE 6 Analysis of Variance for Iron Sludge

Source of variation	Sum of squares	df	Mean square	F
Main effects	500374	10	50037	11835
mole ratio	270584	7	38655	9143
P-concentration	229452	2	114726	27135
pH	336	1	336	79
Interactions	70312	23	3057	723
mole ratio·P-conc	69821	14	498	1180
mole ratio·pH	205	7	29	7
P-conc·pH	286	2	143	34
Explained	570685	33	17293	4090
Residual	465	110	4	
Total	571150	143	3994	

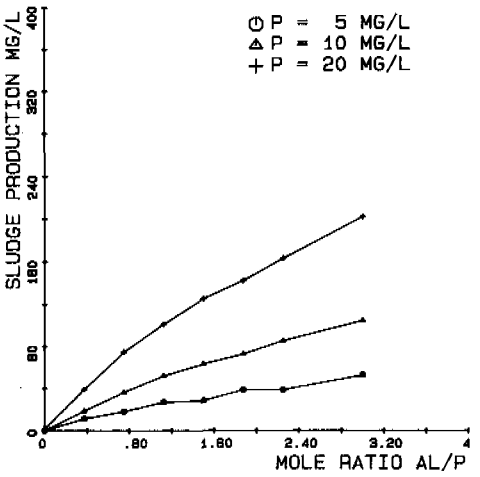

Fig. 1 Sludge production by alum addition

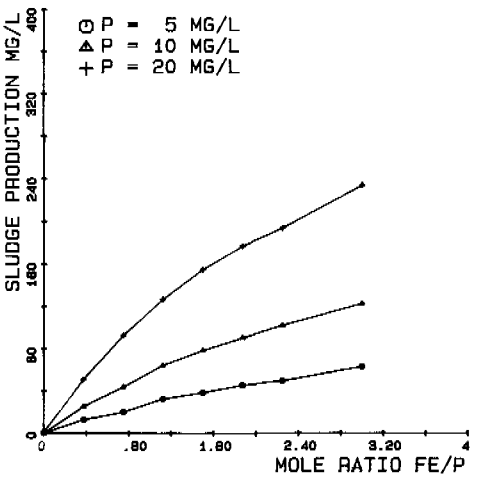

Fig. 2 Sludge production by iron addition

As the error variance is small, F-ratios tend to be high, thus all factors have significant main effects and interactions. In this experiment the F-ratios cover a wide range.
Both tables show that the combined main effects have a much stronger influence than their combined interactions.
The first step is to examine whether the interaction effects are significant. Of the 3 interactions mentioned, only $\beta \cdot P$ is important. A plot of the sludge production lines vs. β for different P-concentrations as shown in figures 1 and 2 does not indicate a clear influence of interaction (the sludge production is plotted as the average of both pH values). Deciding the interactions to be neglected, their variance can be added to the variance for residuals, thus leaving only the main effects as shown in table 7. From this table one can detect a strong effect of β and P, the pH-effect is negligible.

TABLE 7 Analyses of Variance for Alum and Iron Sludge

Source of variation	Sum of squares	df	Mean square	F
	Alum sludge			
Main effects	351182	10	35118	86.8
mole ratio	194046	7	27720	68.5
P-concentration	157067	2	78533	194.1
pH	68	1	68	0.2
Explained	351182	10	35118	86.8
Residual	53802	133	404	
Total	404985	143	2832	
	Iron sludge			
Main effects	500374	10	50037	94.0
mole ratio	270585	7	38654	72.6
P-concentration	229452	2	114726	215.6
pH	336	1	336	0.6
Explained	500373	10	50037	94.0
Residual	70776	133	532	
Total	571150	143	3994	

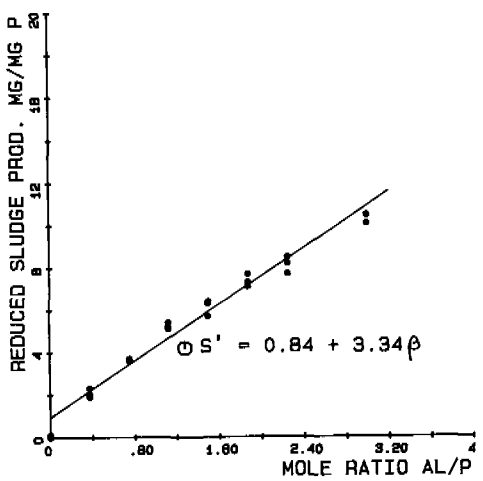

Fig. 3 Reduced sludge production by alum addition

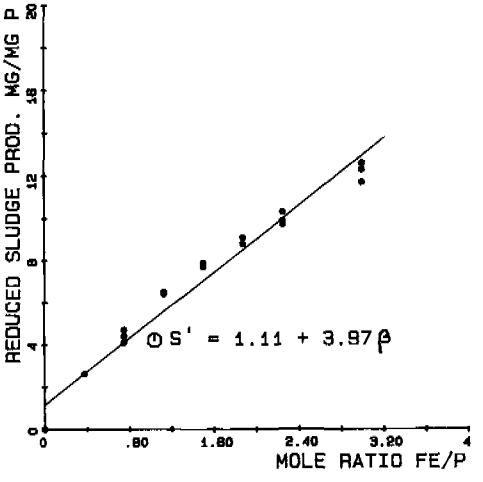

Fig. 4 Reduced sludge production by iron addition

A closer look to figures 1 and 2 show that twofold P-concentrations result in double sludge production values. When production values are divided by the respective P-concentrations, the 3 lines coincide into one line, showing the relationship between β and the "reduced sludge production" S' in mg dry solids per mg influent-P. Figures 3 and 4 show a straight line relationship and least square methods give the equations:

Alum: $S' = 0.84 + 3.34\beta$

$S = (0.84 + 3.34\beta)P \qquad (R = 0.981)$ |1a|

Iron: $S' = 1.11 + 3.97\beta$

$S = (1.11 + 3.97\beta)P \qquad (R = 0.982)$ |1b|

Volumetric sludge production

The experimental data for sludge volumes are less consistent than for mass production. For low dosages there is no question of any measurable volume. This is in contradiction with the measurement of a mass production for the same dosages.
The reason for measuring no volume with low β and P-values is the formation of very light flocs which do not settle. Their presence is visual as a haze in the liquid.
For alum additions in phosphate solutions of 10 mg P/l there is no observable volumetric production through β-values of 1.875. This comes to an absence of a measurable volume up to a dosage of 16.3 mg Al/1. In case of iron addition to a 10 mg P/l phosphate solution, volumes can be measured from β = 0.75. Thus iron flocs have better settling properties, something also known in practice.

MODELING

Regression model

Considering all the experimental variables which effect sludge production, modeling of sludge production can be based on developing a regression model. Such a model is given by the general equation of the regression analysis:

$$S = c_0 + c_1\beta + c_2P + c_3pH + c_{11}\beta^2 + c_{22}P^2 + c_{33}(pH)^2 + c_{12}\beta P + c_{13}\beta pH + c_{23}PpH \qquad |2|$$

where:
S = sludge production, mg/l;
β = mole ratio, Al/P or Fe/P;
P = phosphate concentration, mg P/l;
pH = pH-value; and
c = regression coefficients.
For simplicity not all terms are kept in the equation. The interactions terms including pH and the squared terms are omitted from this equation, as not being relevant. The only remaining interaction β·P is equivalent with the chemical dosing. In the regression analysis a stepwise inclusion of variables into the equation is possible. The order in which the variables are entered is determined by their respective contribution to explained variance. The model becomes:

Alum: $S = -10.297 + 3.233\cdot\beta\cdot P + 0.9\cdot P + 1.378\cdot pH + 1.07$ |3a|

Iron: $S = -23.885 + 3.661\cdot\beta\cdot P + 1.423\cdot P + 3.05\cdot pH + 2.89$ |3b|

TABLE 8 Stepwise Regression Analysis of Sludge Production Data

Variable added to regr. eq.	Alum R^2	Alum change	Iron R^2	Iron change
$\beta \cdot P$	0.97747	0.97747	0.96583	0.96583
P	0.98355	0.00608	0.97482	0.00899
pH	0.98372	0.00017	0.97541	0.00059
β	0.98380	0.00008	0.97582	0.00041

The order in which the terms appear in the equation is from left to right. The effect of each variable is shown in table 8.
The major part of the explained variance can be attributed to the relationship between S and $\beta \cdot P$, to a less extent to the variable P. The introduction of the other variables does not increase the multiple R^2 that much, which can be translated as a negligible effect on sludge production. Thus the Eqs.|3a,b| simplify to:

Alum: $S = 0.82 + 3.30 \cdot \beta \cdot P + 0.80 \cdot P \quad (R = 0.992)$ |4a|
Iron: $S = 1.38 + 3.85 \cdot \beta \cdot P + 1.16 \cdot P \quad (R = 0.987)$ |4b|

Deterministic model

The coagulants used in this experiment, alum and ferric chloride, have both trivalent cations. In the development of the next model no distinction is made any longer between both cations and they will be replaced by the symbol Me.
The amount of Me-cations which have reacted (Me) can be calculated from the added amount (Me(tot)) and the final concentration in the filtrate (Me(rest)) as:

$$Me = Me(tot) - Me(rest) \quad |5|$$

Parts of these cations are fixed as phosphate sludge and precipitated as such. The quantity of sludge is dependent on the removed portion of phosphate (Prem):

$$Prem = P - Prest \quad |6|$$

The remaining protion of Me is precipitated as a metalhydroxide.
Thus, the filtered sludge consists of a mixture of metalphosphates and metalhydroxides:

$$S = MePO_4 + Me(OH)_3 \quad |7|$$

The deterministic model of sludge production can be presented schematically as follows:

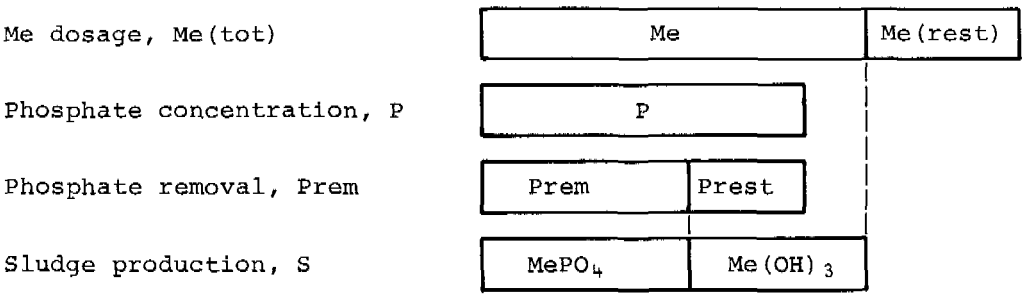

In developing the mathematical model we use the following notations:
k1 = 1/at.weight Me
k2 = 1/at.weight P
k3 = mol.weight $MePO_4$
k4 = mol.weight $Me(OH)_3$
Precipitated as $MePO_4$: k2·k3·Prem, mg/l
Precipitated as $Me(OH)_3$: {Me - k2/k1·Prem}·k1·k4 =
k1·k4·Me - k2·k4·Prem

$$S = k2(k3 - k4)\cdot Prem + k1\cdot k4\cdot Me \qquad (Me \text{ in mg/l}) \qquad |8|$$

The chemical dose can be calculated from the product β·P as:
Me(tot) = k2/k1·β·P
Eq.|8| can be put into the experimental variables β and P:

$$S = k2(k3 - k4)(P - Prest) + k1\cdot k4\cdot\{k2/k1\cdot\beta\cdot P - Me(rest)\} \qquad |9|$$

In this equation two variables were not experimentally fixed, viz. Prest and Me(rest). The question rises if these variables are dependent of the other variables in the equation. An analysis of variance shows Prest to be influenced by β, P and β·P, a result that could be expected. The variable Me(rest) is only slightly dependent on P in the case of alum dosing, but the relationship is not strong (R = 0.37). We don't make a big error when taking Me(rest) as a constant value, merely because Me(rest) values are small compared with the initial concentration Me(tot).
The averages are Al(rest) = 0.11 mg/l and Fe(rest) = 0.10 mg/l.
Substituting these values and the constants k1 to k4 in Eq.|9| gives an equation in which sludge production is expressed in terms of β·P and (P - Prest).

$$\text{Alum: } S = 1.42(P - Prest) + 2.52\cdot\beta\cdot P - 0.318 \qquad |10a|$$
$$\text{Iron: } S = 1.42(P - Prest) + 3.45\cdot\beta\cdot P - 0.191 \qquad |10b|$$

Comparison of models

Eqs.|10a,b| are expressed in the variables (P-Prest) and β·P, while Eqs.|4a,b| from the regression analysis are expressed in terms of P and β·P.
To bring both sets of equations in accordance to each other, a second regression analysis can be performed with the variable (P-Prest), instead of the initial concentration P. The output is:

$$\text{Alum: } S = 2.55(P - Prest) + 2.50\cdot\beta\cdot P + 1.61 \quad (R = 0.998) \qquad |11a|$$
$$\text{Iron: } S = 3.37(P - Prest) + 2.79\cdot\beta\cdot P + 3.50 \quad (R = 0.997) \qquad |11b|$$

Eqs.|10a,b| and |11a,b| should be identical, but a comparison shows that they certainly do not give the same results for sludge production. The regression constants are different, and sludge productions calculated from the deterministic model are lower than the experimental results, for all combinations of β, P and Prest within the experimental range.
This is true because the model was oversimplified in its setup. In developing this model it was assumed that the reaction products of phosphates with Al^{3+} and Fe^{3+} precipitated as $AlPO_4$ and $FePO_4$. This is also found frequently in literature. Nevertheless this assumption has to be revised. A better approach seems to be taking into account an unknown portion of crystalline water, bounded to the flocs, as:
$MePO_4.nH_2O$ and $Me(OH)_3.mH_2O$.
Eq.|9| can be written as:

$$\text{Alum: } S = \frac{44+18n-18m}{31}(P - P_{rest}) + \frac{78+18m}{31} \cdot \beta \cdot P - \frac{78+18m}{27} Me(rest) \quad |12a|$$

$$\text{Iron: } S = \frac{44+18n-18m}{31}(P - P_{rest}) + \frac{107+18m}{31} \cdot \beta \cdot P - \frac{107+18m}{56} Me(rest) \quad |12b|$$

Solving Eqs.|12a,b| and |11a,b| to the unknown constants m and n gives the portions of crystalline water for both chemicals.
When alum is used as coagulant, then $m = 0.028 \approx 0$. If $m = 0$ than $n = 1{,}95 \approx 2$.
This means the formation of $AlPO_4.2H_2O$ and $Al(OH)_3$.
For ferric chloride as coagulant $m = -1.14$ and $n = 2.22$. This result is not easy to explain without more detailed research to the nature of sludge solids. The dry solids analysis can probably cause a change in the solids structure, resulting in a negative m-value.

CONCLUSIONS

- General sludge production data for phosphorus removal processes given in literature have to be used carefully. The calculated examples of sludge production use average values for the concentration of influent phosphorus and removal efficiency. Case studies show a wide range in sludge production data, which are mostly far beyond the calculated values.
- Sludge production is strongly influenced by the mole ratio cation/P and influent P-concentration, only slightly by the pH value.
- For a certain dosing rate, experiments in tapwater show the sludge production to be directly proportional to the influent P-concentration.
- Addition of ferric chloride causes a 1.2-fold higher sludge production compared with the use of alum.
- A regression analysis produces the following model for the sludge production S:
  Alum addition: $S = 1.61 + 2.55\ P(removed) + 2.50 \cdot \beta \cdot P(influent)$.
  Iron addition: $S = 3.50 + 3.37\ P(removed) + 2.79 \cdot \beta \cdot P(influent)$.
Correlation between this model and experimental data is high: $R = 0.998$ (alum) and 0.997 (ferric chloride).
- Comparison of the regression model with a deterministic model proves the formation of $AlPO_4.2H_2O$ and $Al(OH)_3$ as reaction products.

REFERENCES

Adrian, D.D. and Smith Jr. J.E. (1972). Dewatering physical-chemical sludges - Applications of new concepts of physical-chemical wastewater treatment. In: Progress in Water Technology, IAWPR, vol.1, pp. 273-289.

Farrel, J.B. (1974). Sludges generated in phosphate removal processes. In: Proc. United States - Japan Conf. on Sewage Treatm. Technol. (3rd), Tokyo, Japan, pp. 270-282.

Knight, C.H., Mondoux R.G. and Hambley B. (1973). Thickening and dewatering sludges produced in phosphate removal. In: Research Program for the Abatement of Municipal Pollution under Provisions of the Canada - Ontario Agreement on Great Lakes Water Quality, Phosphorus Removal Design Seminar, Conf. Proc. nr. 1.

Schmidtke, N.W. (1980). Sludge generation, handling and disposal at phosphorus control facilities. In: Phosphorus Management Strategies for Lakes, Proc. Conf., pp. 361-390.

STORA (1981). Chemische defosfatering - Methoden en neveneffecten, Rapport STORA, Rijswijk.

Veldkamp, R.G. (1983). Modellering van slibproduktie bij fosfaatverwijdering. Rapport nr. 83-27, Laboratorium voor Gezondheidstechniek, Technische Hogeschool Delft.

Wat. Sci. Tech. Vol.17, Amsterdam, pp.121-132.
Printed in Great Britain.

0273-1223/85 $0.00 + .50

PHOSPHORUS REMOVAL FROM WASTEWATER BY THE CRYSTALLIZATION METHOD

Isao Joko

Kurita Water Industries Ltd, 1723 Bukko-cho, Hodogayaku, Yokohama, Japan

ABSTRACT

To develop a new process for phosphorus removal the calcium phosphate crystallization method has been investigated. The metastable zone of calcium phosphate precipitates which is defined by concentrations of phosphate and calcium ions and pH was determined by batch experiments. Phosphorus in wastewaters can be constantly reduced to a sufficiently low level at the metastable reaction zone under the presence of seed crystals.The crystallization method proved to be practicable as advanced technology for phosphorus removal from wastewater through column tests and 50m^3/day pilot plant tests over 180days with a sewage secondary effluent.

KEYWORDS

Wastewater; Advanced technology; Phosphorus removal; Crystallization; Calcium phosphates; Metastable zone; Seed crystal; Phosphate rock.

INTRODUCTION

In recent years general interest in our environment has grown rapidly. Technology for phosphorus removal from wastewater has been developed rapidly in the last few years. The need for practical phosphorus removal process has arisen as a result of the over-fertilization and eutrophication of the watercourses and impoundments.

The technique of chemical precipitation with metal salts has been almost universally applied for nutrient control. However, chemical precipitation produces a sludge disposal problem that may be extremely troublesome for plant operators. Zoltek (1974) investigated the reaction between soluble inorganic orthophosphate and solid phosphate rock, and has reported that nucleation of apatite on phosphate rock ore has a potential use as a wastewater phosphate removal treatment process. But, in his experiments, a satisfactory

result on the efficiency of phosphorus removal was not obtained.

The purpose of this research was to develop a phosphorus removal process that utilizes crystallization phenomena of calcium phosphate which produce no sludge. To develop the crystallization method for phosphorus removal, batch and column experiments were carried out and a 50m^3/day pilot plant was operated in 1979. This paper is based upon those works (Joko et al., 1980, 1981, 1983).

OPERATIONAL CONDITIONS FOR CRYSTALLIZATION METHOD

Materials and Methods

Synthetic test solutions. All synthetic test solutions were made with distilled water and reagent grade chemicals. Sodium dihydrogen-phosphate, sodium bicarbonate, and calcium chloride were added at the desired molar ratio to distilled water and pH was adjusted with caustic soda and hydrochloric acid solutions.

Seed crystals. Seed crystals were prepared from a phosphate rock. Two types of the seed crystals (Seed-A, Seed-B) which were different in the particle size were prepared for the experiments. The physical properties and chemical composition of the seed crystals are listed in Table 1. Seed-A was used for the batch experiments and Seed-B for the column experiments.

Batch experiments. Batch experiments were performed by using 500ml covered Erlenmeyer's flasks that were immersed in a water bath. At the start of the experiments, Seed-A was added to the reaction vessels containing synthetic test solution. The solution was stirred with a magnetic stirrer. At an interval, aliquots of the solution were taken out from the reaction vessels, filtered through Millipore filters of 0.22μm pore size, and analyzed for total calcium and phosphate.

TABLE 1 Physical Properties and Chemical Composition of the Seed Crystals

Apparent density(g/cm^3)	1.4
BET Surface area(m^2/g)	15.6
Chemical composition(%)	
P_2O_5	34.8
CaO	52.6
F	4.1
Others	8.5
Grain size (mm)	
Seed-A	0.06-0.25
Seed-B	0.5 -1.0

BET = Brunauer-Emmett-Teller

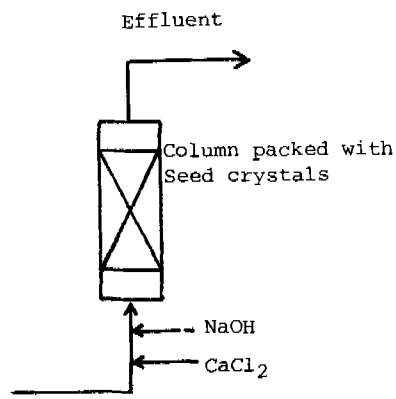

Fig.1. Flow diagram of column experiment

Column experiments. Column experiments were carried out with fixed bed reactors packed with 150-ml of the granular seed crystals (Seed-B). The flow diagram of the column experiments is shown in Figure 1. The synthetic feed solution was passed upward through the seed bed with calcium chloride and caustic soda solutions being fed just before the column. Effluent samples were collected from the top of the column and analyzed for phosphorus, calcium, pH and alkalinity

Analytical methods. Phosphorus concentrations were determined spectrophotometrically by the phosphomolybdate method; Calcium was measured by titration with 0.01M ethylenediamine tetraacetic acid; and alkalinity by titration to pH 4.8 with a 0.02M HCl solution.

Results and Discussion.

Phosphorus removal by precipitation. Phosphorus removal tests with a sewage secondary effluent using the calcium phosphate precipitation method were carried out. Phosphate concentrations in treated water achievable by this method will depend on the solubility of the precipitate of calcium phosphate. The effect of calcium concentration and pH on the phosphorus removal is shown in Figure 2. When calcium concentration and pH are high enough, phosphate ions react with calcium ions to precipitate calcium phosphates.
The reaction can be expressed as follows:

$$3HPO_4^{2-} + 5Ca^{2+} + 4OH^- \longrightarrow \underset{\text{hydroxyapatite}}{Ca_5(OH)(PO_4)_3} + 3H_2O$$

As the calcium concentration in the solution increases, the critical pH value of phosphorus precipitation becomes lower.

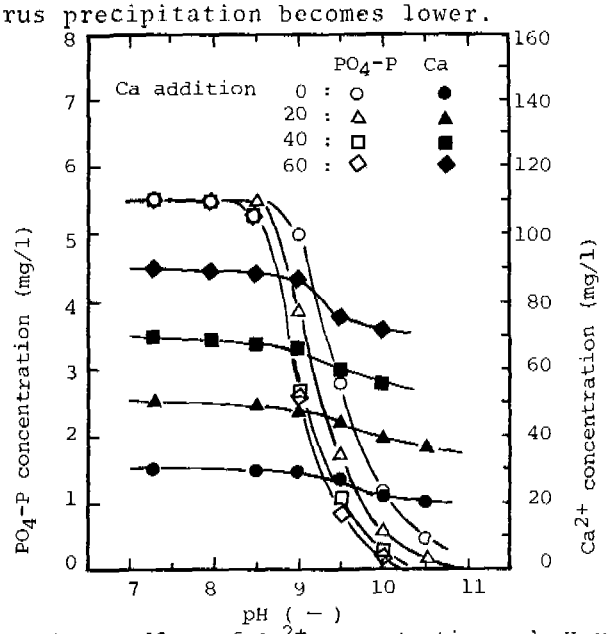

Fig.2. Effect of Ca^{2+} concentration and pH on the phosphorus removal. Initial condition : Test solution=sewage secondary effluent, PO_4-P=5.5mg/l, Ca=31mg/l, M-alkalinity=93mg/l, pH=7.3(-).

Metastable zone of calcium phosphate. Batch experiments were carried out to find out stable operational conditions for phosphorus removal in the continuous operation without phosphate sludge formation. Critical supersaturation curves of calcium phosphate as determined by the experiments are shown in Figure 3. The curve shifts to the high pH region when the phosphorus concentration decreases. From these results, we defined the metastable zone of calcium phosphates. Figure 4 illustrates the metastable zone. The metastable zone is the region between the solubility curve and the critical supersaturation curve. In this region, calcium phosphates do not precipitate by the addition of calcium hydroxide, but they may crystallize out on the surfaces of seed crystals.

The unstable zone above the critical supersaturation curve is the range where a precipitation reaction takes place and phosphorus concentration decreases to a level determined by solubility of calcium phosphates. Any seed crystals are unnecessary in this region for fine crystallization precipitate formation.

Effect of seed crystals addition. Many studies have been made on a growth of calcium phosphates from solution(Walton et al.1967; Nancollas, 1968; 1970), and on the effect of seed crystals for the reaction(Tomazic and Nancollas, 1975; Nancollas and Wefel, 1976; Koutsoukos et al. 1980).

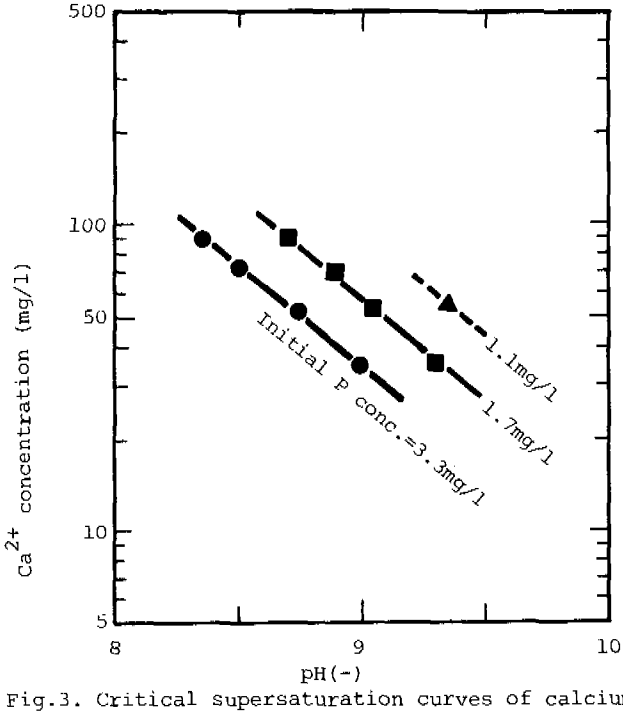

Fig.3. Critical supersaturation curves of calcium phosphates. Condition:M-alkalinity=100mg/l,Temperature=19-21°C, Reaction time=1hr.

In general, at relatively low degrees of supersaturation, nucleation will be induced by the substance itself or by a closely matching foreign mineral. On the other hand, at high supersaturation a large variety of foreign particles will act as seed crystals effectively for the release of the supersaturation.

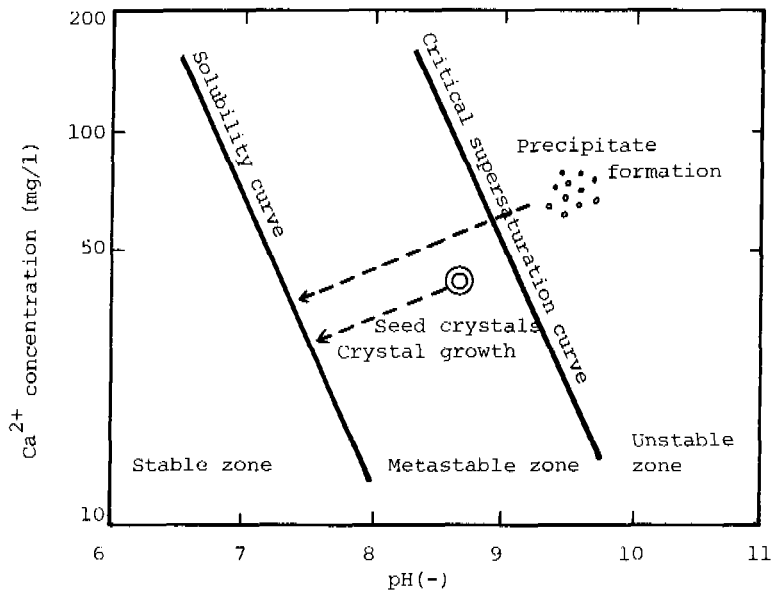

Fig.4. Metastable zone of calcium phosphates

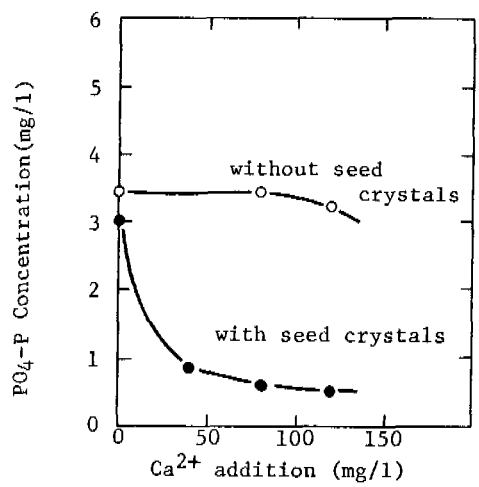

Fig.5.Effect of seed crystals addition on phosphorus removal. Initial condition: PO_4-P=3.5mg/l, seed crystals addition=0.1wt%,pH=8(-),Reaction time=3hr.

Seed crystals were prepared from a phosphate rock for this experiments. Figure 5 shows the results of beaker tests using a 3.5mg/l phosphorus solution of pH8 with or without 0.1 wt% calcium phosphate (hydroxyapatite) seed crystals. With the seed crystals, the phosphorus concentration reduced to 0.8mg/l at 40mg/l of calcium, and decreased further as calcium dose increased. On the other hand, little phosphorus removal was observed even at 120mg/l of calcium dose without the seed crystals.

Effect of calcium. The effect of calcium addition on phosphorus removal was studied with fixed bed reactors packed with 150ml of the granular seed crystals (Seed-B). The results are shown in Figure 6. Under the condition of 45mg/l calcium dose, phosphorus concentrations of the treated water were always below 0.1mg/l during the 52days column operation. On the other hand, without calcium addition, breakthrough of phosphorus occurred after 14 days operation. From these results it was found that the efficiency of phosphorus removal was strongly affected by calcium in water, and phosphorus in water could be removed continuously by adding calcium.

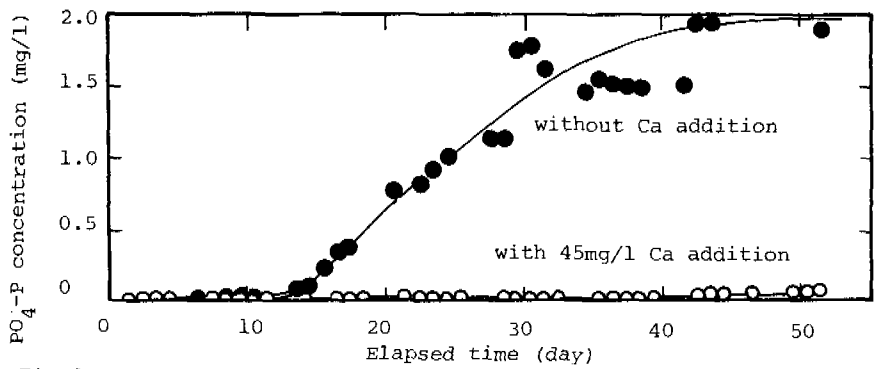

Fig.6. Column test results:Effect of Ca on the efficiency of phosphorus removal. Initial condition:PO_4-P=2mg/l,M-alkalinity=100mg/l, pH=9(-),SV=2hr^{-1}.

Effect of alkalinity of water. The effect of bicarbonate ions on calcium phosphate precipitation has been investigated. It is reported that bicarbonate ions cause increase of phosphate residuals at pH9 - 10.5 because of competitive precipitation with calcium carbonate (Ferguson et al. 1970, 1973).

The effectsof alkalinity of water on the phosphorus removal were studied using the batch and the column systems. Contact timesin the batch experiments were from 1 to 25 hours, and length of the column experiments was for 68days.

Seed-A was used for the batch system and Seed-B for the column system. Alkalinity of the water was adjusted to a desired degree with a sodium bicarbonate solution. The results of the batch experiments are shown in Figure 7, and those of the column experiments in Figure 8. According to the results of the batch experiments, the efficiency of phosphorus removal decreased as the alkalinity of water increased. On the other hand, in the case of the column experiments no difference was observed in the efficiency of phosphorus removal at the steady state under the experimental conditions of alkalinity from 50 to 250mg/1. In the case of the column experiments, a phenomenon was observed that the pH of the effluent was decreased as the alkalinity of water decreased. From these experimental results it seems that the efficiency of phosphorus removal at the steady state was more strongly affected by the pH of water than the alkalinity.

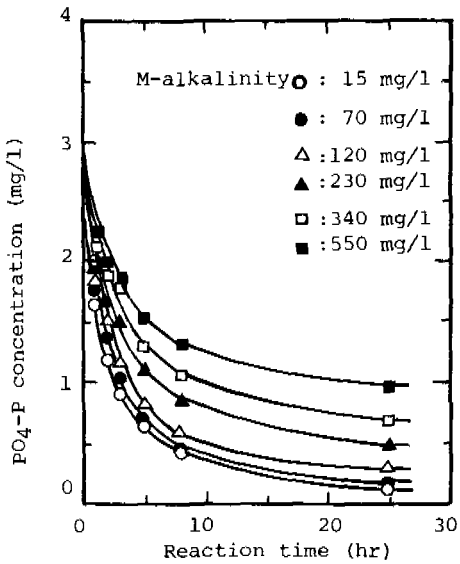

Fig.7.Effect of M-alkalinity of water on the efficiency of phosphorus removal.Initial condition:PO_4-P=3mg/1, Ca=50mg/1,pH=8.5(1),Seed crystals addition=0.1wt%.

Application to a sewage secondary effluent. The column tests were conducted with a sewage secondary effluent. The sewage secondary effluent dosed with calcium chloride at 20-25mg/1 calcium and adjusted to pH9 by caustic soda was passed upward through the test column packed with 300ml of the granular seed crystals (Seed-B). For removal of suspended solids trapped in the bed, a backwash operation was carried out once a day at a flow rate of LV*=30m/hr for about 10min. The results of the continuous flow test are shown in Figure 9. Phosphorus concentrations in the feed varied from 1 to 6mg/1, and those of the treated water were 0.03 to 0.5mg/1 during the test period over 180 days.

* LV = linear velocity

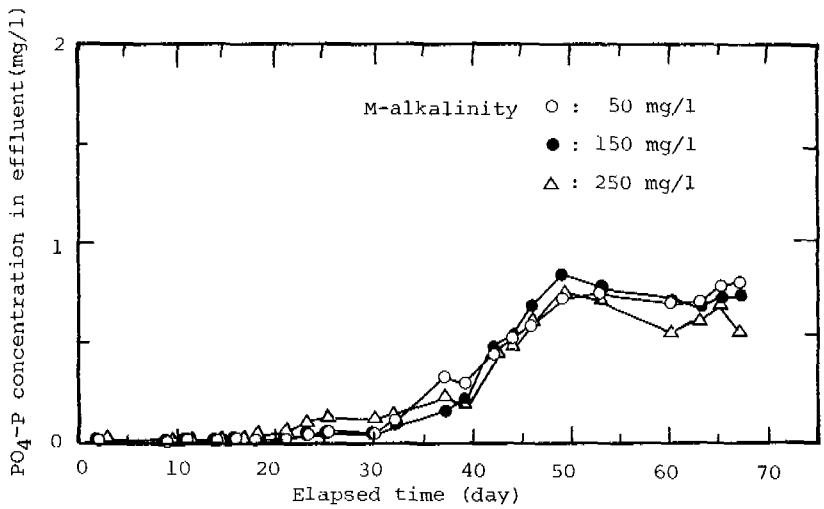

Fig.8.Column test results-Effect of M-alkalinity of water on the efficiency of phosphorus removal . Initial condition:PO_4-P=3mg/1, Ca=40mg/1,pH=9(-),SV=3hr^{-1}. SV = space velocity.

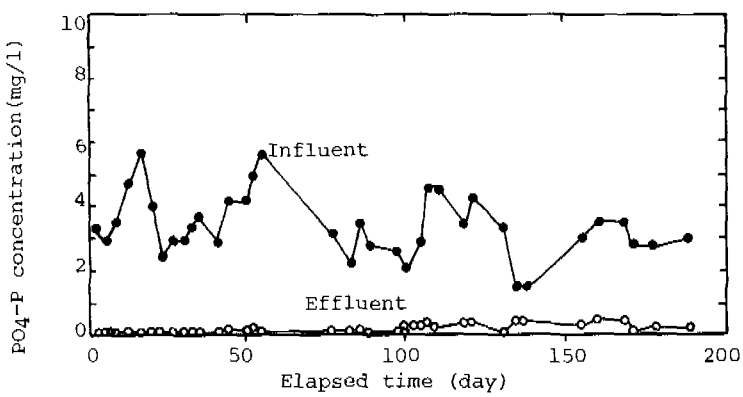

Fig.9.Column test results with a sewage secondary effluent. Condition: Ca addition=20-25mg/1,pH=9(-),SV=2hr^{-1}.

PILOT PLANT TESTS

Specifications and operating conditions. As the crystallization method was proved to be practicable for phosphorus removal from sewage secondary effluent, a pilot plant consisting of a fixed bed up-flow type crystallization reactor packed with the granular seed crystals (Seed-B) and chemical dosing equipment was installed at Yamato Municipal Sewage Works to investigate reliability for a long-term performance. The operation of the plant was started in June 1979. It was operated continuously for about 6 months. The pilot plant specifications and the flow diagram are shown in Table 2 and Figure 10, respectively.

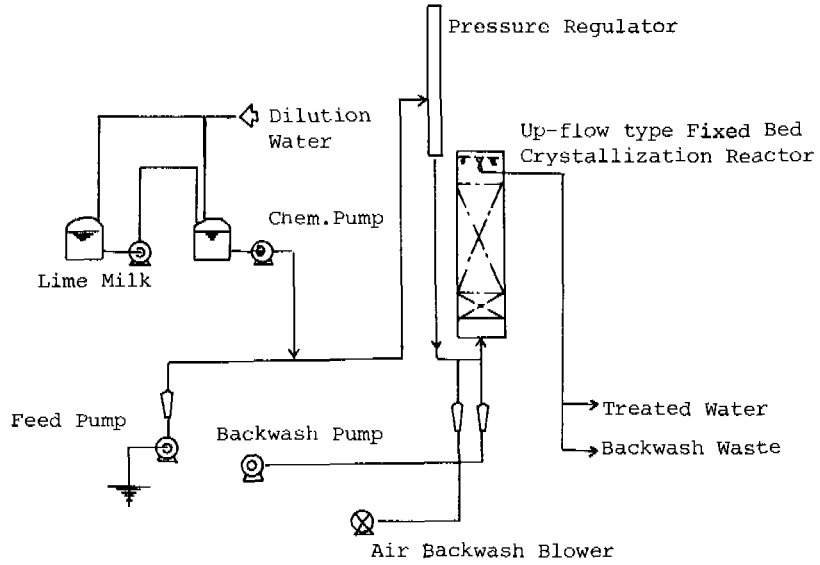

Fig.10. Flow diagram of the pilot plant

TABLE 2 Specification and Operating Conditions of Pilot Plant

Type	Up-flow type fixed bed
Size	900mm$^{\phi}$ x 3,050mm^{H}
Seed crystals	Seed-B
	Packed volume=0.9m^{3}
Flow rate	SV=2.3hr^{-1}
Backwashing	Air-water backwash

Result and discussion. A lime dose of 70mg/l was necessary to raise the pH of feed to the predetermined value of 9, because M-alkalinity of the secondary effluent was as high as 200-300mg/l as $CaCO_3$. The values were high compared to 80-120mg/l of average municipal effluents in Japan. In Figure 11, pH values obtained as a function of lime dose for different M-alkalinity of sewage secondary effluent are shown. For average sewage effluents in Japan, 40-50mg/l lime should be sufficient.

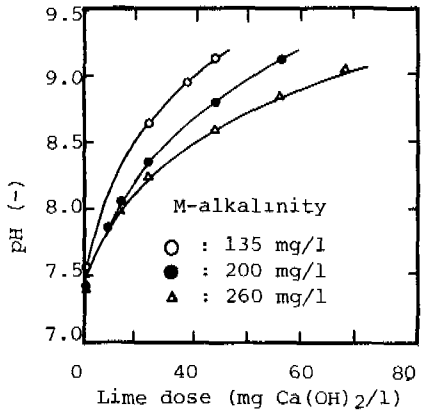

Fig.11. pH values obtained as a function of lime dose for different M-alkalinity of wastewater.

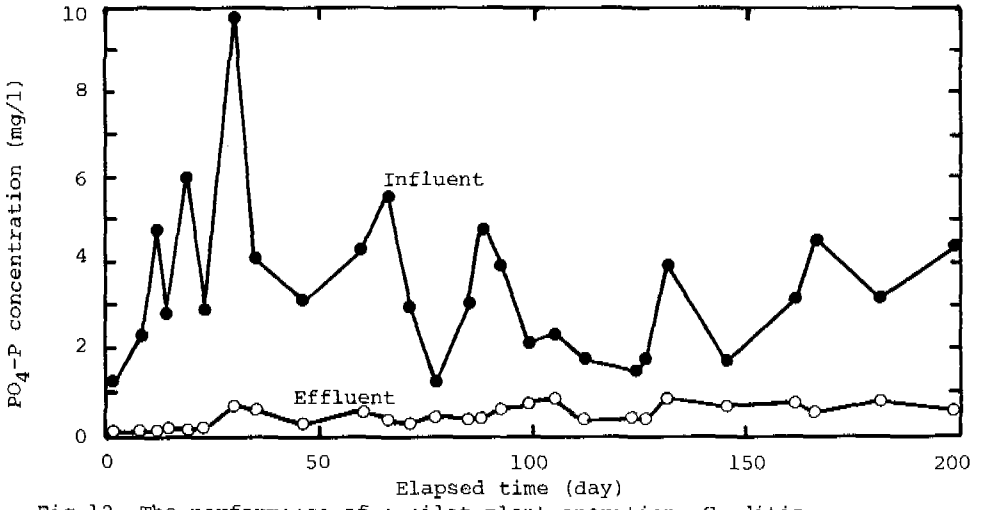

Fig.12. The performance of a pilot plant operation. Condition : Lime dose = 70mg/l, pH=8.5-9, SV=2.3hr^{-1}.

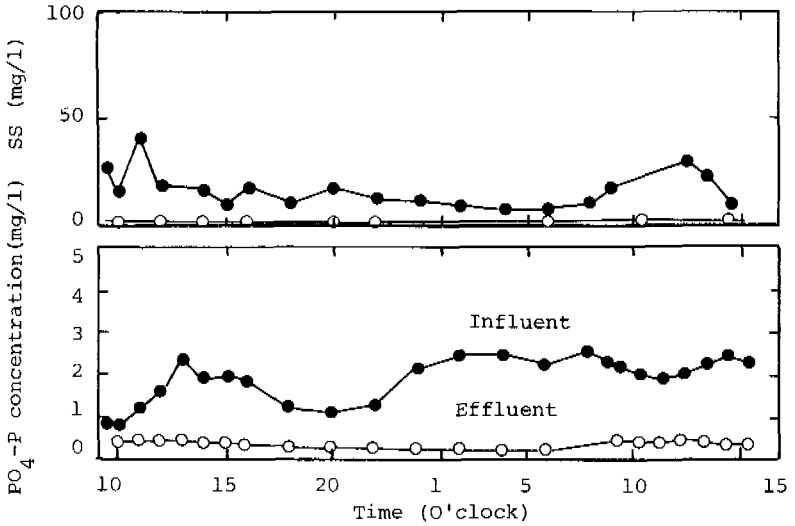

Fig.13. Water quality diurnal changes

Figure 12 shows the performance obtained from the operation continued as long as 200 days.
Phosphorus concentrations in the feed water varied from 1 to 10mg/l, and those of the treated water were always below 1mg/l. Figure 13 shows the stability of this process against varying influent phosphorus and suspended solids concentrations. It was found that phosphorus and suspended solids in the sewage secondary effluent could be removed simultaneously to a sufficiently low level, and the amount of sludge generated was practically negligible.

CONCLUSIONS

1. Phosphorus in wastewater was removed to a sufficiently low level at the metastable reaction zone defined by concentrations of phosphorus, calcium and pH under the presence of seed crystals.
2. Phosphate rock was effective as the seed crystals.
3. Suspended solids in wastewater were removed in the phosphorus removal process by the up-flow type fixed bed crystallization reactor.
4. The efficiency of phosphorus removal was more strongly affected by the operating conditions such as pH and calcium concentration than the alkalinity of water.
5. The problem of sludge production was practically negligible.

At present, three field tests using pilot plants (flow rate : 120m^3/day, 90m^3/day, 80m^3/day respectively) are carrying on at three different sewage treatment plants, and three actual facilities (flow rate : 480m^3/day, 350m^3/day, 90m^3/day respectively) of this process are in operation in Japan.

REFERENCES

Ferguson, J.F., Jenkins, D. and Stumm, W. (1970). Calcium Phosphate Precipitation in Wastewater. Chem. Prog. Symp. Ser., 67, 279-287.

Ferguson, J.F., Jenkins, D. and Eastman, J. (1973). Calcium phosphate precipitation at slightly alkaline pH values. J. Water Pollut. Control Fed., 45, 620-631.

Joko, I., Koizumi, M., Watanabe, A. and Abe, O. (1980). Studies on Phosphorus Removal by Crystallization Method (1)-Reaction Conditions for Phosphate Crystallization -. Jour. Japan Sewage Works Association, 17(197), 43-49.

Joko, I., Koizumi, M., Watanabe, A. and Abe, O. (1981). Studies on Phosphate Removal by Crystallization Method (2)-Crystallization Filtration System -. Jour. Japan Sewage Works Association, 18 (200), 2-11.

Joko, I. (1983). Studies on Phosphorus Removal by Crystallization Method : The Effect of Alkalinity of Water. Env. Cons. Eng., 12, 278-283.

Koutsoukos, P., Amjad, Z., Tomson, M.B. and Nancollas, G.H. (1980). Crystallization of Calcium Phosphates. A Constant Composition Study. J. Am. Chem. Soc., 27, 1553-1557.

Nancollas, G.H. (1968). Kinetics of Crystal Growth from Solution. Journal of Crystal Growth, 34, 335-339.

Nancollas, G.H. and Mohan, M.S. (1970). The Growth of Hydroxyapatite Crystals. Archs. oral Biol., 15, 731-745.

Nancollas, G.H. and Wefel, J.S. (1976). Seeded Growth of Calcium Phosphates : Effect of Different Calcium Phosphate Seed Material. J. Dent. Res., 55, 617-624.

Tomazic, B. and Nancollas, G.H. (1975). The Seeded Growth of Calcium Phosphates. Surface Characterization and the Effect of Seed Material. J. Colloid Interface Sci., 50, 451-461.

Walton, A.G., Bodin, W.J., Furedi, H. and Schwartz, A. (1967). Nucleation of calcium phosphate from solution. Can. J. Chem., 45, 2695-2701.

Zoltek, J. Jr. (1974). Phosphorus removal by orthophosphate nucleation. J. Water Pollut. Control Fed., 46, 2498-2520.

Wat. Sci. Tech. Vol.17, Amsterdam, pp.133-142.
Printed in Great Britain.

0273-1223/85 $0.00 + .50

PHOSPHATE REMOVAL BY CRYSTALLIZATION IN A FLUIDIZED BED

J. C. van Dijk and H. Braakensiek

DHV Consulting Engineers, P.O Box 85, 3800 AB Amersfoort, The Netherlands

ABSTRACT

A new process for the removal of phosphate from effluent from sewage treatment plants is described. The process is based on the crystallization of calcium phosphate in a fluidized bed. The major advantage of the process is the fact that no sludge is produced, but a small quantity of waterfree pellets that can be reused in the phosphate industry. The results of five years of research and development are presented. In 1984 the first demonstration plant will be built. Cost calculations for a full-scale plant are also given.

KEYWORDS

Phosphate removal, fluidized bed, tertiary treatment, calcium phosphate crystallization, pellet reactor.

INTRODUCTION

Conventional methods for the removal of phosphates from wastewater in sewage treatment plants are based on the precipitation of metal phosphates. Iron salts ($FeCl_3$ or $FeSO_4$), aluminum salts ($Al_2(SO_4)_3$) or lime compounds (CaO or $Ca(OH_2)$) are dosed to the wastewater, whereafter a precipitate is formed which can be removed by sedimentation. Depending on the place of application of the chemicals in the treatment process, the precipitate can be removed in the preliminary sedimentation tank, the final sedimentation tank or a tertiary sedimentation tank.
The main disadvantage of the conventional methods is the production of a substantial amount of chemical sludge. Handling, transport and disposal of this sludge lead to increased cost and a solid waste problem, which cannot easily be solved in densely populated areas.

Our paper deals with a new process for the removal of phosphate from wastewater, based on the crystallization of calcium phosphate in a fluidized bed. This method produces no sludge, but only a small amount (4 kg per p.e. per year) of waterfree pellets. These calcium phosphate pellets can be used in the phosphate industry, thus creating a simple and effective method of recycling phosphate.

BASIC PRINCIPLES OF THE SYSTEM

The most typical aspect of the system is a fluidized bed of pellets on which the crystallization of calcium phosphate takes place (see Figure 1). The pellets move freely in the upward flow of the water so that cementing of the pellets is prevented. This is why a certain minimum flow is required.
Because the sedimentation velocity of the pellets is much higher than that of calcium phosphate flocs, the surface load of a crystallization reactor can be much higher than that of a sludge process. The high rate of crystallization allows a very short detention time. In practice, the maximum superficial velocity amounts to some 80 m/h.
Another design parameter often used for fluidized bed reactors is the fixed bed height, which is defined as the height of the grain bed at zero-flow.
During operation the pellets in the reactor increase in diameter. As a bed of large pellets has a small reactive surface (part of) the pellets should be regularly removed and replaced by smaller diameter seed pellets. If only a proportion of the pellets is replaced this procedure can take place during full operation.
The seed pellets can consist either of broken product material or of other materials, such as silica sand.
Caustic soda is the most suitable chemical for use in the crystallization process as it is commercially available as a solution, that can be applied after a simple dilution procedure. Lime may also be used but should be applied as a pure solution for a proper crystallization process.

THEORY

In order to effect crystallization, the wastewater should be supersaturated with respect to calcium phosphate. Solubility products of some calcium phosphates (Sillen and Martel, 1964) are presented in Table 1.

TABLE 1 Solubility products of calcium phosphates
(pK_a = negative logarithm of activity product)

Compound		pK_a
$CaHPO_4.2H_2O$	Dicalcium phosphate	6.5
$Ca_3(PO_4)_2$	Tricalcium phosphate	26.0
$Ca_4H(PO_4)_3$	Octacalcium phosphate	46.9
$Ca_5(PO_4)_3\,OH$	Hydroxiliapatite	57.8
$Ca_5(PO_4)_3\,F$	Fluorapatite	60.4

The solubility product of one or more calcium phosphate compounds can be exceeded by dosing of either Ca^{++}-ions or OH^--ions. In practice, dosing of OH^--ions is most effective as it increases the driving force for the crystallization considerably by the conversion of $H_2PO_4^-$ and HPO_4^{--} to PO_4^{---}, as presented in Table 2 (Stumm and Morgan, 1981). Dosing of Ca^{++}-ions is only required in wastewater with a low natural Ca^{++}-concentration, i.e. soft water.

TABLE 2 Equilibrium constants of phosphorous acid
($pK_{1,2,3}$ = negative logarithm of equilibrium constant)

$H_3PO_4 + H_2O \rightleftarrows H_2PO_4^- + H_3O^+$	$pK_1 = 2.2$
$H_2PO_4^- + H_2O \rightleftarrows HPO_4^{--} + H_3O^+$	$pK_2 = 7.2$
$HPO_4^{--} + H_2O \rightleftarrows PO_4^{---} + H_3O^+$	$pK_3 = 12.2$

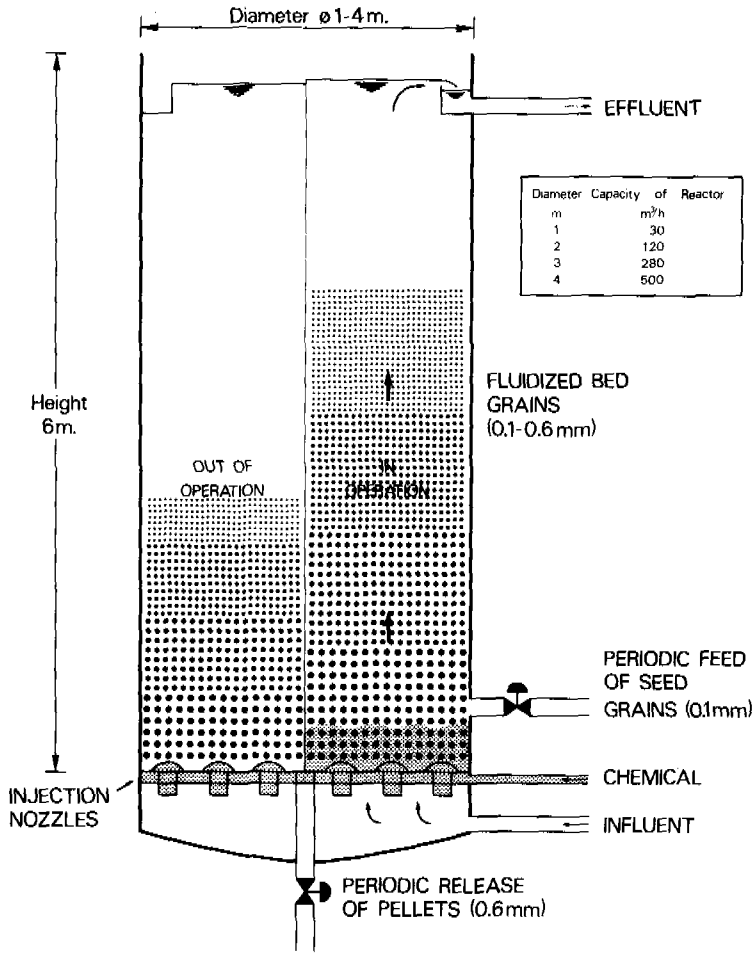

FIGURE 1. BASICS OF FLUIDIZED BED REACTOR

A rise in pH increases the driving force for the crystallization and consequently leads to a lower phosphate content in the effluent from the reactor. However, the pH cannot be increased too much as this will lead to spontaneous nucleation of calcium phosphate in the liquid phase, instead of crystal growth on the seed grains. Spontaneous nucleation occurs when the solubility product of $Ca_3(PO_4)_2$ is exceeded (Nancollas and Wefel, 1976) and is demonstrated by the presence of small flocs in the effluent of the reactor. The effluent becomes turbid and the total phosphate concentration is rather high.
Consequently, the process conditions should be such that crystal growth occurs on the seed grains and spontaneous nucleation is avoided.

It is noted that effluent of sewage treatment plants contains many compounds that may influence the solubility and crystallization of calcium phosphates. Negative effects have been reported from HCO_3^-, Mg^{++}, Sn and organic phosphate, whereas a strongly positive effect has been reported from F^-, in concentrations over 10^{-5} mol/l (Nancollas and Tomazic, 1974, Meyer and Nancollas, 1972).

This implies that the actual solubility product and crystallization rate of calcium phosphate can only be determined by field tests at sewage treatment plants.

RESULTS OF FIELD TESTS

The development of the crystallization process was started by DHV Consulting Engineers in 1978.
Since 1978 DHV has carried out investigations both into the fundamental physical-chemical process conditions as well as into the practical feasibility of the process for removal of phosphate in sewage treatment plants. The complete results have been described in nine reports (DHV Raadgevend Ingenieursbureau, 1978-83). In the present paper a summary of the most important results is given.

* Concentration of soluble ortho-P

The relation between the concentrations of soluble ortho-P, calcium and pH in the effluent from the reactor has been determined at several sewage treatment plants. It was found that neither the composition of the sewage nor the biological process applied influenced the actual solubility of calcium phosphate. For all plants, the concentration of soluble ortho-P in the effluent from the reactor was found to be determined entirely by pH and Ca^{++}-concentration, as presented in Figure 2.
The data of Figure 2 were hardly influenced by such kinetic conditions in the reactor as superficial velocity (range 10-60 m/h), bed height (range 1-3 m) and grain size (range 0.1-0.6 mm). It becomes therefore clear that the reaction rate is not a limiting factor and the effluent of the reactor is in chemical equilibrium. However, from Figure 2 it can be calculated that the actual solubility is much higher than the theoretical solubility. The negative logarithm of the actual activity products is approximately 41-43 for hydroxilapatite, 44-45 for octacalcium phosphate and 24-25 for tricalcium phosphate.

* Concentration of organic-P

Organic phosphate can be incorporated in the crystal lattice only to a limited extent. Data on the removal of organic phosphate are presented in Table 3.

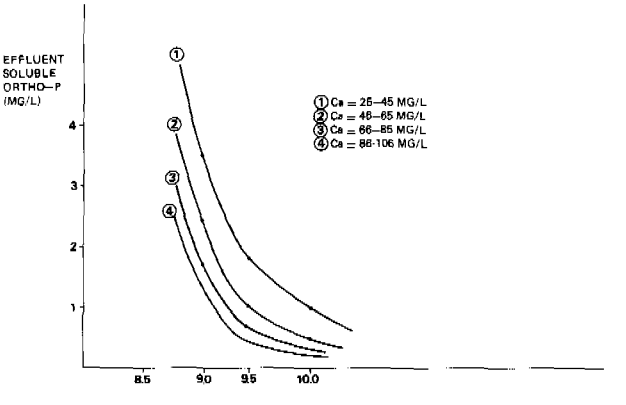

FIGURE 2: CONCENTRATION OF SOLUBLE ORTHO–P IN THE EFFLUENT FROM THE REACTOR

TABLE 3 Reduction of organic-P in the reactor

Sewage treatment plant	Type	Average concentration feed (mg/l)	Average concentration effluent (mg/l)
Wijk bij Duurstede	Oxidation ditch	< 0.1	< 0.1
Weesp	Trickling filter	1.9	1.0
Huizen	Activated sludge	0.5	0.1

The differences in concentration of organic-P in the treatment plants are apparent. The trickling filter plant gives an effluent with a much higher organic-P content than the oxidation ditch and activated sludge plant. In view of the limited removal of organic-P, it can be concluded that the fluidized-bed process is more suitable for the latter type of treatment plants.

* Concentration of filtrable ortho-P

As mentioned before, the effluent from the reactor may contain some phosphate, that can be removed by filtration through a membrane filter. It was found that the following three factors influence the concentration of filtrable ortho-P:

- Composition of the feed

  In the effluent from the sewage treatment plant some suspended matter is normally present, which also contains phosphate.
  As this suspended matter will not be removed in the reactor, the phosphate will also be present in the effluent.
  Table 4 gives some data on the concentration of filtrable ortho-P in the effluent of the reactor at different treatment plants.

TABLE 4 Concentration of filtrable ortho-P in the effluent from the reactor

Sewage treatment plant	Type	Average concentration filtrable ortho-P (mg/l)
Wijk bij Duurstede	Oxidation ditch	0.44
Weesp	Trickling filter	0.47
Huizen	Activated sludge	1.27
Driebergen	Trickling filter	1.27

The concentration of filtrable ortho-P in Huizen and Driebergen proves to be much higher than in Wijk bij Duurstede and Weesp. This is attributed to the final clarifier. In view of the limited removal of suspended matter, it is concluded that the fluidized-bed process is more suitable for treatment plants with a secondary effluent that is low in suspended solids.

Erosion of calcium phosphate from the grains

The turbulence in the reactor should not become too high in order to prevent erosion of the grains.
The turbulence in the reactor can be expressed by means of the velocity gradient G (Kawamura, 1975):

$G = \sqrt{\frac{W}{\eta}}$

G = velocity gradient (s^{-1})
W = power dissipated per unit volume (W/m^3)
η = absolute viscosity (Ns/m^2)

The power dissipated in the reactor can be divided into two parts:

Power dissipated for the fluidization of the bed

This is determined mainly by the submerged weight of the fluidized bed and the expansion of the bed. In practice, the G-value proves to increase with increasing grain size and specific gravity, and is relatively independent of superficial velocity.

Power dissipated at the water distribution nozzles

This is determined by the water velocity at the nozzle outlets. In practice the G-value can be strongly influenced by the size and number of the nozzle openings.

Table 5 gives data on the relationship between G-value and filtrable ortho-P.

TABLE 5 Concentration of filtrable ortho-P for different G-values

Nozzle type	Superficial velocity (m/h)	Grain size (mm)	G-value (s^{-1})	Average concentration filtrable ortho-P (mg/l)
I	40	0.50	330	1.30
II	40	0.50	280	0.90
II	40	0.25	170	0.45
II	10	0.25	170	0.45

The minimum concentration of filtrable ortho-P, which is 0.45 mg/l, approximately equals the concentration in the feed. It turns out that this concentration increases with increasing grain size and increasing turbulence at the inlet (due to nozzle type).

- Homogeneous nucleation of amorphous ortho-P

Homogeneous nucleation of amorphous ortho-P occurs when the supersaturation becomes so high that crystallization does not take place solely at the surface of the seed grains, but also in the liquid.
It was found that several practical measures can be taken to prevent homogeneous nucleation of amorphous ortho-P:
- intensive mixing of caustic soda and water in such a manner as to avoid locally high supersaturation
- mixing of caustic soda and water in the presence of grains with a high specific surface
- recirculation of effluent
- dosing of caustic soda in more than one step
- application of more than one reactor in series

In most of the situations investigated (Dutch sewage treatment plants with an effluent P-concentration of 6-30 mg/l), the latter two measures were not necessary. Recirculation is not strictly necessary either, but allows less sensitive process control.
The mixing of water and reagent was found to be very important, especially in view of the fact that the water inlet nozzles were selected for minimum turbulence. In order to achieve proper mixing of water and caustic soda, it is therefore necessary to strongly dilute the caustic soda and inject it through special nozzles with a relatively small opening.

* Concentration of total-P

The concentration of total-P is equal to the sum of the three parameters mentioned and varies between roughly 1 mg/l (oxidation ditch effluent) and 2 mg/l (trickling filter effluent).

* Consumption of chemicals

The consumption of caustic soda is to a large extent determined by the conversion of CO_2 and HCO_3^- to CO_3^{--} (Stumm and Morgan, 1981).

TABLE 6 Equilibrium constants of carbonic acid
($pK_{1,2}$ = negative logarithm of equilibrium constant)

$CO_2 + 2H_2O \rightleftarrows H_3O^+ + HCO_3^-$	$pK_1 = 6.3$
$HCO_3^- + H_2O \rightleftarrows H_3O^+ + CO_3^{--}$	$pK_2 = 10.3$

Consequently, the caustic soda consumption will be higher for high alkalinity water than for low alkalinity water. In practice, the consumption is approximately 2-3 mmol/l.
For soft waters Ca^{++}-ions also have to be added. This can be done by dosing $Ca(OH)_2$ to the final settling tank of the sewage treatment plant or to the pump buffer tank (see Figure 3). The lime can be dosed to a pH of around 8. Milk of lime can be used for this purpose as a result of the available dissolving time. For hard water lime dosing may also be advantageous in view of cost.

* Production of pellets

It has been established that the pellets consist virtually completely of calcium phosphate and seed material. Other compounds, such as $CaCO_3$, are not present in significant amounts.
The pellets can be used in the phosphate industry and represent an economic commodity. The pellet production is approximately 4 kg per p.e. per year - based on a P-discharge of 1.3 kg per p.e. per year and 40% P-removal in the primary and secondary treatment stages.

COST

The investigations have up to now been carried out on a pilot-plant scale (capacity max. 30 m^3/d). In 1984 a demonstration unit with a capacity of 270 m^3/d will be built.
Cost calculations have been prepared for a plant for 10,000 p.e. (see Figure 3) and are summarized below:

Investment:	buffer tank reactor caustic soda storage and dosing control and electrical equipment	Dfl. 310,000

Annual cost:

1.	depreciation 15 years, interest 10%	Dfl. 40,000
2.	maintenance 3%	Dfl. 9,000
3.	caustic soda 2 mmol/l at Dfl. 0.024/mol	Dfl. 35,000
4.	energy 0.02 kWh/m^3 at Dfl. 0.20/kWh	Dfl. 3,000
5.	pellet disposal	Dfl. 0
	Total	Dfl. 87,000
	Cost per p.e.	Dfl. 8,70
	(1 Dfl. = 0.33 US$)	

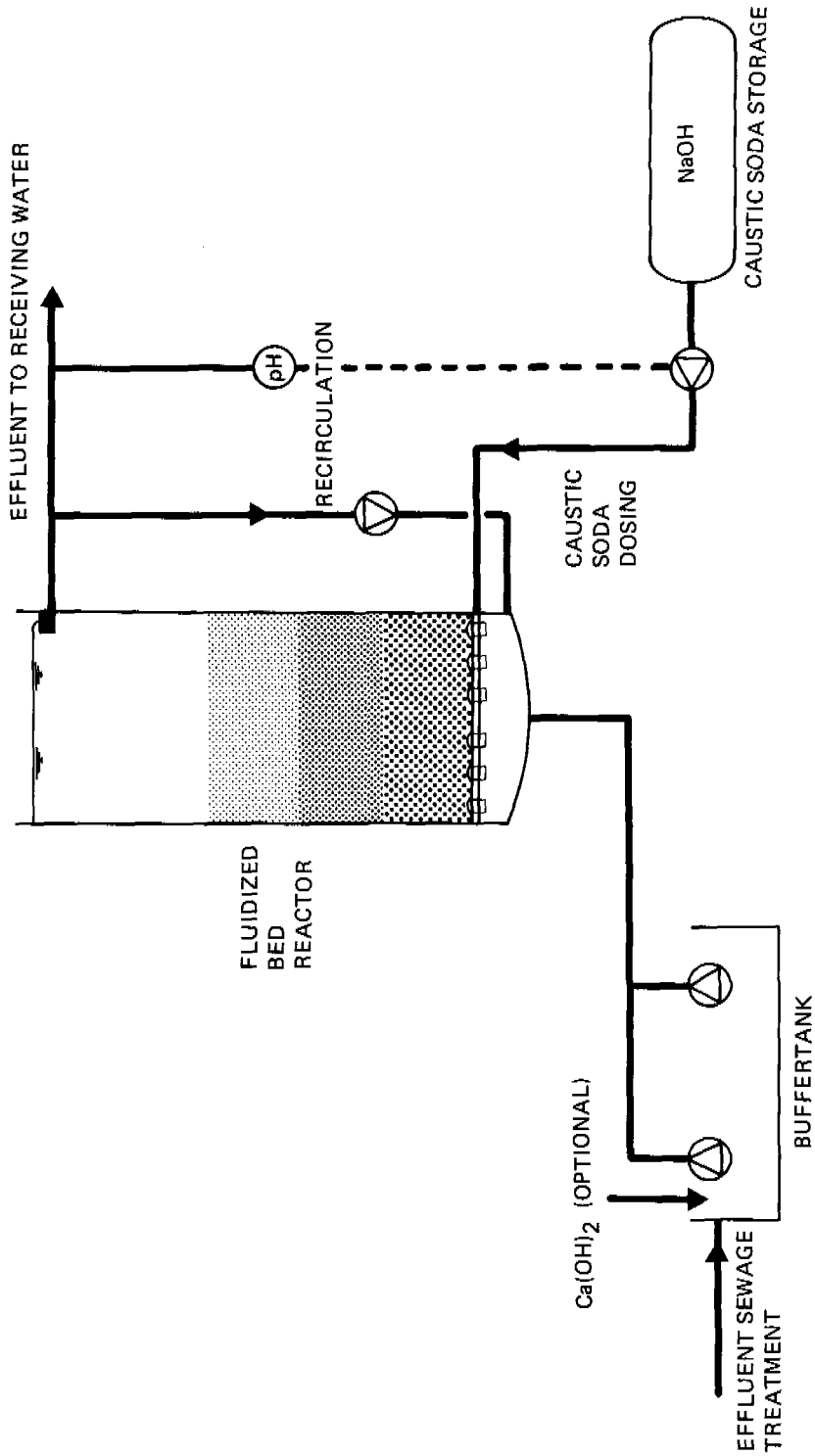

FIGURE 3: TREATMENT PLANT FOR REMOVAL OF PHOSPHATE BASED ON CRYSTALLIZATION IN A FLUIDIZED BED.

ACKNOWLEDGEMENTS

Financial support for the research programme has been given by the Dutch government (through the Dutch Institute for Treatment of Wastewater) since 1979 and by Hoechst Holland BV since 1982. Technical support during the execution of the tests has been given by the Water Control Authorities Amstel en Gooiland and the Province of Utrecht.

LITERATURE

DHV Raadgevend Ingenieursbureau. Fosfaatverwijdering in een gefluidiseerd kristalbed. DHV Raadgevend Ingenieursbureau. Amersfoort, the Netherlands. 9 Reports from 1978-1983 (in Dutch).

Kawamura, S. Design and operation of high-rate filters - Part 2. Journal Am. Water Wrks Ass., Nov. 1975, p. 653-662.

Nancollas, G.H. and Tomazic, B. Growth of calcium phosphate on hydroxilapatite crystals, Effect of supersaturation and ionic medium. Journal of Physical Chemistry, Vol. 78, no. 22, 1974, 2218-2225.

Nancollas, G.H. and Wefel. Seeded growth of calcium phosphate. Effect of different calcium phosphate seed material. Journal Dental Research, August 1976, 617-624.

Meyer, J.L. and Nancollas, G.H. Effect of stannous and fluoride ions on the rate of crystal growth of hydroxilapatite. Journal Dental Research, October 1972, 1443-1450.

Sillen, L.G. and Martell, A.E. Stability constants of metal-ion complexes, Special Publication No. 17, The Chemical Society. Metcalf and Cooper Ltd., London 1964 .

Stumm, W. and Morgan, J.J. Aquatic Chemistry (2nd ed.). John Wiley & Sons, New York 1981.

ANAEROBIC TREATMENT

Wat. Sci. Tech. Vol.17, Amsterdam, pp.143-154.
Printed in Great Britain.

0273-1223/85 $0.00 + .50

BATCH ANAEROBIC METHANOGENESIS OF PHENOLIC COAL CONVERSION WASTEWATER

Phillip M. Fedorak and Steve E. Hrudey

Environmental Engineering and Science Program, Department of Civil Engineering, University of Alberta, Edmonton, Alberta, T6G 2G7, Canada

ABSTRACT

Batch experiments using the Hungate serum bottle technique were used to determine the anaerobic treatability of phenolic (7600 mg/l by 4-aminoantipyrine) wastewater from an H-coal conversion pilot plant. Methane production above controls was achieved at up to 6% V/V dilution. At these levels, inhibitory components in the wastewater retard but do not stop volatile organic acid (VOA) fermentation to methane.

Ether-extracted wastewater was tested at up to 50% V/V on cultures receiving 200 mg/l phenol and was found not to be inhibitory, suggesting that inhibitory components in the wastewater are ether-extractable. Finally, a "reconstituted H-coal" which contained pure phenolic constituents added to ether-extracted H-coal exhibited batch methanogenesis above controls at H-coal dilutions up to 10% V/V. These findings indicate that the ether-extractable inhibitory substances are not one of the major phenolic compounds present in the H-coal wastewater.

INTRODUCTION

Wastewater from coal conversion technologies present a major treatment challenge (Neufeld, 1984). Although aerobic biological treatment technology has received the most attention for these wastewaters, anaerobic processes offer significant advantages in lower energy consumption and sludge production. Anaerobic treatability of phenolics has received increasing attention in recent years (Fedorak and Hrudey, 1984; Boyd et al., 1983; Khan et al., 1982; Khan et al., 1981; Suidan et al., 1980; Ossio and Fox, 1980; Neufeld et al., 1980) but work involving anaerobic treatment of coal conversion wastewaters has not been widely reported.

A study of the batch anaerobic treatability of coal conversion wastewaters was undertaken using a sample of wastewater from the H-coal pilot plant at Catlettsburg, Kentucky (supplied to us by Dearborn Environmental Consulting Services on behalf of the Wastewater Technology Centre, Environmental Protection Service, Environment Canada). This wastewater will be referred to simply as "**H-coal**" throughout this report.

The project aimed to establish at what level, if any, batch cultures could ferment phenolic components of H-coal to methane and to characterize the nature of any inhibition of methanogenesis apparent with this wastewater.

MATERIALS AND METHODS

Analytical Methods

Methane analyses were done using the gas chromatographic (GC) method of Fedorak and Hrudey (1983) and volatile organic acids (VOAs) were analyzed by the GC method outlined by Boone (1982).

Phenolic compounds in the wastewater and cultures were routinely analyzed using an aqueous injection method on 5% Polymetaphenyl ether coated Tenax GC (Bartle et al., 1977). The 4.5 m x 3.2 mm stainless steel column was housed in a Varian (model 1700) GC equipped with a flame ionization detector (FID). The injector, oven and detector temperatures were 250°, 200°, and 350°C respectively. Nitrogen was used as a carrier gas at 17 ml/min. Detector hydrogen and air flows were 30 and 300 ml/min respectively. This method did not resolve the m- and p- isomers of cresol. The relative proportions of these two isomers were determined by extracting the wastewater with methylene chloride using the procedure of Stuermer et al. (1982). The phenolic compounds were analyzed using a 1.8 m x 2 mm glass column packed with GP (80/100) Carbopack C /0.1% SP-1000 (Supelco) housed in a Hewlett Packard (model 5736A) GC. The injection port and FID were at 250°C while the oven was at 225°C. Nitrogen was used as the carrier gas at 13 ml/min. Hydrogen and air flow rates were 30 and 240 ml/min respectively.

Preparation of H-coal and H-coal Derived Test Solutions

Three test solutions were used in these batch culture experiments: unmodified H-coal, ether-extracted H-coal and reconstituted H-coal. Each test solution was pre-reduced prior to being added to the anaerobic cultures. This was done by placing 80-100 ml in a 158 ml serum bottle and adding 1 part per 100 resazurin solution (100 mg/l). The bottle was sealed and then the headspace gas was exchanged 10 times to remove oxygen. This was done by first evacuating the headspace and then filling with O_2-free 30% CO_2 in N_2. After this procedure was complete, 1 part per 100 sodium sulfide solution (25 mg/l $Na_2S \cdot 9H_2O$) was added to lower the redox potential.

The ether-extracted effluent was prepared by extracting 200 ml of H-coal 7 times with 30 ml portions of diethyl ether. The aqueous phase was then drained into a beaker and left overnight to allow dissolved ether to evaporate. The extent of the phenolic removal and the presence of any residual ether were determined by GC analysis.

The reconstituted H-coal was prepared by combining suitable aliquots of 7 concentrated phenolic solutions in ether-extracted H-coal. The volumes and concentrations were as follows: 40 ml phenol (12 250 mg/l), 5 ml o-cresol (9 080 mg/l), 10 ml m-cresol (12 500 mg/l), 5 ml p-cresol (8 030 mg/l), 5 ml 2,5-dimethylphenol (DMP) (1 260 mg/l), 10 ml 3,5-DMP (2 130 mg/l) and 5 ml 3,4-DMP (880 mg/l). A further 18 ml of extracted H-coal and 1 ml resazurin solution were added giving a total volume of 99 ml liquid in a serum bottle which was then sealed. After the headspace gas had been exchanged, 1 ml sodium sulfide solution was added. Based on GC analysis, the concentrations of each phenolic in the reconstituted H-coal were essentially the same as those in the unmodified H-coal wastewater.

Culture Methods

Details on the set up of the batch cultures in serum bottles and the composition of the medium have been given by Fedorak and Hrudey (1984). However, in the present study, smaller aliquots of more concentrated medium were added to the cultures to allow larger volumes of H-coal to be added to a fixed total culture volume of 10 ml. The concentration of the medium was increased by reducing the volume of water added during preparation. The final volumes of the prepared medium were 70 ml when 3 ml aliquots were added to the cultures and 33.3 ml when 1 ml aliquots were added.

All cultures were incubated at 37°C with occasional shaking. Headspace samples were frequently analyzed for methane. After inverting the bottles and allowing the biomass to settle, 3 µl aliquots of supernatant were removed with a Hamilton syringe and analyzed for phenolic content. In all cases, triplicate cultures were established for each test solution.

Cultures containing unmodified H-coal. The final dilutions of H-coal tested in 10 ml cultures are listed in Table 1. Prior to autoclaving, each bottle contained 3 ml medium and an aliquot of 0.5 to 2 ml distilled water (depending on the dose of H-coal to be added). After autoclaving, all additions to the bottles were made using a syringe. The sterile contents were pre-reduced with 0.1 ml sodium sulfide solution and inoculated with 5 ml of domestic anaerobic sewage sludge. Then a suitable aliquot of pre-reduced H-coal was added to each bottle to give the desired final dilution. For example, the 15% (V/V) culture contained 3 ml medium, 0.5 ml distilled water, 5 ml sludge and 1.5 ml H-coal. Two such sets of cultures were established. One set was supplemented with 0.1 ml VOA solution containing 37.5 mg/ml acetic acid and 13 mg/ml propionic acid (pH 7) to test the effects of the wastewater on the conversion of VOAs to methane (Owen et al., 1979). The other set remained unsupplemented.

Cultures containing ether-extracted H-coal. The final dilutions of ether-extracted H-coal tested in 10 ml cultures are listed in Table 1. After autoclaving and pre-reducing with 0.1 ml sodium sulfide, each bottle was inoculated with 3 ml of domestic anaerobic sewage sludge and suitable aliquots of pre-reduced ether-extracted H-coal were added to give the desired final concentration.

Cultures containing reconstituted H-coal. These cultures were set up in the same manner as the unmodified H-coal cultures using pre-reduced, reconstituted H-coal in place of the unmodified H-coal. The final dilutions of reconstituted H-coal tested, including two positive controls (2 and 4% unmodified H-coal), are listed in Table 1.

Statistical Methods

At each time of methane analysis, the data were analyzed using the method of Dunnett (1955) to determine which test solutions produced mean methane levels which were significantly different from the mean control value ($P > 0.05$).

TABLE 1. Summary of Experimental Batch Cultures[1]

Substrates/Controls	H-Coal Concentrations Tested (% V/V)	Medium Volume (ml)	Domestic Sludge Inoculum Volume (ml)
H-Coal: • unmodified	2 4 6 8 10 12 15	3	5
Control: • distilled water	0	3	5
H-Coal: • plus 500 mg/l VOA	2 4 6 8	3	5
Controls: • distilled water plus 500 mg/l VOA	0	3	5
• distilled water	0	3	5
H-Coal: • ether-extracted plus 200 mg/l phenol	2 4 10 15 30 35 40 45 50	1	3
Controls: • distilled water plus 200 mg/l phenol	0	1	3
• distilled water	0	1	3
H-Coal: • ether-extracted and reconstituted to original phenolic concentration	2 4 6 8 9 10 12 14 16	3	5
Controls: • unmodified H-coal	2 4	3	5
• distilled water	0	3	5

[1] Culture volume made up to 10 ml using distilled water.

RESULTS AND DISCUSSION

Chemical Characteristics of the H-coal Effluent

Dearborn Environmental Consultants provided the analysis of the H-coal as summarized in Table 2. The concentration of phenolics in the H-coal was extremely high at 7600 mg/l. However, none of the other measured parameters were likely to be detrimental to the anaerobic process.

The data in Table 3 summarize the GC analyses of phenol and the alkylphenolics in the wastewater. Phenol was clearly the most abundant compound. Considering data in both Tables 2 and 3, phenol accounts for 62% of the phenolics in the H-coal. Since phenol, p-cresol and recently, m-cresol, have been shown to be fermentable (Boyd et al., 1983), the complete anaerobic biodegradation of these three compounds would remove 86% of the phenolics, identified by GC, from the H-coal.

It was unlikely that the full strength wastewater would be amenable to anaerobic degradation. Therefore, a series of dilutions were tested to determine which concentrations would be fermentable and which would be inhibitory.

Batch Cultures Receiving Unmodified H-coal

Batch cultures challenged with proportions of H-coal ranging from 2 to 15% were studied. Figure 1 summarizes the methane concentrations found in the cultures containing 2 to 10% H-coal over a 57 day incubation period. Each culture bottle

TABLE 2. Analysis of H-coal Effluent (Supplied by Dearborn Environmental Consulting Services)

Parameter	Concentration
Organic carbon (mg/l)	7 600
COD (mg/l)	21 100
Phenolics[1] (mg/l)	7 600
Total Kjeldahl nitrogen (mg/l)	267
Nitrite nitrogen (mg/l)	0.2
Nitrate nitrogen (mg/l)	0.8
Ammonia nitrogen (mg/l)	6.4
Total cyanide (mg/l)	0.21
Total phosphorus (mg/l)	5
pH	7.4

[1] 4-aminoantipyrine colorimetric method

TABLE 3. Concentrations of Various Phenolics in H-coal Effluent[1]

Phenolic	Concentration (mg/l)
phenol	4 900
o-cresol	586
m/p-cresol[2]	1 650
m-cresol[3]	1 230
p-cresol[3]	420
2,4/2,5-dimethylphenol[2]	63
3,5-dimethylphenol	213
3,4-dimethylphenol	44

[1] Direct aqueous injection onto Polyphenyl ether coated Tenax GC.
[2] Not resolved by this GC method.
[3] Analysis with Carbopack C column showed the m/p ratio to be 2.9, which allows estimation of m and p-cresol fractions of the m/p peak.

contained fermentable organics which were introduced with the sludge inoculum. Thus, inhibition of the anaerobic process was indicated by reduced methane production in phenol-containing cultures relative to phenol-free control cultures. At concentrations greater than 10%, the methane production was only inhibited to the same extent as the 10% H-coal culture. Three concentrations of H-coal gave enhanced methane levels. These were 2, 4 and 6% which correspond to

152, 304, and 456 mg/l phenolics respectively (based on data in Table 2). Consistent with earlier observations using single fermentable phenolics (Fedorak and Hrudey, 1984), higher concentrations of H-coal (higher concentrations of phenolics) exhibited longer acclimation times. With 2% H-coal, the acclimation time was 12 days; with 4% H-coal, it was 16 days; and with 6% H-coal, it was 43 days. Batch cultures containing 8% H-coal showed varying responses depending upon the domestic sludge sample used for inoculation. In the case shown in Fig. 1, methane concentrations in 8% H-coal cultures were only slightly less than the control values, while in other experiments (data not presented), there was little or no methane production, (i.e. severe inhibition).

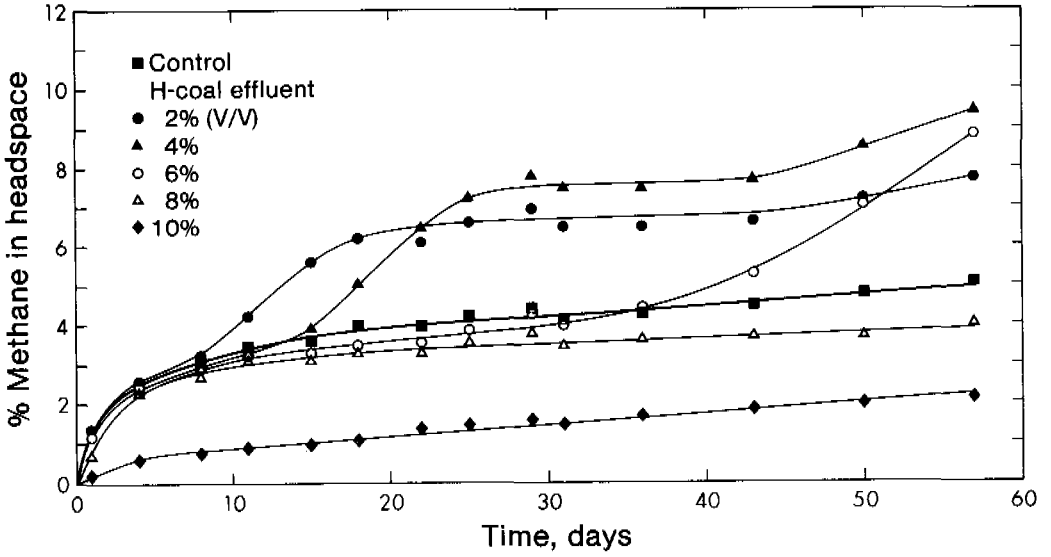

Fig. 1 Methane production in batch cultures containing various dilutions of unmodified H-coal (without VOA supplementation)

After 66 days incubation, the supernatant in a 4% H-coal culture was analyzed by GC for phenolics. Figure 2 compares the resulting chromatogram with that obtained from the analysis of this culture at the time of inoculation (day zero). The selective loss of the phenol and m/p-cresol peaks was observed leaving mainly o-cresol, and presumably the dimethylphenols which were barely detectable.

Phenolic degradation was monitored by comparing changes in the ratios of the area of a given peak to that of o-cresol rather than measuring the absolute concentration of each compound. Since it has been our experience, and there have been no reports in the literature of o-cresol being degraded under anaerobic conditions, o-cresol served as a convenient "internal standard" in the H-coal cultures. Based on the H-coal data in Table 3, the ratio of m/p-cresol to o-cresol was 2.81 and the ratio of m-cresol to o-cresol was 2.09.

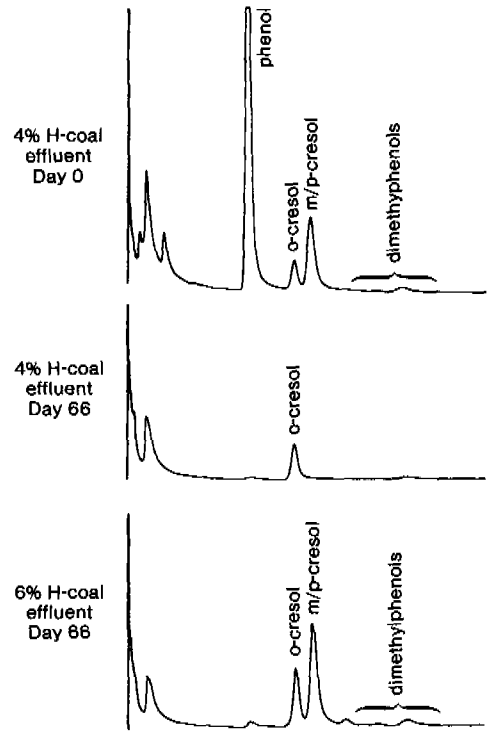

Fig. 2 Substrate analyses of batch cultures containing H-coal at times indicated

The complete loss of the m/p-cresol peak was not always observed in these batch cultures. Often the m/p-cresol to o-cresol ratio decreased to near 2 suggesting the removal of p-cresol but not m-cresol. In some cases, the ratio decreased to zero while in other cases the ratio remained constant. For example, the bottom chromatogram in Fig. 2 shows the phenolics left after 66 days in a culture which contained 6% H-coal. Although phenol had been removed, the m/p-cresol peak remained. Another analysis of this culture after a total of 78 days incubation gave a m/p-cresol to o-cresol ratio of 2.06. This value was very close to the 2.09 ratio expected if only m-cresol remained.

Data gathered from these H-coal cultures clearly show that m-cresol (along with phenol and p-cresol) can be selectively removed from a complex phenolic wastewater, as well as in pure chemical studies such as Boyd et al. (1983). The ability of batch cultures to degrade m-cresol is far more variable than is the case with phenol and p-cresol. Furthermore, cultures which ferment phenol and p-cresol do not always remove m-cresol from the phenolic mixture.

The addition of varying dilutions of H-coal to VOA-supplemented cultures showed that increased inhibition was noted as the H-coal concentration increased (Fig. 3). By day 4, the cultures containing 2% H-coal had produced only 62% of the methane found in the control cultures. The cultures containing 4 and 6% H-coal produced about 40% of the control value while the 8% H-coal culture produced very little methane. The inhibition observed with the three lower concentrations did not persist and methane production in excess of that in the control was observed in the 2 and 4% H-coal cultures after acclimation times of

28 and 34 days respectively. By day 54, the methane concentrations in the 6% H-coal cultures had reached those of the control cultures and there was a slight increase in methane levels found in the 8% H-coal cultures.

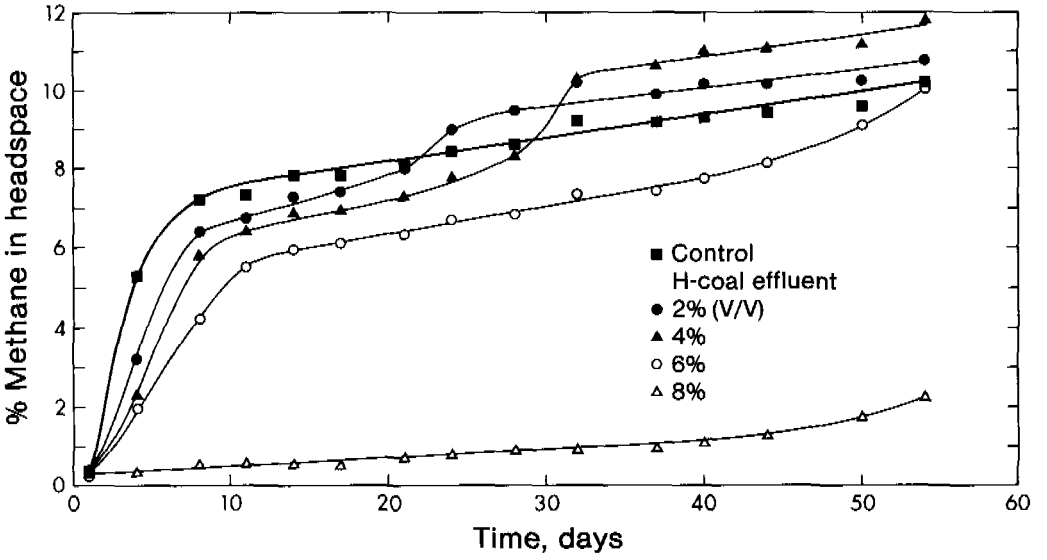

Fig. 3 Methane production in batch cultures containing various dilutions of unmodified H-coal (with VOA supplementation)

These results indicate that at the H-coal concentrations which were fermentable in batch cultures (< 6% V/V) there were components in the wastewater that retarded, but did not stop, the conversion of VOAs to methane.

Batch Cultures Receiving Ether-extracted H-coal

GC analyses of the ether-extracted H-coal showed that 99.8% of the phenol had been removed and that no ether remained. Phenol was used as the indicator of extraction efficiency because it was easily analyzed and it was the predominant compound, accounting for nearly 50% of the organic carbon in the wastewater.

This extraction was intended to remove the majority of the organic compounds from the wastewater while leaving the inorganic species in the aqueous phase. Various dilutions of the extracted aqueous phase were then added to batch cultures containing 200 mg/l phenol to test for inhibition of phenol degradation and/or methane production. Results from these experiments would then suggest whether the inorganic aqueous matrix or the organic fraction of the wastewater was the cause for observed inhibition with the unextracted wastewater.

When the ether-extracted H-coal was added to batch cultures in dilutions up to 50% (V/V), no inhibition of phenol degradation nor methanogenesis was observed. In fact, for higher proportions of extracted H-coal added, higher methane production was observed. These results suggested that there were readily fermentable substrates which remained after ether extraction of the H-coal.

The VOA analysis of unextracted H-coal showed 280 mg/l acetic acid, 160 mg/l propionic acid, 50 mg/l butyric acid and 35 mg/l valeric acid. Analysis of the ether-extracted H-coal showed essentially the same concentrations of VOAs as the unmodified wastewater. Extraction at pH 7 did not remove these compounds and they provided a source of readily fermentable substrates for the methanogenic cultures. Thus, at concentrations up to 50% (V/V), the ether-extracted H-coal was not inhibitory to either the methanogenic or phenol-degrading populations in the sludge.

Cultures Receiving Reconstituted H-coal

Batch cultures which received H-coal at ≥ 10% (V/V) (and sometimes ≥ 8%) could not degrade the phenolics therein and usually exhibited total inhibition of methane formation (Figs. 1 and 3). The total phenolic concentrations in the 8 and 10% H-coal cultures were approximately 608 and 760 mg/l respectively (based on the data in Table 2). It is unlikely that the phenolics alone were responsible for this severe inhibition since the methane production from cultures which received up to 1200 mg/l phenol or 600 mg/l p-cresol was only slightly inhibited (Fedorak and Hrudey, 1984). Similarly, when synthetic mixtures of phenolics were added to batch cultures, the fermentable compounds could be degraded when the total concentrations were near 700 mg/l (Fedorak, 1984).

The results from the extracted H-coal batch cultures clearly showed that neither the inorganic nor non-extractable organic components of this wastewater were causing the inhibition observed in the unextracted H-coal batch cultures. Thus it appeared that some ether-extractable component(s) (presumably organic compound(s)) was (were) responsible for the inhibition. This wastewater contained a variety of other aromatic compounds including quinoline, isoquinoline, methylquinolines, naphthalene, methylnaphthalenes, and fluorene all at concentrations less than 1 mg/l, except 8-methylquinoline which was at 6.6 mg/l (Dearborn Environmental Consulting Services, personal communications). Aniline and 2,4-dinitrophenol were also present at 64 and 107 mg/l respectively. Undoubtedly many other organic compounds were present but there are no other data currently available.

The purpose of this experiment was to remove the organic materials from the H-coal and then to add back the phenolics to their original concentrations in the extracted aqueous phase. This "reconstituted H-coal" was then added to batch cultures to determine whether the mixed phenolics or some other organics were the cause of the inhibition.

The reconstituted H-coal was tested in batch cultures with varying dilutions up to 16% (V/V). The methane production from selected concentrations are shown in Figs 4 and 5. To verify the validity of this approach, batch cultures of 2 and 4% reconstituted H-coal were compared with batch cultures of 2 and 4% unmodified H-coal. The resulting methane concentrations observed from this part of the experiment are shown in Fig. 4. In all cases, methane was produced in excess of the levels found in the control cultures. On the last 3 sampling times (days 41, 44 and 49), there was no statistically significant difference ($P < 0.05$) between the methane concentration produced from the 2% H-coal and that from the 2% reconstituted H-coal. The same was true for the 4% H-coal and 4% reconstituted H-coal.

There was, however, a noticeable difference between the acclimation times of the 4% reconstituted and 4% unmodified H-coal cultures (Fig. 4). The reconstituted H-coal cultures required between 8 and 13 days while the unmodified H-coal cultures required between 16 and 20 days. This distinct difference suggested the presence of an ether-extractable component in the H-coal which caused mild inhibition even when diluted to 4% (V/V).

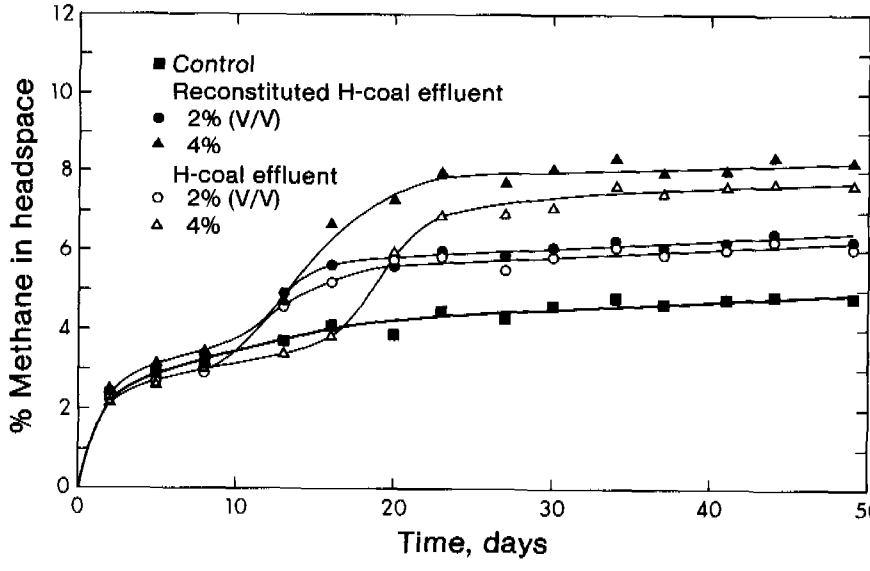

Fig. 4 Methane production in batch cultures containing either unmodified H-coal or reconstituted H-coal

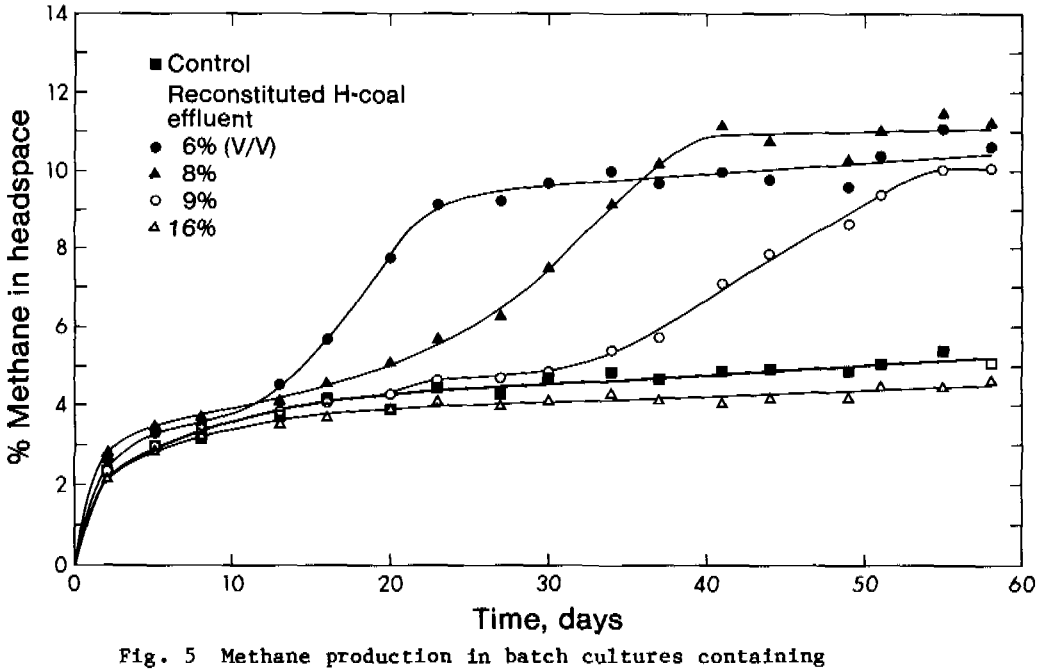

Fig. 5 Methane production in batch cultures containing reconstituted H-coal

A comparison of the methane production from cultures containing reconstituted H-coal (Fig. 5) with the data from cultures containing unmodified H-coal (Fig. 1) clearly shows that the inhibition observed with the unextracted H-coal is not due solely to the phenolic content. The highest proportion of unextracted H-coal which was amenable to anaerobic degradation was 6% (V/V) and the cultures required 43 days to acclimate (Fig. 1). With 6% reconstituted H-coal the acclimation time was only 16 days (Fig. 5). After 20 days incubation, methane production increased in the cultures containing 8% reconstituted H-coal (which was equivalent to a total phenolics concentration of 596 mg/l). Two of the three replicate cultures containing 9% reconstituted H-coal (671 mg/l phenolics) began to degrade these compounds by day 34. Enhanced methane production started in the third culture after 49 days and the rate of gas formation in this culture was much lower than in the other two. By day 55, enhanced methane levels were detected in the cultures containing 10% reconstituted H-coal (746 mg/l phenolics). The latter data were not included in Fig. 5 to avoid congestion.

The highest proportion of reconstituted H-coal tested in batch cultures was 16% (V/V) which contained 1194 mg/l phenolics. Although there was no enhanced methane production from this concentration, the methane produced was not significantly less than that found in the control cultures (Fig. 5). With unmodified H-coal there had been marked inhibition of methane normally produced from organics contained in the sludge inocula at both 10% (V/V) (Fig. 1) and 8% (V/V) H-coal (Fig. 3).

Phenolic analyses done on day 57 for the cultures containing $\leq$ 8% reconstituted H-coal showed that phenol had been removed from each culture. Also by that time, the m/p-cresol peak had been removed from most cultures which received $\leq$ 6% reconstituted H-coal. The exception was one of the triplicate cultures containing 2% reconstituted H-coal in which only p-cresol had been degraded. There appeared to be little degradation of the m- and p-isomers in the 8% cultures.

The results from experiments with the reconstituted H-coal show that ether-extractable compound(s), other than the phenolics, was (were) responsible for observed inhibition in cultures containing unmodified H-coal. These results also agree with data from cultures receiving synthetic mixtures of phenolics (Fedorak, 1984). For example, cultures given 6 phenolics at a total concentration near 700 mg/l could selectively degrade the fermentable phenolics. In the present study, methane production in excess of the controls was observed with cultures given 9 and 10% reconstituted H-coal which corresponded to 671 and 746 mg/l phenolics respectively. Many of the cultures containing reconstituted H-coal were able to completely remove the added m-cresol, further verifying a recent report that this compound is susceptible to anaerobic degradation.

ACKNOWLEDGEMENTS

We acknowledge the fine technical assistance of Valerie Williams and Shauna Mercer. Funding for this project was provided through a research subcontract with Dearborn Environmental Consulting Services on behalf of the Wastewater Technology Centre, Environmental Protection Service, Environment Canada and grant support from the Natural Sciences and Engineering Research Council of Canada.

REFERENCES

Bartle, K.D., Elstub, J., Novotny, M. and R.J. Robinson. (1977). Use of a modified Tenax GC column packing for the direct gas chromatographic analysis of phenols in water at the ppm level. J. Chromatogr., 135, 351-358.

Boone, D.R. (1982). Terminal reactions in the anaerobic digestion of animal waste. Appl. Environ. Microbiol., 43, 57-64.

Boyd, S.A., Shelton, D.R., Berry, D. and J.M. Tiedje. (1983). Anaerobic biodegradation of phenolic compounds in digested sludge. Appl. Environ. Microbiol., 46, 50-54.

Dunnett, C.W. (1955). A multiple comparison procedure for comparing several treatments with a control. J. Am. Statist. Assoc., 50, 1096-1121.

Fedorak, P.M. and S.E. Hrudey. (1983). A simple apparatus for measuring gas production by methanogenic cultures in serum bottles. Environ. Technol. Letters, 4, 425-432.

Fedorak, P.M. and S.E. Hrudey. (1984). The effects of phenol and some alkyl phenolics on batch anaerobic methanogenesis. Water Res., 18, 361-367.

Fedorak, P.M. (1984). Anaerobic Biological Treatment of Phenolic Wastewaters. Ph.D. Thesis, University of Alberta.

Khan, K.A., Suidan, M.T. and W.H. Cross. (1982). Role of surface active media in anaerobic filters. J. Environ. Eng. Div., Am. Soc. Civ. Eng., 108, 269-285.

Khan, K.A., Suidan, M.T. and W.H. Cross. (1981). Anaerobic activated carbon filter for the treatment of phenol-bearing wastewater. J. Water Pollut. Control Fed., 53, 1519-1532.

Neufeld, R.D. (1984). The Treatment of Wastes from the Synthetic Fuels Industry. In D. Barnes, C.F. Forster and S.E. Hrudey (Ed.), Surveys in Industrial Wastewater Treatment, Vol. 2, Pitmans, London. 65-129.

Neufeld, R.D., Mack, J.D. and J.P. Strakey. (1980). Anaerobic phenol biokinetics. J. Water Pollut. Control Fed., 52, 2367-2377.

Ossio, E. and P. Fox. (1980). Anaerobic biological treatment of in-situ retort water. Lawrence Berkeley Lab. Publ. No. LBL-10481, Univ. Calif., 47 pp.

Owen, W.F., Stuckey, D.C., Healy, J.B., Young, L.Y. and P.L. McCarty (1979). Bioassay for monitoring biochemical methane potential and anaerobic toxicity. Water Res., 13, 485-492.

Stuermer, D.H., Ng, D.J. and C.J. Morris. (1982). Organic contaminants in groundwater near an underground coal gasification site in northeastern Wyoming. Environ. Sci. Technol., 16, 582-587.

Suidan, M.T., Cross, W.H. and M. Fong. (1980). Continuous bioregeneration of granular activated carbon during the anaerobic degradation of catechol. Prog. Water Technol., 12, 203-214.

Wat. Sci. Tech. Vol.17, Amsterdam, pp.155-166.
Printed in Great Britain.

0273-1223/85 $0.00 + .50

THERMOPHILIC ANAEROBIC CONTACT DIGESTION OF PALM OIL MILL EFFLUENT

A. Ibrahim,* B. G. Yeoh,** S. C. Cheah,***
A. N. Ma,*** S. Ahmad,*** T. Y. Chew,** R. Raj** and
M. J. A. Wahid*

**Rubb. Res. Inst. of Malaysia, P.O. Box 150, Kuala Lumpur, Malaysia*
***Standards & Ind. Res. Inst. of Malaysia, P. O. Box 35, S. Alam, Malaysia*
****Palm Oil Res. Inst. of Malaysia, Bangi, Selangor, Malaysia*

ABSTRACT

The palm oil industry is one of the major agro-based industries in Malaysia whose production accounts for more than 90% of the world export. The industry, however, also generates enormous quantities of liquid waste with high organic load causing serious pollution problems. In view of the high level of organics, anaerobic pretreatment is usually practised prior to aerobic breakdown. Most of the anaerobic digesters installed at the mills are currently operated under mesophilic conditions. However, the inherently high temperature of the effluent suggests that thermophilic digestion would bring about a much more effective system. This paper reports on results obtained from a pilot plant study on thermophilic anaerobic contact digestion of palm oil mill effluent which has been conducted and includes a microbiological study associated with the investigation.

KEYWORDS

Palm oil mill effluent; high-strength organic waste; anaerobic contact process; BOD; methane; microbiological enumeration.

INTRODUCTION

Palm oil export earnings represent one of the major foreign exchange earners of Malaysia. In 1982, there were 185 mills in the country producing about 3.5 million tonnes of crude palm oil. In the international oil market, Malaysian palm oil accounted for more than 90% of the world export. The processing of the fresh fruit bunches (FFB) into crude palm oil, however, also produced enormous quantities of organic residues (Fig. 1). It has been estimated that about 2.5 tonnes of liquid waste are discharged per tonne of oil processed (Chan, P'ng and Aminuddin, 1983) (Table 1). In terms of population equivalent, the total amount of organic waste produced would equal the amount produced by a population of about 18 million, which is greater than the population of Malaysia. Apart from the organic contents, the waste also contains high levels of nitrogen (Table 2). It is therefore recognised that indiscriminate discharge of the waste into surface waters can precipitate serious pollution problems. In response to possible environmental repercussions,

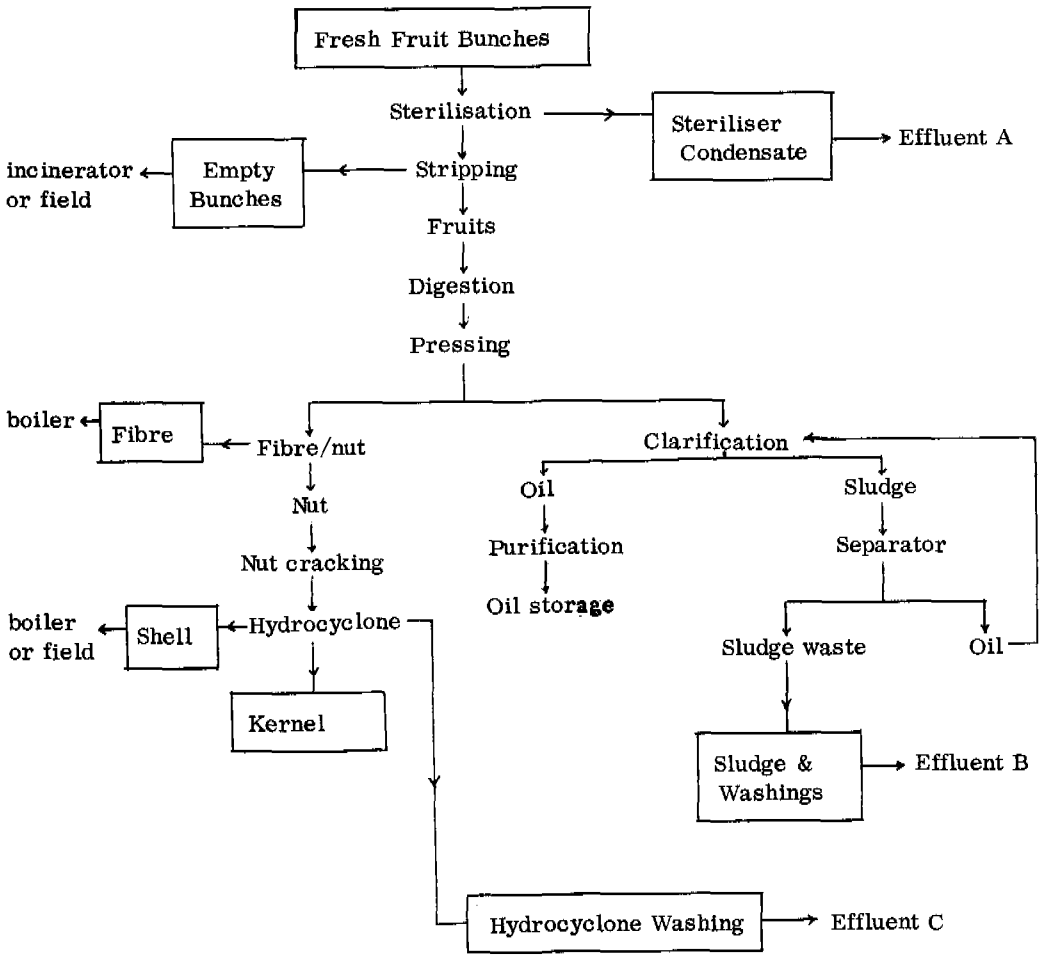

Fig. 1. Sources of palm oil mill effluent

TABLE 1 Effluent Quantities Produced

Nature	Quantity (tonne)	
	per tonne oil	per tonne FFB
Steriliser condensate	0.9	0.12
Clarification sludge	1.5	0.5
Hydrocyclone washings	0.1	0.05

TABLE 2 Average Characteristics of Palm Oil Mill Effluent

Parameter*	Range	Mean
pH	3.4 - 5.2	4.2
BOD	10250 - 43750	22260
COD	15550 - 100380	50710
Total solids	11460 - 78710	40370
Suspended solids	4400 - 53640	17620
Volatile solids	8770 - 71610	33820
Oil and grease	130 - 17970	6110
Ammoniacal nitrogen	4 - 77	35
Total nitrogen	180 - 1360	750

*All parameters, except pH, are expressed in mg/l.

the Government, through the Department of Environment, has formulated regulatory control (Environmental Quality Regulations 1977 (Prescribed Premises) (Crude Palm Oil). The industry has adopted two lines of approach: treatment mainly by biological methods and utilisation chiefly as a source of plantation fertiliser. In view of the high level of organics, anaerobic pretreatment is usually practised prior to aerobic breakdown. A survey (Ma and co-workers, 1981) has indicated that most of the mills employ either the ponding system or tank digestion, both conventional digesters. Anaerobic digestion is rate-controlled by the methanogenesis stage, the slowest stage of the whole process (Loehr, 1977). Consequently conventional digestion processes are dictated by large reactors with high hydraulic retention times of the order of 20 - 40 days. Depleting land area coupled with the need for more efficient digesters have prompted active research into alternative digestion systems. One of the many promising digestion processes is the anaerobic contact digestion. This is basically a completely mixed reactor with provision for sludge recycle, thus able to achieve very high bacterial retention time at low hydraulic retention. The survey (Ma and co-workers, 1981) also showed that most, if not all, of the digesters were operated under mesophilic conditions. It is however recognised that the inherently high temperature of palm oil mill effluent may be exploited to operate the digesters under thermophilic conditions. Studies (ENAA and SIRIM, 1982) have demonstrated the superiority of thermophilic operation.

A pilot plant study on the thermophilic anaerobic contact digestion of POME has been conducted to determine the efficacy and viability of such a system. This paper reports on the results of the investigation.

PILOT PLANT

The flow diagram of the pilot plant is shown in Fig. 2.

Raw palm oil mill effluent (POME) transported by a 2-tonne vacuum truck is charged into a 5 m^3 storage tank after being passed through a 2 mm mesh screen basket for the removal of coarse solids in the effluent. A pump feeds POME continuously into a 10 m^3 digestion tank.

In the digestion tank, organic matter in POME is digested under anaerobic condition and then sent to a 3 m^3 sendimentation tank whereby the supernatant separates from the concentrated digested sludge. The sludge is recycled into the digester and excess sludge is diverted into the sludge tank.

In general, digested liquor is heated by steam but in the pilot plant, an indirect heating system using electric heater is adopted. Agitation and mixing in the digestion tank are achieved by sparging the recirculated biogas.

MATERIALS AND METHODS

Plant Operation

Average characteristics of POME are depicted in Table 2. During this phase of the study, the digester was operated at two temperatures : 45°C and 50°C. At each temperature, the organic loading measured as kg BOD/m^3 day was varied in each experimental run by

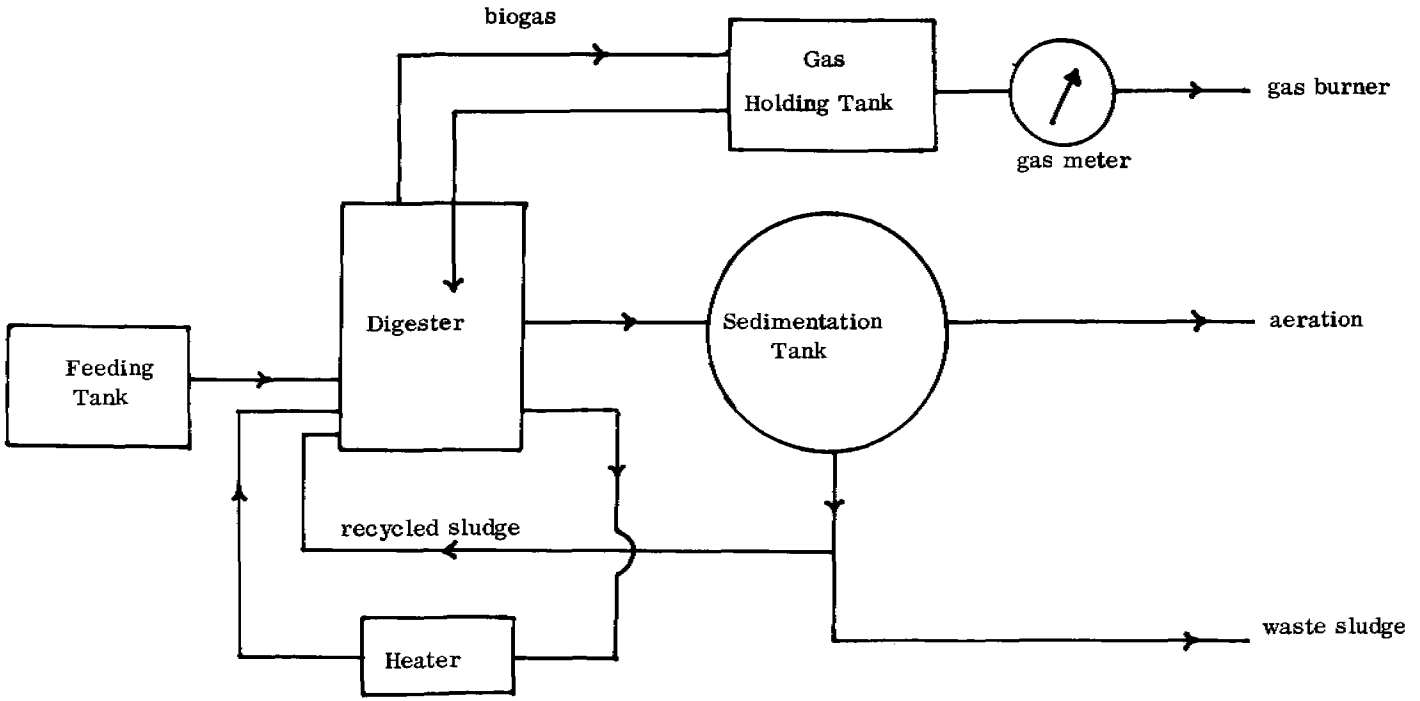

Fig. 2. Flow diagram of the pilot plant

changing the feed flow-rate. Table 3 shows the operation schedule for both Series I (45°C) and Series II (50°C) of the study.

Daily measurements of gas production, pH, gas composition and temperature were undertaken. The digester operating temperature was automatically recorded. Only the carbon dioxide content of the gas was monitored and the methane content was thus determined by difference. Settlability of the digester sludge was also determined daily by measuring SV_{60}.

A steady state operation was assumed when the gas production rates remained constant over a period of about twice the hydraulic retention time. Strategic samples would then be taken for a detailed laboratory analysis. Adequate samples were taken to produce a representative average.

Samples were analysed for their COD, BOD, pH, total solids, volatile solids, suspended solids, volatile suspended solids, total Kjeldahl nitrogen, ammoniacal nitrogen and oil and grease using Standard Methods (APHA, AWWA and WPCF, 1975). Sulphate was precipitated as barium sulphate and determined gravimetrically as such.

TABLE 3 Operational Schedule of Series I and II

	Series 1 (45°C)				Series 2 (50°C)			
Run	1	2	3	4	1	2	3	4
Feed flow-rate (m^3/ day)	1	1.6	1.7	1.3	1.2	1.23	1.4	2.1

Microbiological Study

Enumeration of total anaerobes was made in a complex habitat-stimulating medium (Medium CHS) of the following composition (g or ml per litre): decolorised, clarified digester fluid, 400; K_2HPO_4, 0.45; KH_2PO_4, 0.45; $(NH_4)_2SO_4$, 0.90; NaCl, 0.90; $MgSO_4$ $7H_2O$, 0.09; $CaCl_2.2H_2O$, 0.09; Bacto-peptone, 5.0; yeast extract, 2.5; beef extract, 1.0; glucose, 0.25; cellobiose, 0.25; maltose, 0.25; soluble starch; 0.25; resazurin (0.1% solution), 1.0; cysteine-HCl, 0.25; $Na_2S.9H_2O$, 0.25; pH of the medium was adjusted to 7.2 with 1N Na_2CO_3 solution. The medium was boiled to expel air. Growth of bacteria occured in tubes capped with gas-impermeable butyl rubber stoppers in an atmosphere of CO_2. Bacterial counts were estimated by three different methods : (a) dilution to extinction; (b) most probable number (MPN); and, (c) roll tube according to the method of Hungate (1969) using Medium CHS with 2% agar.

The number of sulphate-reducing bacteria in the digester liquor was estimated in Medium S of the following composition (g, unless stated otherwise, per litre): KH_2PO_4, 0.5; NH_4Cl, 1.0; Na_2SO_4, 3.0; $CaCl_2.6H_2O$, 0.2; $MgSO_4.7H_2O$, 2.0; sodium citrate. $2H_2O$, 5.0; $FeSO_4.7H_2O$, 0.5; yeast extract, 1.0; sodium lactate, 10; ascorbic acid, 7.5 mg; sodium

thioglycollate, 7.5 mg; Na_2SO_3, 3.0.pH of the medium was adjusted to 7.5 with 4 M NaOH solution. The medium was solidified with 1.5% agar. For enumeration, 1 ml diluted sample was added to 9 ml agar medium held molten at 45 - 50°C in a screw-capped tube. Contents of tubes were then shaken gently and allowed to set. The growth medium was overlayed with 1.5% agar up to the brim of the tube to prevent the entry of air. Enumerations of sulphate-reducing bacteria were made by counting the black colonies in the growth medium.

Aerotolerant bacteria in the digester was enumerated by spreading 0.1 ml diluted digester liquor on nutrient agar plates.

RESULTS AND DISCUSSION

Tables 4 and 5 depict the results of Series I and II respectively of the study. In the analysis of the results, attention was only directed towards the organic breakdown and gas production.

TABLE 4 Summary of Results (Series I)

Parameters	Runs			
	1	2	3	4
BOD loading (kg/m^3 day)	1.01	3.02	3.11	2.53
BOD removal rate (kg/m^3 day)	0.97	2.84	2.88	2.37
Gas production (m^3/ day)	17.0	28.0	28.8	23.1
CH_4 (%)	65	65	60	65
Hydraulic retention time (days)	10	6.25	5.9	7.7
BOD removal (%)	96.0	94.0	92.6	93.5

TABLE 5 Summary of Results (Series II)

Parameters	Runs			
	1	2	3	4
BOD loading (kg/m^3 day)	2.4	2.56	2.79	3.44
BOD removal rate (kg/m^3 day)	2.29	2.43	2.54	3.21
Gas production (m^3/ day)	23.2	23.8	27.9	36.4
CH_4 (%)	65	65	65	63
Hydraulic retention time (days)	8.3	8.1	7.2	4.7
BOD removal (%)	95.4	94.9	91.0	93.3

In Series I of the study, four experimental runs were completed at organic loadings ranging from 1.01 to 3.11 kg BOD/m^3 day. The corresponding hydraulic retention times varied from 5.9 to 10 days. The results demonstrated increasing removal rates with increase in loading: from 0.97 to 2.88 kg BOD/m^3 day. However the percentage removal remained fairly consistent around 94 percent. The consequent gas production also increased with increasing loading, ranging from 17 to 28.8 m^3/day.

Four runs were also completed in Series II of the study, at BOD loadings ranging from 2.4 to 3.44 kg/m^3 day. A very low hydraulic retention time of about 4.7 days was recorded at the highest loading. Again the results showed increase in removal rates with increasing loading. There was however insignificant differences in the percentage removal. Gas production varied from 23.2 to about 36.4 m^3/day, recording average methane content of about 65 percent.

At 45°C, the maximum tolerable loading as indicated was about 3.11 kg BOD/ m^3 day while at the higher temperature of 50°C, digester failure started to occur at a loading of 3.44 kg BOD/m^3 day. As suggested by the similar levels of percentage removals in both series, the 5-degree increase in operating temperature did not seem to effect significant differences in digester performance. In Series II, the maximum loading could not be maintained for a significant period of steady state due to the occurrence of spillage of the digester contents. This was thought to be attributed more to the digester design rather than the high organic loading. It was observed that excessive surface scum entered the gas outlet line choking it thus creating the high pressure build-up in the digester. This finally resulted in the spillage of the contents through the vent valve.

Microbiological enumeration in Series I was performed for the number of total anaerobes that can be detected under laboratory conditions. Results showed that there are at least 10^8 anaerobes per ml of digester liquor. In Series II the digester was regularly sampled for enumeration of both total anaerobes and sulphate-reducing bacteria and the results are as shown in Table 6.

The estimated bacterial count is only a reflection of the efficiency of the enumeration method used. The results of Kirsch (1969) indicated that supplementing the medium with digester fluid, as was done in this work, allowed more than 10^8 bacteria to be detectable in 1 ml of sewage anaerobic digester liquor. Other published sewage digesters include that of Ueki and co-workers (1978) who reported 10^6 - 10^7 per ml of digester liquor while Mah and Sussman (1968) estimated the count to be 10^8 - 10^9 ml. The latter also reported aerotolerant bacterial counts of between 10^6 and 10^7 per ml of digester liquor. In a digester treating swine waste, Iannotti, Fischer and Sievers (1978) established that approximately 10^6 aerotolerant bacteria could be detectable per ml digester fluid on standard plate count medium and that this represented only 0.05% of the total population. The results shown here, however, indicated that the aerotolerant population makes up approximately 1% of the total bacterial population of the digester.

The sulphate-reducing bacteria are responsible for the production of H_2S in biogas. Their importance in the breakdown of organic polymers in anaerobic digestion is not fully understood but they have been shown to be present here as well as in digesters treating other wastes. For digesters treating palm oil mill effluent at mesophilic temperatures (28 - 33°C), about 10^5 bacteria can be detected in a ml of anaerobic liquor (Cheah, unpublished data). Toerien, Thiel and Hattingh (1968) have also established that sulphate-reducers occurred in a 30°C digester treating sewage at a count of approximately 3×10^4 - 4×10^4/ml. However, in the 50°C digester reported here, only 10^1 - 10^2 bacterial/ml were detectable representing a reduction of approximately 1000 times in the number of these bacteria in the digester. This finding has important implications in the utilization of biogas for generating electricity by the gas engine system where low concentration of the highly corrosive H_2S in biogas is desirable.

OPERATIONAL PROBLEMS

Some of the operational problems inherent in the pilot plant are listed below :

Scum Formation in Digester

During the operating period of two years, scum build-up occurs due to the presence of oil and grease in the raw effluent. The design has made no provision for its removal. At high loading of POME during Run 4 (Series II), there was carry-over of solids (scum) into the gasline causing choking to occur. The high production and build-up of biogas created a pressure within the digester causing half of the contents to spill out of the vent pipe.

TABLE 6 Enumeration of Bacteria in the Digester: Series II

Run	Sulphate Conc. in anaerobic liquor (mg/l)	No. bacteria per ml anaerobic liquor					
		Total Anaerobes			Sulphate reducers	Aerotolerant bacteria	
		Dil. to extinetion	MPN method	Hungate roll tube method		$26^{o}C$ incubation	$50^{o}C$ incubation
2	309	-	-	-	7.6×10	-	-
3	779	10^{8}	2.0×10^{7}	-	1.4×10^{2}	8.5×10^{6}	1.0×10^{6}
4	626	10^{8}	4.6×10^{7}	2.1×10^{7}	2.1×10^{2}	-	-

Blockage of Pipelines

The choking of pipes due to scum and sediment deposited in the line connecting the digester to the sedimentation tank caused occasional overflow of mixed liquor out of the digester. It was necessary to scrape and remove the thick layer of sediment in the lines. Regular cleaning of the screen basket and the sand trap was required to prevent clogging of the raw waste effluent pump. Moreover, it was necessary to manually remove the scum from the liquid surface of the sedimentation tank to avoid choking of the inlet pipe.

Corrosion and Blockage in Gasline to Burner

The presence of water vapour, hydrogen sulphide and carbon dioxide caused rusting of the mild steel pipelines. Blockage of the gas flow occurred due to presence of water condensate in the line without provision of water drains being made. The gas-line was modified and replaced by PVC pipes.

CONCLUSION

The study has demonstrated that the anaerobic contact digester may be used for the digestion of palm oil mill effluent. At a temperature of 45°C, the digester could be operated at a maximum organic load of about 3.11 kg BOD/ m^3 day, giving a percentage reduction of around 94%. A higher loading of about 3.44 kg BOD/ m^3 day was tolerable at the higher temperature of 50°C. However some limitations in reactor design did not favour operation at these high loading rates. One obvious modification which may require incorporation is a provision for some scum breaking mechanism at the digester surface. It was observed that at high loading, extensive carry-over of scum into the gas outlet occurred. This, coupled with the high rate of gas production, led to high pressure build-up in the reactor. Ultimately this resulted in a spillage of the mixed liquor through the vent. Microbiological analysis of the digester liquor indicated a significant difference in the population of sulphate-reducing bacteria under thermophilic environment. It was found that in the 50°C digester, only 10^1 - 10^2 bacteria/ml were detectable. This is approximately 1000 times less than the number found under mesophilic condition.

ACKNOWLEDGEMENTS

The authors wish to thank the Acting Controller of SIRIM, the Director-General of PORIM and the Director of RRIM for their encouragement and support for the project. The advice of Prof. S.H. Ong, Dr. C.K. John, Dr. K.S. Ong and Dr. C.N. Chong is greatly appreciated. Special thanks are also due to the technical staff of SIRIM, PORIM and RRIM for services rendered.

REFERENCES

APHA, AWWA, and WPCF (1975). Standard Methods for the Examination of Water and Wastewater, 14th ed. American Public Health Association, Washington D. C.

Chan, K. W., T. C. P'ng, and M. R. M. Aminuddin (1983). Palm oil mill effluent utilization and its future research directions in the palm oil industry. Seminar on Land Application of Palm Oil and Rubber Factory Effluents, Serdang, Malaysia.

ENAA, and SIRIM (1982). Report on Demonstration Test for Palm Oil Mill Effluent Treatment Plant. Engineering Advancement Association of Japan, ENAA 1981 - DP - 1.

Hungate, R. E. (1969). A roll tube method for cultivation of strict anaerobes. In J. R. Morris and D. W. Ribbons (Ed.), Methods in Microbiology, vol. 3B. Academic Press Inc., New York. pp. 117 - 132.

Iannotti, E. L., J. R. Fischer, and D. M. Sievers (1978). Medium for the enumeration and isolation of bacteria from a swine waste digester. Appl. Environ. Microbiol., 36, 555 - 566.

Kirsch, E. J. (1969). Studies on the enumeration and isolation of obligate anaerobic bacteria from digesting sewage sludge. Dev. Ind. Microbiol., 10, 170 - 176.

Loehr, R. C. (1977). Pollution Control for Agriculture. Academic Press Inc., New York.

Ma, A. N., C. S. Chow, C. K. John, A. Ibrahim, and Z. Isa (1981). Disposal of palm oil mill effluent in Malaysia - a survey. Proceedings Int. Conf. The Oil Palm in Agriculture in the Eighties, Kuala Lumpur. pp. 1 - 11.

Mah, R. A., and C. Sussman (1967). Microbiology of anaerobic sludge fermentation I : enumeration of non-methanogenic anaerobic bacteria. Appl. Microbiol., 16, 358 - 361.

Toerien, D. F., P. G. Thiel, and M. M. Hattingh (1968). Enumeration, isolation and identification of sulphate-reducing bacteria in anaerobic digestion. Water Res., 2, 505 - 513.

Ueki, A., E. Miyagawa, H. Minato, R. Azuma, and T. Suto (1978). Enumeration and isolation of anaerobic bacteria in sewage digester fluids. J. Gen. Appl. Microbiol., 24, 317 - 332.

FORMATION AND OXIDATION OF SULPHIDES

Wat. Sci. Tech. Vol.17, Amsterdam, pp.167-181.
Printed in Great Britain.

0273-1223/85 $0.00 + .50

OXIDATION OF SULFIDE AND THIOSULFATE AND STORAGE OF SULFUR GRANULES IN *THIOTHRIX* FROM ACTIVATED SLUDGE

P. H. Nielsen

Institute of Biology, University of Odense, Campusvej 55, DK-5230, Odense M, Denmark

ABSTRACT

Thiothrix from activated sludge is, in the presence of oxygen, able to oxidize sulfide and thiosulfate and store many clear sulfur granules at sulfide concentrations less than about 1 mM and thiosulfate concentrations of 0.1-20 mM. On this basis, a sulfur storage test for the identification of Thiothrix in activated sludge was developed. It is shown that the filamentous bacteria, Type 021N (commonly causing bulking in sewage plants), is able to store sulfur granules and thus is a Thiothrix. In enrichment cultures with thiosulfate typical Thiothrix rosettes and motile gonidia are developed, and the presence of a sheath is demonstrated. Filamental diameter varies between 0.8-2.4 μm, the youngest filaments being thinnest. Attempts to isolate Thiothrix have been unsuccesful, but Thiothrix filaments with only a few contaminants are able to grow on solid media with acetate as the only carbon and energy source, indicating the presence of heterotrophic strains. The filamentous organisms of 14 Danish sewage treatment plants are identified, Thiothrix being the most common in 8, and responsible for bulking in 4 plants.

KEYWORDS

Thiothrix; Leucotrichaceae; colorless sulfur bacteria; Type 021N; bulking activated sludge; thiosulfate oxidation.

INTRODUCTION

Filamentous micro-organisms are often observed in wastewater treatment plants (Hünerberg et al., 1970; Cyrus and Sladka, 1970; Farquhar and Boyle, 1971b; van Veen, 1973; Eikelboom, 1975; Strom and Jenkins, 1981). From these more than 20 different filamentous organisms are described, of which some are commonly involved in sludge bulking. One of these groups of organisms is Thiothrix, which is often found in sewage plants receiving wastewater with high concentrations of hydrogen sulfide (Farquhar and Boyle, 1972; Merkel, 1975; Pipes, 1978; Walker, 1982).

Thiothrix was first described by Winogradsky (1888) and has been reported in many habitats with continuously flowing, sulfide rich water. Thiothrix consists of non-motile, ensheathed filaments, showing storage of sulfur granules and frequent growth in typical rosettes. Winogradsky (1888) has stated that the filaments form motile gonidia from the tip, but this motility has not been confirmed (Larkin, 1980).

Harold and Stanier (1955) suggested that Thiothrix is obligately aerobic and chemoautotrophic using sulfide as an energy source, but Larkin (1980) recently isolated some strains of Thiothrix that seem heterotrophic or mixotrophic. However, only a few physiological characteristics of Thiothrix are published.

Sometimes Thiothrix does not contain sulfur granules and then it is morphologically and developmentally similar to Leucothrix mucor and therefore considered as a member of the family Leucotrichaceae (Buchanan and Gibbons, 1974; Raj, 1977). The absence of sulfur granules has caused much confusion in the identification of the organism in activated sludge. To facilitate the identification both Farquhar and Boyle (1971a) and Eikelboom and van Buijsen (1981) have developed sulfur storage tests based on the addition of sulfide to activated sludge and the appearance of sulfur granules.

Eikelboom (1975) described a filamentous organism, Type 021N, which, apart from the absence of sulfur granules, resembles Thiothrix very much. Type 021N is one of the most common filamentous organisms causing bulking in sewage treatment plants of the Netherlands. Type 021N is also very common in plants of the UK, West Germany and the USA (Tomlinson and Bruce 1979; Wagner, 1982, Strom and Jenkins, 1981). Pipes (1978) suggested that Type 021N in fact belongs to Thiothrix.

The two existing sulfur storage tests were used, and in some cases Type 021N stores S-granules. The storage seems to depend on methodological problems concerning the presence and concentration of oxygen and sulfide in the tests. Therefore the conditions under which sulfur storage takes place were determined and a new sulfur storage test for Thiothrix was developed. Further, the morphology, cytology and some physiological characteristics of Thiothrix in activated sludge and in enrichment cultures are described. The presence of Thiothrix in some Danish sewage treatment plants was determined.

MATERIALS AND METHODS

Sources of Thiothrix

The morphological investigations and the enrichment of Thiothrix have been made on bulked activated sludge from an oxidation ditch in Funen, Denmark. This plant, which has discontinuous operation, receives domestic sewage (10-20% of the organic loading), industrial sewage from a slaughter house, sewage from a dairy and sewage from a brewery. The hydraulic loading was about 3000 m^3 per day and the residence time was about 20 hours. The sludge loading is 0.04-0.06 kg BOD_5 (kg MLSS day)$^{-1}$.

Sludge samples from 14 different purification plants in Denmark (Jutland and Funen) were investigated for the presence of Thiothrix

and other filamentous micro-organisms during January to May 1983. The identification was according to the methods of Eikelboom (1975) and Eikelboom and van Buijsen (1981). The samples were stored at 4°C and identified within 72 hours.

Sulfur storage test

To identify Thiothrix in activated sludge two sulfur storage tests with sulfide are used. According to the method of Farquhar and Boyle (1971a) 10 mg $Na_2S.9H_2O$ is added to 100 ml sludge, and the mixture is gently shaken in a flask for 5 minutes. Also the method of Eikelboom and van Buijsen (1981) was used; mixing one part sludge and one part sulfide solution with a concentration of 200 mg $Na_2S.9H_2O$ per 100 ml. This mixture is intermittently shaken to keep the sludge in suspension. In both cases a positive test resulted when S-granules appear within 15-30 minutes.

To study the influence of oxygen and sulfide or thiosulfate concentrations on the storage of S-granules in Thiothrix, 20 ml of filtered (Whatmann GF/C), anoxic water from the outlet of the sewage plant (pH about 7.8) and 0.5 ml sludge with a heavy growth of Thiothrix (without S-granules) was placed in a 250 ml Erlenmeyer flask. The flask was then filled with the desired gas mixture, which had high oxygen tension (air-saturation) or low oxygen tension (1% air and 99% nitrogen). Sulfide or thiosulfate was then added from stock solutions kept under nitrogen, and the flasks were shaken gently in a rotatory shaker at room temperature. The filamentous organisms were investigated for the presence of S-granules using light microscopy, after 15 minutes and subsequently at suitable intervals. The initial sulfide concentration used was 0.1-10 mM at both high and low oxygen tension, while the thiosulfate concentration was 0.01-50 mM at high and 2 mM at low oxygen tension.

Finally, a new sulfur storage test with thiosulfate was developed:

1. Activated sludge was allowed to settle in a bottle, and from the supernatant 20 ml clear water was transferred into a 100 or 250 ml Erlenmeyer flask.
2. The bottle was shaken and 1-2 ml activated sludge was added to the Erlenmeyer flask.
3. Thiosulfate was added to a final concentration of 2mM.
4. The flask was shaken at room temperature overnight.

A positive result gave filaments with clear sulfur granules.

Enrichment culture of Thiothrix

Activated sludge (with heavy growth of Thiothrix) was diluted 10-20 times with filtered water from the sewage plant outlet. 20 ml of this suspension was poured into a Erlenmeyer flask, and thiosulfate was added to a final concentration about 20mM. After gentle shaking for 2-4 days at room temperature the appearance of Thiothrix rosettes was confirmed by light microscopy, and addition of glucose (final concentration about 200 mg l^{-1}) assured further growth. 2-3 days later, many rosettes were observed.

Attempts to isolate Thiothrix were in accordance with the methods of Larkin (1980) and Eikelboom (1975). Growth was tested on solid media containing the basal salt solution from medium I of van Veen (1973) with different combinations of organic sources and thiosulfate, autoclaved in separate bottles.

Physiological characterization

Poly-β-hydroxybutyrate (PHB) has been stained with Sudan Black B, volutin according to the method of Norris and Ribbon (1971) and Gram staining was according to Godinho-Orlandi (1980). Sulfur granules were identified following ethanol extraction after the method of Farquhar and Boyle (1971a).

Light microscopy

Observations were made by light and phase-contract microscopy using a Leitz microscope and preparations were photographed with a Nikon camera using Kodak Panatomic X film 32 ASA.

Electron microscopy

Samples from activated sludge or enrichment culture were washed in 0.1 M phosphate buffer (pH 7.3) and fixed for 30 minutes in 2.5% glutaraldehyde (pH 7.3) at 0°C. After washing with the buffer, the samples were embedded in 1.25% agar and postfixed in 1% OsO_4 for one hour. After washing with the buffer, the samples were stained with 0.5% uranylacetate for 90 minutes, dehydrated in alcohol, washed in propyleneoxide, embedded in araldite and sectioned with a glass knife. Thin sections were picked up on 300-mesh copper grids and stained with lead citrate. Electron micrographs were obtained using a Jeol 100-CX electronmicroscope.

RESULTS

Storage of sulfur granules from sulfide and thiosulfate oxidation

Using the sulfur storage method of Eikelboom and van Buijsen (1981) the Thiothrix filaments of this study show ability to oxidize sulfide and store S-granules in only a few cases. Using a low sulfide concentration (0.4 mM), as proposed by Farquhar and Boyle (1971a), the filaments store a few S-granules when the sludge is vigorously shaken. Granule formation is not very constant.

In the presence of oxygen, oxidation of sulfide and storage of S-granules takes place (Table 1). Thus, at high oxygen tension (air-saturation), more than 90% of the filaments store S-granules during the first 15-120 minutes at sulfide concentrations of 0.1-0.4 mM. At sulfide concentrations greater than 1 mM, however, only a few S-granules are formed in a few filaments. Further, at low oxygen tension (1% air-saturation) nearly all Thiothrix filaments oxidize sulfide and store many S-granules at 0.1-0.2 mM sulfide, while a few or no S-granules are observed at higher sulfide concentrations. Attempts to find a suitable combination of sulfide and air to improve the sulfur deposit test for Thiothrix in activated sludge have been

unsuccessful, since the results are variable e.g. depending on the age of the sludge. No suitable test with sulfide was found. The thiosulfate test gives more reliable results.

TABLE 1 Typical Storage of S-granules in Thiothrix from Oxidation of Sulfide at High Oxygen Tension (Air)

mM Sulfide	Minutes 15	30	60
0.1	++	++	++
0.2	++	++	++
0.4	++	++	++
0.8	+	++	++
1.0	+-	+-	+-
4.0		+-	+-
10.0	-	-	-

++ = many S-granules in more than 90% of the filaments
+ = a few S-granules in more than 90% of the filaments
+- = a few S-granules in some filaments
- = no S-granules

By using thiosulfate instead of sulfide, more than 90% of the filaments at full air-saturation show numerous and large S-granules after incubation for 18-24 hours with thiosulfate concentrations of 0.05-20 mM. Concentrations less than 0.05 or more than 30 mM result in few or no S-granules after 24 hours. Oxidation of thiosulfate and storage of S-granules at 2 mM thiosulfate occur at temperatures from about 0 to 35 °C. At low oxygen tension (1% air-saturation) and 2 mM thiosulfate only few S-granules are seen in the filaments. This is also the case in unshaken flasks at full air saturation. Sulfur storage in the presence of thiosulfate or sulfide under anaerobic conditions was never observed in this study.

Occurrence of Thiothrix in Danish Sewage Treatment Plants

In the activated sludge of the Danish sewage treatment plants investigated, 14 different types of filamentous micro-organisms have been identified. The names of the dominating types are shown in Table 2. Bulking problems are found in 6 out of 14 plants and the most common organism in these plants is Type 021N. However, using the new sulfur deposit test with thiosulfate it was shown that all the filaments previously identified as Type 021N are able to store S-granules (Table 3). Thus, thiosulfate oxidizing *Thiothrix* is observed in 8 plants and responsible for bulking in 4 of them. Further more, after 48 hours thiosulfate oxidizing *Thiothrix* has appeared in sludge samples from all but one of the treatment plants investigated (usually being potentially present in the sludge). The sewage plants with bulking problems caused by *Thiothrix* are all oxidation ditches, that treat either brewery, dairy or slaughter house wastewater and operate discontinuously with a rather low concentration of dissolved oxygen (1-2 mg O_2 l^{-1}).

TABLE 2 Dominating Filamentous Organisms in 14 Sewage Treatment Plants of Denmark

Filamentous Organism *	Dominating in	
	Number of plants	Number of plants with bulking
021N	4	4
0803	4	2
Microthrix parvicella	5	1
Flexibacter	1	0

* Names according to Eikelboom and van Buijsen (1981)

TABLE 3 Occurrence of Thiothrix and Type 021N in 14 Sewage Treatment Plants of Denmark

Filamentous Organism	Number of plants		
	Present	Dominating	With bulking
021N *	8	4	4
Thiothrix *	3	0	0
Thiothrix ** (oxidizing thiosulfate)			
after 24 hours	8	4	4
after 48 hours	13		

* *Identified according to Eikelboom and van Buijsen (1981).*
** Thiothrix including Type 021N, according to the present study.

Enrichment Culture of Thiothrix

At a thiosulfate concentration of about 20 mM in the culture, the formation of characteristic rosettes and gonidia can normally be observed after 2-4 days (Fig. 1a). Glucose or acetate addition secures further growth. When the organic source is added with thiosulfate the filaments grow in long tangles and no gonidia or rosettes are formed although storage of S-granules still takes place. When the thiosulfate has disappeared from the medium, the S-granules of the filaments also disappear, probably being oxidized to sulfate.

From the enrichment culture unsuccessful attempts were made to isolate some strains of Thiothrix. Thus, good growth is observed on medium I of van Veen (1973) with 20 mM thiosulfate, but a few small unicellular contaminants are always attached to the filaments of the colonies. The filaments of Thiothrix are able to grow on solid media without addition of any carbon or energy sources in excess of the impurities of the agar. Addition of an organic source (0.03% yeast extract or acetate (w/v) increased the growth of the bacteria. In the presence of thiosulfate no significant changes in growth are observed, but the diameter of the filaments changes from 1-1.5 µm to 1.5-2.2 µm (Fig. 2).

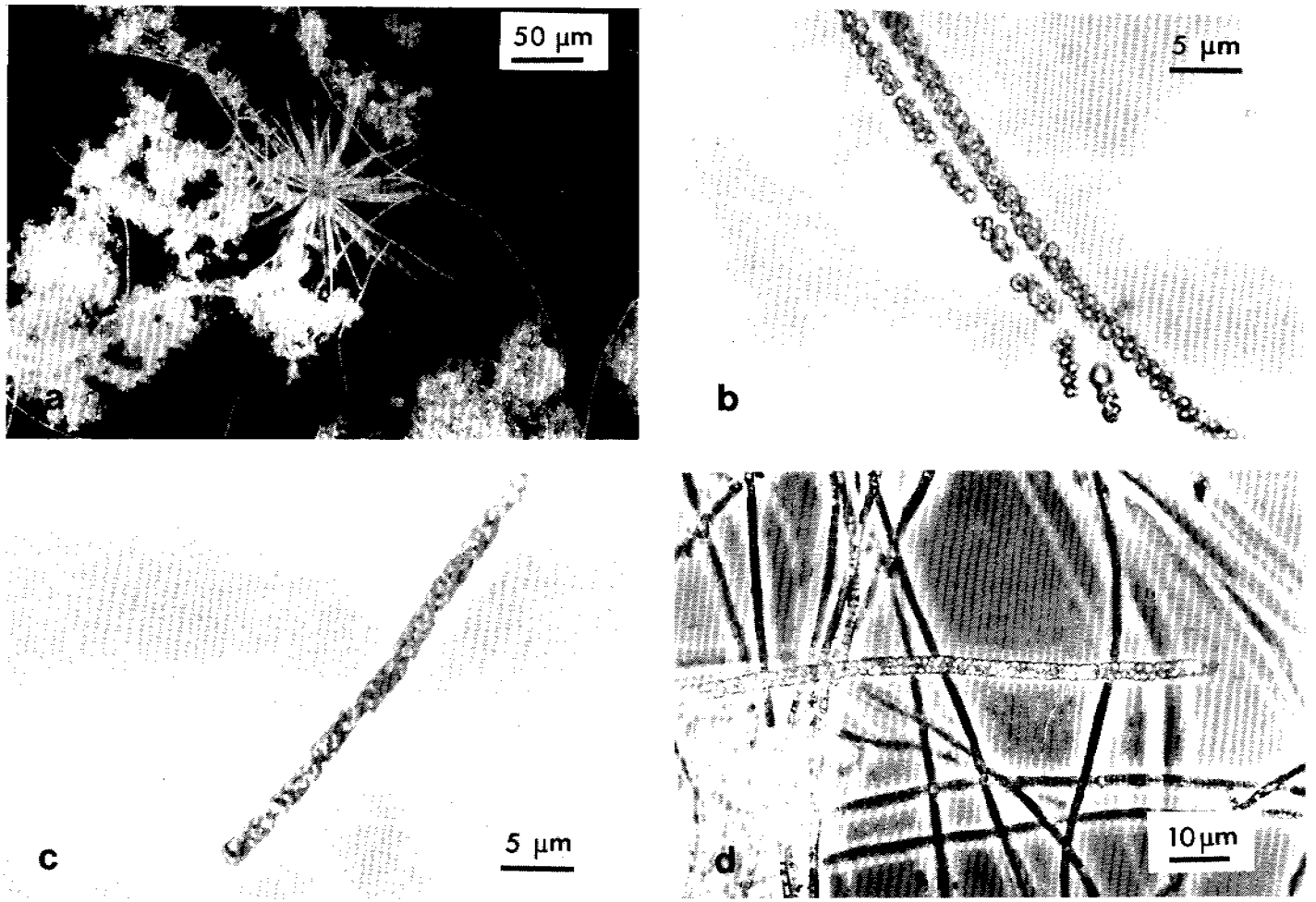

Fig. 1. Thiothrix filaments, rosette and gonidia from activated sludge enriched with 20 mM thiosulfate and 0.03% sodium acetate. 1a. Dark field micrograph showing the appearance of a Thiothrix rosette. 1b. Phase-contrast micrographs of gonidial formation from the tip of a Thiothrix filament. 1c. S-granules extracted from the gonida with ethanol. 1d. "Thick" Thiothrix filament with a diameter of more than 3 µm. The other filaments are of the normal Thiothrix type, without S-granules.

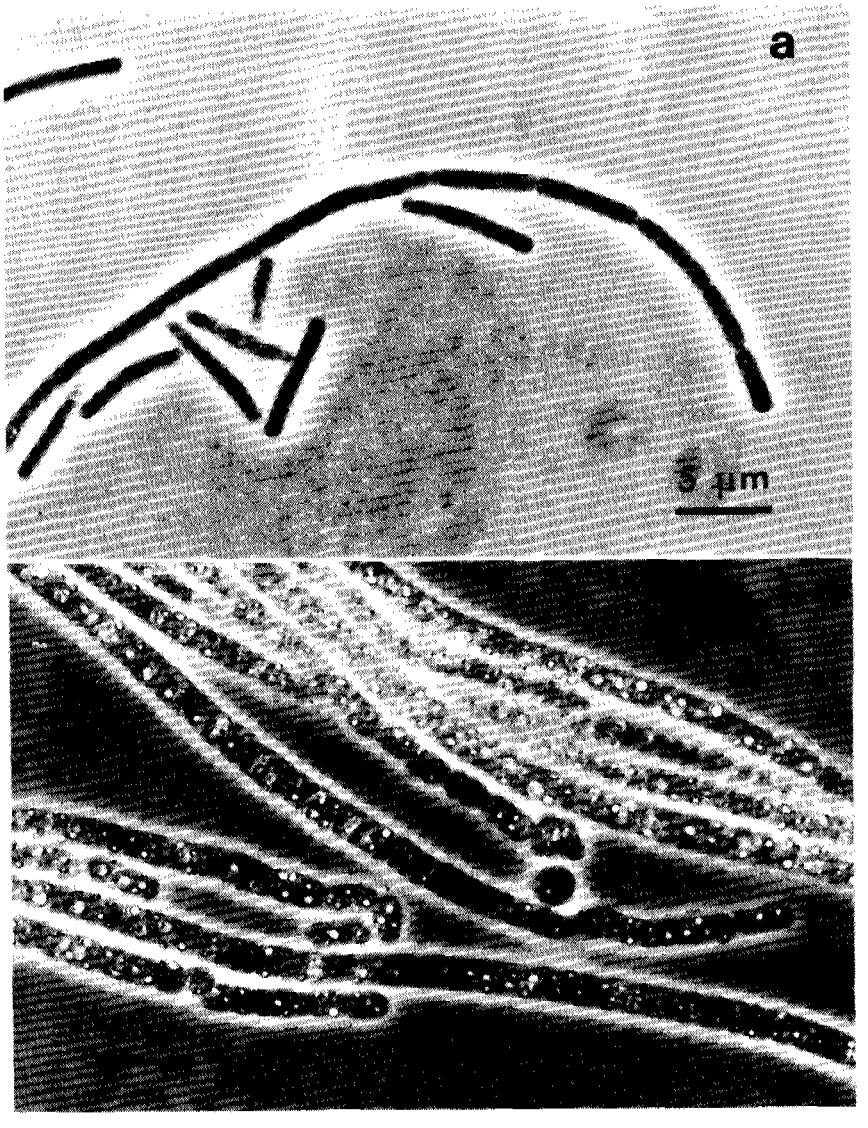

Fig. 2. Growth of Thiothrix on solid medium. Phase-contrast micrographs of growth on 0.03% sodium acetate (2a) and growth on 0.03% sodium acetate plus 20 mM thiosulfate (2b)

In both cases filaments and gonidia are produced. Filaments growing on acetate medium are able to oxidize both thiosulfate and sulfide and form S-granules. When they are transferred to slants containing acetate and thiosulfate with a 1-2 ml salt solution, all the typical characteristics of Thiothrix can be seen.

Morphology

In untreated, activated sludge the Thiothrix filaments are very long, often several mm, with a diameter of 1.4-2.2 μm. Each filament is composed of disc-shaped cylindrical cells with a highly variable form. Square cells, however, occur most often. Cell septa are clearly visible and necroid cells can be present. The filaments are colorless, unbranched and non-mobile with a very delicate sheath which can be seen with electron microscopy. When the growth of Thiothrix in activated sludge is heavy, the filaments often proliferate in ropelike structures. Sometimes true knots are present. Normally the filaments do not taper, but there may be some variation along the filaments. Formation of gonidia and rosettes is only rarely observed.

In enriched sludge the cell septa are hidden by stored S-granules. Most often all cells in a filament contain S-granules, but sometimes cells have many, few and no S-granules in the same filament. After 2-4 days some of the filaments make gonidia (Fig. 1b), with a diameter of 1-1.5 μm and a length of 3-5 μm. The unicellular gonidia wave back and forth just before they separate from the tip of the filaments and move slowly in jerks. Sometimes short chains of cells are liberated instead of single cells. The gonidia sometimes form a holdfast on another Thiothrix filament or form a rosette. Many of the newly formed filaments are rather thin, with diameters down to 0.8 μm, but they get thicker with increasing age.

When Thiothrix grows on solid media containing thiosulfate and acetate, they have nearly the same morphology as the above mentioned, except for the gonidia, which are often thicker with more irregular cells (Fig 2b). Filaments from the media with acetate alone are somewhat thinner (0.8-1.5 μm), and the gonidia are long and thin (Fig. 2a).

In several sludge samples from one of the treatment plants, another type of Thiothrix appears during the enrichment. This type is 3-3.4 μm in diameter and has larger sulfur granules than the normal type. The unicellular gonidia of this type are about 8 μm long (Fig. 1d). Typical rosettes are also formed.

Cytology

The Thiothrix filaments, which are Gram negative, contain various vacuoles and granules. The sulfur granules, identified with ethanol extraction, can be numerous in a single cell. Normally the cells also contain lipid storge vacuoles (PHB) and sometimes a few small volutin granules.

Thin sections of filaments from both the enrichment culture and activated sludge exposed to 2 mM thiosulfate for 24 hours normally show the existence of a sheath, a cell wall of three layers and the presence of intracellular vacuoles, (Fig. 3). The width of the sheath varies, from about 110 nm to 15 nm. In a few cases, no sheath is observed. Sheaths from filaments in the enrichment culture sometimes extend into the holdfast (Fig.3a). The innermost layer of the three-layered cell wall, which is typical for Gram negative bacteria, continues into the cell division septum.

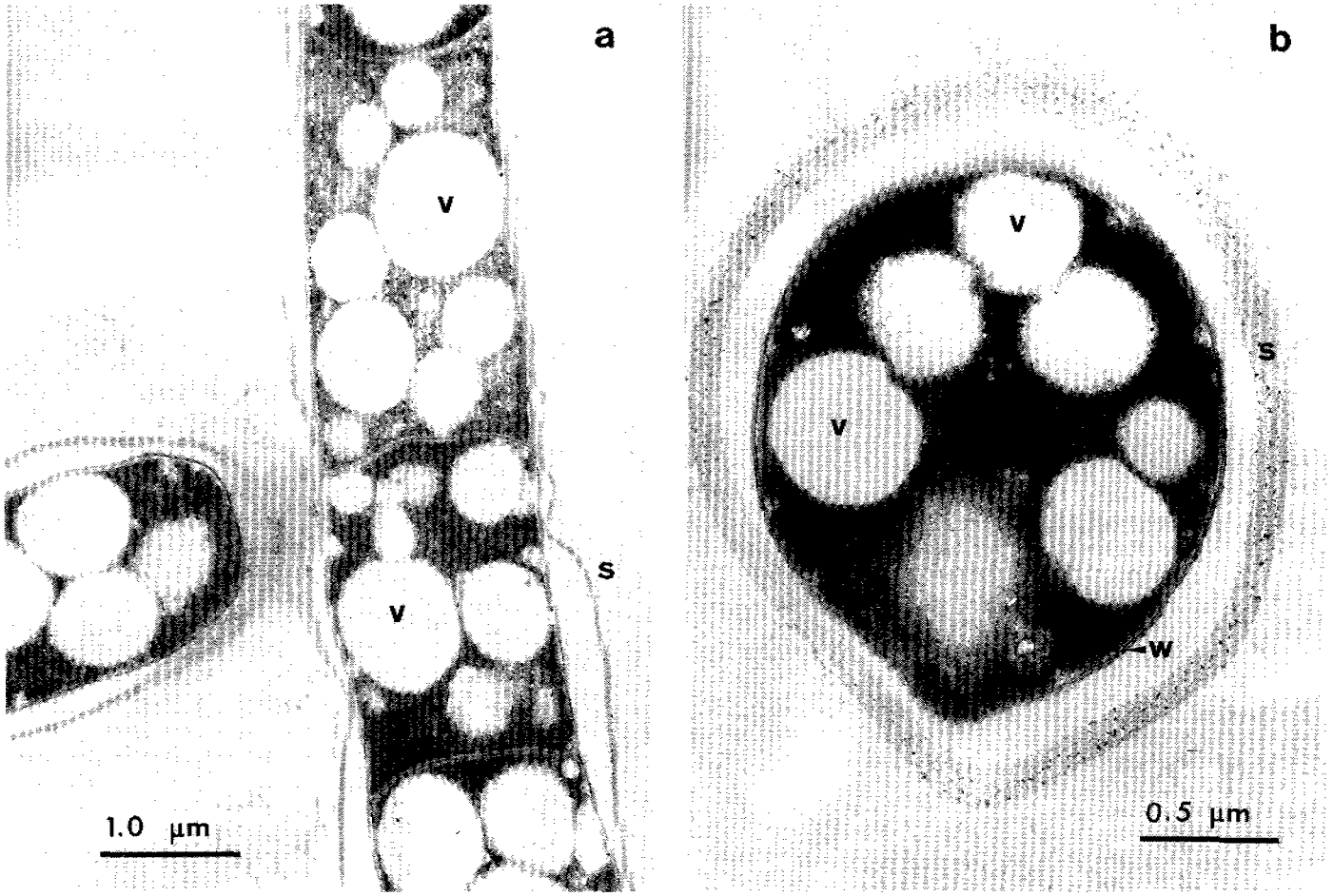

Fig. 3. Electron micrographs of thin sections of Thiothrix filaments from the enrichment culture. 3a. Thin section through a holdfast. 3b. Cross section of a filament: Sheath (S), 3-layered cell wall (W), and vacuoles (V), probably consisting of a lipid, can be seen.

The intracellular vacuoles are probably lipid storage vacuoles and empty spaces where sulfur has been stored. The filaments from the enrichment culture contain many vacuoles, probably caused by the presence of both thiosulfate and an organic source. It is difficult to discern a boundary layer and to distinguish the two kinds of vacuoles, but all the larger vacuoles probably contain lipid. In filaments from activated sludge exposed to thiosulfate (and no organic source), it is sometimes possible to observe inclusion membranes and invaginations of the cytoplasmic membrane.

DISCUSSION

The identification and demonstration of the filamentous bacteria Thiothrix in activated sludge is the subject of much discussion. As shown here the problem is partly methodological and concerns the demonstration of sulfur storage in the organism. Since the Thiothrix filaments do not often contain sulfur granules "in situ", a reliable sulfur storage test is necessary for the identification of this bacteria.

In this study it is shown that sulfur storage due to sulfide oxidation only takes place in the presence of oxygen, and only with sulfide concentrations below about 1 mM. Furthermore the new thiosulfate test has shown that a very common organism, Type 021N, is in fact able to store S-granules under some circumstances. Therefore, compared with the morphological and physiological results, it is very probable that Type 021N belongs to Thiothrix.

In the sulphur storage test of Hünerberg et al. (1970) both air and sulfide were present in the samples. Further Farquhar and Boyle (1971a) used low (0.4 mM) sulfide concentrations and shaken samples. In both cases oxygen was present and Thiothrix was demonstrated as a very common organism in activated sludge. On the other hand, Eikelboom and van Buijsen (1981) used high concentrations of sulfide (4 mM) without controlling for oxygen, thus they found little Thiothrix in activated sludge. Instead they found Type 021N, which morphologically resembles Thiothrix except for the lack of S-granules and sheath. Type 021N was first described by Eikelboom (1975) but he did not test for the ability to oxidize sulfide and store sulfur. However, Eikelboom and van Buijsen (1981) observed few and small S-granules in Type 021N. They also describe two types of Thiothrix that were able to oxidize sulfide and store sulfur very quickly. This implies that oxygen or another usable electron acceptor is present.

In this investigation the sulfur storage from sulfide oxidation in Thiothrix filaments is rather variable at sulfide concentrations below 1 mM. There are probably differences in chemical oxidation of sulfide and in the nutritional stages of the bacteria. Therefore, the tests for sulfur storage from sulfide oxidation were not found suitable in this study.

Thiothrix is known to contain sulfur granules at low sulfide concentrations. Thus, Jones et al. (1982) found good growth at average concentrations of about 2 mM sulfide, but the limits and conditions of sulfur storage were not known. This kind of study requires pure cultures and exact knowledge of the actual concentrations of sulfide and oxygen. Chen and Morris (1972) showed that sulfide in the

presence of oxygen was oxidized to sulfate and thiosulfate within minutes or hours.

The sulfur storage test from thiosulfate, on the other hand, is very effective, reliable and can be used over a broad range of thiosulfate concentrations (best at about 2-10 mM). Effective aeration by shaking or bubbling, however, is necessary. Thiosulfate is, in contrast to sulfide, probably only oxidized to intracellular sulfur by bacteria that normally oxidize sulfur compounds. Skerman et al. (1957) and Maier and Murray (1965) showed that a broad spectrum of normally non-sulfur oxidizing bacteria are able to oxidize sulfide and store S-granules when air is bubbled through the culture. Thus, an S-test based on sulfide and air may give erroneous results.

It is interesting that the times for the formation of S-granules from oxidation of sulfide and from thiosulfate are so different (15-120 minutes and 15-24 hours respectively). This indicates different mechanisms in transport or oxidation of the sulfur compounds.

In the presence of thiosulfate and air the filaments store S-granules and many, mostly younger filaments, produce gonidia, whereupon rosettes are formed. The oxidation of thiosulfate by Thiothrix has been described before e.g. by Caldwell et al. (1975). Motile gonidia are described by Winogradsky (1888) but nobody has hitherto been able to confirm these observations, whereas fragmentation of the filaments under some conditions is described by Bland and Staley (1978) and Larkin (1980). In the present study motile gonidia are often observed in wet mount preparations of the enrichment culture. Gliding on agar surfaces is, however, never observed. The development of gonidia does not take place when an organic source is added to the enrichment culture. This is also the case in Leucothrix, which forms long filaments in media rich in organic matter. Here gonidial formation is induced by unfavorable environmental conditions such as anaerobiosis, starvation, or reduction of incubation temperature (Raj, 1977). The formation of true knots is a characteristic of the family Leucothrichaceae, to which Thiothrix belongs (Buchanan and Gibbons, 1974 and Raj, 1977).

A bacterial sheath is often very difficult to observe without electron microscopy and is probably the reason for the inconsistent observations concerning the presence of sheaths in Thiothrix. Thus Farquhar and Boyle (1971b) have distinguished between three forms of Thiothrix; two without and one with a sheath. Eikelboom and van Buijsen (1981) have described one type with and one without sheaths, besides Type 021N, in which a sheath is not observed. However, several investigators have sometimes seen a "pseudosheath" in Type 021N (Strom and Jenkins, 1981; Eikelboom, personal communication). In the present study nearly all filaments have sheaths, resembling those described by Drawert and Metzner-Küster (1958) and Bland and Staley (1978). However, some filaments have no sheath thus indicating the existence of several types of Thiothrix.

In Thiothrix the diameter of the filaments is often used in the identification and description of different species or types. The diameter, however, is rather variable. Thus, when a small rosette with all filaments having almost the same diameter has been carefully washed, transferred to rinsed sterile filtered wastewater and allowed to grow, filamental diameters of 0.8-2.2 µm have been observed, the youngest filaments being the thinnest. According to Buchanan and

Gibbons (1974) and Fjerdingstad (1979) Thiothrix nivea (Rabenhorst) Winogradsky has a sheath and diameters of 1.4-3.0 µm, thus resembling the filaments described in this study. Probably, many of the thinner filaments are also T. nivea, but other types or species of Thiothrix may be present in the sludge. Filaments with diameters of more than 3 µm are observed rarely, but may belong to another Thiothrix species. Apart from the S-granules it resembles the organism called "Cyanophyceae" by Eikelboom and van Buijsen (1981).

The identification of filamentous micro-organisms in several Danish sewage treatment plants confirm the wide distribution of thiosulfate oxidizing Thiothrix (Type 021N), and this is in accordance with the results of Farquhar and Boyle (1971b) in the USA, who found Thiothrix in 12 out of 16 plants. Further, Tomlinson and Bruce (1979), Strom and Jenkins (1981) and Wagner (1982) all using the identification key of Eikelboom (1975) have found Type 021N as one of the most dominating filamentous organisms in activated sludge, but seldom Thiothrix. However, their Type 021N has probably also been a Thiothrix, which seems responsible for bulking problems in sewage plants in several countries.

The presence of a unit membrane as the boundary of sulfur granules in Thiothrix has been observed by Bland and Staley (1978), and is also observed in some of the filaments in the present study. In some filaments, however, either sulfur inclusion envelopes or invaginations of the cytoplasmic membrane have been established. It is possible that there exist different strains with a different morphology of sulfur inclusion envelopes, an explanation which seems reasonable for Beggiatoa (Strohl et al., 1981).

The physiology of Thiothrix is little known, particularly because of difficulties in isolating the organism. Recently, however, Larkin (1980) has isolated some Thiothrix strains on a solid medium containing only 0.0001% Na-acetate and 0.03% Na-sulfide. Further, Minges et al. (1983) have reported that the strain Thiothrix nivea JP3 is an obligate sulfide or thiosulfate oxidizer. The present attempts to isolate Thiothrix from activated sludge have failed because of difficulties with contaminants. Nevertheless, in 2 cases, colonies with a few contaminants have been developed from single filaments, and growth of these have given some knowledge of the physiology of Thiothrix. Thiothrix are able to grow as heterotrophs on very low concentrations of organic matter like Beggiatoa (Nelson and Castenholz 1981b). Real heterotrophic growth of Thiothrix has never been reported before, and the significance of sulfide and thiosulfate oxidation deserves additional study. The filaments do not contain catalase, so the reduced sulfur compounds may substitute for catalase in peroxide destruction, as suggested for Beggiatoa by Burton and Morita (1964) and Nelson and Castenholz (1981a). Further evidence of the often suggested autotrophic or mixotrophic growth of Thiothrix is still lacking. So the possible protective function of reduced sulfur compounds against peroxides may explain the occurrence of Thiothrix in activated sludge of plants with low oxygen content, often discontinuous operation and sulfide production taking place (Nielsen, P.H., unpublished results). The organic sources, possible growth factors and the feeding pattern may also strongly influence growth of Thiothrix, and further experiments with both pure cultures and activated sludge are necessary to increase our knowledge of the physiology and ecology of this organism.

ACKNOWLEDGEMENTS

I thank E Holm Nielsen for her assistance in the electron microscopy. I also thank Annette Sode and Lee Miller for helpful discussions and linguistic corrections.

REFERENCES

Bland, J.A. and Staley, J.T. (1978). Observations on the biology of Thiothrix. Arch. Microbiol. 117, 79-87.

Brock, T.D. (1981). The Genus Leucothrix. In: Starr, M.P., Stolp, H., Truper, H.G., Balows, A. and Schegel, H.G. (eds.), The Prokaryotes Vol. 1. Springer-Verlag.

Buchanan, R.E. and Gibbons, N.E. (eds.) (1974). Bergey's Manual of Determinative Bacteriology, 8th ed. Baltimore: Williams and Wilkins.

Burton, S.D. and Morita, R.Y. (1964). Effect of catalase and culture conditions on growth of Beggiatoa. J. Bacteriol. 88, 1755-1761.

Caldwell, D.E., Caldwell, S.J. and Tiedje, J.M. (1975). An ecological study of the sulfur-oxidizing bacteria from the littoral zone of a Michigan lake and a sulfur spring in Florida. Plant and Soil 43, 101-114.

Chen, K.Y. and Morris, J.C. (1972). Kinetic of oxidation of aqueous sulfide by O_2. Environ. Science and Technol. 6, 529-537.

Cyrus, Z. and Sladka, A. (1970). Several interesting organisms present in activated sludge. Hydrobiologia 35, 383-396.

Drawert, H. and Metzner-Küster, I. (1958). Fluorescenz- und elektronenmikroskopische Untersuchungen an Beggiatoa alba und Thiothrix nivea. Arch. Microbiol. 31, 422-434.

Eikelboom, D.H. (1975). Filamentous organisms observed in activated sludge. Water Res. 9, 365-388.

Eikelboom, D.H. and van Buijsen, H.J.J. (1981). Microscopic Sludge Investigation Manual. IMG-TNO Rept. A 94A, Delft, The Netherlands.

Farquhar, G.J. and Boyle, W.C. (1971a). Identification of filamentous micro-organisms in activated sludge. J. Wat. Pollut. Control Fed. 43, 604-622.

Farquhar, G.J. and Boyle, W.C. (1971b). Occurrence of filamentous micro-organisms in activated sludge. J. Wat. Pollut. Control Fed. 43, 779-798.

Farquhar, G.J. and Boyle, W.C. (1972). Control of Thiothrix in activated sludge. J. Wat. Pollut. Control Fed. 44, 14-24.

Fjerdingstad, E. (1979). Sulfur Bacteria. ASTM special technical publ. No. 650. Philadelphia.

Godinho-Orlandi, M.J.L. (1980). Microbiology of Sediments in Lakes of Differing Degrees of Eutrophication. Ph.D. thesis. University of Durham.

Harold, R. and Stanier, R.Y. (1955). The genera Leucothrix and Thiothrix. Bacteriol. Rev. 19, 49-64.

Hünerberg, K., Sarfert, F. and Frenzel, H.J. (1970). Ein beitrag zum Blähschlamm. GWF (Wasser-Abwasser) 111, 7-10.

Jones, J.G., Jay, F.M.S. and Hilton, J. (1982). A note on the growth of hiothrix in road drainage ditches. J. Appl. Bateriol. 53, 427-430.

Keil, F. (1912). Beiträge zur Physiologie der farblosen Schwefelbakterien. Beiträgen zur Biologie der Pflanzen. 11, 335-372.

Larkin, J.M. (1980). *Isolation of Thiothrix in pure culture and* observations of a filamentous epiphyte on Thiothrix. Current

Microbiol. 4, 155-158.
Maier, S. and Murray, R.G.E. (1965). The fine structure of Thioploca ingrica and a comparison with Beggiatoa. Can. J. Microbiol. 11, 645-656.
Merkel, G.J. (1975). Observations on the attachment of Thiothrix to biological surfaces in activated sludge. Wat. Res. 9, 881-885.
Minges, C.G., Titus, J.A. and Strohl, W.R. (1983). Plasmid DNA in colorless filamentous gliding bateria. Arch. Microbiol. 134, 38-44.
Nelson, D.G. and Castenholz, R.W. (1981a). Use of reduced sulfur compounds by Beggiatoa sp. J. Bacteriol. 147, 140-154.
Nelson, D.G. and Castenholz, R.W. (1981b). Organic nutrition of Beggiatoa sp. J. Bacteriol. 147, 236-247.
Norris, J.R. and Ribbon, D.W. (eds.) (1971). Methods in Microbiology. Vol. 5A. London. Academic Press.
Pipes, W.O. (1978). Microbiology of activated sludge bulking. Advan. Appl. Microbiol. 24, 85-127.
Raj, H.D. (1977). Leucothrix. CRC Critical Rev. Microbiol. 5, 271-304.
Skerman, V.B.D., Dementjeva, G. and Carey, B.J. (1957). Intracellular deposition of sulfur by Sphaerotilus natans. J. Bateriol. 73, 504-512.
Strohl, W.R., Geffers, I. and Larkin, J.M. (1981). Structure of the sulfur inclusion envelopes from 4 Beggiatoas. Current Microbiol. 6, 75-79.
Strom, P.F. and Jenkins, D. (1981). Identification and significance of filamentous micro-organisms in activated sludge. Paper presented at the 54th annual conference of WPCF, Detroit, Michigan.
Tomlinson, E.J. and Bruce, A.M. (1979). Problems of septicity in biological treatment. Effl. Wat. Treat. Journ. Dec. 1979, 627-639.
Veen, W.L. van (1973). Bacteriology of activated sludge, in particular the filamentous bacteria. Antonie van Leeuwenhoek 39, 189-205.
Wagner, F. (1982). Study of the causes and prevention of sludge bulking in Germany. In: Chambers, B. and Tomlinson, E.J. (eds.) Bulking of Activated Sludge. Ellis Horwood Limited. Chichester.
Walker, A.P. (1982). Quantitative filament counting - a quick, simple method for prediction and monitoring of filamentous bulking. In: Chambers, B. and Tomlinson, E.J. (eds.) Bulking of Activated Sludge. Ellis Horwood Limited. Chichester.
Winogradsky, S. (1888). Beiträge zur Morphologie und Physiologie der Bakterien, Heft I. Zur Morphologie und Physiologie der Schwelfelbakterien. Arthur Felix, Leipzig.

Wat. Sci. Tech. Vol.17, Amsterdam, pp.183-196.
Printed in Great Britain.

0273-1223/85 $0.00 + .50

KINETIC STUDIES OF THE MICROBIOLOGICAL CONVERSION OF SULPHATE TO HYDROGEN SULPHIDE AND THEIR RELEVANCE TO SULPHIDE GENERATION WITHIN SEWERS

G. A. Holder, G. Vaughan and W. Drew

Department of Chemical Engineering, Monash University, Clayton, Victoria, 3168, Australia

ABSTRACT

The relevance of the studies carried out, to the important practical problem of predicting sulphide generation rates within sewers, is discussed in the introduction section of the paper. The predictive equations presently in use are compared, and the desirability of replacing these empirical equations by a more scientific approach based on an analysis of mass transport and biochemical reaction is stressed.

A theoretical analysis of mass transport and metabolism of sulphate during laminar flow in a model sewer is then described. This theoretical section is followed by the description of the laboratory experimental studies. These studies consisted of flowing simulated sewage through tubes containing biofilms of mixed cultures of sulphate reducing bacteria.

The results obtained in the laboratory studies showed that the diffusional resistance in the liquid phase was negligible and that the biological conversion of sulphate to sulphide followed zero order kinetics when mass transfer was not rate limiting. The observed sulphate removal rates gave good agreement with Australian field data for sulphide generation in sewers. The value of the zero order rate constant (measured at 41°C) was 30 mg cm^{-3} h^{-1}.

KEYWORDS

Hydrogen Sulphide. Sulphate-reduction. Sulphide-generation. Sewerage, Sewage, Anaerobic slimes, Biofilm. Rate constant.

INTRODUCTION

The corrosion of concrete sewers which occurs as a result of hydrogen sulphide formation from sulphate-containing sewage has caused concern for many years. The problem arises because bacteria which utilize the sulphate ion as a source of oxygen flourish in warm anaerobic sewage. The enormous expense and hazard caused by the activities of sulphate-reducing bacteria in sewers has provided the stimulus for studies by concerned sewage authorities, research associations and consultants. Early work was carried out in Melbourne by Parker (1945, 1947, 1965) and in California by Pomeroy (1959). One book Thistlethwayte (1972) and one manual,

U.S. E.P.A. (1974) detail the comprehensive investigations which have been carried out on the mechanisms by which the corrosion occurs and the procedures for preventing sulphide formation within sewers. Corrosion resistant linings are expensive. So too is sewer repair. Accordingly the interest in developing design procedures for sulphide control is considerable, as is also evidenced by the most recent literature Meyer (1980), Pomeroy (1977), Nadarajah (1977) and also Lovell (1977) and Roberts (1977).

In order to design effectively for sulphide control a reliable means of predicting the rate of sulphide production is desirable. As a result of studies by the larger sewage authorities in Australia the following empirical correlation has been used to predict the rate of sulphide-sulphur generation in rising mains in which pumps operate continuously (Thistlethwayte, 1972).

$$G_s = 32.2 \times 10^{-6} \times V_s \times [BOD_5]^{0.8} \times [SO_4]^{0.4} \times 1.139^{(t^oC-20)} \qquad (1)$$

where G_s is slime generation rate in lb. of sulphide sulphur/1000 sq. ft. of slime/hr.

V_s is mean velocity of sewage flow in ft./sec.

$[BOD_5]$ is 5 day bio-chemical oxygen demand in mg. O_2/1.

$[SO_4]$ is sulphate expressed as mg.SO_4/1.

and t^oC is temperature in degrees Celsius.

The above equation, which is reproduced here with the symbols and units used in the original publication, was derived from data obtained from investigations into sulphide build-up in pressure ("rising") mains of diameters varying from 0.3 to 1.2 m. and with average stream velocities of from 0.3 to 0.9 m.sec.$^{-1}$ during pumping. The various sewages pumped showed BOD_5 values within an overall range of 90 mg/1 to 800 mg/1 and sulphate contents 42 mg/1 to 660 mg/1. Where pumping stations are operated intermittently a modification of this equation is used.

Other attempts have been made to develop practical correlations for use in forecasting sulphide build-up in sewers. The relevant equations are summarised, together with Thistlethwaytes' equation, in Table 1. Much work in this area has also been carried out in South Africa (1959). As can be seen from Table 1 Pomeroy (1959) correlated biochemical oxygen demand of sewage with sulphide generation rate. Subsequently Pomeroy and Parkhurst (1977) have discussed the forecasting of sulphide build-up rates in partially filled sewers. Boon and Lister (1974) correlated chemical oxygen demand with sulphide build up rate.

TABLE 1. Sulphide generation rates in sewers - predictive equations.

Equation	Source
$G_s = 32.2 \times 10^{-6} V_s [BOD]^{0.8} [SO_4]^{0.4} 1.139^{T-20}$	Australia-Thistlethwayte (1972)
$\emptyset = 0.001 [BOD] 1.07^{T-20}$	USA EPA Pomeroy (1974)
$\emptyset = 0.00023 [COD] 1.07^{T-20}$	England Boon & Lister (1974)
$\Delta C_s = 0.0026.t.C_{EBOD} \left(\frac{1+0.01\ d}{d}\right)$	USA Manuals of Practice. WPCF No. 9 ASCE No. 37.

It should be noted that Thistlethwayte's correlation includes V_s the mean flow velocity of the sewage and also the sulphate concentration, whereas the correlations by Pomeroy and by Boon and Lister do not. Also whereas Thistlethwayte and

Pomeroy include BOD as a parameter, Boon and Lister have preferred to use COD instead. It is therefore difficult to rank the three correlations in order of accuracy without reference to the precise experimental situation. However some idea of the way the three formulae compare is shown by Figure 1. which shows plots of predicted sulphide generation rates in sewers running full at 20°C as a function of BOD_5. We have compared the correlations for COD two to three times greater than BOD, flow velocities in the range 0.3 to 0.9 m s^{-1}, and a fixed sulphate concentration of 100 mg/l. The upper and lower bounds of the rates which Thistlethwayte recorded are shown as dotted lines. All three correlations predict sulphide generation rates of the same order of magnitude.

As emphasised earlier, all three correlations are empirical. Although Thistlethwayte (1972 page 15) does attempt to justify the form of the equation used, the justification does not have any reliable theoretical basis. The unreliability of the procedures presently used for predicting sulphide build-up is evident from the discussion on this subject held at the 8th IAWPR meeting, Sydney (1976) - reference Pomeroy and Parkhurst, (1977).

The purpose of the research programme was three fold. Firstly to show that by applying established chemical engineering principles which deal with mass transport and biochemical reaction, mathematical models can be developed for the sulphate conversion process. Secondly to obtain laboratory experimental data collected with the objective of verifying whether one or more of a number of possible mathematical models might be correct, and thirdly to explore the possibilities of developing a predictive design procedure based on a feasible mechanism (rather than empirically correlated data).

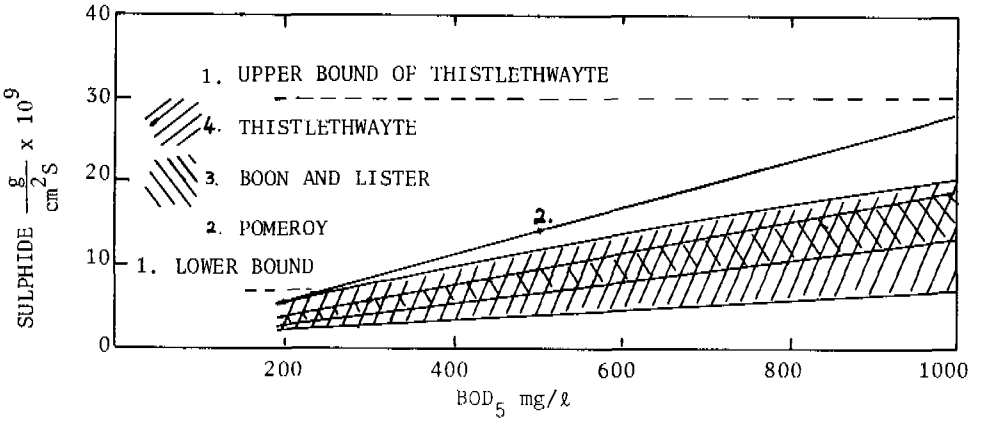

Fig. 1. COMPARISON OF PREDICTED SULPHIDE GENERATION RATES.

MATHEMATICAL MODELS

A schematic model of the processes which are under study is shown in Figure 2. The mathematical models are derived essentially by carrying out a mass balance on an element of fluid in the liquid film and by making the appropriate mathematical substitutions together with a number of simplifying equations. The end result i.e. the mathematical model which is obtained, depends of course on many factors such as the applicability of the mechanistic model, which rate laws are assumed for reaction in the slime, and for transport to the slime and also the validity of the simplifying assumptions. Because the physical laws which apply are in differential form the equations selected have to be manipulated and integrated before relationships between physically measurable quantities can be produced.

It is assumed that Figure 2 is a correct mechanistic model, that the system is at steady state, that the effects caused by growth of the microbial culture during the time the data is collected can be ignored, temperature is constant, the liquid is Newtonian, the slime is homogeneous and of uniform depth, and that all sulphate reduction takes place within the slime. It is further assumed that all other components which are necessary for the bacterial reduction of the sulphate are present in sufficient concentration that they do not limit the rate of reaction.

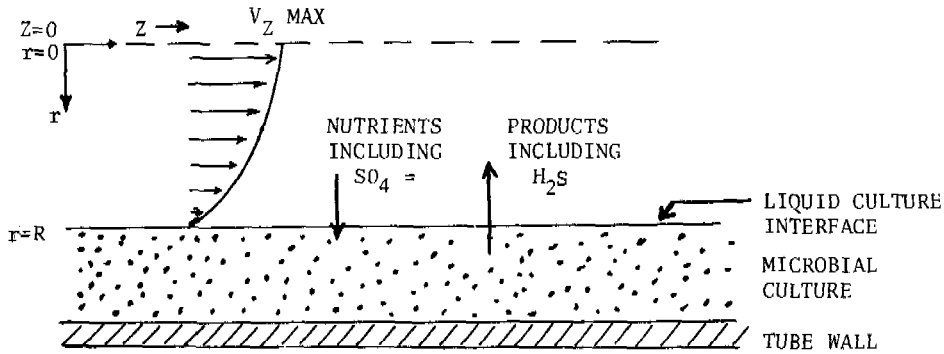

Fig. 2. MECHANISTIC MODEL.

Reynold's number calculations for typical sewers flowing full and for the experiments reported later in this paper show that fully developed laminar flow can be safely assumed. Accordingly by carrying out a momentum balance, the velocity profile (which is drawn in Figure 2) can be expressed in terms of the maximum (mid-line) velocity $V_{z\ max}$ as

$$V_z = V_{z,\ max} \left\{1 - \left(\frac{r}{R}\right)^2\right\} \qquad (2)$$

The transport of sulphate (from here on designated as component A) in the liquid phase is described by the equation of continuity (Bird 1960), expressed in cylindrical coordinates.

$$\frac{\partial C_{al}}{\partial t} + \left|\frac{1}{r}\frac{\partial (rN_{ar})}{\partial r} + \frac{1}{r}\frac{\partial N_{a\theta}}{\partial \theta} + \frac{\partial N_{az}}{\partial z}\right| = R_a \qquad (3)$$

where C_{al} refers to the molar concentration of component A (i.e. sulphate ion) in the liquid phase, N_a refers to the molar flux of A with respect to stationary co-ordinates and R_a is the rate of removal. Because the system is at steady state, is symmetrical, and because there is no removal or production of component A (i.e. sulphate) in the liquid phase the equation of continuity reduces to

$$\frac{1}{r}\frac{\partial (rN_{ar})}{\partial r} + \frac{\partial N_{ar}}{\partial z} = 0 \qquad (4)$$

$$\therefore -D_{al}\left|\frac{1}{r}\frac{\partial}{\partial r}\left(r\frac{\partial C_{al}}{\partial r}\right) + \frac{\partial^2 C_{al}}{\partial z^2}\right| + v_z\frac{\partial C_{al}}{\partial z} = 0 \qquad (5)$$

With axial diffusion considered negligible, this rearranges to

$$v_{z,max}\left|1 - \left(\frac{r}{R}\right)^2\right| \frac{\partial C_{al}}{\partial z} = \frac{D_{al}}{r}\frac{\partial}{\partial r}\left(r\frac{\partial C_{al}}{\partial r}\right) \qquad (6)$$

which is the partial differential equation describing the liquid phase molar concentration of component A, C_{al} (r,z). For the initial condition (z = 0) it is assumed that there exists no radial concentration gradient. That is

$$C_{al}(r,0) = C_{a0}. \qquad (7)$$

Also because of the geometry of the system

$$\left.\frac{\partial C_{al}}{\partial r}\right|_{r=o} = 0 \qquad (8)$$

The remaining boundary condition describes the transport of component A across the liquid-culture interface (r = R), and its form depends upon how the metabolism of component A by the thin layer microbial culture is described.

A number of different choices for the third boundary condition can be made. Two relatively simple realistic alternatives are obtained by assuming that the removal of the sulphate ion within the slime is zero order and that the slime layer is either (a) sufficiently thin that it is fully penetrated or (b) sufficiently thick that it is partially penetrated :

(a) For full penetration the mass flux across the liquid-culture interface is obtained simply by dividing the removal rate by the surface area of the slime-liquid interface.

Thus $$\left.N_{ar}\right|_{r=R} = \frac{k}{2R}(R^{*2} - R^2) \qquad (9)$$

Where k is the zero order rate coefficient for sulphate removal within the slime

$$\therefore \left.\frac{\partial C_{al}}{\partial r}\right|_{r=R} = \frac{-k}{2R D_{al}}(R^{*2} - R^2) \qquad (10)$$

Since the slime thickness is normally very much less than the radius of the tube equation (10) simplifies to :

$$\left.\frac{\partial C_{al}}{\partial r}\right|_{r=R} = \frac{-k\,(R^* - R)}{D_{al}} \qquad (11)$$

(b) For partial penetration the corresponding expressions to those shown above in (a) are obtained by replacing R* (the radius of the tube) by R_c where R_c is the distance from the tube centre to the point in the slime where the sulphate ion concentration drops to zero. R_c is, of course, (unlike R*) dependent on the sulphate ion concentration at the slime-liquid interface. The relationship is given by equation (14) which is derived by applying the equation of continuity (i.e. equation (3)) to the slime phase at steady state making the assumptions that sulphate ion is transported within the slime phase by uniform radial diffusion towards the tube wall whilst being removed at a constant rate.

We thus obtain :

$$D_{as} \frac{1}{r} \frac{\partial}{\partial r} \left(r \frac{\partial C_{as}}{\partial r}\right) = k \qquad (12)$$

At $r = R_c$ $\qquad \frac{\partial C_{as}}{\partial r} = 0 \quad$ and $\quad C_{as} = 0 \qquad (13)$

hence

$$C_{as}\Big|_{r=R} = \frac{k}{2D_{as}} \frac{(R^2 - R_c^2)}{2} + \frac{k}{2D_{as}} R_c^2 \ln \left\{\frac{R_c}{R}\right\} \qquad (14)$$

Since the slime layer is thin relative to the tube radius R_c/R, is close to unity. Replacing $\ln (R_c/R)$ (Perry 5th Edition 2-33) as an infinite series in (R_c/R) causes equation (14) to reduce to :

$$C_{as}\Big|_{r=R} = \frac{k}{2D_{as}} (R_c - R)^2 \qquad (15)$$

$$\therefore \quad (R_c - R) = \sqrt{\frac{2D_{as}}{k}} \cdot \left\{C_{as}\Big|_{r=R}\right\}^{\frac{1}{2}} \qquad (16)$$

Equation (16) shows that the depth of sulphate penetration into the slime is linearly proportional to the square root of its concentration at the slime-liquid interface.

Thus $$k(R_c - R) = \sqrt{2\ k\ D_{as}} \left\{C_{as\ r=R}\right\}^{\frac{1}{2}} = -D_{al} \frac{\partial C_{al}}{\partial r}\Big|_{r=R} \qquad (17)$$

The third boundary condition for the case of partial penetration is therefore :

$$\frac{\partial C_{al}}{\partial r}\Big|_{r=R} = \frac{-\sqrt{2\ k\ D_{as}}}{D_{al}} \left\{C_{al}\ (R,z)\right\}^{0.5} \qquad (18)$$

Solutions to equation (6)

To simplify manipulations it is convenient to introduce the following dimensionless quantities :

$$C_1 = \frac{C_{al}}{C_{ao}} \quad (19) \quad ; \qquad \xi = \frac{r}{R} \quad (20)$$

$$\zeta = \frac{D_{al}\ Z}{V_{z\ max} R} \quad (21) \quad ; \qquad Q = \frac{R}{D_{al}} \sqrt{\frac{2\ k\ D_{as}}{C_{ao}}} \quad (22)$$

Where

C_1 is the fraction of substrate remaining

ξ is dimensionless radial displacement

ζ is dimensionless axial displacement

Q is dimensionless rate parameter

Equation (6) thus becomes :

$$(1-\xi^2)\frac{\partial C_1}{\partial \zeta} = \frac{1}{\xi}\frac{\partial}{\partial \xi}\left\{\xi \frac{\partial C_1}{\partial \xi}\right\} \qquad (23)$$

With the conditions for the two situations considered, tabulated as follows :

Conditions		Full Penetration	Partial Penetration
B.C.1	$C_1\ (\xi,\ 0)$	1	1
B.C.2	$\left.\frac{\partial C_1}{\partial \xi}\right\|_{\xi=0}$	0	0
B.C.3	$\left.\frac{\partial C_1}{\partial \xi}\right\|_{\xi=1}$	Constant	$-Q\{C_1(1,\zeta)\}^{0.5}$

Analytical solutions to (23) using boundary conditions equivalent to those listed above for full penetration are presented in the text by Bird, Stewart and Lightfoot (1960). Unfortunately analytical solutions for the partial penetration case are not available in the literature because the specification for the boundary condition at the slime-liquid interface incorporates sulphate concentration raised to the power 0.5. Accordingly numerical solutions for values of the dimensionless rate parameter Q ranging from 0.1 to 2.5 were computed and are shown in Figure 3 as plots of average concentration (i.e. $\bar{C}_1$) versus the dimensionless distance ζ. The data for $\bar{C}_1$ were calculated as flow-averaged values of C_1 as defined below :

$$\bar{C}_1(\zeta) = \frac{\int_0^1 \xi(1-\xi^2)\ .\ C_1(\xi,\zeta)\ d\xi}{\int_0^1 \xi(1-\xi^2)\ d\xi} \qquad (24)$$

$$= 4\int_0^1 \xi(1-\xi^2)\ .\ C_1(\xi,\zeta)\ d\xi \qquad (25)$$

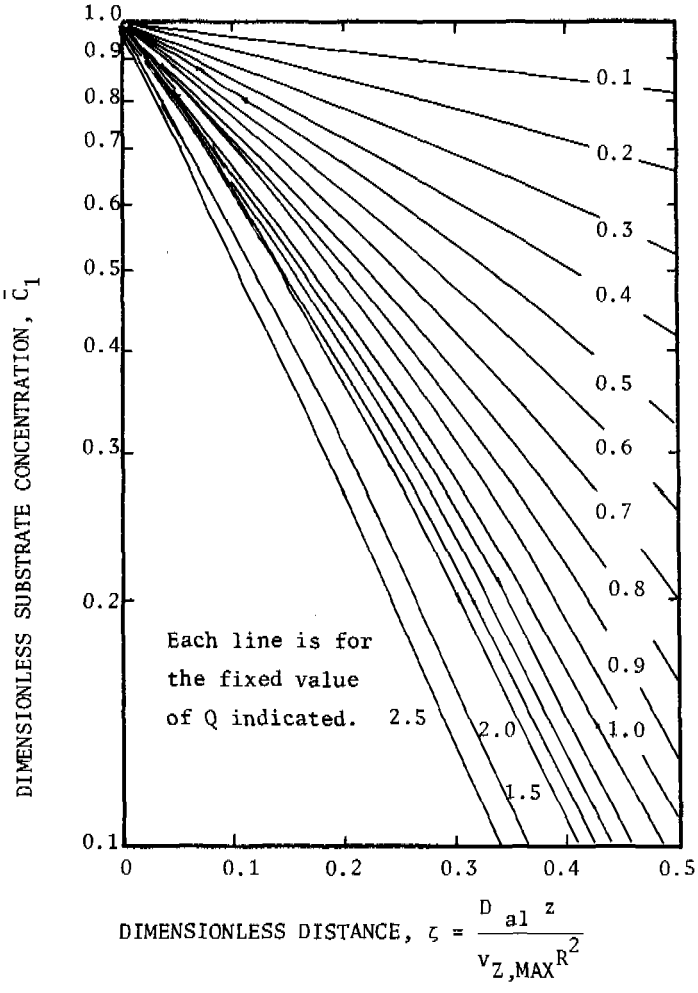

Fig. 3. VELOCITY WEIGHTED AVERAGE DIMENSIONLESS CONCENTRATION $\bar{C}_1$ AS A FUNCTION OF DIMENSIONLESS DISTANCE, ζ, FOR VARIOUS VALUES OF THE DIMENSIONLESS RATE PARAMETER Q. SOLUTIONS FOR THE CASE OF PARTIAL PENETRATION.

EXPERIMENTAL

A schematic diagram of the apparatus and flow scheme used is shown in Figure 4. The cultures were grown in a one-litre mini-fermenter fitted with ports to accept pH, dissolved oxygen and O.R.P. electrodes. Other ports were used for sampling, pH control by the addition of 1N HCl, and recirculation of the culture media through a model sewer. The model sewer consisted of lengths of plasticised PVC tubing of diameter 0.5 to 0.635 cm wound around a 100 cm x 6 cm former, and maintained in a thermostat.

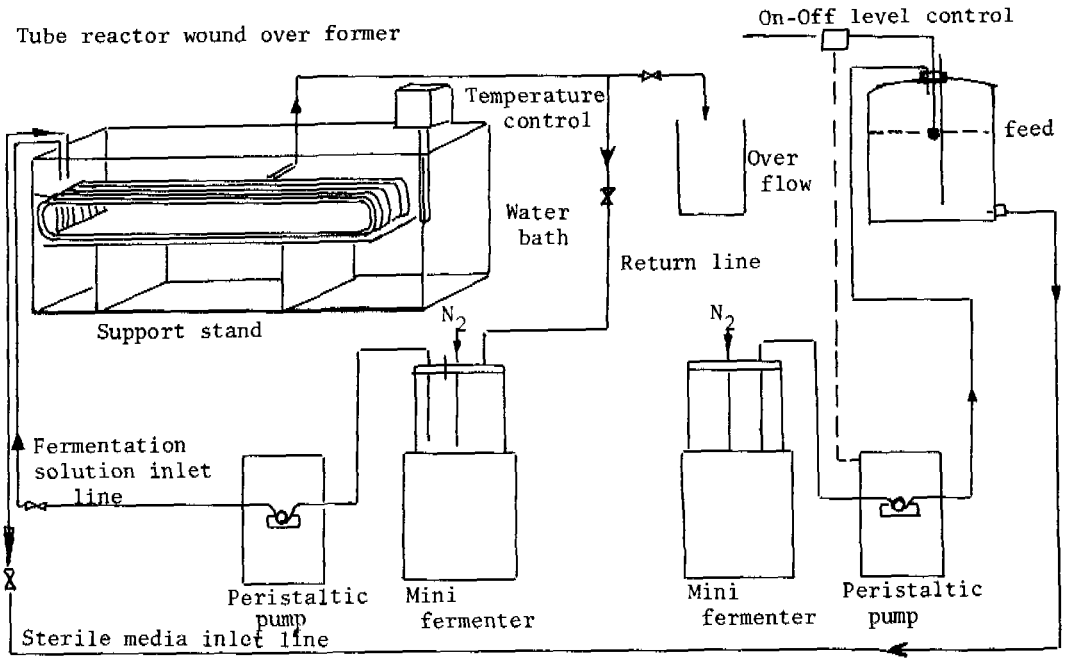

Fig. 4. SCHEMATIC ARRANGEMENT OF APPARATUS FOR TUBULAR REACTOR EXPERIMENTS.

A sample of sediment and water containing sulphate-reducing bacteria was taken from a heavily polluted smelly saline creek near Melbourne. This sample was used to initially inoculate Postgate medium held at room temperature. Subsequent sub-culturing yielded an active stock mixed culture. Culturing and sub-culturing were carried out for a period of one year (during which time batch reactor kinetic studies were carried out) prior to the commencement of the model sewer experiments. All runs were carried out at 41^{o}C because the batch studies had indicated that this was the optimum temperature for culture activity.

Slime growth in the model sewer was readily produced by continuous recirculation of culture media i.e. dispersed bacteria in a synthetic sulphate-containing sewage. When a uniform thin slime layer had formed the system was drained and a flow of sterile synthetic sulphate-containing sewage commenced using a constant-head gravity feed system. Reynold's numbers were in the range 10 to 20 i.e. well within the laminar flow region.

The composition of the synthetic sewage is shown in Table 2. It was based on Postgate's medium, i.e. a solution of sulphate, lactate and other nutrients at pH 7. As can be seen from Table 1. the sulphate ion concentration was, of course, varied in the experimental runs by adjusting the quantity of sodium sulphate in the sterile synthetic sewage. Recirculation of culture media was carried out between all runs so as to continuously recondition the biofilm.

TABLE 2. Composition of Synthetic Sewage.

Component	Concentration g/l.
$K H_2 PO_4$	0.5
NH_4Cl	1.0
$CaCl_2.2H_2O$	0.06
$MgSO_4.7H_2O$	0.06
Yeast Extract	1.0
$FeSO_4.7H_2O$	0.002
Na_2SO_4	0 to 2
Lactate	0 to 5

The theoretical lactic acid requirement for the reduction of sulphate ions is as shown by the following equation :

$$2\ CH_3\ CHOH\ CO_2H + SO_4^{--} \rightarrow 2CH_3COOH + S^{--} + 2H_2O + 2CO_2$$

thus, as can be seen, two moles of lactic acid are required for each mole of sulphate ion. On a mass basis this becomes a ratio of 1.88 : 1.

The corresponding equation in the U.S. EPA (1974) handbook on sulphide control is:

$$2C + SO_4^{--} + 2H_2O \rightarrow 2HCO_3^{-} + H_2S$$

It is also stated in the handbook that 2 moles of carbon would probably, on average, be present in 42g of organic matter. If we assume that the organic matter is present as hydrogen and carbon the ratio of BOD to sulphate on a mass basis is about 1.5 to 1. The theoretical BOD of lactic acid is 7% higher than its mass. The inlet lactate concentrations were always at least twice the inlet sulphate concentrations. The lactate concentration levels were monitored simultaneously with the sulphate to check that an adequate supply of carbon was available to the sulphate reducing bacteria. It is, of course, well established in the microbiological literature that lactate is a preferred carbon source for sulphate reducers.

Samples (c.3ml) were taken for analysis, using a hypodermic syringe pushed through septa located at intervals along the model sewer. Each sample was immediately filtered through Millipore type SC cellulose-acetate paper, to remove any suspended matter, and analysed for sulphate turbometrically (APHA 1975) and for lactate using the procedure detailed by Lawrence (1970).

Measurements of the thickness of the microbial culture to the nearest micron were made using a modified micrometer together with a stereo-microscope. Removable sections of sacrificial tubing were located at the inlet and outlet of the model sewer for this purpose.

The density of the layer of microbial culture was determined by drying at 105°C for 2 hr. sections of tubing of known area and measured slime thickness.

RESULTS AND DISCUSSION

Concentration profiles for sulphate removal are shown in Figure 5 for four typical runs which cover the concentration range 2000 mg/l down to 500 mg/l. As can be seen, within the limitations of experimental error the concentration of sulphate fell linearly along the length of the tube when the concentration of sulphate was high (i.e. certainly above about 500 mg/l). When the inlet sulphate concentration

was 500 mg/1 the profile showed distinct non-linearity - as did all the lower inlet concentrations tested.

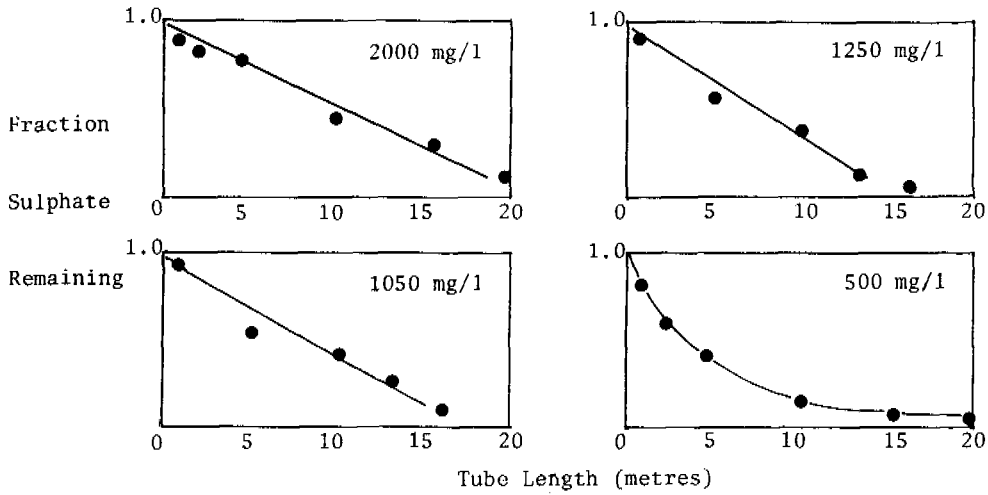

Fig. 5. FRACTION SULPHATE REMAINING VERSUS TUBE LENGTH FOR FOUR DIFFERENT SULPHATE INLET CONCENTRATIONS.

The interpretation of the linear profiles is clearly that the slimes were removing sulphate at a fixed rate regardless of the sulphate concentration. This, in turn, means that the slime layer was being fully utilized (i.e. there was full penetration) and that zero order kinetics applied. The interpretation of the non-linear regions is not quite as straightforward. But the simplest general interpretation is that as the sulphate concentration in the liquid phase falls we eventually reach a situation where sulphate ions are entirely removed within the slime before they can travel to the tube wall, i.e. diffusional limitations result in only a partial penetration of the slime. In these circumstances the depth of penetration is given by equation (16) - which shows that the penetration is proportional to the square root of the sulphate concentration at the surface of the slime layer.

A total of 21 experimental runs were carried out using sulphate inlet concentrations within the range 100 to 2000 mg/1. The experimental data were analysed in the following manner. For each run a line of best fit was determined for the data points on the sulphate concentration profile. From each line of best fit the corresponding initial rate of sulphate removal was computed. Then from the mean measured-depth of culture thickness for each run together with the known inside surface area of the reactor tube and liquid flow rate the initial rate of sulphate removal per cm^3 of slime was calculated for each inlet concentration. The results are shown in Figure 6. As can be seen at the lower concentrations of sulphate (i.e. in the range 0 to about 500 mg/1) the volumetric rate of removal increased as the sulphate concentration increased. This rise in the volumetric removal rate occurs, of course, because the slime is not completely penetrated. Eventually as the inlet sulphate concentration increases full penetration of the slime occurs, the slime is then fully utilized and we move out of the region where diffusional limitations mask the kinetics of the biological reduction of sulphate to sulphide. As can be seen from Figure 6, for the experimental conditions used in these studies, there was evidently full penetration for the nineteen runs carried out using inlet concentrations of 500 mg/1 and higher. The

values for the rate of sulphate removal per unit volume of slime (i.e. the zero order rate constant) were not all identical. The values ranged from a low of 17 mg cm^{-3} h^{-1} to a high of 47.5 mg $cm^{-3}h^{-1}$. Clearly some scatter can be expected due to experimental error - especially in an area of study such as anaerobic biological sulphate reduction. Accordingly a linear regression analysis on the nineteen (full-penetration) results was carried out. It was found that the slope of the relation between the zero order rate constant and the initial sulphate concentration was not significantly different from zero at the 95% confidence limit, with a mean value being obtained for the zero rate constant of 30 mg sulphate cm^{-3} hr^{-1} and a standard deviation of 7.5 mg cm^{-3} hr^{-1}. The largest contributing source of error to the scatter in the data was undoubtedly the measurements of the slime thicknesses using the penetrometer and the sacrificial sections of tubing. The values of the measured slime thicknesses ranged from a low of 28 microns to a high of 59 microns. The mean value for the slime thickness was 41 microns with a standard deviation of 10 microns. An error which caused the measured value of the slime thickness to be too low would produce a high value for the rate constant and vice versa. Figure 7 shows a plot of all the measured values for the slime thickness plotted against the respective calculated values for the zero order rate constants. As can be seen high values for the rate constant tended to be associated with low values for slime thickness, and vice versa.

Comparisons with Field Data

The major sewerage authorities within Australia carried out, for more than 10 years, a cooperative study of sulphide generation within sewers. The findings were edited by Thistlethwayte (1972). The reported range of sulphide-sulphur generation rates was 0.05 to 0.22 lb per thousand square feet of sewer area per hour. Those figures convert to 0.244 to 1,073 g.S m^{-2} hr^{-1}, which in terms of sulphate loss becomes 0.73 to 3.2 g SO_4^- m^{-2} hr^{-1}. The mean value of the zero order rate constant found in the laboratory studies reported here was 30 mg cm^{-3} hr and the mean slime depth $41x10^{-4}$ cm. Accordingly the mean sulphate surface flux is 1.2g SO_4^- m^{-2} hr^{-1} i.e. a figure which agrees well with the range of data reported by Thistlethwayte.

Comparisons with Other Laboratory Studies

No values for the zero order rate constant for biological sulphate reduction could be found in the literature. The general field of anaerobic biological waste treatment is now however of much interest and data on related systems is now appearing in the literature. It is interesting to note that Onuma and Omura in a detailed study reported at the recent Cape Town Conference (1982) gave the zero order rate constants for the aerobic processes of ammonia nitrification to NO_2^- and NO_3^- as 7.26 and 6.37 mg cm^{-3} h^{-1} respectively, at 20°C. The value of 30 mg cm^{-3} h^{-1} which we have obtained for the analogous conversion of sulphate to sulphide is thus about four times larger than the nitrification values. However it should be noted that all runs in the study reported here were carried out at 41°C, because this was the temperature at which the mixed cultures showed maximum activity.

CONCLUSIONS

1. The equations which are presently used for predicting sulphide generation rates within sewers do not have an adequate scientific basis. The present study which takes into account both mass transfer and reaction indicates the route which should be taken to develop improved predictive procedures.
2. Laboratory studies of sulphide generation rates from slimes have given satisfactory agreement with field data obtained in Australian field studies.

3. It has been possible to characterise the sulphate reducing cultures developed in these studies with a single parameter - i.e. the zero reaction rate constant. The value of the zero reaction rate constant was 30 mg SO_4^{--} cm^{-3} h^{-1} at 41°C.

4. The results of this study can be utilised to estimate potential hydrogen sulphide production in sewers.

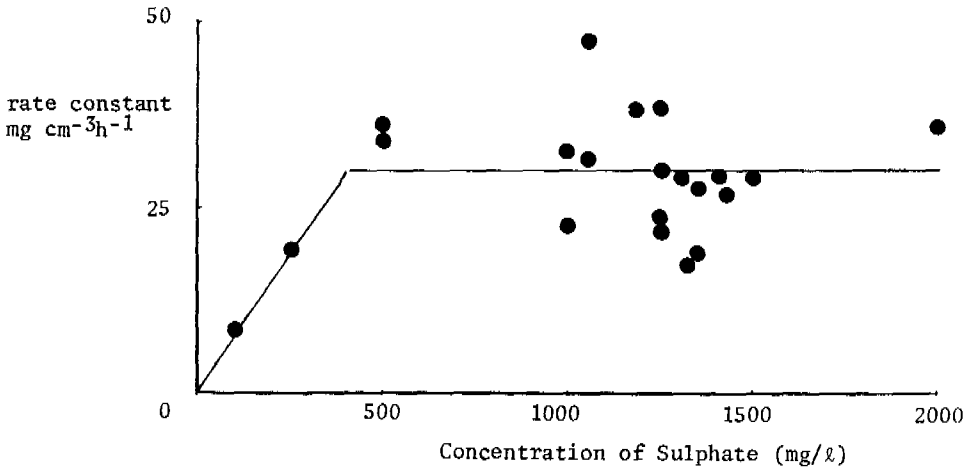

Fig. 6. RATE OF SULPHATE REMOVAL, mg /h per cm^3 OF SLIME, VERSUS INLET SULPHATE CONCENTRATION.

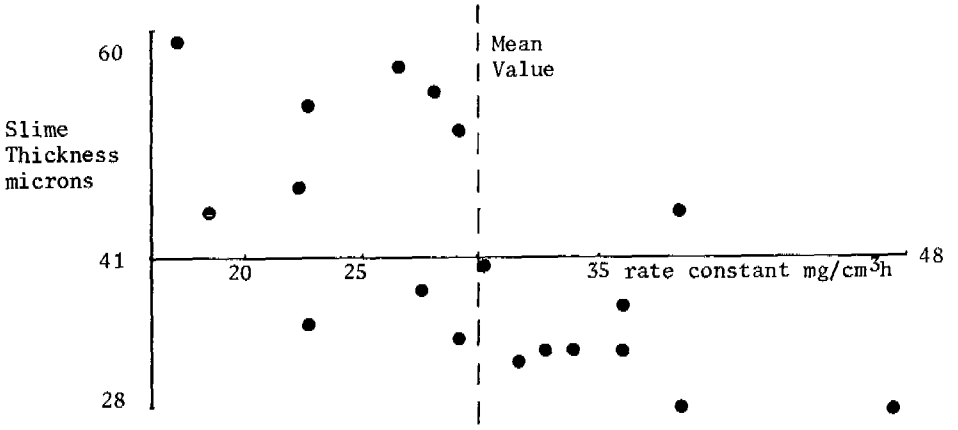

Fig. 7. MEASURED SLIME THICKNESS VS. CALCULATED VALUES FOR THE RATE CONSTANT.

ACKNOWLEDGMENT

Thanks are due to State Rivers and Water Supply, Melbourne, and The Water Research Foundation, Sydney for financial support.

NOMENCLATURE

C_{al}	concentration of component A in the liquid phase g mole cm^{-3}
C_1	dimensionless concentration of A in liquid phase
$\bar{C}_1$	dimensionless velocity-averaged concentration of A (see eqn. 24)
D_{al}, D_{as}	diffusivity of A in liquid and slime respectively
Na	molar flux of A with respect to stationary coordinates
r, θ, Z,	respectively radial, angular, and axial displacement
ξ,ζ	respectively dimensionless radial and axial displacement
Q	dimensionless rate parameter (see eqn. 22)
V_z	liquid velocity in axial direction
k	zero order rate constant mg cm^{-3} h^{-1}
Ra	removal rate of component A (see eqn. 3)
R, R*	radius of liquid flow path and tube radius respectively
Rc	distance from tube centre to the slime depth at which sulphate concentration falls to zero

REFERENCES

Bird, R.B., Stewart, W.E. and Lightfoot, E.N. (1960). *Transport Phenomena.* John Wiley, New York.

Boon, A.G. and Lister, A.R. (1974). *Formation of sulphide in rising main sewers and its prevention.* Water Pollution Research Laboratory, Stevenage, England.

Lawrence A.J. (1970). *A rapid method of estimation of lactic acid in skim milk powder.* Aust. J. Dairy Technol. 25, 198-200.

Lovell, J.W. (1977). *Contribution to discussion.* Prog. Wat. Tech., 9, C37-C39.

Meyer, W.J. *Case study of prediction of sulphide generation and corrosion in sewers.* J.W.P.C.F., 52. No. 11, 2666-2674.(1980).

Nadarajah, A. and Richardson, J. (1977). *Prevention and protection of sewerage systems against sulphide attack with reference to experience in Singapore.* Prog. Wat. Tech., 9, 585-598.

Onuma, M. and Omura, T. (1982). *Mass Transfer Characteristics within Microbial Systems.* Water Sci. Tech., 14, 553-568.

Parker, C.D. (1945). *The corrosion of concrete.* Aust. J. Exp. Biol. Med. Sci., 23, 81-90, 91-98.

Parker, C.D. (1947). *Species of sulphur bacteria associated with the corrosion of concrete.* Nature, 159, 439-440.

Parker, C.D. (1965). *Bacteriology of the corrosion process.* In : *Investigations into the Corrosion of Concrete Sewers by Hydrogen Sulphide.* Melbourne and Metropolitan Board of Works Technical Paper No. A.8, Part 6, also see Part 2.

Pomeroy, R.D. (1959). *Generation and Control of Sulphide in Filled Pipes.* Sewage and Industrial Wastes, 31 (9), 1082-1095.

Pomeroy, R.D. and Parkhurst, J.D. (1977). *The forecasting of sulphide build-up rates in sewers.* Prog. Wat. Tech., 9, 621-628; C37-C39.

Postgate, J.R. (1963). *Versatile medium for the enumeration of sulphate-reducing bacteria.* Appl. Microbiol. 11, 265-267.

Roberts, D.G.M. (1977). *Contribution to discussion.* Prog. Wat. Tech., 9, C37-C39.

South African C.S.I.R. (1959). *Corrosion of Sewers.* CSIR technical report. Pretoria.

Thistlethwayte, D.K.B. (1972) Editor. *The Control of Sulphides in Sewerage Systems.* Butterworth's, Sydney.

U.S.A. E.P.A. (1974) Cincinnatti, Ohio, *Process Design Manual for Sulphide Control in Sanitary Sewerage Systems.*

ACTIVATED SLUDGE

Wat. Sci. Tech. Vol.17, Amsterdam, pp.197-208.
Printed in Great Britain.

0273-1223/85 $0.00 + .50

MIXING AND DETENTION TIME DISTRIBUTION IN ACTIVATED SLUDGE TANKS

H. Bode and C. F. Seyfried

Institut für Siedlungswasserwirtschaft und Abfalltechnik, Universität Hannover, Welfengarten 1, 3000 Hannover, F.R.G.

ABSTRACT

The interrelationship between mixing characteristics and tracer response curves in activated sludge tanks is explained. In some cases the return sludge cycle has a strong influence on the tracer response curves. Results from tracer tests in the field are hard to interpret because the tracer in the return sludge interferes with the initial tracer. Therefore a special evaluation procedure has to be applied. The paper closes with results from a field tracer test study.

KEYWORDS

Activated sludge process, mixing, tracer tests, detention time distribution, stagnant zones.

1. INTRODUCTION

The manner in which wastewater is introduced into the tank and the mixing characteristics of the aeration tank are important parameters in the activated sludge process. They exert considerable influence upon the concentration of residual polluting matter in the effluent (Gould, 1939) and the sludge settling properties (Chudoba, 1973; Rensink, 1974; Wheeler and Jenkins, 1983). Despite decades of intense discussion about these influences, the actual mixing process was rarely investigated. One reason for this is the difficulty of tracer test evaluation due to the circulation of return sludge. Regardless of whether the input signal was an impulse (one single addition) or a step function (continuous addition), tracer particles recirculated through the return sludge prevented definitive conclusions regarding mixing from being drawn.

By additionally observing the tracer concentrations in parallel basins or in the return sludge, the problem of evaluation caused by recirculating tracer particles can be overcome while preserving at the same time the real influence of the return sludge on the mixing pattern (Bode and Seyfried, 1984). To provide a better understanding of the results discussed in the following article, some basic comments on the mixing process in activated sludge tanks are presented first.

2. THEORETICAL TRACER RESPONSE CURVES (WITHOUT RETURN SLUDGE CYCLE)

Instead of using a statistical distribution of different detention times, one plots in tracer tests the tracer concentration at the reactor outlet as a function of time. In the theoretical border cases of plug flow, complete mixing, and mixed tanks in series (n completely mixed tanks in series) the output tracer response curves in Fig. 1 are obtained. In order to achieve a generally valid form of representation

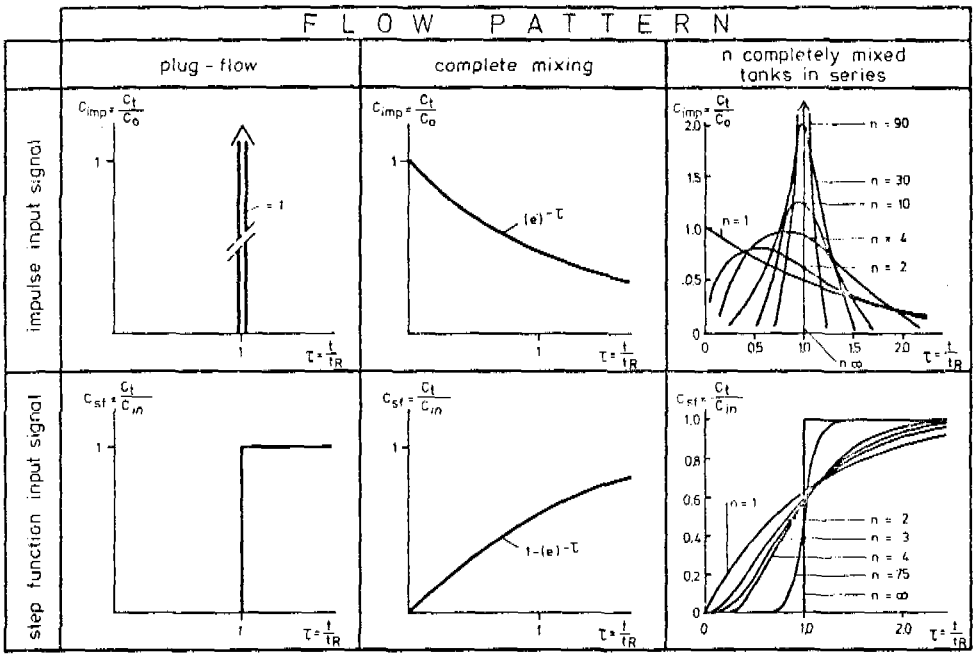

Fig. 1 Output tracer response curves resulting from step function and impulse tracer input signals for different flow patterns

suitable for comparison, effluent concentrations C_t measured at time t are set in proportion either to the calculated initial concentration C_o (in the case of impulse input signals) or to the inflow concentration C_{in} (in the case of step function input signals). The relative effluent concentrations C_{imp} and C_{sf} thus obtained are plotted against the relative detention time $\tau = t/t_R$ (Camp, 1946).

Integration of the tracer response curve produced by an impulse input signal yields a cumulative curve from which the amount of tracer that has flowed out of the system to time τ can be directly obtained. Since the amount of tracer initially in the tank is representative for an influent volume q which has entered at time $\tau = o$, Seyfried (1966, 1974) and Dahlem (1969) chose the ratio $\Delta q/q$ as the ordinate for the cumulative curve, whereby Δq is the component of q still in the tank at time τ (see Fig. 2).

Fig. 1 shows clearly that labelled particles in plug flow do not mix with the tank contents, whereas in complete mixing they are immediately and uniformly distributed over the entire tank contents. The mixing characteristics of tanks in series lie between these two theoretical border cases and approach those of plug flow with increasing tank number n.

3. INFLUENCE OF THE RETURN SLUDGE CYCLE

3.1 FUNDAMENTAL CHANGES IN TRACER RESPONSE CURVES DUE TO PARTIAL RECYCLING OF EFFLUENT (RETURN SLUDGE CYCLE)

If return sludge is fed into the flow of influent wastewater, the velocity of flow increases as given by the continuity equation; the necessary detention time decreases proportionately. This detention time, however, only encompasses one "passage" of the mixed liquor. If one wishes to determine the total time which the wastewater spends in the aeration tank, it has to be taken into account that a portion of the effluent given by $Q_{RS}/(Q_{RS} + Q)$ makes a second "passage". A steadily declining portion of the original volume makes a large number of repeated passages. Whereas the portion of the effluent that flows through the tank only once might have a shorter detention time than if there were no return sludge cycle, summated detention times for the remaining portion are considerably longer than those for no return sludge cycle. The arithmetic mean detention time t_m - relative to all particles - is not, however, altered. (This condition was not always recognized in the literature (Morscheck, H., 1971)). An alteration in the form of the tracer response curve can result, dependent upon the magnitude of the return sludge ratio RSR as well as upon the flow pattern. If one neglects the retention time of the return sludge in the secondary clarifier, the return sludge cycle has the following influence on tracer response curves:

a) PLUG FLOW

In Fig. 2 three cases of cumulative curves of tracer concentrations resulting from impulse input signal illustrate the influence of the return sludge. At time $\tau = o$ a tracer impulse is given to mark the inflowing volume q. In case 1 (RSR = o) the total volume q leaves the tank at time $\tau = 1$.

In case 2 (RSR = 1) the total marked volume reaches the outlet in half the time at t_1, due to the doubled flow $Q + Q_{RS}$ as compared to case 1. However, 50% of the effluent immediately re-enters at the head end of the tank (retention time in the secondary clarifier is neglected) and leaves the tank again at time $t_2 = 1 \cdot \tau$. This bi-

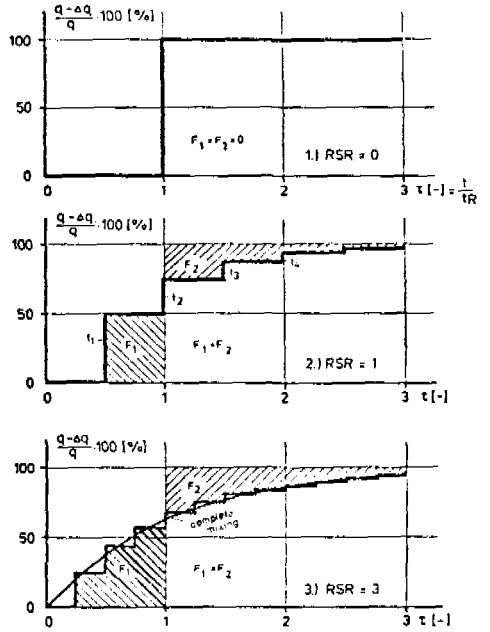

Fig. 2 The cumulative curve of the outflowing tracer at different return sludge ratios in the case of plug flow

section is repeated so that 25% of the original volume leaves the tank for a third time at t_3 = 1,5 τ, 12,5% for a fourth time at t_4, etc.

An increase in the return sludge ratio in a plug flow tank thereby effects a change in the cumulative curve of the tracer response curve. The cumulative curve steadily approaches that of complete mixing. This tendency is even more evident in case 3 where RSR = 3.

b) COMPLETE MIXING

In complete mixing, the return sludge cycle effects no change in the tracer response curve. Just as with plug flow, a component of the effluent, given by the ratio $Q_{RS}/(Q_{RS} + Q)$, immediately re-enters the tank (retention time for secondary clarification is neglected). In a completely mixed tank this component is immediately distributed throughout the entire contents. Since in this type of tank the effluent concentration is identical to that of the contents, the effluent concentration is unaffected by the re-introduction of a portion of the effluent. The completely mixed tank is thereby the only reactor type in which the return sludge cycle does not influence the output tracer response curve.

c) TANKS IN SERIES

In a series of tanks without a return cycle, the tracer response curve varies as a function of the number of tanks n (Fig. 1). Whereas in the border case, n = 1, complete mixing is present, at n = ∞ one is theoretically dealing with plug flow. Accordingly, the return sludge cycle has a varying effect on the tracer response curve and is dependent upon the number of tanks n.

The tracer response curve in a series of many tanks varies more drastically than that in a series of only a few tanks at a given return sludge ratio. This is illustrated by Fig. 3 where the response curves for series of 2 and 4 tanks without a return sludge cycle are compared with those for a return sludge ratio of RSR = 1. The difference is shaded in and is clearly greater for the 4 tanks in series.

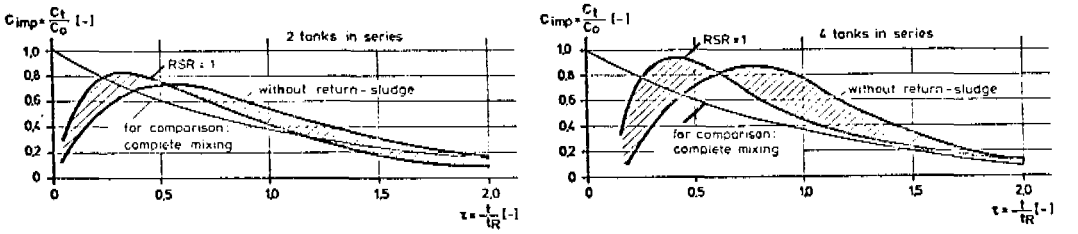

Fig. 3 Influence of the return sludge (RSR = 1) on the output traser response curves for 2 and 4 tanks in series

Fig. 4 shows the tracer response curves for a two tank series at various return sludge ratios.

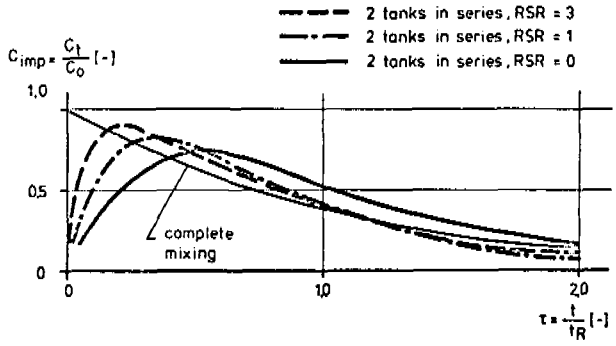

Fig. 4 Influence of the return sludge ratio on the output tracer response curve of two tanks in series

It is evident that by increasing the return sludge ratio, the tracer response curve approaches that of a completely mixed tank.

3.2 IMPAIRMENT OF FIELD MEASUREMENTS DUE TO THE RETURN SLUDGE CYCLE

In field measurements, grab samples from the effluent at a certain time after tracer addition (impulse input signal) contain tracer particles that leave the tank for the first time as well as those from the return sludge. This leads to two further alterations of the tracer response curve other than those described in 3.1. These two additional effects can be roughly described as "time delay due to secondary clarification" and "difficulty of unique correlation between tracer particles and detention time".

The "time delay due to secondary clarification" results from the lag time of the return sludge as it passes through the secondary clarifier and the pipes between the aeration basin and the clarifier. Although this lag time necessarily plays a role in the measurements of the tracer concentration in the effluent of the aeration tank, it is irrelevant for tracer response curves which are intended to describe the mixing characteristics in the aeration tank.

The "difficulty of unique correlation between tracer particles and detention time" becomes evident when one adds up the amounts of all tracer which exit the aeration tank; the sum is greater than the amount of tracer originally introduced. The recirculation of the return sludge leads to the multiple detection of a portion of the tracer. Upon leaving the aeration tank for the first time at t_1, a particular tracer particle is assigned a detention time from the tracer addition at $t_o = 0$ to t_1. The particle re-enters the tank as return sludge and exits for a second time at t_2. Neglecting the fact that the particle was temporarily outside of the aeration tank, a second detention time, $t_2 - t_1$, would be assigned. The detection system, however, is not able to distinguish the particle from others that are leaving the tank for the first time and the particle is incorrectly assigned a detention time from t_o to t_2. The resulting tracer response curve does not reflect the actual mixing processes.

The evaluation method mentioned under 5. is able to eliminate these two effects so that a relevant curve C can be constructed. The real alteration of the tracer response curve described under 3.1 remains unaffected. Due to this real alteration, the possibility of disengaging return sludge pumps during measurements, or of taking other steps which interrupt the return sludge cycle has to be excluded.

4. THE EVALUATION OF MEASURED TRACER RESPONSE CURVES

The desired uniform hydraulic utilization of a tank volume can be impaired by two

factors:

1) By short circuiting flow in which a current of the influent exits the tank very rapidly and in considerably less than the theoretical detention time.
2) By stagnation zones which are only insubstantially involved in the mixing and exchange process of the remainder of the tank.

In short circuiting flow, a portion of the influent flows relatively rapidly into the effluent independent of an otherwise perhaps perfectly normally circulated tank and thereby excludes itself from mixing with the remaining tank contents.

In the evaluation of tracer response curves resulting from measurements in the field, it is rational to compare them with the theoretical response curves for the given tank type (see Fig. 7 (under 6.)). Short circuiting flow can be recognized by the appearance shortly after tracer introduction of tracer concentrations well above the theoretical curve, sometimes fluctuating greatly over short periods.

In addition to a purely optical evaluation of the response curve, it seems desirable to express the complex information contained within the curve as a single parameter or coefficient. This has been attempted with the 50%-value, which defines the point in time at which 50% of all traced particles have left the tank (Dahlem, 1969). This figure, however, has the considerable disadvantage that it can assume identical values for different response curves.

Another figure used for this purpose is the dispersion coefficient (Tomlinson and Chambers, 1979) which, however, in no way investigates the point in time which is to be assigned to the bulk of the tracer as an average exit time but rather describes the deviation from such an average exit time with which the particles leave the tank. Instead of identifying the dispersion coefficient exlusively, it is necessary, for a thorough characterization of the tracer response curve, to incorporate the dispersion coefficient as a supplement to a separate parameter which can describe the average exit time for the bulk of the tracer. It has therefore been occasionally suggested in the literature to establish the ratio between the theoretical detention time $t_R = V/Q$ and the arithmetic mean of the detention times for all traced particles (Ambrose,et al., 1957, Müller-Neuhaus, 1952). This quantity so defined can, however, in measurements over sufficient time periods, only be less than $1 \cdot t_R$ when true dead regions are present. There is no exchange between true dead regions and the remaining tank contents. The circulated tank volume is therefore smaller than assumed. In the field this only occurs with sediments of non-exchangeable substances such as sand. If, however, even the least amount of liquid exchange takes place, then t_m and t_R must be identical within the bounds of experimental error in measurements of sufficient duration.

When in past field measurements, contrary to this finding, values for the ratio t_m/t_R were cited as significantly less than 1, this was due not to dead regions but to stagnation zones and at the same time to premature termination of sample taking. In tracer tests with impulse input signals and the presence of stagnation zones, the extremely low tracer concentrations, detectable even long after tracer addition with sufficiently sensitive measurement methods were neglected.

Despite these problems, in order to be able to make a numerical assertion regarding a measured tracer response curve, the coefficient for comparing mixing characteristics ν is introduced (Fig. 5):

$$\nu = \frac{t^*}{\tau} \; (-) \qquad (1)$$

It holds for t^* that:

$$t^* = \frac{F_1}{F} \cdot t_s + \frac{F_2}{F} \cdot t_R \qquad (2)$$

whereby (see Fig. 5):

F_1 = the amount of tracer having left the tank up to time t_R
F_2 = the amount of tracer having left the tank after time t_R
F = total amount of tracer $F = F_1 + F_2$
t_s = mean detention time for the component of tracer having left the tank up to time t_R.

As the product of the tracer concentration and flow through volume (corresponding to the respective time periods), the areas F represent amounts of tracer having left the tank.

Substitution of Eq. 2 in Eq. 1 yields:

$$\nu = \frac{F_1}{F} \cdot \frac{t_s}{t_R} + \frac{F_2}{F}$$

$$= \frac{1}{F} \left(F_1 \cdot \frac{t_s}{t_R} + F_2\right) \qquad (3)$$

To calculate the parameter t^*, the quantity of particles having left the tank to time t_R is multiplied with the corresponding mean detention time t_s. All particles having left the tank after t_R are assigned the detention time t_R, thereby neutralizing their disproportionately large influence on the mean detention time.

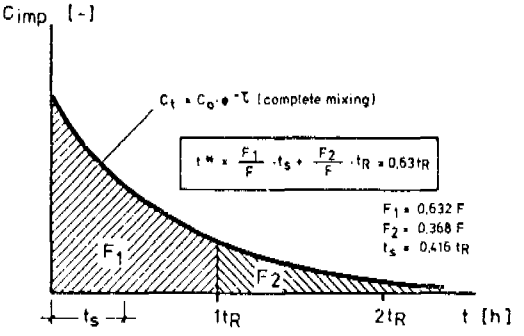

Fig. 5 Determination of t^* in the case of complete mixing

In the case of complete mixing ν becomes 0,63 (Fig. 5) and, in the case of plug flow, 1,0. Whereas values for $\nu > 1$ can neither practically nor theoretically be obtained, it is entirely possible to obtain values less than $\nu = 0{,}63$. These occur in mixing tanks in which stagnation zones are present.

5. DETERMINATION OF THE RELEVANT EFFLUENT CONCENTRATION

Methods for determining the relevant effluent concentration were developed for two different kinds of activated sludge process configurations. The first treats the case of two equally large parallel tanks connected by a common secondary clarifier, the second concerns one line operation plants. Both methods were described in detail by the authors in a previous article (Bode and Seyfried, 1984). They are based on measuring the tracer concentration in the return sludge as well as in the effluent and, in the case of parallel operating lines, also in the effluent of the untraced tank. In the evaluation process of the obtained tracer response curves, a graphical iteration has to be performed which also can be done on a computer. The evaluation results in the relevant effluent tracer response curve C^*, in which the undesired effects of the return sludge are eliminated while the real alteration due to the return sludge remains unaffected (see 3.2).

6. FIELD STUDY

With the help of the methods mentioned, results from seven investigations have been evaluated to date. Of these, the flow measurements from the activated sludge tanks of the municipal treatment plant in Herrenhausen, Hannover, should serve as an example (Bode, 1975).

TEST PARAMETERS

The Herrenhausen municipal treatment plant encompasses two 115 m long tanks (volume = 5,500 m^3 ea.), each equipped with 6 pairs of "mammut rotors" for mixing and aeration of contents. Flow direction is aided by guiding walls at the curves (Fig. 6).

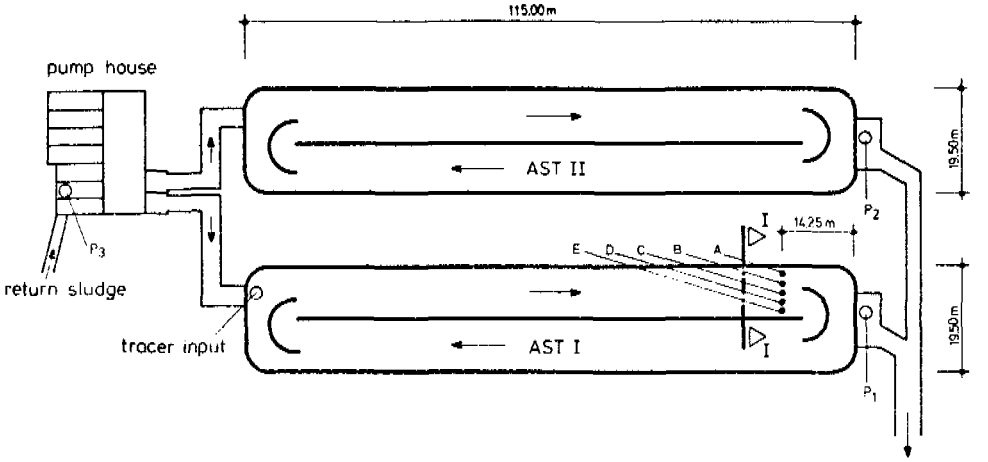

Fig. 6 The activated sludge tanks of the municipal treatment plant Hannover-Herrenhausen with the tracer input and sampling locations

The influent flow of the traced tank I averaged 4,790 m^3/h. 70 kg of lithium chloride (dissolved in 130 l water) were added in the space of 6 seconds. Samples were taken at points P_1, P_2 and P_3 (Fig. 6).

The settled sewage in Herrenhausen is advanced by 4 screw pumps into a closed collection channel, from which point it flows underground into the aeration tank. The return sludge is provided with three additional screw pumps. Due to construction technicalities it was not possible to apply the tracer to just one tank through the influent, and since one tank was to remain unmarked in order to observe the influence of the return sludge on the response curve, the tracer was not able to be applied at the common pumping pit. Therefore, tank I was marked directly by introducing the lithium chloride at the point where the mixed liquor enters the tank subsurface. Care was taken that the tracer was not applied too close to the edge of the tank in order to avoid possible stagnation zones. Since the mixed liquor is also transported in closed pipes to the secondary clarifier, samples were taken directly from the effluent weir.

RESULTS

Fig. 7 shows the corrected response curve C^* which was obtained by using additionally the lithium concentration in the second, untraced parallel tank (P_2) and by applying the first method as mentioned under 5. For purpose of comparison, the theoretical response curve for complete mixing in a tank of equal volume is also pre-

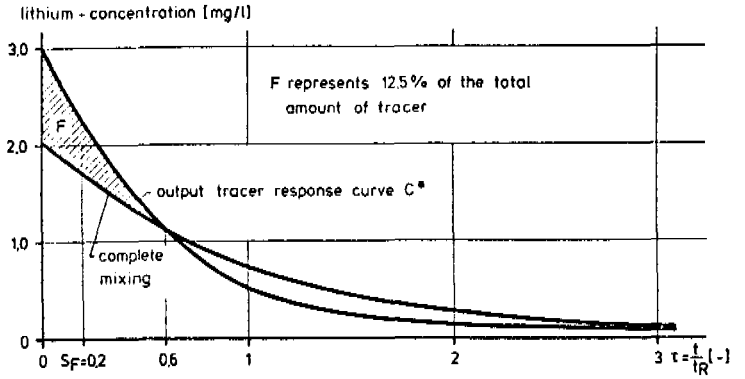

Fig. 7 Corrected output tracer response curve C^* of the tracer study in Hannover-Herrenhausen

sented.

Up to the point $\tau = 0,6$, the concentrations in C^* are greater than the theoretical values. Under complete mixing, 45% of total tracer would have left the tank to this point. In this case, an additional 12,5% of total tracer left the tank in the same amount of time. The initial effluent concentration of C^* was 2,95 mg/l, approx. 45% higher than the theoretical value. Within the theoretical detention time t_R ($\tau = 1$), 74% of the tracer left the tank (with a mean detention time of $t_{m(tR)} = 0,32\ t_R$.) In the same period of time in a completely mixed tank, 63% of the tracer would have left the tank with a mean detention time of $t_{m(tR)} = 0,42\ t_R$ (Fig. 8). These results indicate a relatively great deviation of the mixing characteristics from those of a completely mixed tank. This is supported by the coefficient $\nu = 0,50$, which lies 21% below that of complete mixing and thereby points to the presence of stagnation zones and/or short circuiting flow. Since the wastewater enters the water mass rotating in the tank from the outside and since the outlet is also on the outside of the opposite curve, a certain amount of short circuiting was suspected and consequently confirmed by tracer measurements in the cross section I-I in Fig. 6. The results of these measurements, presented in Fig. 9, represent a "snapshot" of the lithium chloride concentration in the tank cross section 4 minutes after addition of tracer. The arrow P_1 denotes the lithium chloride concentration at the tank outlet and lies in the upper region of curve (a) which represents the cross section distribution. The outflowing tracer concentration is thereby higher than the average concentration for the cross section of flow.

Figs 7 and 9 illustrate that a component of the influent, greater than that for the distribution in a completely mixed tank, appears relatively rapidly in the effluent.

For each particle that flows along the outside of the tank and reaches the outlet before its theoretical time, there is another particle lingering all the longer in the slowly interchanging stagnation zone of the inner region. This is evident from the more horizontal taper of the measured functions as compared to the theoretical functions in Figs 7 and 8. The number of particles that leave the tank only after a multiple of t_R is considerably greater than in a completely mixed tank.

The results make clear that inlet and outlet positions at the opposite curves impair a more uniform and advantageous utilization of the tank volume with respect to the purification process.

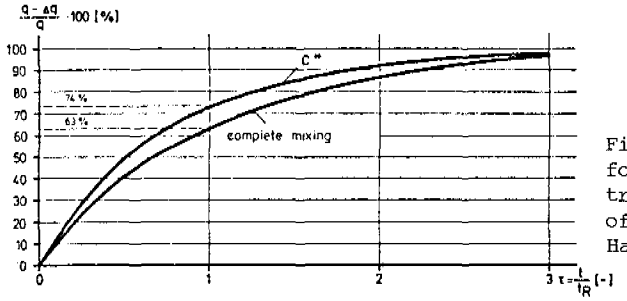

Fig. 8 Cumulative curve for the corrected output tracer response curve C^* of the tracer study in Hannover-Herrenhausen

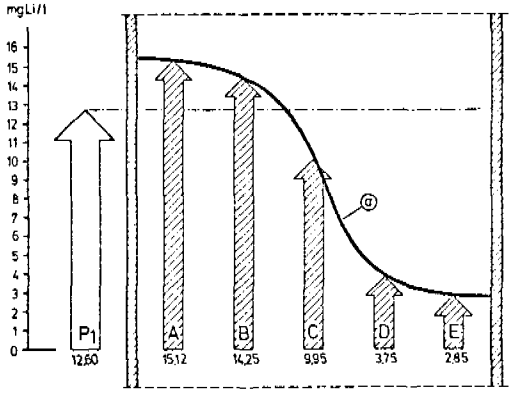

Fig. 9 Cross section I-I of the lithium concentration 4 minutes after tracer addition

7. SUMMARY

The tracer response curves for tanks in plug flow and tanks in series approach the response curves of completely mixed tanks with increasing return sludge ratios RSR.

The degree of hydraulic utilization in aeration tanks can be very precisely determined in field tests employing tracer studies. However, the return sludge cycle, which, due to its influence on mixing characteristics, should not be interrupted during measurements, impedes the acquisition of definitive results considerably; for, in addition to this influence which must be characterized, the return sludge cycle produces invalid relevant concentration distribution for the aeration tank. These invalidities are due to delay of the return sludge in the secondary clarifier on the one hand and multiple detection of tracer particles circulating in the return sludge cycle on the other. Two methods are mentioned with the help of which these invalidities can be characterized and surmounted. One method applies to the case of tanks in parallel flow with common secondary clarification, the other applies to one line operation or several independent parallel lines.

In the field, potentially existing stagnation zones in aeration tanks result in accelerated discharge of a portion of the influent as compared with stagnation-free tanks; this accelerated discharge, however, is compensated for in the mean detention time by the delayed discharge of those particles found in the stagnation zones. In contrast, dead regions result, due to the lack of any liquid interchange whatsoever with the remaining tank contents, in an actual reduction of the mean detention time t_m.

The coefficient ν can serve to characterize the tracer response curve and thereby

the mixing characteristics. ν as a nondimensional quantity yields a mean relative detention time which permits conclusions to be drawn concerning the presence of stagnation zones. The most meaningful application of ν is in comparison with its analogously derived values for the cases of complete mixing and plug flow. In this manner tank forms, aeration devices and mixing devices can be compared and improved.

The results from a field investigation of a tank with rotating flow (mammut rotor tank) demonstrate a clear difference between its tracer response curve and that for a completely mixed tank of equal size. The short circuiting flow apparent there resulted in initial effluent tracer concentrations 45% greater than theoretical value.

NOMENCLATURE

AST	activated sludge tank	(-)
C_{sf}	relative effluent concentration caused by step function input signal $C_{sf} = C_t/C_{in}$	(-)
C_{imp}	relative effluent concentration caused by impulse input signal $C_{im} = C_t/C_o$	(-)
C_t	effluent concentration at the time t	(mg/l)
C_o	theoretical effluent concentration immediately after tracer addition (in the case of complete mixing) ($\hat{=}$ tank concentration)	(mg/l)
C_{in}	inflow concentration of step function input	(mg/l)
C^*	relevant effluent concentration which is significant for the true mixing characteristics of an AST	(mg/l)
n	number of tanks (of equal size)	(-)
P_x	sampling location at x	(-)
q	traced volume of inflow	(m^3)
Δq	rest of q left in the tank	(m^3)
Q	wastewater flow	(m^3/h)
Q_{RS}	flow of return-sludge	(m^3/h)
RSR	return-sludge ratio RSR = Q_{RS}/Q	(-)
t	time	(h)
t_m	mean detention time of all tracer particles	(h)
t_R	theoretical mean detention time, $t_R = V/Q$	(h)
t_s	average detention time of all tracer particles which have left before t_R	(h)
t^*	parameter for calculation ν	(h)
V	volume of a tank	(m^3)
τ	relative detention time, $\tau = t/t_R$	(-)
ν	coefficient for comparing mixing characteristics	(-)

REFERENCES

Ambrose, H., Jr., E. R. Baumann, and E.B. Fowler (January 1957). Three Tracer Methods for Determining Detention Times in Primary Clarifiers. Sewage and Industrial Wastes, Vol. 29, No. 1.

Bode, H. (1975). Durchströmung von Belebungsbecken. Institut für Siedlungswasserwirtschaft, TU Hannover, Dimplomarbeit.

Bode, H., C.-F. Seyfried (1984). Durchströmungsmessungen an Belebungsbecken -Theorie und Praxis -. gwf-wasser/abwasser.

Camp, Th. R. (1946). Sedimentation and the Design of Settling Tanks. American Society of Civil Engineers. Transaction, Paper No. 2285.

Chudoba, J., V. Ottavâ, and V. Madera (1973). Control of activated sludge filamentous bulking. Wat. Res., 7, pp. 1163-1182.

Dahlem, H. (1969). Zur Untersuchung von Aufenthaltszeiten in Belebungsbecken. Gas- und Wasserfach, 110. Jahrgang, Heft 52, S. 1446.

Gould, R.H. (1939). Tallmans Island Works Opens for World's Fair Municipal Sanita-

tion.
Morscheck, H. (1971). Theoretische Überlegungen über die mittleren Aufenthaltszeiten im Belebungsbecken. GWF-Wasser/Abwasser, 112, Jahrgang, S. 248.
Müller-Neuhaus, G. (1952/53). Über die Kennzeichnung der hydraulischen Verhältnisse bei Klärbecken. Wasserwirtschaft 43, S. 7.
Rensink, H. (1974). De involed van het voedings-patroon op het outstaan van licht slib bij verschillende slibbebelastungen. H_2O (7), No. 22.
Seyfried, C.-F. (1966). Fertigkläranlagen für kleine Gemeinden. Kommunalwirtschaft, Heft 9, Deutscher Kommunalverlag Düsseldorf.
Seyfried, C.-F. (1974). The Treatment of Organic Effluents From Non-Food Industries. Federation of European Biochemical Societies. Industrial Aspects of Biochemistry, Ed. B. Spencer.
Tomlinson, E. J., B. Chambers (July 1979). The Effect of Longitudinal Mixing on the Settleability of Activated Sludge. TR 122, Technical Report, Water Research Centre, England.
Wheeler, M., D. Jenkins, and M. Richard (September 1983). The Use of a 'Selector' for Bulking Control at the Hamilton, Ohio, USA, Water Pollution Control Facility, IAWPRC Workshop, Vienna, Austria

Wat. Sci. Tech. Vol.17, Amsterdam, pp.209-219.
Printed in Great Britain.

0273-1223/85 $0.00 + .50

INFLUENCE OF MACROMIXING ON ORGANIC CARBON UPTAKE AND SOLIDS PRODUCTION BY AEROBIC SUSPENDED BIOMASS

S. Elmaleh, T. I. Yoon and A. Grasmick

Laboratoire de Génie Chimique Appliqué aux Biotechnologies, Université des Sciences et Techniques du Languedoc, 34060 Montpellier Cedex, France

ABSTRACT

The influence of macromixing on organic carbon uptake by aerobic suspended biomass has been investigated using two reactors operated in parallel, i.e. a perfectly mixed reactor and a compartmented reactor. Conversion determined on filtrated samples is identical in both of the reactors but with less solids production in the low-dispersed reactor. The reaction rate established on the perfectly mixed reactor shows an apparent first-order with influence of inlet concentration but this relation cannot be used in a mass balance over the compartmented reactor.

KEYWORDS

Suspended biomass ; macromixing ; kinetics ; solids production.

INTRODUCTION

If some works by early investigators have been devoted to characterization of the flow through an activated sludge aeration tank (Thomas and Mac Kee, 1944 ; Murphy and Timpany, 1967 ; Elmaleh and Ben Aim, 1975) and to liquid and even solid phase residence time distribution (Hornut et al., 1980 ; Elmaleh et al., 1982), a few only have tried to enlighten the macromixing influence on conversion.

In theoretical works, the discussion is generally based on the consideration of two extreme flow-patterns ; i.e. plug flow and perfect mixing, and the assumption of a kinetic model derived from the Monod equation or the first-order rate. The main conclusion of this approach is that pollution abatement is better in a plug-flow reactor (Vavilin and Vasilyew, 1978 ; Maxham and Maier, 1978).

On the other hand, the only few experimental works do not provide evidence of any influence of the flow-pattern on conversion and therefore conclude an apparent zero-order kinetics (Kroiss and Ruider, 1977 ; Wolfbauer et al., 1978).

There exists then some contradiction between theoretical predictions and experimental results, which might be solved by systematic and comprehensive runs on a unit where dispersion could easily be varied.

The results should help to understand the pollution uptake kinetics by suspended aerobic biomass and to answer the question : which state of mixedness is optimal ?

MATERIAL AND METHODS

1. Experimental set-up

Two aeration tanks are run in parallel ; reactor A can be compartmented in 2, 4 or 8 equal tanks in series (Fig. 1). Reactor B is a continuous stirred tank reactor (CSTR) of the same 36 liters volume. Both of the reactors are worked without recycle.

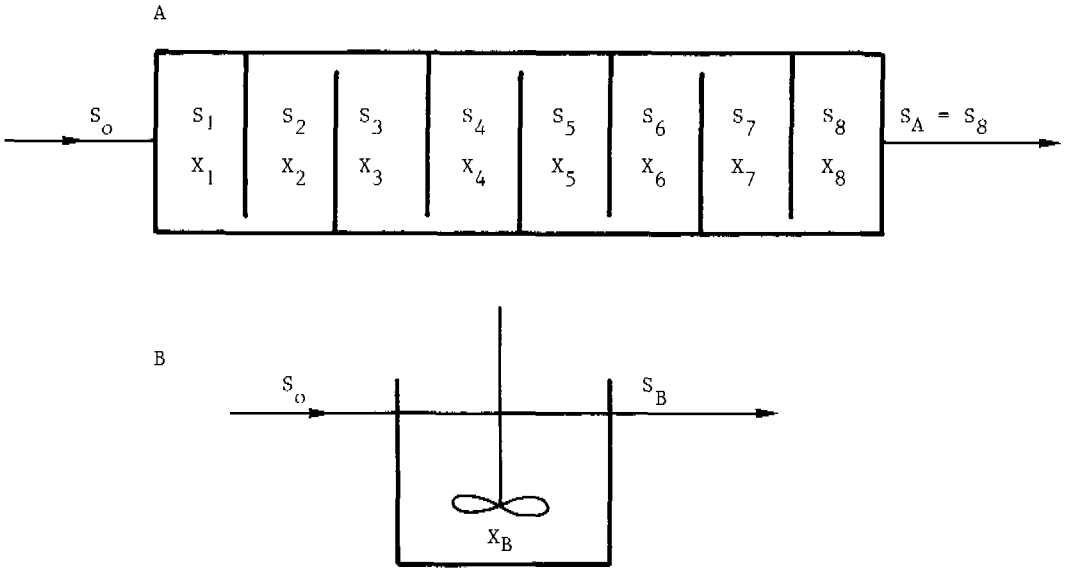

Fig. 1. Reactor A and reactor B.

2. Sewage and microorganisms

Heterogeneous microbial populations were developed from urban wastewater and fed with beef-extract diluted in tap-water.

3. Operating conditions

Reactor B and each compartment of reactor A were perfectly mixed by air-injection with a flow-rate between 4 and 6.6 N m^3/h. Uniform suspended solids concentration was checked in reactor B and each compartment of reactor A.

Liquid phase macromixing was quantified by the macromixing factor defined by Okawa and Ito (1975) :

$$M = - \int_0^\infty \tilde{E} \ \text{Log} \ \tilde{E} \ d\tilde{t} \qquad (1)$$

M decreases from 1, for perfect mixing, to $- \infty$, for plug-flow. M values were determined for each experimental space time value and reported elsewhere (Yoon et al., 1975).

4. Analytical procedure

Organic pollution was characterized by total organic carbon concentration. Measurements were made on clarified samples after 1 hour settling and on filtrated samples (0.45 µm filter).

Total solids concentration was determined by the membrane filtering technique.

RESULTS AND DISCUSSION

1. Total organic carbon conversion

The conversions in reactorsA and B, i.e. respectively $1 - S_A/S_o$ and $1 - S_B/S_o$ are compared for various space time values in Fig. 2.

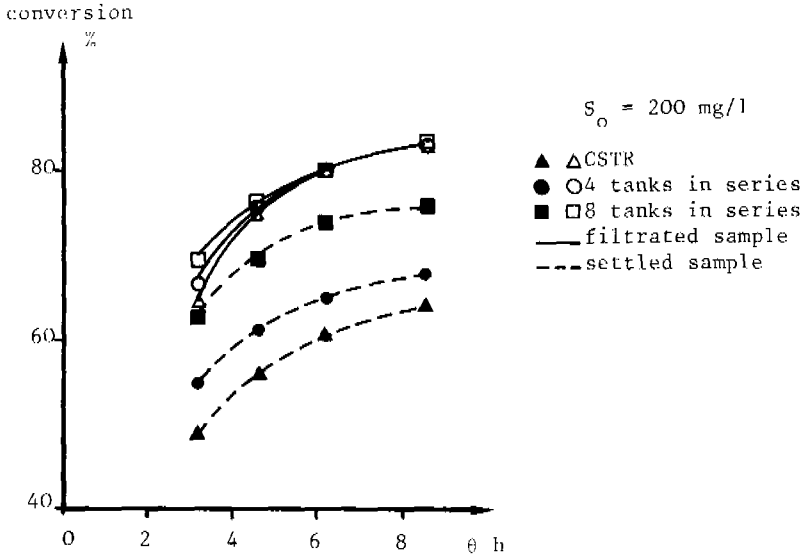

Fig. 2. Conversion in a CSTR and a compartmented reactor against space time

Let us note that :

a) the conversion measured on a filtrated sample does not depend on the liquid-phase dispersion ;

b) the conversion measured on a settled sample is better for the compartmented reactor.

Better flocculation and settleability could explain this last point. The pollution uptake should therefore be zero-order if we consider as substrate the soluble total organic carbon determined by filtration.

In the following discussion, we shall only consider total organic carbon concen-

tration measured on filtrated samples.

2. Total solids production

A solids balance on the j^{th} reactor of n equal tanks-in-series is (Fig. 1) :

$$\frac{n\,(X_j - X_{j-1})}{\theta\,X} = \frac{Y\,n\,(S_{j-1} - S_j)}{\theta\,X} - b \qquad (2)$$

According to equation (2), the plot of experimental results should lead to a straight line allowing calculation of the growth yield Y and the specific loss rate b.

If n = 1, the classical solids balance over a CSTR is obtained :

$$Y\,\frac{S_o - S_B}{\theta\,X_B} = \frac{1}{\theta} + b \qquad (3)$$

Equation (3) shows that the plot of $\frac{S_o - S_B}{X_B}$ against $\frac{1}{\theta}$ is a straight line too.

An example of the straight lines which can be drawn owing to equation (2) is provided by Fig. 3.

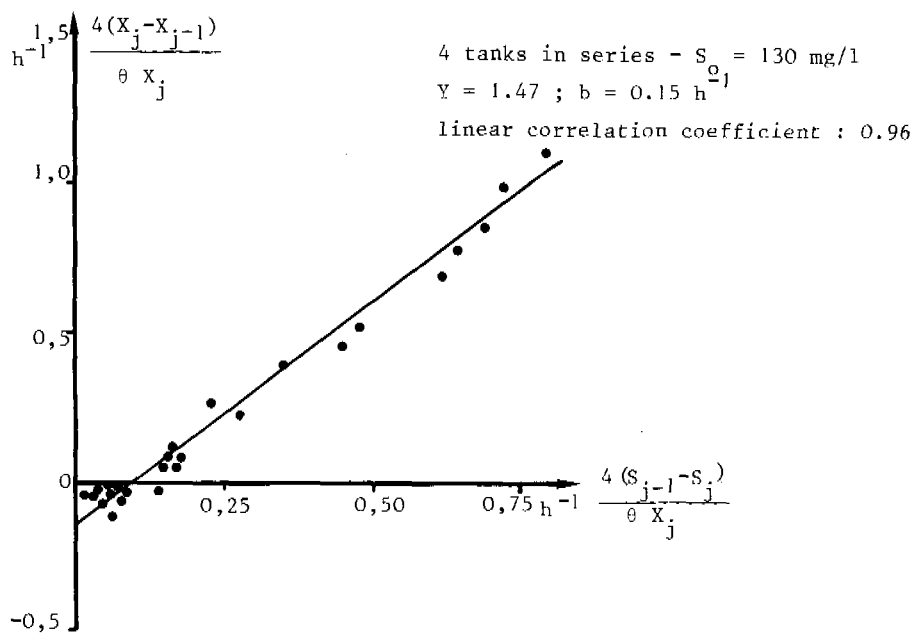

Fig. 3. Example of determination of Y and b.

The tabulation of calculated Y and b-values show that Y may be considered constant and is therefore independent of the liquid-phase dispersion (Table 1).

TABLE 1 Growth Yield and Specific Loss Rate for Various Macromixing Factor Values - S_o = 130 mg/l

Macromixing factor M	Growth yield Y kg SS/kg TOC	Specific loss rate b h^{-1}
1	1.68	0.034
0.909	1.21	0.117
0.898	1.24	0.091
0.872	1.32	0.137
0.863	1.41	0.138
0.852	1.48	0.159
0.831	1.65	0.212
0.824	1.57	0.138
0.803	1.15	0.123
0.752	1.43	0.255
0.720	1.29	0.268
0.680	1.48	0.342
0.621	1.55	0.303
	Mean Y 1.42	
	Accuracy 11 %	

Y values higher than 1 are justified by considering that Y is expressed as the ratio of the mass of total solids produced over the mass of uptaken organic carbon.

On the other hand, b is minimum for perfect mixing and increases when dispersion is decreased ; a linear function between b and the macromixing factor can be established (Fig. 4). The consequence of a higher specific loss rate is that overall sludge production is less in a low dispersed reactor. Let us now consider total solids concentration in each stage of the reactors.

We define an adimensional suspended solids concentration by $\tilde{X} = X/Y\ S_o$ where $Y\ S_o$ is the solids concentration which would be synthesized if all the inlet organic carbon flux was converted to solids. Figure 5 shows that, in perfect mixing, $\tilde{X}$ can be considered as a constant for all experimental space-time and inlet concentration values.

If $\tilde{X}$ is plotted against space time in each compartment of reactor A, a maximum is observed then followed by a rapid decrease (Fig. 5). This maximum corresponds to the second compartment. Let us note that only one curve is needed for fitting all the experimental data obtained for various inlet organic carbon concentration values and that, in any case, solids concentration is much less in the compartmented reactor than in the CSTR.

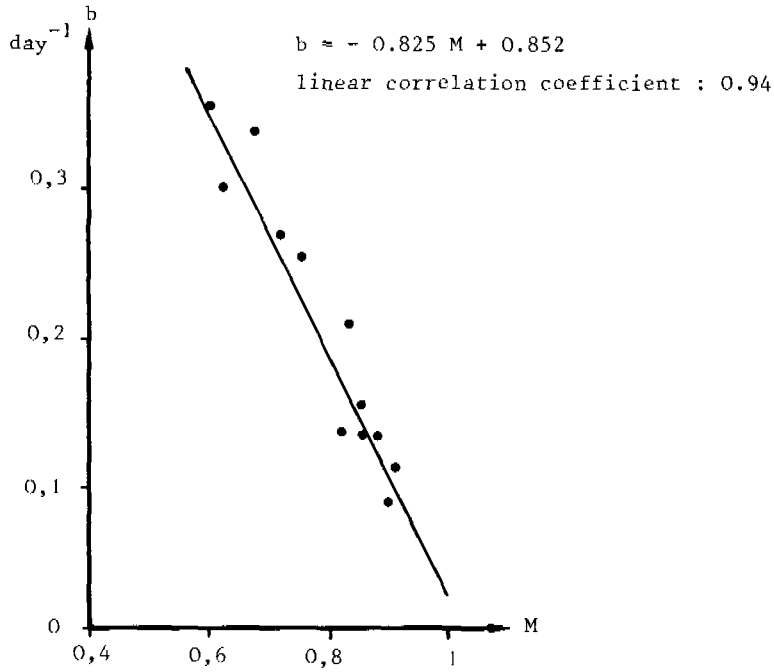

Fig. 4. Specific solids loss rate and macromixing factor

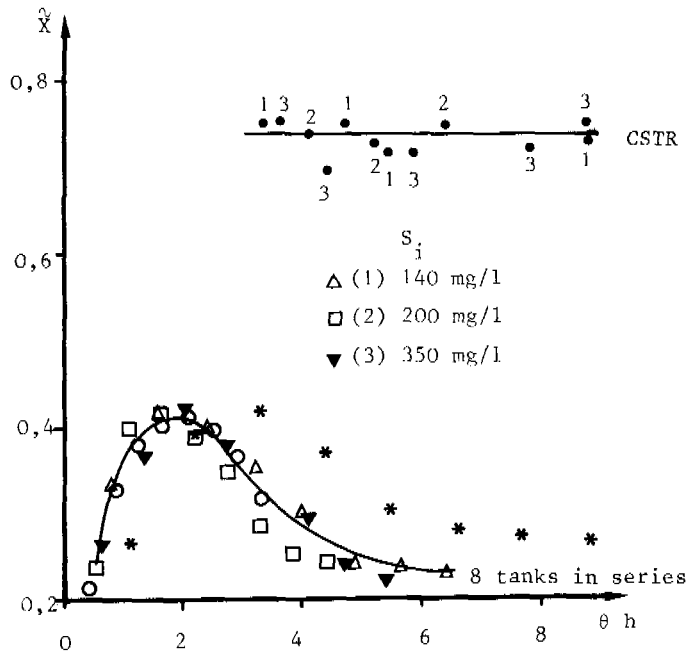

Fig. 5. Adimensional suspended solids concentration against space time

3. Conversion and loading rate

As conversion does not depend on the state of mixedness, the variation of conversion against volumetric loading rate is the same for both of the reactors. But if mass loading rate is plotted, the low-dispersed reactor is dramatically better than the CSTR because of its lower mean solids concentration (Fig. 6).

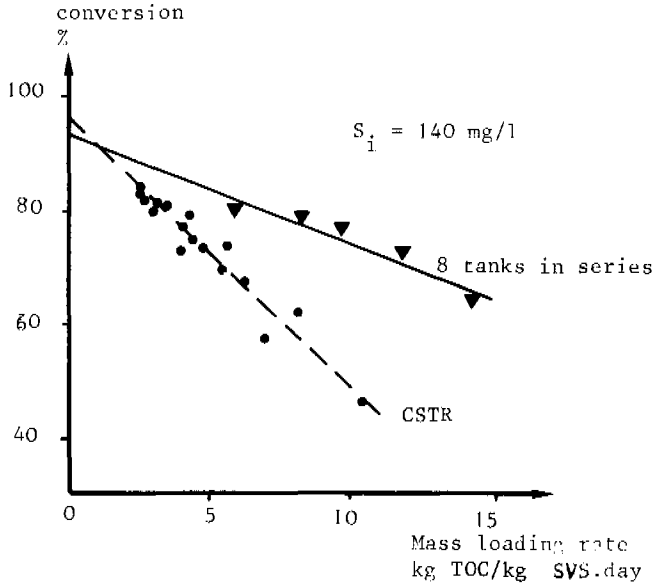

Fig. 6. Conversion against mass loading rate.

4. Organic carbon uptake kinetics

4.1. Perfect mixing

The solids balance in a steady CSTR without recycle is :

$$\mu = \frac{1}{\theta} + b \qquad (4)$$

If reaction rate is zero order, specific growth rate must be independent of substrate concentration ; in fact, μ varies strongly with inlet and outlet concentrations. As suggested by the works of Grady and Williams (1975), Grau et al. (1975) and Elmaleh and Ben Aim (1976), the specific growth rate is plotted against the ratio S_B/S_O (Fig. 7). The straight line which is obtained shows that organic carbon uptake rate is proportional to S_B/S_O :

$$r = \frac{\mu X_B}{Y} = k \frac{S_B}{S_o} X_B \qquad (5)$$

with $k = 0.54\ h^{-1}$.

This last equation can be checked on the substrate mass-balance

$$\frac{S_o - S_B}{\theta X_B} = k \frac{S_B}{S_o} \qquad (6)$$

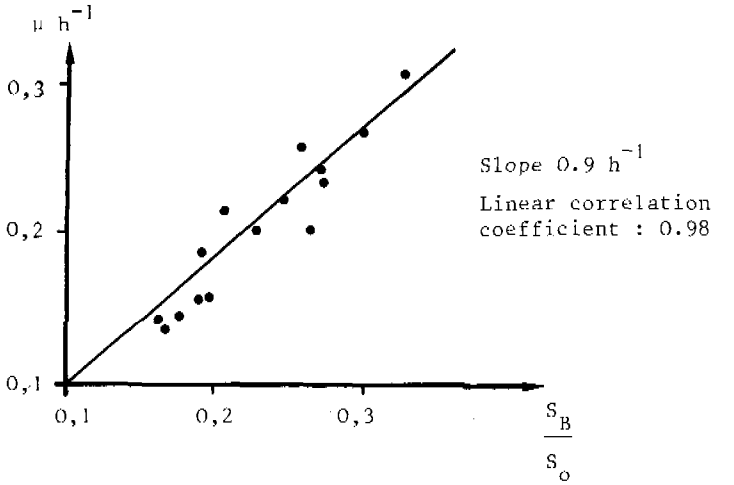

Fig. 7. Specific growth rate in a CSTR.

The plot of $(S_o - S_B)/\theta X_B$ against S_B/S_o gives also a straight line which allows a new calculation of k (Fig. 8).

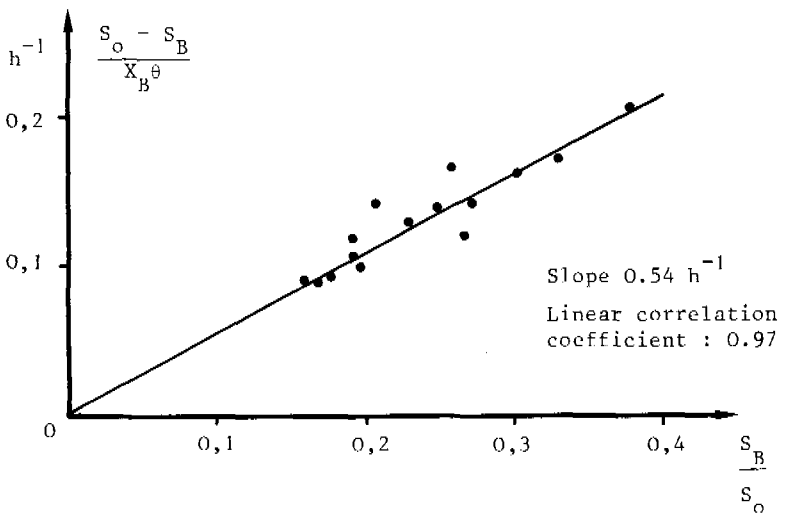

Fig. 8. Specific organic carbon uptake rate in a CSTR.

The same k-value obtained from both of the plots tends to demonstrate the consistency of the experimental data.

Let us note that, in equation (5), X_B/S_o is a constant as $\overset{\gamma}{X}_B = X_B/Y\ S_o$ and Y have been shown constant (Fig. 6). Organic carbon uptake rate can therefore be written

under the following form : $r = k'S_B$ (7)

with $k' = \frac{k X_B}{S_o} = 0{,}50\ h^{-1}$

Equation (7) shows an apparent first-order kinetics ; effluent concentration can then be calculated by an equation similar to Mac Kinney model (1962) :

$$\frac{S_o}{S_B} = 1 + k'\theta \qquad (8)$$

Therefore, reaction rate is not zero-order but it can be expressed by equation (5), i.e. $r = k \frac{S}{S_o} X$, which is apparently first-order in a CSTR.

Can this reaction rate be used in a partially mixed reactor ?

4.2. Partial mixing

If we plot $\frac{S_o - S_j}{S_j}$ against θ_j in the compartmented reactor, we obtain a straight line which is identical to the one drawn by plotting $\frac{S_o - S_B}{S_B}$ against θ for the CSTR, the slope of which being k' (Fig. 9).

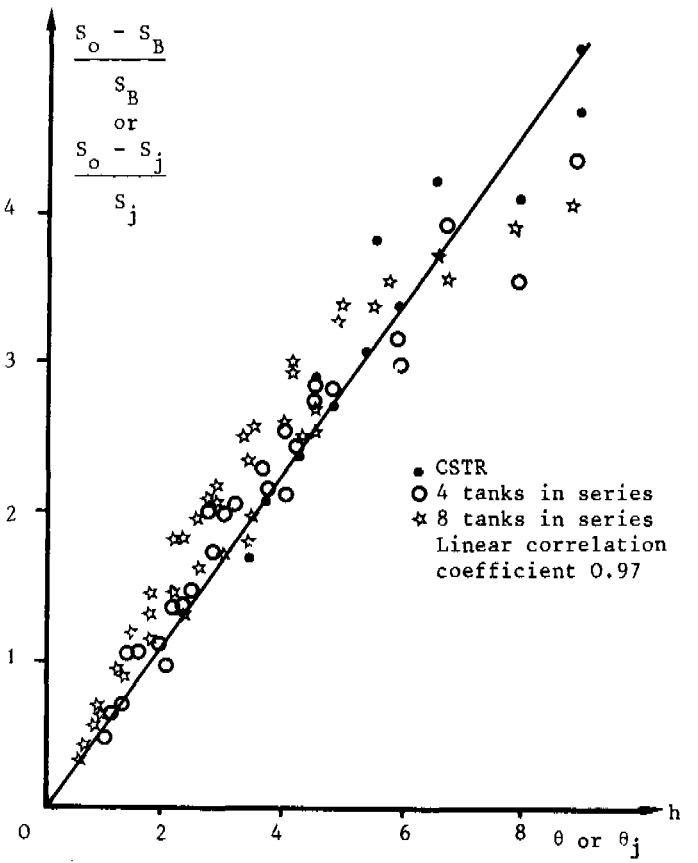

Fig. 9. $\frac{S_o - S_B}{S_B}$ and $\frac{S_o - S_j}{S_j}$ versus space time

The relations of proportionality which can be deduced lead then to the following:

$$\frac{S_o}{S_j} = 1 + \frac{j}{n} k' \quad \text{for the } j^{th} \text{ compartment} \qquad (9)$$

$$\frac{S_o}{S_A} = 1 + k' \quad \text{for the whole reactor} \qquad (10)$$

Equations (9) and (10) are formally identical to equation (8) which is relative to a CSTR with an apparent first-order rate. But the main point is that a mass balance on reactor A based on the reaction established in the CSTR, i.e. equation (5), cannot be used to calculate the conversion. These are surprising results but we must keep in mind that we are dealing with a multicomponent substrate uptaken by a polyculture and a classical approach may not be valid.

CONCLUSIONS

The conclusions create in fact new questions :

a) If a better settleability leads to higher conversion in a low dispersed reactor when settled samples are analyzed, conversion measured on filtrated samples does not depend on the state of mixedness. Is therefore the organic carbon uptake kinetics zero order ?

b) No. The kinetics established on a CSTR provides evidence that reaction rate is proportional to the ratio between outlet and inlet concentration. Can this reaction rate equation be used to calculate conversion in a compartmented reactor ?

c) The reaction rate itself cannot be used in a mass balance over a compartmented reactor. But the mass-balance over a CSTR is still valid to calculate the conversion. This last point emphasizes the care which must be taken when kinetic equations are to be extrapolated from one biological reactor to another.

d) Considering only conversion and solids production, low-dispersed reactors are more efficient than perfectly-mixed reactors and an optimum association to minimize solids production should be found out.

NOTATION

b	Specific solids loss rate	T^{-1}
E	Adimensional residence time distribution	
k	Reaction rate coefficient	T^{-1}
k'	Reaction rate coefficient	T^{-1}
M	Macromixing factor	
n	Number of tanks-in-series	
r	Reaction rate per unit volume	$ML^{-3}T^{-1}$
S	Soluble organic carbon concentration	ML^{-3}
$\tilde{t}$	Adimensional time	
X	Suspended solids concentration	ML^{-3}
Y	Growth yield	

Greek letters

μ	Specific solids growth rate	T^{-1}
θ	Space time	T

REFERENCES

Elmaleh, S., and R. Ben Aim (1975). Représentation de l'écoulement macroscopique dans un bassin d'aération par une cascade de deux mélangeurs parfaits inégaux. *Chem. Eng. J.*, 9, 107.

Elmaleh, S., and R. Ben Aim (1976). Influence sur la cinétique biochimique de la concentration en carbone organique à l'entrée d'un réacteur développant une polyculture microbienne en mélange parfait. *Water Research*, 10, 1005.

Elmaleh, S., and S. Papaconstantinou (1982). Measurement of liquid and solid residence time distribution in biological reactors. In A. Pethö and R.D. Noble (Ed.) *Residence Time Distribution Theory in Chemical Engineering*, Verlag Chemie, Weinheim, pp. 216-222.

Grady, C.P.L., and D.R. Williams (1975). Effect of influent substrate concentration on the kinetics of natural microbial populations in continuous culture. *Water Research*, 9, 171.

Grau, P., M. Dohanyos, and J. Chudoba (1975). Kinetics of multicomponent substrate removal by activated sludge. *Water Research*, 9, 637.

Hornut, J.M., S. Elmaleh, and R. Ben Aim (1980). Détermination du macromélange du liquide et des solides dans une unité à boues activées en fonctionnement normal avec recyclage. *Chem. Eng. J.*, 19 (3), 209.

Kroiss, H., and E. Ruider (1977). Comparison of the plug flow and completely mixed activated sludge process. *Prog. in Wat. Technol.*, 8, 169.

Mac Kinney, R.E. (1962). Mathematics of complete mixing activated sludge. *J. Sanit. Eng. Div.*, 88, 87.

Maxham, J.V., and W.J. Maier (1978). Effect of hydraulic regime on organic polymer uptake in the activated sludge process. *Biotech.Bioengng.*, 20, 1745.

Murphy, K.L., and P.L. Timpany (1967). Design and analysis of mixing for an aeration tank. *J. of San. Eng. Div.*, ASCE, SA5, 1.

Okawa, K., and S.Ito, (1975). A definition of quality of mixedness. *J. of Chem. Eng. of Japan*, 8, (2), 148.

Thomas, H.H., and J.E. MacKee (1944). Longitudinal mixing in aeration tanks. *Sew. Works J.*, 16, 42.

Vavilin, V.A., and V.B. Vasilyev (1978). Mathematical models of biological waste treatment processes for the design of aeration tanks. *Water Research*, 12, 491.

Yoon, T.I., S. Elmaleh, and R. Ben Aim (1979). Caractérisation du degré de macromélange dans un réacteur étage pour l'épuration biologique. *Entropie*, 15, (33), 60.

Wolfbauer, O., H. Klettner, and F. Moser (1978). Reaction Engineering models of biological wastewater treatment and the kinetics of the activated sludge process. *Chem. Eng. Sc.*, 33, (7), 953.

Wat. Sci. Tech. Vol.17, Amsterdam, pp.221-234.
Printed in Great Britain.

0273-1223/85 $0.00 + .50

AN EQUALIZATION CONTROL STRATEGY FOR ACTIVATED SLUDGE PROCESS CONTROL

P. L. Dold,* H. O. Buhr** and G. v. R. Marais***

*Dept. Chemical Engineering, Univ. of Cape Town, South Africa
**Greeley and Hansen Inc., Phoenix, Arizona, U.S.A
***Dept. Civil Engineering, Univ. of Cape Town, South Africa

Abstract

Fluctuations in hydraulic and organic loads cause wastewater treatment plant operating problems, necessitating some form of process control to ensure attainment of design objectives. A comparison of in-plant control with equalization control indicates that the latter is more appropriate for the case of long sludge age nutrient removal activated sludge processes which include anaerobic, anoxic and aerobic zones. A microprocessor-based control strategy is presented for the operation of an equalization tank upstream of the process to reduce, optimally, diurnal fluctuations in both flow and organic load rates. Results from implementation on a 150 $M\ell.d^{-1}$ plant with an in-line equalization tank (4,5 hour mean retention time) demonstrate the successful performance of the control strategy.

INTRODUCTION

Daily cyclic variations in the influent flow and load rates to wastewater treatment plants (WWTP) cause operating problems in areas such as aeration control, settling tank overloading, etc., and may result in plants not removing the concentrations of pollutants for which they were designed. Difficulties encountered in activated sludge process operation and performance due to these deviations from steady state have led to wide interest in the development and application of control procedures for treatment plant operation. Generally two philosophies towards a solution of the problem have achieved prominence; namely,

1. In-plant control, wherein no attempt is made to attenuate variations in the influent flow and load rates, and each treatment unit is controlled separately in such a manner that the cyclic inputs are accommodated optimally by varying oxygen input, feed input points, underflow recycle rate, and so on.

2. Equalization control, wherein the influent flow and organic load rates are regulated to relatively constant values upstream of the biological process, thereby simplifying and/or reducing the control requirements within the plant.

Examination of the requirements for effective control of long sludge age nutrient removal activated sludge processes, many of which are being designed and constructed in South Africa, indicates that in-plant control is not suited, as

yet, to these processes principally for two reasons:

- The complex nature of these multi-reactor processes (which include anaerobic, anoxic and aerobic zones) necessitates a complex in-plant control strategy incorporating feedforward control to account optimally for the occurrence of large disturbances and the large time constants involved. Such a strategy will rely heavily on the predictive power of a dynamic mathematical model of the process incorporating carbonaceous material removal, nitrification, denitrification and biological excess phosphorus removal. While existing models for carbonaceous material removal, nitrification and denitrification may be sufficiently accurate for purposes of feedforward control, it is doubtful whether adequate models describing the dynamics of phosphorus release and uptake exist as yet.

- A summary of the variables which should be monitored and/or manipulated in a nutrient removal process in-plant control strategy is shown in Fig 1. From the Figure it is clear that the control problem is far more complex than that for the aerobic process.* In addition, it is questionable whether available instrumentation is sufficiently reliable for application of such a complex control scheme; as yet problems in this regard are real, making this an important factor in deciding if an in-plant control system should be used. Certainly, complex in-plant control should not be considered if the technical support and infrastructure is not available to provide the necessary back-up services to maintain a range of measuring and control instruments; such back-up does not exist country-wide in South Africa, for example.

In view of the problems implicit in in-plant control, attention has been directed to equalization of flow and load as an alternative basis for control of nutrient removal processes. This paper deals with the development of a microprocessor-based control strategy for the operation of an equalization tank upstream of a biological process to reduce, optimally, fluctuations in both flow and load rates, subject to the volume constraints of the tank; results from full-scale application are presented.

PROBLEM IDENTIFICATION

Theoretically, if the diurnal influent flow and load rate variations could be reduced to yield near-constant inputs of flow and load to a WWTP, then the need for control on the plant (e.g. aeration control) would largely fall away. Yet despite such positive theoretical indications, many researchers concluded that there was little merit in equalization as a control tool. However, an analysis of the basis for these conclusions (Dold, Buhr and Marais, 1982) indicated that these were mainly the result of a lack of understanding of the kinetic behaviour of the activated sludge process. For example:

1. In many cases incorrect parameters were used to assess the effects of equalization. For example, evaluation of equalization performance often was based on effluent COD (or BOD) quality. However, because a large fraction of the influent COD is particulate material, the effluent COD is virtually insensitive to influent COD load rate variations as the particulate material is enmeshed and adsorbed by the sludge mass. Consequently, the use of this parameter as a criterion to assess the effectiveness of equalization is bound to show that little benefit is to be derived from equalization.

---

*For purposes of illustration the three-reactor UCT process configuration has been selected. Other nutrient removal processes incorporate more than three reactors and would no doubt require more complex monitoring networks for application of an in-plant control strategy.

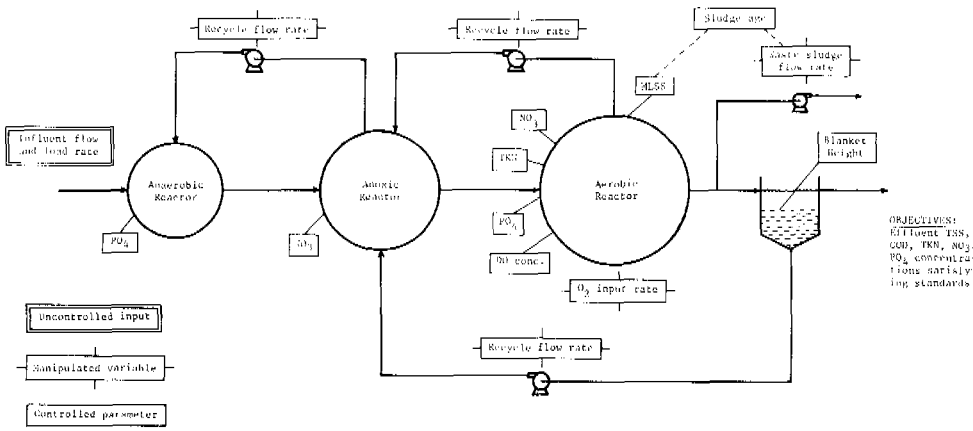

Fig 1: Controlled and manipulated variables in a biological nutrient removal activated sludge process (UCT configuration) for an in-plant control strategy.

2. Much of the work on equalization was conducted on plants operated at very short sludge ages (< 3 days). From kinetic considerations, the response of the oxygen utilization rate in this situation is largely attenuated, even where variations in the influent loading conditions are substantial. Consequently, equalization could demonstrate very little benefit in terms of simplifying the problem of aeration control. This negative conclusion on equalization would have been highly unlikely had the evaluation included plants operated at long sludge ages. At long sludge ages both theoretical predictions and plant experience show that the process responds fairly sensitively to influent load fluctuations.

3. Traditionally the objective in operating an equalization basin was to attenuate flow rate variations. Little emphasis was placed on the deliberate attentuation of load rate variations; the degree of load attenuation that automatically accompanies flow equalization was considered rather as a secondary bonus (EPA, 1974). Therefore, equalization as practised in the past does not necessarily supply an effective control tool because the degree of load equalization associated with flow equalization may not be sufficient to overcome the control problems arising from load rate fluctuations.

4. On settling tank behaviour, the literature often reports negatively on the effects of flow equalization; such reports were found to be associated with plants in which the settling tanks were considerably underloaded. However, for settling tanks loaded to full capacity equalization of the flow showed significant improvement of the effluent quality with regard to solids loss, by reducing the peak load to within the capacity of the tank. (Foess, Meenahan and Harju, 1977; Foess, Meenahan and Blough, 1977; Ongerth, 1979).

The analysis of previous equalization experience brought out one very important feature: namely, that the full benefit of flow and load equalization becomes apparent only in plants operated at long sludge ages; at short sludge ages the benefits from equalization arise essentially from flow equalization alone (e.g. simplified and/or improved settling tank behaviour).

With regard to operation of equalization facilities, very little information is supplied in the literature. The operating procedure generally is regarded as an extension of the approach to equalization design; that is, the tank is sized using the cumulative mass flow hydrograph approach (Rippl method) so that a constant

outflow rate can be withdrawn from the tank - operation involves setting the outflow rate equal to the estimated mean inflow rate each day (EPA, 1974; Speece and La Grega, 1976; Click and Mixon, 1974). Two problems inherent in this operational method were identified by Dold et al. (1982):

1. The tank is sized on the basis of providing complete flow equalization under a selected diurnal influent flow rate pattern. However, the suggested operational procedure provides no solution in the event of the amplitude of the daily input changing to the extent that it no longer is possible to withdraw a constant outflow from the tank without causing either overflow or emptying.

2. Operators experience difficulties in estimating the required outflow rate setting to avoid either overflow or emptying, i.e. there are difficulties in forecasting the mean daily inflow rate. The source of this problem is that the mean inflow (and the flow pattern) changes from day to day, and usually differs significantly between week and weekend days.

In view of the limited attention given to the operational aspects in the literature it, perhaps, could be concluded that the reservations above are unfounded. However, experience at the only equalization facility in South Africa showed problem (2) above to be a real one - it was almost usual for the tank to overflow every day, and only a partial degree of equalization was achieved (see Fig 2). It is evident that, if the equalization tank hold-up is to be used optimally, a predictive technique taking due cognizance of the variability of the influent pattern from day to day and between week and weekend needs to be incorporated in the control procedure, i.e in a control strategy.

CONTROL STRATEGY DEVELOPMENT

Operation of an equalization facility generally will be based on control of the tank outflow rate. Therefore, the essence of the equalization control problem is to determine what would be the appropriate outflow rate from the tank at any instant in time such that variations in both the flow and load rates will be optimally minimized on a continuous basis, within the volume constraints of the system. Two principal requirements of the control strategy structure are apparent:

1. Whenever a control decision is to be taken it is necessary to consider the effect of that decision as a part of the full 24-hour cycle. Because of the interrelation of the parameters flow and load, and because the influent flow and load rate patterns are not identical, no constant output value can be expected simultaneously for both parameters over the daily cycle for optimal equalization - if the flow rate remains constant at the mean value, the load rate could fluctuate quite appreciably, and vice versa. Therefore, a principal function of the strategy is to vary the tank outflow rate over the 24-hour cycle such that both flow and load will fluctuate minimally.

2. The daily cyclic influent flow and load rate patterns are not repeated identically from day to day. Therefore, to obtain near-optimal operation on a continuous basis, it is necessary to reassess control decisions (i.e. tank outflow rate setting) at short intervals (say, half-hourly), taking cognisance of the prevailing tank hold-up and inflow situation.

From the requirements (1) and (2) above it is possible to envisage the overall structure of a flow and load equalization control strategy as follows: At the start of each control interval the current status of the tank hold-up and inflow is accepted; some predictive technique is employed in forecasting the expected influent patterns for the next 24 hours; the outflow rate pattern for the 24-hour cycle to equalize the flow and load optimally is determined; and the required

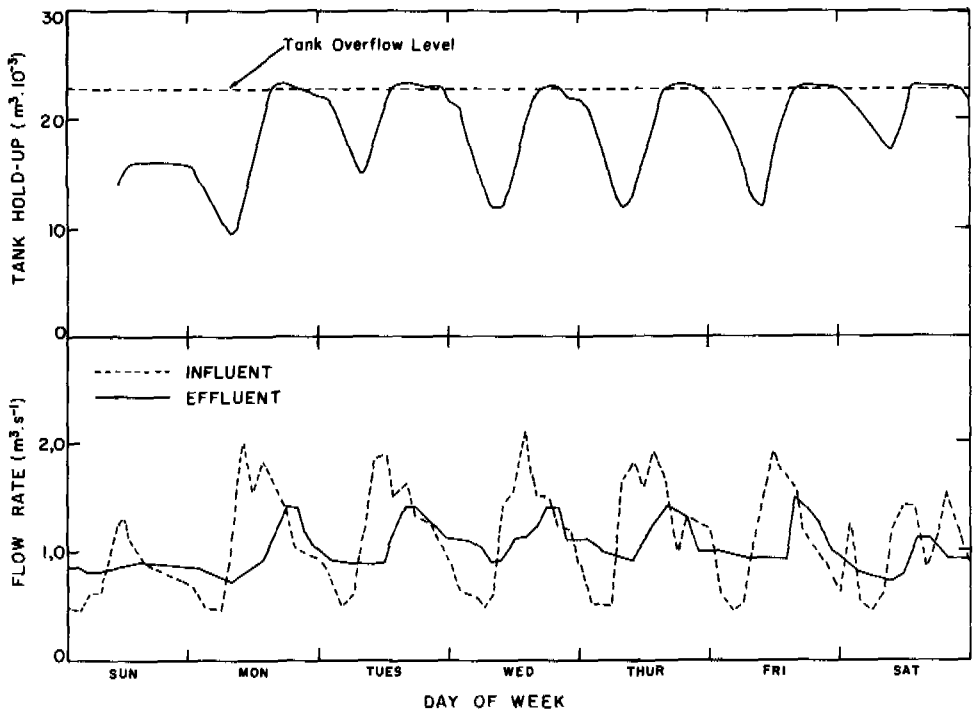

Fig 2: Performance of an in-line equalization tank (4,5 hour mean retention time) at a 150 $M\ell.d^{-1}$ plant where the outflow rate was specified manually.

outflow rate is implemented for the duration of the control interval (half-hour,say), at which time the procedure is repeated.

A primary requirement for implementing the control strategy is the development of a numerical procedure to identify the tank effluent flow and load rates which deviate the least from absolute constancy (for a given tank size under the inputs of flow and load). In developing this numerical optimization procedure it is necessary (1) to attach relative weights to the importance of flow and load equalization, and (2) initially to assume that the daily cyclic influent patterns are repeated identically from day to day.

1. Weighting factor for equalization. As the two interrelated parameters (flow and load) are independent in so far as the calculation procedure for evaluating equalization is concerned a weight must be ascribed to the relative importance of equalization of each. For example, a weight of 1 for flow (and corresponding zero for load) would express the intention to equalize the flow rate without consideration of the load, and so on.

2. Selection of fixed daily cylic influent patterns for the flow and load establishes a basis for the development of a numerical procedure to identify an optimal equalization condition. Acceptance of fixed daily input patterns implies that (1) all tank response variables (hold-up, concentration, flow rate, etc.) necessarily must be the same at the beginning and end of each 24-hour cycle, and (2) mass balance principles

must be obeyed. These conditions serve a most useful function in that, for any proposed calculation procedure to obtain optimal equalization, if the conditions (1) and (2) are satisfied the procedure at least is stable and convergent.

To establish the numerical procedure requires consideration of the situation as encountered in practice: The equalization tank hydraulic response is governed by a simple differential equation relating the change in tank hold-up, V, to the inflow and outflow rates, F_o and F_l, respectively, i.e.

$$dV/dt = F_o - F_l \tag{1}$$

In this equation the influent flow rate, F_o, is, in the terminology of control systems, a "load variable", i.e. an uncontrolled variable which is set by external factors and whose variation must be accommodated by the control system. Of the other two variables, F_l and V, one may be freely manipulated, whereupon the behaviour of the second will be fixed by Eq (1). Therefore, in the numerical procedure to identify an optimal solution for a 24-hour cycle, it is necessary to decide on whether one should either:

1. Determine the tank hold-up profile, V, under the cyclic inputs which results in optimal flow and load equalization, and from this determine the outflow rate profile, F_l, to be applied by the control strategy;
   or
2. Determine the outflow rate profile, F_l, which results in optimal flow and load equalization, and from this determine the hold-up profile, V, associated with F_o and F_l.

In both cases a constraint on the tank hold-up is operative in that the tank must neither empty nor overflow during the cycle. After a thorough investigation the second approach was found to be superior: by maintaining a "smooth" outflow rate profile, the tank acts as a buffer to rapid random variations exhibited by the input pattern in practice. In contrast, by imposing a "smooth" hold-up profile, sharp fluctuations in the influent pattern (about the trend pattern) are transmitted to the downstream process, thereby nullifying, to a degree, the objective of equalization.

Development of a calculation procedure (using the outflow rate profile development approach) that will always advance to the optimal solution (i.e. development of an equalization algorithm) required formulation of an objective function to give an assessment, numerically, of the equalization efficiency: Accepting that the effluent flow and load rates will deviate from the mean over the daily cycle, it is necessary to quantify the combined deviation. This can be accomplished by including two terms in the objective function (error expression) - one for the flow deviation, E_f, and one for the load variation, E_{ld}. By selecting a weighting factor, α, the two components can be summed to provide a measure of the equalization error, E_e, which takes into account the relative importance ascribed to each equalization aspect:

$$E_e = \alpha E_f + (1-\alpha)E_{ld} \tag{2}$$

where $0 \leq \alpha \leq 1$.

Formulation of the components E_f and E_{ld} is subjective. By trial it was found that successful results were obtained if each is calculated on the basis of the squares of the deviations from the respective mean values ($\bar{F}$ and $\bar{L}$), integrated over the 24-hour cycle, i.e.

$$E_f = \int_o^{24} (F/\bar{F} - 1)^2 dt \tag{3}$$

$$E_{ld} = \int_0^{24} (L/\bar{L} - 1)^2 dt \qquad (4)$$

The procedure to determine the optimum outflow rate profile from an equalization tank of a specified size, under known 24-hour inputs of flow and load rate, operates as follows:

(1) Initially an arbitrary outflow rate profile is selected. To maintain consistency with the approach adopted for the control strategy, the profile is divided into a number of adjustment intervals corresponding to the number of control intervals in a 24-hour cycle.

(2) The outflow rate profile, together with the inflow profile, is used to calculate the tank hold-up (volume) response over the cycle. This hold-up profile, together with the influent flow rate and concentration profiles, enable the calculation of the effluent concentration profile and, in turn, the effluent load rate profile. The selected outflow rate profile and the associated effluent load rate profile then can be used to compute a measure of the equalization efficiency from Eq 2.

(3) To determine the optimum outflow rate profile, an iterative procedure is followed whereby the effect of incremental changes in outflow rate at the different adjustment intervals is assessed by each time calculating the associated effluent load profile and the value of the equalization error, E_e. Changes to the profile which result in a decreased E_e value during the procedure are "accepted" until a change in flow rate (increase or decrease) at any of the adjustment intervals no longer improves the equalization efficiency. The final profile is then accepted as the optimum. Two different optimization techniques were used to check that this approach did, in fact, identify the optimal condition.

A necessary condition for the optimum outflow profile is that, under the influent pattern, the associated tank hold-up profile at no point exceeds the physical volumetric limits of the equalization tank, i.e. there is no overflow and/or emptying. It was found that this physical constraint could be incorporated as an integral part of the optimization procedure by adding a penalty error, E_{lm}, to the equalization error, E_e, which increases rapidly when the tank hold-up limits are exceeded, and then using the sum of E_e and E_{lm} as the objective function. In this way changes to the outflow profile which cause the hold-up limits to be exceeded at some point in the cycle will be strongly resisted because, even though the E_e component might decrease, the accompanying increase in E_{lm} will outweigh the decrease. To attain stability in this mechanism it is necessary to select an appropriate weighting factor, β, for the penalty error value, E_{lm}, so that the penalty error component in the objective function is negligible compared to the equalization component if the hold-up limits are not exceeded; the inclusion of a weighting factor is merely a consequence of the units used in the calculation of the penalty error, E_{lm}.

An advantage of the volumetric penalty error approach is that the penalty error can be formulated to allow specification of upper and lower tank hold-up limits within the physical extreme values. This is useful for the analysis of situations where, for example, the tank hold-up may not drop below a specified level for some reason.

Application of the optimization procedure using the combined equalization error and the volumetric limit penalty error still gave rise to certain problems: with small equalization tanks (< 3 hours mean retention time), "spikiness" could develop in the outflow rate profile. One method of accounting for this problem would have been simply to specify a maximum allowable rate of change of outflow

rate in the development of the optimum profile. However, to maintain consistency in the mathematical procedure, a second penalty error, E_s, was included in the objective function to constrain the rate of change of tank outflow rate; this ensures the development of a smooth profile. Large values of E_s in the objective function, while ensuring the development of a smooth outflow rate profile, will favour flow equalization, and will tend to mask the effect of the equalization error weighting factor, α (see Eq 2). To prevent this situation again it is necessary to include a weighting factor, ω, for the penalty error, E_s, to maintain an appropriate balance between the magnitudes of the different components of the objective function.

To summarize, the objective function (or error expression) which was found to result in acceptable behaviour of the equalization algorithm was made up of three components, one of which (E_e) consisted of two parts, i.e.

$$E_t = f(E_e, E_{lm}, E_s)$$

$$= \alpha E_f + (1-\alpha)E_{ld} + \beta E_{lm} + \omega E_s \qquad (5)$$

Application of the Equalization Algorithm

Dold et al. (1982) applied the equalization algorithm to determine optimal performance of a range of equalization facilities under a range of invariant cyclic input patterns i.e. where the 24-hour influent patterns are repeated identically from day to day. These results provide a useful means for evaluating the effects of various parameters on equalization performance. The principal conclusions of this analysis, which included a comparison of in-line and side-line equalization configurations, were:

1. For both in-line and side-line equalization, the efficiency of equalization increases with increasing tank size; however, the rate of improvement decreases with increasing size. Optimal equalization generally requires a tank with a mean retention time (based on the mean inflow rate) in the region of 4 to 6 hours. Very little is gained in equalization efficiency for retention times greater than 6 hours.

2. Almost identical curves of equalization efficiency versus retention time are obtained for influent data collected at different full-scale treatment plants, even though the influent flow and load rate patterns may differ substantially between plants.

3. An important characteristic exhibited by the controlled (effluent) load rate is that, whereas the load rate in the uncontrolled (influent) cycle may fluctuate between a quarter and two to three times the mean (with consequential low and high oxygen demands in the downstream process), the controlled load is virtually constant, with a small drop once every 24 hours. This phenomenon will have a marked effect on aeration control, and will also substantially reduce the cost of providing aeration capacity to meet the peak requirement. The behaviour is illustrated in Fig 3, which is an example of equalization algorithm application.

4. The behaviour of the algorithm over the region where there is a drop in effluent load rate (see 3 above and Fig 3) highlights the superiority of the optimization approach over the subjective response action likely if the control decisions were by human agency. When the tank hold-up approaches its lower limit the algorithm causes the outflow rate to increase, thereby increasing the rate at which the already low tank level is dropping - an action unlikely to be duplicated in manual control. The necessity for this, however, is evident from the objective (to equalize both flow and load): over this period the tank outflow rate is increased slightly to sustain the

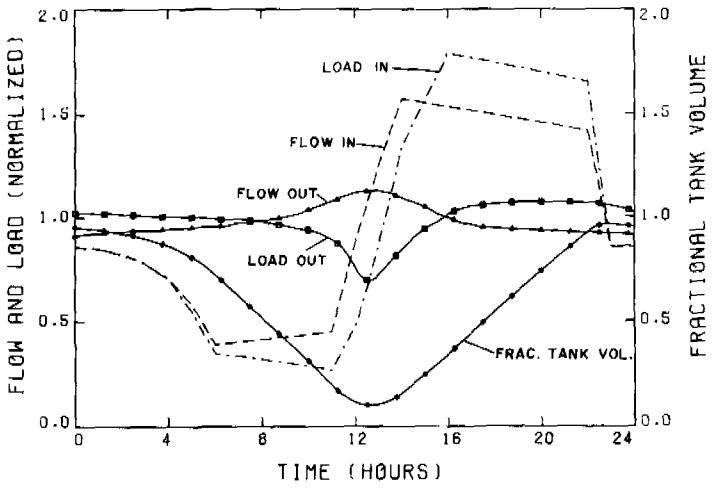

Fig 3: Equalized flow and load rate patterns obtained from application of the equalization algorithm (Mean tank retention time of 5,5 hours).

decreasing load rate.

5. With regard to equalization tank volume requirements, comparison of side-line and in-line equalization indicates that, in the region where effective equalization is achieved, both schemes require the same size equalization tank, i.e. neither scheme results in a decreased volume requirement over the other.

6. With side-line equalization as much as 60 percent of the daily inflow may bypass the equalization tank without reducing the equalization efficiency. This may allow a substantial saving in pumping costs where gravity flow through the tank is not possible. However, the disadvantage with side-line equalization is that the tank no longer acts as a buffer to all of the rapid fluctuations in the influent stream because part of the inflow bypasses the tank. Therefore, where possible in-line equalization should be used in preference to the side-line configuration.

Formulation of the equalization algorithm constituted the first phase in the development of the equalization control strategy. Once this aspect had been completed the next step was incorporation of the equalization algorithm in the control strategy structure outlined prior to development of the control algorithm itself.

Control Strategy

In control strategy operation the equalization algorithm is applied at regular short intervals to determine the optimal outflow rate profile for an ensuing 24-hour cycle under the expected 24-hour input patterns. The actual tank outflow rate for the duration of the short (say, half-hour) control interval is set equal to the value at the start of the calculated optimum profile for the ensuing 24-hour cycle. By re-optimizing operation at regular short intervals to account for the variability of the influent patterns under real-time conditions, near-optimal operation on a continuous basis should be attained.

Successful operation of the control strategy obviously depends to a large degree on the ability to make accurate predictions, at the start of any control interval,

of the expected influent flow and load rate patterns for the ensuing 24-hour cycle. Because the daily input patterns are repeated with relatively small variations from day to day, it was decided that the expected influent patterns should be based on the historical average influent patterns. It was found that, if the influent patterns were very similar from day to day, and if the patterns were close to the mean historical influent patterns, then the control strategy operated very successfully i.e. the daily outputs were very close to the optimal ones obtained under invariant daily inputs. However, when the daily inflow patterns differed substantially from the mean historical patterns, difficulties were encountered, particularly over those part of the cycle when the tank was either near-full or near-empty. This problem was overcome by basing the prediction primarily on the historical inflow and concentration data, but incorporating an adjustment to the inflow data based on differences between actual and historical inflow rates immediately prior to the prediction of the influent profiles for the ensuing 24-hour cycle.

A second problem encountered in the prediction of the expected 24-hour influent patterns based on the historical average patterns was that changes to the influent patterns (as a result of, for example, changes in the sewer collection network) may cause the historical data stored in the microcomputer memory no longer to conform to the daily inputs. To overcome this problem, a mechanism for continuous updating* of the historical inflow rate data was incorporated in the strategy as follows:

> By monitoring the change in tank level over a control interval, and knowing the tank outflow rate, it is possible to compute the inflow rate, and in turn update the historical data stored in the microcomputer memory. In this way, a running average of historical data is maintained; this approach also allows the effect of gradual seasonal changes in flow rate to be automatically incorporated in the operation.

Yet another problem in the prediction of expected 24-hour influent patterns was that the influent patterns differ substantially between weekday and weekend, as illustrated in Figs 2 and 5. An analysis of data for several treatment plants showed that the influent patterns for weekdays and weekend days differ sharply in (1) the form of the flow and load rate patterns and (2) a reduction in the mean daily flow and load rates for the weekends compared to weekdays. This problem was resolved by distinguishing between two types of historical daily inputs - one for weekdays and one for weekend days (and holidays). With this approach application of the control strategy showed that the strategy very effectively evens out the sharp disparity in flow and load rates in the transition from week to weekend, and vice versa. That is, the strategy allows the effect of the change to be spread over an extended period without necessitating any sudden control action.

Accepting that the expected influent profiles for an ensuing 24-hour cycle could be determined, application of the algorithm under real-time conditions (i.e. in the control strategy) nevertheless differs slightly from the application under invariant daily inputs - it became evident that the constraint on maintaining a material balance over a 24-hour cycle must not be imposed when the algorithm is applied under real-time conditons:

> The objective in applying the equalization algorithm, for both invariant daily inputs or for real-time conditions, is to determine the 24-hour outflow rate profile which results in the maximum attenuation of influent flow and load variations; that is, the objective is to maintain the outputs as close as possible to the respective mean values of the expected 24-hour input

*Updating of historical influent concentration data is discussed later.

patterns. In the analysis under invariant inputs, where the daily cyclic influent patterns are repeated identically from day to day, it was necessary to follow mass balance principles over a 24-hour cycle because the daily outflow necessarily equals the daily inflow, and the tank situation (hold-up, concentration, outflow rate, etc) must be identical at the start and end of each 24-hour cycle. Under real-time conditions, in view of the variability of the influent patterns, it is unlikely that the tank situation (hold-up, etc) corresponds identically to the optimal one indicated by the historical influent data at the time that the equalization algorithm is applied - in fact, if, say, a rainstorm has occurred then it is possible that the tank situation is very different from the optimum. Effective long-term operation of the strategy hinges on the expectation that the influent patterns in general will correspond relatively closely to the historical data. Therefore, even if the tank situation is non-optimal when the algorithm is utilized, the action of the strategy should be to endeavour to return the situation to optimality in future cycles (observing the volumetric limits and constraint on rate of change of outflow rate, of course). In order to achieve this action it is necessary to drop the requirement of maintaining a material balance over 24-hour cycles during application of the algorithm; in this way, by allowing either more or less than the daily inflow to leave the tank over 24-hours it would be possible to converge to the optimal condition in future cycles.

Once the mass balance constraint had been dropped it was necessary to ensure that the control strategy would still lead to optimal operation. To this end the strategy was tested, assuming that the actual inputs corresponded exactly to the historical data, but with the starting condition different from the optimal one. It was found that, after one or two cycles, the operation returned to optimality - even though a mass balance was not imposed; once the behaviour had stabilized the daily outflow equalled the inflow and the tank situation was identical at corresponding times in subsequent daily cycles.

Testing the Control Strategy

To test the control strategy a series of simulations (using input data measured at full-scale treatment plants) was devised to check whether or not the conclusions obtained using the algorithm under invariant daily cyclic inputs still hold for the real-time situation. An example of simulated control strategy operation is shown in Fig 4. The results of these simulations indicated that:

- In all cases the conclusions (with regard to tank size, configuration, etc.) obtained under fixed diurnal input patterns also hold under real-time inputs.

- There is only a marginal decrease in performance efficiency with the real-time daily inputs compared to the invariant inputs.

An additional phase of evaluation of the control strategy involved testing the behaviour under unusual input patterns (e.g. storm conditions where there is ingress of stormwater into the sewers) or where aspects of equalization facility design impose constraints on operation (e.g. where floating mixers are used to mix the tank contents and a minimum operating depth is obligatory). The purpose here was to illustrate that, under certain circumstances, situations may arise where emergency action must supersede the action of the control strategy. Dold et al. (1982) have detailed how such instances are incorporated in the control strategy.

CONTROL STRATEGY IMPLEMENTATION

For the implementation of flow equalization the only requirements needed to operate the microcomputer control strategy are the facilities to:

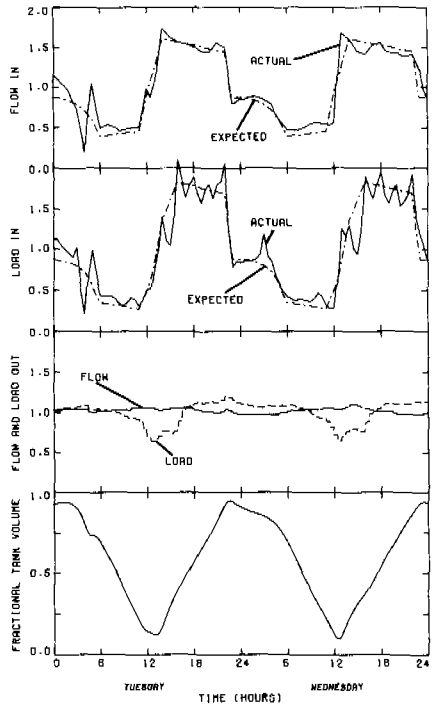

Fig 4: Example of simulated control strategy operation over a two-day period (Mean tank retention time of 5 hours).

- measure liquid level in the tank
- measure tank outflow rate
- specify the setpoint for the outflow rate controller.

These measurements can all be obtained with very reliable, and simple, instrumentation which is stable in the long term - an important aspect in the South African context, to minimize back-up needs.

For implementation of simultaneous flow and load equalization it would appear that continuous monitoring of, say, influent COD concentration also would be required. This would pose a problem because instrumentation required to monitor COD on a continuous basis, and the operation thereof, is both complex and costly - this would nullify, to a degree, the objective of developing an inexpensive and simple alternative to in-plant control. However, continuous monitoring of COD was not found to be necessary; it is sufficient to check the historical COD data stored in the microcomputer memory at intervals of, say, 3 to 4 months. This is so because simulation studies indicated that the system response is relatively insensitive to deviations in actual influent concentration from the historical data for the magnitude of deviation normally encountered. The reason for this insensitivity arises from the fact that the load rate is the product of flow rate and concentration; because the flow rate is accurately accounted for continuously, deviations in concentration affect the load rate only in part. Indeed, the added efficiency in load equalization obtained by continuous COD monitoring is most unlikely to merit the cost of implementation.

The control strategy was implemented at full scale on the 150 $M\ell.d^{-1}$ Goudkoppies WWTP, Johannesburg, which operates as an in-line equalization tank with a mean retention time of approximately 4,5 hours. The tank receives the primary clarifier overflow and is not mixed so that it was not possible to apply the CSTR equations for COD concentration (and load) with any expectation of accuracy. Consequently, in this instance, only the flow equalization aspect of the control strategy was implemented (i.e. $\alpha = 1$ in Eq 2).

On start-up the control strategy behaved exactly according to specification; initially the tank outflow rate was not as constant as would be expected with a tank of this size, but this was due to differences between the roughly estimated historical inflow rate data and the actual influent patterns. However, within a few days the initial historical inflow profiles had been updated to reflect the actual influent patterns more accurately and the control strategy operated with remarkable effectiveness as shown in Fig 5:

1. During the mid-week period the tank outflow rate was maintained very near constant.

2. The strategy handled the transition from week to weekend, and vice versa, in the expected manner by spreading the effect of the step change in daily inflow rate over an extended period.

3. The control strategy removed a considerable work load from the plant operators.

4. The level of equalization efficiency was incomparably higher than that attained when the outflow rate was specified manually, as illustrated by comparing Figs 2 and 5.

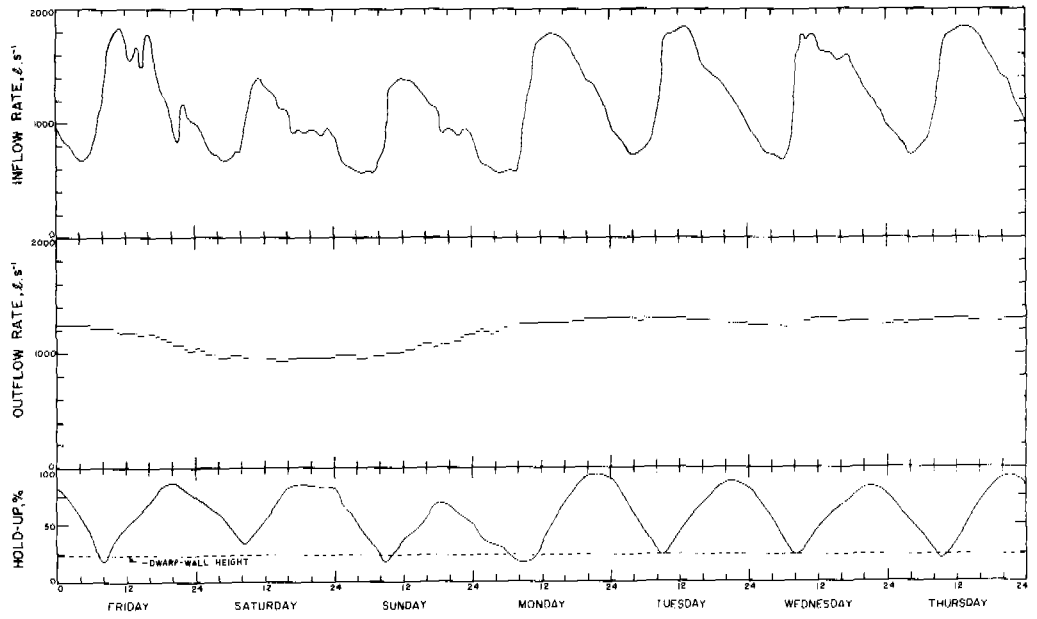

Fig 5: Response behaviour of the Goudkoppies WWTP equalization tank over a period of one week under control strategy operation.

In the case of the implementation at Goudkoppies initial indications are that, even though the tank is un-mixed, the degree of load equalization achieved perhaps exceeds that expected for a completely mixed tank; in particular, when the tank level is low, the drop in load rate does not appear to be as great as that encountered in simulations for a completely mixed tank. It can be surmised, perhaps, that the load rate is partially sustained over this period by solids being flushed out, having settled on the tank base during the remainder of the cycle. This behaviour is possibly specific to the Goudkoppies installation - the tank contains a set of dwarf-walls laid out in such a way that, when the tank level is low, flow is canalized in series fashion and settled solids are scoured from the tank as a result of the increased linear flow velocity along the tank floor. Because of this feature it would be inappropriate to draw any general conclusions as yet on the merits of using an un-mixed tank; however, it would seem that an unmixed tank receiving settled sewage, if designed to scour any particulate material that settles each day (by incorporating dwarf walls), may have considerable practical and economic advantages.

CLOSURE

From both theoretical and experimental points of view the control strategy presented here gives rise to very satisfactory performance of equalization tanks. The success achieved is likely to lead to added interest in equalization, particularly for nutrient removal plants (operated at long sludge ages) - installation of high performance equalization tanks obviates most of the difficulties encountered in the application of in-plant control procedures.

ACKNOWLEDGEMENT

This research was carried out under contract with the Water Research Commission of South Africa. The authors wish to thank the Commission for permission to publish this paper. Gratitude is also expressed to the staff of the City of Johannesburg who assisted in the implementation at the Goudkoppies WWTP.

REFERENCES

Click C N and F O Mixon (1974). Flow Smoothing in Sanitary Sewers, J Water Pollut Cont Fed, 46, No 3, 522-531.

Dold P L, H O Buhr and G v R Marais (1982). Design and control of equalization tanks. Research Report W 42, Dept Civ Eng, Univ of Cape Town.

Environmental Protection Agency (1974). Flow Equalization, Technology Transfer Seminar Publication, Cincinnati, Ohio.

Foess G W, J G Meenahan and D Blough (1977). Evaluation of in-line and side-line flow equalization systems, J Water Pollut Cont Fed, 49, No 1, 120-130.

Foess G W, J G Meenahan and J M Harju (1977). Flow equalization is on the level, Water and Wastes Eng, 96-109.

Ongerth J E (1979). Evaluation of Flow Equalization in Municipal Wastewater Treatment. Report prepared for U S EPA, Cincinnati, Ohio.

Speece R E and M D La Grega (1976). Flow equalization by use of aeration tank volume. J Water Pollut Cont Fed, 48, No 11, 2599-2608.

Wat. Sci. Tech. Vol.17, Amsterdam, pp.235-246.
Printed in Great Britain.

0273-1223/85 $0.00 + .50

THE A-B PROCESS: A NOVEL TWO STAGE WASTEWATER TREATMENT SYSTEM

A. I. Versprille, B. Zuurveen and Th. Stein.

ESMIL International B.V., P.O. Box 7811, 1008 AA Amsterdam, The Netherlands

ABSTRACT

New acts on wastewater disposal demand for higher process stability and effluent quality.
The A-B process, a novel two step treatment system, meets these requirements in a cost effective way.
Five full-scale plants have been put in operation over the last two years.
The objective of this paper is to give an outline of the features of the A-B system in the context of the results of these full-scale plants.
In spite of the extreme high load, the A-stage can be operated at a high reduction rate and is stable. Variations in the organic load and pH- and toxic shocks are leveled out and a constant, mainly soluble effluent is supplied. This implicates a low sludge production in the B-stage. As a consequence higher overall reduction rates are obtained as compared to conventional processes at the same sludge load. Very low and stable final effluent concentrations are observed in all full-scale plants.

Of special interest are the possibilities of upgrading existing conventional treatment facilities, at minor costs, by incorporating the A-B technology.
The A-B process therefore can be considered as a very promising, cost effective alternative for both existing and new wastewater treatment plants in responding to the increasing effluent demands.

KEYWORDS

Wastewater treatment; A-B process; two-stage system; full-scale results; energy and space saving; process stability; upgrading existing treatment plants.

INTRODUCTION

In protecting our surface waters and ground water resources, in many countries, restrictions and taxes are put upon wastewater disposals. Above this, long term plans are being prepared which will lead to gradually increasing requirements in the future.

In Germany the new "Wasserwirtschaftsgesetz" requires for domestic wastewater treatment plants an average BOD in the effluent of five unsettled samples of 25 mg/l. If it is proposed that in 95% of the tests these requirements must be met, this implies that as an operation design value, the treatment plant to be constructed or upgraded should cover an interval "a" to the proposed average of 25 mg/l (fig.1). For the Netherlands, due to the stronger requirements, this "interval" will be even larger.

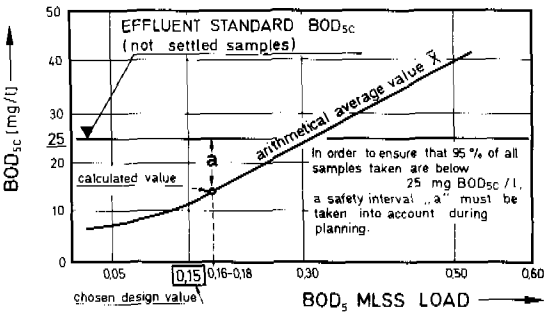

Fig. 1. Effluent BOD values at several sludge loads (from Böhnke, 1983)

In upgrading existing treatment systems or in designing new plants, which should meet higher standards, in principle, the existing scale of conventional systems could cope in many cases; however, only at the expense of a high price in investment as well as in energy.
In general therefore, new systems should be searched for, which preferably meet the following requirements:

better treatment efficiency with higher process stability;
lower specific volume requirements with lower specific construction costs - better performance of existing overloaded treatment plants;
reduction of the specific energy demand;
lower specific annual costs;
increased degradation of sparingly degradable substances.

In the beginning of the seventies a new process was developed by Prof. Dr.-Ing. B. Böhnke and his co-workers of the "Institute für Siedlungswasserwirtschaft" of the Technical University of Aachen, Germany. (Böhnke, 1977, 1978).
From experiments it was concluded that the A-B process meets the stated requirements for new systems.
Esmil adopted the system and became licensee.

Thirty experiments with 16 different wastewaters have been conducted according to the A-B process over the last eight years (Gethke, 1983a, 1983b).
For the present five full-scale plants are operating according to the A-B principles. Another five are planned or under construction as may be seen in table 1.

TABLE 1 Full-Scale A-B Plants

Name	Capacity *	Phase
Krefeld	800.000	in operation
Rheinhausen	170.000	in operation
Haan-Gruiten	10.000	in operation
Pulheim	80.000	in operation
Bad Honnef	35.000	in operation
Rotterdam Dokhaven	470.000	under construction
Köln-Langel	300.000	under construction
Neuenkirchen	44.500	under construction
Salzburg	300.000	planned
Eschweilen	160.000	planned

* Capacity expressed in population equivalents (p.e.)

It is the intention of this paper to illustrate in this context the basic principles and features of the A-B process and to present the results of the first full-scale plants.

THE A-B PROCESS

The reduction process, taking place in an activated sludge plant, is characterized by a fast removal of a relatively big part of the organics from the wastewater, within the first minutes.
This phenomenon, which already had been recognized by Jung (1954), formed the basis for the development of the A-B process.

The basic components of the A-B process are two activated sludge plants in series. A high loaded first or A-stage is followed by a low loaded second or B-stage.
A typical flow sheet is given in figure 2.

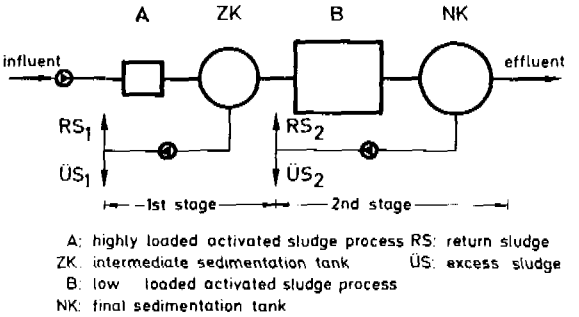

Fig. 2. General flow sheet
A-B process

Characteristics, as compared to other two stage activated sludge processes, are the absence of a presettling tank, the complete separation of the sludge circles of the two stages and the extremely high loaded A-stage (3-6 kg BOD/kg MLSS.day).
Up to 70% of the influent BOD is removed in this stage at low energy costs.

The B-stage is a normal low loaded activated sludge plant with sludge loads in the range of 0,15-0,30 kg BOD/kg MLSS.day.

THE A-B PLANT OF KREFELD

In 1978 Esmil was granted the order for the reconstruction and extension of the wastewater treatment plant of the city of Krefeld according to the A-B principle.
As representative, this full-scale plant will be discussed in more detail.

Wastewater Characteristics

The wastewater is characterized by fluctuations in both composition and load as a result of a high industrial content. The pH may vary from 2 up to 12 and back within some hours and variations in the COD from 200 up to 3,000 mg/l within one day have been established.

After intensive pilot plant experiments the A-B process was selected as the most appropriate system for this type of wastewater (Böhnke, 1976, Diering, 1978).

The plant is designed for 800,000 population equivalents. Some basic parameters are summarized in table 2.

TABLE 2 Design Parameters A-B Plant Krefeld

Capacity	800,000 p.e.
BOD-load	48,000 kg/day
BOD-concentration (av.)	340 mg/l
Flow (av.)	143,000 m^3/day
Flow (max. dwf)	10,200 m^3/hour
Flow (max. rwf)	16,320 m^3/hour

Plant lay-out

Construction was started at the end of 1978. The existing treatment facilities have been incorporated in the design. Reconstruction started behind the existing grit removal (figure 3).

One of the former rectangular primary clarifiers is used as A-stage and the other two have been reconstructed to intermediate (A-stage) clarifiers.

TABLE 3 Design Data A-Stage Krefeld.

Volume	5,100	m^3
Organic load (av.)	9.5	kg BOD/m^3.day
Sludge load (av.)	5.0	kg BOD/kg MLSS.day
BOD-reduction	65	%
OC/Load	0.11	kg O_2/kg BOD
Surface load		
Clarifier (at max. dwf)	3.0	m/h

New are: the sludge return pumping station for the A-stage, the B-stage (low loaded activated sludge plant of the Carrousel type) with rectangular secondary clarifiers and one additional thickener for the mixture of the A- and B-stage sludges.
The thickened surplus sludge is dewatered with centrifuges and incinerated together with the municipal refuse of the city.

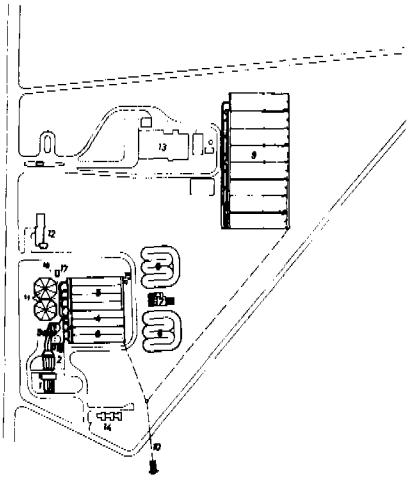

Fig. 3. Lay-out A-B plant Krefeld

Some basic design data of both the A- and B-stage are summarized in tables 3 and 4.

TABLE 4 Design Data B-Stage Krefeld

Volume	30,720	m^3
Organic load (av.)	0.55	kg BOD/m^3.day
Sludge load (av.)	0.15	kg BOD/kg MLSS.day
OC/Load	2.5	kg O_2/kg BOD
Surface load clarifier (at max. dwf)	0.6	m/h

Operation results

The start-up was at the end of 1981.
Actual loads amount to an average of 505,000 p.e.: 63% of the capacity.
Several alternative ways of operation have been tested to deal with this underloading in order to come as close as possible to the design data (Gethke, 1983a, Gruteser 1983a, 1983b).
This could be realized by switching off half of the A-stage.

Table 5 summarizes some results of the first six months of 1983.

TABLE 5 Operation Results A-B Plant Krefeld

	Design	Actual
A-stage		
Reduction rate (%)	65	55
Organic load (kg BOD/m^3.day)	9.5	11.9
Sludge load (kg BOD/kg MLSS.day)	5.0	4.3
S.V.I. (ml/g)	45	37
OC/Load (kg O_2/kg BOD)	0.11	0.06
B-stage		
Reduction rate (%)	90-95	94
Sludge load (kg BOD/kg MLSS.day)	0.15	0.13
S.V.I. (ml/g)	150	130
Total plant		
Capacity (p.e.)	800,000	505,000
Reduction rate (%)	95	98

In spite of the higher load and the so-called facultative way of operation (minimized oxygen input) the reduction rate of the A-stage remains over 50%.

Of special interest are also the high overall reduction rate of 98% and the low S.V.I. in both stages, which result in a 7% SS behind the thickeners.

Besides the advantages of lower energy consumption and less construction volume, one of the major features of the A-B process, as compared to one stage activated sludge processes, is the capability of dealing with relatively big variations of the influent composition (BOD, pH, toxic substances etc.)

Reaction to pH-shock loads. A representative pH-curve is shown for the individual stages in figure 4.

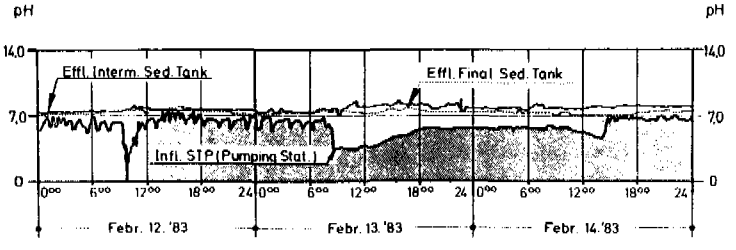

Fig. 4. Reaction of both stages of the A-B plant of Krefeld to pH-shock loads (from Böhnke, 1983).

A very strong acidic shock occurred during the 12th of February (pH ~ 1), followed by an influent pH of 3-4 during the next two days.
This extremely high stress was cushioned by the A-stage and was not discernible in the B-stage influent. The same phenomena have been observed in other A-B experiments (Gethke, 1983c).
An excellent buffering effect of the A-stage is evident.

Reaction to organic shock loads. Table 6 indicates the results of 20 days in the first half of 1983 for which the hydraulic load and/or the organic load exceeded the design loads of 143,000 m^3/day and 98,000 kg COD/day respectively.
In spite of these shock loads the final effluent COD is very stable between 30 and 60 mg/l with an average of 40 mg/l (Diering, 1983a).

TABLE 6 Performance Of The A-B Plant Of Krefeld During Organic Shock Loads

Influent		A-stage			B-stage	Final Effluent	
Flow m^3/day	COD mg/l	Sludge load kg COD / kg MLSS.day	COD mg/l	Reduction %	Sludge load kg COD / kg MLSS.day	COD mg/l	Reduction %
144,888	846	10.7	245	71.0	0.36	50	94.1
193,117	750	29.9	543	27.6	1.14	50	93.3
162,742	959	40.8	262	72.7	0.24	50	94.8
190,730	662	-	325	50.9	0.58	30	95.5
153,359	650	27.9	317	51.2	0.35	30	95.4
264,773	462	7.7	121	78.8	0.21	30	93.5
96,422	1141	7.1	95	91.7	0.07	30	97.4
144,220	705	17.3	288	59.1	0.34	30	95.7
155,907	688	20.0	277	59.7	0.44	30	95.6
173,723	790	16.3	307	61.1	0.39	46	94.2
92,060	1118	9.2	305	72.7	0.26	48	95.7
131,918	818	14.1	241	70.5	0.36	52	93.6
93,577	1280	16.2	277	78.4	0.23	n.a.	-
143,502	712	9.5	345	51.5	0.50	43	94.0
192,727	698	16.5	137	80.4	0.23	10	98.6
255,683	553	61.6	137	60.0	0.74	43	92.2
143,047	251	5.9	221	52.2	0.12	26	89.6
168,432	325	23.9	120	47.4	0.29	49	84.9
186,117	726	35.3	171	48.9	0.86	58	92.0
187,527	603	21.8	290	42.3	0.74	60	88.1
Average							
163.724	732	20.6	263	61.4	0.42	40	93.6

Reaction to toxic shock loads. The compatibility and the high chances of survival of the activated sludge in the A-stage are not only confined to pH- and organic shocks but apparently also include toxic loads. This is indicated by oxygen concentration data in the A- and B-stages at Krefeld (figure 5).
With a constant oxygen transfer in the A-stage, the oxygen concentration changes in an extraordinary manner.
This distinct increase in oxygen concentration implies that the bacteria must be damaged. However, this partial damage or inactivity of the activated sludge in the A-stage is already corrected within 4 hours. The toxic load has practically no effect

on the B-stage.

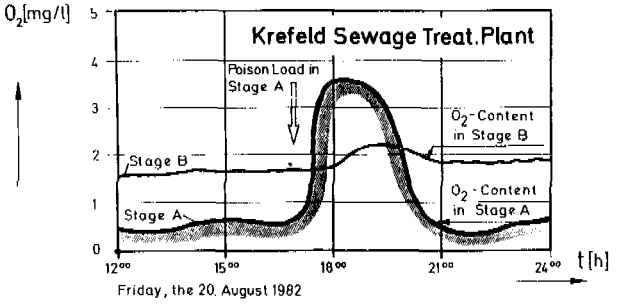

Fig. 5. Consequences of a toxic shock load in the O_2-content in the A- and B-stage at the Krefeld STP (from Böhnke, 1983).

DISCUSSION

It may be concluded that the potential features of the A-B process have been completely fullfilled in the plant of Krefeld. Operation is characterized by a high process stability, resulting in a very stable and high final effluent quality.

Results of the other four full-scale plants are similar. Some typical operating data are summarized in table 7 (Diering, 1983b).

TABLE 7 Operating Data Full-Scale A-B Plants

	Krefeld	Pulheim	Rhein-hausen	Bad Gruiten	Bad Honnef
Capacity (p.e.)					
Design	800,000	80,000	170,000	10,000	35,000
Actual	505,000	26,700	84,000	4,500	50,000
Influent (mg BOD/l)	480	412	214	288	620
Effluent (mg BOD/l)	5-7	6	6	5	4
Effluent (mg COD/l)	30-60	42	52	50	30
Reduction rate A-stage (%)	55	59-62	44	43	55-60
Sludge load B-stage ($\frac{kg\ BOD}{kg\ MLSS.day}$)	0.13	0.05	0.18	0.15	0.13
S.V.I. A-stage (ml/g)	37	40-58	60	50	40-60
S.V.I. B-stage (ml/g)	130	50-70	93	65	70-100

The very low BOD and COD values of the final effluents are

remarkable. The S.V.I. for both stages are low with regard to a normal single stage activated sludge plant.

Of special interest are the results of Haan-Gruiten (Eitner, 1983a, 1983b).
This plant was transformed to an A-B plant by using the existing aerated grit removal as a combined A-stage/grit chamber and the existing primary clarifier for intermediate sedimentation.
The only new item installed is a sludge return pumping station for the A-stage.
The original average index was 225 ml/g. After reconstruction this index dropped to 65 ml/g (figure 6).

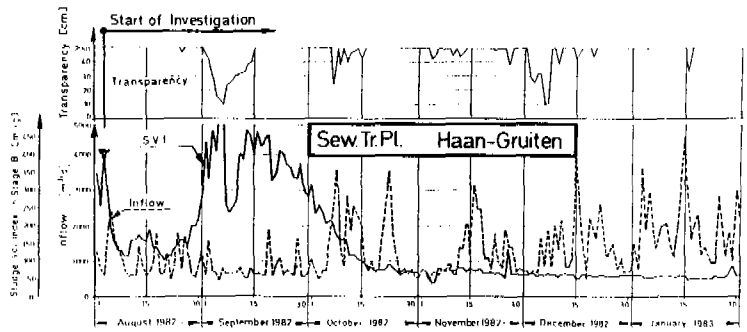

Fig. 6. Response to the S.V.I. in the STP of Haan-Gruiten after conversion to the A-B system. (from Eitner, 1983b).

From this and other observations it can be stated that in general the A-B process leads to a low sludge volume index in both stages. This characteristic of the A-B process permits higher loadings of the clarifiers.

Another key to success of the A-B process is the fact that, despite the extremely high loading, the A-stage can be operated at a high reduction rate and is stable. Variations in organic load and pH and toxic shocks are leveled out and a constant influent with mainly soluble organics is supplied to the B-stage.
The latter results in a low sludge production with as consequence a longer sludge age and a higher reduction rate compared to single stage processes at the same sludge load.

Gethke (1983c) has compared the sludge loads of the B-stage to a single stage activated sludge plant with the same treatment efficiency. The results are given in figure 7.

Results of the five full-scale plants indicate an average total sludge production of 1.5 kg d.s./kg BOD of which 85% is formed in the A-stage (Diering, 1983b). The B-stages of these plants are operated on an average sludge load of 0.13 kg BOD/kg MLSS.day.
The low sludge production in the B-stage results in a sludge age of approximately 25 days, which is almost twice the sludge age of a single stage plant at the same sludge load.

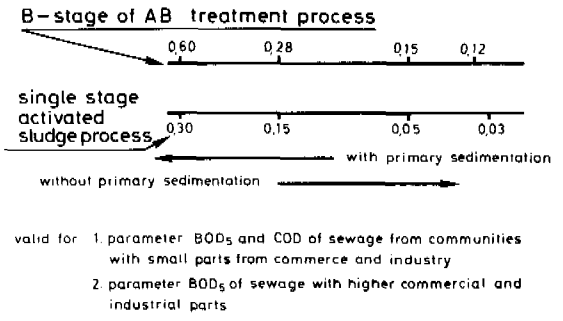

Fig. 7. Sludge loads of the B-stage of the A-B process related to a single stage activated sludge process for equal reduction rates. (from Gethke, 1983c).

This also explains that nitrification has already started in an A-B plant at a sludge load of 0.3 kg BOD/kg MLSS.day.

ECONOMY

The features of the A-B process result both for investment and energy in savings up to 30% compared to equivalent one stage treatment plants.

A comparison for 100,000 p.e. is given in table 8.

To reach a final effluent BOD below 10 ppm and complete denitrification the A-B process may be designed at a sludge load of 4 kg BOD/kg MLSS.day for the A-stage and 0.15 kg BOD/kg MLSS.day for the B-stage.
Equivalent final effluent results can only be obtained in a conventional single stage activated sludge plant at a sludge load of 0.05 kg BOD/kg MLSS.day.
The total treatment volume for the A-B process amounts to approximately 17,370 m^3 compared to 33,140 m^3 for the stabilization plant.
The reduction in treatment volume is 47.5%.

A second example is indicated for a final effluent demand of 13 ppm BOD and complete respectively partial denitrification. In this case the reduction in treatment volume amounts to 25%.

Energy consumption has been calculated for the complete treatment plant including aeration, sludge return pumping station, clarifiers and sludge handling.
In comparison with the stabilization plant the A-B alternative gives a saving in energy consumption of 32%.
For the second example the energy saving results in respectively 16 and 5% for the partial and complete denitrification alternative.

TABLE 8 Comparison A-B Process Versus Conventional One Stage Processes For 100,000 p.e. (Gethke, 1983c)

Position	Treatment volume (m^3)								Energy consumption *
	AS	PC/CA	BS/AT	SC	PT	D	ST	TOTAL	
A-B process F/M B-stage = 0.15	600	1950	5400	4400	900	3600	520	17370	19.6
Conventional one stage process F/M = 0.05	-	-	24000	8500	640	-	-	33140	29.0
A-B process F/M B-stage = 0.28	600	1950	2700	4100	950	3800	550	14650	p 18.7 c 17.8
Conventional one stage process F/M = 0.15	-	1950	8400	4600	830	3240	530	19550	p 22.2 c 18.7

* Incl. biology, sludge return pumping, sludge digestion, sludge dewatering etc. in kWh/p.e..year.

F/M = Sludge load
AS = A-stage
PC = Primary clarifier
CA = Clarifier A-stage
BS = B-stage
AT = Aeration tank
SC = Secondary clarifier
PT = Primary thickener
D = Digester
ST = Secondary clarifier
p = partial denitrification
c = complete denitrification

Of special interest are also the possibilities to upgrade existing conventional single stage activated sludge plants by incorporating the A-B process technology.
By expanding the aerated grit chamber the functions of A-stage and grit removal are combined.
The primary clarifier is modified to intermediate clarifier and only a sludge return pumping station has to be installed additionally.
The advantages of the A-B system are achieved at very low costs.

The A-B process therefore can be considered as a very promising, cost effective alternative for both existing and new wastewater treatment plants.

ACKNOWLEDGEMENT

The assistance by Prof. Dr.-Ing. B. Böhnke and his staff in composing this paper is gratefully appreciated.
Thanks are also expressed to Mrs. Rinske de Groot for typing this manuscript.

REFERENCES

Böhnke, B., Diering, B. (1976). Durchführung von Versuchen zur biologischen Reinigung des Krefelder Abwassers. Abschlussbericht, Institut für Siedlungswasserwirtschaft der RWTH Aachen, Dezember 1976 (not published).

Böhnke, B., (1977). Das Adsorptions-Belebungsverfahren. Korrespondenz Abwasser (KA), 24, No. 2.

Böhnke, B., (1978). Möglichkeiten der Abwasserreinigung durch das "Adsorptions-Belebungsverfahren" - Verfahrenssystematik, Versuchsergebnisse - Schriftenreihe des Instituts für Siedlungswasserwirtschaft der RWTH Aachen, 25, 437-465

Böhnke, B., (1983). Vergleichende Betrachtung von Versuchs- und Betriebsergebnisse der zweistufigen A-B Technik unter besonderer Berucksichtigung mikrobiologischer Reaktionsmechanismen. Korrespondenz Abwasser, 30, no. 7 und 8, 452-461, 530-536.

Diering, B., (1978). Versuchsergebnisse und genereller Entwurf des Klärwerkes Krefeld für 800.000 EW. Wissenschaft und Umwelt - ISU 3, 140-146.

Diering, B., (1983a). Betriebsergebnisse des A-B Klärwerkes Krefeld. Paper presented at the A-B Technology Conference, 26-28 September 1983, Aachen (in preparation).

Diering, B., (1983b). Schlammanfall und Schlammalter in den A- und B-Stufen. Paper presented at the A-B Technology Conference, 26-28 September 1983, Aachen (in preparation).

Eitner, D., (1983a). Untersuchungen zur Nutzung eines belüfteten Sandfanges als Adsorptionsstufe. Korrespondenz Abwasser (KA), 30, No. 2, 104-111.

Eitner, D., (1983b). Belüfteter Sandfang in Kombination mit einer A-Stufe : Betriebsergebnisse der Kläranlage Haan-Gruiten. Paper presented at the A-B Technology Conference, 26-28 September, 1983, Aachen (in preparation).

Gethke, H.-G. (1983a). Betriebliche Erfahrungen und erste Ergebnisse zum Adsorptions-Belebungs-Verfahren in Krefeld. Gewässerschutz-Wasser-Abwasser (GWA), Schriftenreihe des Instituts für Siedlungswasserwirtschaft der RWTH Aachen, 62, (in preparation).

Gethke, H.-G. (1983b). Zusammenfassende Darstellung der Untersuchungen zum Adsorptions-Belebungs-Verfahren. Gewässerschutz-Wasser-Abwasser (GWA), Schriftenreihe des Instituts für Siedlungswasserwirtschaft der RWTH Aachen, 59, 363-404.

Gethke, H.-G. (1983c). Untersuchungen und Anwendung eines zweistufigen Belebungsverfahren mit einer Höchbelastbelebung in der 1. Stufe und einer Schwachbelastbelebung in der 2. Stufe. (Adsorptions-Belebungs-Verfahren - Abschlussbericht) (not published).

Gruteser, K., Diering, B., (1983a). Erste Ergebnisse des Demonstrationsprojektes zum A-B Verfahren in Krefeld: Vorstellung des Projektes, Mesz- und Regeltechnik, Verfahrenstechnik, Reinigungsleistung. Gewässerschutz-Wasser-Abwasser (GWA), Schriftenreihe des Instituts für Siedlungswasserwirtschaft der RWTH Aachen, 59, 405-419.

Gruteser, K., (1983b). Spezifischer Energieaufwand der A-Stufe in Krefeld bei unterschiedlicher Fahrweise. Paper presented at the A-B Technology Conference, 26-28 September 1983, Aachen, (in preparation).

Jung, H., (1954). Die neuzeitliche Abwasserreinigung im Blickwinkel. Kommunalwirtschaft, 17/18, 395-401.

Wat. Sci. Tech. Vol.17, Amsterdam, pp.247-258.
Printed in Great Britain.

0273-1223/85 $0.00 + .50

FLEXIBLE MODELLING OF THE ACTIVATED SLUDGE SYSTEM — THEORETICAL AND PRACTICAL ASPECTS

M. S. Sheffer,* M. Hiraoka** and K. Tsumura**

*Environ. Protection Service, Office of Interior, Jerusalem, Israel
**Dept. of Sanitary Eng., University of Kyoto, Kyoto, Japan

ABSTRACT

For the purpose of optimal modelling, a "Flexible Modelling" method was developed. A flexible set of models consisting of hierarchical mechanistic models derived from a highly detailed structured model by mechanistic simplification was obtained. The performance of a computer program with an algorithm for parameter fitting in the time domain was evaluated by use of simulation. The program was able to estimate the models' parameters, even when using data with different degrees of inaccuracy. A computer program for model selection was developed, whereby the model was selected according to the information required. It was found that for prediction of the dynamic behavior of the MLVSS, the simplest model can supply all the necessary information. For prediction of effluent substrate concentration, the differences between the models' predictions depend on the characteristics of the disturbances and on the values of the models' parameters. The selection of the proper model and updating its parameters can be done by a computer which uses the presented program for model selection and parameter fitting.

KEYWORDS

Heterogenic system; multicomponent substrate; flexible modelling; mechanistic simplification; prediction; parameter fitting; model selection.

INTRODUCTION

The heterogenity and complexity of the activated sludge system raise the question as to whether one model can provide all the different levels of necessary information concerning the system. Steady state models may be sufficient for the purpose of designing a plant, but they are inadequate for its operation and control. A dynamic model should predict the dynamic behavior of the system. However, some models provide over-detailed information which cannot be verified, whilst other models may not provide sufficient information for a specific purpose. Therefore, when using a model, its aims should be clearly defined. When modelling a complex system such as the activated sludge, no one model can be expected to describe all the features of the system. Complete quantification of the micro-biological system necessitates the measurement of an enormous number of reaction rates and an understanding of their complex interaction. Since these are beyond the scope of reasonable measurement techniques, simplified mathematical models are necessary.

JWST AMSTERDAM 1-Q

Storer and Gaudy (1969) have shown that the Monod model is not capable of predicting the lag in specific growth rate that occurs when substrate increases. Therefore, it cannot be expected to accurately predict the dynamics of oxygen utilization. This lag is believed to occur due to the formation of stored mass. Though neglecting the lag may cause discrepancies in the predicted behavior of oxygen utilization, it is quite possible that the predicted dynamic behavior of the raw substrate would be the same, with or without allotting a separate phase for stored mass. Young et al. (1980) have shown that optimal periodic control based on a structured model with a stored mass phase can be substantially different from that based on the Monod model. However, the values of the kinetic parameters used in the two models differed greatly, even for such parameters as the decay rate coefficient which, in principle, should be of the same order in both models. Klei and Sundstrom (1974) examined the differences that exist between using a linear model and the non-linear Monod equation. They found that reasonably small differences exist, for input step changes of up to 30%.

One of the main obstacles in practical usage of models of the activated sludge process for various purposes, is the inflexibility of the presently available modelling approaches. The complexity of the activated sludge biosystem and the variety of conditions to which the system is subjected, may be best dealt with by flexible modelling. The flexible models' structure is composed of a set of mechanistic models and consists of both detailed and simplified forms.

THE SET OF MODELS

There are many constituents in the activated sludge system. There is a wide spectrum of reactions and interactions between the microbial species, organic matter, nutrients and inorganic matter. To mathematically describe such a system in detail would involve enormous complexity. This research takes into account only the most important constituents of the system. Thus, a hierarchial set of models developed by mechanistic simplification, neglects minor reactions and/or combines several interrelated reactions into one overall step.

Fig. 1 is a detailed representation of the volatile part of the biosystem in the aeration tank. Apart from the active mass and inert mass, the volatile part contains a substrate phase which is divided into two components. One is the substrate as it appears in the influent, and the other is the substrate after undergoing presteps to assimilation. These two components are further divided into their dissolved and suspended parts. The detailed model takes into account two separate routes of substrate assimilation, each route consisting of two steps. The first step is the prestep to the growth/assimilation reaction, wherein the suspended substrate undergoes a sorption/entrapment reaction. This reaction is not fully understood and the equation used by Blackwell, after modification (Sheffer, 1982), is used to describe this step (Figs. 1-4 should be consulted for the definition of the state variables):

$$\left(\frac{dXSS}{dt}\right)_{la} = RT_{la} \cdot XSS \cdot \left(f^{*}_{S_{la}} - \frac{XSM}{XA}\right) \cdot XA \qquad (1)$$

la refers to reaction la in Fig. 1.

RT = transfer rate coefficient ($L^3/M.T$)

f^{*}_{S} = maximum fraction of available suspended substrate which can be maintained by the active mass

The pre-assimilation step of the dissolved substrate can be described by a similar equation, with a different transfer rate coefficient. However, since this step is mainly an enzymatic breakdown reaction, the Michaelis-Menton equation is preferable, since it is based on the results of biochemical research.

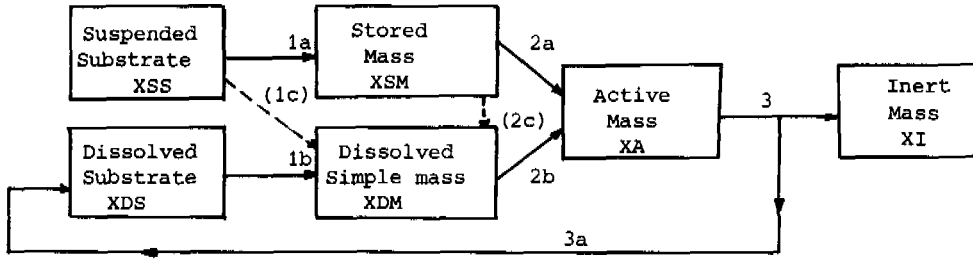

Fig. 1. A detailed representation of the volatile part of the biosystem in the aeration tank

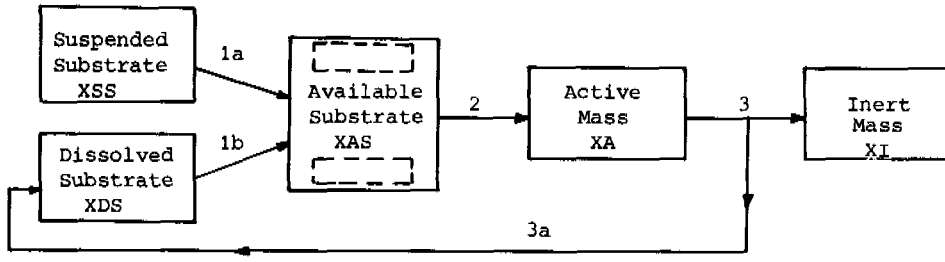

Fig. 2. Mechanistic simplification step 1 - an available substrate phase

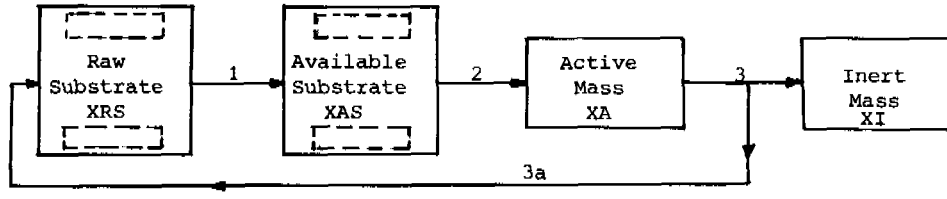

Fig. 3. Mechanistic simplification step 2 - a raw substrate phase

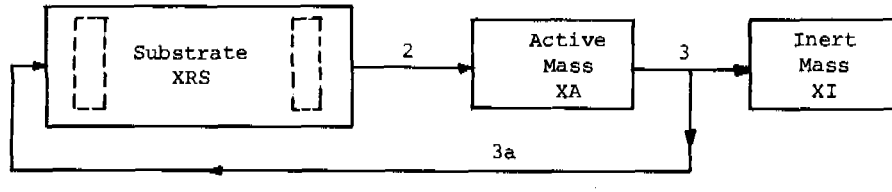

Fig. 4. Mechanistic simplification step 3 - one substrate phase

The concentration of active mass can be used instead of that of the enzymes, since the formation of enzymes and their concentration is proportional to the concentration of the microorganisms:

$$\left(\frac{dXDS}{dt}\right)_{1b} = R_{MM} \cdot \frac{XDS}{K_{MM}+XDS} \cdot XA \qquad (2)$$

R_{MM} = Michaelis-Menton constant (1/T)

K_{MM} = saturation coefficient (M/L^3)

and $_{1b}$ refers to reaction 1b in Fig. 1

The second step in the elimination of substrate from the system is the assimilation/growth reaction. The kinetics of this step can be described by the Monod equation, for both the suspended phase and the dissolved phase, using different values for the growth rate coefficient and the saturation coefficient:

$$\left(\frac{dXA}{dt}\right)_{2a} = RXA_{2a} \cdot \frac{XSM}{KXA_{2a}+KSM} \cdot XA \qquad (3)$$

$$\left(\frac{dXA}{dt}\right)_{2b} = RXA_{2b} \cdot \frac{XDM}{KXA_{2b}+XDM} \cdot XA \qquad (4)$$

RXA = maximum specific growth rate (1/T)

KXA = saturation constant (M/L^3)

and $_{2a}$ and $_{2b}$ refer to reactions 2a and 2b in Fig. 1.

Other subroutes and reactions exist in the system. Suspended substrate may undergo enzymatic solubilization, to become dissolved simple mass (1c). Stored mass may be solubilized before being assimilated (2c). However, for the sake of simplicity, these reactions are not considered here.

The first step in mechanistic simplification is to consider the stored mass and the dissolved simple mass as one phase. Both the suspended substrate and the dissolved substrate undergo a reaction prior to assimilation. The result of these reactions is a system constituent which is ready for assimilation. Considering them as a combined phase — the available substrate (XAS) — avoids the necessity of two separate growth equations containing unmeasureable and undeterminable parameters. Using an available substrate phase also eliminates the question of whether or not suspended mass must be solubilized before being assimilated (Fig. 2). Thus, the second model in the hierarchial set accounts for a prestep to assimilation, wherein the two substrate phases become available substrate for the growth of the organisms:

$$\left(\frac{dXA}{dt}\right)_{2} = RXA \cdot \frac{XAS}{KXA+XAS} \cdot XA \qquad (5)$$

$_2$ refers to reaction 2 in Fig. 2.

It is realized that some of the dissolved substrate may be available for assimilation without undergoing any preparatory reaction. However, since the activated sludge is a heterogenic system with a multicomponent substrate, some degree of generalization is imperative. Thus, the growth/assimilation step and its prestep are presumed for all the dissolved substrate without exception.

The next simplified model is that which takes into account only one phase of substrate in the influent; i.e. considering the biodegradable part of the suspended solids and of the dissolved organic matter in the influent as one phase (Fig. 3).

This substrate phase (the "raw substrate" — XRS), undergoes a sorption/entrapment solubilization step (1) prior to its assimilation. The reactions of the basic components in the model can be described by the following equations:

$$\left(\frac{d(XRS)}{dt}\right)_1 = RT \cdot XRS \cdot \left(f_s^* - \frac{XAS}{XA}\right) \cdot XA \qquad (6)$$

$_1$ refers to reaction 1 in Fig. 3

Reaction 2 and 3a are given by equations 5 and 7 respectively

This model, the basic structured model, is still somewhat detailed, since it contains two stages in the elimination of substrate from the system. In contrast with the researchers that advocate inclusion of a storage phase, some researchers (Patterson et al., 1970) have reached the conclusion that sorption/storage is not significant in the activated sludge process. Support for this belief comes from the detection of an immediate growth response of the activated sludge to an increase in influent substrate, as indicated by a significant activity increase. It would be incorrect to generalize as to whether or not a storage phase should be included in the model. The variety of microorganisms and substrate components present in the system, and the difference in the conditions in which different activated sludge systems are operated, suggest that in some systems it may be important to consider the storage step whilst in other systems it may be neglected. Walter et al. (1968) found that storage was related to the type of substrate and that some substrates showed no evidence of storage. The flexible modelling method provides a means to take the storage phase into consideration when it plays a significant role in the dynamic behavior and to neglect it when all the necessary information can be obtained from simpler models. The basic structured model contains two steps in the elimination of substrate, while its simpler derivative in the hierarchial set takes into consideration only one substrate phase (Fig. 4). In this model, the sorption/entrapment step is neglected, or included in the overall assimilation reaction. This reaction can be described by the Monod formulation as is given in equation 5.

Further simplification may be obtained by reducing the Monod equation to a first order term with respect to substrate concentration. Such a simplification is justified in a system which operates at a removal efficiency of 80% or more, and the effluent substrate concentration is much lower than the saturation coefficient KXA.

The importance of redissolving of dead cells and their function as an additional source of substrate has already been realized (Eckenfelder and Weston, 1956). Grady et al. (1974) showed that the soluble COD of the activated sludge process consists also of microbial excreta. Cell decay is not a process taking place only within the cell walls of bacteria, but also includes lysis and resolubilization of organic substances. From the scientific point of view such a reaction should not be neglected. Therefore, all the models in the hierarchial set contain a "complete mass cycle", i.e. they account for the decay reaction and the resolubilization of the cell decay material (3a), which is subsequently considered to be an additional substrate.

$$\left(\frac{dXA}{dt}\right)_{3a} = Y_2 \cdot RD \cdot XA \cdot \qquad (7)$$

Y_2 = substrate formed per unit active mass decayed

RD = decay rate coefficient (1/T)

DIFFERENCES BETWEEN THE PREDICTIONS OF THE MODELS IN THE FLEXIBLE SET

A comparative simulation program to compare the predictions of the models in the flexible set was performed. The present day inadequacy of sensors and fast analytical methods, makes the use of the highly detailed models impractical for engineering purposes. Therefore, only three models from the flexible set were compared: the basic structured model, the Monod-decay model and the first order-decay model. The comparison was done by simulating variations in the influent, while keeping all other conditions constant. Sinusoidal changes in flow rates and concentration and step changes were simulated. Before the simulation, the models' parameters were adjusted so that the models would predict a similar output for the same constant.

Fig. 5 shows the simulation results for the three models, when subjected to the same sinusoidal change in influent flow rate and concentration. The predicted behavior for three different amplitudes (α = 0.25; α = 0.50; α = 0.75, where α is the fraction of the maximal change in input) is presented. When the amplitude is small (α = 0.25), all three models predict the same behavior in regards to both XRS and MLVSS. However, when the amplitude increases, the differences in the predicted values of XRS are not negligible. The behavior of MLVSS is almost the same for all the models, even for large amplitudes.

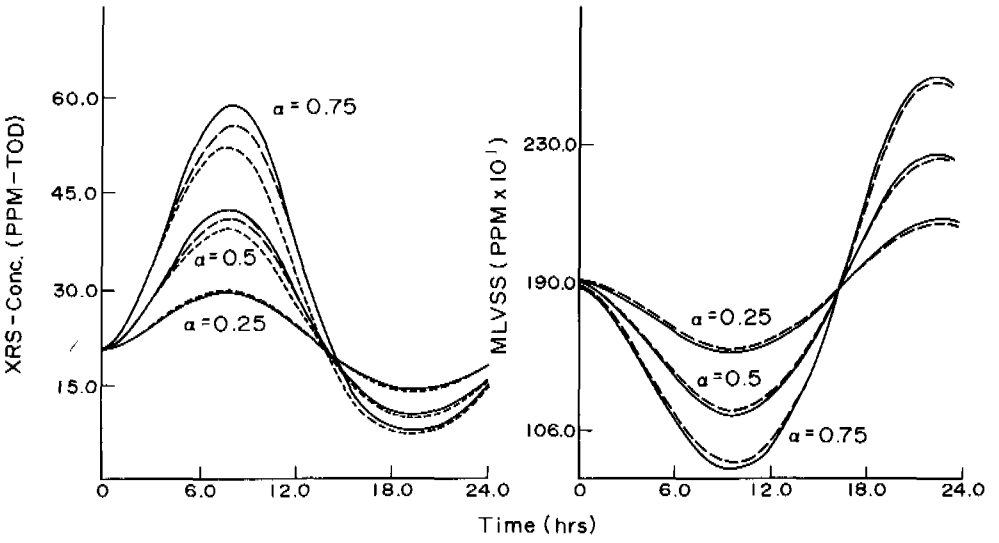

Fig. 5. The models' predictions for sinusoidal changes in influent flow rate and concentration, for 3 different amplitudes

The simulation of a step change demonstrates that the differences in the models' predictions depend on both the magnitude and the characteristics of the step. Three different kinds of step changes were simulated: a volumetric step change, a step change in influent concentration alone, and a combined step change in flow rate and concentration. Differences in the models' predictions are witnessed in the case of the combined step change. When the step change is only in flow rate, there are small differences between the models' predictions. When the step change is only in influent concentration, there are no significant differences between the models' predictions (Fig. 6).

Another factor that affects model prediction and differences between the models in the flexible set of models, is the value of the parameters. An additional set of

parameter values was selected, so that the models continued to predict nearly the same performance with regards to XRS and MLVSS, for the same input. The resultant models' predictions, using the second set of parameters, when the same step changes as simulated with the first set of parameters were applied, is presented in Fig. 7. A comparison of this figure with Fig. 6, shows that when different sets of parameters are selected, the degree of similarity in the predicted dynamic behavior of the models may be quite different. Two different sets of parameters were used for simulating the system with a combined sinusoidal change in flow rate and concentration (Figs. 8 and 9). For both the sinusoidal change and the step change, the change in parameter values has a negligible effect on the dynamic behavior and the differences in the models' predictions with regards to MLVSS. However, it does have an effect on the predicted behavior of XRS according to the three models. This means that the differences between the models' predictions do not depend only on the kind of magnitude of the disturbances, but also strongly depend on the values of the models' parameters.

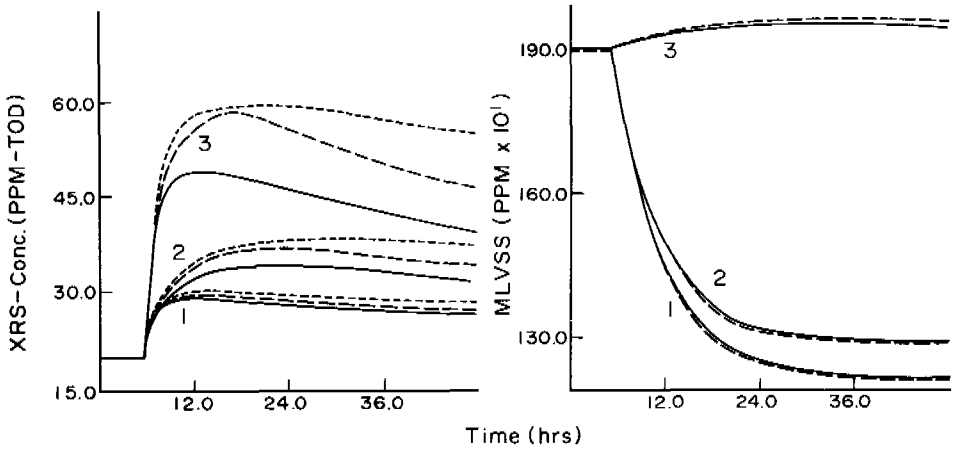

Fig. 6. The models' predictions for 3 kinds of step changes (concentration 1; flow rate 2; combined 3)

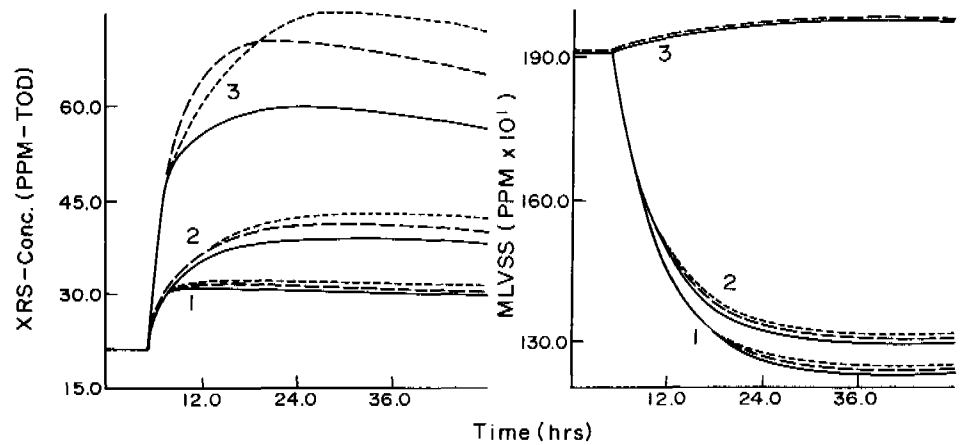

Fig. 7. The models' predictions for step changes using the second set of parameters

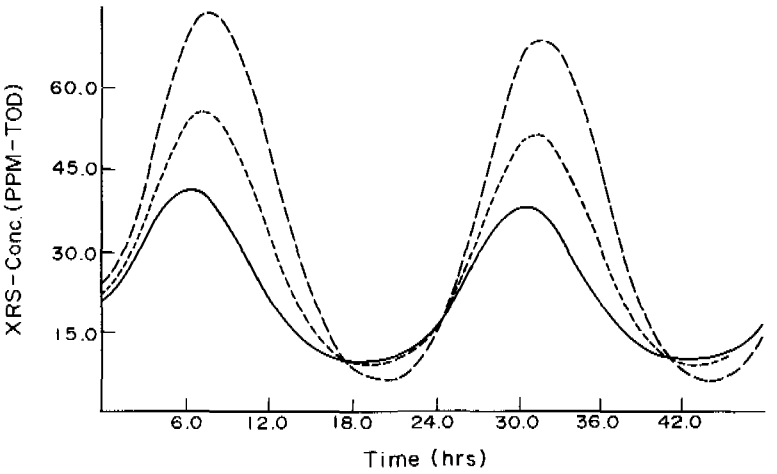

Fig. 8. The models' predictions for a combined sinusoidal change in flow rate and concentration - parameter set a.

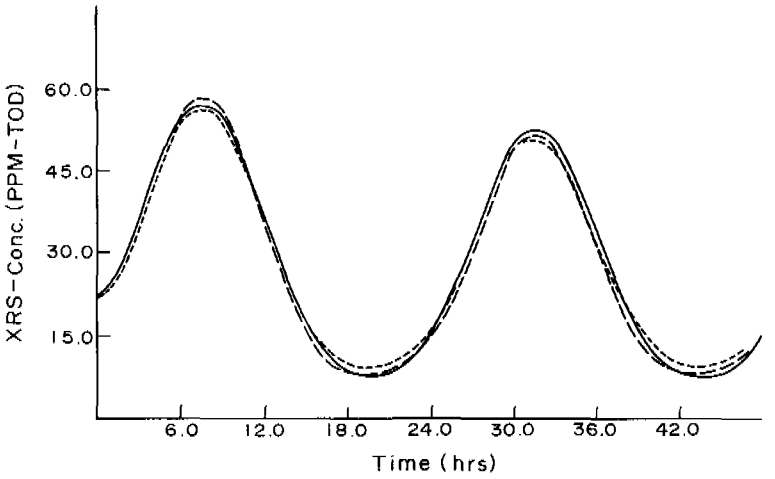

Fig. 9. The models' predictions for a combined sinusoidal change in flow rate and concentration - parameter set b.

PARAMETER FITTING

For practical use of the set of models in real activated sludge systems it is necessary to estimate the models' parameters, so that the models' output can be matched as closely as possible to the system's output. The activated sludge system is a dynamic biological system and its kinetic parameters' values may change during operation, due to internal changes in the microbiological species, changes in the character of the disturbances or environmental changes. Therefore, after obtaining values for the model's parameters for the initial period of time, it is necessary to be able to update these parameter values during plant operation, in order to account for changes in the real system. A program for parameter estimation, that matches the models' prediction to the system's data in the time domain, can be used also as a recursive on-line updating algorithm. That is, when new data are collected, they are fed into the algorithm, to enable an updated estimation of the parameters.

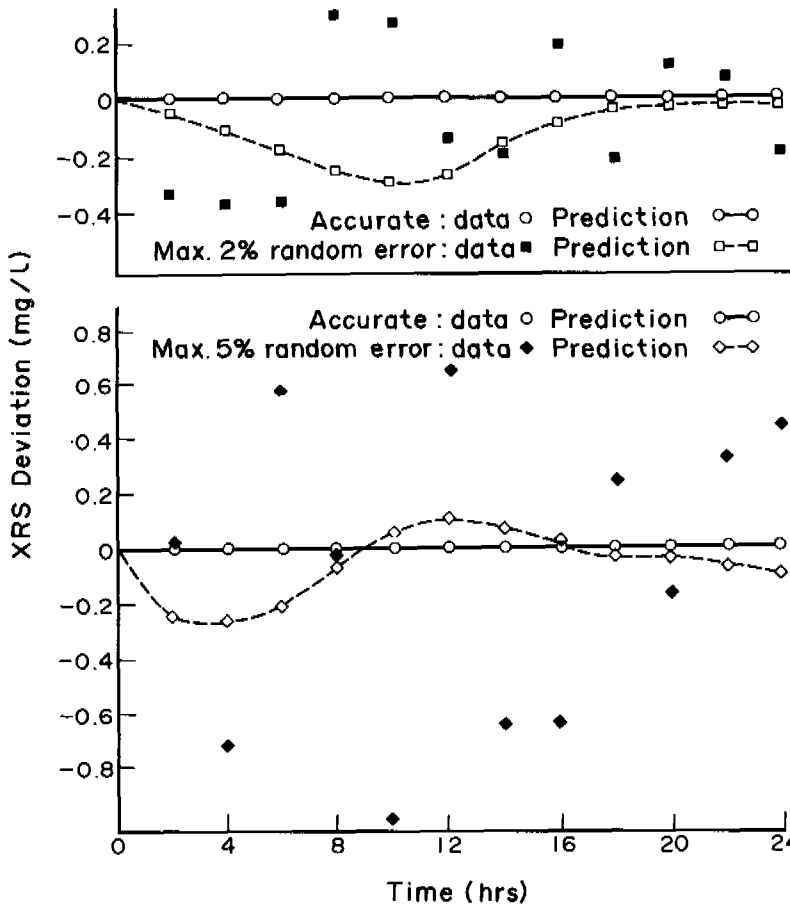

Fig. 10. The structured model's prediction, after using accurate and inaccurate data sets for parameter fitting - deviation from accurate solution

A method developed by Ojika and Wells (1980) is suitable for parameter estimation in the time domain, in dynamic systems described by non-linear differential equations, such as the activated sludge system. Given a model consisting of a set of non-linear equations, initial conditions and initial parameter values, this parameter fitting program enables the determination of the parameter values which best fit a given set of data. The performance of the subroutine MPLSM (1981), which is based on the above mentioned method, was checked with the proposed set of models.

A typical load disturbance in the activated sludge plant has a pattern similar to that of a sinusoidal form with a cycle time of 24 hours. In order to obtain data similar to that of a real system, the structured model was simulated with load disturbances of a sinusoidal form, with a cycle time of 24 hours. In addition, random error components of maximum 2% or maximum 5% were introduced into the simulation results, thus simulating data with different degrees of inaccuracy for the parameter fitting process. A detailed presentation and analysis of the performance of the parameter fitting program appear elsewhere (Sheffer, 1982). Fig. 10 illustrates the prediction of the structured model, after parameter fitting using data set with different degrees of inaccuracy, in comparison with the accurate data and the accurate solution. It can be seen that when the inaccurate data are distributed randomly around the accurate data, the prediction of the model is closer to the accurate solution than the inaccurate data. Thus besides fitting the parameter values, the program can serve as a data refining method and as a corrector of random fluctuations in measurements in real systems.

MODEL SELECTION

The activated sludge system is a complex system and there is a wide range in the degree of complexity of the models which can be used to describe it. Some of the more detailed models are so complex that they are inappropriate for practical use. However, in many situations, the activated sludge process can actually be described satisfactorily by fairly simple models. When selecting a model from the flexible set of models, it is important to select the one that will be the most useful for the specific purpose. When the aim of the model is to obtain the dynamic response of the substrate and the MLSS, it has been shown that relatively simple models may provide satisfactory results, similar to those obtained using complicated models. In order to assure that the model is as simple as possible, each new constant or element of complexity should be shown to be essential, and its ommission should result in failure to describe some important feature of the response.

It has been shown that there are no significant differences with regards to XRS and MLVSS between the various models in the flexible set, as long as the disturbances are of a small or moderate amplitude. However, the differences between the models depend not only on the amplitude of the disturbances, but also on the values of the models' parameters. Since the values of the parameters are specific for each system, it is impossible to know in advance which model from the set should be used for a specific purpose, under specific load conditions. Connecting the input-output data of the system to a computer, would enable to obtain an on-line analysis which could help determine whether the existing load conditions are within the "stability range" of the process and permit the use of a simpler model, or whether a more detailed model is necessary. The problem is further complicated by the non-stationary nature of the activated sludge process. Thus, frequent updating of the models' parameters is required. After determining the purpose of the model, the problem as to which model should be used can be tackled by a computer program for model selection.

It is possible to distinguish between two types of model equivalence/difference. The first type can be defined as a "matching criterion", which quantifies the

degree of similarity between the model and the data. In this research, the least squares criterion is used as the normalized matching criterion (NMC):

$$NMC = \sum_{i=1}^{T} (X_i - D_i)^2 \Big/ \sum_{i=1}^{T} D_i \tag{8}$$

X_i = calculated value

D_i = measured value

If the matching criterion of two models for the same interval of time are equal, the two models can be presumed to be equivalent. However, this type of model equivalence/difference is applicable only retrospectively. It is quite possible that two models be equivalent according to the matching criterion, but still exhibit differences with regards to the prediction of the dynamic behavior in the case of a change in load conditions. Therefore, a second type of model equivalence/difference is necessary. The second type of model equivalence/difference is defined as a "comparison index", which quantifies the difference between the models' predictions. A program which compares the models' predictions, calculates indices for model selection and updates the indices for different load conditions, has been developed. As an example two comparison indices are used. The first index is the number of checking points (out of a total 24 points per day), that the difference between the models' predictions for XRS is larger than 5% and that for MLVSS is larger than 0.5%:

$$Index_1 \quad \sum_{t=1}^{24} IND \tag{9}$$

for XRS: $$IND = \begin{matrix} 0 \text{ if } DIF < 0.05 \\ 1 \text{ if } DIF \geq 0.05 \end{matrix} \tag{10}$$

for MLVSS: $$IND = \begin{matrix} 0 \text{ if } DIF < 0.005 \\ 1 \text{ if } DIF \geq 0.005 \end{matrix} \tag{11}$$

$$DIF = \frac{|x'(t) - x(t)|}{x(t)} \tag{12}$$

$x'(t)$ = the state variable of the simpler model

$x(t)$ = the state variable of the higher model

The second comparison index calculates the average deviation (percent) of the measured state variables (XRS and MLVSS):

$$Index_2 = [\sum_{t=1}^{24} \frac{|x'(t) - x(t)|}{x(t)}] \cdot 100/24 \tag{13}$$

These two indices compare the predictions of XRS and MLVSS. It should be emphasized that similar indices can be calculated for the other system components. Likewise, additional indices can be determined.

According to the purpose of the model, a criterion for model selection, which determines the conditions in which the simpler model can be used and under what conditions it should be replaced by a more detailed model, should be employed. Since the equivalence/difference of the models depends on both the load conditions and on the parameters' values, the program for model comparison should be connected to the program for parameter fitting. The combined system would yield a

program which can work on-line, estimate and update the models' parameters and determine which model should be selected under the existing load conditions, according to the specific purpose of the model.

REFERENCES

Eckenfelder, W.W. and Weston, R.F. (1956). Kinetics of biological oxidation. In: Biological Treatment of Sewage and Industrial Wastes, G.J. McCabe and W.W. Eckenfelder (Eds)., Vol. 1

Grady, C.P.L. and Williams, D.R. (1975). Effect of influent substrate concentration on the kinetic of natural microbial population in continuous culture. Water Res., 9, 642-649.

Klei, H.E. and Sundstrom, D.W. (1974). Automatic control of an activated sludge reactor. J. Water Pol. Cont. Fed., 46, 993-999.

Ojika, T. and Welsh, W. (1980). Modeling problems in ordinary differential equations using the initial value adjusting method. J. of Math. Analysis and Applic., 75, 2-11.

Ojika, T. (1981). MPLSM -- a general subroutine for parameter fitting. Research Mathematical Science. Kyoto University.

Patterson, J.W., Brezonik, P.L. and Puntnam, H.D. (1970). Measurement and significance of ATP in activated sludge. Env. Sci. Tech., 4, 569-574.

Sheffer, S.M. (1982). Modelling and computer control of the activated sludge process. Ph.D. Dissertation. Kyoto University.

Storer, F.F. and Gaudy, A.F. Jr. (1969). Computational analysis of transient response to quantitative shock loading of heterogeneous populations in continuous culture. Environ. Sci. and Technol., 3, 143-152.

Walters, C.E., Engelbrecht, R.S. and Speece, R.E. (1968). Microbial substrate in activated sludge. J. San. Engr. Divs. ASCE, 94, 257-269.

Yeung, S.Y.S., Sincic, D. and Bailey J.E. (1980). Optimal periodic control of activated sludge processes: II. Comparison with conventional control for structured sludge kinetics. Water Res., 14, 77-84.

KINETICS AND AERATION IN AEROBIC TREATMENT

Wat. Sci. Tech. Vol.17, Amsterdam, pp.259-272.
Printed in Great Britain.

0273-1223/85 $0.00 + .50

DETERMINATION OF KINETIC CONSTANTS OF ACTIVATED SLUDGE MICROORGANISMS

J. S. Čech, J. Chudoba and P. Grau

Prague Institute of Chemical Technology, Department of Water Technol. and Environmental Engineering, Suchbátarova 5, 166 28 Prague, Czechoslovakia

ABSTRACT

A respirometric method for measuring kinetic constants of activated sludge microorganisms by means of a simple respirometer was developed and tested by using two types of mixed culture. It has been found that both the maximum substrate removal rate and the half-velocity coefficient are basically lower with the mixed cultures cultivated in a completely-mixed reactor /filamentous/ than with those cultivated in a selector-type reactor /nonfilamentous/.

KEYWORDS

Activated sludge microorganisms; kinetic constants determination; respirometer; substrate removal.

INTRODUCTION

Kinetics of bacterial growth have usually been described by two well-known Monod equations /Monod, 1949/:

$$\frac{dX}{dt} = \mu X \qquad /1/$$

$$\mu = \mu_{max} \frac{S}{K_s + S} \qquad /2/$$

where X is concentration of biomass; S is concentration of a growth-limiting substrate; μ and μ_{max} are, respectively, actual and maximum biomass growth rates; and K_s is saturation or half-velocity coefficient.

Though originally developed for pure cultures and single component substrates, the model has often been used for mixed cultures /activated sludge microorganisms/ and multicomponent substrates /waste waters/. In these cases, however, μ_{max} and K_s are not constant but

variable, depending on a composition of mixed cultures /Peil and Gaudy, 1971; Ghosh and Pohland, 1972/. Shifts in culture population are reflected in changes of overall growth kinetic constants.

The primary purpose of waste water purification is not to cultivate mixed cultures and produce biomass, but to remove organic compounds from solution. It is therefore desirable to express equations /1/ and /2/ in substrate removal terms. The rates of biomass growth and substrate removal are mutually combined by the following relation

$$\frac{dX}{dt} = - Y_{obs} \frac{dS}{dt} \qquad /3/$$

where Y_{obs} is the observed biomass yield coefficient. Combining equations /1/, /2/ and /3/ leads to :

$$- \frac{dS}{dt} \frac{1}{X} = \frac{\mu_{max}}{Y_{obs}} \frac{S}{K_s + S} \qquad /4/$$

After the substitution of r_X for $-(dS/dt)/X$, and $r_{X,m}$ for μ_{max}/Y_{obs}, equation /4/ turns into

$$r_X = r_{X,m} \frac{S}{K_s + S} \qquad /5/$$

where r_X and $r_{X,m}$ are, respectively, actual and maximum substrate removal rates.

Equation /5/ shows the dependence of the substrate removal rate on the actual concentration of a single component substrate. At high values of S /$S \gg K_s$/, $r_X = r_{X,m}$, the substrate being removed with a maximum constant rate. At low values of S /$S < K_s$/, $r_X = (r_{X,m}/K_s)S$, the substrate being removed with a decreasing rate. Consequently, from a practical point of view it is important to know the values of both K_s and $r_{X,m}$ for a given system. For their routine determination, a simple, rapid and sufficiently accurate method should be developed because most of the presently used methods are either tedious or have a limited accuracy. The aim of this paper is to present a simple respirometric method for determining K_S and $r_{X,m}$.

A BRIEF SURVEY OF THE METHODS USED

A review of methods for measuring K_s /and hence also $r_{X,m}$/ was published by Williamson and McCarty /1975/. Generally, these methods can be divided into two groups according to a way of cultivation:

a/ Batch cultivation.
b/ Continuous cultivation without biomass recycling /chemostats/.

Batch cultivation can be carried out with both high and low initial concentrations of biomass. Though this method is simple and rapid, its main disadvantage can be seen in the fact that "it provides estimates of limited accuracy when K_s values are small /less than 20 mg/l/ because of large analytical errors associated with measuring low substrate concentrations" /Williamson and McCarty, 1975/.

In continuous chemostats, hydraulic retention time is the same as mean cell residence time, which equals the reciprocal of observed biomass growth rate. For various mean cell residence times, steady-state concentrations of a given substrate are measured and plotted against the calculated values of r_X, which leads to a relation given by equation /5/. Applying a proper method of linearization of equation /5/, one can obtain both constants by means of a least square method. The main disadvantage of this method can be seen in the fact that a relatively long period is generally required to reach a steady-state, especially for organisms with long generation periods. Moreover, application of this method to mixed cultures containing species with substantially different generation periods is very questionable. Changing the mean cell residence time, for example from 24 to 2.4 h, one makes a severe selection of species in the mixed culture, enriching it with fast growers and reducing a proportion of slow growers. This results in finding inconsistent values of both constants /Ghosh and Pohland, 1972/.

The above-mentioned disadvantages of measuring K_S and $r_{X,m}$ forced Williamson and McCarty /1975/ to develop a new method called the "infinite-dilution" method. Since this method was used in our experiments as a comparative one, it will be briefly described here.

For the infinite-dilution method, a completely-stirred, continuously-fed reactor without recycle and no effluent draw-off is used. When a feed solution is sufficiently concentrated, the flow rates of feed can be kept very small, so that the change in reactor volume over a measuring period is negligible. A mass balance for the substrate in the reactor leads to

$$\frac{dS}{dt} = \frac{Q\,S_o}{V} - r_{X,m}\,\frac{X\,S}{K_S + S} \qquad /6/$$

where V is reaction vessel volume; S_o and S are, respectively, substrate concentrations in the feed solution and in the reactor; Q is feed flow rate.

When the mass flow, QS_o, is maintained at less than the maximum removal rate, $r_{X,m}XV$, a steady-state substrate concentration will be reached within less than an hour if X is sufficiently high /hundreds mg/l/. Over a short period of the experiment, the biomass concentration will change very little and can be assumed constant. At a steady state, ds/dt=0, and thus equation /6/ can be rearranged as follows :

$$\frac{Q\,S_o}{X\,V} = r_{X,m}\,\frac{S}{K_S + S} \qquad /7/$$

This procedure being used, the steady-state substrate concentrations are measured at various substrate mass flow rates and corresponding substrate removal rates. The data obtained are properly treated and both constants are calculated.

The only disadvantage of this method is a need of a simple, sufficiently specific and accurate analytical method for determination

of a substrate tested. This can be overcome by a simple respirometric method described here.

RESPIROMETRIC METHOD FOR MEASURING K_s AND $r_{X,m}$

Description of the Respirometer Used

Any respirometric method requires a suitable respirometer. Of numerous respirometers described in the literature, the simplest one, developed by Lamb and co-workers /1964, 1967/, was adapted and used. It is schematically shown in Fig. 1. In principle, the respirometer

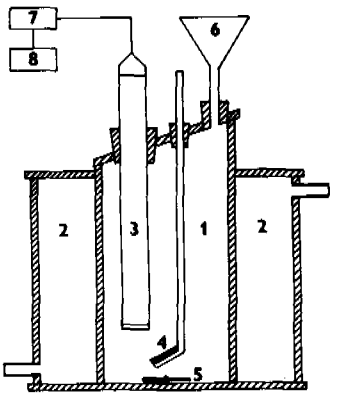

Fig. 1. Scheme of the respirometer used. 1-respirometric cell, 2-water jacket, 3-oxygen electrode, 4-aeration frit, 5-magnetic mixing bar, 6-expansion funnel, 7-oxymeter, 8-recorder.

consists of an oxygen electrode, oxymeter, continuous recorder, and a Perspex respirometric vessel. The respirometric vessel consists of a water jacket enabling it to maintain a constant temperature of 20 °C and of a proper respirometric cell. It is placed on a magnetic mixer so that the content of the cell can be thoroughly stirred. A ceiling of the respirometric cell is oblique in order that air bubbles could easily escape from the cell. Three openings are made in the ceiling. The first serves for inserting the oxygen electrode /through a rubber stopper/, through the second an aeration frit is led to the bottom of the cell, and into the third, located at the top of the oblique ceiling, a rubber stopper with a small funnel is inserted. The opening with the inserted funnel serves for dosing the substrate solution and for escaping air bubbles during periods of aeration. A cross-sectional area of the funnel stalk is small enough to reduce an oxygen absorption during the measurement to a minimum. The working volume of the respirometric cell is 450 ml.

Experimental Procedure and Evaluation of Respirograms

A working concentration of biomass, X_o, is prepared by either thick-

ening or diluting the original suspension. In the case of diluting, washing medium or effluent or supernatant can be used according to the necessity. The working concentration of biomass will generally depend on the level of heterotropic endogenous respiration rate. In order to suppress the process of nitrification, allylthiourea is used in suitable concentrations.

The suspension of activated sludge microorganisms is then transferred into the respirometric cell and aerated to increase the dissolved oxygen concentration to 6-8 mg/l. When these concentrations are reached, the aeration is stopped. A slow decrease in oxygen concentration is due to heterotrophic endogenous respiration. A typical respirogram is shown in Fig. 2 and can be interpreted as follows.

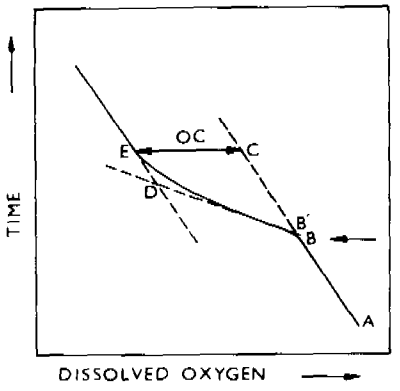

Fig. 2. Recorder chart with a typical respirogram.

During the endogenous phase of respiration, heterotrophic microorganisms utilize oxygen at a constant rate over a relatively long period of time, as demonstrated by the line A-B-C. At time B, a calculated, small volume of concentrated substrate solution is injected into the cell by means of a hypodermic syringe. This dose being known, the initial substrate concentration, S, can be easily calculated. The substrate solution is balanced with all necessary nutrients. Addition of a limited amount of substrate to the respirometric cell causes a temporary increase in respiration rate, as shown by the line B-D. This line is in fact a maximum-value tangent to the curve B-E and means the constant total respiration rate at the substrate concentration S. As the substrate concentration decreases with time, the respiration rate also decreases, being at low concentrations substrate-dependent. When the substrate has been removed /point E/, the respiration rate returns to a value /line D-E/, which is equal to, or perhaps slightly different from, the original endogenous rate.

When the measurement with one concentration is finished, a new dose of substrate can be injected into the cell and a next respirogram is recorded. This can be repeated several times. New reaeration is necessary when the dissolved oxygen concentration drops below 2

mg/l. If corresponding couples of S and r_X are available, a relation given by equation /5/ can be constructed and both constants can be computed.

Evaluating a respirogram, one must first calculate endogenous, $r_{X,e}$, and total, $r_{X,t}$, respiration rates and measure a net oxygen consumption, OC. This data being used, the following rates and coefficients can be computed.

a/ Specific rate of substrate oxidation at concentration S:

$$r_{X,ox} = r_{X,t} - r_{X,e} \qquad /8/$$

b/ Specific rate of substrate removal at concentration S:

$$r_X = \frac{r_{X,ox}}{OC/S} \qquad /9/$$

c/ Coefficient of substrate oxidation:

$$1 - Y = \frac{OC}{S} \qquad /10/$$

d/ Coefficient of biomass yield:

$$Y = 1 - \frac{OC}{S} \qquad /11/$$

All quantities are expressed in oxygen units.

The respirometric method is so sensitive that even substrate concentrations below 1 mg/l bring about recordable changes in respiration rates. This method was tested by using two types of activated sludge cultivated in hydraulically different systems. The method was also verified by comparing it with the infinite-dilution method proposed by Williamson and McCarty /1975/. Results of these experiments are presented below.

DESCRIPTION OF EXPERIMENTS

Cultivation of Stock Activated Sludge

The activated sludge used for respirometric measurements was cultivated in two 6-l continuously-fed units with the temperature maintained at 20°C. Technological parameters are summarized in Table 11 and both units are schematically illustrated in Fig. 3.

The first unit was a selector-type reactor, which was shown to be capable of suppressing the growth of filamentous microorganisms /Chudoba and co-workers, 1973; Heide and Pasveer, 1974; Lee and co-workers, 1982/. The selector consisted of three small tubes, each having volume of 0.25 litres. As the total working volume of the system was 6 litres, a ratio of V_t/V_i was 24. The second unit was a completely-mixed reactor with the total working volume of 6 litres. The multicomponent substrate solution was dosed by a peristaltic pump. Its composition is given in Table 2. All components were dis-

solved in distilled water because both effluents were used for isolation of refractory organic compounds produced by activated sludge microorganisms.

The excess sludge from both units was periodically used for respirometric measurements carried out with individual components of the mixed substrate.

TABLE 1 Technological Parameters of Activated Sludge Units

Parameter	Units	Selector system	Completely-mixed system
Aeration volume	l	6	6
Volume of settlers	l	1.5	1.5
Retention time	h	24	24
Sludge age	d	4.3	4.3
Recirculation ratio	-	1	1
MLSS	g/l	1.54	1.51
SVI	ml/g	62±13	296±196
Volumetric loading	g/l.d		
BOD basis		1	1
COD basis		1.5	1.5
Sludge loading	g/g.d		
BOD basis		0.65	0.66
COD basis		0.97	0.99

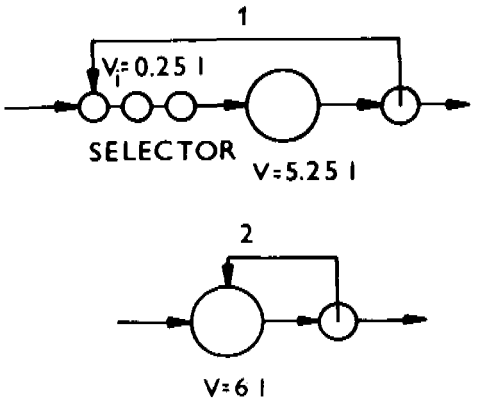

Fig. 3. Schematic outline of laboratory activated sludge units used for stock sludge cultivation. 1-selector system /SE/, 2-completely-mixed system /CM/.

TABLE 2 Composition of Multicomponent Substrate Used for Feeding the Activated Sludge Units

Component		Concentration, mg/l
Valeric acid	/as COD/	300
Glutamic acid	/as COD/	300
Tyrosine	/as COD/	300
Methylalcohol	/as COD/	300
Phenol	/as COD/	300
$NaHCO_3$		300
KH_2PO_4		33.3
$CaCl_2$		27.5
$MgSO_4.7\ H_2O$		30
$FeCl_3.6\ H_2O$		0.38
Trace elements[1/]		à 0.001

1/ Zn,Mn,Co,Cu,Al,Ni,Mo,Cr,Si,F,Sn,I,B.
All components were dissolved in distilled water.
COD-1500 mg/l, BOD_5-1000 mg/l.

Respirometric Measurements

For respirometric measurements, unwashed biomass was used and diluted with effluents when necessary. Initial concentrations of biomass varied from 0.3 to 1.5 g/l. A dose of 1 mg/l of allylthiourea was proved to be sufficient for suppressing totally nitrification. Prior to measuring, the suspension of biomass had been aerated without exogenous substrate at least for one hour.

As measurements with lower substrate concentrations showed higher coefficients of variation, two or three replicates were carried out /not consecutively/ and a mean value was calculated. When calculating values of r_x according to equation /9/, individual values of r_x were divided by a mean value of $r_{x,ox}$ calculated from individual OC/S measurements. Since a slight biomass activation was often observed during measurements, low and high substrate concentrations were alternatively used to equalize this effect.

Analytical Methods

All analyses were carried out according to Standard Methods /APHA, 1976/. Phenol was determined by the p-nitroaniline method.

RESULTS AND DISCUSSION

Relationships between r_x and S are graphically presented for all tested substrates in Figs 4-8.

There exist three methods of linearization of equation /5/, namely:

$$\frac{1}{r_X} = \frac{K_s}{r_{X,m}} \frac{1}{S} + \frac{1}{r_{X,m}} \qquad /12/$$

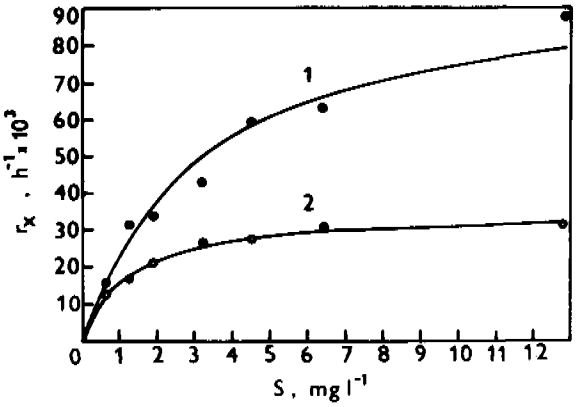

Fig. 4. Relationship between r_X and S for valeric acid. 1-SE, 2-CM.

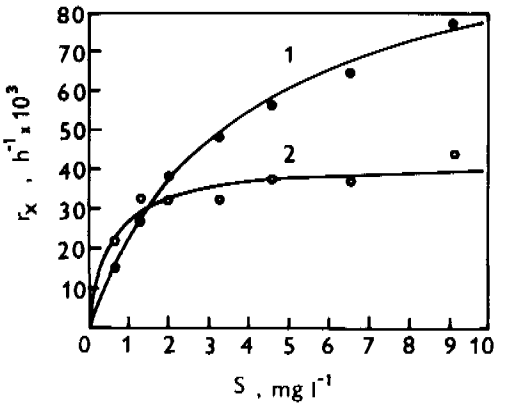

Fig. 5. Relationship between r_X and S for glutamic acid. 1-SE, 2-CM.

$$\frac{S}{r_X} = \frac{K_s}{r_{X,m}} + \frac{S}{r_{X,m}} \qquad /13/$$

$$r_X = r_{X,m} - \frac{r_X}{S} K_s \qquad /14/$$

The last equation was used for computing $r_{X,m}$ and K_s because it seemed to be the best one. Its advantages in comparison with equation /12/ are as follows :

1/ Experimental points are more evenly spread out along the X-axis.
2/ It is less sensitive to the r_X values, which are less accurate, measured at low substrate concentrations.
3/ It is more sensitive to incorrectly measured values, so that they can be easily identified and accordingly omitted.

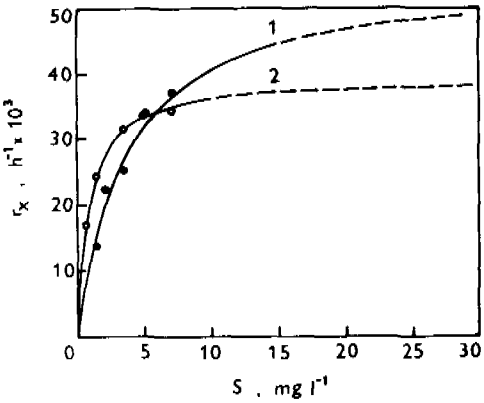

Fig. 6. Relationship between r_X and S for tyrosine. 1-SE, 2-CM.

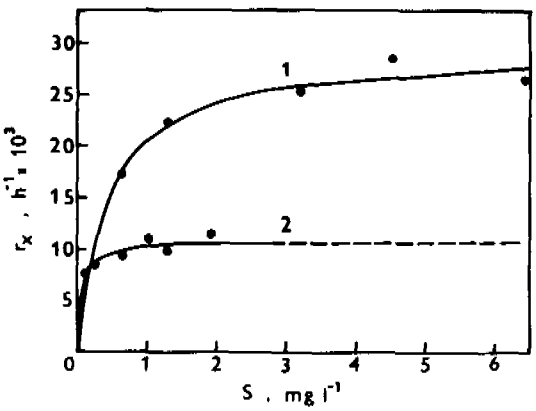

Fig. 7. Relationship between r_X and S for methylalcohol. 1-SE, 2-CM.

With equation /14/, both kinetic constants were computed for individual substrates and mixed cultures. They are summarized in Table 3 together with corresponding correlation coefficients; these vary from 0.83 to 0.99, indicating an acceptable correlation. In Table 3 are also included the coefficients of substrate oxidation, 1-Y, with corresponding coefficients of variation, c_v.

The results presented in Table 3 show that both constants are basically lower with a mixed culture cultivated in the completely-mixed reactor /filamentous/ than with that cultivated in the selector-type

reactor /nonfilamentous/. Thus, the results experimentally proved the hypothesis proposed by Chudoba and co-workers /1973/. The significance of these findings as well as further supporting data will be presented and discussed elsewhere.

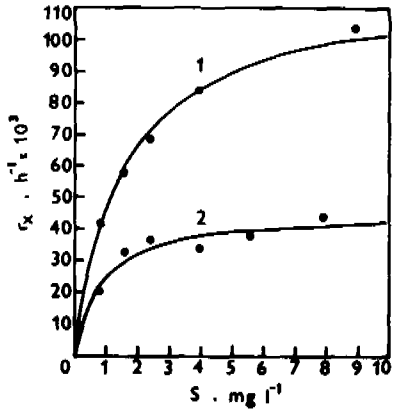

Fig. 8. Relationship between r_X and S for phenol. 1-SE, 2-CM.

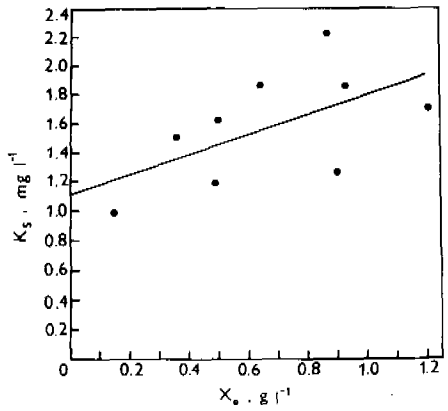

Fig. 9. Relationship between the K_S of phenol determined by the respirometric method and the initial biomass concentration. SE system.

Comparison of the Respirometric and the Infinite-dilution Method

This comparison was carried out with phenol because this can be easily and accurately determined. The results are summarized in Table 4 and show that the respirometric method gives K_S values higher than the infinite-dilution method. It was presumed that this phenomenon could be caused by adsorbing a portion of the substrate on the biomass surface, thus lowering its actual concentration in solution. As the respirometric method is based on the initial sub-

strate concentration calculated and not measured, it cannot reflect this change in solution. In order to prove the adsorption hypothesis, the initial concentrations of phenol were determined in the respirometric cell immediately after injecting a stock solution. The

TABLE 3 Summary of the Results Obtained

Substrate	System	X_o g/l	K_s mg/l	$r_{X,m}$ 3 l/hx10	c_{cor} -	1-Y -	c_{var} %
Valeric acid	SE	1.480	3.20	99	0.93	0.24	16.2
	CM	1.510	1.18	35	0.98	0.28	8.4
Glutamic acid	SE	0.628	3.71	106	0.99	0.25	7.0
	CM	0.768	0.56	42	0.87	0.26	6.8
Tyrosine	SE	0.988	3.66	55	0.85	0.35	7.2
	CM	0.360	0.91	40	0.99	0.40	13.0
Methyl-alcohol	SE	0.832	0.45	30	0.96	0.56	6.5
	CM	0.736	0.06	11	0.83	0.65	12.9
Phenol	SE	0.930	1.49	117	0.98	0.34	6.0
	CM	0.880	0.78	45	0.85	0.44	8.2

TABLE 4 Comparison of the Kinetic Constants of Phenol Determined by two Different Methods

Date /1983/	System	Respirometric method K_s mg/l	Respirometric method $r_{X,m}$ 3 l/hx10	Infinite-dilution method K_s mg/l	Infinite-dilution method $r_{X,m}$ 3 l/hx10
2/23	SE	1.59	44	1.02	44
3/2	SE	1.03	46	0.14	43
3/10	SE	1.77	95	1.10	87
3/15	SE	1.90	127	1.78	183
3/23	SE	1.63	172	1.51	216
4/1	SE	1.20	106	0.32	86
3/21	CM	0.80	77	0.20	66

TABLE 5 Comparison of Calculated /Sc/ and Measured /Sm/ Initial Concentrations of Phenol in the Respirometric Cell

S_c , mg/l	2.28	3.80	5.32	7.60
S_m , mg/l	1.69	2.73	4.08	5.78
Sc/Sm -	1.35	1.39	1.30	1.31

results are presented in Table 5 and show the differences between calculated and measured phenol concentrations to vary from 30 to 40 %. These figures will generally depend on the character of a given substrate.

If the respirometric determination of K_s is influenced by adsorption, then there should exist a relation between the initial biomass concentrations and K_s values. This was really observed as shown in Fig. 9. The substrate adsorption takes place also in the infinite-dilution method. In this case, however, the substrate concentration is determined analytically, so that the actual concentration in solution is always obtained. Though the K_s values obtained by the respirometric method can be expected to be higher than those obtained by the infinite-dilution method, the differences are not so fundamental that these values could not be used for practical purposes.

The K_s values found are much lower than those published by Peil and Gaudy /1971/, but are in good agreement both with those measured by Ghosh and Pohland /1972/ for slow growers and with those measured respirometrically by Painter and co-workers /1968/.

SUMMARY

A respirometric method for measuring kinetic constants of activated sludge microorganisms by means of a simple respirometer was developed and then tested by two types of mixed culture. The main advantages of the method are as follows :

1/ It can be used for those substrates that cannot be easily determined analytically.
2/ It is much more sensitive than the methods based on the biomass growth or substrate removal.
3/ It determines kinetic constants of mixed culture at given technological parameters /loading and mean cell residence time/ without changing its qualitative and quantitative composition.
4/ Practical realization is the simplest of all other methods.

The only disadvantage of this method is that it gives K_s values higher than the comparative infinite-dilution method proposed by Williamson and McCarty /1975/. It has been found that both the maximum substrate removal rate and the half-velocity coefficient are basically lower with the mixed cultures cultivated in a completely-mixed reactor /filamentous/ than with those cultivated in a selector-type reactor /nonfilamentous/.

REFERENCES

APHA /1976/. Standard Methods for the Examination of Water and Wastewater.

Chudoba, J., P. Grau and V. Ottová /1973/. Control of activated sludge filamentous bulking-II. Selection of microorganisms by means of a selector. Water Res., 7, 1389-1406.

Ghosh, S., and F.G. Pohland /1972/. Kinetics of assimilation multiple substrates in dispersed growth systems. Water Res., 6, 99-115.

Heide, B.A., and A. Pasveer /1974/. Oxidation ditch: Prevention and control of filamentous sludge. H_2O /7/, 373-377.

Lamb, J.C.,III, and co-workers /1964/. A technique for evaluating the biological treatability of industrial wastes. J. Wat. Pollut. Control Fed., 36, 1263-1284.
Lee, S-E., B.L. Koopman, D. Jenkins, and R.F. Lewis /1982/. The effect of aeration basin configuration on activated sludge bulking at low organic loadings. Wat. Sci. Tech.,14, 407-427.
Monod, J. /1949/. The growth of bacterial cultures. Ann. Rev. Microbiol., 3, 371-394.
Painter, R.A., R.S. Denton, and C. Quarmby /1968/. Removal of sugars by activated sludge. Water Res., 2, 427-447.
Peil, K.M., and A.F. Gaudy, Jr. /1971/. Kinetic constants for aerobic growth of microbial populations selected with various single compounds and with municipal wastes as substrates. Appl.Microbiol., 21, 253-256.
Vernimmen, A.P., E.R. Henken, and J.C. Lamb,III /1967/. A short-term biochemical oxygen demand test. J. Wat.Pollut. Control Fed., 39, 1006-1020.
Williamson, K.J., and P.L. McCarty /1975/. Rapid measurement of Monod half-velocity coefficients for bacterial kinetics. Biotechnol. Bioeng., 14, 915-924.

Wat. Sci. Tech. Vol.17, Amsterdam, pp.273-278.
Printed in Great Britain.

0273-1223/85 $0.00 + .50

THE POTENTIAL USE OF ENZYMES FOR REMOVAL OF AROMATIC COMPOUNDS FROM WATER

S. W. Maloney, J. Manem, J. Mallevialle and F. Fiessinger

Laboratoire Central, SLEE, 38 rue du Président Wilson, 78230 Le Pecq, France

ABSTRACT

Enzymatic methods have shown promise for removing aromatic compounds from (high strength) industrial waste water. The removal of these compounds was studied at low levels which might be encountered in surface waters which receive some industrial discharge. The results indicate that enzymatic oxidative coupling may be useful in eliminating aromatics which are not well removed in biological or physical water treatment.

KEYWORDS

Biotechnology, enzymatic oxidation, horse radish peroxidase, chlorinated phenol removal, trace organic removal.

INTRODUCTION

An enzymatic method has recently been suggested (Alberti et al. 1981, Klibanov et al. 1980) for the removal of aromatic compounds from water. In this process, wastewaters containing aromatic compounds are treated with horseradish peroxidase (HRP) and hydrogen peroxide. This enzyme catalyzes the oxidative coupling of the dissolved aromatics. The resulting high molecular weight compounds are less soluble in water and can be removed by sedimentation and/or filtration. These studies were conducted at high pollutant concentration (100 mg/L) compared to potable water treatment, where the concentration level for organic compounds is in the ng/L to ug/L range. However, little effect of concentration was noted for one aromatic compound which was studied as low as 0.5 mg/L (Klibanov et al. 1981). Thus, this process may be applicable to drinking water treatment for the removal of aromatic organic pollutants.

Phenolic compounds are examples of aromatic organic pollutants which may arise from a number of sources. They arise from industrial operations such as coking plants and pulp and paper manufacturing (Wolkoff et al. 1974), from wood preservations (Rudling 1970), as well as natural and domestic sources (Baker 1966). Many chlorinated phenolics are toxic (Stanlake et al. 1982, Stecher et al. 1968) and some also present taste and odor problems (e.g., mono and dichlorophenols) in finished drinking water (Smith et al. 1976).

A concern in the use of this enzyme technique for drinking water treatment is the nature of the products of the oxidative coupling, and the fate of these products in the water treatment process. Klibanov and Morris (1981) did not identify specific products but noted that the products were less soluble, high molecular weight polymers. Schwartz and Hutchinson (1981) also noted the formation of biphenyls accounting for 3% of the initial carbon concentration. These would be incomplete polymerization products, but at the low aromatic compound concentrations found in drinking water, they may be the predominant products. Such products may not be removable by sedimentation and/or filtration, and may pass through the treatment process in their altered (polymerized) form.

A further potential problem in drinking water treatment is the presence of competing or interfering compounds. Raw water supplies usually have background organic carbon comprised mainly of humic acids (Mc Carty 1980). Recent data (Pflug 1980) suggest that humic acids may deactivate peroxidase.

The purpose of this paper is to investigate the effectiveness of the peroxidase - hydrogen peroxide system for removal of low levels of phenolic compounds from water. Three compounds, mono-di, and pentachlorophenol, are used as model compounds of aromatic pollutants. The treatment process is characterized both in terms of specific compound removal and removal of its reaction products.

MATERIALS AND METHODS

The phenolic compounds, 2-chlorophenol (2-CP), 2,4-dichlorophenol (2,4-DCP) and pentachlorophenol (PCP) were taken from a phenol test kit (4-4570, Supelco, Inc., Bellefonte, PA). Radio-labelled 2,4-DCP (specific activity = 114 uCi/mg, Amersham International, Amersham, England) was also used to lower the limit of detection, HRP (Type VI, Sigma Chemical Co., St. Louis, MO, E.C. Noo 1.11.1.7) was assayed for activity using the manufacturers' instructions, yielding a value of 250 units per mg. Hydrogen peroxide (30%) was purchased from Prolabo (Paris, France).

The various chlorophenols were mixed in water purified by the Milli-Q system (*Millipore Corp., Bedford, Mass.*) or filtered river water, as noted. Samples of the chlorophenols were placed in 250 ml flasks on a gyratory shaker (Model R 2, New Brunswick Scientific, Edison, NJ). The chlorophenol solution was adjusted to pH 6-7 by a 10 mM phosphate buffer. Peroxide and/or HRP were then added to the solution and the flasks were shaken at 175 ppm for 3 hours. Selected samples were centrifuged (Janetzki K24, Englesdorf, Germany) at 12.000 rpm to remove any suspended material. Afterwards, phenols were analyzed as described below.

High pressure liquid chromatography (HPLC) was used to identify phenols and separate the products of the reaction. The system included a Dupont 870 pump module, 850 absorbance detector and a 4.6 mm X 25 cm Zorbax ODS liquid chromatography column (all from Dupont and Co., Wilminston, DE). Analysis of 2-CP was achieved under the following conditions : mobile phase 33% MeOH in water, while 2,4-DCP and related by products were eluded by application of a binary gradient (0% to 100% of MeOH in water-25 min). For samples of the radio labelled 2,4-DCP, subsamples were collected simultaneously with absorbance detection. These subsamples were analyzed by liquid scintillation counting. Two mL of subsample were mixed with 8 mL of PICO FLUOR 30 and counted on a TRI-CARB 300C (United Technologie Packard, Zurich, Switzerland) liquid scintillation system.

RESULTS

The initial experiments were carried out with pentachlorophenol using the method described by Klibanov and Morris (1981) using 100 mL of PCP, 1 and 5 mM peroxide, and 100 units/L HRP. However, the results did not indicate the 90% removal indicated for other aromatic compounds. At 1 mM the removal was only 15-20%, and at 5 mM the results were only marginally better at 20-30%. Former researchers (Alberti et al, 1980 ; Klibanov et al, 1980 ; Klibanov et al, 1981) had not used PCP, so it was decided to duplicate a formerly successful experiment and confirm the technique.

Table 1 shows the results for several experiments involving 2-CP. The experiments were initiated according to reference Alberti et al (1981), i.e., 1000 units/L HRP, 5 mM peroxide, and 100 mg/L of 2-CP. Although the results did not indicate 99+% removal as previously determined (Alberti et al, 1981), there was substantial removal of 2-CP. Subsequent experiments with 2-CP at lower concentrations indicated that near complete removal (90-95%) of the compound occurred.

TABLE 1 Removal and/or tranformation of 2-chlorophenol by enzymatic oxidative coupling

2-CP (ng/L)	Solvent	Enzyme Concentration units/L	Peroxide Concentration mM	Centrifugation	% Removal
100	Buffer pH7	1000	1	+	75
100	-	1000	1	-	75
100	-	1000	5	+	75-90
100	-	1000	5	-	75-90
10	-	1000	5	+	95
10	-	1000	5	-	95
1	-	1000	5	+	> 95
1	-	1000	5	-	> 95
0.1	-	1000	5	-	> 95
0.01	-	1000	5	-	> 95
0.01	-	100	5	-	> 95
0.01	tap water	100	5	-	> 95
1	Filtered river water	1000	5	-	> 95
0.3	-	1000	1	-	> 95
0.3	-	1000	5	-	> 95
0.3	-	1000	1	-	> 95
0.3	-	100	1	-	> 95

The appearance of a dark precipitate was observed at the higher concentrations as reported in the literature (Klibanov et al, 1981). However, no precipitate was observed for the lower concentrations. Centrifugation did not improve the removal of the 2-CP and was discontinued for most of the experiments, as shown in table 1.

The effects of background organic compounds can also be seen in table 1. Filtered river water was taken from a pilot plant upstream of Paris, France. The total organic carbon (TOC) concentration of this water was approximately 2 mg/L. The results indicate that these background organics, assumed to be humic and fulvic acids, do not interfere with the enzyme reaction, as the removal of the 2-CP is equivalent in Milli-Q water and filtered river water.

The limit of detection of the HPLC method for the chlorophenols is approximately 0.001 mg/L, which is still a high concentration compared to values usually observed in raw water supplies. Furthermore, the method only indicated the disappearance of the 2-CP, and not the appearance of reaction products.

Thus, a set of experiments were conducted with a radio labelled 2,4-DCP. The purpose was to determine a mass balance on the compound and to significantly reduce the limit of detection.

Table 2 shows the results of experiments conducted with the radio labelled 2,4-DCP in tap water and Milli-Q water. This table shows both results only when there was a difference. The differences never exceeded five percent, thus the presence of background organics in the tapwater (organic concentration approximately 2 mg/L) does not appear to interfere with the reaction.

TABLE 2 Removal and/or transformation of 2.4-dichlorophenol by enzymatic oxidative coupling - all values percent removed

2.4-DCP (mg/L)	Enzyme Concentration 100 units/L	100 units/L	10 units/L
240	-	47-42	7-10
120	93-95	-	-
60	> 95	94-92	25-22
24	> 95	95	47-50
10	> 95 (a)	> 95	-
3	> 95	> 95	82-80
0.6	> 95	> 95	> 95
0.06	> 95	> 95	> 95
0.008	> 90	> 90	-
0.0025	> 90	> 90	-

Conditions : Unless otherwise noted, all experiments were run with Milli-Q and tapwater. Where there was a difference, Milli-Q is shown first, e.g. 7% removal at 10 units/L peroxidase and 240 ppa 2,4-DCP. Peroxide concentration is 5 mM. Time of reaction is 3 hours, pH range is 6.5-7.

(a) experiment run at 1 and 5 mM peroxide.

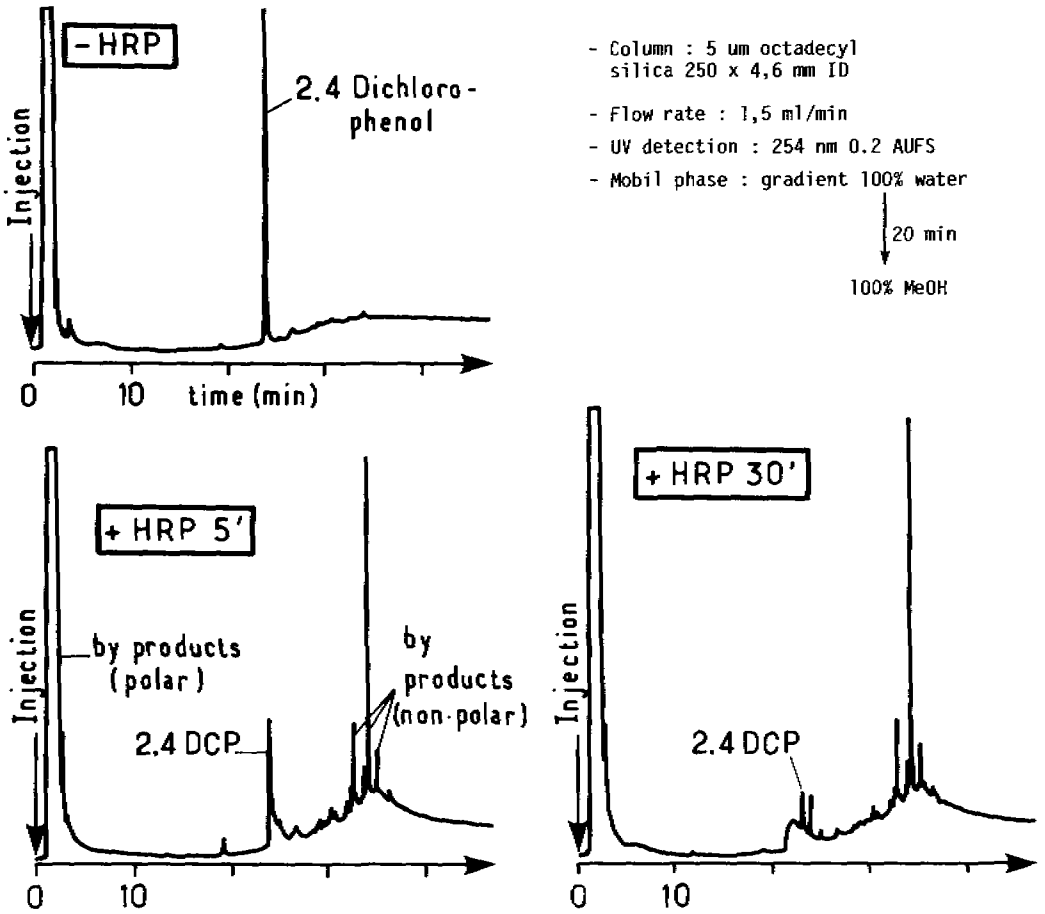

Fig. 1

- At high concentrations, the appearance of several peaks and disappearance of 2,4-DCP is monitored directly on UV absorbance after HPLC. Figure 1 shows an example of chromatograms obtained. The first one corresponds to the 10 mg/L solution of 2,4-DCP before the addition of enzyme . The second and third chromatograms correspond to the remaining 2,4-DCP and related byproducts respectively 5 min and 30 min after the enzyme addition (1000 units/L).

- All concentrations were determined by collecting fractions of the sample after HPLC and analyzing them by liquid scintillation counting. The by-products yield two major fractions, which represent about 65% of the initial radioactivity. They are a highly polar fraction and a high molecular weight non-polar fraction (Figure 1). Further work is needed to determine the potential toxicity and/or mutagenicity of these products.

- Two additional experiments were conducted with and without centrifugation at low 2,4-DCP concentrations (0.1 and 0.0025 mg/l) to determine if the products of the reaction could be removed from the water by settling. The results indicate that the products are not removed but only transformed.

CONCLUSION

The results of these experiments indicate that the peroxidase-peroxide system is effective in eliminating chlorinated phenols at low levels from drinking water supplies, but does not remove their products from the water. Further work is necessary to determine if these by-products present a potential risk for the human health and if they are removed in other unit processes. The enzymatic procedure offers an alternative to the standard treatments, for example for sporadic taste and odor problems associated with chlorinated phenols (Smith et al, 1976).

REFERENCES

Alberti, B.N., and Klibanov, A.M. (1981). Enzymatic removal of dissolved aromatics from industrial aqueous effluents. Biotechnology and Bioengineering Symposium. No.11 John Wiley and Sons, New York, 373-9

Baker, R.A. (1966). Phenolic analyses by direct aqueous injection gas chromatography. J. of American Water Work Association. V. 58, 751-60.

Klibanov, A.M., Alberti, E., Morris, D. and Felshin, L.M. (1980). Enzymatic removal of toxic phenols and anilines from waste waters. J. Applied Biochemistry. V.2, 414-21.

Klibanov, A.M. and Morris, E.D. (1981). Horseradish peroxidase for the removal of carcinogenic aromatic amines from water. Enzyme Microbiology and Technology. 3, 119-22.

McCarty, P.L. (1980). Organics in water...an engineering Challenge. J. Environmental Engineering Division. ASCE. 106, 1.

Pflug, Z. (1980). Effect of humic acids on the activity of two peroxidases. Z. Pflannernechr. Bodenkd. 430-40.

Rudling, L. (1970). Determination of pentachlorophenol in organic tissues and water. Water Research, 4, 533-7.

Schwartz, R.D. and Hutchinson, D.B. Microbial and enzymatic production of 4,4' dihydroxybiphenyl via phenol coupling. Enzyme Microbiology and Technology, (1981), 3, 361.

Smith, J.G., Lee, S. and Netzer, A. (1976). Model studies of aqueous chlorination : the chlorination of phenols in dilute aqueous solutions. Water Research. 10, 985-90.

Stanlake, G.J. and Finn, R.K. (1982). Isolation and characterization of a pentachlorophenol degrading bacterium. Applied and Environmental Microbiology. 44, 1421-7.

Stecher, P.G. et al. The Merck index. Eighth edition, Merck and company, Inc. Rahway, N.J. (1968).

Wolkoff, A.W. and Larose, R.H. (1974). A highly sensitive technique for the liquid chromatographic analysis of phenols and other environmental pollutants. J. of Chromatography. 99, 731-43.

Wat. Sci. Tech. Vol.17, Amsterdam, pp.279-289.
Printed in Great Britain.

0273-1223/85 $0.00 + .50

DEVELOPMENT OF POLLUTANT SPECIFIC MODELS FOR TOXIC ORGANIC COMPOUNDS IN THE ACTIVATED SLUDGE PROCESS

Andrew T. Watkin and W. Wesley Eckenfelder, Jr.

Vanderbilt University, Department of Civil and Environmental Engineering, Box 6222 Station B, Nashville, Tennessee 37235, U.S.A.

ABSTRACT

The concept of pollutant specific models in completely mixed biological recycle reactors is developed. Pollutant specific Monod constants are developed by considering substrate utilization, cell growth, and endogenous decay rates based solely on influent and effluent specific pollutant concentrations. In this way, models are developed which predict specific pollutant removal in biological reactors. Three nonvolatile compounds are evaluated; namely, phenol, 2,4-dichlorophenol, and 2,4-dinitrophenol and their respective specific Monod constants determined. A pollutant specific model for concurrent biodegradation and volatilization is also developed. A mathematical method for evaluating the pollutant specific Monod constants independent of volatilization kinetics is derived for the volatile compounds dinitrobenzene and carbon tetrachloride. Control strategies are discussed which emphasize the rate limiting pollutant concept. Conclusions are drawn as to the applicability and limitations of pollutant specific models.

KEYWORDS

Pollutant specific models; toxic pollutants; volatilization; activated sludge; rate limiting pollutant; minimum attainable effluent concentration.

INTRODUCTION

The majority of research which considers the biological treatability of toxic pollutants has been conducted within the past seven years. This research has been conducted attempting to quantify, categorize, and predict degradation rates of various toxic pollutants in the activated sludge process. The focus of this paper is on the activated sludge process due to its predominate use in the United States, Feiler (1980); however, the basic concepts are applicable to all aerobic biological treatment systems. The overall mechanism for the removal of toxic pollutants is known to be quite complex. For the purpose of constructing a model based on fundamental principles, the removal of toxic pollutants has been broken down into the following three mechanisms:

1) Biodegradation; 2) Absorption onto Solids; 3) Volatilization.

Existing data pertaining to adsorption of toxic pollutants onto solids is sparse and poorly understood. For this reason, this paper will focus on biodegradation and volatilization.

In the past, researchers have largely developed biokinetic data for toxic pollutants using conventional surrogate parameters such as BOD, COD, and TOC to quantify biokinetic constants. This paper will present biokinetic constants for specific toxic pollutants in multisubstrate environments. Modeling methods for both non-volatile and volatile substrates will be developed for several toxic pollutants. The power of pollutant specific models will become quite evident once the reader understands the potential reduction in analytical and process control effort in treatment plant operations.

Pollutant Specific Biological Model

Monod (1949) first developed the equation for single substrate removal by a pure culture in a completely mixed reactor called a chemostat. Monod's basic equation is as follows:

$$\frac{dX}{Xdt} = \mu = \frac{\mu_m S}{K_s + S} \tag{1}$$

where X = biomass concentration, mg/l,
μ = specific growth rate, m^{-1},
S = substrate concentration, mg/l
K_s = saturation constant, mg/l.

The saturation constant is defined as the substrate concentration at which μ is equal to one half the maximum specific growth rate, μ_m. The advantage of the Monod equation is that it mathematically bridges the gap between zero and first order biological kinetics.

Complications arise when wastewaters are encountered with multiple substrates and mixed microbial populations. The difficulty of measuring mixed substrate influent levels has generally been overcome by the use of surrogate parameters such as BOD, TOC, and COD. When studying mixed cultures it is seen that the species are in a continuous state of change with respect to diversity and population. These microbial changes can have a large effect on the observed kinetic growth constants. A method which is widely used to dampen or add capacitance to such a system is the so-called recycle activated sludge reactor. Such a reactor allows the variability of the microbial population to be controlled by controlling the average residence time of the microbes in the reactor.

The appropriateness of Monod kinetics for specific toxic pollutant biodegradation was well illustrated by Tabak and Barth (1978). They demonstrated that the degradation of benzidene in completely mixed reactors ranged between zero and first order with the breakpoint at about 0.5 ppm. Shamat and Maier (1980) found similar behavior in degradation studies of several chlorinated pesticides. It is a reasonable assumption that many toxic pollutants are likely to demonstrate Monod kinetic behavior in the activated sludge process. For this reason, the Monod model will be used in developing a pollutant specific model.

At this point a concept which will become fundamental to the development of a model for toxic pollutant removal in the activated sludge process will be introduced. The concept is quite analogous to the design strategy for nitrification systems, where the nitrifying bacteria are considered to be a fixed proportion of

the active biomass of the system at steady state conditions. This assumption makes use of the idea that a set fraction of the active biomass in a steady state reactor will specifically degrade a given organic compound, and that this pollutant specific fraction of the active biomass will exhibit Monod type reaction kinetics. Therefore, in an activated sludge reactor, if sludge wasting is representative of the entire microbial population, then the ratio of biomass growth attributable to a specific toxic pollutant to that attributable to all substrates will remain fixed. The biological reaction rate, S_o-S/Xt, may then be calculated for a specific toxic pollutant in a mixed substrate feed using the overall mixed liquor volatile suspended solids and the specific toxic pollutant concentrations. Since the ratio of the cell yield coefficients for the specific toxic pollutant to the total substrate is a constant, the excess cell growth will be mathematically absorbed into the biokinetic constants. This assumption theoretically enables one to calculate biokinetic constants which are specific to a toxic pollutant and allows for the prediction of specific toxic pollutant effluent concentrations. The goodness of fit of the resulting model will partially reflect the validity of this assumption.

The mathematics of applying Monod kinetics to a completely mixed continuous flow reactor have been developed by Lawrence and McCarty (1970) and others; the resulting equations are based on both substrate and biomass balances. Once the biokinetic constants have been determined for a specific substrate the following equation can be used to predict the reactor performance for a specific pollutant:

$$S^* = \frac{K_s^*(1+b^*\theta_c)}{\theta_c(Y^*k^*-b^*)-1} \qquad (2)$$

where k^* = maximum pollutant specific substrate utilization rate, $days^{-1}$,
S^* = pollutant specific effluent concentration, mg pollutant/l,
K_s^* = pollutant specific saturation constant, mg pollutant/l,
Y^* = pollutant specific cell yield coefficient, mg VSS/mg pollutant,
b^* = species specific endogenous decay coefficient, $days^{-1}$,
θ_c = mean cell residence time or sludge age, days.

It is important to note that as seen in Equation 2, the effluent specific substrate concentration is solely a function of sludge age at steady state conditions. Biokinetic constants for three nonvolatile toxic organics are presented in Table 1. The 95% confidence limits for these Monod constants ranged from plus or minus 28 to 260% partially due to the low number of data points and numerical error propagation.

TABLE 1 POLLUTANT SPECIFIC MONOD CONSTANTS FOR NON-VOLATILE COMPOUNDS

Compound	No. of Sample Points	k^*, day^{-1}	K_s^*, mg/l	b^*, day^{-1}	Y^*	Calculated Using Data From
2,4-DCP	7	0.18	1.3	0.065	3.1	Fuentes (1982)
2,4-DNP	3	0.38	8.2	0.15	2.9	Kincannon & Stover (1982)
Phenol	6	1.51	0.026	0.29	0.75	Rozich et al. (1983)

Plots of specific pollutant effluent concentration and sludge age are shown in Figures 1, 2, and 3 for phenol, 2,4-dichlorophenol, and 2,4-dinitrophenol, respectively. Fuentes (1982) demonstrated that 2,4-dichlorophenol does not

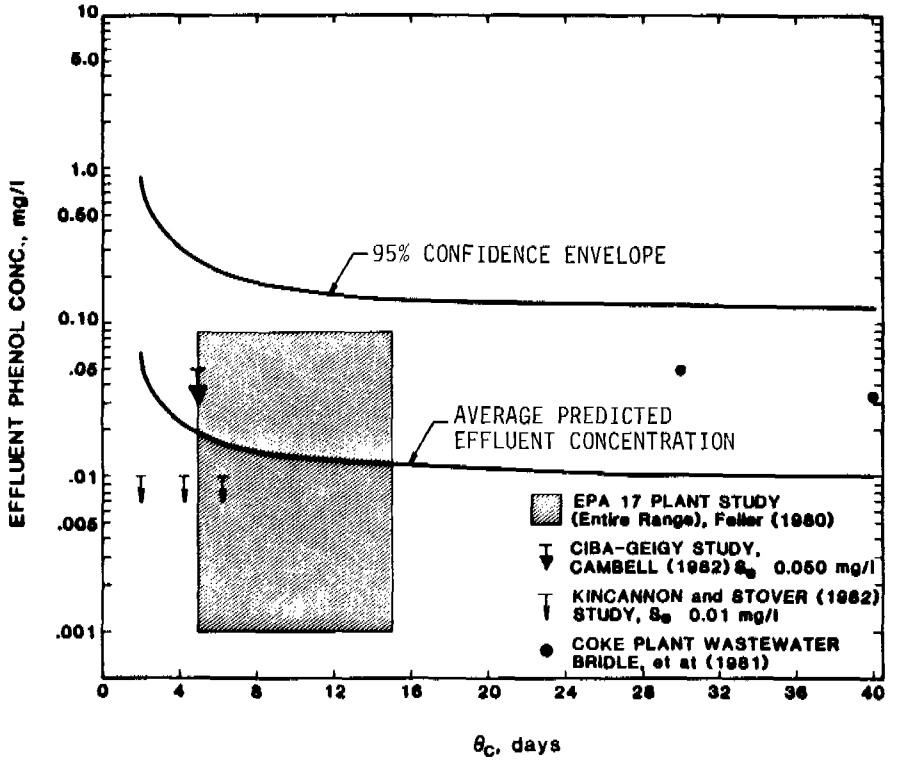

Fig. 1. Effluent phenol concentration versus sludge age

significantly volatilize or adsorb onto biological solids. Volatilization and adsorption were approximately zero and 0.03 percent removal on a throughput basis, respectively, in a reactor with a sludge age of approximately 8 days and a hydraulic retention time of approximately 15 hours. Kincannon and Stover (1982) demonstrated that both volatilization and adsorption were approximately zero for phenol and 2,4-dinitrophenol at sludge ages and hydraulic retention times of approximately 6 days and 8 hours, respectively.

Figures 1 through 3 illustrate that each pollutant has a minimum attainable effluent concentration. This phenomena occurs at sufficiently low specific substrate concentrations when the endogenous decay rate is greater than the specific growth rate. Mathematically, this can be seen by dividing the numerator and denominator of Equation 2 by θ_c and then taking the limit as θ_c approaches infinity which results in the following equation:

$$S^*_{min} = \frac{K^*_s b^*}{Y^* k^* - b^*} \qquad (3)$$

where S^*_{min} = the minimum achievable specific pollutant concentration. This phenomena has also been recognized by Grady and Lim (1980) for surrogate parameters such as BOD, TOC, and COD. It is not readily evident that the minimum attainable substrate concept is entirely applicable to specific toxic pollutants.

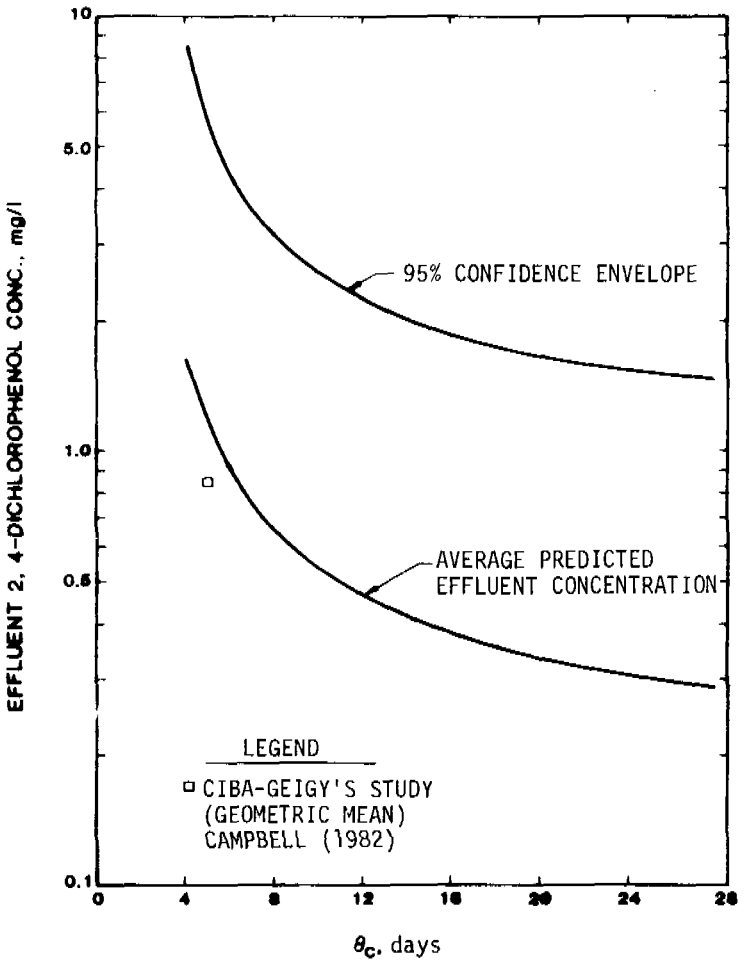

Figure 2 - Effluent 2,4 Dichlorophenol Concentration Versus Sludge Age

However, for consistency Table 2 lists minimum levels of treatment of phenol, 2,4-dichlorophenol, and 2,4-dinitrophenol in the activated sludge process. The 95% confidence limits for these minimum levels ranged from plus or minus 488 to 970% due to the low number of data points and numerical error propagation.

Volatilization

Volatilization or air stripping is known to be a significant removal mechanism for many toxic pollutants in the activated sludge process. The rate of volati-

lization in a completely mixed reactor with steady air flow is known to follow first order kinetics as follows:

$$\frac{dS}{dt} = -K_v S \tag{4}$$

where K_v = overall first order volatilization constant,
S = pollutant concentration in the reactor,
t = time.

Once K_v is identified for a given aeration basin, then Equation 4 can be incorporated with Equation 1 to yield a concurrent biodegradation/volatilization model by using a simple mass balance technique. Therefore, one must first identify methods of determining overall first order volatilization constants for toxic pollutants. This method will be illustrated for both surface and diffused aeration.

TABLE 2 MINIMUM ATTAINABLE EFFLUENT CONCENTRATIONS IN THE ACTIVATED SLUDGE PROCESS FOR SELECTED ORGANIC POLLUTANTS AT INFINITE SLUDGE AGE

Compound	S^*_{min}, mg/l
Phenol	0.0089
2,4-Dichlorophenol	0.17
2,4-Dinitrophenol	1.3

Matter-Müller et al. (1981) and Roberts et al. (1982) have shown through film transfer theory that when the Henry Law constant for a volatile compound is greater than approximate 0.1 (dimensionless) that the liquid film resistance dominates and the relationship between oxygen and volatile organic mass transfer coefficients is described as follows:

$$\beta_i = \frac{K_{L,i}}{K_{L,O_2}} = \left[\frac{D_{L,i}}{D_{L,O_2}}\right]^{\Omega} \tag{5}$$

where β_i = the ratio of the mass transfer coefficients of volatile substance i to oxygen,
$K_{L,i}$ &
K_{L,O_2} = the mass transfer coefficients of substance i and oxygen, respectively,
Ω = the model dependent exponent relating the dependence of K_L on D_L ranging from 0.5 to 1.0.

Roberts et al. (1982) has experimentally found Ω to equal 0.66 on the average for chloroform, trichloroethane, carbon tetrachloride, trichloroethylene, and tetrachloroethylene. Therefore, in actual reactor application we can rewrite Equation 5 by taking advantage of the fact that the interfacial gas-liquid characteristics will be the same for both oxygen and the volatile organic compound of concern in a given reactor as follows:

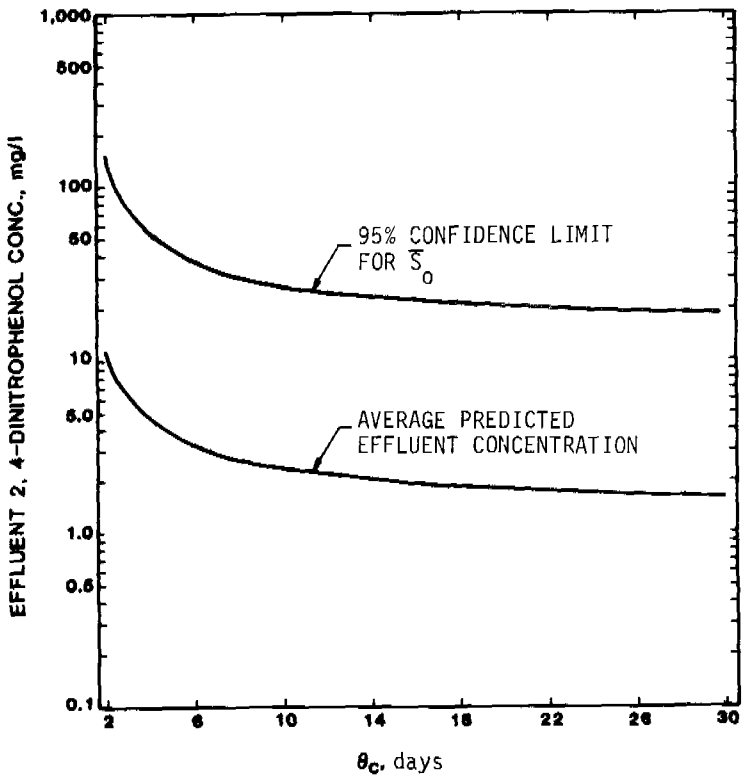

Figure 3 Effluent 2,4-dinitrophenol Concentration Versus Sludge Age

$$\beta_i = \frac{K_{L,i}{}^a}{K_{L,O_2}{}^a} = \left[\frac{D_{L,i}}{D_{L,O_2}}\right]^{.66} \tag{6}$$

where a is the interfacial area per unit volume.

For surface aeration we can write the following mass transfer expression for the volatile compounds in a completely mixed reactor assuming that the equilibrium concentration of the compound in the liquid phase is essentially zero.

$$\frac{dS}{dt} = -\beta_i K_{L,O_2}{}^a S_{L,i} \tag{7}$$

where $S_{L,i}$ is the concentration of compound i in the liquid phase. It is readily apparent that the overall volatilization constant, K_V, described in Equation 4 can be expressed as $\beta_i K_{L,O_2}{}^a$.

For diffused bubble aeration Roberts (1982) develops the following expression for the mass transfer of volatile compounds from a completely mixed reactor:

$$\frac{dS_{L,i}}{dt} = \frac{Q_G H_i}{V_L}\left[1-\exp\left[-\frac{K_{L,i}aV_L}{H_i Q_G}\right]\right]S_{L,i} \qquad (8)$$

where Q_G = volumetric air flow rate
V_L = volume of the reactor
H_i = dimensionless Henry's Law constant.

Here again it is readily apparent that the overall volatilization constant, K_V, as described in Equation 4 can be described as follows:

$$K_V = \frac{Q_G H_i}{V_L}\left[1-\exp\left[-\frac{K_{L,i}aV_L}{H_i Q_G}\right]\right] \qquad (9)$$

Matter-Müller (1981) illustrates that the mass transfer rates of volatile organics in diffused bubble aeration is dependent on both the mass transfer rate coefficient, $K_{L,i}$, and the degree of saturation in the exit gas; while in surface aeration mass transfer rates are restricted only by the mass transfer coefficient. The result is that surface aeration is more efficient in volatile organic compound removal. These conclusions were also substantiated by Roberts, Munz and Dändliker (1982).

Concurrent Biodegradation/Volatilization Model

Few attempts have been made by investigators to model simultaneous Monod biological kinetics and first order stripping kinetics in a completely mixed activated sludge reactor. Such an analysis must begin by considering a mass balance around a completely mixed reactor. Figure 4 illustrates the system boundary for the mass balance.

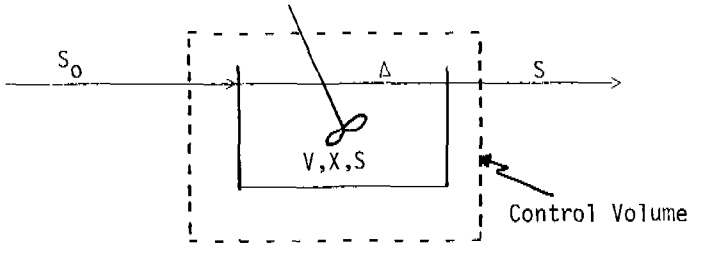

Fig. 4. Control volume for a completely mixed reactor

Considering biological Monod kinetics and first order volatilization the following mass balance can be written for the substrate at steady state conditions:

$$\frac{S_o - S}{\theta} = \frac{kXS}{K_s+S} + K_V S \qquad (10)$$

where θ = hydraulic residence time,
k = the maximum rate of substrate utilization per unit weight of biomass, time^{-1}.

By multiplying Equation 10 by $(K_s + S)$ we get:

$$K_s\left[\frac{S_o-S}{\theta}\right] + S\left[\frac{S_o-S}{\theta}\right] = K_sK_vS + K_vS^2 + kXS \tag{11}$$

By dividing Equation 11 by K_s and grouping constants we obtain,

$$\frac{1}{K_s}\left[S\left[\frac{S_o-S}{\theta}\right] - K_vS^2\right] - \frac{k}{K_s}XS = K_vS - \left[\frac{S_o-S}{\theta}\right] \tag{12}$$

Finally, by dividing Equation 12 by the quantity $S(S_o-S/\theta) - K_vS^2$, we obtain the following linear form:

$$\frac{K_vS - \left[\frac{S_o-S}{\theta}\right]}{S\left[\frac{S_o-S}{\theta}\right] - K_vS^2} = -\left[\frac{k}{K_s}\right]\frac{XS}{\left[S\left[\frac{S_o-S}{\theta}\right] - K_vS^2\right]} + \frac{1}{K_s} \tag{13}$$

It is seen in Equation 13 that by linear regression of the rather complex variables,

$$\frac{K_vS - \left[\frac{S_o-S}{\theta}\right]}{S\left[\frac{S_o-S}{\theta}\right] - K_vS^2} \quad \text{and} \quad \frac{XS}{S\left[\frac{S_o-S}{\theta}\right] - K_vS^2}$$

that the "true" Monod constants, independent of volatilization effects, may be determined. Equation 13 allows for the determination of growth parameters based on actual substrate metabolism in cases where absorption is found to be insignificant.

The effluent concentration for a specific organic compound may be predicted by the quadratic solution of Equation 13 as follows:

$$S = \frac{-\left[K_v + \frac{k}{K_s}X - \frac{S_o}{K_s\theta} + \frac{1}{\theta}\right] \pm \left\{\left[K_v + \frac{k}{K_s}X - \frac{S_o}{K_s\theta} + \frac{1}{\theta}\right]^2 - 4\left[\frac{K_v}{K_s} + \frac{1}{K_s\theta}\right]\left[-\frac{S_o}{\theta}\right]\right\}^{1/2}}{2\left[\frac{K_v}{K_s} + \frac{1}{K_s\theta}\right]} \tag{14}$$

In the above development it should be noted that the cell yield and endogenous decay characteristics are mathematically absorbed into the steady state biomass concentration, X. Biological treatability data from Kincannon and Stover (1982) for nitrobenzene and carbon tetrachloride were analyzed by linear regression of Equation 12 and the resulting Monod constants are reported in Table 3. The 95% confidence limit for this Monod constant ranged between plus and minus 160 to

400% due to the few data points available and numerical error propagation.

TABLE 3 POLLUTANT SPECIFIC MONODS CONSTANTS FOR VOLATILE COMPOUNDS

Compound	No. of Data Points	Degrees of Freedom	k^*,day^{-1}	K_s^*,mg/l
Nitrobenzene	3	1	0.32	3.9
Carbon Tetrachloride	6	4	0.011	0.029

Calculated Using Data From: Kincannon and Stover (1982)

Discussion

The concept of pollutant specific models has significant impact on biological process control. Pollutant specific models allow the designer, operator, and regulator to determine the single pollutant or group of pollutants which are rate limiting in the activated sludge process, provided that the compound is treatable to acceptable standards. Here we can define the rate limiting pollutant(s) as the pollutant(s) which requires the highest sludge age(s) to meet effluent requirements. Note that the rate limiting pollutant could also be a conventional surrogate parameter such as BOD, COD, or TOC. Once the rate limiting pollutant(s) is identified then a treatment plant can monitor only the rate limiting pollutant(s) to insure effluent compliance. This assumes the variability of the influent wastewater characteristics is statistically quantifiable and accounted for when determining the rate limiting pollutant. This simplified operation and design strategy would greatly reduce operating efforts and costs.

The following factors should be considered when using pollutant specific models:

1) The effects of cosubstrate degradation on specific pollutant biokinetic constants needs further study. Due to the relatively poor fit of the model as seen in Figures 1 through 3 it is apparent that the assumption of specific microorganisms which are capable of degrading only a single pollutant is likely to be in error. Therefore, the biokinetic constants require adjustment when different cosubstrates are present. Such an adjustment could likely take the form of coefficients, say α, β, σ, and ζ, which relate the biokinetic constants determined from the test wastewater blend to that of the particular wastewater blend of concern. Equation 2 could then be modified by these coefficients for a particular wastewater of concern as follows:

$$S^* = \frac{\alpha K_s^*(1+\zeta b^*\theta_c)}{\theta_c(\sigma Y^*\beta k^* - \zeta b^*)-1} \qquad (15)$$

Equation (15) is given only for discussion purposes and the method for predicting α, β, σ, and ζ is not readily apparent at this time.

2) The concept of a minimum achievable effluent concentration, S^*_{min}, demands consideration in the design and operation of biological waste treatment processes. If required effluent quality cannot be achieved biologically, then alternate treatment processes must be evaluated.

3) When completely mixed reactors are used the effluent concentration must be below the inhibitory range for each compound considered. This is typically the case in municipal treatment plants; however, for some industrial applications inhibition may be of concern.

4) If adsorption onto biological or other suspended solids is known to be significant, this effect must be considered when developing design models.

5) Mass transfer rates of volatile organic compounds vary greatly depending on the type of aeration device used and should be considered in aerator design.

The use of the pollutant specific models for volatile and non-volatile organic pollutants is recommended where possible. The lack of data and poor correlation of biological kinetic constants greatly limits the present use of such models. However, as more data is collected, compiled, and analyzed, more significance can be placed on the use of pollutant specific models. The rate limiting pollutant concept has tremendous potential in the design, operation, and regulation of biological systems for the removal of toxic pollutants, once a more substantial data base is gathered.

REFERENCES

Beltrame, P.L., Carniti, P. and Pitea, D. (1982). Kinetics of biodegradation of mixtures containing 2,4-dichlorophenol in a continuous stirred reactor. Water Research, 16, 429.

Briddle, T.R., Bedford, W.K. and Jank, (1981). Biological nitrogen control of coke plant wastewaters. Prog. Wat. Tech., 12, Toronto, Pergamon Press.

Cambell, I. (1982) Laboratory scale studies of activated sludge systems containing Ciba-Geigy wastewater. Ciba-Geigy Corp., Cranston, R.I.

Feiler, H. (1980). Fate of priority pollutants in publicly owned treatment works - interim report. U.S. Environmental Protection Agency, EPA-440/1-80-301.

Fuentes, H.R. (1982). The fate of 2,4-dichlorophenol and 4,6-dinitro-o-cresol in continuous flow complete mixed aerobic activated sludge systems. Ph.D. Dissertation, Vanderbilt University.

Grady, C.P.L. and Lim, H.C. (1980). Biological wastewater treatment - theory and applications, Marcel Dekker, Inc., New York.

Kincannon, D.F. and Stover, E.L. (1982). Determination of activated sludge biokinetic constants for chemical and plastic industrial wastewaters. EPA Draft Report, Cooperative Agreement CR-806343-01-02.

Lawrence, A.W. and McCarty, P.L. (1970). Unified basis for biological treatment design and operation. J. Sant. Engr. Div., ASCE, 3, 757.

Matter-Müller, C., Gujer, W. and Giger, W. (1981). Transfer of volatile substances from water to the atmosphere. Water Research, 15, 1271-1279.

Monod, J. (1949). Growth of bacterial cultures. Annual Review of Microbiology, 3.

Rozich, A., Gaudy, A.F. and D'Adamo, P. (1983). Predictive model for treatment of phenolic wastes by activated sludge. Proc. 37th Industrial Waste Conference, Ann Arbor Science, Ann Arbor.

Roberts, P.V., Munz, C., Dänkliker, P. and Matter-Müller, C. (1982). Volatilization of organic pollutants in wastewater treatment-model studies. Draft-EPA Report, Contract No. R-806631.

Roberts, P.V. and Dänkliker, P. (1982). Mass transfer of volatile organic contaminants from aqueous solution to the atmosphere during surface aeration. Submitted to Environmental Science and Technology.

Shamat, N.A. and Maier, W.J. (1980). Kinetics of Biodegradation of Chloronated organics. J. WPCF, 52, 2158.

Tabak, H.H. and Barth, E.F. (1973). Biodegradability of benzidene in aerobic suspended growth reactors. J. WPCF, 552-558.

Wat. Sci. Tech. Vol.17, Amsterdam, pp.291-302.
Printed in Great Britain.

0273-1223/85 $0.00 + .50

THE KINETIC ANALYSIS OF BOD AND NITROGEN REMOVAL IN AN OXIDATION DITCH

Y. Terashima* and M. Ishikawa**

**Dept. of Sanitary Engng., Faculty of Engng., Kyoto Univ., Kyoto City, Japan*
***Dept. of Civil Engng., Faculty of Engng., Yamaguchi Univ. Ube City, Japan*

ABSTRACT

The simultaneous removal of nitrogen as well as organic substances is one of important characteristics of the oxidation ditch process. To describe this phenomena, synthetic kinetic models including the rates of BOD oxidation, nitrification, denitrification, DO and alkalinity changes, and sludge growth were proposed in this study. Rate equations for these mechanisms were mainly based on Monod type kinetics taking into account several limiting effects among these mechanisms. To develop the design procedure, these kinetic models were combined with the tank-in-series model having circulating and back flows. They were analyzed numerically for typical design and operating conditions. From these computer simulations, successful results to explain these complicated phenomena and several design and operating bases were obtained.

KEYWORDS

Oxidation ditch ; kinetics ; BOD oxidation ; nitrification ; denitrification.

INTRODUCTION

Recently in Japan, much attention has been devoted to the oxidation ditch process as a small scale simple sewage treatment process, which is needed especially for the sewage system in rural areas. This process has the following principal advantages : 1) easy maintenance and lower operating cost, 2) less production of excess sludge, and 3) reduction of nitrogen as well as BOD.
The oxidation ditch process circulating the mixed liquor in an oval ditch is one of many activated sludge processes. The main operating conditions and representative values are BOD loading : 0.1-0.2 kgBOD/m^3.day, BOD·SS loading : 0.03-0.05 kgBOD/kgSS·day, MLSS : 3000-4000 mg/l, sludge retention time : 15-30 days, aeration time : 24-48 hours, return sludge ratio : 50-150%. The removal efficiencies reported are 90-95% of BOD and SS, 50-90% of Total-N, and 30-60% of Total-P.
The stable and relatively high removal efficiency, especially for BOD and nitrogen, can be explained by the following facts :
1) The circulating flow is steady and concentrations are stable and low, because

the feed is diluted 50-300 times with the circulating mixed liquor.
2) The DO distribution decreasing in the flow direction, that gives a suitable condition to denitrifying bacteria, is established by using a brush or caged rotor aerator placed across the ditch at only one or two positions.
3) Nitrifying and denitrifying bacteria are hardly washed out, because the less the amount of excess sludge becomes, the larger the sludge retention time (SRT) becomes.
Although the oxidation ditch process has noticeable characteristics, the mechanism of removal is very complicated, and the modeling of the phenomena has not been established, because BOD oxidation, nitrification, and denitrification occur concurrently and successively.
These reactions are concerned with many factors such as DO, pH, temperature and alkalinity among others, as shown in Table 1.

Table 1 Factors Influencing BOD oxidation, Nitrification & Denitrification

	Temperature	pH	DO	Alkalinity	BOD	NH_4	NOx	Biomass
BOD oxidation	○	○	○		○			○
Nitrification	○	○	○	○		○		○
Denitrification	○	○	○		○		○	○

○ : large influencing factor

The oxidation ditch process for BOD and nitrogen removal can be regarded as the process having both of the functions of a single sludge nitrification-denitrification process and an extended aeration process. Therefore, the modeling of kinetics is performed based on Ishikawa's study [1] of the nitrification and denitrification in nightsoil treatment and Batchelor's research [2] on a single-sludge system .

KINETIC DEVELOPMENT

In biological waste water treatment, the metabolic reactions of oxidized, nitrified, nitrafied, denitrafied, and denitrified bacteria could be fifteen, as shown in Table 2, corresponding to their respiration, growth, and endogenous respiration stages. For the oxidation ditch process in which all of these reactions are probable, however, it is difficult and impractical to develop the kinetic models based on all of them. Therefore, the following assumptions are taken as practical simplifications :
(A) Bacteria biomass is not considered in every species. The sum of all bacteria is regarded as one kind of the biomass to be considered. Every species of bacteria in the biomass acts as a metabolic tissue.
(B) The sum of nitrite and nitrate is indicated as NOx, which is only one form of oxidized nitrogen. Because high nitrite concentrations are not usually observed in the oxidation ditch process, the rates of nitrification and denitrification are taken to be proportional to the removal rates of ammonia and NOx, respectively.
From these assumptions, fifteen metabolic reactions in Table 2 can be reduced to nine, consisting of oxidizing, nitrifying and denitrifying reactions.

BOD removal

For an ordinary activated sludge process, the kinetic model of BOD removal has almost been established by many investigators. For the single reactor in which

Table 2 Classification of Metabolic Reaction

	Respiration	Growth	Endogenous Resp.
Aerobes	$C_xH_yO_z$ (BOD) + O_2 → K_{11}, X_1 → CO_2 (NH_3) + H_2O	$C_xH_yO_z$ + NH_3 + O_2 → K_{12}, X_1+dX_1 → CO_2 + H_2O	O_2 → K_{13}, X_1-dX_1 → CO_2 NH_3 + H_2O
Nitrite B.	NH_3 + O_2 → K_{21}, X_2 → NO_2 + H^+, H_2O	NH_3 CO_2 + O_2 → K_{22}, X_2+dX_2 → NO_2 + H^+, H_2O	O_2 → K_{23}, X_2-dX_2 → NO_2 CO_2 + H^+, H_2O
Nitrate B.	NO_2 + O_2 → K_{31}, X_3 → NO_3	NH_3 NO_2 CO_2 + O_2 → K_{32}, X_3+dX_3 → NO_3 + H^+, H_2O	O_2 → K_{33}, X_3-dX_3 → NO_3 CO_2 + H^+, H_2O
Denitrite B.	NO_3 + $C_xH_yO_z$ → K_{41}, X_4 → NO_2 + CO_2, H_2O	NO_3 + $C_xH_yO_z$ → K_{42}, X_4+dX_4 → CO_2 + H_2O OH^-	NO_3 → K_{43}, X_4-dX_4 → NO_2 + CO_2, H_2O
Denitrate B.	NO_2 + $C_xH_yO_z$ → K_{51}, X_5 → N_2 + CO_2, H_2O OH^-	NO_2 + $C_xH_yO_z$ → K_{52}, X_5+dX_5 → CO_2 + H_2O OH^-	NO_2 → K_{53}, X_5-dX_5 → N_2 + CO_2, H_2O OH^-

BOD removal and denitrification occur concurrently, however, it is necessary to take further into account the loss of BOD that is caused by the denitrification, as shown by the mass balance equation (1).

The sum of BOD removed = (the loss by oxidation) + (the loss by denitrification) (1)

The kinetic model for this case, therefore, is expressed as follows, based on the Monod type kinetics :

$$\frac{1}{X}\frac{dS}{dt} = -\frac{Us \cdot S}{Ks + S}\frac{DO}{Ko + DO} - \alpha \left(\frac{dC_3}{dt}\right)_B \qquad (2)$$

where X : biomass of MLVSS (mg/l)
S : concentration of BOD (mg/l)
Us : maximum rate of BOD removal (hr^{-1})

Ks : saturation coefficent for BOD (mg/l)
DO : concentration of dissolved oxygen (mg/l)
Ko : saturation coefficient for DO (mg/l)
(dC_3/dt) : rate of denitrification
α : exchange coefficient (g/g)

As indicated by the right hand first term, BOD oxidation is influenced by the DO concentration. This idea has been adopted by a few scholars[3]. The right hand second term is introduced based on the above consideration. The exchange coefficient can be calculated by the following equations :

$$(CH_2O)_6 + 8NO_2 \longrightarrow 4N_2 + 2H_2O + 6CO_2 + 8OH \qquad (3)$$

$$5(CH_2O)_6 + 24NO_3 \longrightarrow 12N_2 + 18H_2O + 30CO_2 + 24OH \qquad (4)$$

When nitrite and nitrate are denitrified, the theoretical oxygen demands (ThOD) in Eq.(3) and (4) are calculated to be 1.71 and 2.85 g per nitrogen unit gram, respectively. By assuming that BOD is equal to 2/3 ThOD, the exchange coefficients become 1.14 and 1.90 respectively.

Nitrification

Nitrifying bacteria are autotrophic and perform respiration. The nitrifying reaction rate is usually expressed by Monod's kinetics.

$$-\frac{dN}{dt} = \frac{Un \cdot N}{Kn + N} \qquad (5)$$

where dN/dt : the rate of nitrification (mg/l·hr)
Un : maximum rate of ammonia removal (hr^{-1})
Kn : saturation coefficient for ammonia (mg/l)
N : concentration of ammonia (mg/l)

In most cases, the Kn value is small (0.5-2 mg/l). Therefore, this rate can be shown as a zero-order reaction.

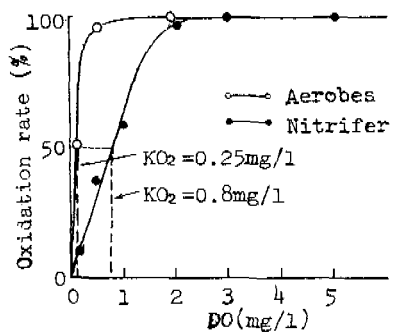

Fig.1 The effect of DO on the rate of oxidation by Aerobes and Nitrifer

The relationship between the nitrifying rate and the DO concentration is shown in Fig.1. The nitrifying rate is largely influenced by dissolved oxygen. When DO is below 0.2 mg/l, the nitrifying reaction occurs very slowly, but when DO is more than 2.0 mg/l, it proceeds rapidly.
Although the influence of pH on nitrification has been investigated extensively,

the influence of alkalinity has scarcely been studied.

Fig.2 The effect of alkalinity on the nitrification rate

From Fig.2, which was obtained by the authors [4] from experiments on nitrification and denitrification in an aeration tank, it is observed that the nitrifying rate decreases at an alkalinity below 150 mg/l. Almost all of the waste water in Japan shows an alkalinity below 150 mg/l.
Consequently, the authors propose the following kinetic model taking account of the influences of DO and alkalinity :

$$\frac{1}{X}\frac{dC_1}{dt} = -\frac{U_1 \cdot C_1}{K_1 + C_1}\cdot\frac{DO}{Ko + DO}\cdot\frac{A}{Ka + A} \qquad (6)$$

where C_1 : concentration of ammonia-nitrogen (mg/l)
U_1 : maximum rate of nitrification (hr^{-1})
K_1 : saturation coefficient for nitrification (mg/l)
Ko : saturation coefficient for DO (mg/l)
A : concentration of alkalinity (mg/l)
K_a : saturation coefficient for alkalinity (mg/l)

U_1 and K_1 are the same as Un and Kn, respectively. The value of K_a obtained from Fig.2 is 100 mg/l.

Overall change of NOx-N

It is stressed that denitrification, such as that observed in the oxidation ditch or aerobic digestion processes, takes place concurrently with nitrification, in one reactor. Many investigations including that of Pasveer [5] and the authors [1] have shown this fact. On this point, the oxidation ditch process differs fundamentally from the separated processes for nitrification and denitrification. From these considerations, combining the nitrification rate shown by Eq.(6) and denitrification rate described below , the overall change of NOx-N can be expressed as follows:

$$\frac{1}{X}\frac{dC_2}{dt} = \frac{U_1 \cdot C_1}{K_1 + C_1}\cdot\frac{DO}{Ko + DO}\cdot\frac{A}{Ka + A} - \frac{U_2 \cdot C_2}{K_2 + C_2}\cdot\frac{S}{Ks + S}\cdot\left(1 - \frac{DO}{Ko + DO}\right) \qquad (7)$$

where C_2 : NOx-N (mg/l)
U_2 : maximum rate of denitrification (hr^{-1})
K_2 : saturation coefficient for denitrification (mg/l)

Denitrification

Denitrifying microorganisms are facultative and heterotrophic bacteria which need

organic carbon for denitrification. In the oxidation ditch process, a portion of the organic substances in the influent and mixed liquor is consumed as the electron donor. Consequently, the denitrification in an oxidation ditch is probably influenced by the relatively low concentration of BOD. On the other hand, many studies on denitrification indicate that there exists DO inhibition. Bauman[7] maintained that the DO concentration of 0.5 mg/l was the highest limit for denitrification. Sharma et al [8] showed that the influence of DO could be based on Monod type kinetics, and they obtained the saturation coefficient (Ko) of 0.1 mg/l.

From these considerations, the nitrogen gas generation by denitrification can be shown as follows assuming Monod type kinetics for NOx-N, BOD and DO :

$$\frac{1}{X}\frac{dC_3}{dt} = \frac{U_2 \cdot C_2}{K_2 + C_2}\cdot\frac{S}{Ks + S}\cdot\left(1 - \frac{DO}{Ko + DO}\right) \qquad (8)$$

Sludge growth and DO and alkalinity changes

As indicated above, the concentrations of sludge as biomass and DO are principal factors controlling the rate of BOD oxidation, nitrification and denitrification. Also, alkalinity is closely related to nitrification. The changes of these are written as follows :

$$\frac{dX}{dt} = a\left(\frac{dS}{dt}\right)_B + b\left(\frac{dC_1}{dt}\right)_B + c\left(\frac{dC_3}{dt}\right)_B - dX \qquad (9)$$

$$\frac{d\,DO}{dt} = -a'\left(\frac{dS}{dt}\right)_B - b'\left(\frac{dC_1}{dt}\right)_B - d'X + K_La\,(DO_S - DO) \qquad (10)$$

$$\frac{dA}{dt} = -e\left(\frac{dC_1}{dt}\right)_B + f\left(\frac{dC_3}{dt}\right)_B \qquad (11)$$

where
- a : yield coefficient of the removal of BOD
- b : yield coefficient for nitrification
- c : yield coefficient for denitrification
- d : microbial decay coefficient (hr^{-1})
- a' : oxygen-use coefficient for BOD oxidation
- b' : oxygen- use coefficient for nitrification
- d' : oxygen- use coefficient for energy of maintenance (hr^{-1})
- K_La : over-all oxygen transfer rate (hr^{-1})
- DOs : saturation concentration of dissolved oxygen
- e : decrease of alkalinity for nitrifying
- f : increase of alkalinity for denitrifying

The Eq. (9) consists of the rate of biomass sludge growth from BOD oxidation , nitrification, and denitrification and the rate of biomass consumption by endogenous respiration. The values of the coefficients a,b,c,d were obtained from the literature[1)-4)] on the treatment of domestic waste water. Eq. (10) shows that the change of DO comes from the BOD oxidation, nitrification, sludge decay, and oxygen supply. In the case of the oxidation ditch process, it must be noticed that the waste water is aerated partially and that overall oxygen transfer rate coefficient K_La reflects the effect on oxygen transfer from the water surface as well as from the aerator. The Eq.(11) represents the alkalinity change due to consumption by nitrification and production by denitrification. These biochemical reactions are shown as follows :

$$NH_4 + 2O_2 + 2HCO_3 \longrightarrow NO_3 + 2H_2CO_3 + H_2O \qquad (12)$$

$$16NO_3 + 3(CH_2O)_6 \longrightarrow 8N_2 + 28CO_2 + 20H_2O + 16OH \qquad (13)$$

From Eq.(12) and (13), the alkalinity consumption and production are

calculated to be 7.14 and 3.57 g as $CaCO_3$ per unit gram of nitrogen, respectively.

MIXING DESCRIPTION

Another important problem concerned with the oxidation ditch process is the description of the mixing regime. Mixing in an aeration tank is classified into four types, complete mixing, plug-flow, tank-in-series, and dispersion models. For the oxidation ditch process, it is necessary to take account of the back-flow as well as the circulation flow, as shown in Fig.3.

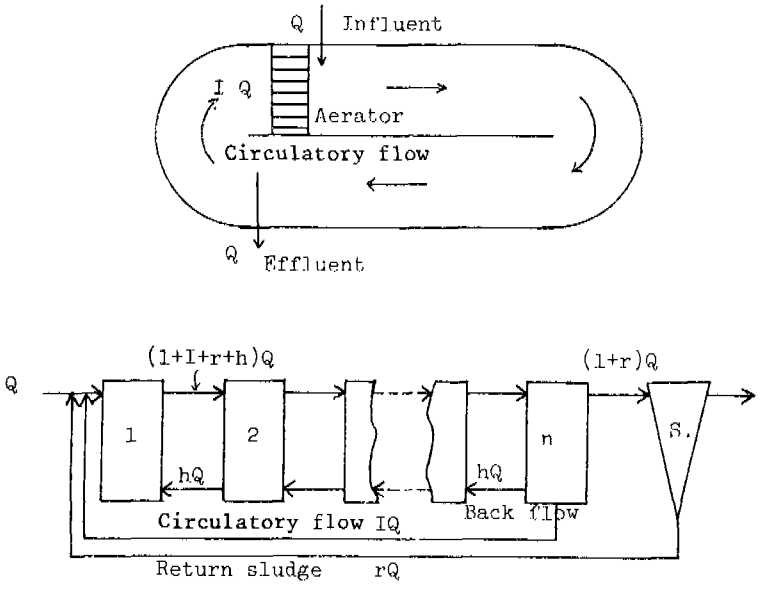

Fig.3 Schematic of oxidation ditch and tank-in-series model

Therefore, the authors adopted the following mixing model proposed by Ishikawa one of the authors, which is the tank-in-series model including back-flow :

Material balance

The first tank

$$\frac{V}{n}\frac{dC}{dt} = Q\{C_0 + (I + r)C_n + hC_2 - (1+h+I+r)C_1\} \qquad (14)$$

The i th tank

$$\frac{V}{n}\frac{dCi}{dt} = Q\{(1+h+I+r)C_{i-1} + hC_{i+1} - (1+2h+I+r)C_i\} \qquad (15)$$

The n th tank

$$\frac{V}{n}\frac{dCn}{dt} = Q\,(L+h+I+r)(C_{n-1} - C_n) \qquad (16)$$

Initial conditions

$$Ci = 0 \quad \text{at } t=0$$
$$C = C^{\bullet}\, V/Q\ \delta(t) \quad \text{at } Ci \neq 0 \qquad (17)$$

where C , Ci, Cn : concentrations of 1st, i th, and n th tank (mg/l)
V : tank volume (m^3)
n : tank number
C˜ : average concentration in the tank (mg/l)
$\delta(t)$: Dirac's δ function
Q : feed-flow (m^3/day)
I : circulation flow ratio
h : back-flow ratio
r : return sludge ratio

For the ditch divided into ten tanks, the degree of mixing was calculated by these equations and the Dirac's delta response method.

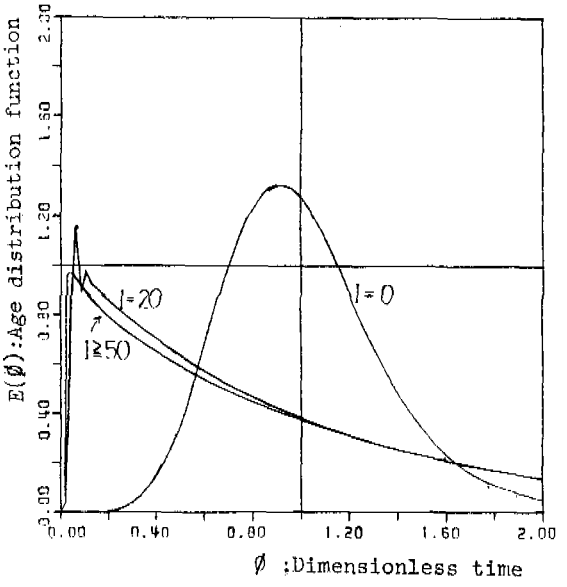

Fig.4 Delta response for circulation flow (n=10.0, h=0.0)

Fig.4 shows the concentration responses to the delta input under several circulation-flow ratios (0-50 Q). These indicate that the mixing in the oxidation ditch process is similar to complete mixing. However, the complete mixing model can't be adopted because of the boundary condition of the tank-aeration.

COMPUTER SIMULATION

The change of waste water quality in the oxidation ditch was simulated on the basis of the rate and mixing models indicated above using computer techniques. Kinetic coefficients for the rate models were obtained from the literature[2)-4)] and related studies by the authors[1)]. Table 3 presents kinetic and stoichiometric coefficients. Influent waste water quality and other design and operating conditions were assumed as shown in Table 4, by taking into account usual instances.

Also, it was assumed in these simulations that the oxidation ditch consisted of five completely mixed tanks in series with circulation and back-flows, that only the first tank was aerated, and that the excess sludge was not withdrawn from the settling tank.

Based on these assumptions, several factors related to optimum design and

retention time (SRT), the positions of the influent, effluent and aeration, and others were discussed.

Table 3 Kinetic and Stoichiometric Coefficient

Us	(hr^{-1})	0.2 [1)—5)]	b	(-)	0.17 [3), 4)]
U_1	(hr^{-1})	0.03 [1)—5)]	c	(-)	- [3), 4)]
U_2	(hr^{-1})	0.02 [1)—5)]	d	(hr^{-1})	0.002 [3), 4)]
Ks	(mg/l)	100 [1)—5)]	a'	(-)	0.34 [3), 4)]
K_1	(mg/l)	0.5 [1)—5)]	b'	(-)	4.57 [3), 4)]
K_2	(mg/l)	0.1 [1)—5)]	d'	(hr^{-1})	0.0008 [3), 4)]
Ko	(mg/l)	0.1 [1)—5)]	K_La	(hr^{-1})	2-3
K_A	(mg/l)	100.0 [5)]	DOs	(mg/l)	8.0
θ	(-)	1.14-1.90	e	(-)	7.14
a	(-)	0.70 [3), 4)]	f	(-)	3.57

Table 4 Influent quality and design conditions

Influent		value	Design condition		value
BOD_5	S_0	200 mg/l	Feed flow	Q	1 Q m^3/day
NH_4-N	C_1	50 mg/l	Volume	V	6 -36 Q m^3
NOx-N	C2	0 mg/l	Circulate flow	I	100 Q m^3/day
N_2 -N	C_3	0 mg/l	Return sludge	r	1 Q m^3/day
Alkalinity	A	150 mg/l	MLSS	X	3000 mg/l
SS	X	0 mg/l	Over all oxygen transfer rate	K_La	2 hr^{-1}
DO	DO	0.01 mg/l			

RESULT AND DISCUSSION

The results of the simulation of the change of water quality in the five tanks in series were shown in Fig.5-10. It is observed that BOD, NH_4-N, and NOx-N or alkalinity, respectively, increase or decrease little in the flow direction. The oxidation ditch seems to be a completely mixed tank. However, it is noticeable that DO decreases from the first tank aerated to the last tank, especially in the cases of large hydraulic retention times. Figure 11 shows the relationships between the water quality in the last tank and HRT. In the case of DO, the concentration also in the first aerated tank is shown in this figure. The value of BOD decreases with the increase of HRT for this continuous system. The same holds true for the first order reaction as expected for the Monod reaction in the relatively low concentration region. The concentration of NH_4-N is reduced together with alkalinity by nitrification in the region of HRT less than about 20 hours. Beyond this, it increases again because the decrease of alkalinity limits the rate of nitrification, as observed in Japan where the alkalinity of sewage is relatively low. The concentration of NOx-N increases with HRT to a plateau state. A very low concentration of NOx-N at a small HRT indicates the occurrence of denitrification, and the high plateau concentration at a large HRT indicates that denitrification as well as nitrification are inhibited, mainly because of the increase of DO and the decrease of alkalinity, respectively. As a result, the concentration of total nitrogen (T-N) as the sum of NH_4-N and NOx-N decreases and then increases with HRT. To obtain a better understanding, the relationships

between the removal ratios of BOD, NH -N and T-N and the hydraulic retention time are shown in Fig.12.

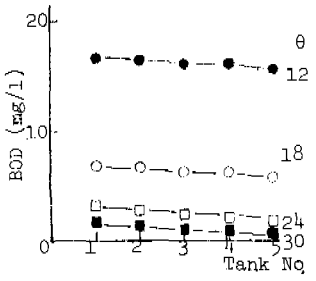

Fig. 5 Change of BOD in tank-in-series model (Retention time θ ;hrs)

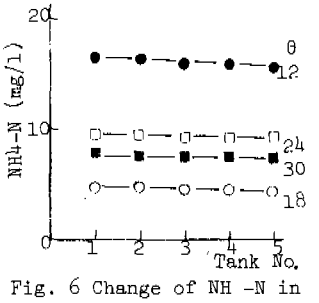

Fig. 6 Change of NH -N in tank-in-series model (Retention time θ ;hrs)

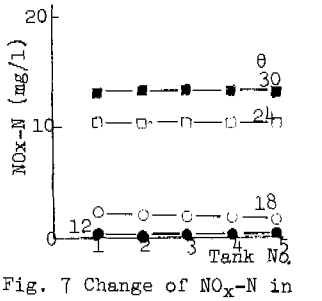

Fig. 7 Change of NO_x-N in tank-in-series model (Retention time θ;hrs)

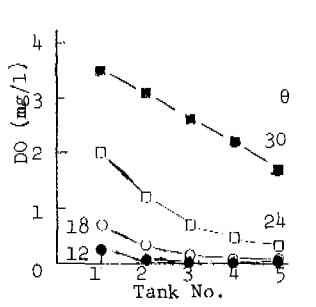

Fig. 8 Change of DO in tank-in-series model (Retention time θ ;hrs)

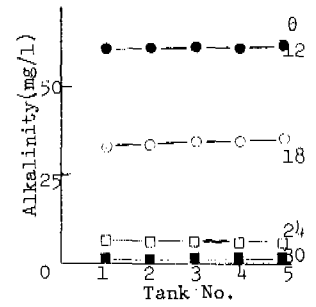

Fig. 9 Change of alkalinity in tank-in-series model (Retention time θ ;hrs)

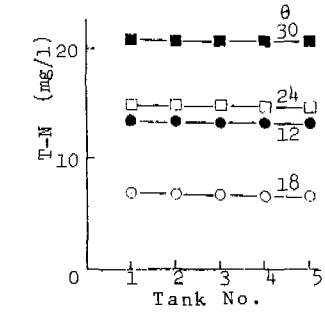

Fig. 10 Change of T-N in tank-in-series model (Retention time θ ;hrs)

Based on the above simulation results, several analyses were performed as follows:

(1) Tank volume and other design and operating criteria

The tank volume of an oxidation ditch is usually decided on the basis of empirical HRT, BOD loading or nitrogen loading. By performing simulations as indicated above, however, it is possible to decide the HRT and tank volume so as to ensure the removal efficiencies needed for both BOD and nitrogen. In this simulation, the HRT to maintain both a 90% removal of BOD and 80% for T-N is between 13 and 23 hours, as shown in Fig.11. Using the influent concentrations and these HRT values, the loadings of BOD, BOD·SS, T-N, and T-N·SS are calculated to be 0.23-0.37 kg/m^3·day, 0.08-0.12 kg/kg·day, 0.06-0.09 kg/m^3·day, and 0.02-0.03 kg/kg·day, respectively. These would be useful indications for practical designs.

(2) Method of aeration

Many kinds of aerators have been recently developed. In order to remove nitrogen as well as BOD, however, any aerator needs to establish such an oxygen distribution decreasing in the flow direction like that for a HRT of 24 or 18 hours as shown in Fig.8. The DO to maintain both the 90% removal of BOD and 80% removal of T-N is estimated to be in the range of 0.3-2 mg/l in the first tank and almost zero in the last tank. Therefore, it isn't efficient to supply excess oxygen and also to use two aerators for nitrogen removal.

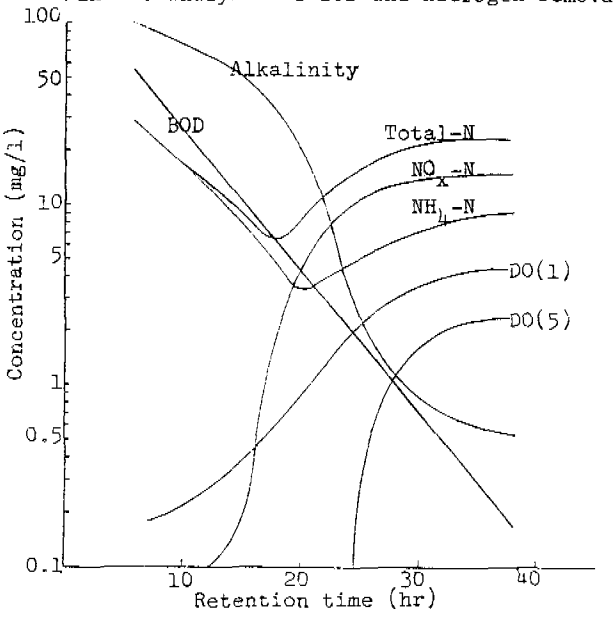

Fig. 11 The relationship between retention time and water quality in the 5th tank.(DO;in the 1st and 5th tanks)

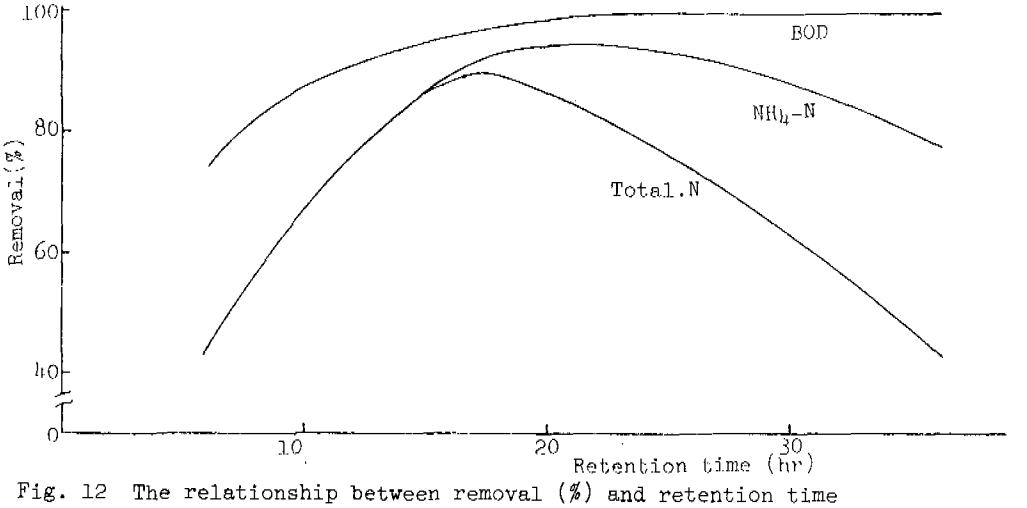

Fig. 12 The relationship between removal (%) and retention time

(3) Effect of alkalinity

The reduction in alkalinity has a large effect on the nitrification of NH_4-N, and consequently on the denitrification of NOx-N. In Fig.10, it can be observed that the alkalinity corresponding to the minimum NH_4-N concentration is about 20 mg/l, and that an alkalinity less than 20 mg/l makes the nitrification rate smaller. It is obvious that the alkalinity at any HRT comes from the equilibrium of production and consumption by denitrification and nitrification, respectively.

(4) Positions of influent and effluent

From the above discussions, it seems effective to introduce raw waste water into the ditch at a position which has low DO and high NOx-N concentrations, to

promote denitrification. By an additional simulation, it was shown that the maximum removal ratio of T-N could be improved by 5% when introducing it to the last tank.

(5) Sludge growth rate and sludge retention time (SRT)

The sludge growth rate and SRT are also significant factors in the oxidation ditch process. In this simulation, the calculated values are in the range of 40-70 mg SS/day and 43-70 days, respectively. Such large values of HRT assure enough holding of the nitrifiers without washing out from the ditch.

CONCLUSIONS

The oxidation ditch process can be characterized fundamentally by its inherent simultaneous reactions of organic substrates and nitrogen, and by its flow and mixing patterns. In this work, synthetic kinetic models including the rates of BOD, oxidation, nitrification, denitrification, DO and alkalinity changes, and sludge growth were proposed, mainly based on Monod type kinetics and several limiting effects among these phenomena. Then the tank-in-series model with circulation and back-flow was combined with these kinetic models to form predictive models.

The results obtained from computer simulations for the typical design and operating conditions are as follows : (1) Predictive models proposed can reasonably explain the change of waste water quality in the oxidation ditch ; (2) The oxidation ditch can be regarded as an almost completely mixed tank, except for DO ; (3) There is an optimum hydraulic retention time for the removal of NH_4-N or T-N ; (4) For the simultaneous removal of BOD and T-N or NH_4-N, one point aeration would be better to establish the distribution of DO, decreasing to almost zero at the end of the flow. Also the introduction of waste water before aeration is effective ; (5) Alkalinity has a large effect on nitrification. Low alkalinity at a large HRT causes the increase of NH_4-N and T-N ; (6) For the assumed treatment requirements of the removal efficiency more than 90 and 80 % respectively for BOD and T-N, the design criteria of HRT was obtained to be 13-23 hours in this study. Also other suggestive design criteria were obtained.

ACKNOWLEDGMENT

The authers would like to express their acknowledgment to Dr. H.Nakanishi for his advice, and to Mr.H.Ozaki for his help on the computer simulations.

REFERENCES

1) Ishikawa,M. and Nakanishi,H. (1983). Proc. of Environ.&Sani. Eng. Research, Japan Society of Civil Eng.,19,196-206
2) Batchelor,B. (1982). J.WPCF 54,1493-1504
3) Hashimoto,S. and Furukawa,K. (1978). J.Japan Sewage Work Association, 15, (175),20-29
4) Ishikawa,M. (1983).The Most Simplified Nitrogen Removal System, The Report of Japan Iron Steel Association.
5) Pasveer,A. (1960). " Waste Treatment " P.C.G.ISAAC
6) Sharma,B. and Ahlert.R.C. (1977). Water Research,11,897-925
7) Bauman,R.E. (1975)," Process Design mannual for Nitrogen Control ",EPA.

Wat. Sci. Tech. Vol.17, Amsterdam, pp.303-311.
Printed in Great Britain.

0273-1223/85 $0.00 + .50

STEADY STATE MEASUREMENT OF OXYGENATION CAPACITY

Kees de Korte and Peter Smits

Public Works Amsterdam, Sewerage and Drainage Department, Wibautstraat 3, 1091 GH Amsterdam, The Netherlands

ABSTRACT

The usual method for OC measurement is the non-steady state method (reaeration) in tapwater or, sometimes, in activated sludge. Both methods are more or less difficult and expensive. The steady state method with activated sludge is presented. Fundamentals are discussed. For complete mixed aeration tanks, plug flow systems with diffused air aeration and carousels the method is described more in detail and the results of measurements are presented. The results of the steady state measurements of the diffused air system are compared with those of the reaeration method in tapwater. The accuracy of the measurements in the 3 systems is discussed. Measurements in other aeration systems are described briefly. It is concluded that the steady state OC measurement offers advantages in comparison with the non-steady state method and is useful for most purposes.

KEYWORDS

OC measurement, steady state, activated sludge, respiration rate, complete mixed, diffused air, carousel.

INTRODUCTION

An important reason for measuring the OC is to check the guaranteed values of OC and efficiency of aeration equipment. A commonly used method is the reaeration method (non-steady state condition) in tapwater. Sodium sulphite is used to set the initial oxygen concentration at zero. The reaeration method is also used with activated sludge instead of sodium sulphite. The first method is more expensive than the second because of the use of chemicals and tapwater. Both methods however need much preparation in advance and only a few measurements can be made in one day. That is probably the reason that in the few cases that an OC measurement is carried out, mostly only the maximum OC is measured. Especially when energy saving is the object, it is desired to know the OC and the efficiency at different capacities of the aeration system. When the aeration system consists of more than one unit, many measurements are required. This can be done at relatively low cost by the presented method. This method is characterised by the use of activated sludge as oxygen consumer and steady state conditions during measurement.

OC MEASUREMENT UNDER STEADY STATE CONDITIONS

The system considered is an aerated and complete mixed compartment. A flow passes through the compartment (Fig. 1):

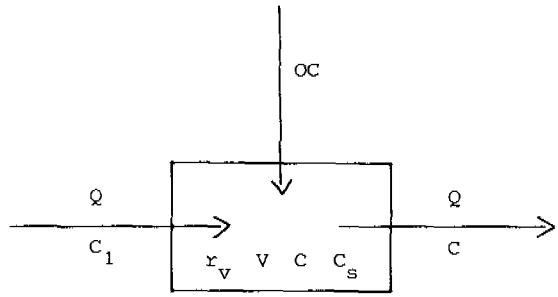

Fig. 1. The aerated complete mixed compartment

OC = oxygenation capacity of aeration system (kg/h)
Q = flow through the system (m^3/h)
r_v = respiration rate in the system (mg/l.h)
V = volume of the system (m^3)
C_1 = oxygen concentration in incoming flow (mg/l)
C = oxygen concentration in system (mg/l)
C_s = oxygen saturation (mg/l)

For steady state condition the following oxygen balance can be made for the compartment:

in (flow)	$Q\ C_1\ 10^{-3}$	kg/h
in (aeration)	$OC\ (C_s-C)/C_s$	kg/h
out (flow)	$Q\ C\ 10^{-3}$	kg/h
consumption	$r_v\ V\ 10^{-3}$	kg/h

The oxygen balance results in:

$$OC = (Q\ (C-C_1) + r_v\ V)\ \frac{C_s}{C_s-C}\ 10^{-3} \qquad (1)$$

The respiration rate r_v is determined in a sample taken from the system. The sample is aerated in a closed respirometer at the same temperature as in the system. At an oxygen concentration of approx. 6 mg/l the air supply is closed and the oxygen concentration decreases. The respiration rate r_v is calculated as the rate of decrease between 5 and 3 mg/l. In that oxygen concentration range the measured respiration rate is independent of the oxygen concentration. At oxygen concentrations lower than the critical concentration C_c, the measured respiration rate decreases due to diffusion limitation in the activated sludge flocs. From Heide et al. (1979) it can be concluded that for most sludges C_c is about 0.5 - 1.5 mg/l under usual conditions. To ensure that the measured respiration rate corresponds to the actual respiration rate in the system, the oxygen concentration in the system must be higher than 3 mg/l. The oxygen saturation C_s is measured in a filtered sample taken from the system. A pressure correction must be made for the oxygen saturation of diffused air systems. In general the pressure at half the immersion depth of the diffusers is used.

Before measurements can be done, steady state conditions must be present. This means that all parameters of eq. 1 must be constant (or at least constant enough). The respiration rate r_v is strongly influenced by the addition of wastewater. It is advisable to measure under endogenous conditions.

The endogenous respiration rate can decrease slowly, but in comparison to the much faster variations in oxygen concentrations it can be considered constant. In a carousel it can take a very long time (up to hours) to achieve a constant flow Q after starting the aerators. Depending on the type of aeration system and local circumstances, the oxygen concentration C usually is constant after a short time.

OC MEASUREMENT IN COMPLETE MIXED AERATION TANKS

In complete mixed aeration tanks (with surface aerators) the oxygen concentration is the same at any place.

Preparations. Preferably the measurements are done using endogenous activated sludge. This means that the wastewater flow must be stopped for several hours. Return-sludge pumping must be stopped in aeration tanks with more than one aerator and unknown distribution of the return-sludge over the different compartments. In other cases pumping can be continued if desired.
If necessary the suspended solids of the activated sludge can be adjusted in advance to meet the requirements for the respiration rate. The resulting oxygen concentration C in the aeration tank can be estimated from:

$$C = C_s - \frac{r_v \, V \, C_s}{1000 \, OC} \qquad (2)$$

For good measurements C has to be in the range of 3 mg/l to approx. 80 % of C_s.

Measuring procedure. First the return-sludge flow Q and the volume V of the aeration tank are determined. During the entire measurement period the respiration rate r_v is measured with short intervals of time. After each change of OC the oxygen concentration C in the aeration tank and the oxygen concentration in the return-sludge C_1 are measured. When both are constant the next change in OC is made. Afterwards the oxygen saturation C_s is determined. For the calculation of the OC eq. 1 is used.

Accuracy. The accuracy of the result mainly depends on:
- the measurement of C
  0,2 mg/l difference in C = 8 mg/l with C_s = 10 mg/l gives 10 % difference in OC. 0,2 mg/l difference in C = 5 mg/l with C_s = 10 mg/l gives 4 % difference in OC.
- the determination of r_v
  with good equipment the accuracy of the determination of r_v can be better than 5 %.

With return-sludge the accuracy of Q and C_1 have little influence on the result.

Note. Some complete mixed aeration tanks are equipped with more than one aerator. Each aerator influences a certain compartment of the tank. The volume of such a compartment can be determined from the flow pattern, which is clearly visible at the surface of the aeration tank. The OC of each aerator must be measured separately.

Results. Measurements have been carried out in the sewage treatment plant Huizen. Two aerators were present in the aeration tank. During the measurements a flow of 690 m^3/h return-sludge was pumped to the compartment of aerator 1. It then flowed through the compartment of aerator 2 to the final settling tank. The activated sludge was endogenous because more than 12 hours before measuring the wastewater flow was directed to an adjacent aeration tank. For hours the respiration rate was very constant. First, 16.9 and a few hours later 16.8 mg/l.h. Some additional data:

- total volume of aeration tank 1505 m^3
- temperature activated sludge 9.6 °C
- oxygen saturation 11.40 mg/l
- beta factor 0.996

For both aerators the OC was measured at 4 immersion depths. The immersion depth of both aerators was changed at the same time. It took 45 minutes to reach the steady state condition. All oxygen concentrations were measured with the same portable oxygen meter. With a second one the measurements of the first one were checked. The results are shown in Fig. 2.

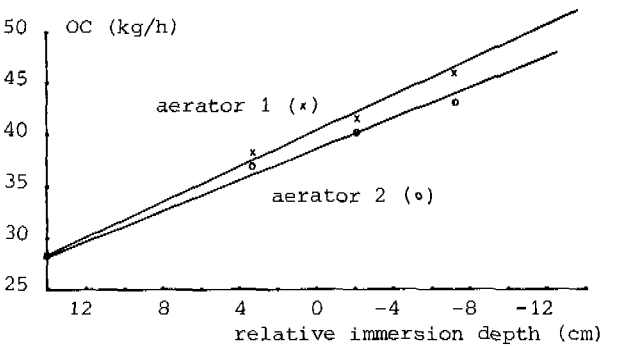

Fig. 2. OC measurements in Huizen

OC MEASUREMENT IN PLUG-FLOW AERATION TANKS

In plug-flow aeration tanks (with diffused air aeration) compartments with different OC can be present as a result of differences in number and/or positioning of the diffusers and of course the air flow rate. The OC in a compartment has to be measured in a representative section of it.

Preparations. Preferably the measurements are made using endogenous activated sludge and without return-sludge. In principle it is also possible to measure during normal operation. This can only be done when the condition is fulfilled that over a sufficient distance on both sides of the section where the measurement takes place, the oxygen concentration C and the respiration rate r_v are the same as in this section. The desired respiration rate can be estimated and adjusted in the same way as for complete mixed aeration tanks, using eq. 2.

Measuring procedure. During the entire measurement period the respiration rate r_v is measured with short intervals of time. After each change of air flow rate the oxygen concentration C is measured. When C is constant, the next change can be made. Afterwards the oxygen saturation C_s is determined. A correction for pressure is made. Usually half of the immersion depth of the diffusers is taken as the pressure. The results are calculated with eq. 1 with $C = C_1$.

Accuracy. The accuracy depends on the measurement of C and the determination of r_v and is the same as for complete mixed aeration tanks.

Results. Measurements have been carried out during normal operation in the treatment plants Amsterdam-West and Amsterdam-Zuid.

In Amsterdam-West during a period of two weeks, 8 measurements were carried out. They were done in the same compartment of an aeration tank using the same air flow rate. The results are shown in Fig. 3. Theoretically a straight line is

obtained. For C = 0, the OC per unit volume (40 mg/l.h) can be read on the vertical axis in the same units as the respiration rate.
The results indicate an accuracy of 10 % of the individual results.

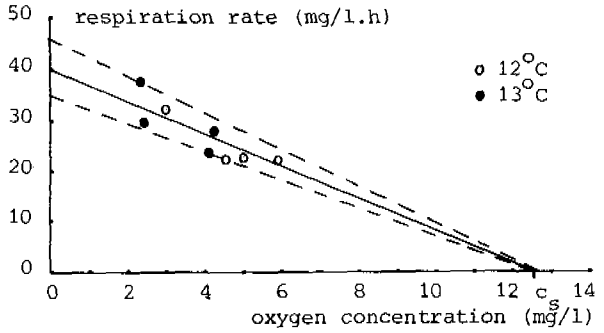

Fig. 3. Accuracy of individual OC measurements

In Amsterdam-Zuid the effect of air flow rate on OC and efficiency has been investigated in a compartment of 589 m^3. The immersion depth was 4 m.

TABLE 1 OC-Measurements Amsterdam-Zuid

Air Flow Rate m^3/h	OC kg/h	Efficiency kg/kWh
610	53	4.5
740	58	4.1
1100	84	4.0

The designed air flow rate is 310 - 1040 m^3/h. For the air flow rates of 610 and 740 m^3/h 7 separate OC measurements have been made. The measured OC-range for 610 m^3/h is 46.5 - 60.7 kg/h (standard deviation 4.9) and for 740 m^3/h the range is 48.3 - 62.4 kg/h (standard deviation 5.7).
In Fig. 4 and Fig. 5 the results are shown together with the results of measurements in tapwater with the re-aeration method. These measurements were done in 1977 by the RIZA (State Institute on Wastewater Treatment).

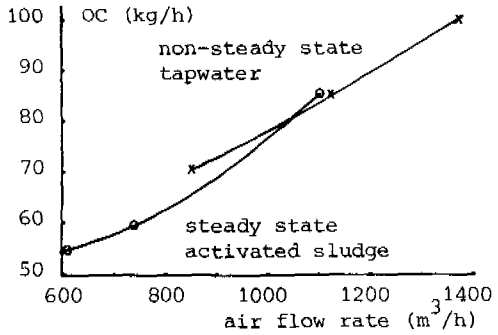

Fig. 4. Comparison of two different OC measurement methods (Amsterdam-Zuid)

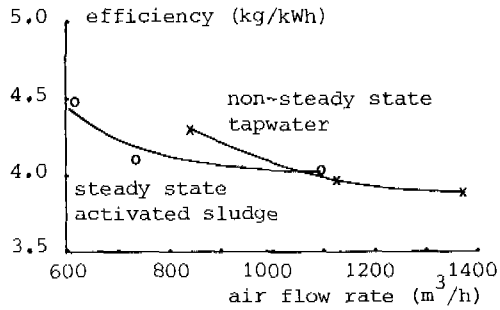

Fig. 5. Comparison of different efficiency measurement methods

The results show good agreement. The lower OC and efficiency in the recent measurement may be caused by some clogging of the diffusers during the 5 years between both measurements.

OC MEASUREMENT IN CAROUSELS

Carousels are oxidation ditches with one or more turbine aerators. The activated sludge flows through the aeration tank and passes complete mixed compartments where it is aerated, followed by a plug flow compartment without aeration. The oxygen profile is shown in Fig. 6.

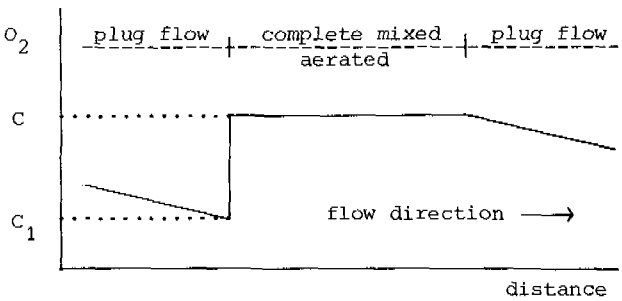

Fig. 6. Oxygen profile in carousels

Preparations. Solids content and respiration rate r_v must be the same in all parts of the aeration tank. This means that wastewater addition must be stopped a long time before measuring can take place. The measurements are preferably made with endogenous activated sludge. Because of the mixing characteristics in the circuit, return-sludge must be stopped to prevent a part of the flow having a different oxygen concentration, unless the return-sludge is added in a complete mixed part of the circuit. Normally no special care has to be taken for the respiration rate r_v. Only extreme high or low respiration rates can cause difficulties due to very high or very low oxygen concentrations in the complete mixed compartments. Attention has to be paid to the flow Q. Depending on local circumstances the flow and the OC can be more or less strongly related. It can take a long time before there is a constant flow in the circuit.

Measuring procedure. Two methods are possible. The first one is the "oxygen-rise" method. The OC of each individual aerator can be determined.

At first the flow Q is determined. Flow velocity measurement with propeller-type devices in activated sludge is not only difficult as a result of frequent interference by dirt but also very time-consuming. Another, in any case easier, method is velocity measurement with a mainly submerged buoy (Fig. 7).

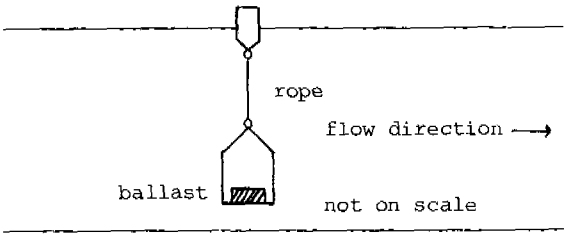

Fig. 7. Submerged buoy

Measurements on several places at the cross-section and at various depth may be necessary to obtain appropriate results.
The volume V of the complete mixed aerated compartment can be estimated by means of the mixing pattern that is visible upstream of the aerator, assuming that the downstream situation is similar.
The oxygen concentration C_1 just upstream of the aerated compartment and the oxygen concentration C in the aerated compartment are measured. The OC is calculated according to eq. 1 (note that V is the volume of the aerated complete mixed compartment). Especially at high Q and low OC the difference $C - C_1$ can be very small. In that case the second method can be used when $C_1 > C_c$. With the "oxygen-consumption" method the total OC for the aeration tank is determined. An oxygen balance for the whole aeration tank can be made for steady state conditions. It can take several hours before steady state is accomplished. Calculations are made according to eq. 3:

$$OC = r_v \, V_{tot} \frac{C_s}{C_s - C} \, 10^{-3} \qquad (3)$$

Eq. 3 is derived from eq. 1. At steady state and with $C_1 > C_c$ the oxygen increase in the aerated compartment equals the oxygen decrease in the non-aerated compartment:

$$Q \, (C - C_1) = r_v \, (V_{tot} - V) \qquad (4)$$

V_{tot} is the total volume of the aeration tank. Substitution of eq. 4 in eq. 1 results in eq. 3. This method can only be used for carousels with one aerator.

Accuracy. For the "oxygen-rise" method the result mainly depends on $Q \, (C - C_1)$ and less on $r_v \, V$, which contributes 10 - 40 % to the total result; this depends on Q and OC. The accuracy of the determination of Q is estimated at 5 - 10 %. The accuracy of the difference $C - C_1$ is about 0.1 mg/l, resulting in 5 % for an oxygen rise ($= C - C_1$) of 2 mg/l and 20 % for an oxygen rise of 0.5 mg/l. For the "oxygen-consumption" method the accuracy is the same as for complete mixed aeration tanks.

Results. Measurements have been done in two carousel plants.

In Beemster the OC of the 3 aerators has been measured at various immersion depths according to the "oxygen-rise" method. The results are shown in Fig. 8.

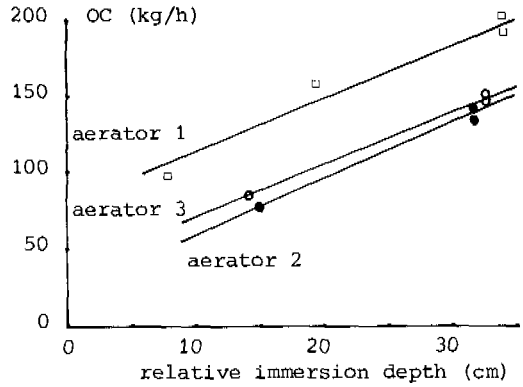

Fig. 8. OC measurements in Beemster

In Hazerswoude the OC of the aerator has been measured using the "oxygen-consumption" method because $C - C_1$ was too small (about 0.5 mg/l) due to a high flow (0.5 m/s). Steady state was reached at $C = 8.05$ mg/l and $r_v = 9.5$ mg/l.h. With $C_s = 10.59$ mg/l and $V = 1650$ m^3 the OC at maximum capacity results in 65 kg/h.

OC MEASUREMENT WITH ROTOR AERATORS

In aeration tanks with rotor aerators, usually no complete mixed compartment is present that includes the entire cross-section. Consequently the flow Q cannot be determined. The OC can be determined using the "oxygen-consumption" method as described for carousels using eq. 3. The oxygen concentration C is determined just downstream of the rotor.

OC MEASUREMENT IN CIRCUITS WITH DIFFUSED AIR AERATION

The method that should be used depends on the arrangement of the aerators. When the aerators are distributed homogenously over the aeration tank, the OC can be measured in the same way as in complete mixed systems.

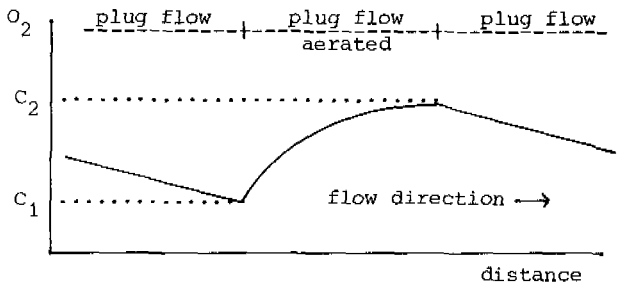

Fig. 9. Oxygen profile in circuits with intermittent diffused air aeration

This method can also be applied for Schreiber systems with moving aerators or combinations of moving and fixed aerators when no important changes in oxygen concentration are observed during periods without aeration. For systems with aerators concentrated on a limited number of places, the oxygen profile is shown in Fig. 9.
For $C_1 > C_c$, the respiration rate r_v is constant. When r_v, Q, C_1, C_2, C_s and the length of the aerated zone are measured the OC can be calculated. As the OC cannot be expressed explicit in an equation, the use of a computer may be helpful.

DISCUSSION AND CONCLUSIONS

OC measurement at steady state conditions with (endogenous) activated sludge is practicable for various aeration systems and results in values representative for the practical conditions during measurement. The result includes the influence of the alpha and beta factor. The alpha factor, which influences the oxygen transfer coefficient, depends on the waste characteristics (in particular surface active agents) and the type of aeration system. Because the waste characteristics in the aeration tank change during treatment, the alpha factor is not constant. With increasing degree of treatment, the influence of the alpha factor decreases. The beta factor, which influences the oxygen saturation, depends on the dissolved solids. In most cases the oxygen saturation is hardly influenced and the oxygen saturation in activated sludge is practically the same as in pure water. The accuracy obtained depends on the type of aeration system and local circumstances and will be good enough for most purposes. Steady state OC measurement has a number of advantages in comparison with the non-steady state method with activated sludge and with tapwater in particular:

- no chemicals are used
- no special equipment (pumps, tanks etc.) is necessary
- preparations in advance are limited
- hydraulic conditions (mixing and flow patterns) are stable
- one or two portable oxygen meters and a meter for respiration rate are the only instruments
- measurement procedure is simple and the measurement can be done by one or two persons, depending on the type of aeration system
- calculations are easy

It can be concluded that steady state OC measurement is easy to do, is not labour-intensive and consequently can be performed at low cost. The results are satisfactory for most purposes.

REFERENCES

Heide, B.A. and Kruize, R.R. (1977). Zuurstofoverdracht en denitrificatie in actief-slib. H2O, 12, 337-343.

INDUSTRIAL WASTEWATER TREATMENT

Wat. Sci. Tech. Vol.17, Amsterdam, pp.313-324. 0273-1223/85 $0.00 + .50
Printed in Great Britain.

REMOVAL OF IRON CYANIDE FROM GOLD MILL EFFLUENTS BY ION EXCHANGE

D. T. Vachon

Environment Canada, Environmental Protection Service, Wastewater Technology Centre, Burlington, Ont. L7R 4A6, Canada

ABSTRACT

Using a strongly basic anion exchanger (Rohm & Haas Amberlite IRA-958) laboratory ion exchange tests were conducted on the removal of iron cyanide from synthetic and actual gold mill effluents. Variables examined included the effects of pH, concentration and hydraulic loading of the feed on the resin exchange capacity and resin column utilization. The results showed ion exchange to be an effective method of removing iron cyanide to concentrations of less than 3 mg/L. Tests with synthetic gold mill effluents gave resin exchange capacities ranging from 13 to 34 mg CN_{Fe}/mL resin depending on the concentration of iron, copper and zinc cyanides in these solutions. When raw barren bleed was tested, an exchange capacity for the ferro/ferricyanides was determined to be ~6 to 8 mg CN_{Fe}/mL resin. For chlorinated barren bleed, a resin exchange capacity of 14 mg CN_{Fe}/mL resin was observed. A capacity of 19 mg CN_{Fe}/mL resin was achieved for tailings pond decant.

Regeneration with 15% NaCl provided mixed results with recoveries ranging from 40 to 100% of the iron cyanide exchanged by the resin. Upon multiple exchange-regeneration cycles, the resin lost 25% of the exchange capacity for total cyanide during the first cycle. Subsequently, the loss in exchange capacity was approximately 1% per cycle. Pilot scale tests were considered essential prior to full scale system design.

KEYWORDS

Wastewater treatment, iron cyanide, removal, ion exchange, gold mill effluent.

BACKGROUND

Effluents from most Canadian gold mills contain elevated levels of cyanide in the form of free cyanide and metal cyanide complexes, particularly those of zinc, copper, nickel and iron.

The major waste streams from gold milling which contain cyanide are the barren bleed (discarded mill solution) and a slurry containing the leached ore. Both

streams are discharged to a tailings pond where the solids settle out. The resulting clear supernatant that discharges from the pond (tailings pond decant) may have elevated levels of cyanide. Because of the known toxicity of cyanide to fish at levels as low as 0.03 mg/L (Leduc et al, 1982), a number of Canadian gold mills have recently installed alkaline chlorination systems to remove cyanide from their effluents. Although this process is effective in removing most cyanide species, it does not remove iron cyanide. Therefore, in some situations, the concentrations of iron cyanide in the treated effluents can be excessive leading to toxicity problems in the receiving water.

One process that has been reported to be effective in treating metal cyanide bearing wastewaters is ion exchange (Zabban and Helwick, 1980; Trachtenberg and Murphy, 1979; Bessent et al, 1979). Trachtenberg and Murphy (1979) described studies on iron cyanide removal from leachate from a storage dump of discarded linings from aluminum reduction cells. Data from the full scale treatment system showed an average reduction from 48 mg/L CN_{Fe} to <0.5 mg/L (99%) at a hydraulic loading of 0.13 mL/min/mL resin. However, no information was provided pertaining to wastewater volumes treated before regeneration or exchange capacities. Bessent et al (1979) reported on the use of ion exchange for the treatment of coke plant wastewaters at pilot scale. The coking effluents were first treated with ferrous sulfate to convert the free cyanide to ferrocyanide. The ferrocyanide was then removed by an ion exchange process employing Amberlite IRA-958 resin. Based on these pilot scale studies, they concluded that for a full scale application, the average resin loading would be 11 mg CN_{Fe}/mL resin at a nominal concentration breakthrough of 10 mg/L of iron cyanide. Breakthrough would occur after ~200 bed volumes if the influent cyanide concentration was ~80 mg/L and the hydraulic loading rate was 0.13 mL/min/mL resin.

Although ion exchange has been used for iron cyanide removal from miscellaneous industrial effluents, only limited information is available with respect to the treatment of gold mill effluents. Halbe et al (1979) and Trautman and Ommen (1981) discussed ion exchange as a wastewater treatment alternative for the Homestake Gold Mine, Lead, South Dakota, USA, to attain compliance with a total cyanide discharge limitation of <0.02 mg/L. Halbe et al (1979) during development work, reported iron (presumably iron cyanide) removals in excess of 97% from one mill wastewater. Influent levels were 5 to 6 mg CN_T/L and Fe <1 mg/L. Hydraulic loadings applied to a 90 mL resin bed of Amberlite IRA-958 were 0.33, 0.5, and 0.67 mL/min/mL resin. Iron levels in the effluent remained < 0.1 mg/L after 2 200 bed volumes of wastewater had passed through the column. In both of the previous papers, however, no data were provided on resin loading, essential data for full scale system design.

This lack of specific data necessitated the laboratory study reported in this paper. The purpose of the study was to evaluate the feasibility of using ion exchange to treat effluents of a gold mill that had installed an alkaline chlorination system. The resin's exchange capacity and the effective utilization of the resin column was determined to permit design of a pilot plant.

MATERIALS AND METHODS

Exchange Resin

Amberlite IRA-958 (supplied by Rohm and Haas) is an acrylic, strongly basic anion exchanger which is highly selective for ferrocyanide. The ion exchange column removes cyanides as follows:

$$X[\text{Resin-N-R}_3^+ + Cl^-] + Fe(CN)_6^{X-} \rightarrow [(\text{Resin-N-R}_3^+)_X + Fe(CN)_6^{X-}] + XCl^-$$

where X = 4 in ferrocyanide and X = 3 in ferricyanide. Once the resin is exhausted, it is regenerated with aqueous sodium chloride as follows:

$$[(\text{Resin-N-R}_3^+)_X + (\text{Fe(CN)}_6^{X-})] + \text{NaCl} \rightarrow X\ [\text{Resin-N-R}_3^+ + \text{Cl}^-] + \text{Na}_X\text{Fe(CN)}_6^{X-}$$

The exchange capacity of the resin for iron cyanide has been reported to be 19 to 37 mg CN_{Fe}/mL resin from a waste stream containing varying concentrations of ferrocyanide and ferricyanide (Avery and Waitz, 1977).

Test Solutions

Cyanide solutions used in the tests consisted of synthetic and actual gold mill wastewaters. Initial studies used pure solutions of ferrocyanide and ferricyanide and a simulated barren bleed containing copper, zinc and iron (ferro/ferri) cyanides with pH adjustment using NaOH pellets. Samples of barren bleed and tailings pond decant collected from a western Canadian gold mill were used in subsequent studies. Some tests were run using the wastewater as received whereas for others, the wastewater was first treated by the alkaline chlorination process in the laboratory. Table 1 presents the characteristics of the wastewaters used in the tests. Total cyanide (CN_T) and weak acid dissociable cyanide (CN_W) (namely copper and zinc cyanides) were analyzed according to the methods described by Conn (1981). Iron cyanide (CN_{Fe}) was determined as the difference of these two cyanide forms (namely $CN_{Fe} = CN_T - CN_W$). Heavy metals were analyzed by atomic absorption spectroscopy.

TABLE 1 Raw and Treated Gold Mill Effluents

Parameter*	Raw Barren Bleed	Treated Barren Bleed	Raw Tailings Pond Decant	Treated Tailings Pond Decant
CN_T	365-385	54-60	21-27	13-15
CN_W	290-300	1.0	10-11	1.0
Fe	25-30	17-22	5-8	4-7
Zn	60-68	0.2	0.03	0.02
Cu	180-210	<0.5	8-12	<1.0

* Concentrations in mg/L.

Batch Tests

These tests were conducted to determine the maximum resin exchange capacities for total and iron cyanide. Using synthetic solutions, the effects of hydraulic loading , initial cyanide concentration and pH level were investigated. Gold mill effluents were tested to evaluate the effluent matrix effect on maximum resin loadings. The apparatus set-up is shown in Figure 1. The micro column (2 mL disposable pipet) contained a known amount of resin (100 to 450 mg) and 200 mL of test solution was continuously cycled through the resin for six hours at a pre-selected resin hydraulic loading. Preliminary tests had indicated that six hours of contact time was more than sufficient to reach equilibrium between the resin and the aqueous phase.

Continuous Flow Tests

To determine the effective utilization of the exchange capacity of the resin and to provide design data for pilot or full scale application continuous flow tests

were conducted. The "effective" exchange capacity of the resin was determined when breakthrough of total or iron cyanide occurred in the effluent. Breakthrough profiles for the various cyanide forms were also investigated. The apparatus used for these tests is also shown in Figure 1. The column, a 25 mL buret, contained resin volumes of 10-15 mL. The test solution was run through the column on a "once-through" basis. Breakthrough was determined qualitatively by adding a few drops of the effluent to highly acidic solutions of ferrous sulphate or ferric sulfate. A blue (Prussian Blue) or bluegreen (Turnbull's Blue) colour indicated breakthrough of iron cyanide.

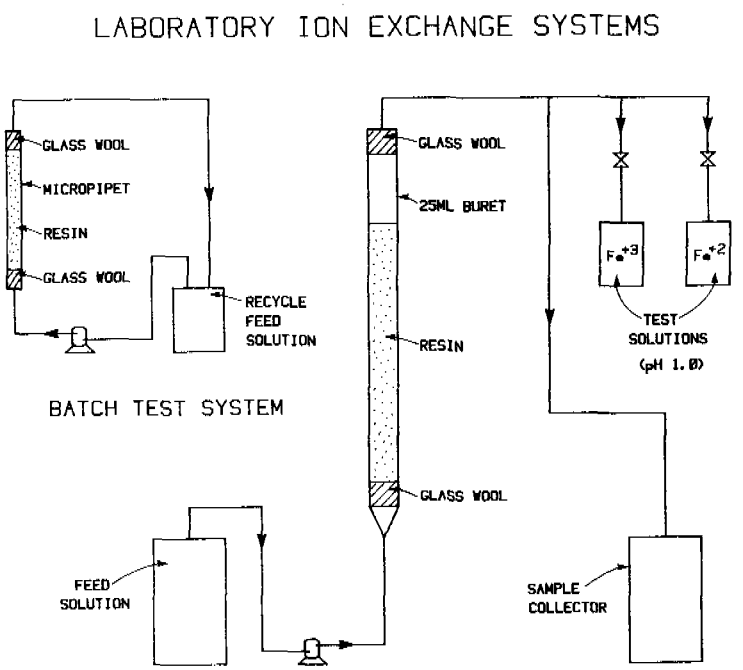

Fig. 1. Laboratory apparatus for ion exchange studies

The ion exchange column was regenerated using a NaCl solution. The resin manufacturer recommended using 3 to 4 bed volumes of the regenerant solution. In this study, regeneration of the resin was continued until there was no indication of iron cyanide in the eluant solution. This procedure lead to the use of excessive volumes of regenerant solution in some cases. Samples of the influent, effluent and regenerant solutions were collected at regular intervals for quantitative analysis of cyanide and heavy metal concentrations.

Field Test

Apparatus similar to that used for the laboratory continuous flow tests was used in a test conducted at a gold mill. Tailings pond decant was collected in two

batches with each batch providing test solution for ~40 h. This wastewater was fed at a hydraulic loading of 0.38 mL/min/mL resin. The resin volume used in this test was 29 mL. Samples were collected at regular intervals from the effluent and analyzed for cyanides and heavy metal concentrations.

RESULTS AND DISCUSSION

Batch Tests

Table 2 summarizes the data from the batch tests. Tests 1 to 11 were conducted to assess the effects of initial cyanide concentration, hydraulic loading and solution pH on exchange capacity for total and iron cyanide. In general, it was observed that the exchange capacity increased under conditions of increasing cyanide concentration, lower hydraulic loading and increasing pH. A reduced exchange capacity was noted for iron cyanide during the tests on the simulated barren bleed (metal cyanide solution) and the raw gold mill wastewaters. This was attributed to competition for exchange sites by copper and zinc cyanides which were also present in the test solutions. The exchange capacity for iron cyanide in test 18 (treated barren bleed) was only 6 mg CN_{Fe}/mL resin which was totally unexpected as this was significantly less than any of the other results. On closer inspection of the results, it was found that residual chlorine was present in the test solution and the lower exchange capacities were attributed to this factor.

TABLE 2 Results of Batch Tests

Test	Feed Solution	Initial $[CN_T]$ mg/L	Hydraulic Loading (mL/min/mL resin)	pH	Resin Exchange capacity (mg/mL resin) CN_T	CN_W	CN_{Fe}	Fe	Cu	Zn
1	Ferrocyanide	250	0.8	7.7	22		22	6.7		
2	Ferricyanide	500	0.4	7	35		35	8.0		
3	Ferrocyanide	500	0.4	7	17		17	7.8		
4	Ferrocyanide	1000	0.4	7	35		35	8.0		
5	Ferrocyanide	250	0.7	8.5	17		17	4.3		
6	Ferrocyanide	250	0.9	9.8	14		14	3.8		
7	Ferrocyanide	500	0.4	9	35		35	9.7		
8	Ferrocyanide	250	0.8	10.9	29		29	10.5		
9	Ferrocyanide	250	0.7	11.9	28		28	10.4		
10	Ferrocyanide	250	0.6	12.4	29		29	(6.7)		
11	Ferrocyanide	500	0.4	12	46		46	12.3		
12	Ferricyanide	390	0.4	12.2	34		34	7.1		
13	Ferro/Ferri-cyanide	390	0.4	12.1	39		39	(24)		
14	Ferro/Ferri-cyanide	390	1.4	11.6	26		26	6.5		
15	Metal cyanide	710	0.4	11.6	36	16	20	10.1	3.9	3.4
16	Metal cyanide	470	0.7	11.9	37	11	26	13.3	5.5	(44)
17	Raw Barren Bleed	390	0.4	12	25	13	12	2.5	12.5	0
18	Treated Barren Bleed	60	0.4	12	6	-	6	0.4	-	-
19	Raw Tailings Pond Decant	27	1.2	10.7	23	8.2	15	5.5	9.9	-
20	Treated Tailings Pond Decant	13	1.5	12	18	-	18	4.0	-	-

Continuous Flow Tests

Table 3 summarizes the data from the continuous flow tests. The breakthrough levels detected for iron cyanide in most of the tests were < 3 mg/L. For total cyanide, however, the concentrations ranged from 0.6 to as high as 245 mg/L. In the latter cases, the majority of the cyanide was weak acid dissociable cyanide (copper and zinc cyanides). The "effective" exchange capacities for the resin were calculated based on the mass of cyanide (CN_T or CN_W) or metals exchanged by the resin at breakthrough. The exchange capacities determined in these continuous flow tests, in general, were 10 to 50% less than those found in the batch tests.

TABLE 3 Results of Continuous Flow Tests

Test	Feed Solution	Initial $[CN_T]$ (mg/L)	Hydraulic Loading (mL/min/mL resin)	Breakthrough Point $[CN_{Fe}]$ (mg/L)	Breakthrough Point $[CN_T]$ (mg/L)	Breakthrough Point Number of Bed Volumes	Effective Exchange Capacity (mg/mL Resin) CN_T	CN_W	CN_{Fe}	Fe	Cu	Zn
1	Ferrocyanide	110	0.41	1.8	1.8	280	30		30	11		
2	Ferricyanide	290	0.40	3.0	3.0	120	34		34	13		
3	Ferro/Ferri cyanides	210	0.31	2.6	2.6	120	25		25	8.2		
4	Iron, Copper Zinc cyanides	470	0.30	0	5	50	24	11	13	4.7	6.1	8.0
5	Raw Barren Bleed	378	0.30	0.5	64	75	26	20	5.7	2.0	14	1.1
6A	Raw Barren Bleed	365	0.40	<0.1	62	90	27	20	5.8	2.6	17	
7	Raw Barren Bleed	370	0.28	2.2	31.6	70	26	20	6.0	1.7	13	2.6
8	Raw Barren Bleed	365	0.09	0	109	100	26	18	7.6	2.9	15	
9	Raw Barren Bleed	378	1.7	10	245	80	~19	~14	~5	~2	~9	~3
10	Treated Barren Bleed	54	0.30	3.3	3.3	280	14		14	4.5		
11	Tailings Pond Decant	15	0.37	0.4	0.6	1480	>21	~1	>20	>10		
12	Field Test	20	0.38	3.0	16.5	1840	26	6.7	19	7.8	4.3	

The resin showed capacities from pure solutions of iron cyanide (Tests 1-3) of~25-34 mg CN/mL resin at pH 12.0 and at a hydraulic loading of 0.3 to 0.4 mL/min/mL resin. These values are similar to those reported by Avery and Waitz (1977). As the data in Table 3 show, the presence of copper and zinc cyanide in the solution adversely affected the uptake of iron cyanide by the resin. This is understandable since zinc and copper cyanide will be expected to compete with iron cyanide for the exchange sites on the resin. Exchange capacities of 19-27 mg CN_T/mL resin and 5-8 mg CN_{Fe}/mL resin were observed for the tests in which raw barren bleed was used. These capacities are ~ 25% lower than those observed for the synthetic iron cyanide solutions and are attributed to the uptake of zinc, copper and other exchangeable cyanide forms present in the barren bleed. Because breakthrough was measured in terms of iron cyanide, the concentrations of copper and zinc in the ion exchange column

effluent reached high levels during the test. This caused an increase in the uptake of total cyanide. The result was an increase of total cyanide exchange capacity over the value determined for the synthetic barren bleed (test 4). For treated barren bleed, the exchange capacity for iron cyanide was higher than that observed for raw barren bleed. This was expected because alkaline chlorination removes almost all the copper and zinc cyanides and leaves additional exchange sites available for iron cyanide. Also, the total cyanide uptake was much lower than in the previous tests using raw barren bleed.

Treated tailings pond decant was used in test 11. The level of metal cyanides other than iron cyanide was minimal in the treated decant sample. No significant breakthrough of total cyanide in the effluent was noted even after 1 480 bed volumes of wastewater had passed through the column. This indicated very effective polishing of a cyanide contaminated effluent stream of which the major constituent was iron cyanide. Actual exchange capacities for total and iron cyanide would be greater than the values determined from test 11 since at the time of the test's termination, significant breakthrough of the cyanides had not occurred.

Figure 2 illustrates the breakthrough curve of iron cyanide for a ferrocyanide solution. As shown, the iron cyanide concentration in the effluent increased rapidly from 1.8 to 68 mg/L following breakthrough. This represents a favourable situation where the exchange band (or wave front) is very narrow in the resin column which means a maximum utilization of the resin. Figure 3 illustrates the breakthrough curve of simulated barren bleed. In this case, breakthrough of the cyanide species is more gradual than in the former case and represents a wider exchange band in the resin column with poor utilization of the exchange medium. The high copper concentrations in the effluent in excess of the feed concentration show that copper cyanide (represented by metallic copper) initially taken up on the resin was later displaced by iron cyanide.

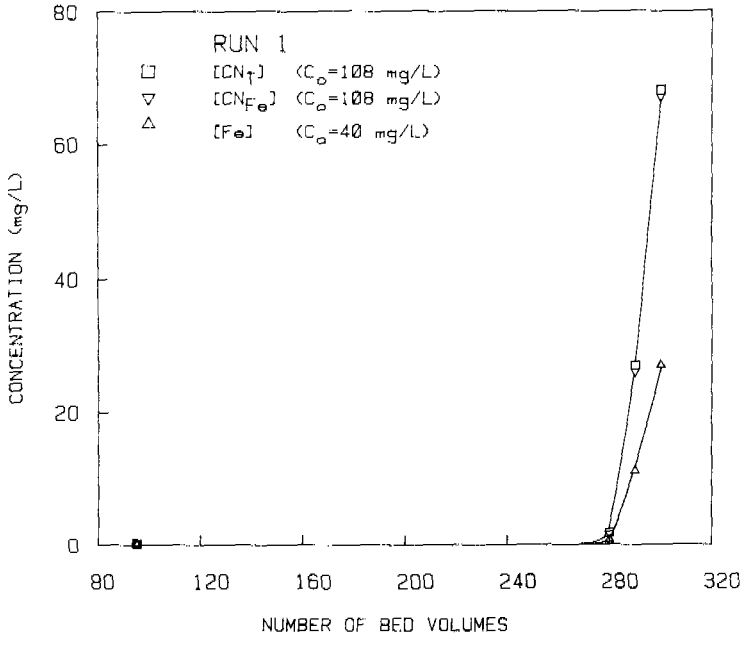

Fig. 2. Breakthrough curve for ferrocyanide solution

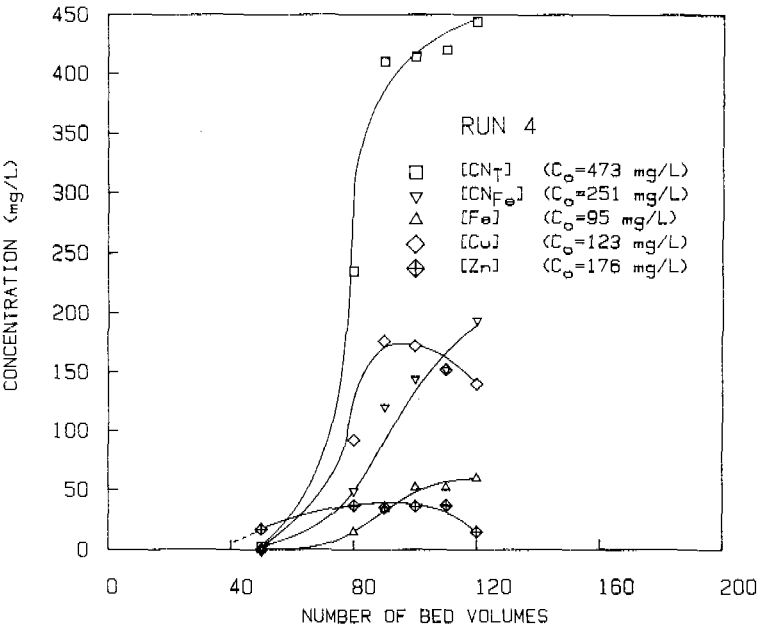

Fig. 3. Breakthrough curve for simulated barren bleed

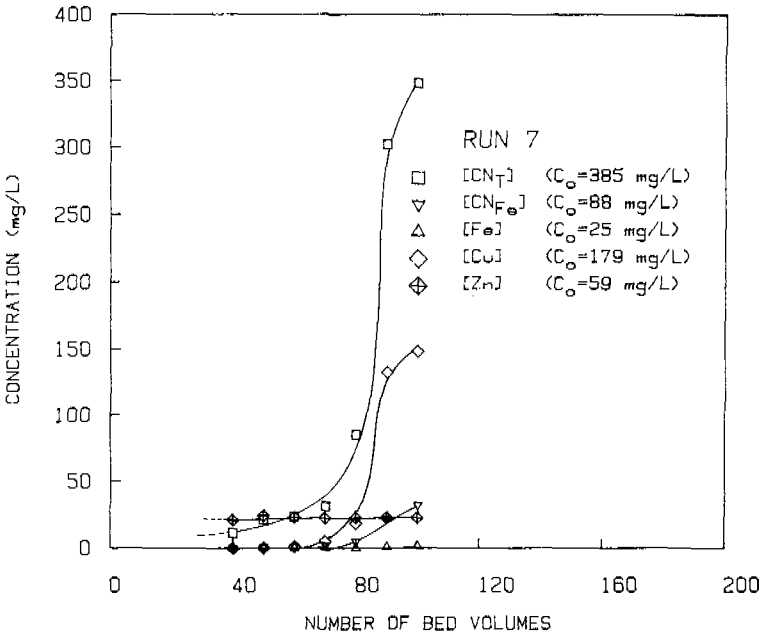

Fig. 4. Breakthrough curve for raw barren bleed

Zinc cyanide displayed a peculiar exchange pattern. Its presence was noted almost immediately in the effluent but at a relatively constant concentration of ~20% of the influent level (Figure 4). This implies that some zinc cyanide is "poisoning" the resin. This "poisoning" appears to be "permanent uptake" of zinc cyanide at certain exchange sites that are not available for the uptake of iron cyanide. While this aspect is important in evaluating exchange capacities, the necessary work to properly assess this problem was not undertaken during this study.

Field Test

The data for the field test are presented in Table 3. A breakthrough of 3.0 mg/L for iron cyanide was observed after 1 840 bed volumes of tailings pond decant had been treated. At this point, exchange capacities were 26 mg CN_T/mL resin and 19 mg CN_{Fe}/mL resin. The breakthrough profiles for this test are presented in Figure 5. Leakage of iron cyanide from the column was gradual after 1 000 bed volumes of the wastewater had been treated. In contrast, the total cyanide concentration in the column effluent increased rapidly following treatment of ~ 800 bed volumes. Assuming a discharge limit for total cyanide < 1 mg/L, termination of a run would be required after 800 bed volumes. If suitable pretreatment had been applied, and the ion exchange was used only for removing iron cyanide from the wastewater, nearly 1 600 bed volumes would have been treated before exceeding the assumed effluent limit.

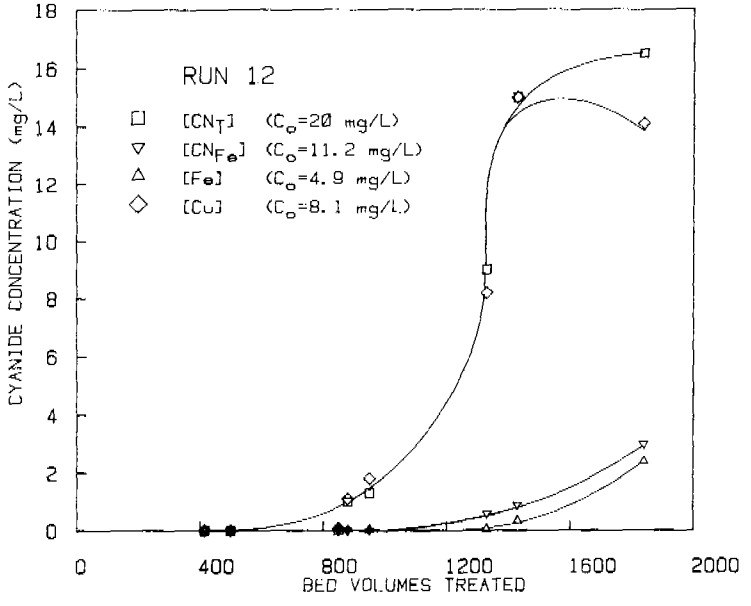

Fig. 5. Breakthrough curve for tailings pond decant

Regeneration

Table 4 presents the results of resin regeneration for the continuous flow tests (Table 3). Generally, regeneration was incomplete when a 10% NaCl solution was used but improved considerably with a 15% NaCl solution. For the runs using test solutions containing a high proportion of iron cyanide, good recoveries (≥80%)

were achieved for both total and iron cyanide. An exception was the low recovery in test 3. In this case, the low recovery was perhaps due to a very high hydraulic loading during regeneration (0.31 mL/min/mL resin). It is generally accepted that the hydraulic loading during regeneration should be low; 0.03 to 0.07 mL/min/mL resin.

TABLE 4 Regeneration Results

Test	Regenerant Solution	% Regen. Volume to Feed Volume	% Recovery					
			CN_T	CN_W	CN_{Fe}	Fe	Cu	Zn
1	15% NaCl	4	80		80	100		
2	15% NaCl	80	95		95	85		
3	15% NaCl	16	66		66	63		
4	15% NaCl	18	60	100	60	57	83	0
5	10% NaCl	12	66	74	45	62	77	2
6A	10% NaCl	17	76	76	75	78	79	
7	15% NaCl	23	71	83	40	46	91	2
8	10% NaCl	17	76	80	69	58	86	
9	10% NaCl	11	Not available					
10	15% NaCl	7	98		98	100		
11	15% NaCl	3	86	60	87	66	-	
12	15% NaCl	<3	88	53	99.8	94	70	

Poor recoveries of iron and total cyanide were noted when high levels of copper and zinc cyanides were present. Regeneration was incomplete although significant volumes of regenerant solution were used. As discussed earlier, another problem that was observed was poisoning of the resin by zinc cyanide. Other authors have observed this and found that zinc can only be eluted effectively with NaOH solution. It was not within the scope of this study to address the problem of ultimate disposal of the iron cyanide, but it can be precipitated as Prussian Blue and separated from the regenerant solution, and then incinerated, buried or sold according to Avery and Waitz (1977).

Multicycling

Some limited testing was done using raw barren bleed to evaluate the resin exchange capacity after several cycles of use and regeneration. The data related to the loss of exchange capacity after repeated regeneration are presented in Table 5. A loss of ~25% of the resin capacity for total cyanide was noted

TABLE 5 Results of Multicycle Ion Exchange Studies on Raw Barren Bleed

Test	Cycle	Initial $[CN_T]$ (mg/L)	Hydraulic Loading (mL/min/mL resin)	Breakthrough Point		Number of Bed Volumes	Effective Exchange Capacity (mg/mL Resin)				
				$[CN_{Fe}]$ (mg/L)	$[CN_T]$ (mg/L)		CN_T	CN_W	CN_{Fe}	Fe	Cu
6A	1	365	0.40	0	62	90	27	20	6.8	2.6	17
6B	2	365	0.40	1	134	90	21	14	6.8	2.5	12
6C	3	365	0.40	12	159	90	19	13	5.8	2.3	11
6D	4	365	0.40	8	144	90	20	14	6.1	2.3	12
6E	5	365	0.40	11	161	90	18	13	5.9	2.2	9.2
6F	6	365	0.40	5	152	90	19	13	6.4	2.2	11
6G	7	365	0.40	11	159	90	19	13	5.9	2.2	9.5

following the first cycle. Most of this loss of exchange capacity appeared to be for weak acid dissociable cyanide. The reduction in exchange capacity for iron cyanide is shown in Figure 6 and was <15%. The loss in exchange capacity noted for total cyanide in the first three cycles represents the reduced exchange capacity for copper (and zinc) cyanide. After the third cycle, equilibrium was achieved, and no further decrease in exchange capacity was observed. The reduced exchange capacity of the resin is attributed to "poisoining" by zinc cyanide as discussed earlier. Reducing zinc concentrations in the feed or improving removal of zinc from the exhausted resin during regeneration should increase the overall resin loadings for both total and iron cyanide.

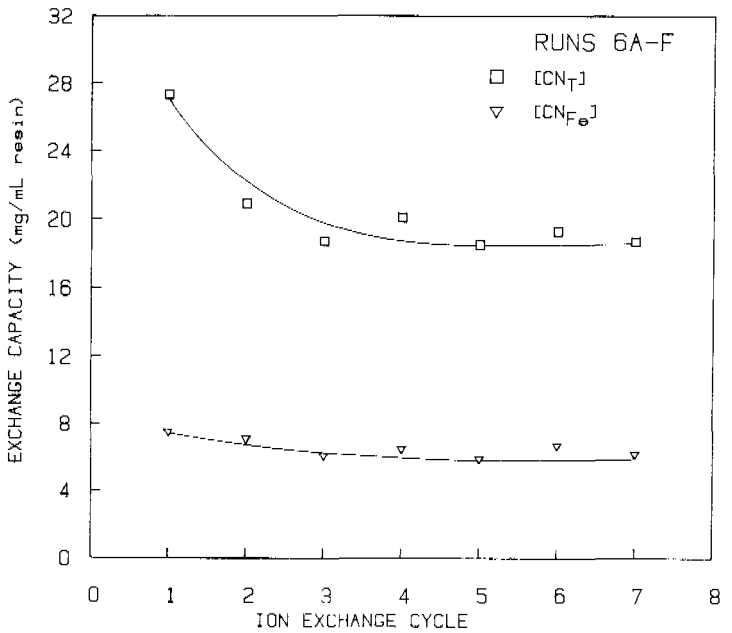

Fig. 6. Loss of resin exchange capacity over 7 cycles

CONCLUSIONS AND RECOMMENDATIONS

The removal of iron cyanide from synthetic and actual gold mill effluents was effectively demonstrated in laboratory and field studies. In the initial screening, the general trend observed was that the exchange capacity increased under conditions of increasing cyanide concentration, lower hydraulic loading and increasing pH. Resin exchange capacities for synthetic solutions were 24 to 34 mg CN_T/mL resin and 13 to 34 mg CN_{Fe}/mL resin. Treated mill effluents containing a high proportion of iron to total cyanide concentration gave exchange capacities of 14 to >21 mg CN/mL resin. These capacities were approximately 50 to 80% of those obtained with synthetic solutions.

Lower exchange capacities were observed for raw mill effluents. In these feed solutions, copper and zinc cyanides competed with iron cyanide and claimed a significant portion of the exchange capacity. Values observed for raw barren bleed were 26 mg CN_T/mL resin and 5-7.6 mg CN_{Fe}/mL resin. Post-treatment after ion exchange would be required in order to remove the weak acid dissociable

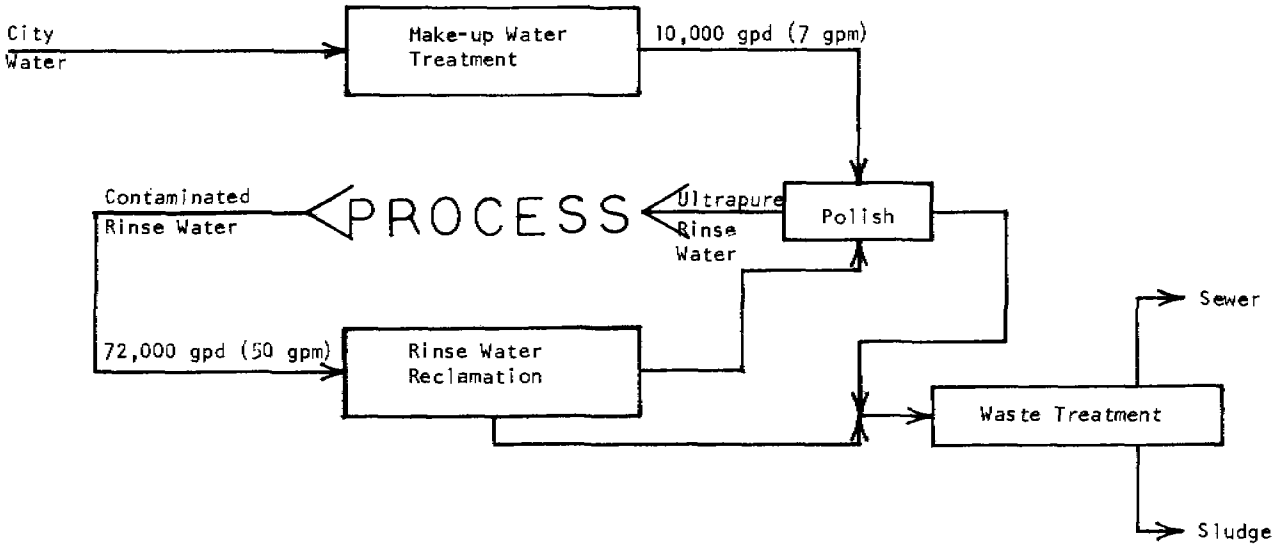

FIGURE 1. WATER RECLAMATION AND WASTE TREATMENT PROCESS SCHEMATIC

Rinse water reclamation system. Accumulating the contaminated rinse waters and purifying them to a quality of approximately 300,000 ohm/cm.

Make-up water system. Purifying city water to replenish that portion of the rinse water discharged to the Waste Treatment System. This system is also sized to supply the total process flow requirement in the event that the Rinse Water Reclamation System is shut down for any reason.

Polishing system. Polishing the combined streams from the rinse water reclamation recirculation loop and Make-up Water System to produce a volume of 72,000 gpd of 18 megohm/cm quality rinse water.

Waste treatment system. Accumulating all toxic wastes from the Rinse Water Reclamation and Polishing Systems and producing a dewatered sludge for disposal in a landfill and a clarified effluent suitable for discharge to the sewer authority.

PROCESS DETAILS

The devices are prepared by electroplating the following metals on a special ceramic substrate:

Permalloy (nickel-iron)
Nickel
Copper
Gold

Each plating line consists of an acid pretreatment bath, a spray rinse, the plating bath and another spray rinse. The rinses flow into a common drain, and then into a 5000 gallon storage tank feeding the Rinse Water Reclamation System.

Figure 2 illustrates the equipment details for the complete system.

RINSE WATER RECLAMATION SYSTEM

The contaminated rinse waters are continuously pumped through an activated carbon filter to remove low molecular weight organic contaminants and into a reverse osmosis unit for further purification. The reverse osmosis unit utilizes a semi-permeable membrane to remove dissolved ionic and high molecular weight organic contaminants. Approximately 90% of the feed volume is pumped through the membrane as purified water (permeate) while the remaining stream (concentrate) contains the bulk of the contaminants, and is directed to the Waste Treatment System. This reverse osmosis unit is sized to treat as much as 72,000 gpd of contaminated rinse water. The permeate accumulates in a 5000 gallon storage tank from which it is pumped through another activated carbon filter to remove any trace of low molecular weight organic contaminants, then through a pair of two-bed (cation-anion) automatic deionizers to further remove ionic contaminants. Each two-bed deionizer unit has an ionic adsorption capacity of 344,000 grains (5,882,400 ppm), and the regenerant waste is directed to the Waste Treatment System. The purified water passes through an ultrafiltration unit designed to remove particulate matter and such organic contaminants as bacteria and virus which may have been picked up in the activated carbon filters or deionizers. The ultrafiltration unit operates similarly to the reverse osmosis unit in that most of the water is pumped through a semi-permeable membrane as permeate, and the concentrate stream exits to the Waste Treatment System. 95% of the feed water becomes permeate, most of which is directed to the Polishing System for polishing up to 18 megohm/cm quality for reuse as ultrapure rinse water; the rest of the permeate is continuously recirculated back to the 5000 gallon storage tank.

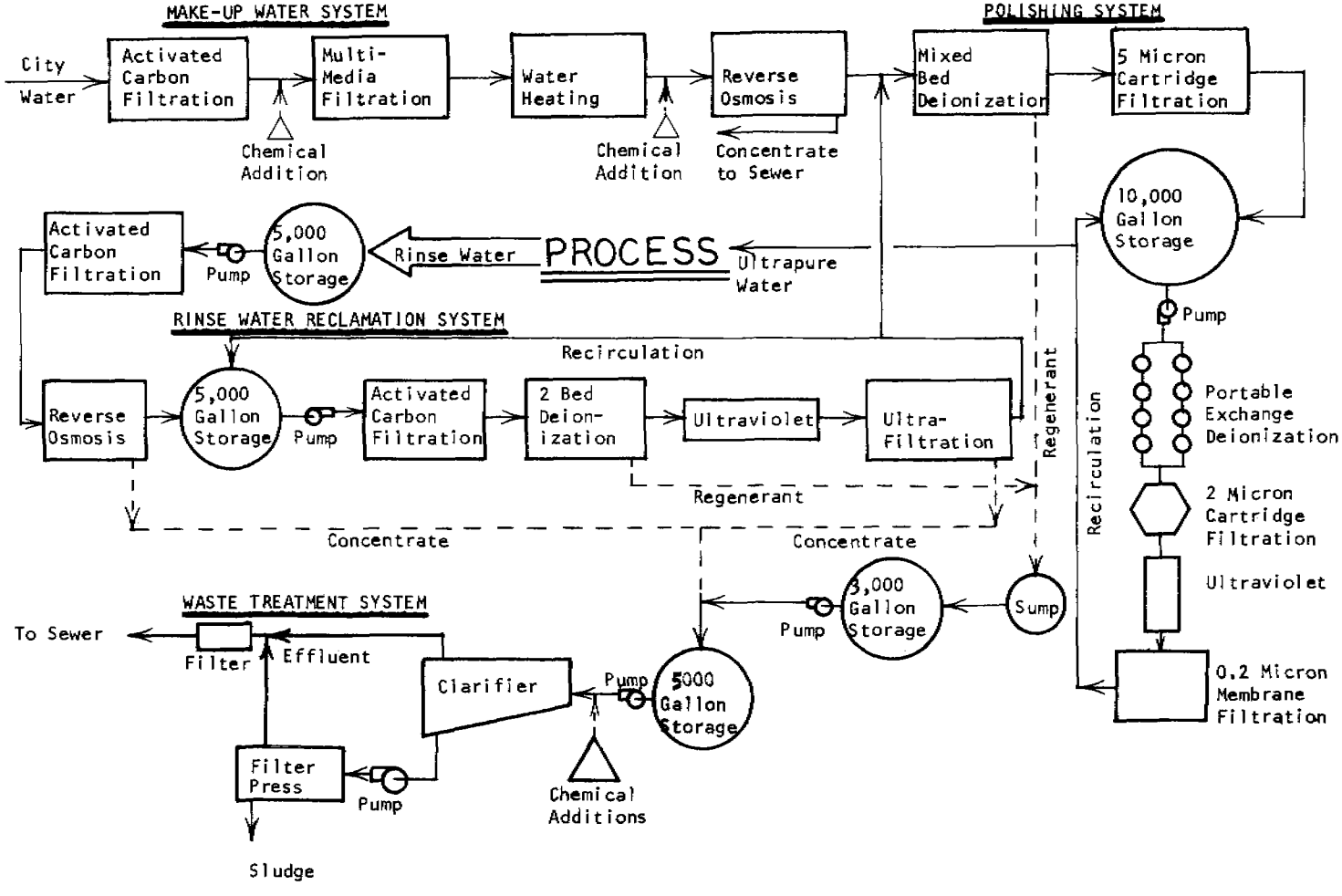

FIGURE 2. CONTINUOUS WATER RECLAMATION AND WASTE WATER TREATMENT SCHEMATIC

The total dissolved solids concentration (TDS) of the feed stream to the reverse osmosis unit does not exceed 800 ppm. Operating at 90% recovery, with thin film composite spiral wound membrane elements, the permeate TDS is 140 ppm.

The stream directed to the two-bed deionizers is a mixture of the reverse osmosis permeate and recirculation loop; operating at full capacity, the TDS of this stream is 136 ppm. Each two-bed unit can process at least 43,000 gallons of the above feed stream before requiring regeneration. At the maximum flow rate of 72,000 gpd, each unit regenerates approximately every 16 hours.

MAKE-UP WATER SYSTEM

To supply make-up water to replace that lost to the Waste Treatment System (concentrate from the RO and UF units and regenerant from the deionizers), and also to serve as an emergency source of total rinse supply in the event of a breakdown of the Rinse Water Reclamation System, the Make-up Water System is designed to purify as much as 72,000 gpd of city water. This system includes activated carbon filtration to remove chlorine and low molecular weight organics, a multimedia filter to lower the suspended solids level, water heaters to warm the water to 77°F., and a reverse osmosis unit capable of producing up to 50 gpm of purified water, which is then directed to the Polishing System.

Based on a feed water TDS of 170 ppm, operating at 70% recovery and utilizing spiral wound cellulose acetate membrane elements, the reverse osmosis unit produces a permeate quality of 17 ppm TDS.

Should the Rinse Water Reclamation System require shut-down for any reason, the Make-up Water System is capable of producing a sufficient quantity and quality of water to bypass the reclamation system without affecting the production of the semiconductor devices.

POLISHING SYSTEM

The purified water from both the Rinse Water Reclamation and Make-up Water Systems is blended and polished up to 18 megohm/cm quality in this system. This combined flow of 72,000 gpd, with a quality of approximately 200,000 ohm/cm is directed to automatic mixed-bed deionizers and then through 5 micron filter cartridges to remove particulate matter which may have been picked up in the deionizers. Each mixed-bed deionizer requires regeneration no more frequently than once every eight days.

The resulting stream is directed to a 10,000 gallon storage tank where it is continuously purified by recirculating through portable exchange mixed-bed deionizers, 2 micron cartridge filters, an ultraviolet light and 0.2 micron cartridge membrane filters.

The exchange deionizers ensure that the ionic contaminants in the water are held at a concentration less than 0.03 ppm (18 megohm/cm); the 2 micron cartridge filters are to remove particulate matter from the deionizers and the ultraviolet irradiation unit is designed to minimize bacteria growth in the pure water. The 0.2 micron membrane filters are cartridge filters utilized to prevent passage of fine particulate material or large organic agglomerate. The water is continuously recirculated back to the 10,000 gallon storage tank with as much as 72,000 gpd directed to the process as ultrapure rinse water.

WASTE TREATMENT SYSTEM

Occasional plating bath dumps, regenerant waste from the automatic mixed-bed deionizers in the Polishing System and from the two-bed deionizers in the Rinse Water Reclamation System is fed to a sump and from there to a 3000 gallon storage tank for accumulation and equilization. It is then pumped to a 5000 gallon storage tank where it mixes with the concentrate streams from the reverse osmosis and ultrafiltration units in the Rinse Water Reclamation System. Sodium hydroxide and calcium chloride are stoichiometrically added to this mixed waste as it is pumped to a slant-tube clarifier to facilitate precipitation of the resulting insoluble heavy metal hydroxides. A sludge pump directs the precipitated material to a one cubic foot filter press for dewatering and the resulting sludge is placed in drums for hauling to a disposal site. The effluent from the clarifier and filter press meets MWCC discharge limits and is filtered to remove suspended solids and then sewered. The Waste Treatment System is designed to process a continuous flow of as much as 20,000 gpd.

SUMMARY

Because of the extremely high value of the products produced in this facility and to minimize the possibility of treatment system shut-down, each pump has a spare plumbed in and ready to run. In addition, each system has been over-sized to allow the bypass of an entire system in the event of a serious break-down.

The high technology processes of reverse osmosis, ultrafiltration, automatic deionization and activated carbon filtration have been used extensively to produce ultrapure rinse waters for the electronic manufacturing industries; however, the concept of extensive reclamation of these waters is new and relatively unproven.

This case history confirms the feasibility of continuous rinse water reclamation and underscores the simplicity of design possible to accomplish this recovery.

As the cost of raw water and waste discharge increases and consistency of quality becomes more uncertain, the concept of reclamation and minimal discharge is the "wave of the future" in this and many other industries.

OPERATING COST SUMMARY

Operating costs for each sub-system are summarized below. These data include materials and electrical energy costs only, and do not include labor.

Rinse Water Reclamation System

Total daily operating cost = $71.04/day
Total operating cost/1000 gallons = $2.37/1000 gallons

Make-up Water System

	Normal Flow	Maximum Flow
Total daily operating cost =	$100.96/day	$293.04/day
Total operating cost/1000 gallons =	7.02/1000 gal	2.85/1000 gal

Polishing System

Total daily operating cost = $56.49/day

Total operating cost/1000 gallons = $2.37/1000 gallons

Waste Treatment System

Total daily operating cost = $22.82/day
Total operating cost/1000 gallons = $1.14/1000 gallons

Overall operating costs assuming maximum flows and full operation of the Rinse Water Reclamation System:

Daily cost $251.31/day
Cost/1000 gallons = $11.31/1000 gallons

Estimation of overall operating costs based on the assumption that the Rinse Water Reclamation System is not operating is not practical because the Waste Treatment System would have to be significantly increased in size, with the attendant increase in capital and operating cost. In actuality, if the Reclamation System were temporarily shut down, an exemption permit would be obtained from the MWCC to allow temporary discharge of toxic wastes.

The attached operating cost data provide details of each system component and the associated operating costs.

OPERATING COST DATA

Rinse Water Reclamation System

The contaminated rinse water, (maximum flow - 72,000 gpd) is pumped through a series of purification processes and into a recirculation loop to continuously remove most of the contaminants. Approximately 62,000 gpd is blended with 10,000 gpd from the Make-up Water System, polished up to 18 megohm/cm quality and directed to the process for rinsing purposes.

Operating costs are calculated on purification of the maximum flow of 72,000 gpd over a 16 hour/day period.

Two distribution pumps with 5 Hp motors to supply water from the 5000 gallon holding tank to the activated carbon filters.

Operating cost = 4.7 kwh x 16 hours x $0.02677/kwh = $2.01/day = $0.03/1000 gal

Two 42" diameter activated carbon filters. Operating costs include backwash water and periodic carbon replacement. Backwashing utilizes 2000 gallons of water and the frequency is every day. Carbon replacement is expected to be every six months.

Backwash water cost/day = 2000 x 0.75/1000 gal = $1.50/day = $0.02/1000 gal

Carbon replacement cost/day = 23 ft^3 x $55/$ft^3$ ÷ 125 = $10.12/day = $0.14/1000 gal

Total operating cost = $11.62/day = $0.16/1000 gal

One reverse osmosis unit operating at 90% recovery, producing approximately 65,000 gpd of purified water (permeate) which is directed into a 5000 gallon storage tank feeding the recirculation loop.

Operating costs include replacement membrane elements, electrical usage of the high pressure pump, cleaning chemicals and rinse water and prefilter cartridge costs.

Membrane element replacement (two year life)	$ 64.00/day
Electrical costs (47 kwh x 16 hour/day x $0.02677/kwh)	20.13/day
Cleaning chemicals and rinse water costs	0.47/day
5 micron prefilter cartridge costs	5.04/day
Total operating cost/day	= $ 89.64/day
Total operating cost/1000 gal	= $ 1.25/1000 gal

Two distribution pumps with 5 Hp motors to supply water from the 5000 gallon permeate holding tank and supply flow to the recirculation loop.

Operating cost = 4.7 kwh x 24 hours x $0.02677/kwh = $3.02/day = $0.04/1000 gal

Two 36" diameter activated carbon filters. Operating costs include backwash water and periodic carbon replacement. Backwashing utilizes 1400 gallons of water and the frequency is every other day. Carbon replacement is expected to be every six months.

Backwash water cost/day = 1400 x 0.75/1000 gal x 1/2 = $0.53/day = $0.01/1000 gal

Carbon replacement cost/day = 17 ft^3 x $55/$ft^3$ ÷ 125 = $7.48/day = $0.10/1000 gal

Total operating cost = $8.01/day = $0.11/1000 gal

Duplex automatic two-bed DI units operating alternately with each two-bed unit containing a total exchange capacity of 344,000 grains. Based on the average permeate quality of 136 ppm total dissolved solids, each two-bed unit requires regeneration after 43,000 gallons. Based on an average continuous recirculation flow of 65,000 gpd, each two-bed unit requires regeneration every 16 hours. Operating costs include regenerant chemicals usage, rinse water usage and resin replacement.

Chemicals usage per regeneration

34 gallons 20° Be′ HCl @	$0.95/gal	= $32.30
18 gallons 50% NaOH @	$1.50/gal	= 27.00
	Total	$59.30

$59.30 ÷ 2 = $29.65/day

Rinse water usage @ 2605 gallons/regeneration =

2605 x $0.75/1000 gal ÷ 2 = $0.98/day

Resin replacement

Cation resin life expected to be ten years and replacement cost $65/$ft^3$. Each two-bed unit contains 17 ft^3 of cation resin and total daily cost = $ 0.44/day.

Anion resin life expected to be five years and replacement cost $250/$ft^3$. Each two-bed unit contains 19 ft^3 of anion resin and total daily cost = $4.22/day

Total resin cost = $4.66/day

Two-bed DI operating costs summary:

Chemicals cost	=$29.65/day
Rinse water cost	= 0.98/day
Resin replacement cost	= 4.66/day
Total cost	=$35.29/day
Cost/1000 gal	=$0.49/1000 gal

One ultraviolet light utilizing 9.152 kwh electrical energy with a total operating cost of $0.25/day = $0.003/1000 gallons.

One ultrafiltration unit operating at a minimum of 95% recovery and providing final filtration for the rinse water reclamation recirculation loop.

Operating costs include replacement of membrane elements, electrical usage of the pump and cleaning chemicals and rinse water usage.

Membrane element replacement (two year life)	= $12.80/day
Electrical costs (18.8 kwh x 16 hour/day x $0.02677/kwh)	= 8.05/day
Cleaning chemicals and rinse water costs	= 0.35/day
Total operating cost/day	= $21.20/day
Total operating cost/1000 gal	= $ 0.29/1000 gal

Make-Up Water System

Under normal operating conditions, this system will produce 10,000 gpd to be blended with 62,000 gpd from the Rinse Water Reclamation System and the total flow polished up to 18 megohm quality for process rinsing. In the event of a breakdown in the Rinse Water Reclamation System, the Make-up Water System is designed to supply the entire process water requirement of 72,000 gpd.

Operating costs have been calculated for two flows, "normal" (14,400 gpd) and "maximum" (103,000 gpd).

Following is an equipment list for the system identifying each operating cost component and summarizing the total costs for each flow.

One 42" diameter activated carbon filter - operating costs include water used in the backwash cycle and periodic carbon replacement. Each backwash cycle uses 2000 gallons of water, and the carbon capacity of the 42" diameter tank is 23 ft^3 Raw water cost is $0.75/1000 gallons and carbon cost is $55/$ft^3$.

	Normal Flow	Maximum Flow
Frequency of backwash	one/month	one/week
Backwash water cost	$0.01/day	$0.03/day
Frequency of carbon replacement	12 months	six months
Carbon replacement cost	$5.06/day	$10.12/day
Total daily operating cost	$5.07/day	$10.15/day
Total operating cost per 1000 gallons of water processed	$0.35/1000 gal	$ 0.10/1000 gal

One 36" diameter multi-media filter; operating costs include a coagulant added to produce a 2 ppm concentration and water used in backwash cycle (1800 gal).

	Normal Flow	Maximum Flow
Coagulant usage	0.24 lb/day	1.72 lb/day
Coagulant cost/day	$0.78/day	$5.55/day
Backwash frequency	every three days	every two days
Backwash water cost/day	$0.45/day	$0.68/day
Total operating cost/day	$1.23/day	$6.23/day
Total operating cost/1000 gal	$0.09/1000 gal	$0.06/1000 gal

Two gas fired water heaters to raise the temperature of the water to approximately 77°F for most efficient membrane processing and product rinsing. The mean water temperature over the course of the year is estimated to be 55°F, so a 22°F temperature increase is required to bring the water to 77°F. Heat requirement is as follows: Btu/day = Δ temp (°F) x lb day. Cost of natural gas is estimated to be $5.50 x 10^{-6}/Btu.

Normal Flow

14,400 gal/day x 8.33 lb/gal x 22°F = 2,638,944 Btu/day

Cost/day = $14.51
Cost/1000 gallons = $1.01/1000 gal

Maximum Flow

103,000 gal/day x 8.33 lb/gal x 22°F = 18,875,780 Btu/day

Cost/day = $103.82
Cost/1000 gal = $1.01/1000 gal

One reverse osmosis unit. 70% of the filtered and heated feed water is pumped through the membrane and is blended with the Rinse Water Reclamation System recirculation water prior to polishing in the mixed-bed deionizer. Operating costs include HCl used to lower the pH of the feed water to 6.5, hexametaphosphate dispersant added to a concentration of 2 ppm, replacement membrane elements, electrical usage of the high pressure pumps, membrane cleaning chemicals and rinse water, and prefilter cartridge costs and the cost of the entire water supply.

	Normal Flow	Maximum Flow
HCl costs ($/day)	$ 0.79	$ 5.99
Hexametaphosphate costs ($/day)	0.60	4.29
Membrane element replacement (2 year life)	64.00	64.00
Electrical costs ($/day)	2.24	16.11
Cleaning chemicals and rinse water ($/day)	0.04	0.16
5 micron prefilter cartridge costs ($/day)	1.68	5.04
Total water cost ($/day)	10.80	77.25
Total operating cost ($/day)	$ 80.15/day	$172.84/day
Total operating cost ($/1000 gal)	$ 5.57/1000 gal	$ 1.68/1000 gal

Polishing System

Two 30" diameter automatic mixed-bed deionizers operating alternately each with an exchange capacity of 165,000 grains. Based on an average feed water quality of 4½ ppm (0.263 gpg), and continuous flow of 72,000 gpd from the combined streams of the make-up water reverse osmosis permeate and rinse water reclamation recirculation loop, each deionizer requires regeneration every eight days. Operating costs include regenerant chemicals usage, rinse water usage and resin replacement.

The mixed-bed deionizers and other components of the polishing loop will operate at a constant recirculating flow of 72,000 gpd, and costs are based on the assumption that this entire flow is used for process rinsing daily.

Chemicals usage per regeneration:

15 gal 20°Be' HCl @ \$0.95/gal = \$14.25
10.8 gal 50% NaOH @ \$1.50/gal = \$16.20
Total = \$30.45/regeneration

\$30.45 ÷ 8 = \$3.81/day

Rinse water usage @ 2155 gallons/regeneration:

2155 x \$0.75/1000 gal ÷ 8 = \$0.20/day

Resin replacement:

Cation resin life expected to be ten years and replacement cost \$65/ft^3. Each mixed-bed unit contains 7½ ft^3 of cation resin, and total daily cost = \$0.20/day.

Anion resin life expected to be five years and replacement cost \$250/ft^3. Each mixed-bed unit contains 11½ ft^3 of anion resin, and total daily cost = \$2.30/day.

Total resin cost = \$2.50/day

Mixed-bed operating costs summary:

Chemicals cost	3.81/day
Rinse water cost	0.20/day
Resin replacement cost	2.50/day
Total mixed bed DI costs	= \$6.51/day
Cost/1000 gal	= \$0.09/1000 gal

Two distribution pumps with 5 Hp motors to supply water from the 10,000 gallon storage tank to the polish/recirculation loop. Operating costs are assumed to be only the electrical consumption of each pump @ 4.7 kwh each x 16 hours = 75.2 kwh /day. 75.2 kwh/day x \$0.02677/kwh = \$2.01/day or \$0.03/1000 gal.

Eight portable exchange deionization tanks for final polishing are exchanged every twelve weeks at a cost of \$584/exchange.

$$\$584 \times \frac{52}{12} \div 250 = \$10.12/\text{day}$$

\$ 10.12/day ÷ 72,000 x 1000 = \$0.14/1000 gal

Two filter housings containing 10 two micron cartridges each and requiring changing once every three months.

Operating cost = $2 \times 10 \times \$65 \times \frac{12}{3} \div 250 = \$20.80/\text{day} = \$0.29/1000$ gal

Two filter housings containing 15-0.2 micron cartridges each and requiring changing once every six months.

Operating cost = $2 \times 15 \times \$70 \times \frac{12}{6} \div 250 = \$16.80/\text{day} = \$0.23/1000$ gal

One ultraviolet light utilizing 9.152 kwh electrical energy.

Total operating cost = $9.152 \times 0.02677 = \$0.25/\text{day} = \$0.003/1000$ gal

Waste treatment system. The regenerant wastes from the deionization units, concentrate streams from the reverse osmosis and ultrafiltration units in the Rinse Water Reclamation System and backwash from the activated carbon filters in the Rinse Water Reclamation System are directed to the Waste Treatment System which is sized to continuously treat a maximum flow of 20,000 gpd.

Operating costs are based on this flow and consist of electrical consumption of the various pumps and chemicals usages.

Total pump electrical cost - 6.6 kwh x 16 hours x \$0.02677/kwh = \$2.82/day

Total chemicals costs \$20.00/day

Total daily cost = \$22.82/day
Total cost/1000 gal = \$ 1.14/1000 gal

Wat. Sci. Tech. Vol.17, Amsterdam, pp.337-350.
Printed in Great Britain.

0273-1223/85 $0.00 + .50

DEVELOPMENT OF A NEW PROCESS FOR TREATING URANIUM MINING EFFLUENTS

P. M. Huck, W. B. Anderson and R. C. Andrews

Department of Civil Engineering, University of Alberta, Edmonton, Alberta, T6G 2G7, Canada

ABSTRACT

Decants from Canadian uranium mining tailings areas are treated to remove radium-226 prior to discharge into the environment. This paper describes the development of a new treatment process for these effluents. This new process differs from existing systems in that it involves the use of a fluidized bed to facilitate $(Ba,Ra)SO_4$ coprecipitation on a granular medium of high surface area. No solids separation step is required, as the granular material is free draining. The new process has been demonstrated to provide radium-226 removal efficiencies consistently exceeding 90% in contact times of about 20 seconds. These short times are in contrast to times on the order of days for conventional pond systems or hours for mechanical systems involving stirred tank precipitation reactors.

KEYWORDS

Barium-radium sulphate; coprecipitation; factorial optimization; fluidized bed; path of steepest ascent; precipitation; radium-226; tailings effluents; uranium effluents.

INTRODUCTION

The mining and milling of uranium ores results in large quantities of waste solids (tailings) after processing. Included in these wastes are all the radioactive isotopes from the uranium, actinium and thorium decay series. The tailings are discharged in slurry form to impoundment areas where the solids settle out of the slurry. In regions having a net excess of precipitation over evaporation, the liquid used to transport the tailings is discharged from the tailings impoundment areas to surface waters. These effluents or decants contain little suspended material but appreciable quantities of dissolved materials; of particular concern for environmental protection is the amount of radium-226 being discharged to the aquatic environment. This isotope has an extremely high radiotoxicity.

Canadian uranium mine/mill tailings decants are treated with barium chloride to remove radium-226. Historically, this has been accomplished in large ponds which

provide an opportunity for a $(Ba,Ra)SO_4$ precipitate to form and subsequently settle. As environmental requirements have become more strict, two deficiencies have become apparent with this type of treatment system: acceptable total radium-226 levels are difficult if not impossible to achieve and the radium-bearing sludge which accumulates in the ponds presents a disposal problem on mine closure. Preliminary studies (IEC, 1980) have suggested that it may be acceptable to return the sludge produced by barium chloride treatment systems to tailings areas for final disposal. If this proves feasible, treatment systems which produce an easily-handled residue on an ongoing basis would be beneficial, in avoiding a final disposal problem.

Within the last few years, effort has been expended in Canada on improving treatment systems. This work was partly in response to a suggested Atomic Energy Control Board target level for tailings decants of 10 pCi/L total radium-226 (Huck, 1982). A mechanically based system has been developed, consisting of barium chloride addition to stirred tank reactors for precipitation, and granular media filtration for solids separation (Averill et al., 1983). This process offers improved effluent quality, reduces treatment time from days to hours and produces sludge on a continuous basis for on-going disposal rather than at the end of a mine's life. However, the filtration step is critical and must be carefully designed and operated. To date, only one full scale system has been placed into service.

OBJECTIVE AND PROCESS CONCEPT

The objective of the research reported herein was to develop a radium-226 removal process for tailings pond effluents which would be superior to pond systems but simpler than a mechanically based stirred tank/filtration system. Previous work by two of the authors (Huck and Anderson, 1983) had demonstrated that, under certain conditions, significant quantities of radium-226 could deposit on surfaces during barium chloride treatment. Pilot scale studies of the mechanical treatment system mentioned previously had recognized the role which surface effects could play (Averill et al., 1983). Seeley (1977) had also postulated adsorption of $RaSO_4$ on particle surfaces in a study on the leaching of uranium tailings.

The concept of the new treatment system was to induce the radium to deposit on existing surfaces of granular material in a reactor rather than in/on a precipitate created in the bulk of solution. The granular material, being free draining, could subsequently be separated from solution readily, eliminating the need for a separate liquid-solid separation step in the process. This granular material, once loaded with radium-226, should be easily handled and could be disposed of directly if it consisted of sand or some other low value material obtained locally at a uranium mine. To maximize the extent and rate of removal, the type of process required was one having high surface area, such as a packed or fluidized bed. To avoid plugging of the bed as particles grew and influent suspended solids were removed, the logical choice was a fluidized bed. In general, such a bed in which precipitation is induced is uncommon.

This paper reports the results of initial laboratory testing of the process and confirmatory field experiments.

MATERIALS AND METHODS

A laboratory scale fluidized bed reactor was designed and fabricated as illustrated in Fig. 1. The reactor consisted of a 2.5 cm internal diameter, 2.15 m high clear acrylic column with 16 sample ports located at 0.1 m and 0.2 m

intervals in the bottom and top portions respectively. A cone-shaped section was provided at the top to minimize carryover of fines. The column was supported on a free standing structure situated in a tray to contain spills. The column media was sieved silica sand, supported on 3 mm diameter glass beads. Actual media depths used in testing did not exceed 240 mm. Untreated tailings pond effluent was delivered to a port at the base of the column by a variable speed peristaltic pump. Similarly barium chloride feed solution was pumped through an injection port located at the sand/bead interface. This port extended into the centre of the column in an effort to ensure proper mixing of the barium chloride and the influent.

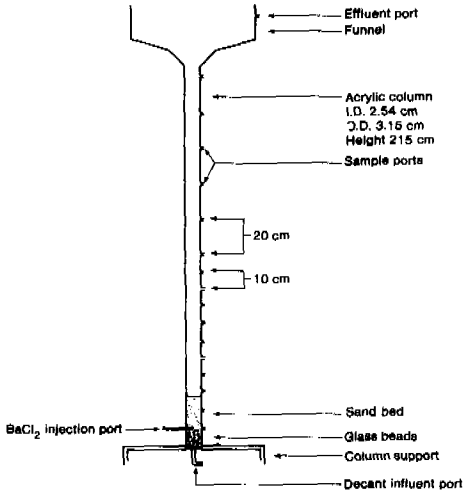

Fig. 1 Fluidized bed reactor apparatus (not to scale)

TABLE 1 Mean Tailings Pond Effluent Characteristics

Parameter*	Ontario mine	Saskatchewan mine**		Field Experiments Run 1	Run 2	Run 3
Radium-226						
Total	267	404	65	759	630	923
Dissolved	128	285	39	727	544	540
Ca	560	280	280	Not measured		
Mg	4	228	228	Not measured		
Hardness-total (as $CaCO_3$)	1410	1270	1270	Not measured		
SO_4	1535	1220	1220	Not measured		
NO_3-N	52	14	14	Not measured		
Fe - total	0.06	0.16	0.16	Not measured		
pH	9.5	7.3	7.3	8.1	8.0	7.8

* All units mg/L except pH and radium-226 (pCi/L).
** Effluent of two activity levels used in selected tests.

The mean water quality of the tailings pond effluents used in this phase of testing is shown in Table 1. Effluent was shipped to the laboratory in 23 L

plastic containers and in some cases lined 200 L drums. Radium-226 activity levels were determined by a modification of the radon de-emanation technique from Standard Methods (APHA-AWWA-WPCF, 1980). Dissolved radium is defined as that remaining in the sample after passage through a 0.45 μm filter. Other parameters were determined using procedures from Standard Methods except pH and NO_3-N, which was measured with an Orion Research Microprocessor Ionanalyzer 901.

HYDRAULIC TESTING

Initial tests were performed on the column using deionized water to experimentally verify calculated fluidization velocities. Equations outlined by Stathis (1980) were used to determine minimum fluidization velocities (V_{mf}) based upon mean particle diameter. Fluidization flow rates and corresponding fluidization numbers (the ratio of actual velocity to V_{mf}) were calculated for sand sieve fractions with mean diameters of 0.505 mm and 0.326 mm. These sizes were selected as being practical yet requiring minimum amounts of tailings effluent to attain fluidization for laboratory experimentation. Mercury manometers were used to measure the headloss through the 60 mm and 120 mm bed depths tested. A reasonable agreement was obtained between the theoretical and actual fluidization velocities (Table 2) although some channelling was observed below a fluidization number of 2.0.

TABLE 2 Experimental Verification of Calculated Fluidization Velocities

Mean Grain Diameter	Minimum Fluidization Velocity*	
	Calculated	Actual
0.326	11.4	14.8
0.505	22.9	21.7

* Units are cm/min except grain diameter which is mm.

In addition, some experiments involving dye injection were performed to observe the mixing characteristics of a barium chloride solution entering the column, and to observe any changes in column flow induced by sampling of effluent above the fluidized bed. For the purposes of these experiments, deionized water was used in place of decant, and methylene blue dye was used to trace the flow. Visual observations (confirmed photographically) concluded that the barium chloride solution mixed evenly in the fluidized bed. Complete mix as opposed to plug flow behaviour was evident. Injecting dye above the bed illustrated smooth streamlines, characteristic of laminar flow. Rapid collection of a sample (130 mL in <10 seconds) appeared to draw liquid almost exclusively from above the sample port as opposed to slow collection which drew liquid exclusively from below the port. These observations confirmed that rapid collection of samples was preferable, particularly when bed disturbance was to be avoided.

PHASE ONE TESTING

The first phase of testing was designed to confirm the hypothesis that radium-226 coprecipitating with barium in sulphate and/or carbonate form would adhere to the sand surfaces present in the fluidized bed. It was also designed as an initial kinetics test, to determine how quickly the column achieved steady state. This first phase examined uranium tailings pond effluents originating from two separate geographical regions in Canada. One mill was located in northern Saskatchewan, the other in Ontario. Both mills employed a sulphuric acid leach process.

For both decants, total and dissolved radium-226 percentage removals consistently ranged from 75 to 95%. These very encouraging results were obtained despite the fact that initial testing involved small bed heights, short contact times in the bed (approximately 30 seconds) and completely unoptimized conditions.

PHASE TWO TESTING

Factorial Optimization Experiments

After the initial testing had confirmed the viability of the process concept, it was decided to examine five factors in an effort to optimize the radium removal efficiency of the system. These factors were: mean sand diameter, unexpanded sand bed height, fluidization number, $BaCl_2$ feed solution strength, and $BaCl_2$ dose.

Factorial experiments were used to investigate the significance of the factors individually and in combination. Path of steepest ascent (PSA) experiments were employed to arrive at optimum conditions quickly. These experiments when combined with factorial design experiments, in a procedure known as "response surface methodology" are used to assist in process optimization. A PSA is a vector through n-dimensional space which points in the direction of the greatest change in the response parameter measured in the factorial experiment. The PSA is calculated by ratio based on the levels tested and responses observed for each factor in the factorial design (Averill et al., 1983).

The results for each factor are summarized below. Two experiments are described in detail later.

Mean Sand Diameter

Sieved silica sand particles with mean diameters of 0.326 and 0.505 mm were compared as it was hypothesized that the smaller diameter particles would increase radium removals because of their greater surface area in beds of equal height. Removal efficiencies did not however differ significantly in any tests and it was concluded that even the larger diameter particles had sufficient surface area to facilitate any deposition that was likely to occur under the conditions tested.

Unexpanded Bed Height

It was hypothesized that increased bed height would improve radium-226 removal due to the corresponding increase in both available surface area and contact time. Test results supported the hypothesis with a 240 mm high bed demonstrating a slightly better ability to remove dissolved radium than did a 120 mm high bed. There did not appear to be any significant difference in the ability of the bed to remove particulate radium. As with mean sand particle diameter the height of the smaller bed (at 120 mm) may have been sufficient to accomodate most if not all deposition that was likely to occur.

Fluidization Number

Fluidization numbers investigated were 1.1, 1.5, 2.0, 2.5 and 3.0. It was hypothesized that as fluidization number increased (as a result increasing flow and decreasing contact time) radium removal efficiency would decrease. This in fact was not observed under any of the conditions investigated and it was again

suspected that conditions under which the tests were performed were sufficient to permit any deposition that was likely to occur.

Barium Chloride Feed Solution Strength

Barium chloride feed solution strengths of 0.25 mg/mL and 0.50 mg/mL (as Ba^{+2}) were investigated and found to show no significant difference in radium-226 removal ability.

Barium Chloride Dose

Of the five factors investigated, barium chloride dose was found to be the most critical. Nine dosages (ranging from 4 to 28 mg/L as Ba^{+2}) were examined and it was found that the ability of the system to remove radium increased significantly up to a dose of 14 mg/L (as Ba^{+2}) whereupon radium-226 activity levels in treated effluent tended to stabilize.

It was encouraging to note however that even at the low dose of 4 mg/L the system was still able to remove 81% of the radium contacting the bed. When dosed in excess of 14 mg/L the system consistently removed 91 to 98% of the radium originally present in the untreated tailings pond effluent.

Table 3 lists conditions, that based upon preliminary testing, appeared to be approximately optimal or at least a compromise between optimal and practical. The barium chloride dose is in the range of doses used in pond and mechanical systems.

TABLE 3 Approximate Optimal Conditions for Radium-226 Removal With Bench Scale System

Condition	Optimum Level
Fluidization number	3.0
Bed height	240 mm
Sand diameter (mean)	0.505 mm
$BaCl_2$ dose (as Ba^{+2})	16 mg/L
$BaCl_2$ feed solution strength (as Ba^{+2})	0.50 mg/mL

Some factors were not investigated, either because of problems that would be encountered in a laboratory situation, or because they were perceived to be of less importance. These factors include pH variation of the untreated tailings pond effluent, temperature variation and fluidization numbers in excess of 3.0.

It was decided that temperature and pH variation were factors that would be better suited to examination in a field situation. It is unlikely that fluidization numbers in excess of 3.0 would have to be used in a scaled up system but the information may be important if it should ever be necessary to discharge large volumes of decant from a tailings area in a short period of time.

Two experiments which completed this phase are described in detail below. The first involved untreated tailings pond effluent of a relatively high initial radium-226 activity level, and the second involved effluent of a relatively low initial radium-226 activity level.

Experiment 1

The objective of this experiment was to investigate the significance of varying $BaCl_2$ feed solution strength and fluidization number on radium-226 removal in the fluidized bed with a tailings pond effluent of relatively high radium-226 concentration.

A two variable matrix was set up (Table 4) which examined five fluidization numbers and two $BaCl_2$ feed solution strengths. Fixed conditions included sand bed height at 240 mm, mean sand diameter at 0.505 mm and $BaCl_2$ dose (as Ba^{+2}) at 16 mg/L. These conditions had been determined in factorial experiments to be optimal with regard to experimental apparatus and tailings pond effluents being used. A new sieved silica sand bed was used for each trial.

Radium-226 removal in the fluidized beds was excellent (Table 4). Dissolved radium-226 activity levels immediately above the bed (i.e., following treatment) ranged from 12 to 42 pCi/L with a mean of 21 pCi/L, excluding one anomalous value. Total radium-226 activity levels immediately above the bed were also excellent and closely paralleled dissolved values; levels ranged from 13 to 42 pCi/L, with a mean of 25 pCi/L.

TABLE 4 Radium-226 Remaining in Column Effluent and Percentage Removed (Normal Decant)

Trial Number*	$BaCl_2$ Solution Strength (mg/mL as Ba^{+2})	Fluidization Number	Radium-226 Remaining (pCi/L) Dissolved	Total	Radium-226 Removed (%)** Dissolved	Total
8	0.25	1.1	143	16	50	95
5	0.50	1.1	25	22	92	95
3	0.25	1.5	14	24	95	95
2	0.50	1.5	42	13	86	97
1	0.25	2.0	18	41	94	91
7	0.50	2.0	19	42	93	87
6	0.25	2.5	12	28	96	94
4	0.50	2.5	28	17	91	96
9	0.25	3.0	22	26	92	92
10	0.50	3.0	13	18	95	95
-	0.25	mean	25 ***	27	94 ***	93
-	0.50	mean	17	22	91	94

* With the exception of trial numbers 9 and 10, trials were performed in random order.

** Based on the following untreated tailings pond effluent radium-226 activity levels:

	Trials 1-6	Trials 7-10
dissolved (pCi/L)	301	285
total (pCi/L)	448	330

*** Excluding the value for trial 8.

These test results confirmed that a $BaCl_2$ feed rate of 16 mg/L yielded consistently high radium removal efficiencies supporting the results of earlier

optimization testing.

Although it was anticipitated that fluidization number might be critical, no definite trend could be discerned within the range of values examined. It is important to note however that experimental conditions bordered on the optimum and if these conditions deteriorated, effects of altering one variable would become more exaggerated. The fact that fluidization number did not appear critical is encouraging. This will undoubtedly prove to be advantageous, as effluent discharge rates from uranium mills vary with daily production and in response to spring thaw and heavy precipitation. Treatment systems must be able to accommodate increased flow capacity without a deterioration in effluent quality.

It would appear that $BaCl_2$ feed solution strength is not critical over the range examined, as percentage removals for each level were quite similar (Table 4). This characteristic is also advantageous both at the experimental level and in practice, in that solution strengths may be altered to accommodate capacities of existing equipment. Space requirements and capital costs for the $BaCl_2$ feed system can be reduced by increasing $BaCl_2$ solution strength. More concentrated $BaCl_2$ solutions will be investigated in future experiments.

Experiment 2

This experiment was conducted shortly after the experiment discussed previously and had the same objectives. The only difference was that the radium-226 activity levels in the untreated tailings pond effluent were much lower; at 70 pCi/L and 51 pCi/L for total and dissolved radium respectively, they were 5 to 6 times less than those of the previous experiment. Fixed conditions were as in that experiment namely a bed height of 240 mm, mean sand diameter of 0.505 mm and $BaCl_2$ dose of 16 mg/L (as Ba^{+2}). Fluidization numbers of 1.5 and 2.5 were however not examined.

TABLE 5 Radium-226 Remaining in Column Effluent and Percentage Removed (Dilute Decant)

$BaCl_2$ Solution Strength (mg/mL as Ba^{+2})	Fluidization Number	Radium-226 Remaining (pCi/L) Dissolved	Total	Radium-226 Removed (%)** Dissolved	Total
0.25	1.1	4	2	92	97
0.25	1.1	2	3	96	96
0.50	1.1	6	2	88	97
0.25	2.0	2	3	96	96
0.50	2.0	4	2	92	97
0.25	3.0	2	3	96	96
0.50	3.0	6	3	88	96
0.25	mean	3	3	95	96
0.50	mean	5	2	89	97

* Based on the following untreated tailings pond effluent radium-226 activity levels: dissolved = 51 pCi/L
total = 70 pCi/L

** Some dissolved radium-226 activity levels exceed total values; this is attributed to sample variability and sample values near detection limits.

Test results indicated that effluent radium levels were exceptionally low with no values exceeding 6 pCi/L (Table 5). Percentage removals were equally impressive with mean values ranging from 90 to 97% for the 0.25 and 0.50 mg/mL Ba^{+2} feed solutions. Again there did not appear to be any real difference in efficiency of radium removal with respect to fluidization number or strenth of the $BaCl_2$ feed solution.

This experiment does however have important implications in that the process was demonstrated to be as effective in removing radium-226 from decants containing low levels of radium as from those containing higher initial levels of radium. It indicates that for a strong decant, two columns in series could achieve radium-226 levels well within suggested Canadian target levels of 10 pCi/L total radium-226.

MASS BALANCE EXPERIMENTS

Mass balance experiments were conducted to confirm that the radium-226 being removed from the tailings decant was in fact being removed by the deposition of barium-radium sulphate (or carbonate compounds) on the sand particles in the fluidized bed and not on some other portion of the test apparatus.

Results indicated that the majority of the radium being removed by the system was being deposited in the fluidized bed. As was suspected some radium was detected in the column influent feed lines, lower column walls, and on the glass bead support layer. Total amounts however were insignificant when compared with those observed in the sand bed.

FIELD TESTING

While experiments in the laboratory demonstrated consistent radium removal efficiencies, the process was not considered to be at steady state. Such a condition would only exist when there was a significant buildup of precipitate on the sand. To achieve this, and to test the system over an extended period with decant directly from a tailings pond, the bench scale apparatus was transported to a Canadian uranium mill for field tests. Several experiments, including an extended run, were conducted over a two week period.

Untreated tailings effluent was trucked daily in a polyethylene drum from the tailings pond to the test apparatus, which was located in the mill. The system was run for approximately 11 to 12 hours per day and shut down at night. During the extended run the system was not drained, nor was any condition altered with the exception of a planned increase in fluidization number on day three.

Run Number 1 - Control

The objective of this control run was to duplicate radium-226 removal efficiencies obtained in the laboratory using a set of conditions at which the system was demonstrated to be consistently capable of removing in excess of 90% of the influent radium. Experimental conditions are listed in Table 6.

The system was run for 10 hours during which time 210 L of decant was pumped through the bed. The influent radium levels were considerably higher than experienced in laboratory testing. Radium-226 removal efficiencies were very good, both in terms of actual amounts of radium remaining in solution and percentage removed (Table 7). A mean total radium-226 activity level remaining in the treated effluent of 77 pCi/L represented 90% removal, and a mean dissolved radium-226 activity level of 22 pCi/L represented 97% removal. On the basis of

similar percentage removals, these results were considered to confirm earlier laboratory results.

TABLE 6 Experimental Conditions - Control

Condition	
Fluidization number	3.0
Upflow velocity (m/hr)	41
$BaCl_2$ dose - as Ba^{+2} (mg/L)	16.0
$BaCl_2$ feed solution strength-as Ba^{+2} (mg/mL)	0.50
Unexpanded bed height - dry (mm)	240
Expanded bed height (mm)	350
Sand diameter - mean (mm)	0.505
Untreated effluent temperature (°C)	19.0
Untreated effluent pH	8.1
Contact time - in bed (sec)	18

TABLE 7 Radium-226 Remaining in Treated Tailings Effluent and Percentage Removed (Field Testing - Control Run)

Hour	Radium-226 Remaining (pCi/L) Dissolved	Total	Radium-226 Removed (%)* Dissolved	Total
1.0	-	79	-	90
2.0	-	40	-	95
3.0	12	22	98	97
4.0	-	50	-	93
5.0	-	71	-	91
6.0	-	80	-	90
7.0	34	28	95	96
8.0	-	87	-	89
9.0	-	113	-	85
10.0	19	196	97	74
mean	22	77	97	90

* Based on the following untreated tailings pond effluent radium-226 activity levels: dissolved = 727 pCi/L
total = 759 pCi/L

Run Number 2 - Reduction of $BaCl_2$ Dose

The objective of this run was to determine if a gradual reduction of $BaCl_2$ dose would result in a reduction of the treatment system's ability to remove radium-226 from the untreated effluent or if, once the system had been operating for several hours, the dose could be reduced without affecting radium removal efficiency.

Conditions were as described in the previous control experiment with the exception of the $BaCl_2$ dose which was decreased as shown in Fig. 2. This was accomplished through appropriate reduction of the $BaCl_2$ feed solution strength.

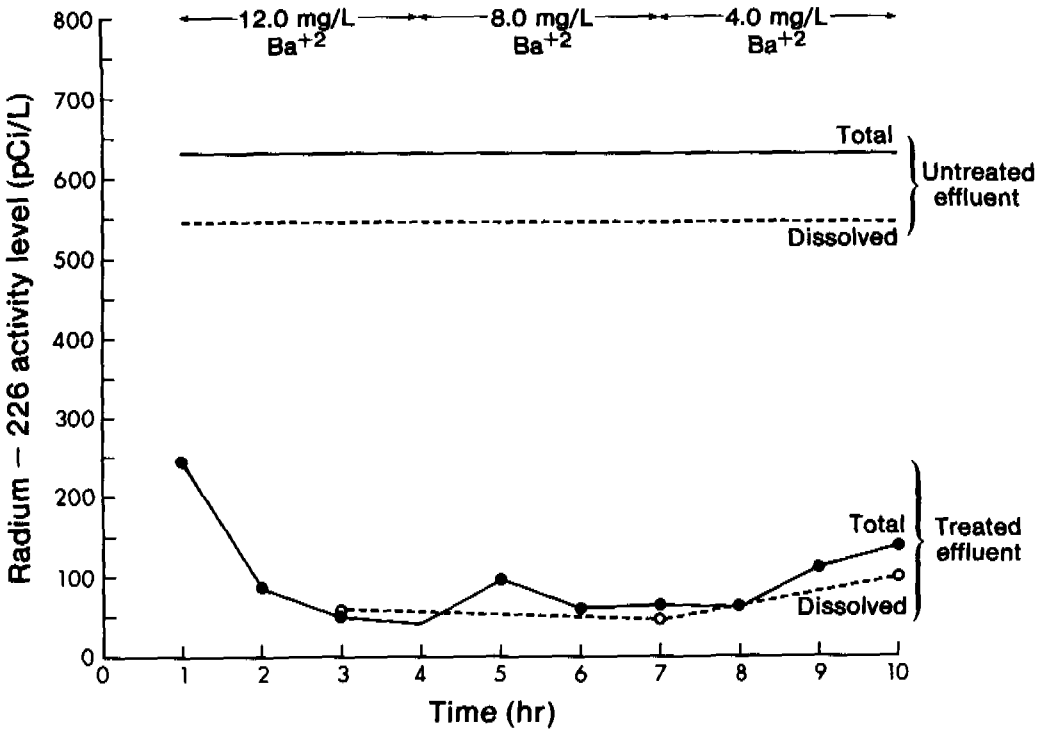

Fig. 2 Radium-226 remaining in treated tailings effluent (dosage reduction experiment)

Fig. 2 and Table 8 illustrate the effect of reducing $BaCl_2$ dosage on the ability of the fluidized bed system to remove radium-226 from untreated tailings pond effluent. $BaCl_2$ dosages in the 8-12 mg/L range were not as efficient as those in the 16 mg/L range used in previous tests but radium removals of around 90% appeared attainable. Reducing the dose to 4 mg/L however did show a significant decrease in the system's efficiency to about 82-84%. These results were in total agreement with what had been previously observed in laboratory bench scale runs.

TABLE 8 Mean Radium-226 Remaining in Treated Tailings Effluent and Percentage Removed for Dosage Reduction Experiment

$BaCl_2$ Dose mg/L (as Ba^{+2})	Radium-226 Remaining (pCi/L) Dissolved	Total	Radium-226 Removed (%)* Dissolved	Total
12.0	58	57**	89	91**
8.0	46	73	92	89
4.0	97	103	82	84

* Based on the following untreated tailings pond effluent radium-226 activity levels: dissolved = 544 pCi/L
total = 630 pCi/L

** Excluding the apparently anomalous value of 244 pCi/L obtained at hour 1.0

Despite the decreased radium removal efficiency at lower $BaCl_2$ doses it was encouraging to note that even the 4 mg/L dose achieved removals in excess of 80%. These results are significant in that there is a safety margin in the event of a $BaCl_2$ feed solution flow reduction or error in feed solution preparation. The use of lower doses will be investigated further in columns with a complete coating of precipitate on the media. Lower doses are advantageous economically and from an environmental point of view as they reduce the bulk of waste material that will have to be handled and stored.

Run Number 3 - Extended Run

The objective of this phase of experimentation was to determine if large quantities of untreated tailings pond effluent could be treated in a single fluidized bed without a reduction in radium-226 removal efficiency of the system. Using the conditions shown in Table 9, the system was run approximately 11 hours per day over 8 1/4 days for a total of 94.5 hours of operation and a throughput of 1750 L. The system was shut off at night but not drained. The bed was flushed daily by temporarily increasing the upflow velocity. However, little visible suspended matter was removed from the bed by this procedure.

Table 9 Fixed Experimental Conditions - Extended Run

Condition	Value*
Fluidization number (at initiation of run)	3.0
Upflow velocity (m/hr)	41
$BaCl_2$ dose - as Ba^{+2} (mg/L)	16.0
$BaCl_2$ Feed solution strength - as Ba^{+2} (mg/mL)	0.50
Unexpanded bed height -dry (mm)	240
Initial sand particle diameter - mean (mm)	0.505
Contact time - in bed (sec)	18

* A fluidization number of 1.5 was used from hours 0.0 - 22.5. Upflow velocity was 20 m/hr and contact time in bed was 24 sec (all other conditions remained the same). The fluidization number was increased to 3.0 at hour 22.5. It decreased gradually thereafter because of media growth.

Results of this phase of field testing were extremely encouraging with mean radium removal efficiencies of 94% for dissolved radium and 95% for total radium. These percentages represent a mean dissolved radium-226 activity level in treated effluent of 33 pCi/L and a mean total activity level of 44 pCi/L based on mean untreated effluent activity levels of 540 pCi/L dissolved and 923 pCi/L total radium-226 (Fig. 3). The system was consistently capable of removing high percentages of radium, and was relatively unaffected by fluctuating untreated effluent radium activity levels. The system removed on average nearly 400 pCi/L of particulate radium (total minus dissolved) probably by some type of cementation process.

It was also encouraging to note that there was no decrease in radium removal efficiency even when the run was terminated following treatment of 1750 L of effluent over a period of 94.5 hours in a bed which was only 25.4 mm in diameter and 240 mm in height.

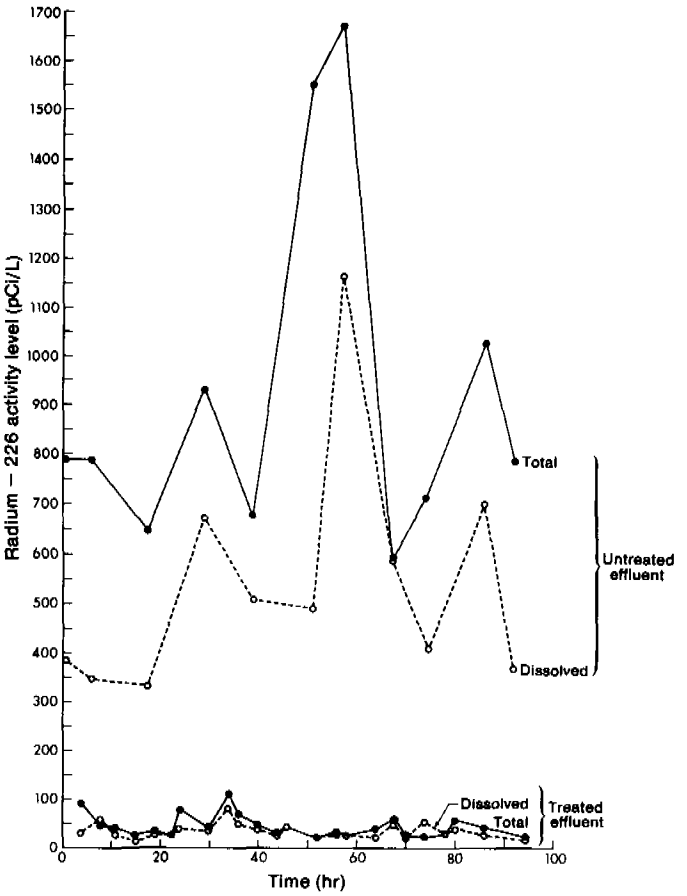

Fig. 3 Radium-226 remaining in treated tailings effluent (extended run)

Following termination of the run the sand was dried and for the first time the $(Ba,Ra)SO_4$ coprecipitate which had depositied on the sand particles was clearly visible. This had not been observed previously, presumably because of the limited length of earlier test runs.

No plugging was observed in the bed although some was observed in the glass bead support when suspended matter trapped in the beads pushed the upper portion of the support bed directly into the $BaCl_2$ flow. Unlike the sand particles, the beads were not fluidized and $(Ba,Ra)SO_4$ coprecipitate formed on the beads causing localized plugging and subsequent channelling of the decant through the sand bed. By the termination of the run this channelling probably reduced contact time to approximately 10 seconds, based on visual observation. There was however, no noticeable reduction in the radium removal efficiency of the system.

Further work is planned to increase radium removals and to test the system under cold weather operation. Following this, scaleup to a larger diameter column will be undertaken.

CONCLUSIONS

1. A new radium removal process for uranium mining effluents has been successfully developed and tested at bench scale. In this fluidized bed process barium chloride is used to precipitate radium-226 directly onto the surface of a free draining granular material.

2. The process provides total radium-226 removals of 90 to 95% in a contact time of approximately 20 seconds. This time is orders of magnitude less than that required by existing pond and mechanical systems, while the barium chloride dose is similar.

3. The short contact time and absence of a solids-separation step make the process simple and compact. It is anticipated that it would be considerably cheaper than conventional processes.

4. Percentage removals appear to be independant of average influent radium-226 activity levels. Strict effluent requirements can be met by operation of two reactors in series, if necessary. It is expected, however, that additional process optimization can improve effluent levels even further.

5. The process appears to be relatively insensitive to moderate changes in major operating parameters and to short-term increases in influent activity levels.

ACKNOWLEDGEMENTS

The authors wish to acknowledge the following: the financial support of the Natural Sciences and Engineering Research Council of Canada; facilities provided by the Faculty of Engineering, University of Regina, Regina, Saskatchewan, Canada (with whom the authors were associated during initial stages of the study); and the contribution to the initial experiments of visiting scholar Bing Song Xu from the Peoples' Republic of China.

REFERENCES

APHA-AWWA-WPCF (1980). Radium-226 by radon in water, in Standard Methods for the Examination of Water and Wastewater, 15th Ed., 590-602.

Averill, D.W., Moffett, D., Webber, R.T., Whittle, L. and Wood, J.A. (1983). Joint government-industry program for the removal of radium-226 from uranium mining effluents. Final Report, II, Wastewater Technology Centre, Environment Canada, Burlington, Ontario.

Huck, P.M. (1982). Removal of radium from uranium mining effluents-current status and new directions. Waste Treatment and Utilization, 2, Pergamon Press, Toronto, Ontario, Canada.

Huck, P.M. and Anderson, W.B. (1983). Deposition of ^{226}Ra on surfaces during precipitation and leaching of $(Ba,Ra)SO_4$. Water Res., 17, No. 10, 1403-1406.

IEC Consultants, Inc. (1980). Placement of radium/barium sludge in tailings areas. Atomic Energy Control Board Report, INFO-0019, Ottawa, Ontario, Canada.

Seeley, F.G. (1977). Problems in the separation of radium from uranium ore tailings. Hydrometallurgy, 2: 249-263.

Stathis, T.C. (1980). Fluidized bed for biological wastewater treatment. Journal of the Environmental Engineering Division, Proceedings of the American Society for Civil Engineers, 106, No. EE1.

NITRIFICATION AND DENITRIFICATION

Wat. Sci. Tech. Vol.17, Amsterdam, pp.351-366.
Printed in Great Britain.

0273-1223/85 $0.00 + .50

DYNAMICS OF NITRIFICATION IN A BIOLOGICAL FLUIDIZED BED REACTOR

Slawomir W. Hermanowicz* and Jerzy J. Ganczarczyk

Dept. of Civil Engineering, University of Toronto, Toronto, Ont., M5S 1A4, Canada
**Present address: Dept. of Civil Engineering, University of California, Berkeley, CA 94720, U.S.A.*

ABSTRACT

Dynamics of nitrification in a biological fluidized bed reactor was investigated with numerical simulations and experimentally in a small scale reactor. A mathematical model was developed describing reactor dynamics, substrate removal and biomass development. Variable microbial activity was used as a quantitative representation of the state of the microorganisms. External and internal mass transfer limitations were considered in substrate removal modelling. The effects of biofilm growth on reactor hydrodynamics and on substrate removal kinetics were incorporated into the model. In the experimental part, the performance of the nitrifying fluidized bed was monitored as the influent concentration was varied following an irregular square wave pattern. The observed changes of the effluent concentration depended not only on actual conditions but also on the past history of the system. Further analysis was carried with the help of the developed model. The concept of variable microbial activity was instrumental in explanation of the microbial dynamics. Predictive capacities of the properly calibrated model were demonstrated.

KEYWORDS

Nitrification dynamics; biological fluidized bed; mathematical model; microbial activity; orthogonal collocation.

INTRODUCTION

Biological nitrification has become an established method of nitrogen control in wastewater treatment. Several review papers have been published (Painter, 1970; USEPA, 1975; Sharma & Ahlert, 1977) presenting in an organized way the substantial amount of accumulated knowledge on the subject. However, most of this knowledge is relevant only to steady-state conditions which are rarely encountered in full-scale operations. Only few authors analysed the dynamics of nitrification in an activated sludge system (Poduska & Andrews, 1975; Beck, 1981). Even less is known about the dynamics of nitrification in a biological fluidized bed reactor (BFBR). Recently, these reactors have gained a considerable interest particularly for wastewater treatment. Since this technology has been successfully applied to the

nitrification process (Jeris and others, 1977; Gauntlett, 1981; Nutt and others, 1982) the understanding of the dynamics of such systems becomes quite important. As compared to the completely mixed chemostat (which can adequately represent most of the activated sludge processes), the BFBR is a much more complex system. Substrate concentration and biomass concentration varies within the reactor. Since microorganisms form a film around carrier particles diffusional limitations become significant outside and inside the biofilm. Biomass growth and removal is closely linked to physical characteristics of the reactor, like porosity, bed expansion and solid mixing intensity. Better understanding of this intricate system is necessary for its appropriate design and operation, and for adequate evaluation of its performance. A mathematical model of a BFBR can be a useful guide for this task.

In the present work a dynamic model of a BFBR was developed and applied to a nitrifying biological bed. An analysis of the dynamics of nitrification in the BFBR was carried out experimentally in a small scale installation and was followed by numerical simulations with the use of the developed model.

STRUCTURE OF THE MODEL

The basic concept of a BFBR consists in cultivating microorganisms in the form of biofilm attached to the surface of carrier particles. Therefore, any model of the BFBR should consist of three major parts:
- reactor model;
- model of substrate removal in the biofilm;
- biomass development model.

Reactor Model

Substrate removal takes place in a reactor of length L filled with a carrier forming a fluidized bed of the height L_s with a porosity ε as shown in Fig. 1. The space in the reactor (column) above the fluidized bed ($x>L_s$) constitutes an outlet zone. Proper modelling of the outlet zone (usually neglected by many authors) may become important when concentration changes are rapid compared to the outlet zone hydraulic detention time. In other cases the contribution of the outlet zone becomes minimal. In the present model, though, it will be retained for a more general approach. The flow of liquid is directed upward with the velocity u (based on empty reactor cross-section) and axial dispersion D_L. Radial gradients of concentration and biomass are neglected, resulting in a one-dimensional model. Mass balance of a substrate in the reactor can be expressed under the above assumptions by Eq. 1 in which c is substrate concentration in the bulk of liquid. The first term in Eq. 1 describes substrate accumulation, the second term represents a transfer of substrate with the liquid, and the third term - liquid dispersion. The function R denotes substrate removal due to biological activity. The removal rate displays a discontinuity at the top of the bed ($x=L_s$) since no substrate occurs in the outlet zone ($R=0$ for $x>L_s$). At this point the dispersion coefficient also changes from D_{LB} in the bed to D_{LO} in the outlet zone.

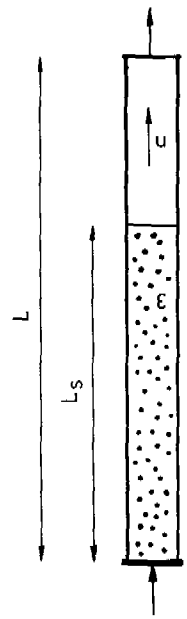

Fig. 1 Fluidized bed reactor model

$$\varepsilon \frac{\partial c}{\partial t} + u \frac{\partial c}{\partial x} - D_L \varepsilon \frac{\partial^2 c}{\partial x^2} + R = 0 \qquad (1)$$

Boundary conditions for Eq. 1 under assumption of a plug flow both at the inlet to the reactor ($x<0$) and in the exit pipe ($x>L$) (Wehner and Wilhelm, 1956; Cauwenberghe, 1966) are:

for $x = 0$ and for $x = L$

$$c_o(t) = c(0,t) - \frac{D_L}{u} \left.\frac{\partial c}{\partial x}\right|_{x=0} \qquad \left.\frac{\partial c}{\partial x}\right|_{x=L} = 0 \qquad (2a)$$

Two additional boundary conditions are required since the removal rate, R, has a discontinuity at $x=L_s$. Most natural conditions can be established for the interface between the bed and the outlet zone to reflect the continuity of substrate concentration and flux as formulated by Cauwenberghe (1966):

$$c(x=L_s^-,\ t) = c(x=L_s^+,\ t) \qquad (2b)$$

$$D_{LB} \left.\frac{\partial c}{\partial x}\right|_{x=L_s^-} = D_{LO} \left.\frac{\partial c}{\partial x}\right|_{x=L_s^+} \qquad (2c)$$

where L_s^- and L_s^+ relate to the conditions immediately below and above the interface ($x=L_s$), respectively.

In many applications it may not be possible to estimate the coefficients D_{LB} and D_{LO} separately. Instead an average coefficient D_L may be evaluated for the whole reactor and this approach is followed in the present work. Michelsen and Ostergaard (1970) described a few methods for estimation of D_L from the residence time distribution.

The porosity of a biological fluidized bed depends on the thickness of the biofilm and thus it varies within the bed and also with time. In Eq. 1 ε is, therefore, a function of the position x, biofilm thickness δ, liquid velocity u, and particle size d. In the present work the porosity was calculated using a method described by Hermanowicz and Ganczarczyk (1983). In the outlet zone the porosity is equal to 1.

Substrate Removal Model

Substrate removal, which takes place within the biofilm, can be presented as a succession of the following steps:
- diffusion of substrate through the liquid film around the particle;
- diffusion of substrate within the biofilm;
- removal (uptake) of substrate by the microorganisms in the biofilm.

In the present work, it was assumed that the biofilm is growing on inert spherical particles of diameter d and its thickness δ is uniform everywhere on the surface of the particle. The thickness, however, can vary along the bed. Substrate removal within the biofilm can be described by the diffusion equation:

$$\frac{\partial c'}{\partial t} - \frac{D_{eff}}{r^s}\frac{\partial}{\partial r}\left(r^s \frac{\partial c'}{\partial r} \right) + R_i = 0 \qquad (3)$$

in which c' is the concentration of a substrate in the biofilm at the distance r from the center of the particle, D_{eff} is an effective substrate diffusivity, R_i represents an intrinsic removal rate, and s is a geometry factor (s=0,1,2 for flat, cylindrical and spherical coordinates, respectively). In practice, since biofilm thickness is relatively small, a steady state in the biofilm is rapidly approached and $\partial c'/\partial t$ can be taken as 0. The time constant of Eq. 3 is $\tau = \delta^2/D_{eff}$. At common values of $\delta = 50\,\mu$ m and $D_{eff} = 2 \cdot 10^{-5}$ cm^2/s, τ = 1.25 s, which is short compared with the time scale of concentration changes. The term R_i represents an intrinsic removal rate which depends on the physiology of microorganisms. The intrinsic removal rate is generally expressed as a product of the specific removal rate, q, and the biomass concentration or biofilm density, X, in the form $R_i = X \cdot q$. The most widely used description of the specific substrate utilization rate, q, is, after Michaelis and Menten (1913):

$$q = Q_m \cdot c/(c + K) \qquad (4a)$$

Several years later Monod (1942) described the specific growth rate of bacteria, μ, in the same mathematical form:

$$\mu = \mu_m \cdot c/(c + K) \qquad (4b)$$

The growth rate and the removal rate are related through a yield coefficient, Y: $\mu = q \cdot Y$. The original equation (Eq. 4a) was derived from the kinetics of a two-step enzymatic reaction under steady-state conditions. Transient dynamic behaviour of microbial cultures cannot be adequately described by Eqs. 4. The need of a more realistic model was recognized by Powell (1967), Ierusalimsky (1967), and Ramkrishna and co-workers (1967). The ideas presented by these authors were further developed theoretically and experimentally by Young and Bungay (1973), and by Chi and Howell (1976). In these works separate components of living microorganisms were identified and a specific structure imposed on biomass previously assumed to be homogeneous. In the present work a simple approach of Powell (1967) is followed. The growth rate, μ, is expressed as a product of yield, Y, activity, Q, and concentration function, G(c):

$$\mu = Y \cdot Q \cdot G(c) \qquad (5)$$

The activity, Q, is a dynamic variable and the rate of its change is assumed proportional to itself and another function of concentration, F(c). Because of the association of activity with RNA content in the cell, Powell called it a "Q-substance" which becomes "diluted" in the biomass during its growth. Thus

$$dQ/dt = Q \cdot F(c) - \mu \cdot Q \qquad (6)$$

It was further postulated by Chi and Howell (1976) that at a steady state activity, $\tilde{Q}$, can vary between a minimum value, Q_{min}, and a maximum one, Q_m, similarly to RNA content in microbial cells, as reported by Ierusalimsky (1967):

$$\tilde{Q} = (Q_m - Q_{min})\,\tilde{\mu}/\mu_m + Q_{min} \qquad (7)$$

It is generally accepted that the steady-state growth rate, $\tilde{\mu}$, is adequately described by the Michaelis-Menten-Monod type of equation (Eq. 4). Introducing from Eq. 4 into Eq. 7 and setting $\alpha = Q_{min}/Q_m$ yields

$$\tilde{Q} = Q_m \, (\tilde{c} + \alpha \cdot K)/(\tilde{c} + K) \qquad (8)$$

Comparing Eqs. 4 and 5 with $\tilde{Q}$ expressed by Eq. 8 yields $G(c) = c/(c + \alpha K)$ and

$$\mu = Y \cdot Q \cdot c/(c + \alpha \cdot K) \qquad (9)$$

The intrisic removal rate R_i is derived from Eq. 9:

$$R_i = \mu \cdot X/Y = Q \cdot X \cdot c/(c + \alpha K) \qquad (10)$$

It should be noted that the mathematical form of Eq. 10 is identical with the Michaelis-Menten-Monod equation, but with the substitution of αK for K. The activity Q is nc longer constant and its rate of change is expressed by Eq. 6. To find F(c) it should be noted that at steady state $F(\tilde{c}) = \tilde{\mu}$, thus

$$F(\tilde{c}) = \mu_m \, \tilde{c}/(\tilde{c} + K) = Q_m \cdot Y \cdot \tilde{c}/(\tilde{c} + K)$$

and

$$dQ/dt = Y \cdot Q \cdot Q_m \cdot c/(c + K) - Y \cdot Q^2 \cdot c/(c + \alpha \cdot K) \qquad (11)$$

The major feature of the above presented model consists in that any immediate change of growth rate caused by a change of concentration is smaller than that resulting from the Monod model (since it was assumed $\alpha<1$) but if the concentration c is held constant the growth rate gradually approaches a steady-state value through the changes of activity Q. At the steady state the variable activity model is exactly equivalent to the Monod model but at transient conditions it is different as the growth rate (or the substrate removal rate) depends not only on the concentration at the present time but also on a history of the microbial culture. The activity Q can be regarded as a representation of the physiological state of the microorganism and constitutes a record of system past performance.

Combining Eq. 10 with the diffusion equation (Eq. 3) (with $\partial c'/\partial t=0$ and $s=0$) yields the following equation for the concentration in the biofilm:

$$D_{eff} \frac{d^2c'}{dr^2} - Q \, X \frac{c'}{c' + K_s} = 0 \qquad (12)$$

where $K_s = \alpha \cdot K$ represents an "apparent" half-saturation constant. The overall removal rate per unit volume of the biofilm, R_{iv} can be expressed by the following equation:

$$R_{iv} = \eta \cdot Q \cdot X \cdot c_s/(c_s + K_s) \qquad (13)$$

where η is an efficiency factor and c_s is the concentration at the surface of the biofilm. Atkinson and Davies (1974) solved Eq. 12 numerically and approximated the effectiveness factor with an analytical function. This function was incorporated in the described model. It was later reported (Atkinson & How, 1974; Mulcahy, Shieh & LaMotta, 1981) that Eq. 12 could be applied to relatively thin spherical biofilms (for which a geometry factor s=2) provided the thickness of the biofilm was replaced by an effective thickness, δ_e, equal to the ratio of biofilm volume to its surface area.

If external mass transfer limitations cannot be neglected then the flux of substrate through the liquid film around the particle has to be equal to the overall removal rate:

$$k_f (c - c_s) = \eta \cdot \delta_e \cdot Q \cdot X \cdot c_s/(c_s + K_s) \quad (14)$$

The concentration c_s can be found by solving Eq. 14 yielding the removal rate R (per unit volume of the bed) to substitute into Eq. 1 :

$$R = \frac{6(1-\varepsilon)}{D} \cdot \eta \cdot \delta_e \cdot Q \cdot X \cdot \frac{c_s}{c_s + K_s} \quad (15)$$

Biofilm Development Model

The third part of the model describes biofilm development. At present, mechanisms of biomass growth and removal in a fluidized bed are only partially understood. For the purpose of this model it will be assumed that the amount of biomass grown, m, is proportional to the amount of substrate utilized. The removal rate of the biomass is assumed proportional to the amount of biomass. Thus,

$$dm/dt = Y \cdot V \cdot \eta \cdot Q \cdot X \cdot c_s/(c_s + K_s) - k_d \cdot m \quad (16)$$

The last term $k_d \cdot m$ (with k_d being an overall biomass removal coefficient) represents biomass removal due to all processes including microbial decay, sloughing and attrition. Obviously, this is a very simple approach but it is similar to the expression of microbial decay as presented by Powell (1967). The rate of removal of the biomass due to sloughing was also reported to be proportional to the amount of biomass (Bryers & Characklis, 1981). It seems, therefore, that Eq. 16 can be used for the intended purpose, at least as a first approximation. Transforming Eq. 16 and applying Eq. 13 to a spherical particle yields the following equation for biofilm thickness changes in the bed:

$$\frac{d\delta_e}{dt} = \frac{d+2\delta_e}{d+6\delta_e} \{ Y \cdot \eta \cdot \delta_e \cdot Q \cdot c_s/(c_s+K_s) - k_d \cdot \delta_e \} \quad (17)$$

SUMMARY OF THE MODEL AND SOLUTION METHODS

In the BFBR both activity, Q, and biofilm thickness, δ, are functions of time and positions in the bed. Thus, ordinary derivatives in Eqs. 11 and 17 should be replaced by partial derivatives. Since substrate concentration in the biofilm varies with the distance from the particle surface the activity Q should also follow these changes. A description of activity changes in the biofilm would require an additional partial differential equation for each particle which would excessively complicate the model. For biofilms of moderate thickness the change of activity across the biofilm is smaller than that of the concentration and it seems reasonable to retain the bulk concentration, c, in Eq. 11. Therefore, the dynamic model of the BFBR can be presented as the set of 3 partial differential equations: Eq. 1 - substrate mass balance, Eq. 11 - activity changes and Eq. 17 - biofilm thickness changes, with Eq. 15 describing the overall rate of substrate removal in the biofilm and with the boundary conditions of Eq. 2 and the conditions describing the initial distribution of substrate, biomass and activity in the reactor.

Solving this set of equations is complicated because the set is a "stiff" one which means that it describes a number of processes with very different time scales. For the flow of the liquid through the reactor the time scale is in the order of magnitude of the reactor hydraulic detention time, i.e. few minutes. The

time scale for the changes of microbial activity is in the order of several hours. The development of the biomass is even slower since the time scale is measured in days, especially for nitrifiers for which the growth rate is low. It means that the solution of the model is a combination of several components which are changing at very different rates. This fact is very important for the stability and accuracy of numerical solutions. Successful solution was achieved with the orthogonal collocation method (Finlayson, 1972; Villadsen & Stewart, 1967; Villadsen & Michelsen, 1978). In the method applied in the present work the concentration function c was approximated with a sum of orthogonal Legendre polynomials that satisfies the differential equation in a number of points (called collocation points). By using this method the partial differential equation (Eq. 1) was transformed into a set of ordinary differential equations of first order. The details of the application of orthogonal collocation to this model are reported elsewhere (Hermanowicz, 1982).

As it was previously noted the function R in Eq. 1 has a discontinuity at the top of the bed ($x=L_s$). Since the concentration function c and its first derivative are continuous, as implied by Eqs. 2b-c, the second derivative of $\partial^2 c/\partial x^2$ must be discontinuous at $x=L_s$. Approximation of this discontinuity with continuous polynomials was very difficult and numerical experiments have shown that even with 12 collocation points, the solution was not stabilized. To avoid this problem the concentration function c was approximated separately in two regions: in the bed (for $x<L_s$) and in the outlet zone (for $x>L_s$) with two sets of polynomials with a condition of continuity of the function c and its first derivative was imposed at $x=L_s$. The improvement in the stability of the solution with separate approximations was quite dramatic even with only two collocation points in each region. For further work four collocation points in the bed and two in the outlet zone were chosen as a trade-off between the accuracy and the speed of computations.

A sophisticated multi-step predictor-corrector method (DIFSUB) developed by Gear (1971) was used to integrate the resulting set of ordinary differential equations with high efficiency.

EXPERIMENTAL INSTALLATIONS AND METHODS

An experimental installation (Fig. 2) was set up to investigate the performance of a biological fluidized bed reactor. The inside diameter of the column was 5.1 cm and the total length 245 cm. The column was filled with quartz sand of the size 20x30 US mesh and the average diameter (determined under a microscope) of 0.832 mm. The density of sand was determined at 2.63 g/cm^3. Commercial oxygen (99.5% purity) was used in the oxygenation device (4). The DO concentration in the effluent was generally at high levels of 10 to 15 mg/L and never dropped below 6 mg/L. During all experiments the value of pH was controlled with an automatic controler by dosing an alkaline solution of sodium carbonate and sodium hydroxide. The installation was seeded with a sample of nitrifying activated sludge from the Humber Water Pollution Control Plant, Toronto, Ont. The influent was prepared by dilution of stock ammonia solution with tap water to obtain required concentrations. The stock solution was prepared by dissolving 128.71 g ammonium chloride, 75.43 g ammonium sulphate, 2.3 g potassium phosphate dibasic, and 1.7 g potassium phosphate monobasic in tap water to the volume of 1 liter resulting in the concentration of 50 g/L NH_4-N. No other nutrients were added as it was assumed that tap water was a sufficient source of the required micronutrients. Successful growth of nitrifiers indicated that this assumption was justified. The concentration of ammonia was measured with the phenate method according to Standard Methods (1976) and also with an Orion 95-10 Ionselective electrode following the manufacturer's instructions. Samples of sand covered with the

biomass were periodically collected at different depths of the bed and the dry mass and the volatile fraction of collected solids were determined following Standard Methods (1976). Some of the sand particles covered with the biofilm were also measured under a microscope. More detailed description of the experimental methods can be found elsewhere (Hermanowicz, 1982).

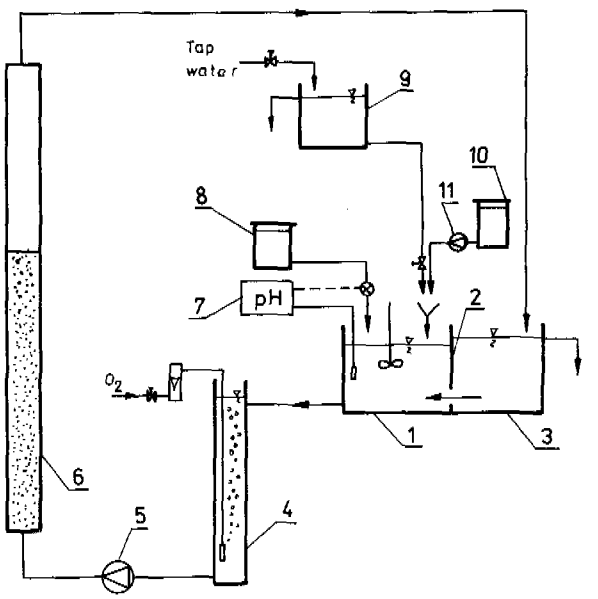

Legend:

1 - feed tank
2 - perforated baffle
3 - recycle tank
4 - oxygenator
5 - variable speed pump
6 - fluidized bed
7 - pH controller
8 - alkaline solution tank
9 - constant head water tank
10 - substrate stock solution tank
11 - peristaltic pump

Fig. 2. Scheme of the experimental installation

SCOPE OF THE STUDY AND EXPERIMENTAL SETUP

In the present work the performance of the BFBR was expressed in terms of the remaining ammonia concentration in the effluent resulting from the periodic changes of the influent concentration. The concentration of ammonia in the influent was varied in the form of an irregular square wave. This pattern of changes was relatively simple from the experimental standpoint, yet because of the variable length of high and low concentration periods it could amplify the effects of the "history" of a bacterial culture on its present performance. The samples of the influent and the effluent were collected every six hours and analysed as described before. The runs lasted from 11 to 15 days each and were separated by stabilization periods of more than one month each. During these periods the operational conditions of the system remained constant. The system was closely observed and the next run was started when the effluent concentration of ammonia stabilized at a constant level.

The operational conditions of the four runs are presented in Table 1. In the present work the terms "influent concentration" and "influent flow" refer to the mixture of water and the concentrated stock solution flowing to the tank (1) from tanks (9) and (10). The hydraulic detention time is defined as the ratio of fluidized bed volume to inluent flow rate. Constant pH of 8.0 was maintained in the feed tank during the period of the study.

TABLE 1. Operational Conditions of Continuous Experiments

Run	Liquid velocity u	Detention time (1)	Bed height	Influent concentration(2) low	Influent concentration(2) high	Biomass concentration(3)	Substrate load (4) low	Substrate load (4) high
	cm/s	min	cm	mg/L NH_4-N		mg/L	mg NH_4-N/mg VS d	
1	0.986	69.4	115	20	45	4800	0.18	0.43
2	0.965	68.0	140	35	65	5400	0.23	0.45
3	1.225	34.4	152	20	45	7500	0.21	0.41
4	1.239	34.9	152	35	65	8400	0.28	0.48

Notes: (1) - detention time based on bed volume and influent flow rate
(2) - average concentration
(3) - average value for the bed and the run
(4) - at low or high influent concentration, respectively

RESULTS AND ANALYSIS OF DYNAMICS

The influent and effluent concentrations are presented in the lower part of Fig. 3 for one of the four runs. The concentration of ammonia in the effluent generally followed the pattern of the influent concentration but some important differences among the runs were clearly visible. In all runs, after a step increase of the influent concentration, the concentration in the effluent also increased but after an initial peak a decreasing trend was observed. The magnitude of the initial peak and the rate of subsequent decrease varied significantly in different runs. At first, it was attempted to analyze the results of the experiments in "conventional" terms by correlating influent and effluent concentrations, applied load and volumetric loading of the bed in various ways. The values of loads used in this analysis were averaged over the whole bed and over the time of application (e.g. substrate loads presented in Table 1 were averaged over the periods of low and high concentrations, respectively). This analysis did not bring any conclusive results as it might been expected but it indicated that the performance of this biological system depended on its past "history" regarded as a sequence of physiological states of the bacterial culture. Similar findings were reported earlier by few other authors (Chi & Howell, 1976; Daigger & Grady, 1982). In present situation the effects of microbial adaptation were masked to some extent by the changes of the biomass concentration. Further investigations of the dynamics of the BFBR were accomplished with the use of the mathematical model described in previous sections.

Use of the mathematical model for the studies of the dynamics of BFBR required numerical values of several parameters. It was decided to estimate the following four parameters from the observed data:

- maximum substrate removal rate, Q_m;
- "apparent" half-saturation constant, K_s;
- "true" half-saturation constant, K;
- biomass removal coefficient, k_d.

These parameters were selected because of their importance in the model and also because their numerical values reported in the literature were widely scattered or not available at all. Other parameters were either directly measured like flow rates, bed height) or calculated from the formulae reported in the literature. Table 2 lists these parameters together with the source of information. The

initial values of biofilm thickness and the concentration in the reactor were measured at the beginning of each run and the initial values of activity were calculated from the concentration values under assumption of steady-state conditions prior to each run. More details about these parameters were presented elsewhere (Hermanowicz, 1982).

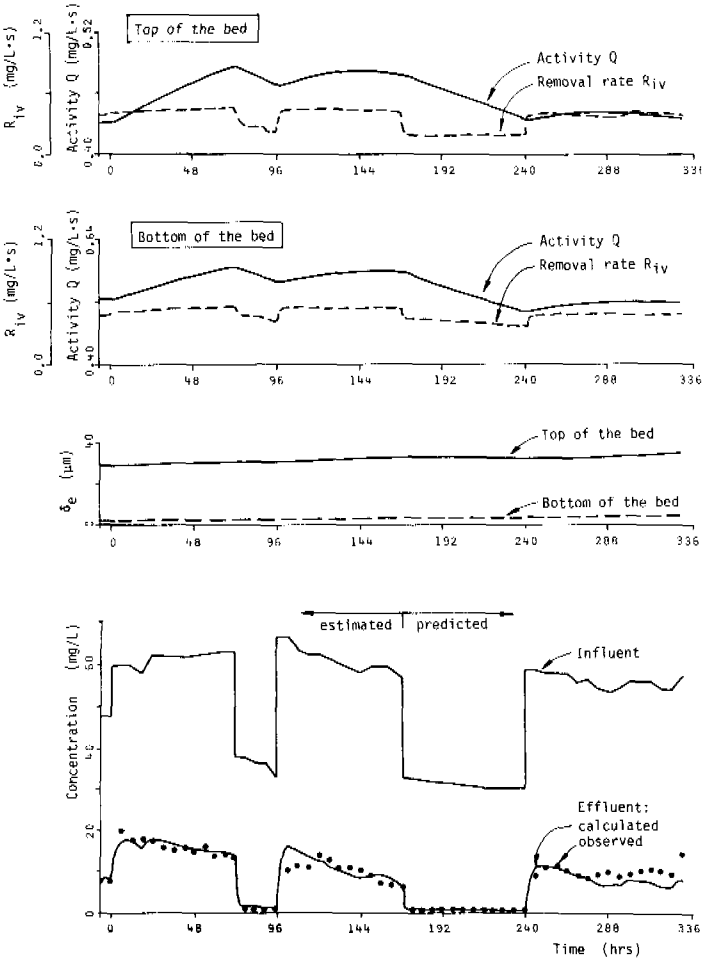

Fig. 3. Dynamics of nitrification - run No. 4 (explanations in text)

The previously described model was enlarged to accomodate the peripheral parts of the experimental installation. The recycle tanks and the oxygenator were modelled as one completely mixed tank and the corresponding differential equation was added to the original set.

The possibility of manipulating with four parameters gave quite a flexibility in fitting the model to the observed data. Since three of four parameters (Q_m, K_s, K) were related to each other at the basic level of the model (through the Monod and activity equations) it was expected that the model could be fitted reasonably well over a range of parameters. In view of this it was decided to check also the

predictive capacities of the model as another test of its validity. Estimation of the parameters in each run was carried out by using only a part of the data, generally from the beginning of the run to the end of the second period of high concentration. The extent of these data is marked in Fig. 3. After the estimation the obtained values of the parameters were used to generate the solution for the entire period of the run. Estimation of the parameters was carried out using two methods: quasilinearization (Bellman and others, 1967; Lee, 1968) and a modified simplex method (Johnson, 1974). The simplex method was employed first to provide some initial estimates of the parameters. Then, quasilinearization with its quadratic convergence was utilized to find more precise values.

TABLE 2. Parameters of the Model

Parameter	Value	Reference
Reactor length, L	245 cm	experimental
Bed height, L_s	variable	experimental, Table 1
Liquid velocity, u	variable	experimental, Table 1
Axial dispersion, D_L	variable	Hermanowicz (1982)
Dry biomass density, X	0.108 g/cm_3	Hermanowicz (1982)
Mass transfer coefficient, k_f	variable	Wilson & Geankoplis (1966)
Influent flow rate	variable	experimental
Initial biofilm thickness, δ_e	variable	Hermanowicz (1982)
Yield, Y	0.29	McCarty (1965)
Effective diffusivity, D_{eff}	$1.7 \cdot 10^{-5} cm^2/s$	Williamson & McCarty (1976)
Porosity, ε	variable	Hermanowicz & Ganczarczyk, (1983)
Estimated parameters		
Maximum removal rate, Q_m		
"Apparent" half-saturation constant, K_s		
"True" half-saturation constant, K		
Biomass removal coefficient, k_d		

It should be noted that the biomass removal coefficient k_d was estimated at higher values for runs No. 1 and 2 than for runs No. 3 and 4. A possible explanation of this fact may be related to the liquid velocity in the bed which was lower during the first two runs. This would indicate that the mechanical attrition by the particles was a major mechanism of biomass removal rather than the hydraulic sloughing since at lower liquid velocities contacts between particles are enhanced due to smaller bed porosity.

The results of the numerical simulations are shown in Fig. 3. The part of the data marked "estimated" served for parameter estimation and the numerical simulation was continued (at the estimated parameter values) to form a "predicted" part of the effluent concentration curve. The agreement between the predicted and observed concentrations was quite acceptable for all runs. The middle graph in Fig. 3 represents the changes of the biofilm thickness during the run. These results were not always accurate enough since no provision for solids mixing or segregation in the bed was included in the model. In this simple approach a particle was assumed to stay within the same region in the bed for all the time but the growth of the biofilm and resulting bed expansion were accounted for. In some cases this simplification led to the prediction of a "reverse" bed stratification wheras in other runs (e.g. run No. 4) the predictions generally

corresponded to the observed biomass profile in the bed. The mixing and stratification phenomena in a BFBR clearly require further studies.

TABLE 3. Estimated Values of Model Parameters

Run	Q_m	K_s	K	k_d	$\alpha = K_s/K$
	d^{-1}	mg/L NH_4-N	mg/L NH_4-N	d^{-1}	-
1	0.62	2.18	4.30	1.15	0.51
2	1.68	0.21	4.08	1.68	0.05
3	0.94	0.16	1.56	0.44	0.10
4	1.10	1.45	21.1	0.57	0.05

The two upper graphs in Fig. 3 convey essentially the same information but for different parts of the reactor. The solid line represents the changes of the activity Q and the dotted line the corresponding changes of the removal rate. These graphs present the most important results of the analysis of the BFBR dynamics. When the influent concentration was raised the activity also increased. This, in turn, caused the removal rate to increase. As a result the substrate concentration in the effluent decreased but because the changes of the activity were slower than that of the influent concentration the removal rate lagged behind the concentration and a concentration peak was formed. When the influent concentration (and thus the amount of substrate) was reduced the activity of the microorganisms decreased adjusting their consumption. The magnitude of this drop depended on the length of the low-concentration period. This mechanism could explain different responses of the system to identical influent concentration changes.

The parameter $\alpha = K_s/K$ reflects the ability of a microbial culture to dynamically respond to a change of substrate concentration. This parameter was defined as a ratio of minimum to maximum activity of the microorganisms. The estimated values of α (Table 3) were within the range of 0.05 to 0.10 with the exception of run No. 1. These low values indicated a large capacity of microorganisms to change their substrate uptake in response to its availability. In the case of run No. 1 the relatively high value of $\alpha = 0.51$ was probably caused by a difference in microbial population. During this run ammonia was oxidized only to nitrite indicating that the number of active cells of Nitrobacter was very low. The lack of symbiotic interaction between Nitrosomonas and Nitrobacter and nitrite accumulation could possibly affect the physiological response of Nitrosomonas resulting in a higher value of α. It is intended to study this subject further.

To demonstrate the significance of the concept of microbial activity numerical simulations were performed under the same conditions as described previously but with the removal rate calculated from the classical Michaelis-Menten equation by setting $K_s = K$ or $\alpha = 1$ in the model. The results of this simulation at the conditions corresponding to run No. 4 are shown in Fig. 4. The results for other runs displayed a similar character. Since the removal rate depended only on the actual concentration in the reactor the effluent concentration closely followed the pattern of the influent and neither peaks nor declines were displayed.

The concept of microbial activity seems, therefore, essential in explaining the dynamics of the biological reactor. The activity can be regarded as a quantitative representation of the state of the microorganisms or as a record of

their past performance. At this point a word of caution is appropriate. The values of the activity presented in this work were obtained from the numerical calculations based on the observed influent and effluent concentrations. Thus, the activity constitutes a mathematical representation of microbial physiology which was useful in the analysis of the dynamics but its strictly physiological interpretation was not advanced at this time. Nonetheless, the results of this work show that the concept of the activity was very helpful in the analysis of the dynamics of a microbial system and that the model utilizing it could reasonably well predict the performance of such system despite the lack of thorough understanding of the physiological phenomena involved.

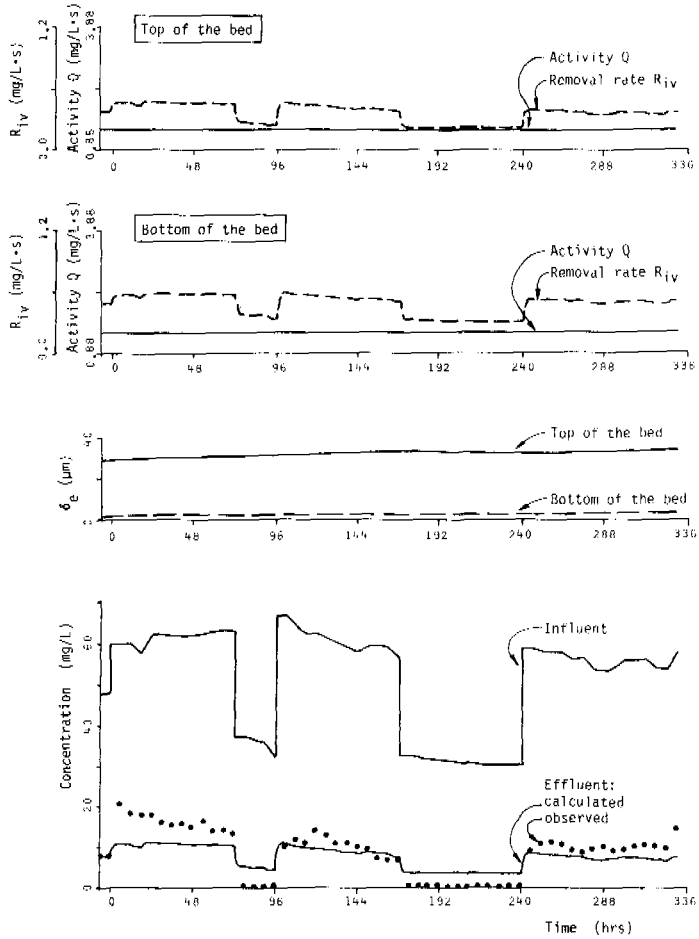

Fig. 5. Simulation results with Michaelis-Menten kinetics (run No. 4)

SUMMARY AND CONCLUSIONS

1. A dynamic mathematical model of a biological fluidized bed was developed. The model incorporated three parts of the system: reactor, substrate removal mechanism, biomass development.
2. The rate of substrate removal depended on the activity of microorganisms as proposed by Powell (1967). The changes of activity, which can be regarded as a

record of physiological states of the microorganisms, were included in the model.
3. The removal of substrate in the biofilm was modelled following Atkinson and Davies (1974) with modifications to include external mass transfer limitations.
4. An orthogonal collocation method combined with a multi-step predictor corrector integrating procedure was used to solve the set of partial differential equations forming the model.
5. The dynamic performance of the experimental fluidized bed could not be explained in the classical terms of substrate loading and biomass concentration.
6. The dynamic model could reasonably well describe the observed data and predict future performance of the nitrifying BFBR.
7. Analysis of the experimental data with the aid of the developed model indicated that the activity of the microorganisms was not constant. The concept of variable activity was critical in explaining the dynamics of the system.

ACKNOWLEDGMENTS

The present work constituted a part of a Ph.D. program of Mr. S.W. Hermanowicz which was carried out under the supervision of Professor J.J. Ganczarczyk at the Department of Civil Engineering, University of Toronto. The authors wish to thank Professors Monomoi and Harada of the Technological University of Nagaoka and Professor Matsumoto of the Tohoku University for their help and valuable comments. The financial support of Mr. Hermanowicz through the University of Toronto Open Fellowship and Ontario Graduate Scholarship is gratefully acknowledged.

NOMENCLATURE

c - substrate concentration in the bulk of liquid
c' - substrate concentration in the biofilm
$\tilde{c}$ - steady state substrate concentration
$c_o(t)$ - concentration at the inlet to the reactor
c_s - concentration at the surface of the biofilm
d - clean particle diameter
D - biocoated particle diameter
D_{eff} - effective substrate diffusivity in the biofilm
D_L - liquid axial dispersion (average)
D_{LB} - liquid axial dispersion in the bed
D_{LO} - liquid axial dispersion in the outlet zone
K - "true" half-saturation constant
k_d - biomass removal and decay coefficient
k_f - external mass transfer coefficient
$K_s = \alpha \cdot K$ - "apparent" half-saturation constant
L - length of the reactor
L_s - expanded height of the bed
m - amount of biomass (Eq. 16)
q - specific substrate removal rate
Q - microbial activity
$\tilde{Q}$ - steady state value of microbial activity
Q_m - maximum specific removal rate and maximum activity
Q_{min} - minimum microbial activity
r - radial distance from the center of a particle
R - substrate removal rate per unit volume of the bed
R_i - intrinsic removal rate in the biofilm
R_{iv} - removal rate per unit volume of the biofilm

s - geometry factor (Eq. 3) s=0,1,2 for plane, cylindrical and spherical coordinates, respectively
t - time
u - superficial liquid velocity
V - biofilm volume
Y - microbial yield coefficient
x - position in the reactor
X - biomass concentration, dry biomass density

$\alpha = Q_{min}/Q_m$ - "variability" coefficient (Eq. 8)
δ - biofilm thickness
δ_e - effective biofilm thickness
ε - bed porosity
η - effectiveness factor
μ - specific growth rate
$\tilde{\mu}$ - steady state value of the specific growth rate
μ_m - maximum specific growth rate

REFERENCES

Atkinson, B., Davies, I.J. (1974). The overall rate of substrate uptake (reaction) by microbial films. Part I. A biological rate equation. Trans. Instn. Chem. Eng., 52, 248-259

Atkinson, B., How, S.Y. (1974). The overall rate of substrate uptake (reaction) by microbial films. Part II. Effects of concentration and thickness with mixed microbial films. Trans. Instn. Chem. Eng., 52, 260-267

Beck, M. (1981). Operational estimation and prediction of nitrification dynamics in the activated sludge process. Water Research, 15, 1313-1330

Bellman, R., Jacquez, J., Kalaba, R, Schwimmer, S. (1967). Quasilinearization and the estimation of chemical rate constants from raw kinetic data. Math. Biosci., 1, 71-76

Bryers, J., Characklis, W. (1981). Early fouling biofilm formation in a turbulent flow system: overall kinetics. Water Research, 15, 483-491

Cauwenberghe, A.R. (1966). Further note on Danckwerts' boundary conditions for flow reactors. Chem. Engng. Sci., 21, 203-205

Chi, C.T., Howell, J.A. (1976). Transient behaviour of a continuous stirred tank biological reactor utilizing phenol as an inhibitory substrate. Biotechn. Bioengng:, XVIII, 63-80

Daigger, G.T., Grady, C.P.L. (1982). The dynamics of microbial growth on soluble substrates. A unifying theory. Water Research, 16, 365-382

Finlayson, B.A. (1972). The Method of Weighted Residuals and Variational Principles. Academic Press, New York

Gear, C.W. (1971). The automatic integration of ordinary differential equations. Commun. ACM, 14, 176-179 & 185-190

Gauntlett, R.B. (1981). Removal of ammonia and nitrate in the treatment of potable water. In Cooper, P.F., Atkinson, B. (Ed.), Biological Fluidised Treatment of Water and Wastewater. Horwood, Chichester. pp. 48-60

Hermanowicz, S.W. (1982). Dynamics of nitrification in a biological fluidized bed reactor. Ph.D. Thesis, Dept. Civil Engineering, University of Toronto.

Hermanowicz, S.W., Ganczarczyk, J. (1983). Some fluidization characteristics of biological beds. Biotechn. Bioengng., XXV, 1321-1330

Ierusalimsky, N.D. (1967). Bottlenecks in metabolism as growth-rate controlling factors. In Powell, E.O. (Ed.), Microbial Physiology and Continuous Culture., Her Majesty's Stationery Office, London. pp.23-33

Jeris, J.S., Owens, R.W., Hickey, R., Flood, F. (1977). Biological fluidized bed treatment for BOD and nitrogen removal. J. Water Poll. Control Fed., 49, 816-831

Johnson, L.E. (1974). Computers, models and optimization in physiological kinetics. CRC Crit. Review Bioengng., 2, 1-37

Lee, E.S. (1968). Quasilinearization and Invariant Imbedding. Academic Press, New York.

McCarty, P.L. (1965). Thermodynamics of biological synthesis and growth. In Baars, K. (Ed.), Proc. Second Internl. Conf. Water Pollution Research. Tokyo, 1964., Vol. 2., Pergamon Press, New York

Michaelis, L., Menten, I. (1913). Die Kinetik der Invertinwirkung. Biochem. Z., 49, 33-48

Michelsen, M.L., Ostergaard, K. (1970). The use of residence time distribution data for estimation of parameters in the axial dispersion model. Chem. Engng. Sci., 25, 583-592

Monod, J. (1942). Recherches sur la croissance des cultures bacteriennes. Herman et Cie., Paris

Mulcahy, L.T., Shieh, W.K., LaMotta, E.J. (1981). Simplified mathematical models for a fluidized bed biofilm reactor. AIChE. Symp. Ser., 77 (209), 273-294

Nutt, S.G., Melcer, H., Marvan, I.J., Sutton, P.M. (1982). Treatment of coke plant wastewater in the coupled pre-denitrification-nitrification fluidized bed process. Presented at 37th Annual Purdue Industr. Waste Conf., Lafayette

Painter, H.A. (1970). Review of literature on inorganic nitrogen metabolism in microorganisms. Water Research, 4, 393-450

Poduska, R.A., Andrews, J.F. (1975). Dynamics of nitrification in the activated sludge process. J. Water Poll. Control Fed., 47, 2599-2619

Powell, E.O. (1967). The growth rate of microorganisms as a function of substrate concentration. In Powell, E.O. (Ed.), Microbial Physiology and Continuous Culture., Her Majesty's Stationery Office, London. pp.34-55

Ramkrishna, D., Fredrickson, A.G., Tsuchiya, H.M. (1967). Dynamics of microbial cell propagation: Models considering inhibitors and variable cell composition. Biotechn. Bioengng., IX, 129-170

Richardson, J.F. (1971). Incipient fluidization and particulate systems. In Davidson, J.F., Harrison, D. (Eds.). Fluidization. Academic Press, London. pp.25-64

Sharma, B., Ahlert, R.C. (1977). Nitrification and nitrogen removal. Water Research, 11, 897-925

Standard Methods (1976). Standard Methods for the Examination of Water and Wastewater., 14th ed., APHA, Washington, D.C.

USEPA (1975). Process Design Manual for Nitrogen Control. U.S. Environmental Protection Agency

Villadsen, J.V., Stewart, W.E. (1967). Solution of boundary value problems by orthogonal collocation. Chem. Engng. Sci., 22, 1483-1495

Villadsen, J.V., Michelsen, M.L. (1978). Solution of Differential Equation Models by Polynomial Approximation. Prentice Hall, Englewood Cliffs, N.J.

Wehner, J.F., Wilhelm, R.H. (1956). Boundary conditions of flow reactor. Chem. Engng. Sci., 6, 89-93

Williamson, K., McCarty, P.L. (1976). Verification studies of the biofilm model for bacterial substrate utilization. J. Water Poll. Control Fed., 48, 281-296

Wilson, E.J., Geankoplis, C.J. (1966). Liquid mass transfer at very low Reynolds numbers in packed bed. IEC Fundamentals, 5, 9-14

Young, T.B., Bungay, H.R. (1973). Dynamic analysis of a microbial process: A system engineering approach. Biotechn. Bioengng., XV, 377-393

Wat. Sci. Tech. Vol.17, Amsterdam, pp.367-383.
Printed in Great Britain.

0273-1223/85 $0.00 + .50

MODELING, OPTIMIZATION AND DESIGN OF FLUIDIZED BEDS FOR BIOLOGICAL DENITRIFICATION

Th. J. Nieuwstad

University of Technology, Department of Civil Engineering, Laboratory of Sanitary Engineering, Stevinweg 4, 2628 CN Delft, The Netherlands

ABSTRACT

A mathematical model for fluidized bed denitrification has been derived, based on the fluidization theory and on zero order kinetics for biological nitrate reduction with nitrite as an intermediate product. Bed expansion, particle size, sludge concentration and nitrate and nitrite concentration can be calculated as a function of the height in the bed. Complete optimal conditions were not found using carrier materials of various specific gravities and with sizes above a radius of 0.2 mm, which was arbitrarily chosen as the smallest carrier particle. However, for each size and type of carrier material an optimal thickness of the biomass layer has been calculated for a standard type of wastewater at constant flow rate. For the kinetic and other constants used in this study, graphs are presented which can be used in the design of fluidized beds for denitrification.

KEYWORDS

Denitrification, pilot-scale fluidized bed, optimization, design, modeling.

INTRODUCTION

In recent years growing attention has been paid to wastewater treatment in fluidized beds (Cooper & Wheeldon, 1980; Cooper & Atkinson, 1981) and biological denitrification in this type of reactor is the subject of many papers (Jeris and others, 1974, 1975, 1977; Scott & Hancher, 1976; Bosman and others, 1978; Eggers & Terlouw, 1979; Mulcahy and others, 1980, 1981; Pitt and others, 1980; Shieh, 1980; Stephenson & Murphy, 1980; Klapwijk and others, 1982; Patton and others, 1982; Shieh and others, 1982; Vossoghi and others, 1982).
Mathematical models for fluidized bed denitrification have been published. In most of these models (Shieh, 1980; Mulcahy and others, 1980, 1981; Shieh and others, 1982) no attention has been paid to the intermediate product nitrite, which can reach considerable concentrations (Jeris and others, 1974; Eggers & Terlouw, 1979; Vossoghi, 1982). In modeling, most authors assume a constant particle size. However, a particle size gradient must exist along the fluidized bed (Eggers & Terlouw, 1979; Shieh and others, 1981) as a consequence of sludge growth. Bed expansion and biomass concentration in relation to particle size and flow rate have been calculated, using the fluidization theory, for denitrifying (Scott & Hancher, 1976; Shieh, 1980; Shieh and others, 1982) and other types of fluidized beds (Stathis, 1980, Tsezos & Benedek, 1980; Shieh

and others, 1981; Boening & Larsen, 1982).
However, no model has been published which describes simultaneously the profiles of the nitrate and nitrite concentration, the particle size, and the biomass concentration along the height of the fluidized bed.
Aim of the research described in this paper was to derive such a model, to verify it experimentally for a pilot-scale denitrifying fluidized bed and to demonstrate its usefulness for design purposes.

MODEL DERIVATION

Fluidization, Bed Expansion and Biomass Concentration

The particles in a fluidized bed for denitrification generally contain a nucleus of an inert carrier material like sand which is surrounded by a layer of biomass (sludge) in which the biological processes can occur. Both the carrier material and the particles are assumed to be spherical.
According to Richardson and Zaki (1954) the superficial upflow velocity v_s, the sedimentation velocity of a single particle v, and the porosity of the bed p are related by the formula:

$$v_s = v\, p^n \tag{1}$$

The value of the exponent n depends on the Reynolds number Re for a single particle and is approximated by:

$$n = 4.26 - 0.73 \log Re \tag{2}$$

For a fluidized particle with radius R the drag force exerted by the liquid equals the gravitational force, or:

$$C_w.\pi R^2.\tfrac{1}{2} g_w v^2 = (4/3)\pi R^3 (g_p - g_w)\, g \tag{3}$$

where the average specific gravity of the particle g_p is given by:

$$g_p = r_m^3 (g_m - g_s)/R^3 + g_s \tag{4}$$

Rearranging (3) and combining with (4) leads to:

$$C_w Re^2 = (64/6)(g_w g/\eta^2)(r_m^3(g_m - g_s) + R^3(g_s - g_w)) \tag{5}$$

When the right hand term of (5) is known from experiment (R, g_s) and constant values (g_m, g_w, g, r_m, η) , the Reynolds number can be calculated from an empirical relation (Smith & Stammers, 1973):

$$\log Re = (\log C_w Re^2 - 1.365)/1.318 \tag{6}$$

From $Re = 2 g_w v R/\eta$ then follows the settling velocity of a single particle, while a combination of (2) and (6) gives a shortcut to the value of the exponent n:

$$n = 5.02 - 0.554 \log C_w Re^2 \tag{7}$$

Using the calculated values of v and n and the superficial velocity v_s from experimental conditions, (1) gives the bed porosity p.
The volume of the biomass V_b per unit of bed volume is given by the difference in total particle volume (1-p) and the volume of the carrier material in the particles. The last mentioned volume is calculated from the number of particles N, multiplied by the volume of carrier material per particle, or:

$$V_b = (1-p) - 4\pi r_m^3 N/3 = (1-p) - (4\pi r_m^3/3)(3(1-p)/4\pi R^3) =$$
$$= (1-p)(1 - r_m^3/R^3) \tag{8}$$

When the dry solids density g_b of the biomass, in kg of dry solids per m^3 of biomass, is known from experiment, the biomass or sludge concentration S follows from:

$$S = g_b V_b \tag{9}$$

Denitrification, Sludge Growth, and Particle Growth

The reduction of nitrate to nitrogen by microorganisms in an anaerobic medium and in the presence of a carbon source can be described as a two step process with nitrite as an intermediate product (Eggers & Terlouw, 1979; Hermans & Van Haute, 1975; Mudrack, 1970; Jeris and others, 1977).
In simplified equations:

$$NO_3^- + \text{carbon source} \rightarrow NO_2^- + \text{cells}$$

$$NO_2^- + \text{carbon source} \rightarrow N_2 + \text{cells}$$

No accurate sludge yield factors for both steps are known, and the assumption that both yields are about equal is reasonable (Eggers & Terlouw, 1979). This means that, when all the nitrate should have been reduced to nitrite, half of the sludge has been produced, while the second half will grow upon further reduction of nitrite.
In a fluidized bed the sludge growth increases the radius of the particles. From the fluidization theory as treated above it appears that the porosity of the bed will increase with the thickness of the biomass layer on the carrier material. The bed will expand and, in the experimental set up which is described later, reach the sludge removal system. When a part of the biomass is removed, such a "nude" particle will sink to the bottom of the column and start to grow again. In the steady state a particle size gradient will exist along the column, and consequently the porosity p, the particle concentration N, and the biomass concentration S will vary with the height in the bed (Eggers & Terlouw, 1979; Shieh and others, 1981).
As in no part of the fluidized bed accumulation of particles can occur, in the steady state through each cross section of the bed a constant number of growing particles will be going upward, while the same number of nude particles will be going downward. Let this number be N_t ($s^{-1}m^{-2}$).
For a differential length dl of the bed all the sludge formed during reduction is transported upward by these N_t particles. A sludge balance over distance dl at position l from the bottom of the bed gives:

$$N_t 4\pi R_l^2 (dR_l/dl) = -v_s(Y_v(dC_l/dl) + \tfrac{1}{2}Y_v(dC_{nl}/dl)) \qquad (10)$$

in which Y_v is the volumetric sludge yield factor in m^3 biomass/kg nitrate reduced, which for nitrite is half the value for nitrate. Integration of (10) with starting condition l=0, $R_l=R_0$, $C_l=C_0$, $C_{nl}=C_{n0}$ leads to:

$$(R_l^3 - R_0^3) = (C_0 + \tfrac{1}{2}C_{n0} - C_l - \tfrac{1}{2}C_{nl}).3v_sY_v/4\pi N_t \qquad (11)$$

The unknown factor $3v_sY_v/4\pi N_t$ is found by realizing that at the top of the column the particle size and concentrations can be measured as $R_l=R_L$, $C_l=C_L$, and $C_{nl}=C_{nL}$. Calculating the factor, substituting into (11), and rearranging leads to:

$$R_l^3 = (R_L^3 - R_0^3)(C_0 + \tfrac{1}{2}C_{n0} - C_l - \tfrac{1}{2}C_{nl})/(C_0 + \tfrac{1}{2}C_{n0} - C_L - \tfrac{1}{2}C_{nL}) + R_0^3 \qquad (12)$$

For a well designed fluidized bed $C_L+C_{\frac{1}{2}nL}$ will be close to zero and may be neglected compared to $C_0 + \tfrac{1}{2}C_{n0}$.
Formula (12) relates the particle size profile to the concentration profiles of nitrate and nitrite provided the particle size and concentrations at the bottom and top of the bed are known. Through the fluidization theory the bed expansion and biomass concentration are related to the substrate concentration profiles.

Nitrate and Nitrite Reduction in the Particles

To describe the kinetics of nitrate and nitrite reduction, the following assumptions have been made:
- the particles are spherical.
- both nitrate and nitrite reduction follow zero order kinetics in substrate and first order in biomass concentration.
- reduction of nitrate always produces nitrite, which is reduced in a consecutive

reaction.
- the carbon source (methanol) is never rate limiting.
- the biomass layer is homogeneous.
- pH, nitrogen gas, and carbon dioxide have no influence.
- diffusion of nitrate and nitrite in the biomass follow Fick's law.
- there is mass transfer resistance between the particles and the bulk of the liquid.

At low concentrations the biomass layer on the particles might be incompletely penetrated by the substrate (Fig. 1). As nitrite is an intermediate product its penetration depth always must be higher than for nitrate.

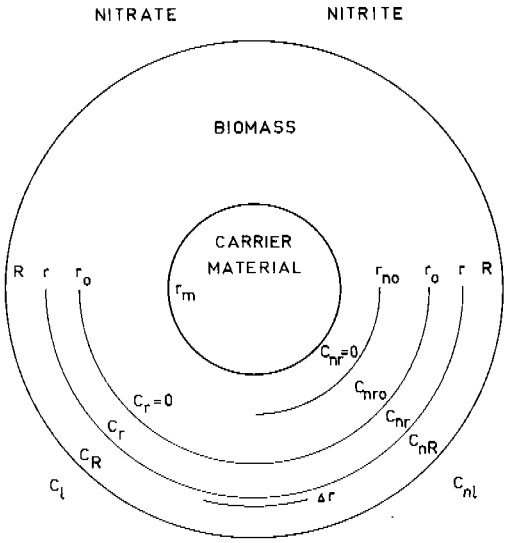

Fig. 1. Biomass covered particle.

Nitrate. For a shell in the biomass layer with thickness dr the mass balance for nitrate leads to:

$$(d^2C_r/dr^2) + (2dC_r/rdr) = K/D \qquad (13)$$

in which K is a zero order rate constant expressed in $kgNO_3^-$-N/(m^3 biomass. second). With the boundary conditions $C_r=C_R$ at r=R and $dC_r/dr=0$ at $r=r_0$ the solution of (13) is:

$$C_r = C_R + K(r^2 - R^2)/6D + Kr_0^3(1/r - 1/R)/3D \qquad (14)$$

in which r_0 is the penetration depth of nitrate which lies between R and r_m.
The relation with the nitrate concentration in the liquid phase C_l, at height l from the bottom of the column, is found from the fact that all nitrate that is reduced in the particle in the biomass layer between r_0 and R is transported into the particle by mass transfer from the liquid:

$$4\pi R^2k(C_l - C_R) = 4\pi(R^3 - r_0^3)K/3 \qquad (15)$$

Elimination of the surface concentration C_R from (14) and (15) gives for the nitrate concentration in the particle as a function of r:

$$C_r = C_l - K(R^3 - r_0^3)/3kR^2 + K(r^2 - R^2)/6D + Kr_0^2(1/r - 1/R)/3D \qquad (16)$$

Remembering that by definition at $r=r_0$ $C_r=0$, substitution into (16) produces a cubic equation in r_0:

$$(2K/k - 2KR/D)r_0^3 + (3KR^2/D)r_0^2 + (6R^2C_1 - 2KR^3/k - KR^4/D) = 0 \qquad (17)$$

When the constants k, K, and D and the values of R and C_1 are known, r_0 is found as that specific root of (17) which value is between R and r_m. If no root is found in this region, the biolayer is completely penetrated by nitrate and $r_0=r_m$. When r_0 is known, the nitrate concentration profile in the biolayer can be calculated from (16). Knowledge of r_0 is important because the volume of nitrate reducing biomass is calculated using this value.

Nitrite. Treatment of the nitrite concentration profile and reduction rate in the particle is very complicated. There are three possibilities:
1. When nitrate penetrates onto the carrier material, nitrite will also do so and the whole biolayer is active in nitrite reduction.
2. When nitrate penetrates to a radius r_0, and nitrite still will reach the carrier material, again the whole biomass is active in nitrite reduction.
3. When neither nitrate nor nitrite penetrate onto the carrier material (Fig. 1) for both substrates only a part of the biolayer is active, and two zones can be recognised:
$r_0 < r < R$, where nitrite is produced from nitrate, and reduced.
$r_{n0} < r < r_0$, where only nitrite is reduced and reaches zero concentration at the penetration depth of nitrite, r_{n0}.
Mathematical treatment of case 3 along lines given for nitrate leads to very complicated expressions for the nitrite concentration profile in both zones. For shortness only the cubic equation from which the penetration depth of nitrite can be calculated is given:

$$(2K_n/k_n - 2K_nR/D_n)r_{n0}^3 + (3K_nR^2/D_n)r_{n0}^2 + 6R^2C_{n1} + 2(K - K_n)R^3/k_n$$
$$+ (K - K_n)R^4/D_n - (2K/k_n - 2KR/D_n)r_0^3 - 3KR^2r_0^2/D_n = 0 \qquad (18)$$

When the constants and experimental values R and C_{n1} are known, and r_0 has been calculated from (17), r_{n0} is found as that specific root of (18) which value is between r_m and R. When no root in this region is found, r_{n0} equals r_m and we consider case 2 in which the total biomass layer is reducing nitrite.
An example of calculated nitrate and nitrite profiles in a particle is given in Fig. 2.

Overall Reaction in the Fluidized Bed

As in the fluidized bed plug flow is approximated, dispersion effects are neglected. When at a height l from the bottom of the column at particle radius R_l and bed porosity p_l the penetration depths of nitrate and nitrite are r_{0l} and r_{n0l}, respectively, the change in nitrate and nitrite concentration over a differential length dl is given by:

$$-v_s\, dC_l/dl = K(1 - p_l)(R_l^3 - r_{0l}^3)/R_l^3 \qquad (19)$$

$$-v_s\, dC_{nl}/dl = K_n(1-p_l)(R_l^3 - r_{n0l}^3)/R_l^3 - K(1-p_l)(R_l^3 - r_{0l}^3)/R_l^3 \qquad (20)$$

in which the right hand term of (20) is the production of nitrite from nitrate. Equations (19) and (20) cannot be solved analytically. Nitrate, nitrite, particle size, and biomass profiles have been calculated by stepwise integration following Euler's method with a step length of 0.1 m. For a given set of conditions (R_0, R_L, v_s, C_0, C_{n0}) the bed length for complete reduction is found when the nitrate and nitrite concentration become zero. This means that in calculating the particle size profile with (12), C_L and C_{nL} may be set at zero. An example of a calculated profile is given in the experimental part, Fig. 4.

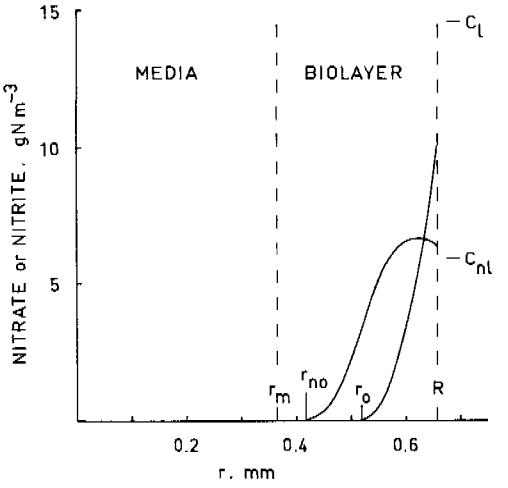

Fig. 2. Nitrate and nitrite penetration into biomass layer.

Parameter Sensitivity

The final model equations (1) - (9), (12), and (17) - (20) contain a great number of constants. The fluidization and kinetic part were separately tested for their sensitivity for the value of the constants (Nieuwstad, 1983).
Fluidization. The biomass concentration S, calculated from (9), was used for testing. Of course (9) implies that g_b must be known accurately. For normal wastewater temperature and salt contents g_w may be set at 1000 kg.m^{-3}. The wet sludge density g_s changed S 6% over the range 990-1020 kg.m^{-3}. Unfortunately, it is very difficult to determine g_s. However, in literature values close to 1000 kg m^{-3} are mentioned (Tsezos & Benedek, 1980). Giving g_w and g_s equal values of 1000 kg.m^{-3} and taking g=9.81 m.s^{-2} simplifies (5) to:

$$C_w Re^2 = 1.046\ 10^5\ r_m^3(g_m-1000)/\eta^2 \qquad (21)$$

Kinetic part. Sensitivity was tested by calculating the bed height for 95% removal of nitrate and 90% removal of nitrite from a model wastewater containing 30 g nitrate and 2 g nitrite nitrogen per m^3. Roughly speaking all constants (K, K_n, k, k_n, D, D_n) must be known within about 10% to predict the bed height within 10%.

EXPERIMENTAL VERIFICATION OF THE MODEL

Pilot Plant

A flow scheme of the pilot plant is given in Fig. 3. The influent, 8-12 m^3.h^{-1} of nitrified wastewater from a pilot activated sludge plant, is pumped upward at a controlled flow rate through a column 5 m high and 0.81 m wide. Just before the entrance into the column excess methanol is added. No special attention has been paid to the inlet system. The influent enters the bottom cone tangentially and passes a perforated plate and a 0.2 m bed of gravel. Above this the microorganisms were supported by sand grains. Starting up of the system took about four weeks.
At 0.3 m below the top of the column an impeller serves as a sludge removal mechanism.

The sheared off sludge and any particles carried over from the fluidized bed arrive in a sand trap. Sand is collected and returned into the bed with the aid of an air-lift. Sludge particles pass the sand trap and are carried away with the effluent. Recirculation of denitrified effluent makes it possible to study the effect of variation in upflow rate regardless of the limited influent flow. Furthermore, the fluidized bed is protected for settling when the influent is stopped.
Sludge and water samples were taken from the top of the column and through sampling ports along the column wall.

Carrier Material

A sieved sand fraction of 0.5-1.0 mm was used as carrier material for the micro-organisms. Consequently, the bio-particles will not be uniform, but all possible sizes of sand grains will be covered with biomass layers of various thickness. As a compromise it was assumed that the bed could be treated as if it contained only sand grains with the modal radius (0.365 mm) of the sand fraction: the modal grain is the most abundant one in a sieved fraction. One kg of carrier material contained $N_m = 1.76\ 10^6$ modal grains which is the real number of particles in a kg of sand.

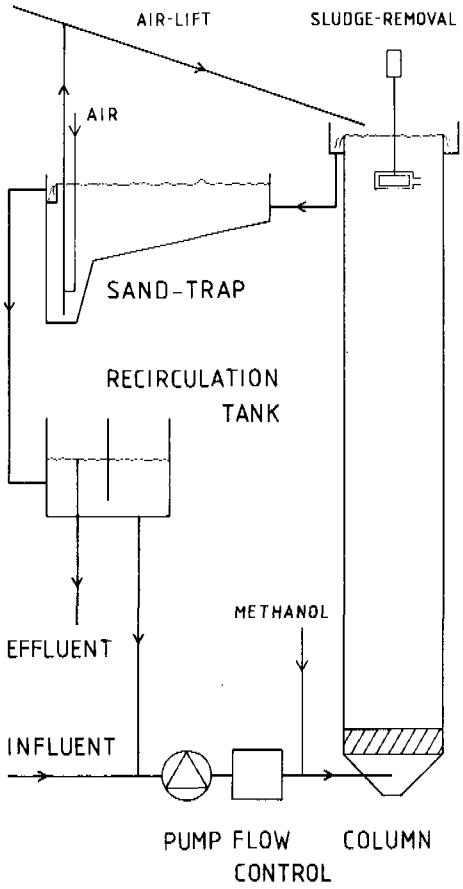

Fig. 3. Flow scheme pilot-plant.

Methods

For the top of the fluidized bed porosity (p) was found from the total volume of the settled particles in a 1 litre sample and from the porosity of these settled particles. The biomass concentration (S), particle size (R), and dry solids density (g_b) were determined by drying, weighing, glowing, and weighing again of known volumes of settled particles and separate determination of the ash content of sheared-off sludge containing no carrier material. Details of these procedures are given elsewhere (Nieuwstad, 1983).
For lower parts of the column it was only possible to determine the particle size and consequently biomass concentration profiles could not be measured experimentally. The dry solids sludge yield factor Y_s was calculated from the increase in suspended solids in the effluent compared to the influent divided by the decrease in nitrate concentration. The volume yield factor was calculated from $Y_v=Y_s/g_b$.
Zero order nitrate and nitrite reduction rate constants (K_s and K_{sn} in s^{-1}) were measured in batch experiments with homogenized sludge from the fluidized bed. The reduction rate constants per unit of volume of biomass (K and K_n) were calculated by multiplication with the biomass dry solids density.
Nitrate, nitrite, and suspended and volatile solids were determined following standard methods.
To find good values for the diffusion coefficients and mass transfer constants was a great problem. From column profile calculation it was finally decided to use the values presented in Table 2, which fulfil the relation of Beek (1971).

Results and Discussion

Overall performance of the fluidized bed. After starting-up the fluidized bed has been in continuous operation for a period of more than four months. Process conditions and influent and effluent quality for 26 days are summarized in Table 1. On the average, the nitrate concentration was lowered from 50.0 to 0.9 $gN.m^{-3}$, or 98% removal, at an empty column retention time - based on influent flow - of 0.3 h and at a temperature of 10.2°C. The nitrite concentration was unchanged at 1.0 $gN.m^{-3}$ because of the fact that this intermediate product could not be removed completely, in particular at flow rates above 20 $m^3.h^{-1}$. Nevertheless, the total removal of nitrate plus nitrite nitrogen was 96%.
During passage through the column the pH increased by one unit from about 7 to about 8.

Sludge properties. The average sludge dry solids yield factor Y_s appeared to be 0.80 kg dry solids/kg nitrate nitrogen, which value fairly well agrees with literature data in the range of 0.64-1.00 for denitrification with methanol as a carbon source. The average dry solids density of the biomass (g_b) of 97 $kg.m^{-3}$ is within the range of 30-150 $kg.m^{-3}$ as reported by Shieh and others (1981) for various attached growth systems. No relation has been found between g_b and the thickness of the biomass layer (particle size) as reported by Shieh and others (1981).
The average volume yield factor was found to be 0.0093 m^3 of sludge per kg nitrate nitrogen. However, this value is of no importance in model calculations.
Testing the fluidization theory. As the sludge concentration in a fluidized bed is very important in determining its capacity, agreement between measured and calculated biomass concentration will be a justification for the use of the fluidization theory. The measured sludge concentration S, the sludge concentration calculated from the particle size (S)c and the difference between both values ΔS at the top of the bed are given in Table 1. The average value of ΔS is 0.46, with standard deviation 2.13. A t-test for S=0 gave t=1.11, well within the 95% confidence limits. This means that it is allowed to use the fluidization theory for sludge concentration calculation.
Profile calculations. The constants used in profile calculations are summarized in Table 2. The kinetic and mass transfer constants and the diffusion coefficient are

dependent on temperature. Furthermore, wastewater quality fluctuations and changes in sludge properties might influence all constants except r_m and g_m. These changes of course are not predictable. Therefore, during the experimental period a number of measured profiles were compared with calculated values using the constants from Table 2 regardless of any temperature or other effect. Not neglected of course was the effect of temperature on wastewater viscosity.
An example of a calculated profile and the measured points is given in Fig. 4. As shown, the fit between measured points and calculated curves is not very good, how-

TABLE 1 Process Conditions Pilot-Plant Fluidized Bed Denitrification

Date	General Process Conditions							Top of The Fluidized Bed				
	Flow, $m^3.h^{-1}$		Temp.	NO_3^-, gN^{-3}		NO_2^-, $gN.m^{-3}$		Part. Radius	Dry Solids Density	Sludge conc., $kg.m^{-3}$		
	In-fluent	Column	°C	In	Out	In	Out	R_L mm	g_b $kg.m^{-3}$	Exp. S	Calc. (S)c	Diff. ΔS
27-10-81	10.1	15.2	13.0	46	2.3	2.1	2.0	0.767	70.1	29.3	28.9	-0.4
28-10-81	10.1	15.2	13.3	39	0.1	1.0	0.1	0.771	74.5	31.7	30.8	-0.9
02-11-81	8.9	19.2	14.5	41	0.2	0.2	0.1	0.735	73.5	28.6	27.8	-0.8
03-11-81	9.4	19.2	15.4	54	0.5	0.7	0.1	0.731	77.2	30.0	29.5	-0.5
09-11-81	9.1	24.8	12.7	60	0.5	0.3	1.0	0.740	80.5	27.9	26.3	-1.2
10-11-81	9.1	24.8	12.1	59	0.9	1.5	1.8	0.717	83.2	27.4	27.1	-0.3
16-11-81	8.7	30.4	11.0	52	1.7	0.6	3.1	0.701	84.5	23.6	24.1	+0.5
17-11-81	8.8	30.4	10.3	57	2.7	0.3	2.1	0.676	89.9	27.4	25.5	-1.9
23-11-81	8.6	29.6	13.2	48	0.4	0.3	0.9	0.652	94.1	28.0	28.2	+0.2
03-12-81	8.8	15.2	9.8	-	-	-	-	0.676	114.4	47.6	45.4	-2.2
07-12-81	9.0	15.2	10.0	-	-	-	-	0.687	92.5	37.7	36.9	-0.8
10-12-81	9.2	15.2	9.7	37	0.1	1.5	0.1	0.685	103.8	42.6	41.2	-1.4
15-12-81	9.2	15.2	7.8	34	0.2	0.9	0.2	0.690	102.8	42.0	40.2	-1.8
16-12-81	9.1	15.2	7.9	40	0.2	1.1	0.2	0.686	105.3	42.9	41.2	-1.7
22-12-81	8.7	19.2	6.3	37	1.0	0.8	0.7	0.668	98.8	30.3	34.2	+3.9
23-12-81	8.7	19.2	8.1	39	0.5	1.4	0.8	0.668	98.2	30.1	34.8	+4.7
05-01-82	6.4	24.8	10.5	52	1.6	0.3	1.4	0.630	85.0	25.2	27.1	+1.9
07-01-82	6.9	24.8	7.7	64	2.8	1.2	2.0	0.638	89.0	26.3	27.5	+1.2
12-01-82	7.8	29.6	7.6	41	2.3	0.8	2.5	0.630	96.3	22.3	26.8	+4.5
14-01-82	9.0	29.6	7.8	43	2.1	1.5	2.6	0.613	100.8	22.8	28.0	+5.2
01-02-82	8.6	15.2	8.7	49	0.2	0.5	1.1	0.672	104.7	42.1	41.1	-1.0
03-02-82	8.6	15.2	9.2	66	0.9	1.2	0.4	0.658	109.0	43.2	42.8	-0.4
24-02-82	5.1	15.2	9.1	51	0.2	2.2	0.2	0.734	125.5	49.0	49.9	+0.9
25-02-82	5.6	15.2	9.3	53	0.2	2.0	0.2	0.718	114.9	44.0	45.8	+1.8
01-03-82	5.3	15.2	9.2	66	0.2	1.3	0.1	0.728	122.8	47.6	48.9	+1.3
02-03-82	5.6	15.2	9.0	73	0.2	0.9	0.2	0.727	122.7	47.5	48.7	+1.2

ever satisfying. Qualitatively the same was observed for other profile measurements. Better fits for individual experiments could sometimes be obtained by varying the constants.
The irregular and sometimes illogic scattering of measured points around the curves partly might be due to sampling particles and water together through the sampling ports on the column, followed by separation of sludge and water for analysis. Perhaps this procedure gave errors because of the high reaction rate. Attempts to produce measured curves with a better smoothness by changing the sampling procedure lead to more complicated procedures without any improvement.
Measurements also might be inaccurate because of ever changing patterns of short-circuiting and dead water in the fluidized bed, especially in the lower part of the column. If any, this deviation from ideal flow does not seem to have a serious adverse effect on the overall performance of the bed.

TABLE 2 Constants for Profile Calculations

Symbol	Value		Symbol	Value
r_m	0.365	mm	K_n	$2.7\ 10^{-4}$ $kg.m^{-3}.s^{-1}$
g_m	2,640	$kg.m^{-3}$	k	$1.4\ 10^{-5}$ $m.s^{-1}$
g_s	1,000	$kg.m^{-3}$	k_n	$1.4\ 10^{-5}$ $m.s^{-1}$
gb	97	$kg.m^{-3}$	D	$3.2\ 10^{-10}$ $m^2.s^{-1}$
K	$5.6\ 10^{-4}$	$kg.m^{-3}.s^{-1}$	D_n	$3.2\ 10^{-10}$ $m^2.s^{-1}$

Figure 4 shows that the intermediate product nitrite can reach considerable concentrations: up to 10 $gN.m^{-3}$ or about 30% of the starting nitrate concentration. The bending of the nitrate curve above a bed height of about 1.5 m, suggesting a deviation from zero order kinetics, in fact is caused by the decreasing penetration depth of the substrate into the biomass layer, making a part of the biomass inactive in the upper part of the bed. This decrease in effectivity has a stronger effect on the overall rate of reduction than the increase in sludge concentration from 34 to 38 $kg.m^{-3}$ going from the bottom to the top of the column.
The usefulness of the model in optimization and design of fluidized beds for biological denitrification will be demonstrated in the next sections.

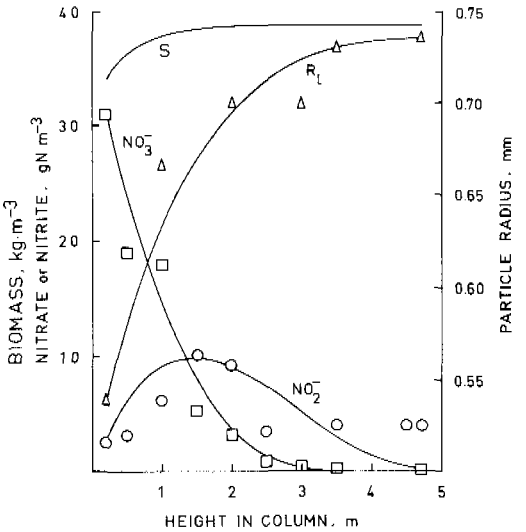

Fig. 4. Nitrate, nitrite, particle size and sludge concentration profiles in a fluidized bed for denitrification (v_s=29 $m.h^{-1}$).

OPTIMIZATION

General Considerations

When the nitrate and nitrite concentration, the temperature, and the various constants are known, the design parameters for a fluidized bed for denitrification are:
- media size, r_m
- media specific gravity, g_m
- particle size at the bottom of the column, R
- particle size at the top of the bed, R_L
- superficial velocity, v_s
- bed height, L.

When a combination of the first five parameters has been chosen, the bed height L for the desired conversion can be calculated. The capacity of the column, defined as m^3 of wastewater per unit of reactor volume per hour, then can be calculated. The highest capacity is the optimal design.
In search for the optimal conditions some restrictions have been made:
- the wastewater contains 30 g nitrate nitrogen.m^{-3} and has a temperature of 10°C.
- a final concentration of 1.5 g nitrate plus nitrite nitrogen.m^{-3} (95% conversion) must be reached.
- carrier materials might be:
  anthracite g_m = 1600 kg.m^{-3}
  sand „ = 2640 „
  garnet(I) g_m = 3200 kg.m^{-3}
  garnet(II) „ = 4300 „
  magnetite „ = 5050 „
- media size r_m in the range 0.1-0.6 mm.
- the difference (R_0-R_L)= 0.1 mm in all cases.
- superficial velocity in the range 19.5-58.0 m.h^{-1} (0.0054-0.0163 m.s^{-1}), or 10-30 $m^3.h^{-1}$ for the pilot plant described in this paper.
- the porosity of the fluidized bed must be higher than 0.45.
- maximum bed height 6.8 m.

Furthermore it has been assumed that particle size control is giving no problems: the sludge removal device in the top of the bed produces particles with the desired radius R_0.

Results of Optimization Calculations

For various values of the design parameters profile calculations gave the column height for 95% conversion of the standard wastewater. As an example, the results for various sand particles at a flow rate of 29 m.h^{-1} are presented in Fig. 5. Clearly, a sand particle with r_m = 0.35 mm, R_0 = 0.45 mm, and R_L = 0.55 mm gives the best result. When the difference between R_0 and R_L is increased above the value of 0.1 mm used here, generally a longer column will be necessary to reach 95% conversion. Figure 6a gives the 95% removal bed height as a function of the superficial velocity for various media densities. Figure 6b gives the treatment capacity of the bed as a function of flow rate. The treatment capacity decreases with flow rate and increases with media specific density, though above 4000 kg.m^{-3} no further improvement was found. At these high densities the sludge layer around the grains must be rather thick to get enough bed expansion. These thick biomass layers are not fully penetrated by nitrate and so become less effective.
In Fig. 7a optimal particle size has been plotted against flow rate for garnet(II) as carrier material. At lower flow rates, optimal conditions are found for smaller particles. Qualitatively, the same effect has been found for the other carrier materials, as can be seen from Fig. 7b, where optimum media radius has been plotted against flow rate for five specific gravities.
For optimal particles, the difference between r_m and R_0 is 0.10 or 0.15 mm, with an average value of 0.13 mm. This means that, when the design value of r_m has been chos-

en, $R_0 = r_m + 0.13$ mm and $R_L = r_m + 0.23$ mm. However, these values only will be valid for nitrate concentrations near the value of 30 $gN.m^{-3}$ used in the above calculations. From the Figures 5-8 it is seen that, though for each media size at each flow rate an optimal biomass cover is found (Fig. 5), no true optimal design for a fluidized bed denitrification column is possible. The use of the graphs presented here in the design of fluidized beds will be demonstrated in the last section of this paper.

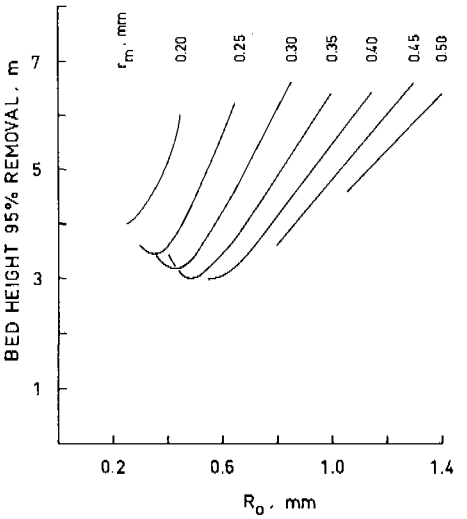

Fig. 5. Bed height for 95% nitrate removal from standard wastewater as a function of particle and media size (g_m=2640 $kg.m^{-3}$, v_s=29 $m.h^{-1}$ at 10°C).

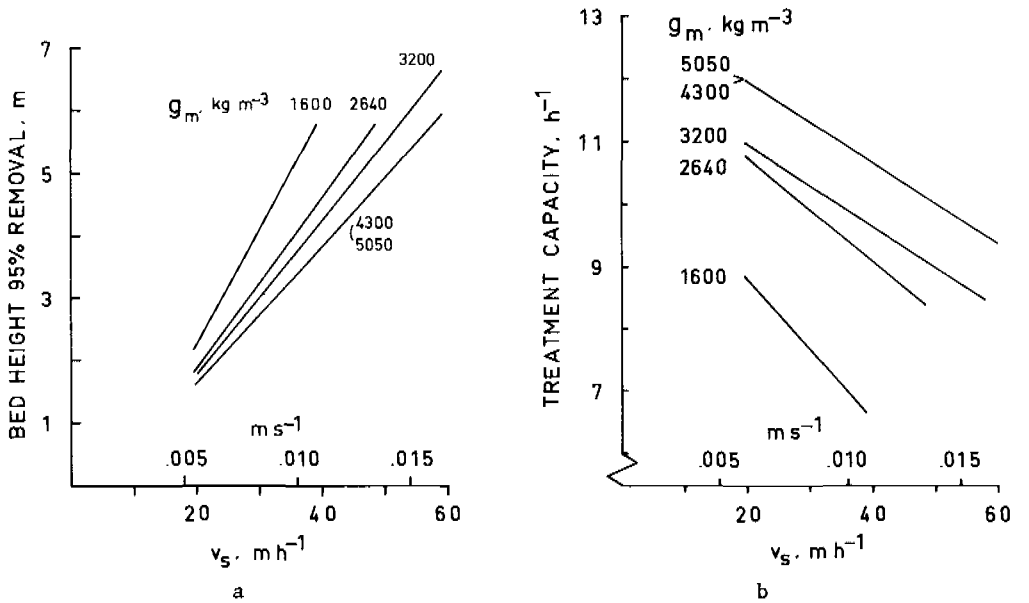

Fig. 6. Bed height for 95% removal (a) and treatment capacity (b) as a function of flow rate and carrier material specific gravity using optimal particle size

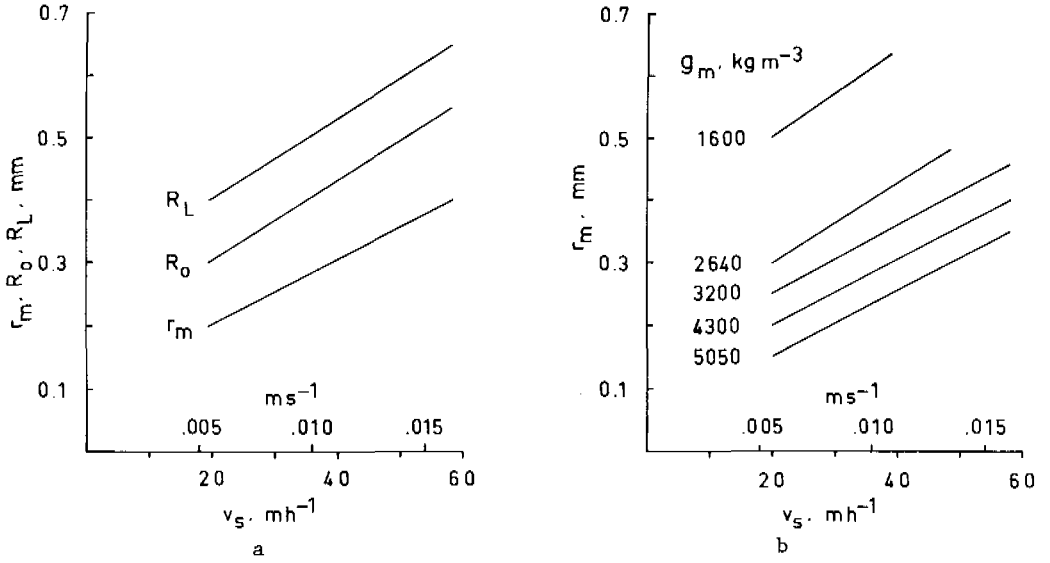

Fig. 7. Optimal media and particle size for garnet-II (a) and optimal media size (b) for other carrier materials as a function of flow rate (temp. 10°C).

Temperature and Concentration Effects

The above calculations are valid for a temperature of 10°C. At higher temperatures two effects are expected:
- An increase in the values of the kinetic and mass transfer constants and the diffusion coefficient, resulting in a shorter necessary bed length.
- A decrease in wastewater viscosity, resulting in lower bed expansion.

Consequently, without addition of carrier material, the particles must grow to reach the sludge removal device again. This will lead to a higher amount of sludge in the column. Calculations using the constants for 10°C demonstrated (Nieuwstad, 1983), that for standard wastewater the bed length at 20°C is about 7% shorter than at 10°C. Generally, for a design at 10°C no problems are to be expected at higher temperatures. The nitrate concentration in the wastewater of course has a strong influence on the necessary bed length. Calculations for a certain design demonstrated (Nieuwstad, 1983), that the bed length for other concentrations than the design value is about linearly proportional to the influent nitrate concentration.

DESIGN

The design of a fluidized bed for denitrification of a hypothetical wastewater is given assuming that:
- all constants are known and have the values used in this paper.
- maximum nitrate concentration is 30 gN.m^{-3}.
- the lowest temperature is 10°C.
- the graphs from Fig. 6, 7, and 8 are valid for this wastewater.
- the flow to be treated is 1000 m^3.h^{-1}
- the nitrate reduction must be above 95%.
- by technological restrictions the maximum cross section of a fluidized bed is limited at 5 m^2.
- particle size control by the sludge removal system gives no problems.

- media sizes below a radius of 0.2 mm are impractical.
- above the top of the bed we need a freeboard of 0.5 m.

The media content of a fluidized bed is calculated from:

$$WM = \sum_{i=1}^{i=L/\Delta l} (1-p_l) g_m F \Delta l \, r_m^3/R_l^3 \qquad (22)$$

with: WM = weight of carrier material, kg
F = cross section of column, m^2
i = step number

In Table 3 the results for two designs are presented. The first one is an optimal design in which was chosen the plant with the lowest total bed volume. The second one is a design based on the wish to use columns with a height of 5 m and a bed height of 4.5 m using sand as carrier material.

TABLE 3 Design of Fluidized Beds for Denitrification

	Lowest Bed Volume	Sand Bed of 4.5 m
Flow, $m^3.h^{-1}$	1,000	1,000
Influent nitrate, $gN.m^{-3}$	30	30
Number of columns	10	5
Superficial velocity, $m.h^{-1}$	20	40
Media s.g., $kg.m^{-3}$	4,300	2,640
Bed height, m	1.7	4.5
Column height, m	2.2	5.0
Media radius, mm	0.20	0.43
Bottom particle radius, mm	0.33	0.56
Top particle radius, mm	0.43	0.66
Total column volume, m^3	110	125
Total bed volume, m^3	85	113
Total freeboard volume, m^3	25	13
Total media weight, kg	23,700	50,400
Media weight per column, kg	2,370	10,080
Effluent nitrate, $gN.m^{-3}$	0.0	0.0
Effluent nitrite, $gN.m^{-3}$	1.5	1.2

Design with Minimum Bed Volume

Figure 6b shows that the highest treatment capacity will be realized with carrier material of high specific gravity, for which has been chosen garnet-II, and at low superficial velocity, 20 $m.h^{-1}$. At these conditions Fig. 6a gives a bed height of 1.7 m, and with 0.5 m freeboard a column height of 2.2 m. Figure 7b gives the media radius as 0.20 mm, from which the bottom and top particle radii follow as 0.33 and 0.43, respectively. The number of columns has been calculated from flow, superficial velocity, and maximum cross section. Table 3 also gives the total column, bed and freeboard volume as well as the media weight per column and for the total plant. The expected effluent nitrate and nitrite concentrations have been calculated.

Design of a 4.5 High Sand Bed

For a 4.5 m high sand bed Fig. 6a gives the superficial velocity as 40 $m.h^{-1}$. Figure 7b gives a media radius of 0.43 mm, from which the bottom and top particle radii follow as 0.56 and 0.66 mm, respectively. Five columns will be needed to treat the design flow, producing an effluent containing no nitrate and 1.2 g nitrite nitrogen per m^3.

Decision

One will have to decide on an economic basis which design is favoured. Calculation of construction, maintenance, and operation costs is beyond the scope of this paper. For practical reasons, a design with the least possible number of columns might be preferred above the design with the lowest bed volume. For the two examples given in Table 3, the fluidized sand bed system will need only half the number of pumping, flow control, and sludge removal equipment - but with double capacity - compared to the lowest bed volume design.
For the hypothetical wastewater flow a system with four 5.5 m columns with garnet-II with radius 0.35 mm perhaps still would be more economic. A three column system would need a bed height of about 7 m at a flow rate of 67 $m.h^{-1}$ using garnet-II at 0.45 mm. Disadvantage of those designs might be the very high flow rate which might create problems with flow distribution.

CONCLUSIONS

1. The bed expansion in a fluidized bed with biomass covered particles can be described by the relation of Richardson and Zaki (1954).When a sieved fraction of carrier material is used, the modal radius and real number of particles per kg of carrier material have to be used in modeling.
2. The sludge concentration in the bed can be calculated from the superficial velocity, the particle size, and the biomass dry solids density.
3. Nitrate reduction through nitrite follows zero order kinetics in both substrates and first order kinetics in sludge concentration.
5. Deviations of overall kinetics from zero order are caused by:
a. partial substrate penetration into the biomass (diffusion limitation);
b. a sludge concentration gradient along the fluidized bed.
6. The particle size profile in a fluidized bed is related to the substrate conversion.
7. A complete model for biological denitrification in a fluidized bed has been derived and verified. Disadvantage is that a great number of constants need to be determined experimentally.
8. The bed volume needed for nitrate reduction decreases with increasing media specific gravity and decreasing flow rate. However, a truly optimal condition doesn't exist.
9. The model can be used in designing denitrifying fluidized beds, for which purpose graphs are presented in Fig. 6-7. These graphs have to be recalculated for other sets of constants for another wastewater quality.

ACKNOWLEDGEMENTS

The author wishes to thank Mr. J.H. de Wit for his attention to the pilot-plant and Mrs. M.A.Th. Verhoeff-Korpel and Messrs. M.A.C.M. Huybregts and R.C.M. Duyvesteijn for collecting and analyzing the samples.

LIST OF SYMBOLS

C_1, C_0, C_L	nitrate concentration height 1, bottom, top	$kgN.m^{-3}$
C_{n1}, C_{n0}, C_{nL}	nitrite concentration height 1, bottom, top	$kgN.m^{-3}$
C_r, C_R	nitrate concentration in particle at r, at R	$kgN.m^{-3}$
C_{nr}, C_{nR}, C_{nr_0}	nitrite conc. in particle at r, at R, at r_0	$kgN.m^{-3}$
C_w	friction coefficient	
D, D_n	diffusion coefficient nitrate, nitrite	$m^2.s^{-1}$
F	cross section of column	m^2
g	gravitational acceleration	$m.s^{-2}$
gp	average specific gravity of particle	$kg.m^{-3}$

g_b	dry solids density of biomass	$kg.m^{-3}$
g_m	specific gravity of carrier material	$kg.m^{-3}$
g_s	specific gravity of wet biomass	$kg.m^{-3}$
g_w	specific gravity of water	$kg.m^{-3}$
k, k_n	mass transfer constant nitrate, nitrite	$m.s^{-1}$
K, K_n	zero order rate constant nitrate, nitrite	$kg.m^{-3}.s^{-1}$
K_s, K_{sn}	zero rorder rate constant nitrate, nitrite	s^{-1}
l	height in fluidized bed	m
Δl	step length	m
L	bed height	m
n	exponent Richardson & Zaki	
N	particles per unit of bed volume	m^{-3}
N_m	particles per kg of carrier material	kg^{-1}
N_t	number returning particles per m^2 of column	m^{-2}
p, p_l	void fraction (porosity) bed, at height l	
r	radius in biomass layer	m
r_0, r_{n0}	radius where nitrate or nitrite conc. zero	m
r_{0l}, r_{n0l}	as above, at height l	m
r_m	radius of particle of carrier material	m
R, R_l, R_0, R_L	radius particle, at height l, bottom, top	m
Re	Reynolds' number	
S, $(S)c$	biomass concentration, calculated value	$kg.m^{-3}$
V_b	volume of biomass per unit of bed volume	
v	sedimentation velocity single particle	$m.s^{-1}$
v_s	superficial upflow velocity	$m.s^{-1}$
WM	total carrier material in a column	kg
y_s	sludge dry solids yield factor	
y_v	volumetric sludge yield factor	$m^3.kg^{-1}$
η	dynamic viscosity of water	$kg.m^{-1}.s^{-1}$

REFERENCES

Beek, W. J. (1971). Mass transfer in fluidized beds. In J. F. Davidson and D. Harrison (Eds.), Fluidization, Academic Press, London/New York. Chap. 9, pp. 431-470.

Boening, P. H. and V. F. Larsen (1982). Anaerobic fluidized bed whey treatment. Biotech. Bioeng., 24, 2539-2556.

Bosman, J., A. A. Eberhard and C. J. Baskir (1978). Denitrification of a concentrated nitrogenous industrial effluent using packed column and fluidized bed reactors. Prog. Wat. Tech., 10, 297-308.

Cooper, P. F. and B. Atkinson (1981), (Eds.). Biological fluidized bed treatment of water and wastewater. Horwood, Chichester.

Cooper, P. F. and H. V. Wheeldon (1980). Fluidized- and expanded-bed reactors for wastewater treatment. Wat. Pollut. Control, 79, 286-306.

Eggers, E. and T. Terlouw (1979). Biological denitrification in a fluidized bed with sand as carrier material. Water Res., 13, 1077-1090.

Hermans, J. and A. van Haute (1975). Theorie en praktijk van de biologische nitrificatie en denitrificatie van afvalwaters. H_2O, 8, 322-328.

Jeris, J. S., C. Beer and J. A. Mueller (1974). High rate biological denitrification using a granular fluidized bed. J. Water Pollut.Control Fed., 46, 2118-2128.

Jeris, J. S. and R. W. Owens (1975). Pilot-scale, high-rate biological denitrification. J. Water Pollut. Control Fed., 47, 2043-2057.

Jeris, J. S., R. W. Owens, R. Hickey and F. Flood (1977). Biological fluidized-bed treatment for BOD and nitrogen removal. J. Water Pollut. Control Fed., 49, 816-831.

Klapwijk, A., J. C. M. van der Hoeven and G. Lettinga (1981). Biological denitrification in an upflow sludge blanket reactor. Water Res., 15, 1-6.

Mudrack, K. (1970). Untersuchungen über die Anwendung der mikrobiellen Denitrifikation zur biologischen Reinigung von Industrieabwasser. Veröffentlichungen des Instituts für Siedlungswasserwirtschaft der Technische Universität Hannover, Heft 36.

Mulcahy, L. T., W. K. Shieh and E. J. LaMotta (1980). Kinetic model of biological denitrification in a fluidized bed biofilm reactor (FBBR). Prog. Wat. Tech., 12, 143-157.

Mulcahy, L. T., W. K. Shieh and E. J. LaMotta (1981). Simplified mathematical models for a fluidized bed biofilm reactor. AIChE Symp. Ser., 77, 273-285.

Nieuwstad, Th. J. (1983). Modeling, optimization and design of fluidized beds for biological denitrification. Laboratory of Sanitary Engineering, Report Nr. 83-28.

Patton, B. D., C. W. Hancher, W. W. Pitt and J. F. Walker (1982). Design of fluidized-bed biological denitrification systems. Oak Ridge National Laboratory, Report Nr. ORNL/TM-7628, DE 82 007131.

Pitt, W. W., C. W. Hancher and B. D. Patton (1980). Biological reduction of nitrate wastewater using a fluidized-bed bioreactor. CIM Bulletin, 73, 161-170.

Richardson, J. F. and W. N. Zaki (1954). Sedimentation and fluidization. Part I. Trans. Inst. Chem. Eng., 32, 35-53.

Scott, C. D. and C. W. Hancher (1976). Use of a tapered fluidized bed as a continuous bioreactor. Biotech. Bioeng., 17, 1393-1403.

Shieh, W. K. (1980). Suggested kinetic model for the fluidized bed biofilm reactor. Biotech. Bioeng., 22, 667-676.

Shieh, W. K., L. T. Mulcahy and E. J. LaMotta (1982). Mathematical model for the fluidized bed biofilm reactor. Enzyme Microb. Technol., 4, 269-275.

Shieh, W. K., P. M. Sutton and P. Kos (1981). Predicting reactor biomass concentration in a fluidized-bed system. J. Water Pollut. Control Fed., 53, 1574-1584.

Smith, J. M. M. and E. Stammers (1973). Fysische transportverschijnselen I. Delftse Uitgeversmaatschappij B.V., Delft, pp. 55-62.

Stathis, T. C. (1980). Fluidized bed for biological wastewater treatment. J. Env. Eng. Div., 106(EE1), 227-241.

Stephenson, J. P. and K. L. Murphy (1980). Kinetics of biological Fluidized bed wastewater denitrification. Prog. Wat. Tech., 12, 159-171.

Tsezos, M. and A. Benedek (1980). A method for the calculation of biological film volume in a fluidized bed biological reactor. Water Res., 14. 689-693.

Vossoghi, M., M. Laroche, J. M. Navarro, G. Faup and A. Leprince (1982). Denitrification en continu à l'aide de microorganismes immobilisés sur des supports solides. Water Res., 16, 995-1002.

Wat. Sci. Tech. Vol.17, Amsterdam, pp.385-397.
Printed in Great Britain.

0273-1223/85 $0.00 + .50

MATHEMATICAL MODEL OF SIMULTANEOUS ORGANIC OXIDATION, NITRIFICATION, AND DENITRIFICATION IN ROTATING BIOLOGICAL CONTACTORS

Yoshimasa Watanabe,* Sumio Masuda,*
Kiyoshi Nishidome** and Chalermraj Wantawin***

*Department of Civil Engineering, Miyazaki University, Miyazaki 880, Japan
**Department of Civil Engineering, Kagoshima Technical College, Hayato 899-51, Japan
***Department of Chemical Engineering, King Mongkut's Institute of Technology, Bangkok, Thailand

ABSTRACT

Simultaneous organic oxidation and nitrification rates in the RBC are given using a mathematical equation. The equation was derived from a hypothesis stating that intrinsic oxygen uptake rate of the biofilm has a constant value at a fixed temperature, independent of the composition of the aerobic bacteria. Based on this hypothesis, empirical equations are proposed to describe the profile of intrinsic organic oxidation and nitrification rates. Computer simulation of the simultaneous organic oxidation and nitrification was carried out to confirm the empirical equations. The mathematical model of the simultaneous nitrification and denitrification is discussed and was tested by computer simulation.

KEYWORDS

Rotating biological contactor;molecular diffusion;organic oxidation;nitrification; denitrification;biofilm;computer simulation.

INTRODUCTION

The authors(1,2,3) developed a steady-state biofilm kinetics for the soluble substrate and applied it to the nitrification and denitrification in Rotating Biological Contactors(RBC). This kinetics is described as the process of molecular diffusion with a simultaneous zero-order intrinsic biochemical reaction. The authors demonstrated that their biofilm kinetics was completely applied to the anaerobic denitrification in a submerged RBC. A partially submerged RBC, which is usually referred to as an RBC, has no steady-state substrate concentration profile within the biofilm, even though the bulk substrate concentration is the steady state, since the biofilm rotates alternately into the air and water. The authors(3,4) carried out a simulation of the nitrification in a partially submerged RBC to determine the substrate profiles within the biofilm. After considering the simulated substrate profiles, a mathematical model was proposed to predict the substrate removal rate at a given bulk substrate concentration. As shown in previous papers(3,4,5), the proposed model well described the pure nitrification in a partially submerged RBC. In the pure nitrification, ammonia is the only interesting substrate if enough inorganic carbon has been added. However, many kinds of wastewater such as domestic sewage contain both soluble organic matter and ammonia. Therefore, the process of molecular diffusion with simultaneous organic oxidation and nitrification occurs in the biofilm used to treat such wastewater. These two biochemical reactions influence each other, since both are aerobic reactions. The oxygen penetration depth in the biofilm changes with the rotation of the disk. This penetration forms a zone within the biofilm where aerobic and anaerobic atmospheres appear

alternately. Simultaneous nitrification and denitrification would be expected in such a zone. The authors(9,10)carried out experimental investigations on the above phenomenon and found out that it is mainly influenced by disk rotating speed,loadings of organic matter and ammonia,biodegradability and diffusivity of organic matter,water temperature,and the partial pressure of oxygen in the air phase.
In the present paper,the authors present a mathematical model of simultaneous organic oxidation,nitrification,and denitrification. Computer simulation results are also reported to confirm the proposed mathematical model.

MATHEMATICAL MODEL FOR A PARTIALLY SUBMERGED RBC

After considering the computer simulation results of nitrification,the authors(4,5) developed a mathematical model for a partially submerged RBC. The model is summarized below. In our model,the substrate removal rate was determined using the submerged disk area. This rate can be converted to the removal rate on the total disk area by multiplying it by the ratio of the submerged disk. The substrate removal rate at a given bulk substrate concentration is expressed by Eqs.(1) and (2) for a partly and fully penetrated biofilm,respectively.
A partly penetrated biofilm($\lambda_1=\sqrt{2DC_s/R}\,/L_a \leq 1$):

The soluble substrate removal rate can be calculated by using the bulk first-order removal rate(F_1) and the parameter λ_2.

$$F= F_1/(1 + \lambda_2) = K_d C_b/(1 + \lambda_2) \tag{1}$$

The parameter λ_2 is calculated by the following procedure.

(1) Calculation of the parameter λ_3

$\lambda_3= L_d\sqrt{2R/D}$

(2) Calculation of C_s

$C_s= (2C_b+\lambda_3^2 - \lambda_3\sqrt{\lambda_3^2+4C_b})/2$

(3) Calculation of the parameter λ_2

$\lambda_2=\sqrt{DC_s/2R}\,/L_d$

A fully penetrated biofilm($\lambda_1 \geq 1$):

The soluble substrate removal rate is constant,independent of the bulk substrate concentration. In an aerobic treatment,the substrate removal rate is calculated from the oxygen flux to the biofilm.

$$F=F^*=(F_{oa} + F_{ow})/(R_o/R)=(F_{oa} + F_{ow})/a \tag{2}$$

Oxygen flux to the biofilm rotating in the air phase:

$$F_{oa}= D_o(C_o^* - C_{so,a})/L_w =\sqrt{2D_oR_oC_{so,a}} \tag{3}$$

$$C_{so,a}=(2C_o^* + \alpha - \sqrt{\alpha^2 + 4\alpha C_o^*})/2$$

$$\alpha =(2R_oL_w^2)/D_o$$

Oxygen flux to the biofilm rotating in the water phase:

$$F_{ow}= D_o(C_{bo} - C_{so,w})/L_d =\sqrt{2D_oR_oC_{so,w}} \tag{4}$$

$$C_{so,w}=(2C_{bo} + \beta -\sqrt{\beta^2 + 4\beta C_{bo}})/2$$

$$\beta =(2R_oL_d^2)/D_o$$

SIMULTANEOUS ORGANIC OXIDATION AND NITRIFICATION

Experimental Investigation

Three completely mixed-flow type units with disk diameter of 30 cm were used. Units 1,2,and 3 consisted of 13,15,or 10 disks,respectively,mounted 2 cm apart on a horizontal shaft. Half the diameter of each disk was submerged. The experimental variables were (a)hydraulic loading,(b)influent concentration of organic matter,and (c) - type of organic matter(glucose,starch,or ethylene glycol). Water temperature was in the range of 23°-27°C and pH 7.8-8.2. The disk rotational speed was fixed at 8.5 rpm and influent ammonia concentration at 45 g/m^3. The experimental conditions are summ-

arized in Table 1. Reduction of ammonia in simultaneous organic oxidation and nitrification consists of reduction due to nitrification and cell synthesis. Eq.(5) shows the ammonia removal rate in simultaneous organic oxidation and nitrification.

$$F_a = F_n + F_g \tag{5}$$

Ammonia removal rate is defined as follows:

$$F_a = Q(C_{ia} - C_{ea})/A_w \tag{6}$$

The mass balance of the oxidized nitrogen in a completely mixed-flow RBC is

$$V_b(dC_{bn}/dt) = QC_{in} - QC_{en} + F_nA_w \tag{7}$$

If the influent contains no oxidized nitrogen,Eq.(7) becomes Eq.(8) at steady state.

$$C_{en} = F_nA_w/Q \tag{8}$$

Assuming that the ratio of oxidized organic matter to ammonia for the cell synthesis is constant,i.e.,$F_g=kF_c$,Eq.(9) is obtained by combining Eqs.(5) and (8).

$$(C_{en}/F_a)/(A_w/Q) = 1-k(F_c/F_a) \tag{9}$$

Combining Eqs.(6) and (9) gives Eq.(10).

$$C_{en}/(C_{ia} - C_{ea}) = 1 - k(F_c/F_a) = 1 - (k/a_c)(a_cF_c/F_a) \tag{10}$$

Experimental data in Runs 4,5,6 and 7 were plotted as shown in Fig.1. Based on Fig.1, the relationship among F_a,F_n,and F_c is given by Eq. 11.

$$F_a = F_n + F_g = F_n + 0.1a_cF_c \tag{11}$$

a_c was experimentally determined as 0.71 gO_2/g oxidized glucose,0.55 gO_2/g oxidized starch,and 0.63 gO_2/g oxidized ethylene glycol(6).Heukelekian et.al(7) reported 0.50 -0.74 gO_2/g oxidized glucose and 0.22-0.68 gO_2/g oxidized starch. Fig.2 shows the

Table 1 Experimental Conditions

Run No.	Organic matter	Influent Conc.	Hydraulic loading	Water Temp.
1	Glucose	36 g/m^3	2.5-7.6 liters/m^2h	27°C
2	Glucose	75	2.5-10.6	25
3	Glucose	180	2.0-7.1	25
4	Starch	233	1.7-7.6	25
5	Starch	57-490	2.6	23
6	Ethelene glycol	30-200	5.7	25
7	Ethylene glycol	60-190	3.6	25

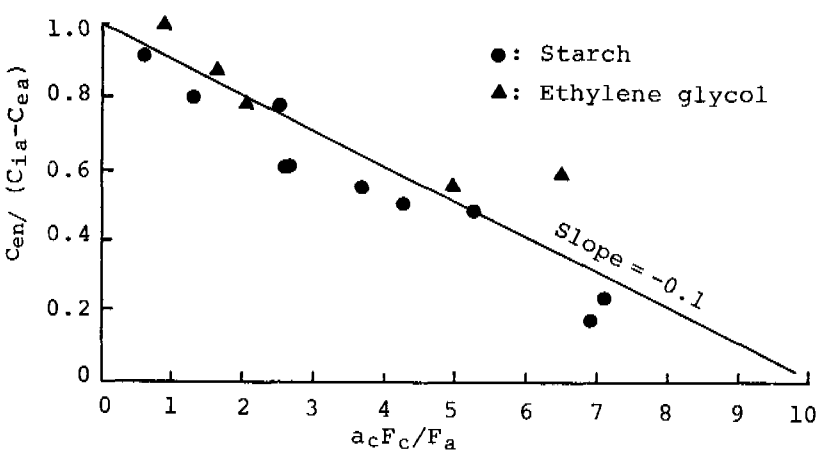

Fig.1. Plot of experimental data for the verification of Eq.(10)

effect of organic oxidation on the relationship between the ammonia removal and bulk ammonia concentration in Run 5. F_n was calculated using the experimental values of F_a and F_c. In Eq.(11), a_c was assumed as 0.55 gO_2/g oxidized starch. Fig.3 shows the relationship between the starch oxidation rate and bulk starch concentration in Run 5. The solid line in Fig.3 shows the same relationship for pure starch oxidation which had been calculated by the mathematical analysis explained in the following section.

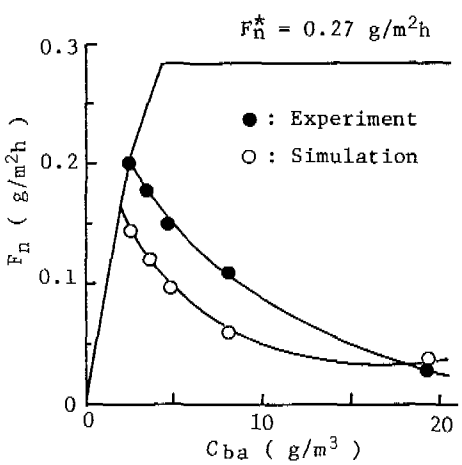

Fig.2. Effect of organic oxidation on nitrification rate

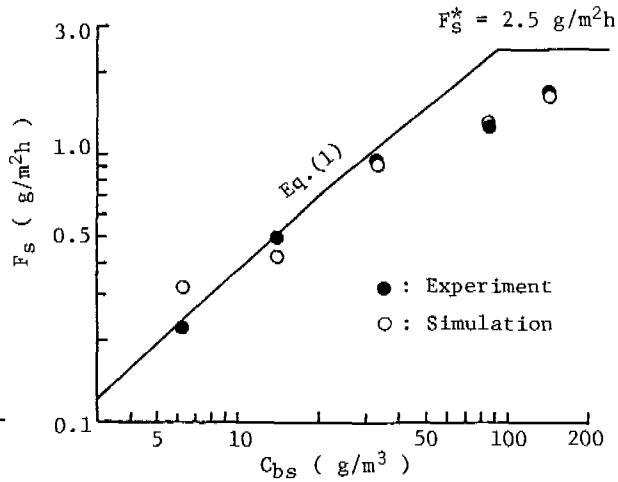

Fig.3. Starch oxidation rate with simultaneous nitrification

Mathematical Analysis

For the mathematical analysis of simultaneous organic oxidation and nitrification, the authors have made the following hypothesis:
"The intrinsic oxygen uptake rate of the biofilm has a constant value at a fixed temperature, independent of the composition of the aerobic bacteria".
This hypothesis can be mathematically expressed by Eq.(12) in the case of simultaneous organic oxidation and nitrification.

$$R_O = a_n R_n^* = a_n R_n + a_c R_c = a_c R_c^* \qquad (12)$$

From the data of the nitrification experiment, the authors(8) obtained an intrinsic nitrification rate of 5.2×10^3 g/m³h(23.5°C) for pure nitrification. Therefore, the intrinsic starch oxidation rate for pure starch oxidation at the same temperature was calculated as follows:

$$R_S^* = (a_n R_n^*)/a_s = (4.33\times5.2\times10^3)/0.55 = 4.1\times10^4 \text{ g/m}^3\text{h}$$

In previous papers(4,5), R_S^* was estimated at 3.0×10^4 g/m³h. Considering Eq.(12), however, the authors have estimated R_S^* at 4.1×10^4 g/m³h in this paper. The molecular diffusion coefficient of starch was calculated as 2.4×10^{-6} m²/h by using the Wilk and Chang equation(4). Under starch rate limiting, the starch oxidation rate for pure starch oxidation is given by Eq.(13).

$$F_S = \sqrt{2D_S R_S^* C_{ss}} \qquad (13)$$

Graphically described, Eq.(13) is given by an oblique line having a slope of 1/2(Fig.4), if R_S^* and D_S are 4.1×10^4 g/m³h and 2.4×10^{-6} m²/h, respectively. The data in Fig.4 were obtained by converting the measured bulk starch concentration to a starch concentration at the biofilm surface(Eq.(14)).

$$C_{bs} = C_{ss} + (F_S/K_d) \qquad (14)$$

The relationship between the bulk starch concentration and starch oxidation rate

was calculated using Eq.(1) for the starch and Eq.(2) for oxygen rate limitings. The following numerical values were used in the calculation: $D_O=8.8\times10^{-6}$ m^2/h, $R_O=a_S R_S^*=2.2\times10^4$ g/m^3h, $L_W=5.0\times10^{-5}$ m, $L_d=6.0\times10^{-5}$ m, $C_O^*=8.5$ g/m^3 and $C_{bo}=3.0$ g/m^3. The starch oxidation rate in the oxygen rate limiting was calculated as follows:

$$F_S^* = F_O/a_S = (F_{Oa} + F_{Ow})/a_S = 2.5 \text{ g/m}^2\text{h}$$

where F_{Oa} was determined to be 1.02 from Eq.(3) and F_{Ow} 0.38 g/m^2h from Eq.(4). Bulk starch concentration at the transition from the starch to oxygen rate limiting was calculated using our mathematical model. F_S^* and C_{bs}^* are expressed by Eqs.(15) and (16), respectively.

$$F_S^* = \sqrt{2D_S R_S^* C_{ss}^*} \tag{15}$$

$$C_{bs}^* = C_{ss}^* + (F_S^*/K_d) \tag{16}$$

Therefore, C_{ss}^* was calculated as 32 and C_{bs}^* as 94 g/m^3. The calculated relationship between F_S and C_{bs} can be shown graphically by the solid line in Fig.3. Fig.3 demonstrated that the reduction of the starch oxidation rate due to simultaneous nitrification is negligible until the bulk starch concentration reaches about 40 g/m^3 (the corresponding BOD is about 20 g/m^3), but because the inner part of the aerobic biofilm consists of both heterotrophic and nitrifying bacteria, it becomes remarkable in the bulk starch concentration

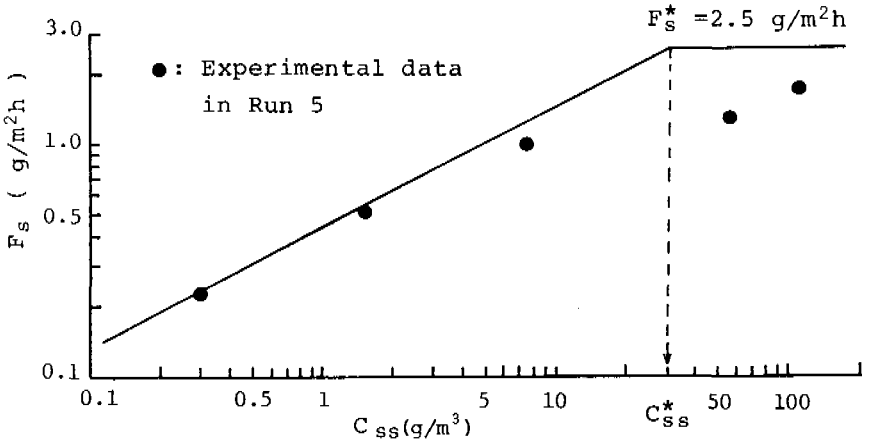

Fig.4. Starch oxidation rate vs. starch concentration at the biofilm surface

Based on Eqs.(3) and (4) and the hypothesis expressed by Eq.(12), the authors have reached the following conclusion :"the amount of oxygen supplied to the biofilm is the same under a fixed disk operating condition, independent of the composition of aerobic bacteria". This conclusion is mathematically expressed by Eq.(17).

$$F_O = F_{Oa} + F_{Ow} = a_n F_n^* = a_n F_n + a_c F_c = a_c F_c^* \tag{17}$$

In dimensionless form, Eq.(17) becomes Eq.(18).

$$F_n/F_n^* = 1 - (1/a_n)(a_c F_c/F_n^*) = 1 - 0.23(a_c F_c/F_n^*) \tag{18}$$

Introducing Eq.(11) into Eq.(18) gives

$$F_a/F_n^* = 1 - 0.13(a_c F_c/F_n^*) \tag{19}$$

The experimental data in Runs 1 to 7 were plotted as the relationship between F_n/F_n^* and $a_c F_c/F_n^*$ and are shown in Fig.5. Fig.5 gives the experimental verification of Eq.(18).

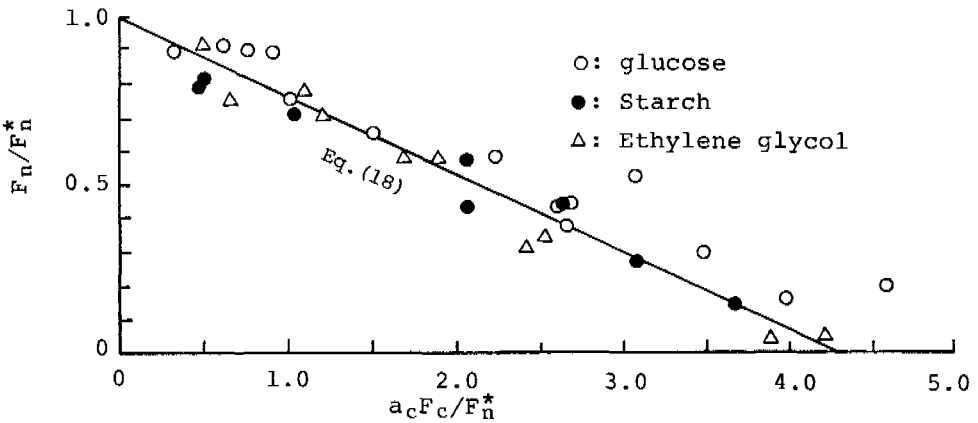

Fig.5. Plot of experimental data for the verification of Eq.(18)

Computer Simulation

Computer simulations were carried out to determine the change in the ammonia,starch and oxygen profiles in the biofilm attached to a partially submerged RBC. The basic equation for the simulations was Eq.(20).

$$\partial C_i/\partial t = D(\partial C_i^2/\partial Z^2) - R_i \qquad (20)$$

The simulation procedure has already been discussed in previous papers(3,4). In a biofilm,with simultaneous organic oxidation and nitrification,the density of the nitrifying bacteria would gradually increase with the depth of aerobic biofilm,while the density of the heterotrophic bacteria would decrease under the same conditions, because of the difference in the specific growth rates of both bacteria. The authors have proposed the emprical formulae(Eqs.(21) to (23)) to express the above phenomenon derived from Eqs.(11) and (12).

Intrinsic nitrification rate:

$$R_n/R_n^* = Z/(K_n + Z) \qquad (21)$$

Intrinsic organic oxidation rate:

$$R_C/R_C^* = K_n/(K_n + Z) \qquad (22)$$

Intrinsic ammonia removal rate:

$$R_a/R_a^* = (Z + 0.1K_n a_n)/(K_n + Z) \qquad (23)$$

The simulations were conducted for the experimental conditions in Run 5. Table 2 shows the numerical values used in the simulations.

Table 2 Numerical constants used in the simulation(for 23.5°C)

Biofilm Thickness	900 μm
Attached-water layer thickness	50 μm
Diffusion layer thickness	70 μm
Max.intrinsic starch oxidation rate	4.1×10^4 g/m^{3}h
Max.intrinsic nitrification rate	5.2×10^3 g/m^{3}h
Diffusion coefficient of oxygen	8.8×10^{-6} m^2/h
Diffusion coefficient of starch	2.4×10^{-6} m^2/h
Diffusion coefficient of ammonia	7.5×10^{-6} m^2/h
Oxygen requirement of starch oxidation	0.55 gO_2/g oxidized starch
Oxygen requirement of nitrification	4.33 gO_2/g oxidized ammonia
Disk rotating speed	8.5 rpm

The saturation constant(K_n) was changed to match the simulated results with the experimental results. Fig.6 shows the simulated profiles of starch,ammonia,and dissolved oxygen in Run 5.

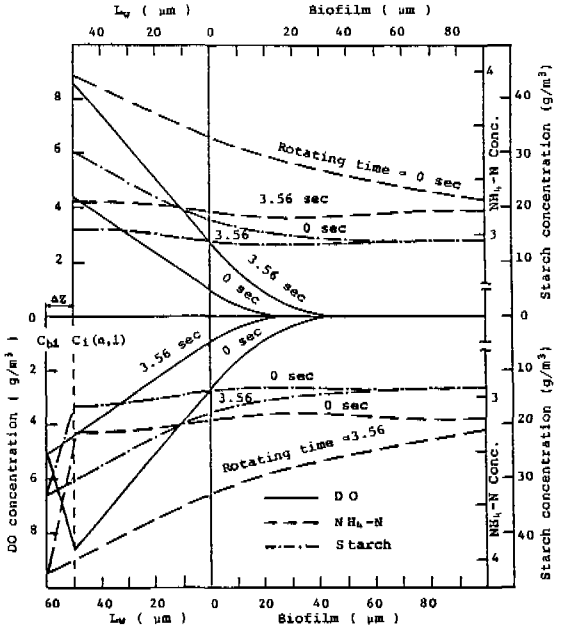

Fig.6. Simulated profiles of starch,ammonia and DO (Run 5,C_{ba}=4.6,C_{bs}=33 g/m^3)

Using the simulated substrate profiles,the substrate removal rates can be calculated by Eq.(24).

$$F_i=(D_i/N\Delta Z)\sum_{n=1}^{N}(C_{bi} - C_i(n,1)) \quad (24)$$

where the submerged biofilm surface is divided into N elemental surfaces,and the biofilm depth is divided into sub-layers, each of them ΔZ thick.

Fig.7 shows the relationship between the bulk starch concentration and the value of K_n giving the best fit. Comparison of the simulated and the experimental starch oxidation rate is shown in Fig.3. The simulated nitrification rates were plotted along with the experimental data in Fig.2.

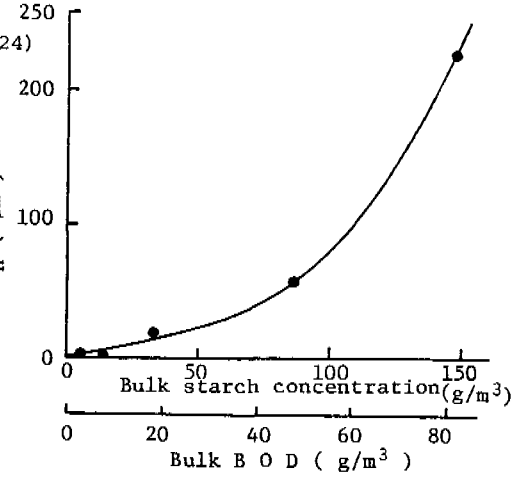

Fig.7. Relationship between K_n and C_{bs}

SIMULTANEOUS NITRIFICATION AND DENITRIFICATION

Experimental Investigation(9,10,11)

The experimental unit was a closed-type RBC with a completely mixed-flow as shown in Fig.8. Artificial wastewater containing methanol,ammonia,inorganic carbon,and trace elements was fed into it. Water temperature was fixed at 30°C and the pH of the bulk water at 8.0. The phenomenon of simultaneous nitrification and denitrification was confirmed by measuring the amount of nitrogen gas in the air phase. Experimental results verified that the amount of nitrogen gas increased. It was almost the same as the theoretical value calculated

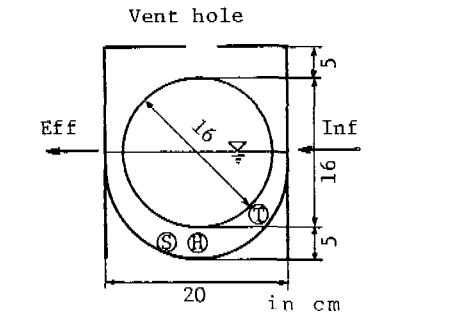

Disk number : 20
Disk diameter : 16 cm
Disk thickness : 0.5 cm
Disk space : 1.0 cm
Disk area : 0.82 m²
Thermometer : T
Heater : H
Thermostat : S

Fig.8. Closed-type RBC unit

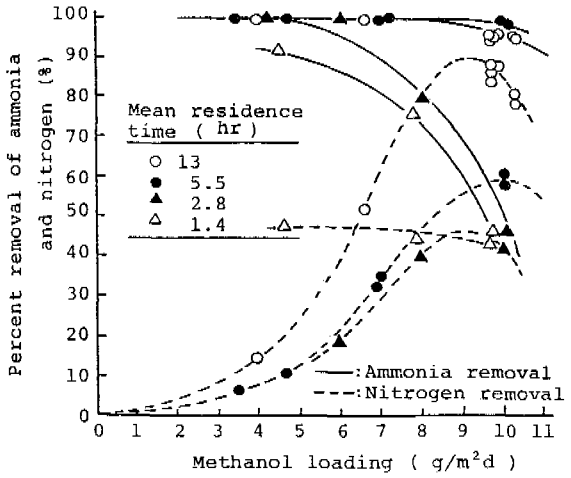

Fig.9. Experimental data on simultaneous nitrification and denitrification (partial pressure of oxygen=0.21 atms.)

from the amount of denitrified nitrogen. This fact would confirm the phenomenon of simultaneous nitrification and denitrification in the RBC. The factors influencing the phenomenon were also examined. Experimental results demonstrated that the efficiency of simultaneous nitrification and denitrification is influenced by the ammonia and organic loadings, biodegradability and diffusivity of organic natter, mean residence time, water temperature, and the partial pressure of oxygen in air phase. Fig.9 shows the relationship among the percent removals of ammonia and nitrogen, mean residence time, and methanol loading at a fixed ammonia loading of 1 g/m²day. The effect of a partial pressure of oxygen on the ammonia and nitrogen removal rates was examined by an experiment in which the vent holes were closed. Steady state operation at an oxygen pressure of .21 atms had been completed before the vent holes were closed. The partial pressure of oxygen decreased with the elapsed time after the vent holes were closed. Fig.10 shows several examples of the experimental results. It took about 6 hours to decrease the partial pressure of oxygen from 0.21 to 0.05 atms.

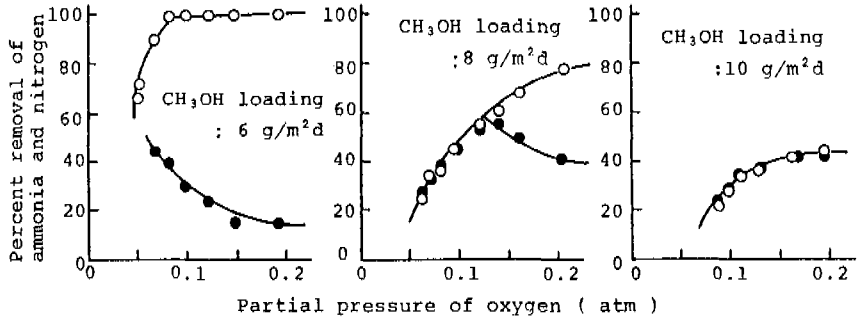

Fig.10. Effect of partial pressure of oxygen on simultaneous nitrification and denitrification (mean residence time=2.8 hrs, ammonia loading=1 g/m²day)

Computer Simulation

Computer simulations were carried out to determine the relationship between the partial pressure of oxygen in the air phase,and the ammonia and nitrogen removal rates. The simulation model was the same as that used in the simulation of simultaneous organic oxidation and nitrification. As mentioned above,the experiment to determine this relationship was conducted for about 6 hours. Therefore,the profiles of the intrinsic organic oxidation and nitrification rates were fixed in the simulations, because 6 hours would be too short a time to significantly change the profiles. Intrinsic nitrification and organic oxidation rates are given in Eqs.(21) and (22). Considering the fact that applied organic loading was higher than that in the experiment for simultaneous organic oxidation and nitrification,the follwing modification was made.

Intrinsic reaction rates in an aerobic biofilm:

$$R_n/R_n^*=\gamma \text{ and } R_c/R_c^*=1-\gamma \quad \text{at } 0 \leq Z \leq Z_o \tag{25}$$

$$R_n/R_n^*=(Z - Z_o)/(K_n + (Z - Z_o))$$
$$R_c/R_c^*= K_n/(K_n + (Z - Z_o)) \quad \text{at } Z \geq Z_o \tag{26}$$

Intrinsic reaction rates in an anaerobic biofilm:

$$R_d=R_d^* \tag{27}$$

$$R_c=2.5R_d \tag{28}$$

Eq.(28) means that 2.5 grams of methanol is oxidized per unit gram of denitrified nitrogen. Z_o is mainly a function of the organic loading during the steady state period. Facultative denitrifying bacteria are assumed to exist in their maximum density within the biofilm. They act as heterotrophic bacteria in the aerobic biofilm and denitrifying bacteria in the anaerobic biofilm.Table 3 shows the numerical constants used in the simulation. Table 4 shows the experimental data for which the simulations were made.

Table 3 Numerical constants used in the simulation(for 30°C)

Biofilm thickness	900 μm
Attached-water layer thickness	50 μm
Diffusion layer thickness	70 μm
Intrinsic nitrification rate	8000 g/m^3h
Intrinsic denitrification rate	3000 g/m^3h
Intrinsic methanol oxidation rate	9000 g/m^3h
Diffusion coefficient of ammonia	9.0×10^{-6} m^2/h
Diffusion coefficient of oxygen	10.4×10^{-6} m^2/h
Diffusion coefficient of methanol	7.5×10^{-6} m^2/h
Diffusion coefficient of nitrate	7.2×10^{-6} m^2/h
Disk rotating speed	7.5 rpm

Table 4 Experimental data for the simulation

	P_o(atm.)	C_{ba}(g/m^3)	C_{bn}(g/m^3)	C_{bm}(g/m^3)	C_{bo}(g/m^3)
Run 1	0.21	0.5	22.0	1.3	1.0
Run 2	0.18	0.5	20.0	1.3	0.9
Run 3	0.11	7.0	0.2	8.5	0.1
Run 4	0.08	20.0	0.1	56.0	0.1

P_o: Partial pressure of oxygen in the air phase.
C_{ba}:Bulk ammonia concentration.
C_{bn}:Bulk nitrate concentration.
C_{bm}:Bulk methanol concentration.
C_{bo}:Bulk DO concentration.

Figs. 11 and 12 show the profiles of intrinsic methanol oxidation and nitrification rates which gave the best fit for the simulated and experimental results. The simulation determined the values of K_n and Z_o to be 70 μm and 30 μm, respectively.

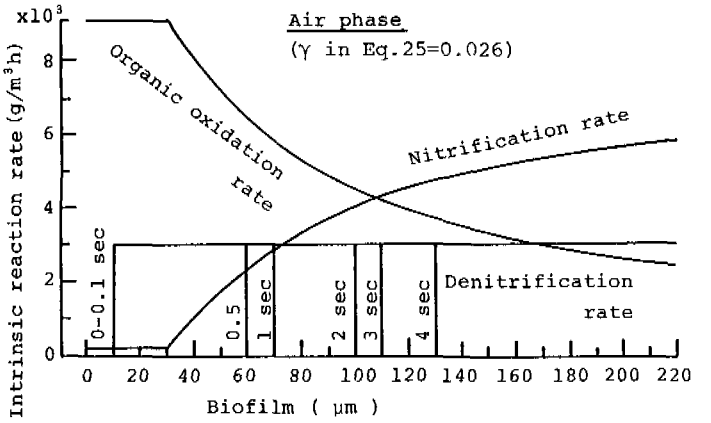

Fig.11. Profiles of intrinsic reaction rates during the air phase

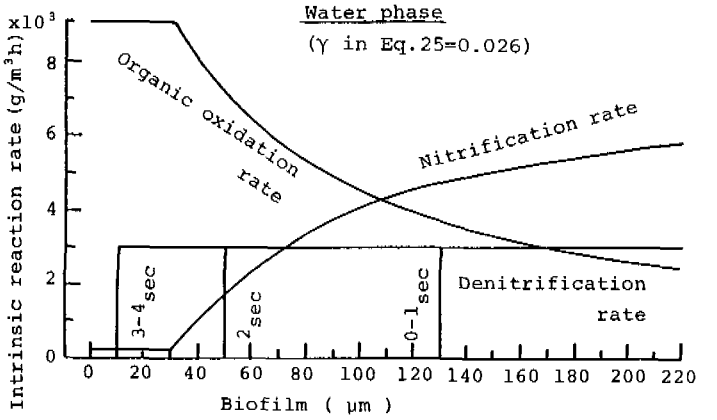

Fig.12. Profiles of intrinsic reaction rates during the water phase

Fig.13 shows the simulated dissolved oxygen profile. Considering the simulated profile shown in Fig.13, the profile of intrinsic denitrification rate is shown in Figs 11 and 12 as a function of the disk rotating time during the air and water phases. Fig.14 shows the comparison of the experimental and simulated rates of nitrification and denitrification.

SUMMARY AND CONCLUSIONS

Both heterotrophic and autotrophic nitrifying bacteria inhabit the biofilm to use for the treatment of wastewater containing organic matter and ammonia. The activities of these bacteria vary, depending on the treatment conditions. The present paper dealt with the mathematical model of simultaneous organic oxidation and nitrification. Based on the hypothesis stating that the intrinsic oxygen uptake rate of the biofilm has a constant value at a fixed temperature, independent of the composition of the aerobic bacteria, the authors proposed the following mathematical relationship for the simultaneous organic oxidation and nitrification rates:

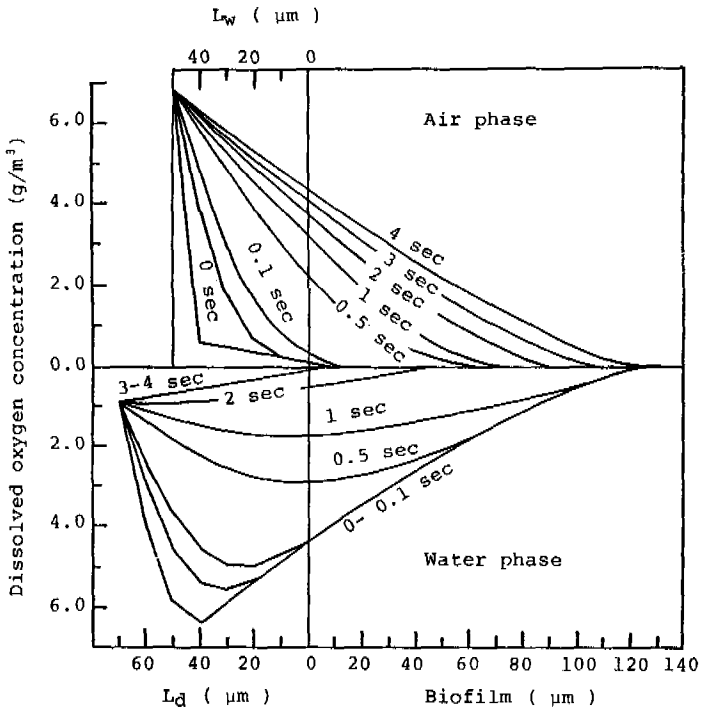

Fig.13. Simulated profile of DO in simultaneous nitrification and denitrification(Run 2)

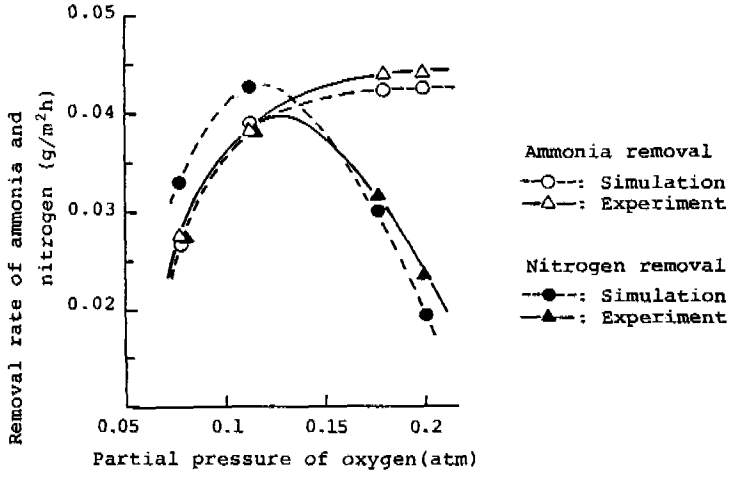

Fig.14. Comparison of experimental and simulated rates of nitrification and denitrification

$$F_n/F_n^* = 1 - (1/a_n)(a_c F_c/F_n^*)$$

The above equation was verified using experimental data. A computer simulation of simultaneous organic oxidation and nitrification was also carried out. The following empirical equations were used for the simulation.

Intrinsic nitrification rate profile:

$$R_n/R_n^* = Z/(K_n + Z)$$

Intrinsic organic oxidation rate profile:

$$R_c/R_c^* = K_n/(K_n + Z)$$

The simulated organic oxidation and nitrification rates almost coincided with the experimental results.

The phenomenon of simultaneous nitrification and denitrification in an RBC was investigated experimentally and with a computer simulation. The simulation model was the same as that used for simultaneous organic oxidation and nitrification, except for the introduction of the action of facultative denitrifying bacteria. The simulated profile of dissolved oxygen showed that denitrification occurs mainly in a zone formed within the biofilm where aerobic and anaerobic atmospheres alternately appear. The depth of such a zone depends on factors such as the loadings of organic matter and ammonia, water temperature, and the partial pressure of oxygen in the air phase. Comparing the simulated and experimental results of simultaneous nitrification and denitrification, the proposed mathematical model was found to be almost completely satisfactory.

ACKNOWLEDGEMENTS

This research was supported by the research grant from the Kajima Foundation.

NOMENCLATURE

Symbol	Dimension	Description	Symbol	Dimension	Description
A_w	m^2	Submerged disk area	$C_{so,w}$	g/m^3	DO conc. at biofilm surface during water phase
C_b	g/m^3	Bulk substrate conc.			
C_{ba}	g/m^3	Bulk ammonia conc.			
C_{bn}	g/m^3	Bulk nitrate conc.	D	m^2/h	Molecular diffusion coefficient of substrate
C_{bo}	g/m^3	Bulk DO conc.			
C_{bi}	g/m^3	Bulk conc. of substrate i	D_o	m^2/h	Molecular diffusion coefficient of DO
C_{ea}	g/m^3	Effluent ammonia conc.	D_s	m^2/h	Molecular diffusion coefficient of starch
C_{en}	g/m^3	Effluent nitrate conc.			
C_i	g/m^3	Conc. of substrate i within biofilm	F	g/m^2h	Substrate removal rate
			F_a	g/m^2h	Ammonia removal rate
C_{ia}	g/m^3	Influent ammonia conc.	F_c	g/m^2h	Organic oxidation rate
C_{in}	g/m^3	Influent nitrate conc.	F_c^*	g/m^2h	Max. organic oxidation rate
C_o^*	g/m^3	Saturation conc. of DO			
C_s	g/m^3	Substrate conc. at biofilm surface	Fn	g/m^2h	Nitrification rate
			F_n^*	g/m^2h	Max. nitrification rate
C_{ss}	g/m^3	Starch conc. at biofilm surface	F_s	g/m^2h	Starch oxidation rate
			F_s^*	g/m^2h	Max. starch oxidation rate
C_{ss}^*	g/m^3	C_{ss} at transition from starch to oxygen rate limiting	F_o	g/m^2h	Oxygen flux to biofilm
			F_{oa}	g/m^2h	Oxygen flux to biofilm during air phase
C_{bs}	g/m^3	Bulk starch conc.			
C_{bs}^*	g/m^3	C_{bs} at transition from starch to oxygen rate limiting	F_{ow}	g/m^2h	Oxygen flux to biofilm during water phase
			K_d	m/h	Mass transfer coefficient
$C_{so,a}$	g/m^3	DO conc. at biofilm surface during air phase	K_n	m	Saturation constant
			L_a	m	Aerobic biofilm depth
			Ld	m	Diffusion layer thickness

Symbol	Dimension	Description	Symbol	Dimension	Description
L_w	m	Attached-water layer thickness	R_s	g/m^3h	Intrinsic starch oxidation rate
R	g/m^3h	Intrinsic substrate removal rate	R_s^*	g/m^3h	Max. intrinsic starch oxidation rate
R_a	g/m^3h	Intrinsic ammonia removal rate	R_o	g/m^3h	Intrinsic oxygen uptake rate
R_a^*	g/m^3h	Max. intrinsic ammonia removal rate	a	-	R_o/R
R_c	g/m^3h	Intrinsic organic oxidation rate	a_c	-	Oxygen requirement of organic oxidation
R_c^*	g/m^3h	Max. intrinsic organic oxidation rate	a_n	-	Oxygen requirement of nitrification(4.33)
R_d	g/m^3h	Intrinsic denitrification rate	a_s	-	Oxygen requirement of starch oxidation(0.55)
R_d^*	g/m^3h	Max. intrinsic denitrification rate	k	-	Constant
			Z	m	Biofilm thickness
			Z_o	m	Constant

REFERENCES

(1) Watanabe,Y. and Ishiguro,M.(1978).Denitrification Kinetics in a Submerged Biological Disk Unit.Progress in Water Technology,Vol.10,Nos.5/6,pp187-195.

(2) Watanabe,Y.,Ishiguro,M. and Nishidome,K.(1980).Nitrification in a Rotating Biological Disk Reactor.Progress in Water Technology,Vol.12,pp.233-251.

(3) Watanabe,Y.,H.E.Bravo and Nishidome,K.(1982).Simulation of Nitrification and Its Dynamics in a Rotating Biological Contactor.Wat. Sci. Tech.,Vol.14 pp.811-832.

(4) Watanabe,Y. et.al.(1982).Kinetics and Simulation of Nitrification in a Rotating Biological Contactor.Proceedings of the 1st International Conference on Fixed-Film Biological Processes.

(5) Watanabe,Y.,Ishiguro,M.and Masuda,S.(1983).Mathematical Model of Rotating Biological Contactor and Its Application to Nitrification and Denitrification Processes.Documentation of the International Seminar on Rotating Biological Discs Oct. 6-8,1983,Fellbach,pp.41-62.

(6) Thanantaseth,C.(1981).Kinetic Model of Biological Oxidation in Rotating Biological Contactors.Master's thesis,Environmental Engineerng Division,AIT.

(7) Heukelekian,H. and Rand,M.C.(1955).Oxygen Demand of Pure Organic Compounds, Sewage and Industrial Wastes,No.27.

(8) Watanabe,Y.,Nishidome,K. and Ishiguro,M.(1982).Simulation of Nitrification Process in a Rotating Biological Contactor.Journal of Japan Sewage Works Association,Vol.19,No.223,pp.30-39.

(9) Masuda,S,Ishiguro,M and Watanabe,Y.(1979).A Study on Nitrogen Removal in a Rotating Biological Contactor.Journal of Japan Sewage Works Association,Vol.16, No.187,pp.24-32.

(10)Masuda,S,Watanabe,Y. and Ishiguro,M.(1982). A Study on Nitrogen Removal in a Rotating Biological Contactor(11).Journal of Japan Sewage Works Association, Vol.19,No.215,pp.12-20.

(11)Masuda,S.,Watanabe,Y. and Ishiguro,M.(1982).Simultaneous Nitrification and Denitrification in a Rotating Biological Contactor.Proceeding of the 1st international conference on Fixed-film Biological Processes.

Wat. Sci. Tech. Vol.17, Amsterdam, pp.399-408. 0273-1223/85 $0.00 + .50
Printed in Great Britain.

THE APPLICATION OF PREDENITRIFICATION NITRIFICATION TECHNOLOGY FOR TRACE CONTAMINANT CONTROL

H. Melcer* and S. G. Nutt**

**Environment Canada, Wastewater Technology Centre, P.O. Box 5050, Burlington, Ontario, L7R 4A6, Canada*
***Canviro Consultants Ltd., 178 Louisa Street, Kitchener, Ontario, N2H 5M5, Canada*

ABSTRACT

Predenitrification nitrification (PDN) technology was applied in two stage anoxic-aerobic systems treating coke plant wastewaters and coal liquefaction process condensates. Both activated sludge and biological fluidized bed modes of operation were investigated for their potential to remove ammonia, phenol, thiocyanate, cyanide and a wide range of trace organic contaminants. It was demonstrated that during nitrification of these complex wastewaters, simultaneous removal of most of the conventional and trace organic contaminants was achieved. Specifically, of the base/neutral extractable organic compounds, only di-n-butyl phthalate was consistently found in treated effluent samples at greater than trace levels (0.01 mg/l). It appears that trace organic contaminant control in complex industrial wastewaters can be achieved by the application of PDN technology.

KEYWORDS

Predenitrification, nitrification, biological fluidized bed, coke plant wastewater, coal liquefaction wastewater, trace contaminants, polyaromatic hydrocarbons, heterocyclic nitrogenous compounds.

INTRODUCTION

Extensive work has been carried out on the application of biological nitrogen control to complex ammonia-bearing industrial wastewaters. At Environment Canada's Wastewater Technology Centre (WTC) in Burlington, Ontario, development of biological nitrogen control technology has been in progress since the mid-1970s. Single and separate sludge systems have been evaluated in suspended growth and fixed-film reactor configurations for both municipal and industrial wastewaters. Predenitrification nitrification (PDN) using solids retention time (SRT) control was found to be the most efficient and cost-effective method of nitrogen control investigated (Sutton et al., 1979; Wilson et al., 1981).

In PDN systems, denitrification is accomplished in an anoxic first stage reactor where organic carbon in the raw wastewater provides the energy source and serves as the electron donor for the denitrification reaction. The conversion of

ammonia to nitrate and oxidation of any biodegradable organics not removed in the first stage are carried out in an aerobic second stage reactor. Depending upon the ratio of carbon to nitrogen in the feed, PDN will reduce or even eliminate the need for supplemental organic carbon. The anoxic removal of raw wastewater organics by denitrification also significantly reduces oxygen requirements. In addition, coupling the nitrification and denitrification reactions results in a net savings in alkalinity requirements. In recognition of these economic advantages, this technology has been applied at full-scale to wastewaters generated by the organic chemical industry (Bridle et al., 1979), gas plants (Graham, 1980) and by-product coke plants (Roper et al., 1982).

A major component of the WTC program addressed the removal of nitrogen and trace organic contaminants from coke plant wastewaters using PDN technology. This, in part, was stimulated by concern over the level of contaminants being discharged to the Great Lakes. Apart from human health considerations, the levels of ammonia, cyanide, thiocyanate, phenolics and trace organics such as polyaromatic hydrocarbons and heterocyclic nitrogenous compounds were thought to be deleterious to the aquatic ecology of the receiving waters. Current work is examining the feasibility of applying PDN for the simultaneous removal of nitrogen and trace organic contaminants from coal liquefaction process condensates.

Several workers (Downing et al., 1964; Hockenbury and Grady, 1977; Wood et al., 1981) have shown that nitrifying organisms are inhibited by a wide range of organic compounds. It is this sensitivity to inhibitory compounds that is exploited in applying biological nitrogen control technology to the removal of trace contaminants. This approach was conceived as a result of the considerable problems that were experienced in the measurement of trace organic contaminants in industrial wastewaters, whose complex organic matrices interfered with analytical protocols. Low and highly variable recoveries resulted; the analytical procedures were long, tedious and required expensive equipment. The use of surrogate parameters such as COD and FOC was considered for monitoring the removal of trace contaminants. This method, however, has not proven to be successful (Hannah and Rossman, 1982). Thus it is postulated that an approach which makes use of the sensitivity of the nitrifiers to inhibitory trace contaminants would eliminate or reduce the need for trace organic contaminant measurement to a more reasonable and less expensive monitoring level. Although it is recognized that nitrification is the key element in this approach, PDN is regarded as the most cost effective biological nitrogen removal technology and is, therefore, applied in this context.

EXPERIMENTAL PROGRAM

The trace organic contaminant data presented for coke plant wastewater treatment are drawn from two phases of work. In the first phase, PDN was utilized in a single-sludge suspended growth mode. Three bench-scale activated sludge systems were set up in the flow configuration illustrated in Fig. 1 and operated over a range of hydraulic retention times (HRTs) and SRTs (Table 1). Low levels of powdered activated carbon (PAC) were added. Details of operating and analytical procedures have been reported elsewhere (Bridle et al., 1980, 1981). Complete nitrification and denitrification were achieved at total system HRTs of 2.5-3.0 days. In the second phase of work, PDN was utilized in a two stage separate-sludge fixed-film reactor system. The flow schematic for the pilot-scale fluidized bed system is illustrated in Fig. 2. Table 1 presents a summary of the operating conditions evaluated. Details of operating and analytical procedures have been reported elsewhere (Nutt et al., 1981, 1983a). Effluent quality was similar to that achieved with the suspended growth system

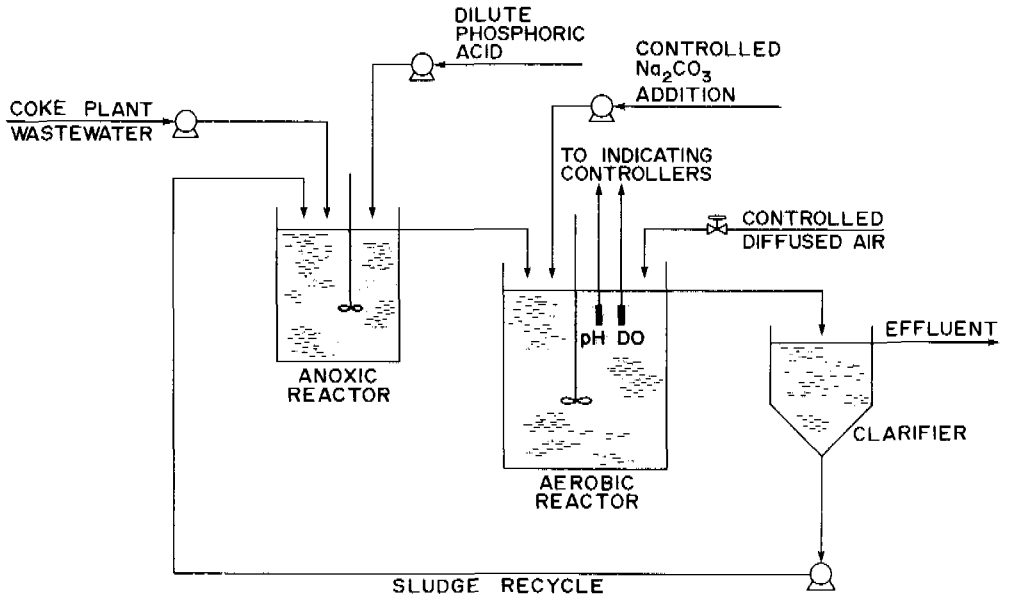

Fig. 1. Two-stage suspended growth process flowsheet

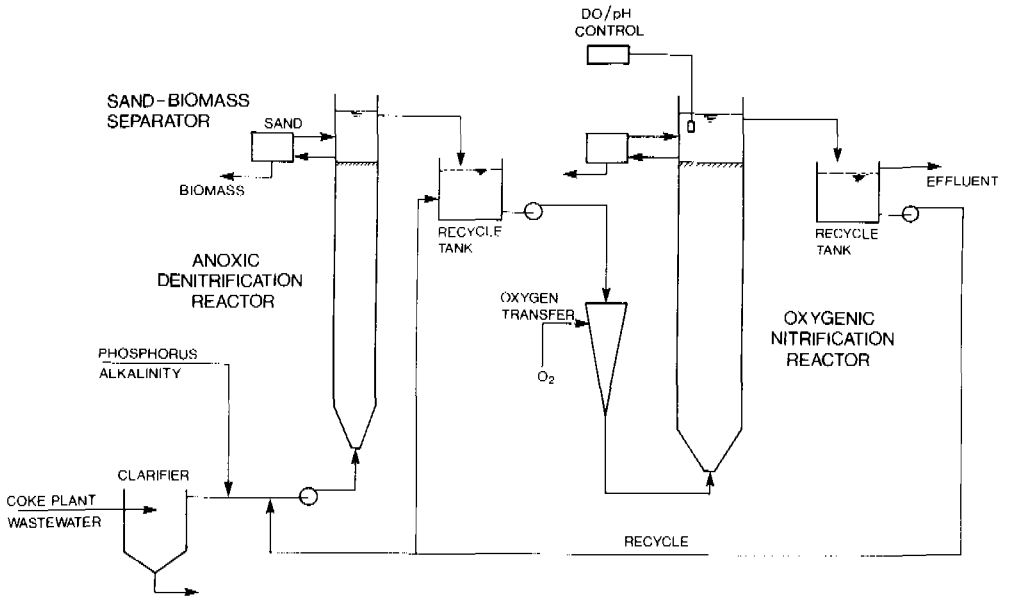

Fig. 2. Two-stage biological fluidized bed process flowsheet

TABLE 1 Summary of Operating Conditions

Reactor Type	Wastewater Feed Type	Reactor Operating Conditions			
		HRT(day)		SRT(day)	
		DN	N	DN	N
Suspended Growth	Coke Plant	0.5 -1.0	1.1 -3.0	10-15	20-45
Fluid Bed	Coke Plant	0.08-0.41	0.58-1.46	5.6-320	52-140
Fluid Bed	Coke Plant & BF Blowdown[2]	0.01-0.11	0.14-0.73	13-47	72-650
Fluid Bed	Coal Liquefaction Process Condensate	0.63	4.13	135[1]	

[1]Total system SRT.
[2]BF - Blast furnace.

but at the significantly reduced HRT of 16 h and without PAC addition. Subsequently, the coke plant wastewater was diluted with two to three parts of blast furnace blowdown water and the HRT was further reduced to 4.5 h while maintaining the same effluent quality (Melcer et al., 1982; Nutt et al., 1983b). Table 2 summarizes pertinent characteristics of the three wastewater feeds in terms of conventional contaminants.

TABLE 2 Raw Wastewater Characterization

Parameter[1]	Coke Plant Wastewater	Coke Plant Wastewater & BF Blowdown	Coal Liquefaction Process Condensate[2]
	Suspended Growth System	Coupled Fluidized Bed System	
FOC[3]	680	776	215	1415
Phenolics	300	483	119	818
TKN	180	181	111	143
NH_3N	88	80	66	113
SCN	240	361	98	75
TCN	8.0	8.2	1.8	0.1

[1]All parameters expressed as median concentrations in mg/l.
[2]Diluted to a 20 per cent concentration with tap water.
[3]Filtered organic carbon.

The coupled fluidized bed PDN technology is now being evaluated for the treatment of coal liquefaction process condensates. Samples of coal liquefaction process condensate were obtained from the H-Coal pilot facility in Catlettsburg, Kentucky. Illinois No. 6 Coal was the feedstock at the H-Coal pilot plant when these samples were collected. Limited pretreatment was carried out at Catlettsburg. This consisted of steam stripping for acid gas removal and partial extraction of phenol with light oil. The resulting wastewater was diluted to a 20 per cent feed strength with tap water. Fluidized bed operating conditions are defined in Table 1. Conventional parameter characterization data are presented in Table 2.

The majority of trace contaminants occurring in coke plant wastewaters and coal liquefaction process condensates are base/neutral extractable compounds resulting from the destructive distillation of coal. The prominent types are polyaromatic hydrocarbons, phthalate esters and heterocyclic nitrogenous compounds. GC/MS protocols were used to measure trace organic contaminants. Detailed concentration and recovery data are reported elsewhere (Melcer and Nutt, 1983). The data presented in this paper are not corrected for recovery data. For base/neutral contaminants, recoveries were generally in the range 60 to 90 per cent. The phenolics, also, were a prominent group of trace contaminants remaining in the treated effluents. They are acid extractable compounds and, when measured by GC/MS protocols, inconsistent and low recoveries were achieved. Hence data for total phenolics, as measured by the 4-aminoantipyrene (4-AAP) method, are presented in lieu of those measured by GC/MS protocols. Interpretation of trace organic contaminant data is, therefore, focussed on the base/neutral compounds.

RESULTS

Raw Wastewater Characteristics

Table 2 presents a summary of conventional parameters for the three wastewater feeds, coke plant wastewater, the coke plant wastewater/blast furnace blowdown water mixture and coal liquefaction process condensate. Detailed characterization of these wastewaters have been previously reported (Bridle et al., 1980; Nutt et al., 1981; Melcer and Nutt, 1983). Concentration data for trace organic contaminants found consistently in the raw wastewaters are presented in Table 3. The lower levels of contaminants in the mixed feed reflects the dilution of the coke plant wastewater by the blast furnace recycle blowdown. No data for the coal liquefaction process condensate were available.

Of the acid extractable contaminants, phenol and 2,4-dimethyl phenol were found in most samples but at levels significantly lower than those determined by the traditional 4-AAP method for total phenolics. Similar differences have been reported by Wilson et al. (1982). Total phenolics data only are presented (Table 2) rather than data for individual phenolics as determined by GC/MS protocols.

The levels of conventional parameters and base/neutral organic contaminants were consistent with other observations (U.S. EPA, 1980; Wilson et al., 1982; Wong Chong and Hall, 1981). Shown in Table 3 are those base/neutral contaminants with mean concentrations for all samples greater than the detection limit (0.01 mg/l). Relatively high concentrations of some heterocyclic nitrogenous compounds (carbazole, indole, isoquinoline and quinoline) were found.

Removal of Contaminants

The removal of conventional contaminants is summarized in Table 4. In general, high quality effluents were produced. Solids retention time control ensured almost complete nitrification and minimized the substrate inhibition effect of phenolics, thiocyanate and cyanide previously reported for these types of wastewaters (Neufeld and Valiknac, 1979; Neufeld et al., 1980). In almost all cases, ammonia oxidation efficiencies were 99 per cent or greater. Lower conversions were measured for the more complex coal liquefaction process condensate feed. Treated effluent thiocyanate concentrations were generally in the range 1 to 2 mg/l. The relatively high levels of effluent total cyanide reflected the significant fraction of refractory complexed cyanide that is present in coke plant wastewater. Periodic analyses indicated that the cyanide

TABLE 3 Base/Neutral Extractable Organic Contaminants in Raw Wastewaters

Contaminant	Mean Concentration (mg/l ∓ std. dev.)		
	Coke Plant Wastewater		Coke Plant Wastewater & BF Blowdown
	Suspended Growth System[1]	Coupled Fluidized Bed System[2]	
Polyaromatic hydrocarbons			
Anthracene and/or Phenanthrene	T[3]	0.08 ∓ 0.09	ND[4]
Chrysene	0.01[5]	ND	ND
Fluoranthene	T	0.02 ∓ 0.02	ND
Fluorene	T	0.01 ∓ 0.01	ND
Indenopyrene	T	ND	ND
Naphthalene	2.28[5]	0.04 ∓ 0.03	T
Pyrene	T	0.02 ∓ 0.02	ND
1,3 and/or 1,4 dichlorobenzene	ND	0.06 ∓ 0.10	0.03 ∓ 0.03
Di-n-butyl phthalate	ND	0.04 ∓ 0.07	1.20 ∓ 1.40
Di-ethyl phthalate	0.80[5]	T	ND
Bis(2-EH)phthalate	0.07[5]	ND	ND
Heterogenous nitrogenous compounds			
Benzonitrile	ND	ND	0.01 ∓ 0.01
Isoquinoline	++	2.33 ∓ 3.27	1.02 ∓ 1.33
2-methyl naphthalene	ND	0.04 ∓ 0.05	ND
Indole	++	6.34 ∓ 10.25	6.65 ∓ 4.26
4-methyl quinoline	ND	0.11 ∓ 0.11	0.11 ∓ 0.13
7A-methyl quinoline	ND	0.54 ∓ 0.82	0.11 ∓ 0.08
7B-methyl quinoline	ND	0.58 ∓ 1.06	ND
2,6- and/or 2,7-dimethyl quinoline	ND	0.04 ∓ 0.03	ND
2,4-dimethyl quinoline	ND	0.02 ∓ 0.03	ND
3,4- and/or 5,6-benzoquinoline	ND	0.09 ∓ 0.07	ND
Carbazole	++	0.98 ∓ 0.92	0.52 ∓ 0.40
2- and/or 8-methyl quinoline	ND	0.52 ∓ 0.82	0.15 ∓ 0.18
Quinoline	++	7.22 ∓ 5.89	5.56 ∓ 4.33
7,8-benzoquinoline	ND	0.03 ∓ 0.04	0.02 ∓ 0.02
Aniline	ND	0.11 ∓ 0.24	0.45 ∓ 0.52
Dibenzofuran	ND	0.03 ∓ 0.04	ND

[1]These samples were screened for the heterocyclic nitrogenous compounds listed. ++ indicates that significant quantities were observed but were not assigned values due to a lack of standards at the time of analysis.
[2]For coke plant wastewater alone, the mean is based on 4 samples. For the mixed feed, the mean is based on 7 samples.
[3]T - trace amounts (less than 0.01 mg/l) detected in more than one sample.
[4]ND - not detected in any sample.
[5]Where no std. dev. is given, data are for mean of 2 determinations.

TABLE 4 Removal of Conventional Contaminants

Parameter[1]	Coke Plant Wastewater		Coke Plant Wastewater & BF Blowdown	Coal Liquefaction Process Condensate
	Suspended Growth System	Coupled Fluidized Bed System		
FOC	38.0 /91.9-96.0	52.6 / 90.6-95.1	23.0 / 85.2-90.8	117/91.7
Phenolics	0.06/99.7-99.9	0.14/>99.9	0.09/>99.9	2.1/99.7
NH_3N	0.9 /98.7-99.8	1.2 / 98.8-99.9	1.4 / 95.9-99.2	13.3/88.2
SCN	1.1 /99.4-99.6	2.2 / 99.2-99.6	0.7 / 99.2-99.7	---
TCN	5.7 /18.0-52.0	5.1 / 12.5-57.8	0.7 / 10.1-72.9	---
NO_TN[2]	19.8 / ---	2.8 / ---	2.1 / ---	17.5/---

[1]Parameters are expressed as median effluent data in mg/l / range of removals in percent.
[2]NO_TN - total oxidized nitrogen.

amenable to chlorination in the treated effluent had been reduced to the level of detection. This level of effluent quality has been similarly reported for the full-scale treatment of coke and gas plant wastewater (Roper et al., 1982). From these data, it may be concluded that despite the presence of the potentially inhibitory contaminants defined in Tables 2 and 3, nitrification could be successfully achieved in these complex wastewaters. Complete denitrification was consistently achieved. The effluent oxidized nitrogen concentration was controlled by the rate of recycle from the nitrification reactor to the denitrification reactor.

Examination of the trace organic contaminant data in Table 5 shows that very few base/neutral contaminants were present in the treated effluents from the PDN systems. Shown in Table 5 are those base/neutral contaminants with mean concentrations for all samples greater than the detection limit (0.01 mg/l). Di-n-butyl phthalate was the only trace contaminant consistently measured in all effluents. Three other phthalate esters were found in at least two effluents. Similar observations were made in a U.S. EPA survey (1980). Phthalate esters are common plasticizers and their consistent presence may indicate contamination of samples. Although care was taken during sample collection to prevent contact with plastic materials, many components of both the bench-scale and pilot-scale systems were made of plastic substances.

Other than the phthalate esters, the only other base/neutral extractable contaminant consistently detected at greater than trace concentrations was 7A-methyl quinoline although it was present only in the treated coke plant effluent from the fluid bed system. This performance was achieved despite the presence, in the influent, of some heterogenous nitrogenous contaminants at concentrations in excess of 1 mg/l (Table 3).

As was the case in untreated wastewaters, the concentration of phenolic contaminants as measured by GC/MS procedures was lower than that determined by wet chemical methods. The maximum phenol concentration measured in treated effluent by GC/MS techniques was 0.01 mg/l compared to concentrations of total phenolic compounds in the range 0.05 to 0.20 mg/l for coke plant effluents and up to 2.1 mg/l for coal liquefaction effluent as determined by the 4-AAP method (Table 4).

TABLE 5 Base/Neutral Organic Contaminants in Treated Effluents

Contaminant	Mean Concentration (mg/l ∓ std. dev.)			
	Coke Plant Wastewater		Coke Plant Wastewater & BF Blowdown	Coal Liquefaction Process Condensate
	Suspended Growth System[1]	Coupled Fluidized Bed System[2]		
Polyaromatic hydrocarbons				
Acenaphthylene	ND[3]	T[4]	ND	ND
Anthracene and/or Phenanthrene	T	T	ND	ND
Fluoranthene	T	T	ND	ND
Pyrene	T	T	ND	ND
1,3- and/or 1,4-dichlorobenzene	ND	ND	T	T
Di-n-butyl phthalate	0.01	0.02∓0.03	0.12∓0.22	0.83
Di-ethyl phthalate	0.03	T	ND	ND
Bis-(2-ethyl hexyl) phthalate	0.01	T	ND	0.19
Butyl benzene phthalate	0.03	ND	ND	0.26
Heterogenous nitrogenous compounds				
Isoquinoline	ND	T	ND	-[5]
3,5-dimethyl pyridine	ND	T	ND	-[5]
Indole	ND	T	ND	-[5]
2- and/or 8-methyl quinoline	ND	T	ND	-[5]
7A-methyl quinoline	ND	0.01∓0.01	ND	-[5]
2,6- and/or 2,7-dimethyl quinoline	ND	T	ND	-[5]
2,4-dimethyl quinoline	ND	T	ND	-[5]
3,4- and/or 5,6-benzoquinoline	ND	T	ND	-[5]
Carbazole	ND	T	ND	-[5]
Quinoline	ND	T	ND	-[5]
7,8-benzoquinoline	ND	T	ND	-[5]

[1]Mean based on 8 samples.
[2]For coke plant wastewater alone, the mean is based on 8 samples. For the mixed feed, the mean is based on 7 samples. For the coal liquefaction process condensate, data are for one sample only.
[3]ND - not detected in any sample.
[4]T - trace amount (less than 0.01 mg/l) detected in more than one sample.
[5]Sample was not analyzed for HNCs.

From this work, it would appear that the presence of nitrifiers in the PDN treatment scheme can be associated with very high effluent quality as defined by trace organic contaminant data. Limited fish toxicity work was initiated to demonstrate further the high quality of treated effluent from PDN systems. Treated effluent from the suspended growth PDN system was subjected to 96 h static bioassay tests using juvenile rainbow trout (Salmo gairdneri) and was found to be non-lethal (Bridle et al., 1980). Further bioassays are in progress on treated effluent from the fluidized bed system.

This work has developed data which demonstrate that the use of PDN technology can effect a simultaneous removal of trace organic contaminants. It emphasizes the potential of using nitrifiers as a surrogate measure of trace contaminant control during treatment of complex industrial wastewaters.

CONCLUSIONS

1. The predenitrification nitrification technology achieved a high degree of conventional and trace contaminant removal from coke plant wastewater and coal liquefaction condensate. Of the base/neutral extractable organic contaminants examined, only di-n-butyl phthalate was consistently found at greater than trace levels in effluent samples from suspended growth and fluidized bed systems. Three more phthalate esters and 7A-methyl quinoline were the only other base/neutral contaminants observed at more than trace levels in effluent samples.

2. The ability to achieve a high degree of trace contaminant removal during nitrification emphasizes the potential of using nitrifiers as a surrogate measure of trace contaminant control during treatment of complex industrial wastewaters.

ACKNOWLEDGEMENTS

This work was co-sponsored by Dofasco Inc., Hamilton, Ontario and Environment Canada. The extensive support of the Organic Analytical Group of the Wastewater Technology Centre is gratefully acknowledged. The technical assistance provided by Dorr-Oliver Inc. is also gratefully acknowledged.

REFERENCES

Bridle, T.R., Climenhage, D.C. and Stelzig, A. (1979). Operation of a full-scale nitrification-denitrification industrial waste treatment plant. J. Wat. Poll. Contr. Fed., 51(1), 127-139.

Bridle, T.R., Bedford W.K. and Jank B.E. (1980). Biological treatment of coke plant wastewaters for control of nitrogen and trace organics. Presented at 53rd Annual WPCF Conf., Las Vegas, Nev.

Bridle, T.R., Bedford W.K. and Jank B.E. (1981). Biological nitrogen control of coke plant wastewaters. Wat. Sci. & Tech. 13(1), 667-680.

Downing, A.L. and co-workers. (1964). Effect of inhibitors on nitrification in the activated sludge process. Jour. Inst. Sew. Purif., 63, 537.

Graham, N.A. (1980). The Waterton gas plant activated sludge installation. Presented at the 30th Can. Chem. Eng. Conf., Edmonton, Alta.

Hannah, S.A. and Rossman L. (1982). Monitoring and analysis of hazardous organics in municipal wastewater -- a study of 25 treatment plants. EPA-600/D-82-376. NTIS, Springfield, Va.

Hockenbury, M.R. and Grady, C.P.L. (1977). Inhibition of nitrification -- effects of selected organic compounds. J. Wat. Poll. Contr. Fed., 49(5), 768-777.

Melcer, H. and co-workers (1982). Combined treatment of coke plant wastewater and blast furnace blowdown water in a coupled fluidized bed system. Accepted for publication in J. Wat. Poll. Contr. Fed.

Melcer, H. and Nutt S.G. (1983). Removal of trace organic contaminants from coke plant wastewater and blast furnace blowdown in a biological fluidized bed system. Presented at the U.S. EPA on Iron and Steel Poll. Abatement Tech., Chicago, Ill.

Neufeld, R.D. and Valiknac, T. (1979). Inhibition of phenol biodegradation by thiocyanate. J. Wat. Poll. Contr. Fed., 51(9), 2283-2291.

Neufeld, R.D., Hill, A.J. and Adekoya, D.O. (1980). Phenol and free ammonia inhibition to Nitrosomonas activity. Water Res., 14, 1695-1703.

Nutt, S.G., Melcer H. and Pries J.H. (1981). Two-stage biological fluidized bed treatment of coke plant wastewater for nitrogen control. Presented at 54th Annual WPCF Conf., Detroit, Mich.

Nutt, S.G. and co-workers (1983a). Treatment of coke plant wastewater in the coupled pre-denitrification nitrification fluidized bed process. Proc. 37th Ind. Waste Conf., Purdue Univ., W. Lafayette, Ind., 527-536.

Nutt, S.G. and co-workers (1983b). Treatment of coke plant wastewater with or without blast furnace blowdown water in a two-stage biological fluidized bed system. Proc. Symp. on Iron & Steel Poll. Abatement Tech., EPA-600/9-83-016, U.S. EPA, Cincinnati, Ohio, 300-316.

Roper, R.E., James J.A. and Long G. (1982). Biological treatment at Citizens Gas and Coke Utility. Presented at Indiana Wat. Poll. Contr. Assoc. Conf., Indianapolis, Ind.

Sutton, P.M. and co-workers (1979). Single Sludge Nitrogen Removal Systems. COA Report No. 88, Environment Canada, Ottawa, Ont.

U.S. Environmental Protection Agency. (1980). Development Document for Proposed Effluent Limitations Guidelines, New Source Performance Standards and Pretreatment Standards for the Iron and Steel Manufacturing Point Source Category, Vol. II, EPA 440/1-80/024b, U.S. EPA, Cincinnati, Ohio.

Wilson, R.W. and co-workers (1981). Design and cost comparison of biological nitrogen removal processes. J. Wat. Poll. Contr. Fed., 53(8), 1294-1302.

Wilson, L.W., Buchianeri B.A. and Tracy K.D. (1982). Assessment of the biological treatment of coke plant wastewater with addition of PAC. Proc. Symp. on Iron & Steel Poll. Abatement Tech., EPA-600/9-81-021, U.S. EPA, Cincinnati, Ohio, 424-445.

Wood, L.B., Hurley, B.J.E. and Matthews, P.J. (1981). Some observations on the biochemistry and inhibition of nitrification. Water Res., 15(5), 543-551.

Wong Chong, G. and Hall J.F. (1981). Single-stage nitrification of coke plant wastewater. Proc. Symp. on Iron and Steel Poll. Abatement Tech., EPA-600/9-81-017, U.S. EPA, Cincinnati, Ohio, 395-455.

Wat. Sci. Tech. Vol.17, Amsterdam, pp.409-419.
Printed in Great Britain.

0273-1223/85 $0.00 + .50

ELEVATED NITRITE OCCURRENCE IN BIOLOGICAL WASTEWATER TREATMENT SYSTEMS

J. E. Alleman

Sch. Civil Engrg., Purdue University West Lafayette, Indiana 47907, U.S.A.

ABSTRACT

The initial conversion of ammonium to nitrite by Nitrosomonas has traditionally been regarded as the rate-limiting step for nitrification metabolism. This perspective implicitly assumes that subsequent oxidation of nitrite by Nitrobacter occurs more rapidly, and that NO_2^- concentrations are consequently maintained at low, sub-mg/L values. However, numerous bench- and full-scale nitrification systems have reportedly encountered elevated nitrite concentrations. Several concerns are generated by this circumstance, including: a) an increased chlorine demand, b) an increased effluent nitrogenous oxygen demand, c) potential nitrite toxicity, and d) possible nitrosamine formation. This paper consequently provides an overview of seven conditions which could lead to elevated nitrite occurrence in biological nitrification systems.

KEYWORDS

Nitrite; nitrification; Nitrosomonas, Nitrobacter; biological wastewater treatment.

INTRODUCTION

Although nitrite (NO_2^-) plays a critical intermediary role in nitrification, it is generally regarded as a nominal (i.e. sub-part-per-million) constituent of nitrified wastewater effluents (Randall and Buth, 1983). This circumstance stems from the corresponding metastable character of the nitrite species, such that nitrate (NO_3^-) represents the traditionally expected product of nitrifying systems.

In the context of sequential Nitrosomonas - Nitrobacter activity, as depicted by Figure 1, the initial conversion of ammonium to nitrite by Nitrosomonas has consequently been viewed as the rate limiting step for complete conversion to nitrate (Benefield and Randall, 1980). Based on this assumption of low-level nitrite presence, there is also a growing trend toward the use of a combined oxidized nitrogen test (i.e. cadmium reduction) in lieu of specific NO_2^- and NO_3^- analyses (Randall and Buth, 1983). Both attitudes reflect a disregard for the potential occurrence of nitrite.

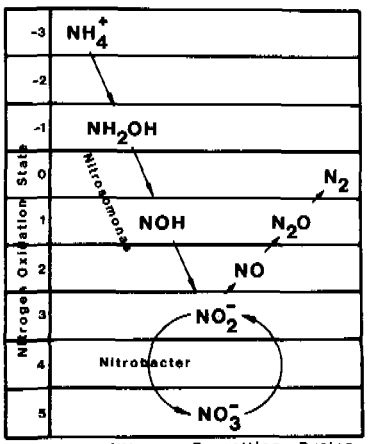

Figure 1 Nitrogen Transitions During Nitrification-Denitrification

Despite this expectation of low-level nitrite presence, though, sizable nitrite concentrations have been observed in numerous nitrification studies and facilities (Warington, 1891; Fowler et al., 1912; Symons and McKinney, 1958; Downing et al., 1964; Knowles et al., 1965; Tomlinson et al., 1966; Prakasam et al., 1972; Focht and Chang, 1975; Voets et al., 1975; Anthonisen et al., 1976; Smith et al., 1978; Verstraete et al., 1977; Alleman, 1978, Colt, 1979; Beccari et al., 1979; Fenlon and Mills, 1980; Hill and Neufeld, 1980; Quinlan, 1980; Sauter and Alleman, 1981; Woods, 1981; Chiesa, 1982; Jones and Paskins, 1982; Tanaka and Dunn, 1982; Alleman, 1983a; Roper et al., 1983; Senanayake, 1983; and Silverstein and Schroeder, 1983). In most instances, these elevated nitrite concentrations were an unexpected consequence of the given environmental conditions. The literature also covers a number of studies in which enhanced nitrite formation was actually the desired goal instead of nitrate production (Smith et al., 1978; Colt, 1979; Prakasam et al., 1978; Alleman, 1983a; and Senanayake, 1983). Whether by intent or circumstance, however, the fact remains that significant nitrite levels can arise in nitrified effluents.

Recognition of this potential conveys several environmental concerns. First, there is the fact that nitrite itself may impose toxic effects on microbial metabolism (Bollag and Henninger, 1978). Secondly, incomplete nitrification yields only a partial reduction of the nitrogenous oxygen demand on a receiving water body. The chlorine demand for disinfection of this effluent would also increase, particularly since nitrite selectively reacts with free chlorine (White, 1981). Finally, the relative reactivity of a nitrite product would raise concerns about nitrosamine formation (Voets et al., 1975; and Ralt and Tannenbaum, 1981).

On the other hand, several investigators have suggested that nitrite may actually be the preferred nitrification product (in comparison to nitrate) if subsequent denitrification is to be achieved (Focht and Chang, 1975; Smith et al., 1977; Colt, 1979, Prakasam et al., 1978; Sauter and Alleman, 1981; Alleman, 1983a; and Senanayake, 1983). In this regard, a pivotal nitrite intermediate between these oxidative and reductive reactions could essentially short-circuit or streamline the involved pathway (Sauter and Alleman, 1981). This would be advantageous in terms of reducing the successive electron acceptor (i.e. O_2) and donor (i.e. organic carbon) demands through nitrification-denitrification metabolism.

Nitrite should, therefore, not be disregarded as a nominally important nitrogen species. Under certain conditions it can represent the dominant effluent nitrogen species, and at concentrations which may warrant close attention.

This article is intended to outline the conditions under which an elevated nitrite concentration might be realized in a nitrification system. These conditions may be condensed to the following listing:

1. Reduced Temperatures,
2. Limiting O_2 or CO_2 Presence,
3. Elevated pH,
4. Free Ammonia Presence,
5. Elevated Solids Wastage,
6. Acute Process Loadings, and
7. Cryptic Nitrate Reduction.

Laboratory results of bench-scale nitrification studies will also be presented to demonstrate that a nitrite or nitrate product can be regulated by manipulating certain of these conditions.

NITRIFIER CHARACTERISTICS

The circumstance of partial/incomplete nitrification depends on either a stimulation of Nitrosomonas and/or an inhibition of Nitrobacter. In either case, the rates for nitrite production and consumption would become unbalanced with a resultant accumulation of the partially oxidized intermediate.

An assessment of the reasons why this disruption occurs requires an understanding of the involved bacteria. Summaries of literature documentation on metabolic characteristics for both nitrifying bacteria are provided by Table 1.

TABLE 1

Nitrifier Genus	μ_m (hrs^{-1})	q_m (hrs^{-1})	Y (mg/mg)	K (mg/L)	b (hrs^{-1})	Optimum pH
Nitrosomonas	0.04-0.08	0.3-1.5	0.04-0.05	0.6-3.6	0.002	7.9-8.2
Nitrobacter	0.02-0.06	0.3-2.0	0.02-0.04	0.3-1.7	0.002	7.2-7.6

References: Sharma and Ahlert, 1977; Alleman, 1983a
Abbreviations: μ_m-max.sp.grwth rate; q_m -max.sp.sub.utiliz.rate; Y-theo. cell yield; K -satur.coeff.; b-decay coeff.

These autotrophs derive limited energy from their substrates and have correspondingly low cell yields and specific growth rates. Each of these attributes may possibly be considered advantageous since sludge production is minimized. However, their slow growth rates are also detrimental because of the inherent delay in recovering from population losses. Furthermore, problems related to competition with heterotrophs over essential nutrients may be linked to these reduced growth rates (Stover and Kincannon, 1976).

A comparison of growth characteristics for both nitrifiers indicates that Nitrobacter is the more fragile of the two. This observation contrasts the general perspective that Nitrosomonas represents the weak link in nitrification. However, Nitrosomonas are believed to be capable of outcompeting Nitrobacter under stressful conditions (i.e. limiting oxygen or inorganic carbon , low temperature conditions, etc.) (Jones and Paskins, 1982).

Along similar lines, the saturation coefficient for Nitrosomonas appears to be slightly greater than for Nitrobacter. Hence, a given Nitrosomonas population would likely have a better ability to handle a short-term increase in substrate loading.

The data on optimal pH values shows that Nitrobacter prefers a somewhat less basic environs. This preference appears consistent with its sensitivity to free ammonia which would be aggravated at a higher pH.

A composite profile on the nitrifiers is that of slow-growing autotrophic microorganisms whose subsistence hinges on expedient and thorough substrate oxidation. Both organisms are susceptible to environmental stress, with Nitrobacter apparently being more sensitive than Nitrosomonas.

STRESS CONDITIONS FOR NITROBACTER

1. Reduced Temperatures

Quinlan (1980) studied the behavior of both nitrifier organisms at temperatures ranging from 0^{o} to 45^{o} C. Nitrite production exceeded subsequent oxidation at the low end of this range. Thermal enrichment of cold-weather nitrification reactors was suggested as a means to avoid potential problems with nitrite build-up, particularly for concentrated nitrogen loadings.

Laboratory studies conducted by Randall and Buth (1983) indicated that sizable effluent nitrite concentrations would occur in the range of 10^{o} to 17^{o} C. Related analyses by these investigators of operating data at a full-scale facility revealed a nitrite build-up for aeration basin temperatures below 11^{o} C. Observed nitrite values at this time were beyond 9 mg/L and exceeded the nitrate level for extended periods.

Comparable reports of full-scale nitrite attenuation during cold-weather operation of nitrification systems have been provided by Chiesa (1982) and Woods (1981). As expected, all three of these aberrant nitrification operations reported significant increases in chlorine demand due to reduction of free chlorine by the nitrite species.

2. Limiting O_2 or CO_2 Presence

Payne (1979) and Boon and Laudelot (1962) have both suggested that Nitrobacter activity might be selectively retarded under conditions of low oxygen tension. Laboratory experimentation by Mines (1983) with oxygen-limited nitrification reactors which resulted in a consistent nitrite product appears to support this possibility. Although free ammonia stress (as addressed in a following section)

was mentioned as a possible contributing factor, Mines believed that Nitrobacter was unable to compete for its critical electron acceptor under O_2 limited conditions.

Jones and Paskins (1982) also observed an elevated nitrite formation in nitrification reactors subjected to low carbon dioxide tension. A metabolic shortcoming in Nitrobacter's competition for anabolic carbon was again cited as a probable cause for this nitrite build-up. In addition, these investigators reported that a temporary accumulation of nitrite would occur under conditions of increased oxygen tension.

3. Elevated pH

Batch nitrification studies by Sauter and Alleman (1981) at four separate pH levels (i.e. 6.8, 8.4, 9.2, 10.2) are depicted by Figures 2a→2d. The pH=6.8 system (see Fig. 2a) realized only a nominal

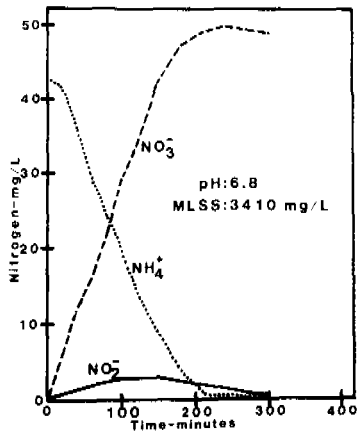

FIG.2a Batch Nitrification at pH:6.8

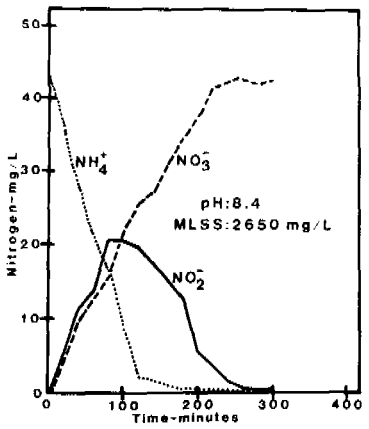

FIG.2b Batch Nitrification at pH:8.4

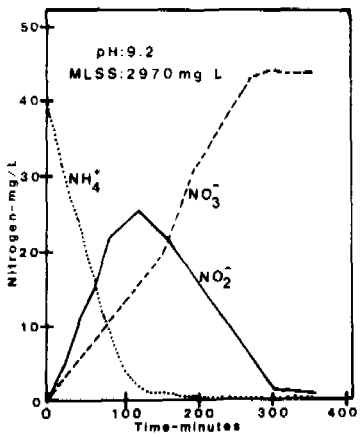

FIG.2c Batch Nitrification at pH:9.2

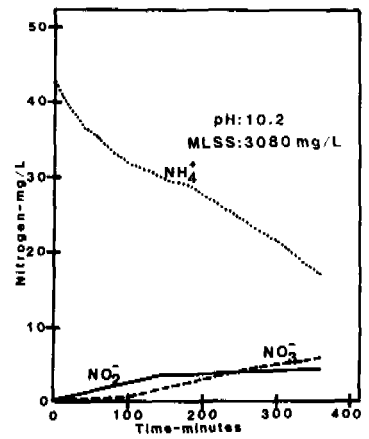

FIG.2d Batch Nitrification at pH:10.2

nitrite involvement since the specific reaction rates for ammonium oxidation and nitrate production were balanced (respectively, 0.113

days^{-1} and 0.117 days^{-1}). However, as pH was increased, the observed ammonium oxidation rates progressively surpassed nitrate production. In turn, intermediate nitrite formation also increased. At pH =10.2, though, the activity of either nitrifier had been curtailed. These results indicate that a nitrite build-up could arise in relation to pH levels beyond the optimum value for Nitrobacter. Indeed, Smith et al. (1978) employed this strategy to selectively obtain a nitrite endpoint during bench-scale investigation of abbreviated nitrification-denitrification ($NH_4^+ \rightarrow NO_2^- \rightarrow N_2$) metabolism.

Furthermore, Fenlon and Mills (1980) similarly observed a nitrite build-up in nitrification units subjected to an elevated pH.

4. Free Ammonia Presence

The factor most commonly linked with elevated nitrite occurrence is free ammonia presence. NH_3 stress on Nitrobacter was initially documented in the late 1800's and has subsequently received extensive investigation due to its ecological/agricultural significance (Warington,1891).

Based upon results published by Anthonisen et al. (1976) and others (Prakasam et al., 1972), it appears that Nitrobacter retardation will initially develop at NH_3 concentrations as low as 0.05 mg/l. This value is approximately two orders of magnitude below the level for an equivalent effect on Nitrosomonas.

The pK value for the ammonium-ammonia couple, 9.25, is only one or two units above the typical, and preferred, pH of a nitrifying reactor. Hence, Nitrobacter inhibition could occur at total ammonium-nitrogen levels of only a few mg/L, with no simultaneous effect on Nitrosomonas.

The impact of free ammonia stress conceptually reinforces the sequential character of complete nitrification. Unless Nitrosomonas provides thorough oxidation of influent ammonium, Nitrobacter will be liable to NH_3 exposure. Stepwise denitrification also exhibits a comparable dependence upon successive conclusions of the involved reductive steps (Payne, 1976).

The circumstance of free ammonia stress on nitrification has been associated with nitrification startups, acute process loading spikes, and batch or plug flow type reactors. Figure 3 provides a related profile of the chronological nitrogen transitions observed during the start-up of a full-scale nitrification facility.

To demonstrate this effect on batch reactor operations, a series of sequencing batch reactor (SBR) experiments were conducted at various aerated REACT lengths. These bench-scale units were supplied with a synthetic waste stream (i.e.prepared from trypticase soy broth) and maintained on a cyclic FILL-REACT-SETTLE-DRAIN routine (Colt, 1979; Alleman, 1983a; Senanayake, 1983).

The results of the 3 hr REACT system shown by Figure 4a solely indicated a nitrite endpoint. Ammonium oxidation continued through most of the period such that free ammonia stress on Nitrobacter would have been sustained throughout REACT aeration. Being unable to procure energy by producing nitrate, it was inevitable that Nitrobacter would not have been retained in the mixed liquor.

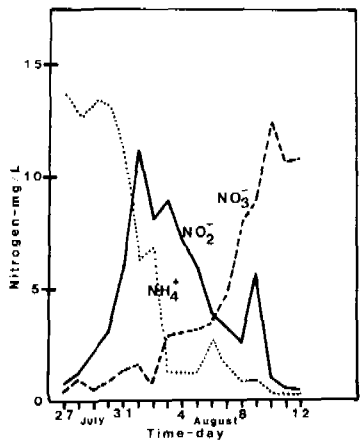

Figure 3. Nitrite Buildup During Full-Scale Nitrification Startup

After switching REACT to a 5 hr duration, the nitrite endpoint evolved to nitrate over a period of several weeks. Figure 4b tracks the typically observed nitrogen transitions once this regime had been stabilized. Significant nitrite formation again developed in apparent correlation to NH_3 presence. Peaking midway through the period, nitrite then dropped to a sub-ppm level at the conclusion of the 5hr REACT aeration period. Nitrate production started at the onset of aeration and increased in rate as the ammonium level declined.

With REACT at 9 hrs, an intermediate nitrite hump was again observed (see Figure 4c). However, the NO_2 spike was lower in concentration and dropped more quickly than had been observed with the 5 hr REACT.

These results demonstrated an ability to manipulate the nitrite and nitrate endpoints in periodic reactors by controlling the duration of REACT aeration and the related pattern of free ammonia stress. Tomlinson et al. (1966) also found that a 50% decrease in batch aeration time resulted in a a major shift to a nitrite endpoint.

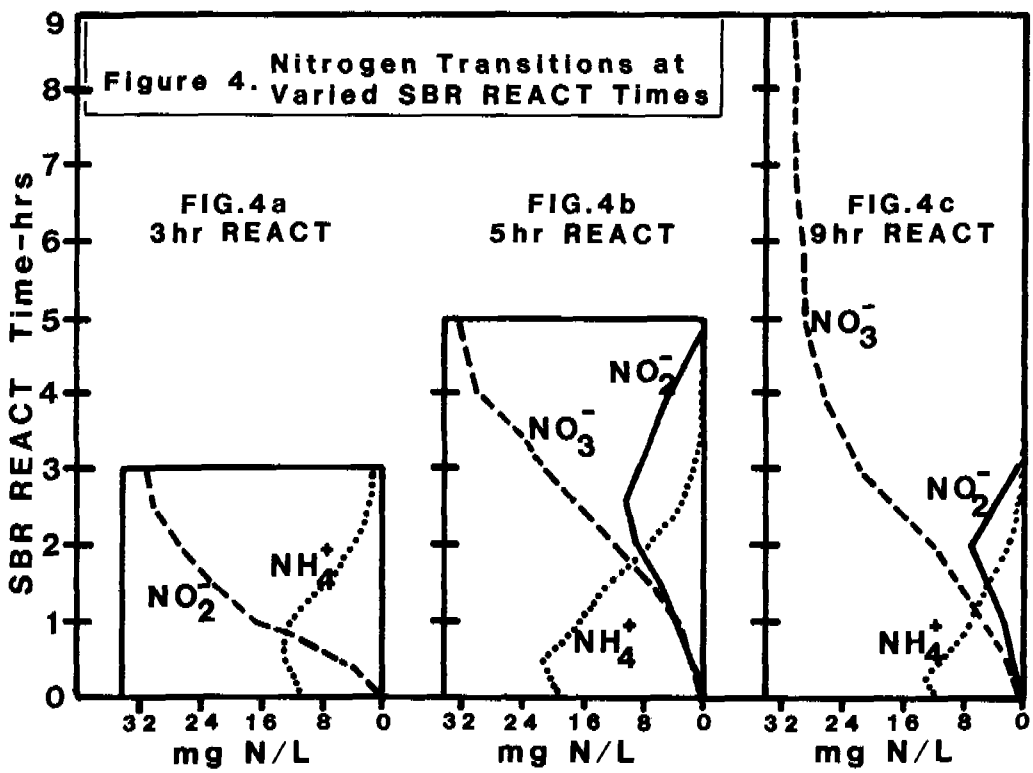

Although both the 5 and 9 hr REACT studies appeared to carry initial periods of free ammonia stress, their production of a nitrate product demonstrated viable Nitrobacter activity. Given sufficient time beyond the initial period of free ammonia stress for complete NO_2 oxidation, Nitrobacter was successfully retained in the system.

5. Excess Solids Wastage

Beccari et al. (1979) determined that effluent nitrogen species could be switched between NH_4^+, NO_2^-, and NO_3^- by controlling the mean cell residence time (MCRT) of continuous flow reactors. Representative plots of these species in relation to MCRT are given by Figure 5.

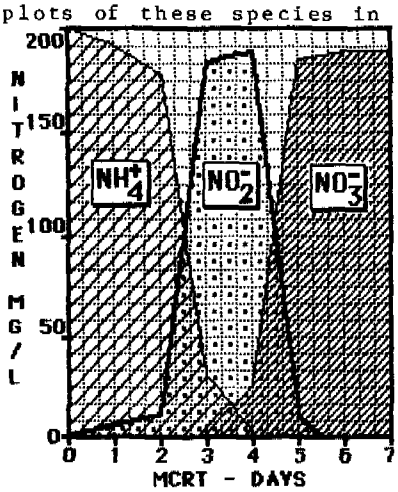

FIGURE 5. Effluent Nitrogen Variations According to MCRT Change

These transitions are figuratively analogous to the classic profiles of downstream nitrogen conversion.

Retention of nitrifiers in a mixed liquor depends upon their respective growth characteristics. Neither is retained much below an MCRT of 2 days and until about 4 days only Nitrosomonas are present. Control of solids wastage within this intermediate MCRT range could consequently result in a predominant nitrite product.

Complete nitrification by a high MCRT system may also be disrupted through excessive, acute solids wastage. Figure 6 depicts a representative nitrogen profile observed at a full-scale nitrification facility (Alleman, 1983b). After an accidental decrease in MLSS from 5000 to 2800 mg/L, both the effluent NH_4^+ and NO_2^- values increased immediately. After this wastage had been stopped, the discharged ammonium level declined steadily. However, effluent nitrite remained elevated for several days. Such behavior also reflects the performance associated with startup of a nitrification system, as was depicted in Figure 3.

6. Acute Process Loadings

Roper et al. (1982) and Prakasam et al. (1972) both documented the effect of process loading on nitrification behavior. Roper et al. (1982) found that a shock ammonium ion input to a continuous-flow reactor system resulted in a sizable increase in effluent nitrite.

Working with elevated process loadings, Prakasam et al. (1972) also found that Nitrobacter activity would be retarded. This latter study clearly recognized the unique circumstance of enhanced nitrite production, referring to the involved pathway as nitritification.

The negative effects of a short-term increase in nitrogen loading may relate to a temporary production of free ammonia stress and to the relative saturation coefficients for the nitrifiers. The K_s values given by Table 1 indicated that both autotrophs have low coefficients and that Nitrobacter has the lower value of the two. A given population of Nitrosomonas and Nitrobacter organisms would, therefore, have only a nominal opportunity to adapt to an acute process loading. Coupled with this limitation, Nitrobacter would also suffer from the

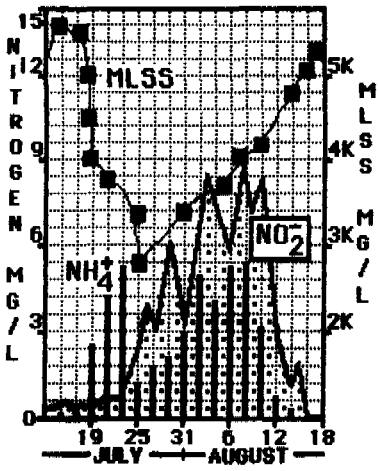

FIGURE 6. Full-Scale Nitrite Buildup After Excess Solids Wastage

related stress of an ammonium-ammonia build-up.

7. Cryptic Nitrate Reduction

Each of the preceding conditions dealt with a circumstance of incomplete oxidation through the nitrification pathway, However, elevated nitrite presence may also be linked with nitrate reduction.

This scenario involves complete conversion of influent ammonium to nitrate (via Nitrosomonas and Nitrobacter, followed by partial NO_3^- reduction back to NO_2^- (see Figure 1. As such, these dual mechanisms for nitrate formation (i.e. NH_4^+ to NO_2^- and NO_3^- to NO_2^-) would exceed the Nitrobacter oxidation capacity. Kirsch and Etzel (1983) identified this type of behavior, and related elevated nitrite presence, in their study of an industrial nitrification facility.

The 'cryptic' attribute for this condition stems from the unexpected incorporation of a nitrate reduction step during nitrification treatment. A number of bacteria, though, appear capable of completing this reaction under truly aerobic conditions (Hirsch et al., 1961; Payne, 1973). Anoxic respiration may also be a contributing factor in relation to interstitial oxygen-deficient biomass zones.

SYNOPSIS

The traditional perspective on nitrite-nitrogen is that it represents a nominally important effluent species. However, several full-scale nitrification facilities have reported operational (i.e. increased chlorine demand) and performance (i.e. increased effluent nitrogenous oxygen demand) difficulties associated with nitrite build-up.

This paper, therefore, provides a comprehensive overview of the conditions which contribute to a formation of elevated nitrite levels in biological wastewater treatment systems. A manipulation scheme was also reported with data obtained from bench-scale sequencing batch reactors whereby a nitrite or nitrate product could be selected.

ACKNOWLEDGEMENT

Support for this research was provided by the U.S. National Science Foundation on Grant No. CME-6006856.

REFERENCES

Alleman, J.E. (1983a). A streamlined approach to biological nitrogen removal in wastewater treatment. U.S. National Science Foundation, Grant No. CME-8006856-Final Report, Washington, D.C., pp.112.

Alleman, J.E. (1983b). Characterization of nitrification performance at AWT facilities. Report to Indianapolis, IN. Dept. Public Works,

December, pp.18.
Alleman, J.E. (1978). Nitrogen removal from wastewater using sequencing batch reactors. Doctoral dissertation, University of Notre Dame, Notre Dame, IN., pp.188.
Anthonisen, A.C., Loehr, R.C., Prakasam, T.B.S., and Srinath, E.G. (1976). Inhibition of nitrification by ammonia and nitrous acid. Jour. Water Pollut. Control Fed., 48, 835-850.
Beccari, M., et al. (1979). A critical analysis of nitrification alternatives. Water Research, 13, 185-195.
Benefield, L.D. and Randall, C.W. (1980). Biological process design for wastewater treatment, Prentice Hall, Inc., Englewood Cliffs, NJ.
Bollag, J.M. and Henninger, N.M. (1978). Effects of nitrite toxicity on soil bacteria under aerobic and anaerobic conditions. Soil Biol. Biochem., 10, 377-381.
Boon, B. and Laudelout, H. (1962). Kinetics of nitrite oxidation by Nitrobacter winogradskyi. Biochem. Jour., 85, 440-448.
Chiesa, S.C. (1982). Personal Communication. Cleveland, OH, September.
Colt, J.S. (1979). Streamlined nitrogen removal from wastewater using batch activated sludge treatment. Unpublished masters thesis, University of Maryland, College Park, MD, pp.102.
Downing, A.L., Painter, H.A. and Knowles, G. (1964). Nitrification in the activated sludge process. Jour. Inst. Sew. Purif., 130-158.
Fenlon, D.R. and Mills, P.J. (1980). On farm aerobic treatment of piggery wastes. The effect of residence time and storage on effluent quality. Water Research, 14, 805-808.
Focht, D.D. and Chang, A.C. (1975). Nitrification and denitrification processes related to wastewater treatment. Advances in Applied Microbiology, 19, 153-186.
Fowler, G.J., Ardern, E. and Lockett, W.T. (1912). The influence of waste liquor from sulfate of ammonia plants on the purification of sewage. Jour. Soc. Chem. Indust., XXXI, 10, 471-477.
Hill, A.J. and Neufeld, R.D. (1980). Influence of un-ionized ammonia and inorganic carbon on biological nitrification. Proc. 34th Purdue Industrial Waste Conf., Ann Arbor Science, Publ., 73-85.
Hirsch, P., Overrein, L. and Alexander, M. (1961). Formation of nitrite and nitrate by actinomycetes and fungi. Jour. Bacter., 82, 442-448.
Jones, G.L. and Paskins, A.R. (1982). Influence of high partial pressure of carbon dioxide and/or oxygen on nitrification. Jour. Chem. Technol. Biotechnol., 32, 213-223.
Kirsch, E.D. and Etzel, J.E. (1983). Personal communication. Purdue University, West Lafayette, IN., November.
Knowles, G., Downing, A.L. and Barrett, M.J. (1965). Determination of kinetic constants for nitrifying bacteria in mixed culture, with the aid of an electronic computer. Jour. Gen. Microbiol., 38, 263-278.
Mines, R.O. (1983). Oxygen transfer studies in the completely mixed activated sludge process. Unpublished doctoral dissertation, Virginia Polytechnic Institute and State University, Blacksburg, VA.
Payne, W.C. (1979). Personal Communication. University of Maryland, College Park, MD, November.
Payne, W.J. (1976). Denitrification. Trends in Biochemical Sciences, October, 220-222.
Payne, W.J. (1973). Reduction of nitrogenous oxides by microorganisms. Bacter. Reviews, 37, 409-452.
Prakasam, T.B.S., Lue-Hing, C. and Loehr, R.C. (1978). Nitrogen control in wastewater treatment systems by microbial nitrification

and denitrification. Microbiology - 1978, 372-379.
Prakasam, T.B.S. and Loehr, R.C. (1972). Microbial nitrification and denitrification in concentrated wastes. Water Research, 6, 859-869.
Quinlan, A. (1980). The thermal sensitivity of nitrification as a function of the concentration of nitrogen substrate. Water Research, 14, 1501-1507.
Ralt, D. and Tannenbaum, S.R. (1981). The role of bacteria in nitrosamine formation.N-Nitroso Compounds. ACS Symposium Series, 157-164.
Randall, C.W. and Buth, D. (1983). Nitrite build-up in activated sludge resulting from temperature and toxicity effects. Jour. Water Pollut. Control Fed., [presently being reviewed].
Roper, R.E., James, J.A. and Long, G. (1982). Biological pretreatment at Citizens Gas & Coke utility. Presented at the Indiana Water Pollut. Control Assn. Conf., Indianapolis, IN, 10 November.
Sauter, L.J. and Alleman, J.E. (1981). A streamlined approach to biological nitrogen removal. Proc. ASCE Specialty Conf. Environ. Engr. New York, NY, 296-306.
Senanayake, S. (1983). Substrate inhibition for streamlined nitrogen removal in the sequencing batch reactor. Unpublished masters thesis, University of Maryland, College Park, MD, pp.104.
Sharma, B. and Ahlert, R.C. (1977). Nitrification and nitrogen removal. Water Research, 11, 897-925.
Silverstein, J. and Schroeder, E.D. (1983). Performance of SBR activated sludge processes with nitrification/denitrification. Jour. Water Pollut. Control Fed., 55, 377-382.
Smith, E.D., Sweazy, R.M., Wells, D.M., Peeples, M.L., Baskett, R.C., and Ramsey, R.H. (1978). Development of an unconventional approach to nitrification-denitrification. Final Report, OWRT No. A-035-Tex, Tech University, Lubbock, TX, 162 pp.
Stover, E.L. and Kincannon, D.F. (1976). Effects of COD:NH_3 ratio on a one stage nitrification activated sludge system. Water & Sewage Works, 31, 120-123.
Symons, J.M. and McKinney, R.E. (1958). The biochemistry of nitrogen in the synthesis of activated sludge. Sewage and Industrial Wastes, 30, 874-890.
Tanaka, H. and Dunn, I.J. (1982). Kinetics of biofilm nitrification. Biotechnol. Bioeng., XXIV, 669-689.
Tomlinson, T.G., Boon, A.G. and Trotman, C.N.A. (1966). Inhibition of nitrification in the activated sludge process of sewage disposal. Jour. Applied Bacterial., 29, 266-291.
Verstraete, W., Vanstaen, H. and Voets, J.P. (1977). Adaptation to nitrification systems treating highly nitrogenous water. Jour. Water Pollut. Control Fed., 49, 1604-1608.
Voets, J.P., Vanstaen, H. and Verstraete, W. (1975). Removal of nitrogen from highly nitrogenous wastewaters. Jour. Water Pollut. Control Fed., 47, 394-398.
Warington, R. (1891). On nitrification. Jour. Chem. Soc., 59, 484-490.
White, G.C. (1981). Problems of disinfecting nitrified effluents. Proc. ASCE Specialty Conf. on Environ. Engrg., New York, NY, 497-511.
Woods, K. (1981). Personal Communication, Western Branch WWTP, MD,

Wat. Sci. Tech. Vol.17, Amsterdam, pp.421-432.
Printed in Great Britain.

0273-1223/85 $0.00 + .50

SINGLE SLUDGE ANOXIC-AEROBIC SYSTEMS FOR BIOLOGICAL TREATMENT OF COKE PLANT WASTEWATERS

M. Beccari, A. C. Di Pinto, R. Passino, R. Ramadori and V. Tandoi

Water Research Institute, CNR, Via Reno 1, 00198 Rome, Italy

ABSTRACT

A study on the biological treatment of coke plant liquid wastes, with high concentration of ammonium nitrogen and phenols, is presented. The anoxic-aerobic single sludge process is used, with the phenols as electron donors in the denitrification process; the inhibiting effect of toxic substances present in the wastewater is prevented by means of dilution. Tests were conducted in a laboratory scale plant to determine the minimum dilution ratio necessary to avoid inhibition and the parameters required for the designing of a full scale plant. Finally the basic design considerations of a wastewater treatment plant for a 1000 t/d coke plant are reported and capital and running costs are evaluated.

KEYWORDS

Coke plant wastewater , biological treatment, single sludge process, nitrification/denitrification, capital and running cost evaluation.

INTRODUCTION AND DEFINITION OF OBJECTIVES

The main problems met within the biological treatment of coke plant liquid wastes are due to the presence of inhibiting substances (Barker and Thompson, 1973; Beccari and others, 1980) and the high content of ammonium nitrogen. Inhibition can be kept under control by means of an appropriate dilution of the wastewater, especially in the case in which completely mixed biological reactors are used. With regard to the high carbonaceous substrate demand for denitrification due to the high ammonium nitrogen content, a preliminary study (Beccari and others, 1983) shows the possibility of using the phenols as electron donors in the single sludge process.

This work sets out to verify the biological treatability of a coke plant discharge using a bench-scale continuous anoxic-aerobic single sludge plant. The main objectives of the study were:

- Evaluation of the lowest possible dilution necessary to prevent inhibitory effects on the nitrifying biomass. (Tests were first conducted with a synthetic wastewater and then with a real coke plant discharge);
- Determination of process main parameters so that a full-scale treatment plant could be designed and related costs estimated.

Downstream of the biological treatment process, polishing by adsorption on activated carbon was foreseen to obtain a residual phenol concentration in compliance with Italian guidelines.

EQUIPMENT AND EXPERIMENTAL

Wastewater Characterization

Table 1 shows the composition of the synthetic solution used during

TABLE 1 Composition of synthetic solution simulating coke plant wastewaters

SUBSTANCE	CONCENTRATION
Phenols (1)	2500 mg/l
Ammonium nitrogen	3000 mg/l
Thiocyanates	500 mg/l (such as CNS^-)
Thiosulphates	100 mg/l (such as $S_2O_3^=$)
Sulphides	100 mg/l (such as $S^=$)
Sulphates	60 mg/l (such as $SO_4^=$)
Chloride	1500 mg/l (such as Cl^-)
Alkalinity	212 meq/l
Aromatic Bases (2)	200 mg/l

(1) - Phenol 2000 mg/l + o-Cresol = 125 mg/l + m-Cresol - 125 mg/l + Catechol = 100 mg/l + methyl-Catechol = 75 mg/l + Resorcinol 50 mg/l + methyl-Resorcinol = 15 mg/l + Benzochinon - 10 mg/l

(2) - Pyridin = 15 mg/l + Aniline = 75 mg/l + Quinoline = 75 mg/l + Carbazol - 20 mg/l + Indol - 15 mg/l

the first test stage. The concentrations of the components were chosen on the basis of mean values to be found in the Italian cokery waters. Data from the literature were used to define the percentage distribution of the aromatic bases (Bark and others, 1972; Bridle and others, 1980) and the compounds contained in the phenol fraction (Ashmore and others, 1967).
From some analyses of the real discharge used during the second testing phase, concentrations of the main substances were seen to be very similar to those assumed in the synthetic wastewaters.
Both synthetic solution and real discharge were diluted with tap water before feeding to the biological plant.

Materials and Methods

The continuous bench-scale plant is shown in Fig. 1. Wasting of sludge and addition of the phosphorus necessary for bacteria synthesis were carried out at pre-established time intervals. During tests with the

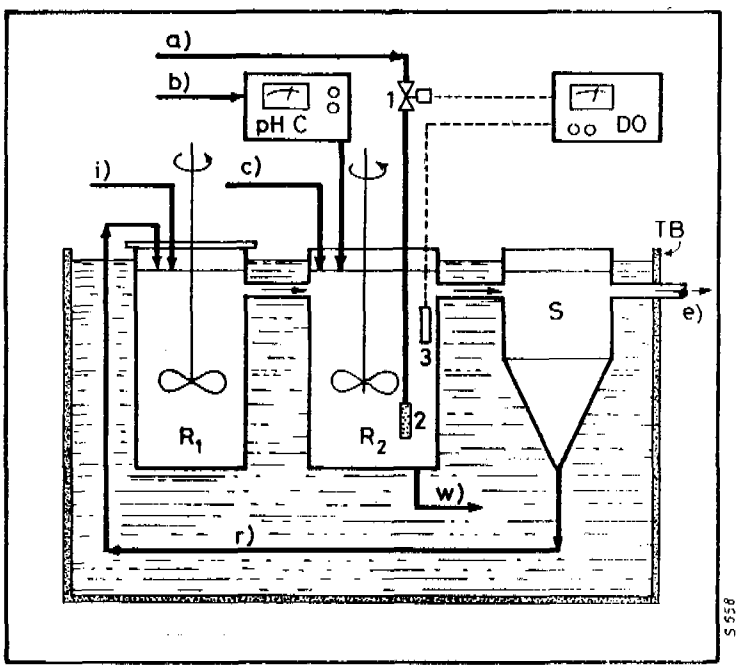

Fig. 1 - Continuous bench-scale anoxic-aerobic unit. R_1 = anoxic reactor (volume 5 l), R_2 = aerobic reactor (volume 7 l), S = settling tank, pHC = pH control, TB = thermostatted bath, DO = dissolved oxygen detector, a = air, b = Na_2CO_3 solution, C = K_2HPO_4 solution, e = effluent, i = influent, r = recycle, W = sludge waste, 1 = electrovalve, 2 = air diffuser, 3 = dissolved oxygen probe.

synthetic wastewater, components were added according to a time sequence that increased solution complexity gradually so as to verify possible component toxicity. Suspended solids, volatile suspended solids and ammonium nitrogen were determined according to National Research Council, 1972, phenol and thiocyanates according to Institution of Gas Engineers, 1967 and nitrates and nitrites according to Strickland and Parson, 1972.
Adsorption tests were conducted using a glass column (i.d.: 2.5 cm; height: 20 cm) filled with 48.7 g of 12 x 40 mesh granulated Filtrasorb 400 activated carbon (Chemviron). Carbon was boiled in distilled deionized water, dried at 150 °C for 3 h and then stored in a dessicator until used. The down-flow tests were operated at a hydraulic loading rate of 5 m/h with a solution of 20 mg/l of C_6H_5OH in distilled water. The phenol concentration used was the same as that found in the effluent from the bench-scale continuous plant when treating the real discharge. Hourly samples were taken at different column heights so that phenol concentration in the liquid phase could be recorded throughout the whole height of the column.

RESULTS

Biological Plant Tests

Three sets of tests were conducted.
The first set was performed keeping both the plant feed flow rate (0.25 l/h) and dilution ratio (1 vol. synthetic solution, see Table 1, + 19 vols. tap water) constant and gradually increasing the complexity of the synthetic coke plant discharge. Table 2 reports the results obtained in stady state conditions when the plant was fed with a solution containing all components foreseen.
In the second set of tests the same flow rate as adopted in the first set was mantained, but the ratio between synthetic wastewater and tap water up to a minimum dilution of 1 vol. of synthetic solution + 3 vols. of tap water was varied. Fig. 2 plots total phenol, ammonium nitrogen and oxidated nitrogen concentration patterns against increases in load (i.e. in synthetic wastewater / tap water ratio).
In the third set of tests the same flow rate was kept but a real discharge instead of the synthetic one was used. During this set of tests, the dilution ratio was varied progressively. Table 3 reports the results obtained in steady state conditions for the maximum real discharge/tap water ratio tested before the inhibiting effects on the nitrifying biomass could reduce nitrification efficiency appreciably.

Carbon Adsorption Column Tests

Fig. 3 gives the breakthrough curves obtained at 4 different bed heights.

TABLE 2 Laboratory scale plant: Results of test at 1:20 dilution ratio (1 volume of synthetic solution + 19 volumes of tap water).

PARAMETER			Feed inlet	Anoxic reactor	Anoxic reactor outlet	Aerobic reactor	Aerobic reactor outlet
Analytical data	Total phenols	mg/l	123		6		1
	CNS^-	"	26		0.6		0.5
	S^{--}	"	5				
	$S_2O_3^{--}$	"	5				
	Aromatic amines	"	10				
	NH_4-N	"	156		29		0
	NO_2-N	"	0		0.2		0
	NO_3-N	"	0		69		99
	Suspended solids	"					12 (*)
Working conditions	Volume	l		5		7	
	Hydraulic retention time	h		20		28	
	Sludge age	d		42		58	
	Biomass concentration	mg MLSS/l		1442		1406	
	pH			7.4		7.5	
	Temperature	°C		26		26	
	Dissolved oxygen	mg/l		0		2.5	
	Biomass nitrogen content (referred to SS)	%			8.7		
	Volatile solids/total solids ratio	%			87		
	Recycle ratio				4.1		
Process parameters	Denitrification rate					0.052 kg NO_3-N/kgVSS·d	
	Nitrification rate (**)					0.104 kg NH_4-N/kgVSS·d	
	Specific phenol consumption ratio					1.7 kg C_6H_5OH/kg NO_3-N	
	Net growth yield coefficient					0.20 kg VSS/kg C_6H_5OH removed	
Process performance	Phenol removal efficiency				99.2 %		
	Nitrification efficiency				100 %		
	Nitrogen removal efficiency				36.2 %		

(*) effluent from settling tank

(**) $k_N = 0.37 \frac{\text{kg } NH_4\text{-N}}{\text{kg VSS·d}}$ from supplementary batch tests

ANALYSIS OF RESULTS

Biological Plant Tests

From the data obtained, it appears that a coke plant discharge can be treated biologically using a single sludge anoxic-aerobic system obtaining removal efficiencies for major pollutants more than satisfactory.

TABLE 3 Laboratory scale plant: results of test at 1:6.3 dilution ratio (1 volume of coke plant wastewater + 5.3 volumes of tap water).

	PARAMETER		Feed inlet	Anoxic reactor	Anoxic reactor outlet	Aerobic reactor	Aerobic reactor outlet
Analytical data	Total phenols	mg/l	400		28		20
	CNS^-	"	40		1		0.5
	NH_4-N	"	600		300		10
	NO_2-N	"	0		3		3
	NO_3-N	"	0		78		374
	Suspended solids	"					30(*)
Working conditions	Volume	l		5		7	
	Hydraulic retention time	h		20		28	
	Sludge age			40		47	
	Biomass concentration	mg MLSS/l		2720		2310	
	pH			7.5		7.5	
	Temperature	°C		25		25	
	Dissolved oxygen			0		2.5	
	Biomass nitrogen content (referred to SS)	%			8.5		
	Volatile solids/total solids ratio	%			86		
	Recycle ratio				1		
Process parameters	Denitrification rate				0.11	kg NO_3-N/kg VSS·d	
	Nitrification rate				0.25	kg NH_4-N/kg VSS·d	
	Specific phenol consumption ratio				1.7	kg C_6H_5OH/kg NO_3-N	
	Net growth yield coefficient				0.13	kg VSS/kg C_6H_5OH removed	
Process performance	Phenol removal efficiency				95.0 %		
	Nitrification efficiency				98.3 %		
	Nitrogen removal efficiency				35.8 %		

(*) effluent from settling tank

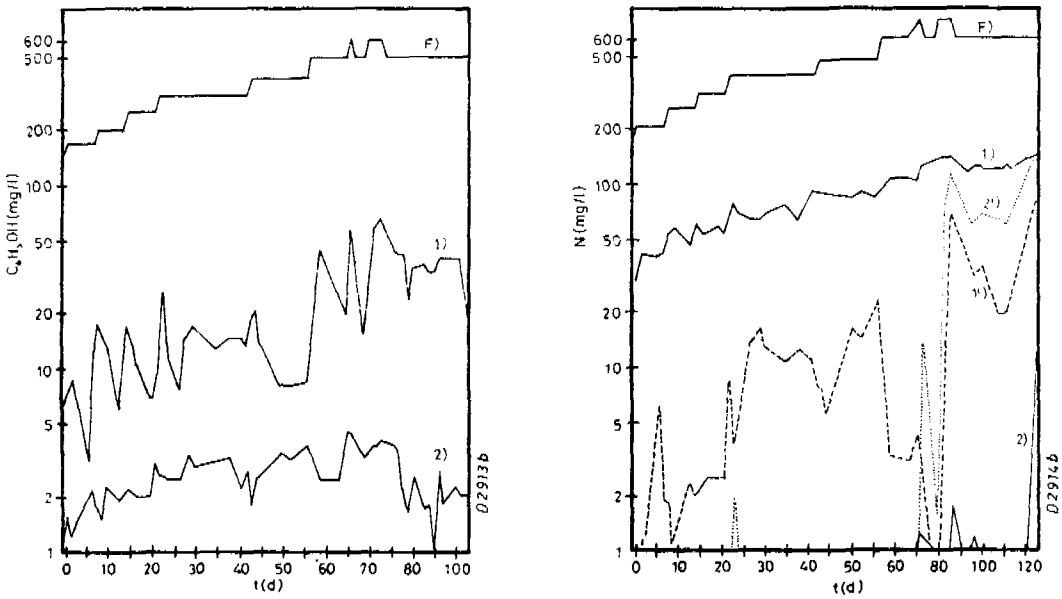

Fig. 2 - Test results at increasing loads. F = phenol or NH_4-N in the feed (synthetic wastewater + tap water); 1: phenol or NH_4-N leaving the anoxic reactor; 1': NO_2-N leaving the anoxic reactor; 2: phenol or NH_4-N leaving the aerobic reactor; 2': NO_2-N leaving the aerobic reactor.

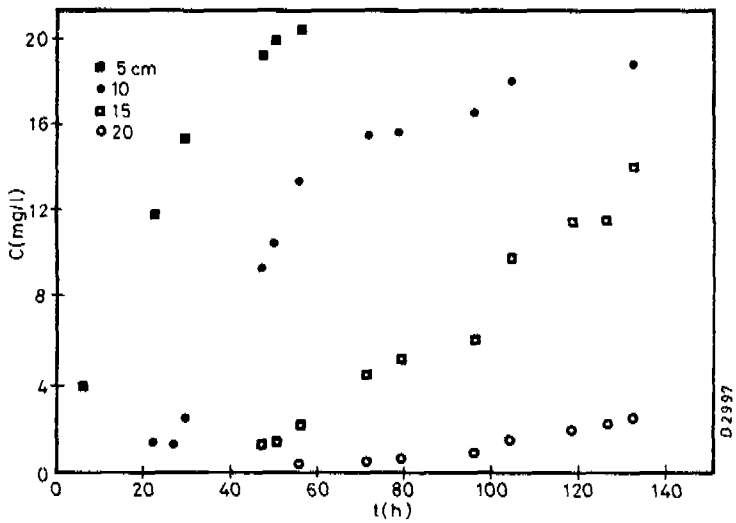

Fig. 3 - Breakthrough curves obtained from column adsorption tests.

Tests conducted with synthetic wastewater do, in fact, show that biomass - and the nitrifying biomass in particular - can be acclimatized to the potentially inhibiting components in the coke discharges without having to adopt excessively high dilutions. More specifically, the minimum dilution compatible with a good treatment pattern was found to be 1 volume synthetic discharge + 4 volumes tap water. When tests were conducted with a real discharge, the dilution required did not increase appreciably (1 volume raw discharge + 5.3 volumes tap water).
Concentration of nitrate nitrogen in the final effluent was found to be far higher than allowed by Italian law (20 mg/l). This was due to the fact that NH_4-N/C_6H_5OH ratio in the water to be treated (1.2 in the synthetic wastewater and 1.5 in the real one) is notably higher than the experimentally-found ratio between oxidized nitrogen and phenols reacting in the denitrification reactor (approximately 0.6). As for main kinetic parameter values, it was seen that, with the exception of ammonia oxidation in the synthetic discharge tests, the nitrification and denitrification rates determined corresponded to the maximum removal rates because testing was always conducted at non-limiting substrate conditions.

Carbon Adsorption Column Test

The correlation between bed height (H) and test duration (t) necessary to determine the characteristic parameters of the Bohart-Adams equation (Bohart and Adams, 1920) was obtained from the breakthrough curves in Fig. 3. This equation enabled calculation of the adsorption zone height (14 cm) and time (84 d) needed for a phenol concentration in the effluent from a 3-m column to reach the maximum value allowed by Italian law (0.5 mg/l).

TECHNICAL AND ECONOMIC EVALUATIONS OF A FULL-SCALE PLANT

Basic Design Considerations

Reference is hereafter made to a discharge treatment plant for coke ovens that produce 1000 t of coke a day. It is assumed that 0.25 m^3 of discharge are produced for every ton of coke.
A correct dimensioning of biological reactors, bearing in mind the process parameters determined by the laboratory scale tests enables virtually negligible ammonium nitrogen and phenol residual concentrations to be obtained. However, considering the Italian limit for effluent phenol concentrations (0.5 mg/l) and the inevitable quality fluctuations of a full-scale plant effluent, provisions must be made for adsorption treatment on activated carbon columns downstream of biological treatment. Adsorption columns were dimensioned on the basis of the same residual concentrations in the biological plant effluent as those detected in the laboratory tests with the real discharge (20 mg/l). Moreover it was decided to adopt a conservative ratio of 1:7 (1 volume raw discharge + 6 volumes dilution water). The follow-

ing main pollutant concentrations in the raw discharge were assumed: total phenols, 2500 mg/l; ammonium nitrogen, 3800 mg/l; thiocyanates, 500 mg/l. Furthermore, the concentration of suspended solids in the final effluent was assumed to be 20 mg/l. Table 4 summarizes the values

TABLE 4 Dimensioning parameters for component units

Component Unit	Parameter
Equalization tanks:	- Hydraulic retention time: 4h - Specific stirring power installed: 15 W/m^3
Pumping station:	- Pump pressure head: 0,6 bar - Pump efficiency: 0.70
Anoxic reactors:	- Biomass concentration(*): 3000 mg SS/l - Denitrification rate: 0.05 kgNO_3-N/kg VSS·d - Specific phenol consumption ratio: 1.7 kg phenol/kg NO_3-N - Specific stirring power installed: 15 W/m^3 - Net growth yield: 0.2 kg VSS/kg phenols
Aerobic reactors:	- Biomass concentration(*): 3000 mg SS/l - Nitrification rate: 0.25 kg NH_4-N/kg VSS·d - Oxygen required for nitrification: 4.6 kg O_2/kg NH_4-N - Efficiency of oxygenation: 1.6 kg O_2/kWh absorbed
Settling tanks:	- Overflow rate: 0.5 $m \cdot h^{-1}$ - Hydraulic retention time (referred to supernatant): 7 h
Pumping and recycling stations:	- Recycling ratio: 2:1 - Pump pressure head: 0.3 bar - Pump efficiency: 0.70
Adsorption columns:	- Hydraulic loading rate: 5 $m.h^{-1}$ - Height of each column: 3 m
Thickeners:	- Sludge residence time: 20 h - Solids load: 30 kg SS/m^2.d - Concentration of thickened sludges: 20 kg SS/m^3
Aerobic digesters:	- Hydraulic retention time: 12 d - Specific oxygen consumption ratio: 2.3 kg O_2/kg VSS removed - Mechanical efficiency of oxygenation: 1.6 kg O_2/kWh absorbed - Volatile solids reduction: 50%
Drying beds:	- Specific area: 200 m^2/1000 inhabitants

(*) Biomass characteristics: VSS/SS = 0.85; nitrogen ponderal fraction (referred to SS) = 0.085

of the design parameters for the various units.

Cost Evaluation

Plant costs for each operating unit (excluding adsorption and regeneration of activated carbon) have been obtained by correlations with a statistical processing of cost data from 35 treatment plants throughout Italy and from design estimates (National Research Council, 1981). Plant costs for the adsorption and regeneration of the activated carbon section were obtained from Perrich, 1981.
Table 5 summarizes capital costs.

TABLE 5 Capital cost (10^6 Italian Liras)

Operating Units	Civil works	Electromechanical equipment
Equalization tanks	40	14
Pumping station		8
Anoxic reactors	280	91
Aerobic reactors	168	254
Settling tanks	89	82
Recycling pumping stations		13
Adsorption columns		250
Activated carbon regeneration furnace		350
Thickeners	10	31
Aerobic digestors	13	10
Drying beds	20	
Electrical equipment and hydraulic network		515
Accessory works	277	
Total Plant Cost	897	1618

Amortization costs were determined on the basis of 15 years for the electromechanical equipment and 30 years for the civil works and on an annual interest on capital of 10%.
As for running costs, basic data were obtained from experience and specialized tests (National Research Council, 1981; Perrich, 1981; U.S. Environmental Protection Agency, 1978). Table 6 reports the calculated running costs.
To conclude, the overall cost for a treatment plant as outlined above (including amortization and running costs) is estimated to be 799.10^6 Italian liras per year. The specific treatment cost per m^3 of raw coke plant discharge is 8750 liras (5.3 U.S. $ per m^3).

TABLE 6 Running Costs

Item	10^6 Italian Liras/yr
Staffing	168
Power	131
Operation and Maintenance	49
Chemicals(*)	143
Total	491

(*) Activated carbon, alkali and phosphorus make-up.

CONCLUSIONS

The main results may be summarized as follows:
By using the anoxic-aerobic single sludge process it is possible to obtain very high efficiency in the treatment of a coke plant discharge diluted with 5-6 volumes of water (98% nitrification and 95% phenols removal).
Nitrogen removal efficiency (assimilative and dissimilative) is approximately 35%; low efficiency is only due to the low phenol/ammonium nitrogen ratio in the raw discharge.
Cost analysis on a full scale plant designed on the basis of the test results showed a specific cost of approximately 9000 liras per m^3 of raw discharge, including amortization (approximately 2000 liras, i.e. 1.2 U.S. $, per t of coke produced).
Treatment costs may be reduced by ammonia stripping before the biological treatment; this would be facilitated by high temperature, high pH and the favourable free ammonia/combined ammonia ratio of the raw discharge. Use of fluidized beds in the denitrification stage might also reduce costs. Furthermore, conservative figures have been assumed for design calculations (specific production of waste and phenol concentration in the final effluent were especially overestimated), and consequently costs are also overestimated.

ACKNOWLEDGEMENT

The authors wish to thank Mr. Franco Duranti for his valid assistance with the experimental and analytical aspects of this work.

REFERENCES

Ashmore, A.G., J.R. Catchpole, and R.L. Cooper (1967). The biological

treatment of carbonization effluents. Wat. Res., 1, 605-624.

Bark, L.S., R.L. Cooper, and K.C. Wheatstone (1972). The determination of organic bases in carbonization effluents. Wat. Res., 6, 117-126.

Barker, J.E., and R.J. Thompson (1973). Biological removal of carbon and nitrogen compounds from coke plant wastes. U.S. Environmental Protection Agency, EPA-R2-73-167.

Beccari, M., R. Passino, R. Ramadori, and V. Tandoi (1980). Inhibitory effects on nitrification by typical compounds in coke plant wastewaters. Envir. Technol. Lett., 1, 245-252.

Beccari, M., R. Passino, R. Ramadori, and V. Tandoi (1983). Denitrification kinetics in the treatment of phenol wastes in a single-sludge system. Envir. Technol. Lett., 4, 163-172.

Bohart, G.S., and E.Q. Adams (1920). Some aspects of the behavior of charcoal with respect to chlorine. J. Am. Chem. Soc., 42, 523-544.

Bridle, T.R., W.K. Bedford, and B.E. Jank (1980). Biological treatment of coke plant wastewaters for control of nitrogen and trace organics. Proceedings 53rd Conf. Wat. Pollut. Contr. Fed.

Institution of Gas Engineers (1967). Recommended analytical methods for gas works and coke oven effluents. Booklet N° 1.

National Research Council, Water Research Institute (1972). Analytical methods for water. Booklet N° 11.

National Research Council, Water Research Institute (1981). Costs of domestic wastewater treatment plant. Booklet N° 46.

Perrich, J.R. (1981). Activated adsorption for wastewater treatment. C.R.C. Press, Inc.

Strickland, J.D.H., and T.R. Parson (1972). A practical handbook of seawater analysis. Fisheries Research Board of Canada, (II Ed.).

U.S. Environmental Protection Agency (1978). Energy conservation in municipal wastewater treatment. Report 430/9-77-011.

Kinetics and Aeration in Aerobic Treatment

Industrial Wastewater Treatment

Nitrification and Denitrification